

ERDC/CHL TR-02-8

Coastal and Hydraulics Laboratory



**US Army Corps
of Engineers®**
Engineer Research and
Development Center

Biscayne Bay Field Data Volume 2, Plates and Appendices

Robert McAdory, Thad C. Pratt, Martin T. Hebler,
Timothy L. Fagerburg, and Richard Curry

July 2002



The contents of this report are not to be used for advertising, publication, or promotional purposes. Citation of trade names does not constitute an official endorsement or approval of the use of such commercial products.

The findings of this report are not to be construed as an official Department of the Army position, unless so designated by other authorized documents.



PRINTED ON RECYCLED PAPER

Biscayne Bay Field Data

Volume 2, Plates and Appendices

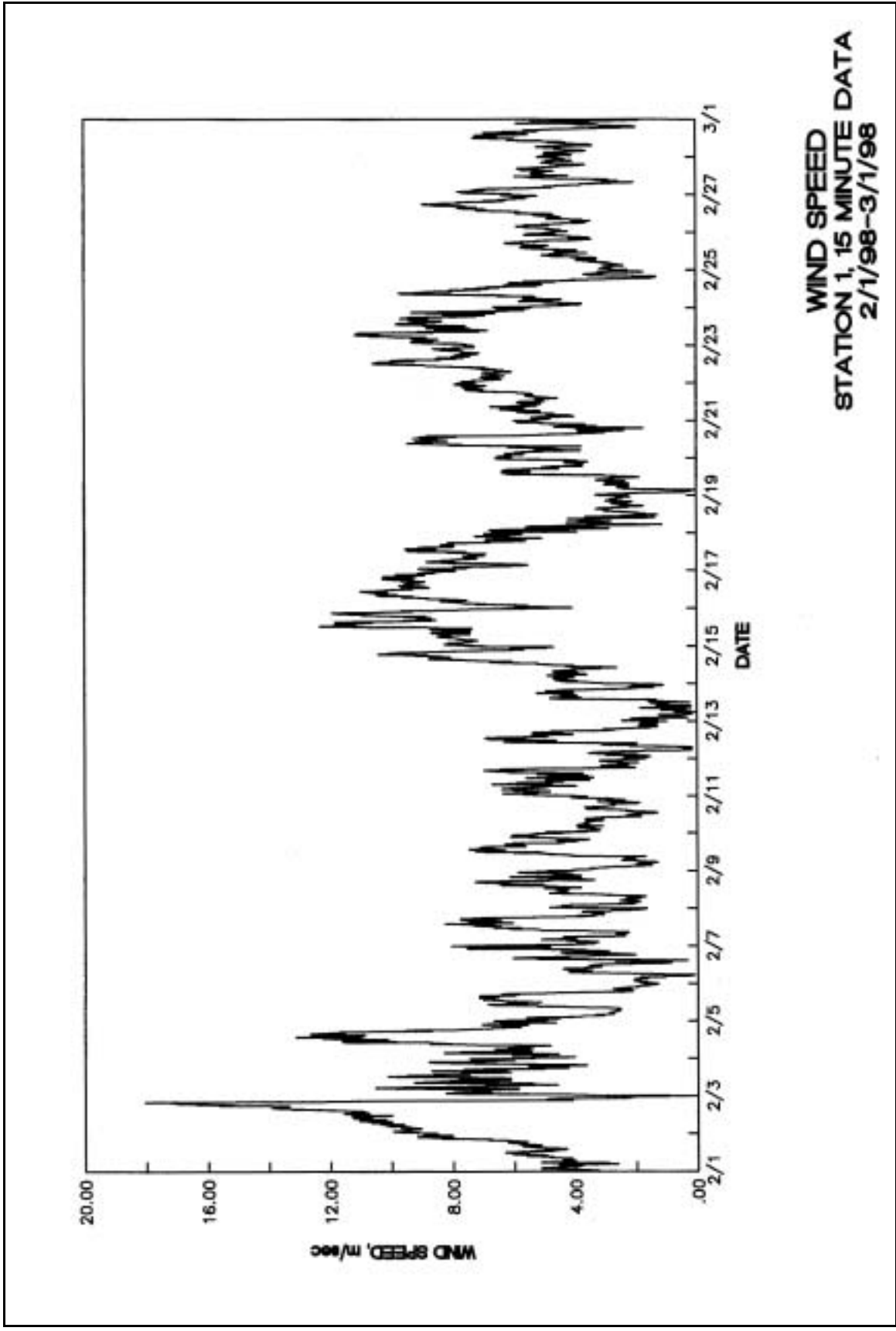
by Robert McAdory, Thad C. Pratt,
Martin T. Hebler, and Timothy L. Fagerburg
Coastal and Hydraulics Laboratory
U.S. Army Engineer Research and Development Center
3909 Halls Ferry Road
Vicksburg, MS 39180-6199

Richard Curry
Biscayne National Park
9700 SW 328th Street
Homestead, FL 33034-5634

Final report

Approved for public release; distribution is unlimited

Prepared for U.S. Army Engineer District, Jacksonville
P.O. Box 4970
Jacksonville, FL 32232-0019



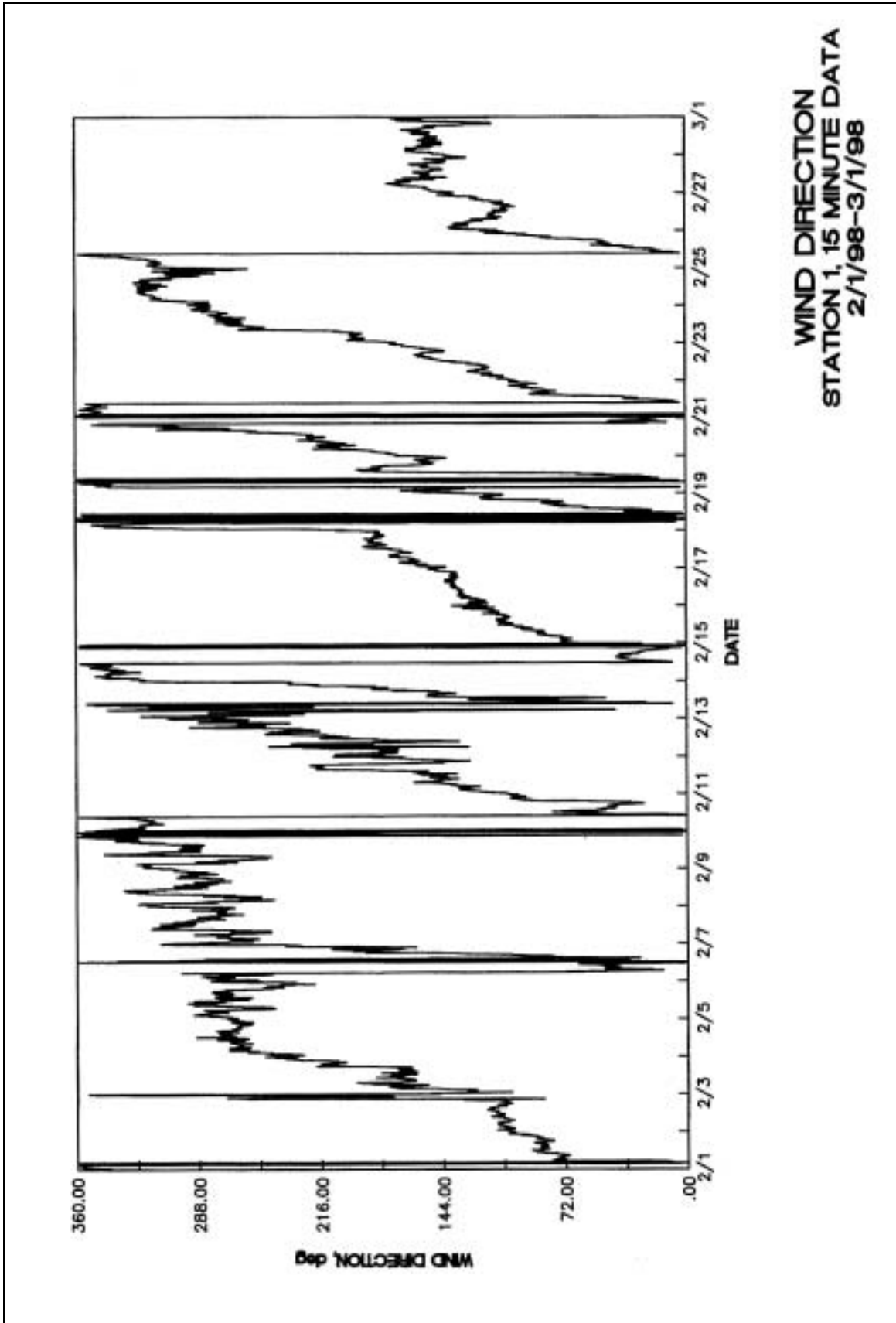
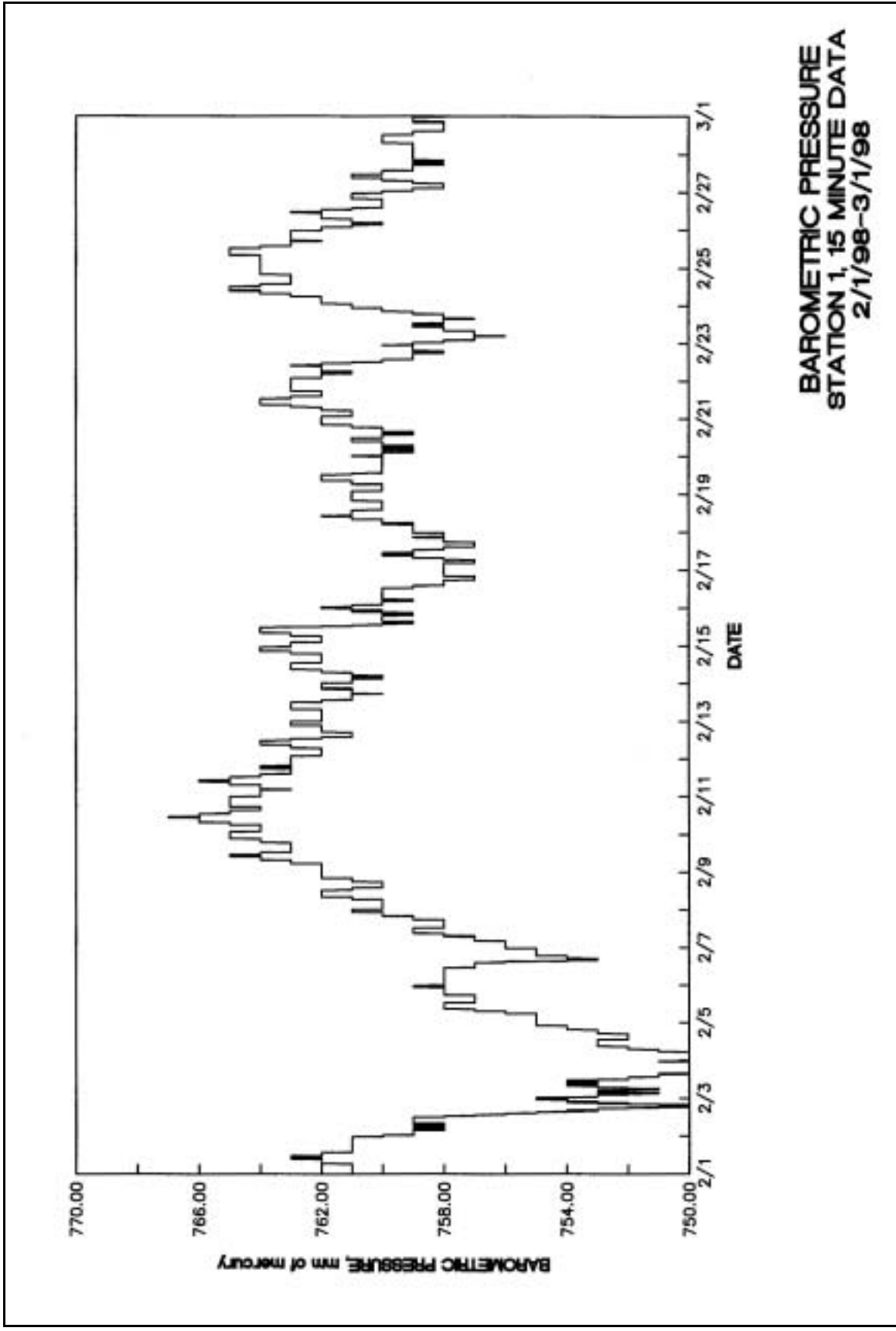


Plate 2



**BAROMETRIC PRESSURE
STATION 1, 15 MINUTE DATA
2/1/98-3/1/98**

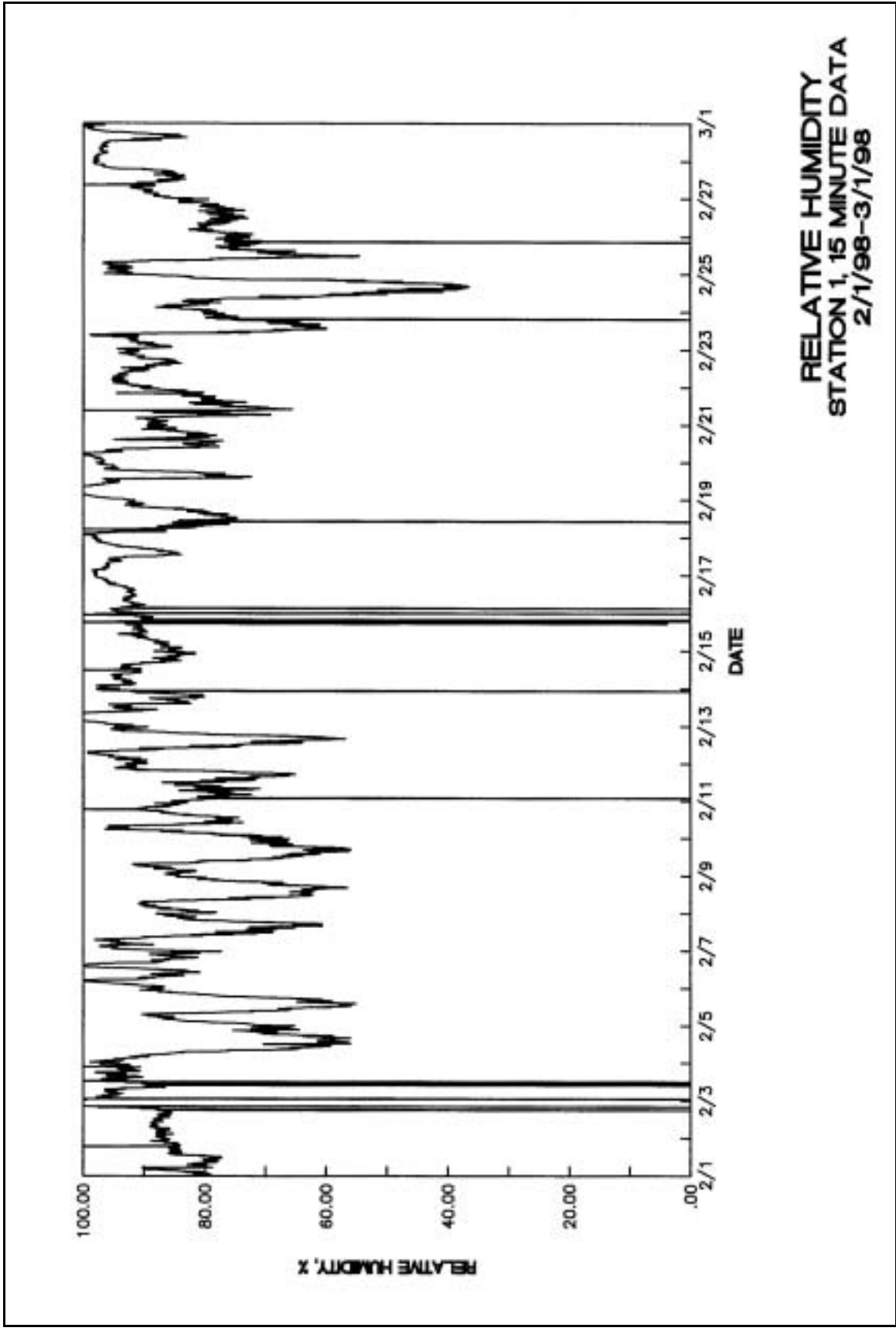
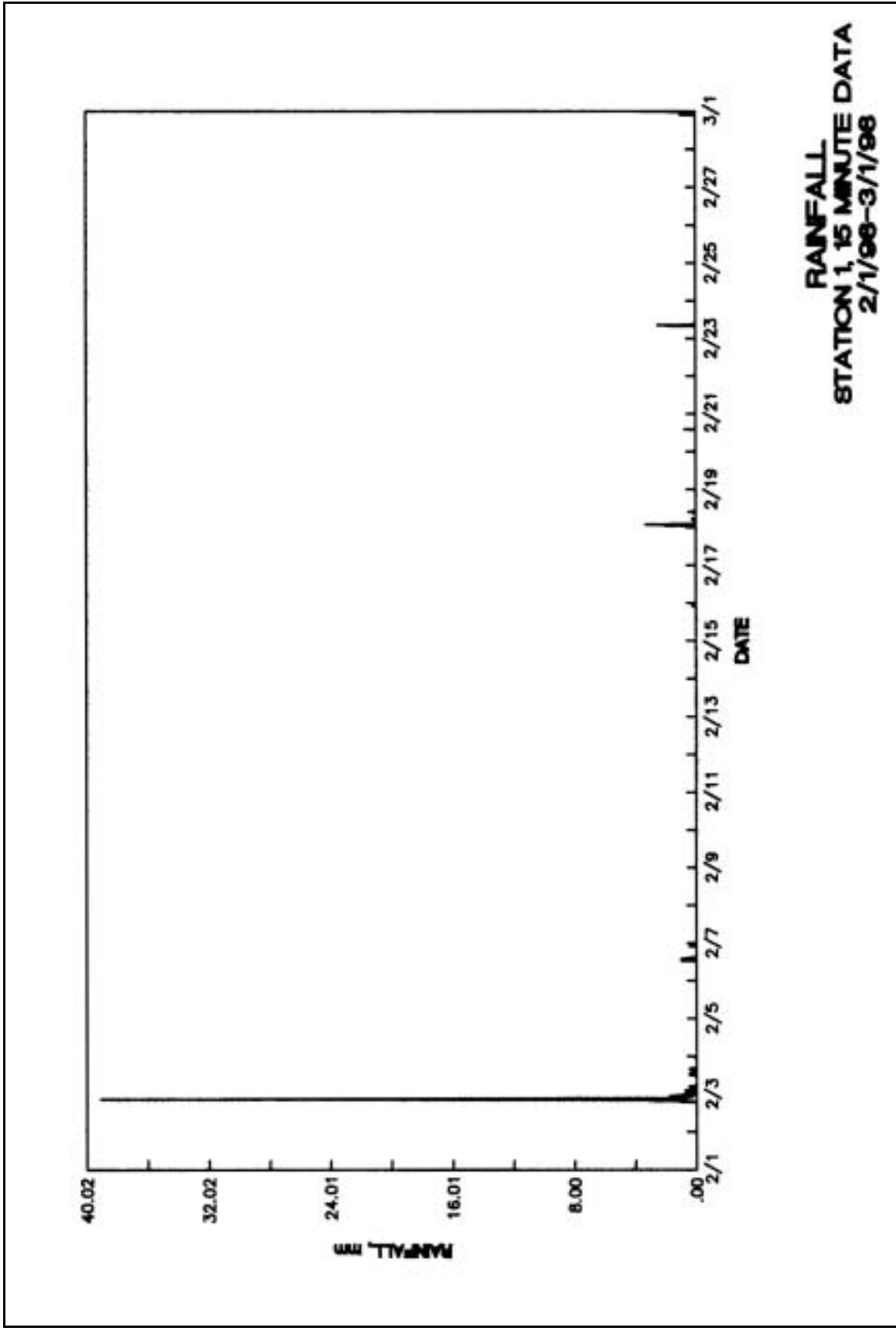


Plate 4



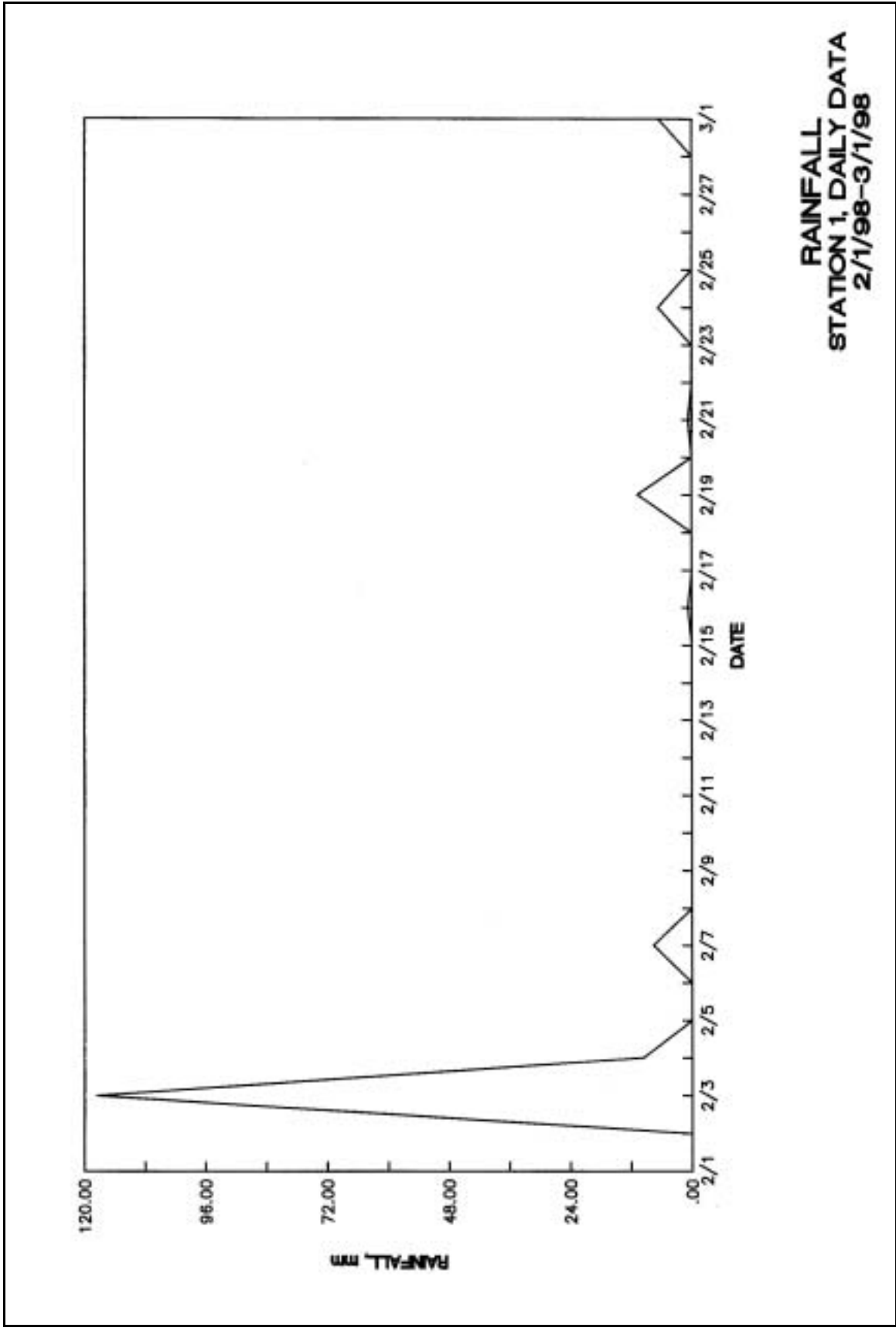
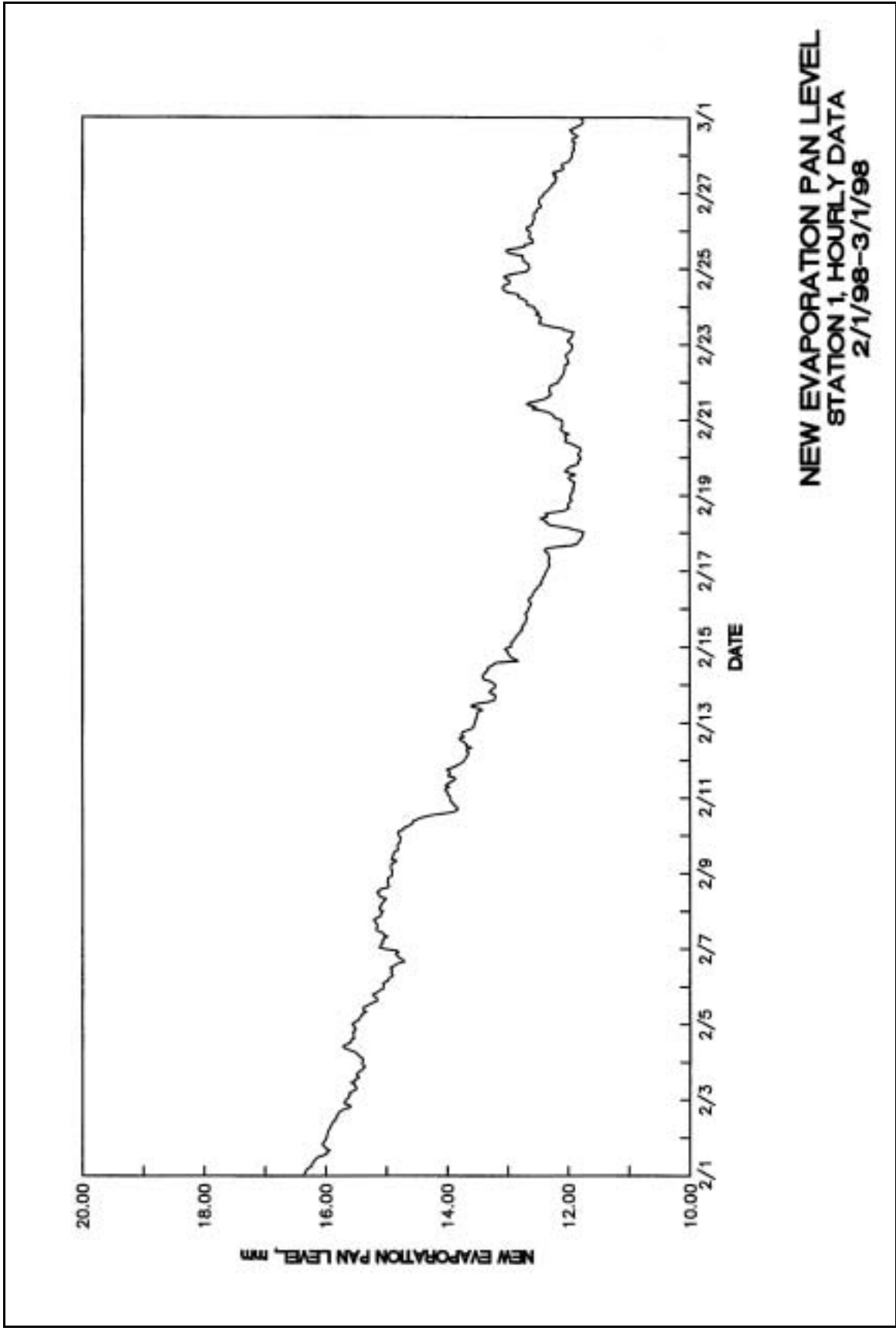


Plate 6



**NEW EVAPORATION PAN LEVEL
STATION 1, HOURLY DATA
2/1/98-3/1/98**

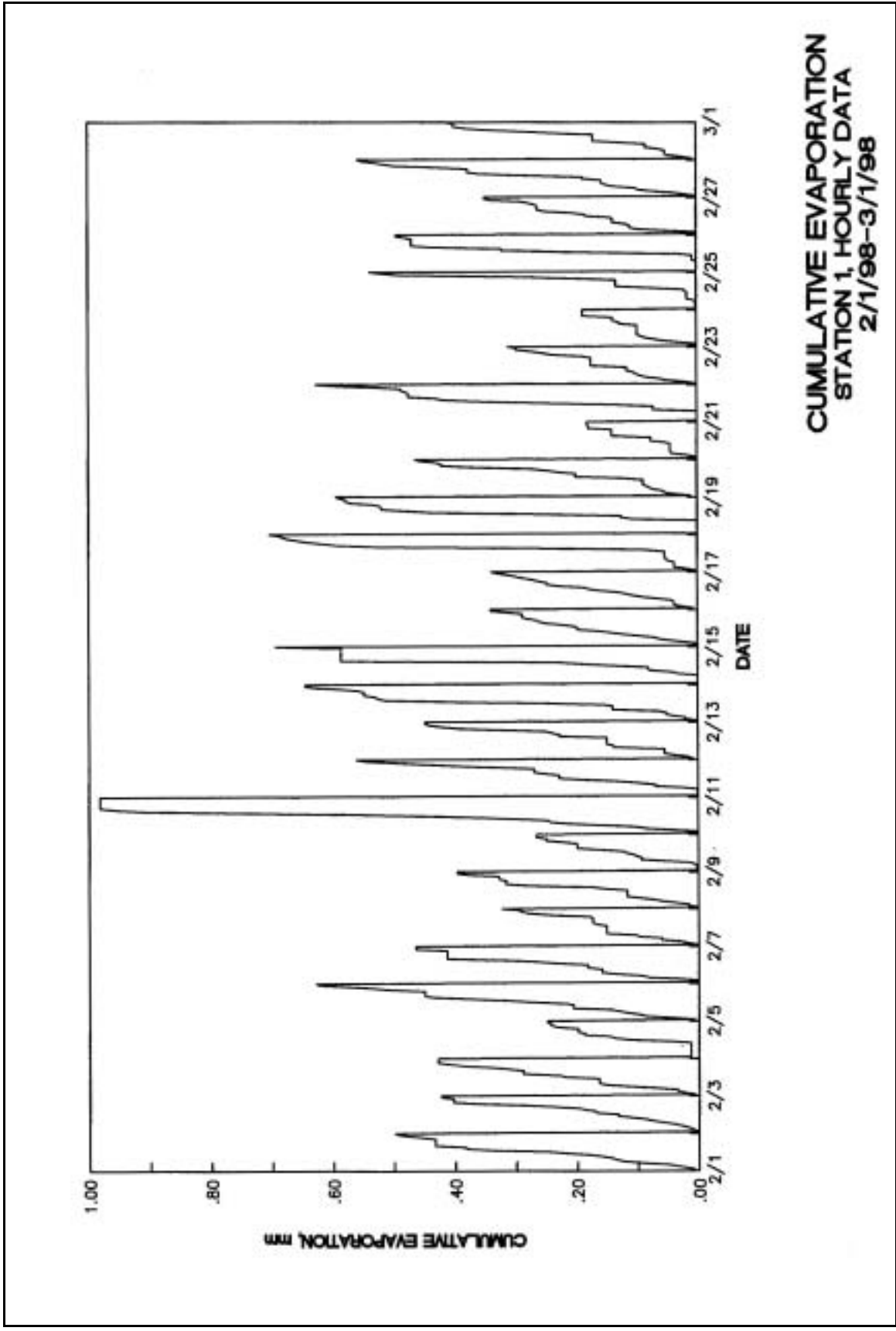
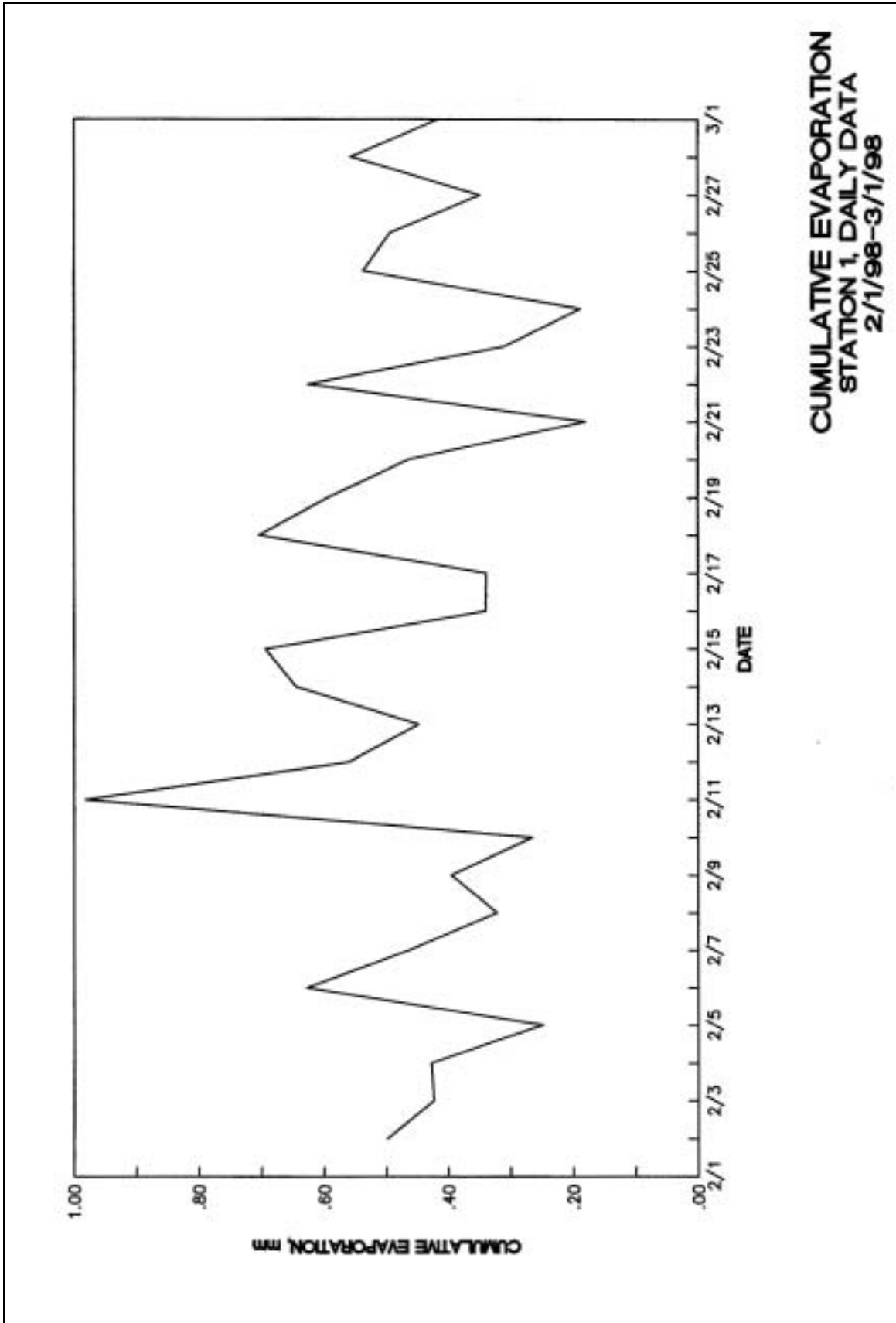


Plate 8



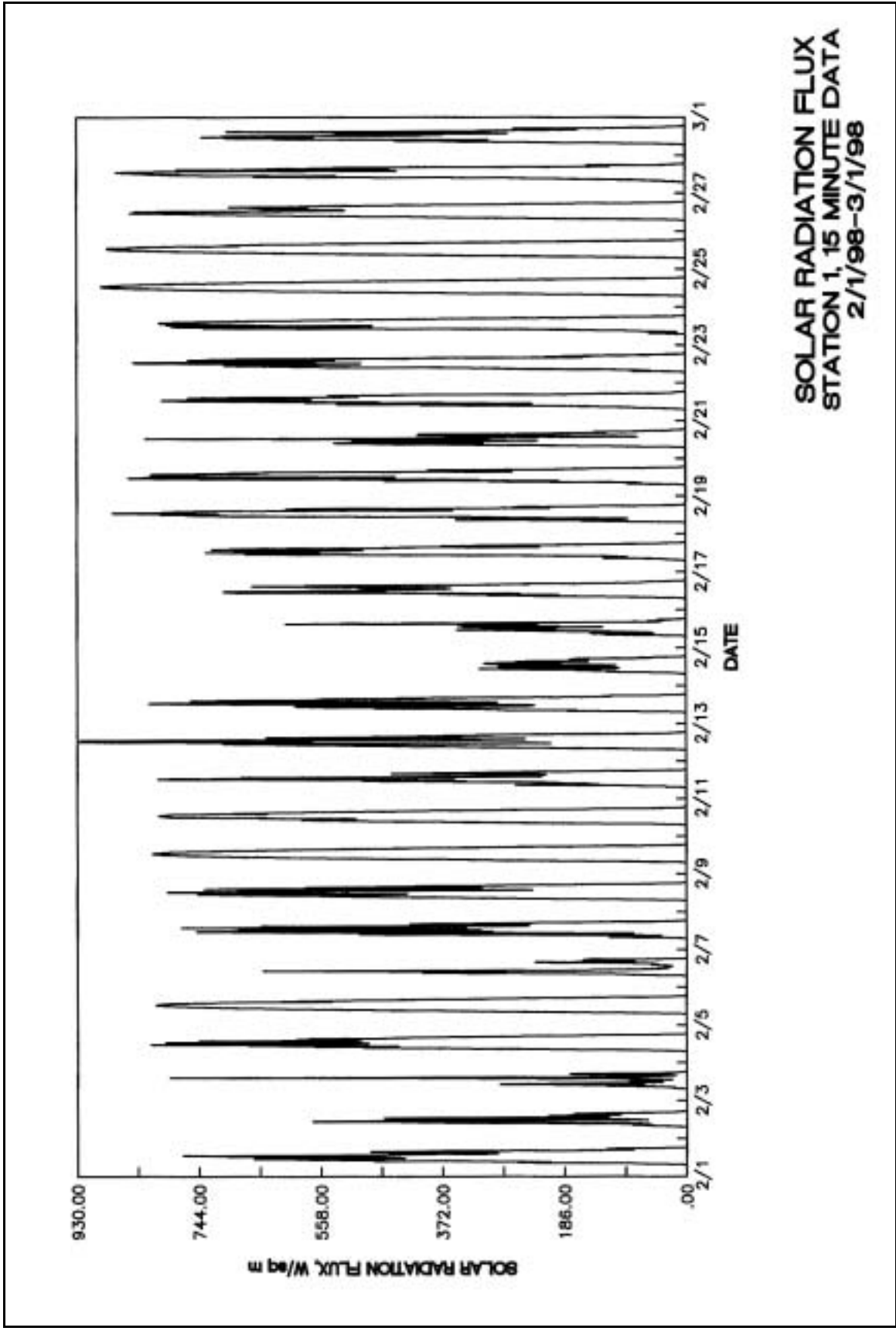
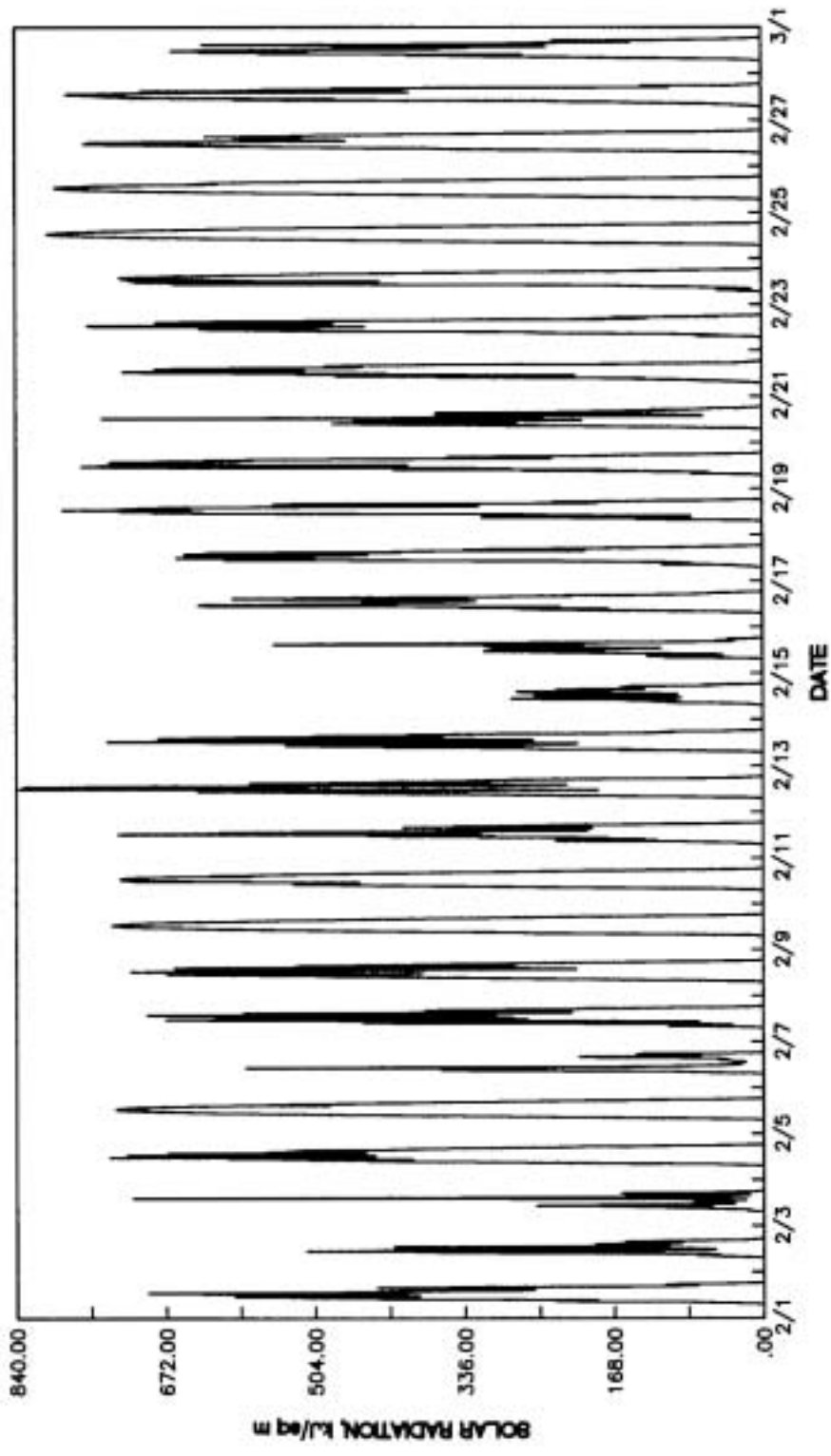


Plate 10



**SOLAR RADIATION
STATION 1, 15 MINUTE DATA
2/1/98-3/1/98**

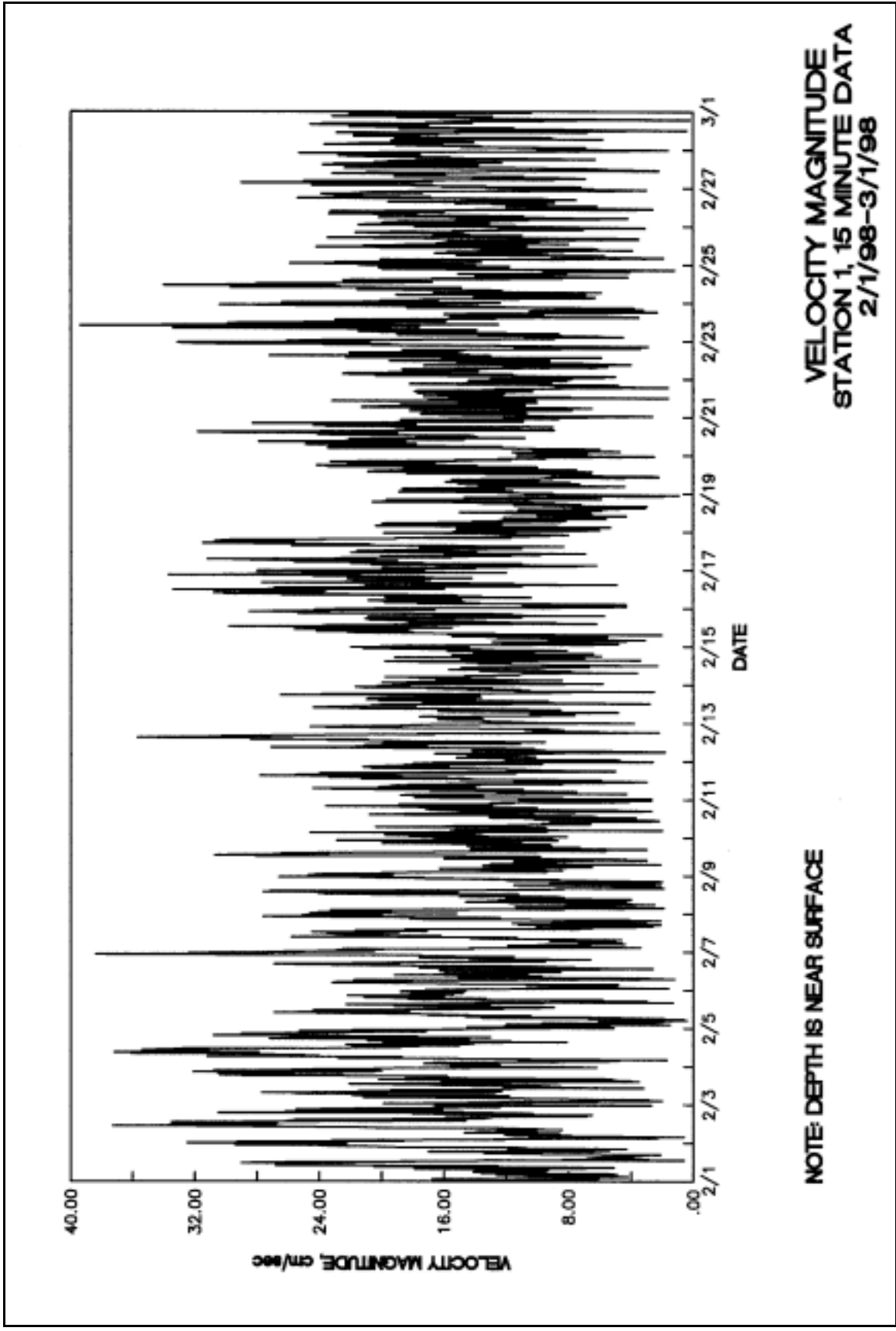
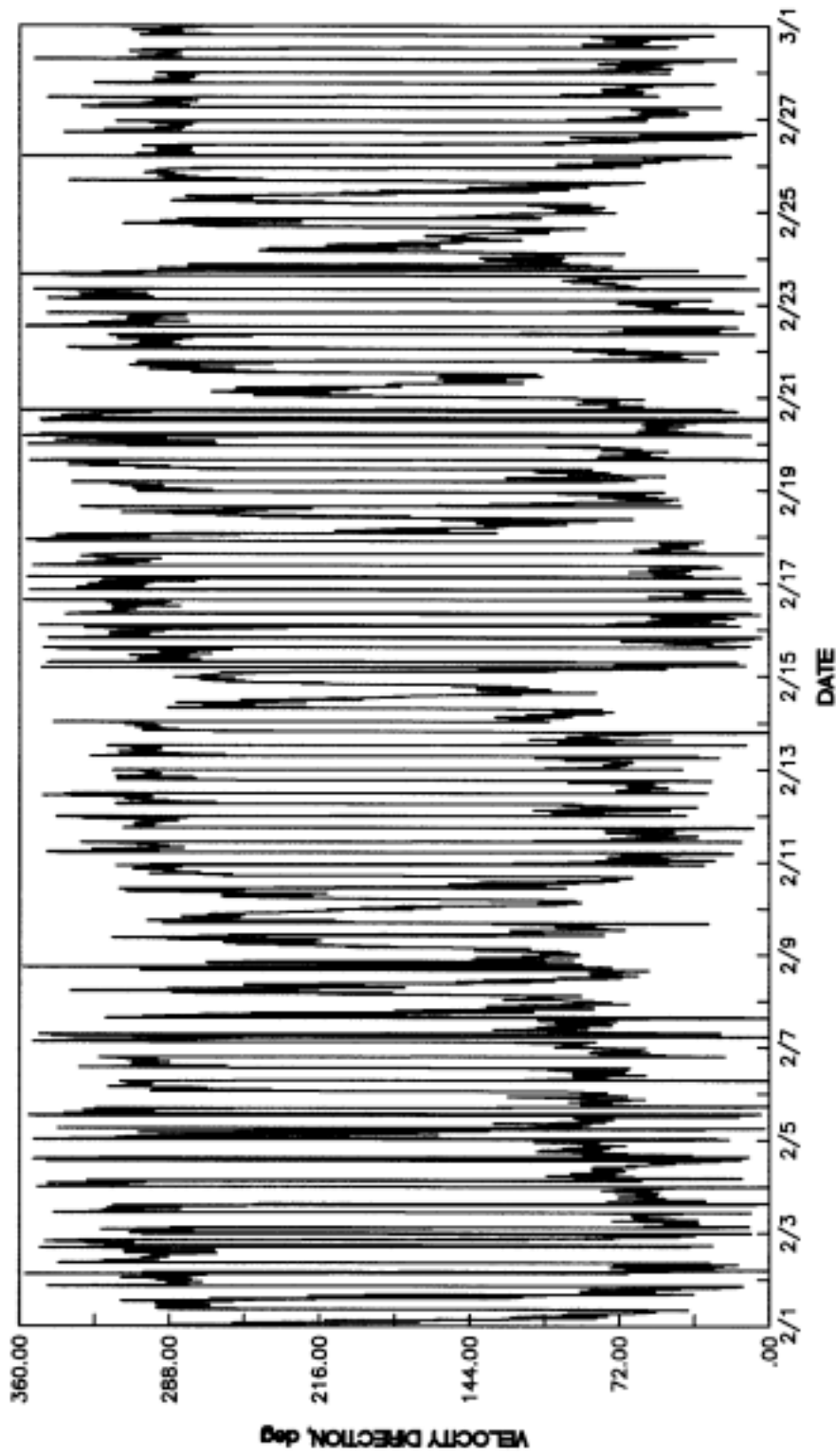
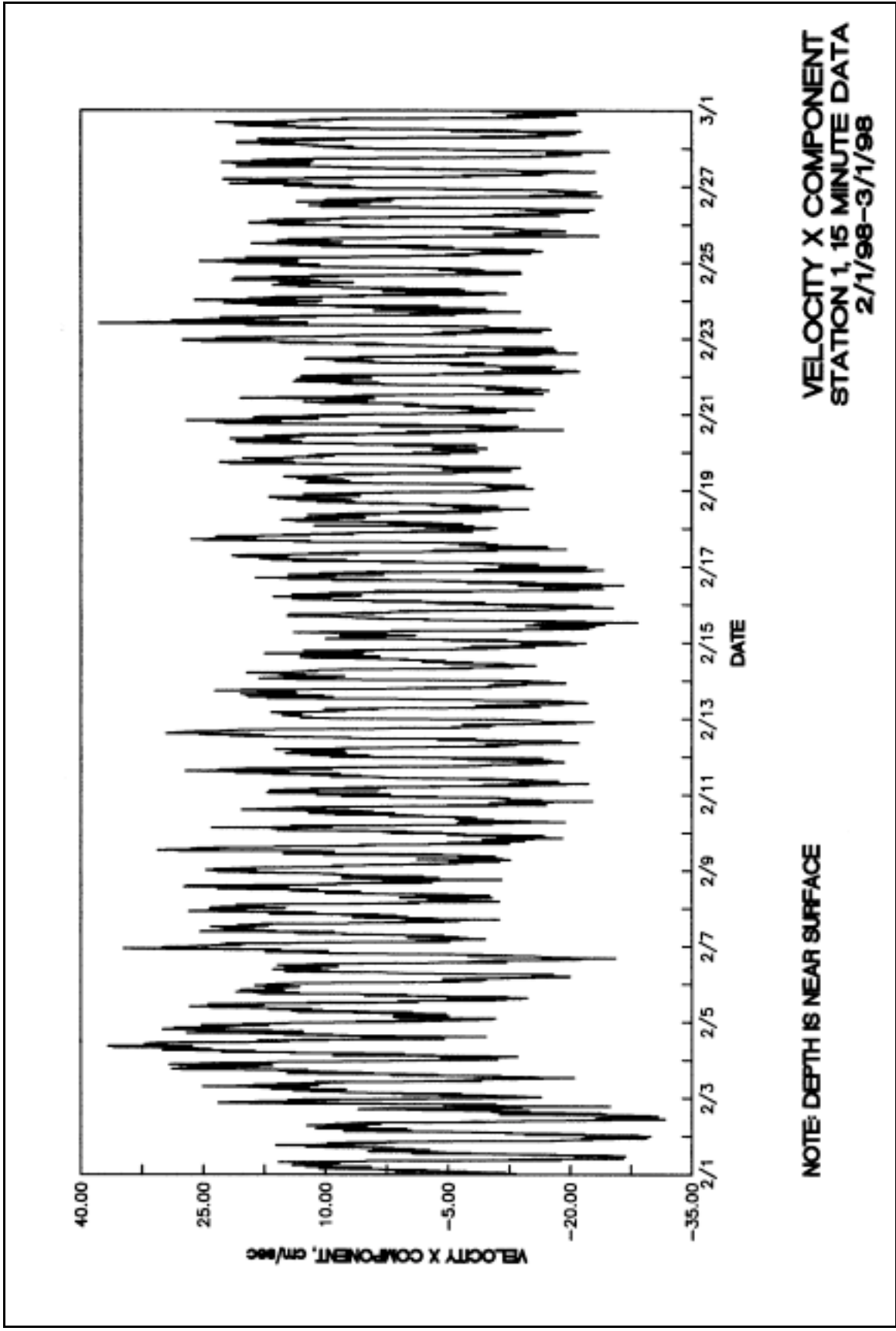


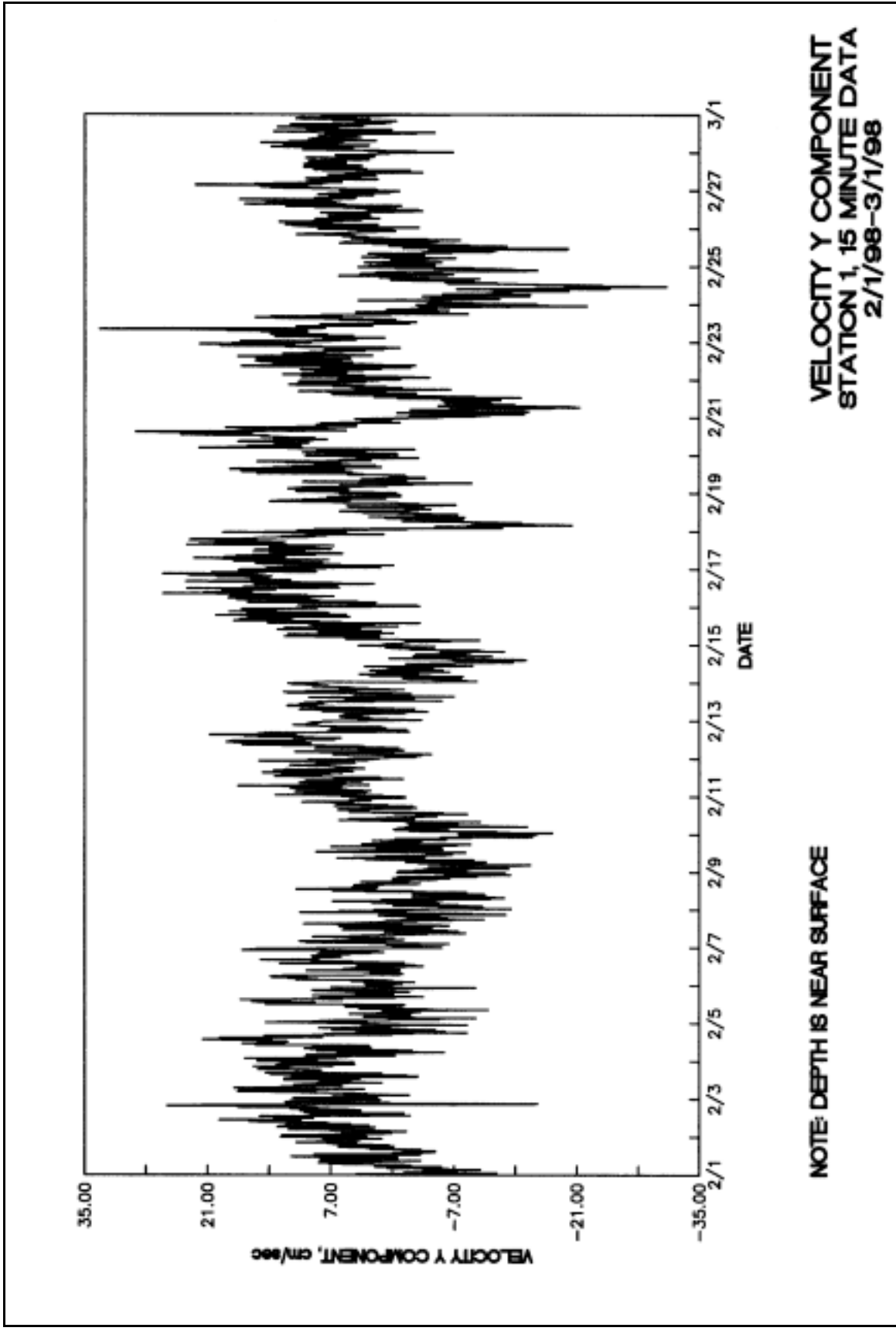
Plate 12



**VELOCITY DIRECTION
STATION 1, 15 MINUTE DATA
2/1/98-3/1/98**

NOTE: DEPTH IS NEAR SURFACE





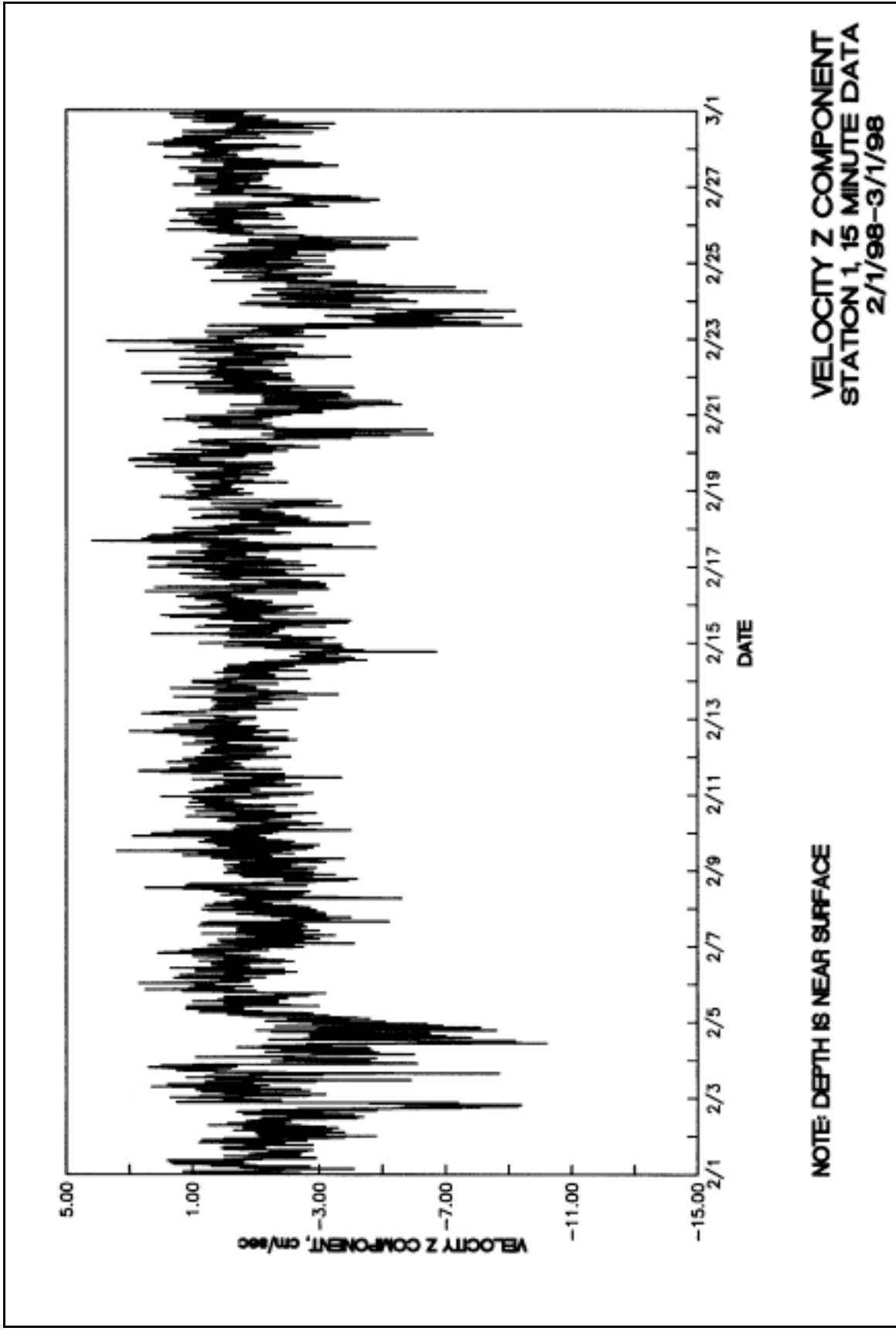
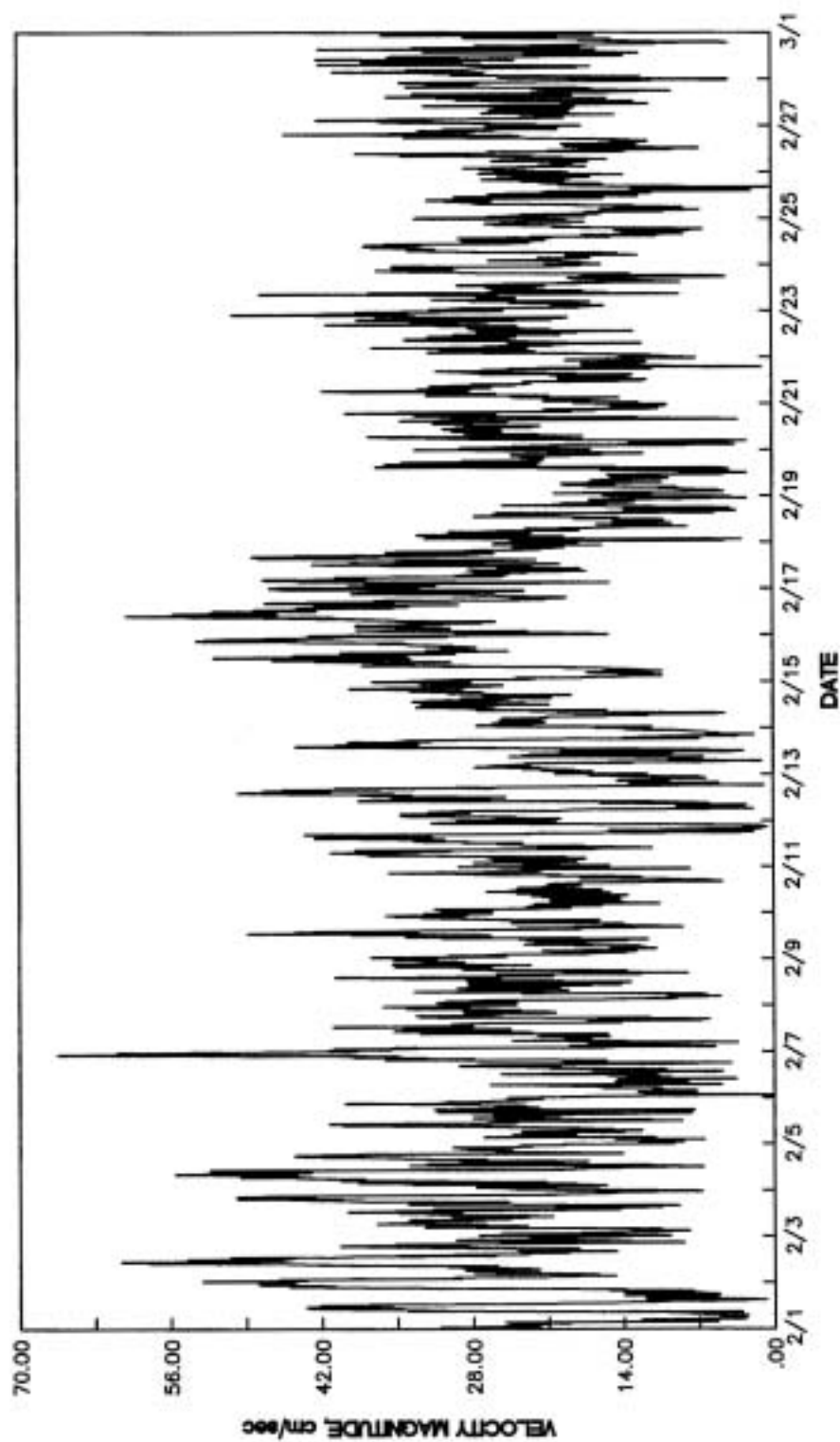
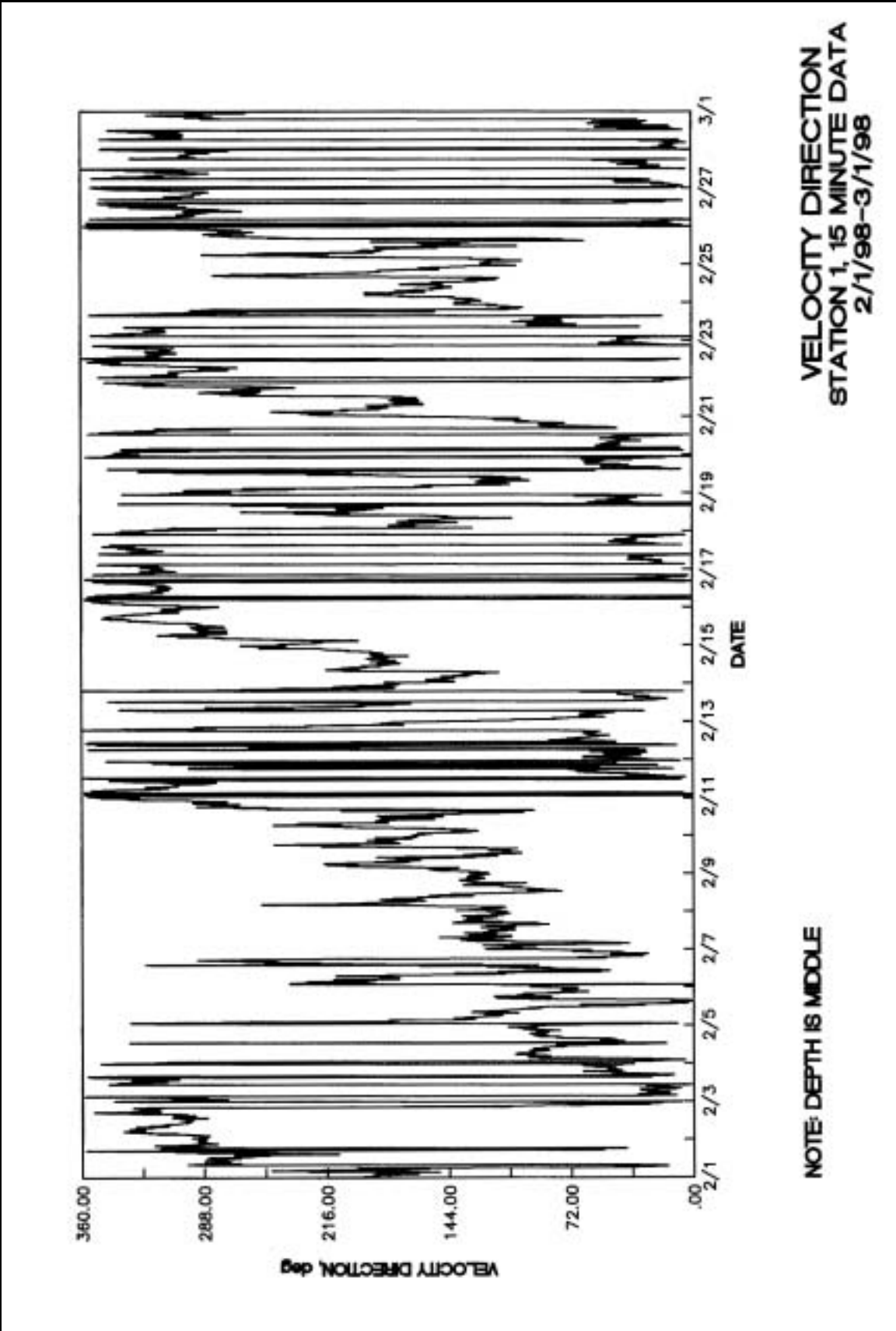


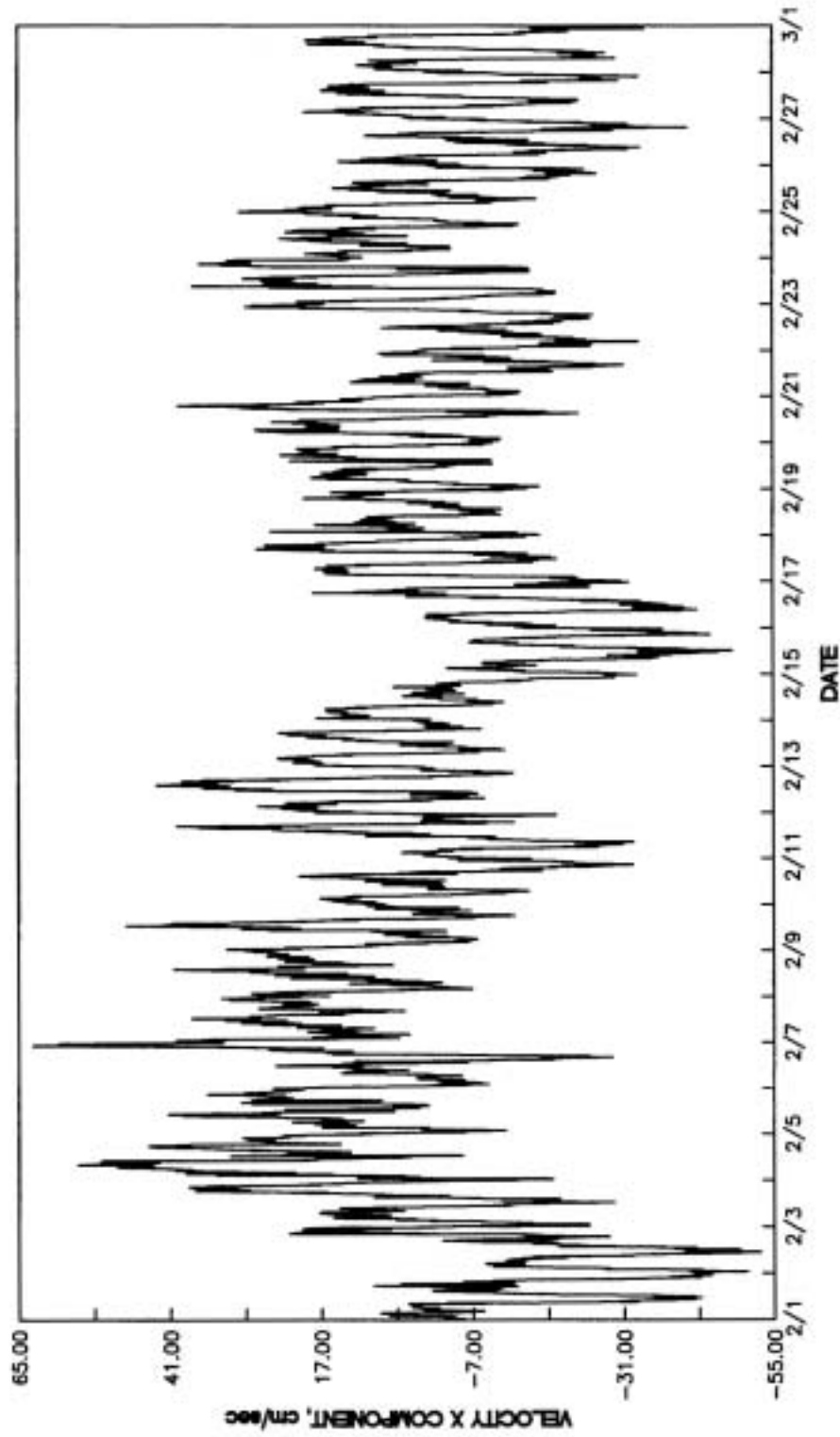
Plate 16



**VELOCITY MAGNITUDE
STATION 1, 15 MINUTE DATA
2/1/98-3/1/98**

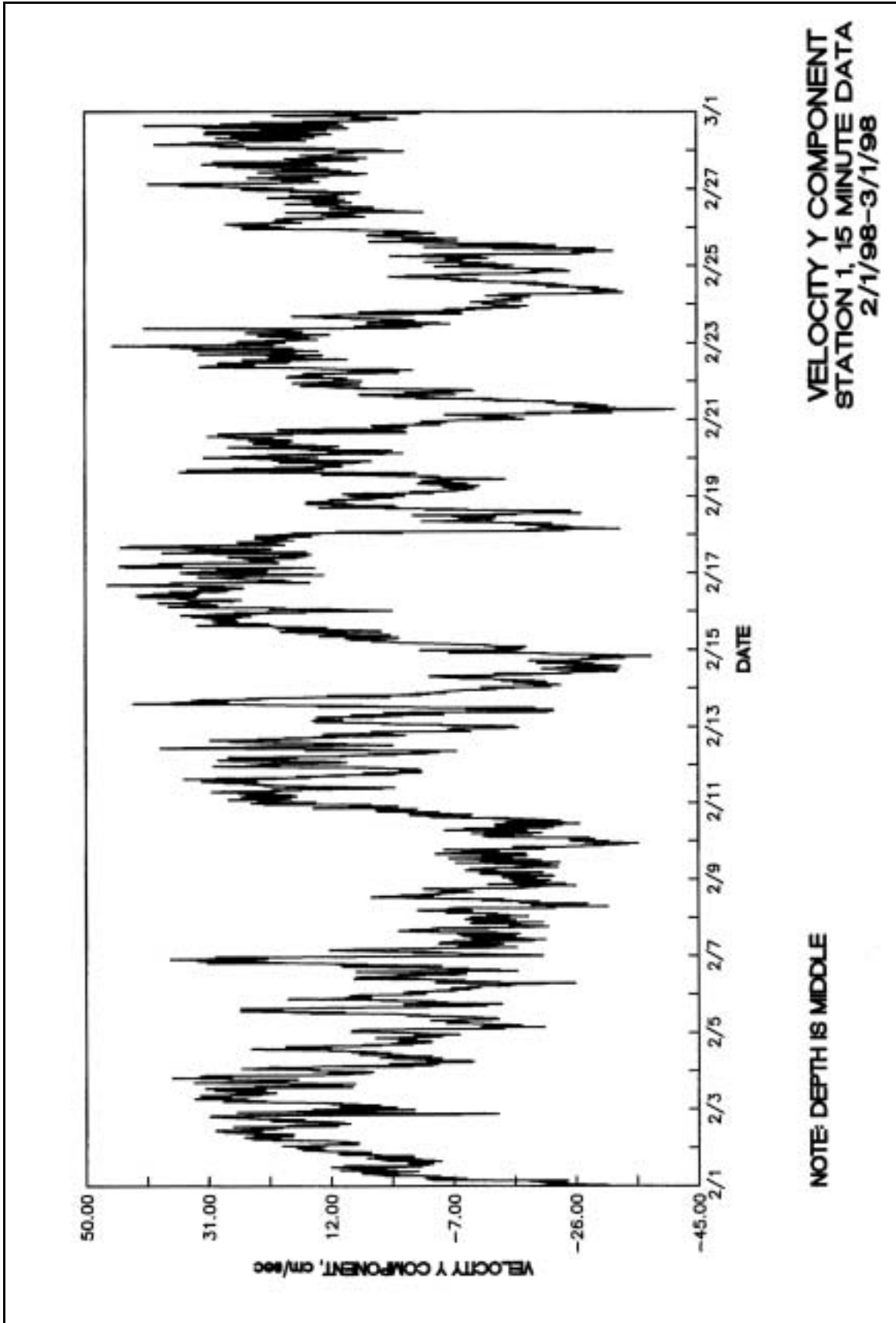
NOTE: DEPTH IS MIDDLE

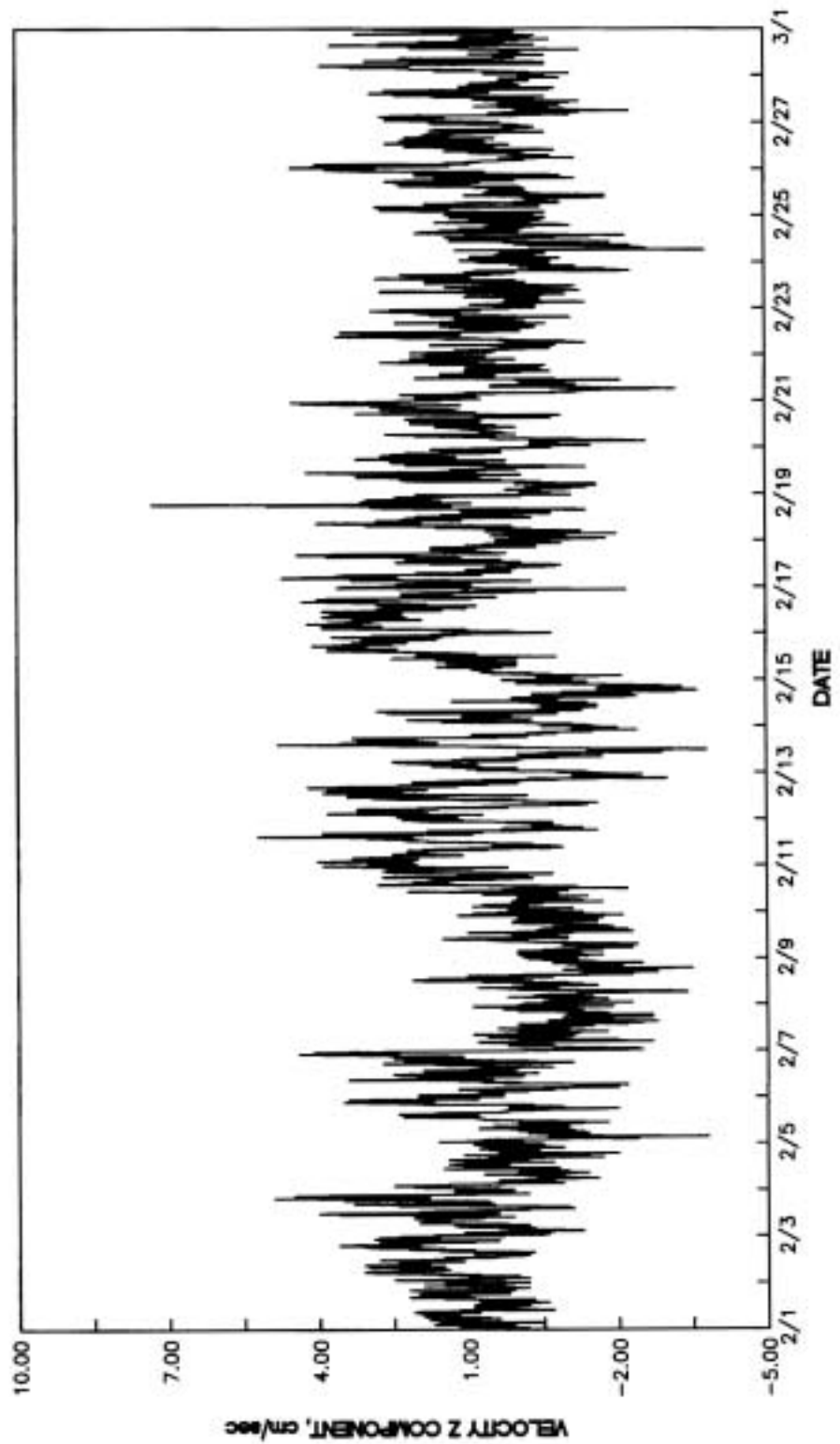




**VELOCITY X COMPONENT
STATION 1, 15 MINUTE DATA
2/1/98-3/1/98**

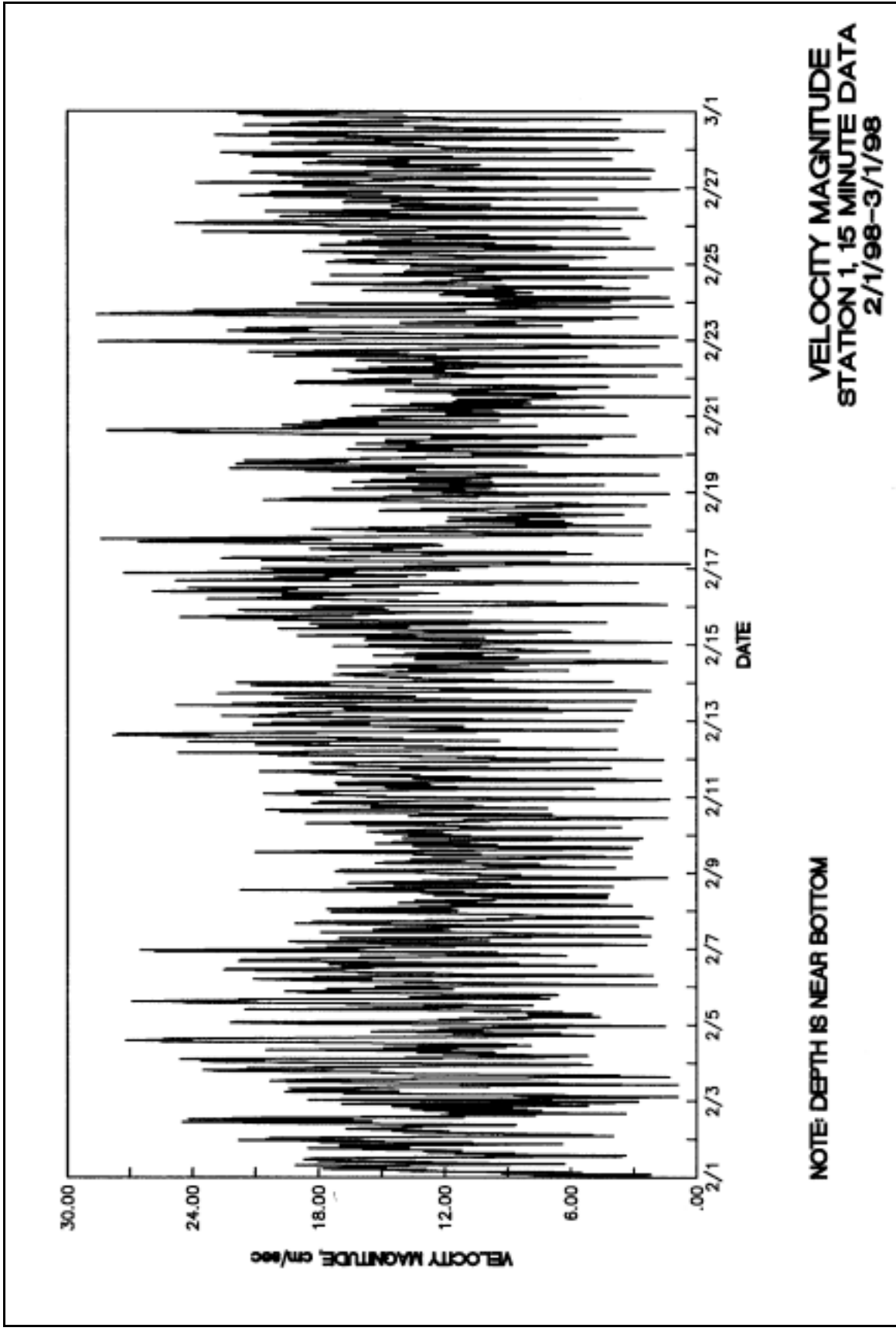
NOTE: DEPTH IS MIDDLE

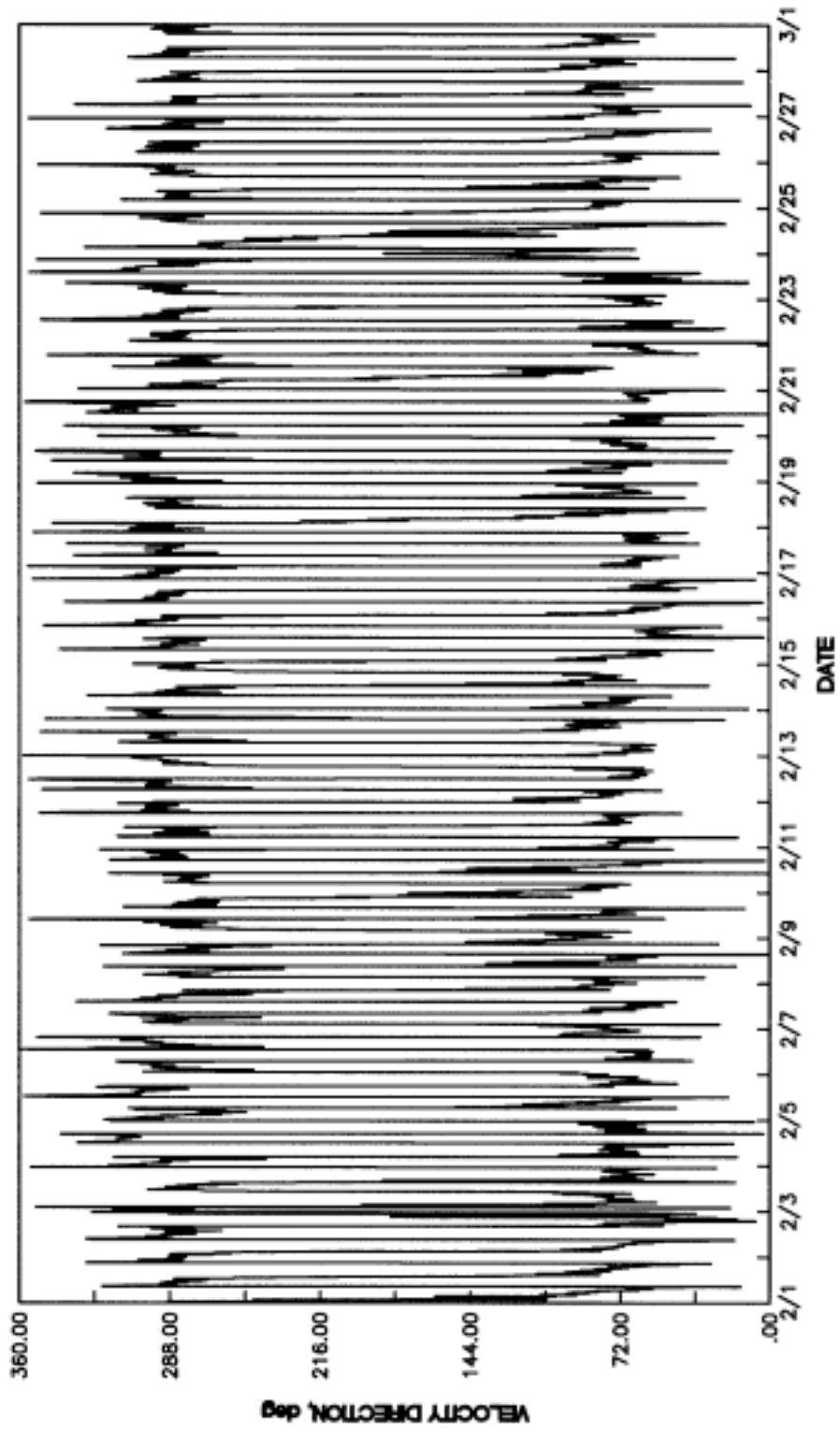




**VELOCITY Z COMPONENT
STATION 1, 15 MINUTE DATA
2/1/98-3/1/98**

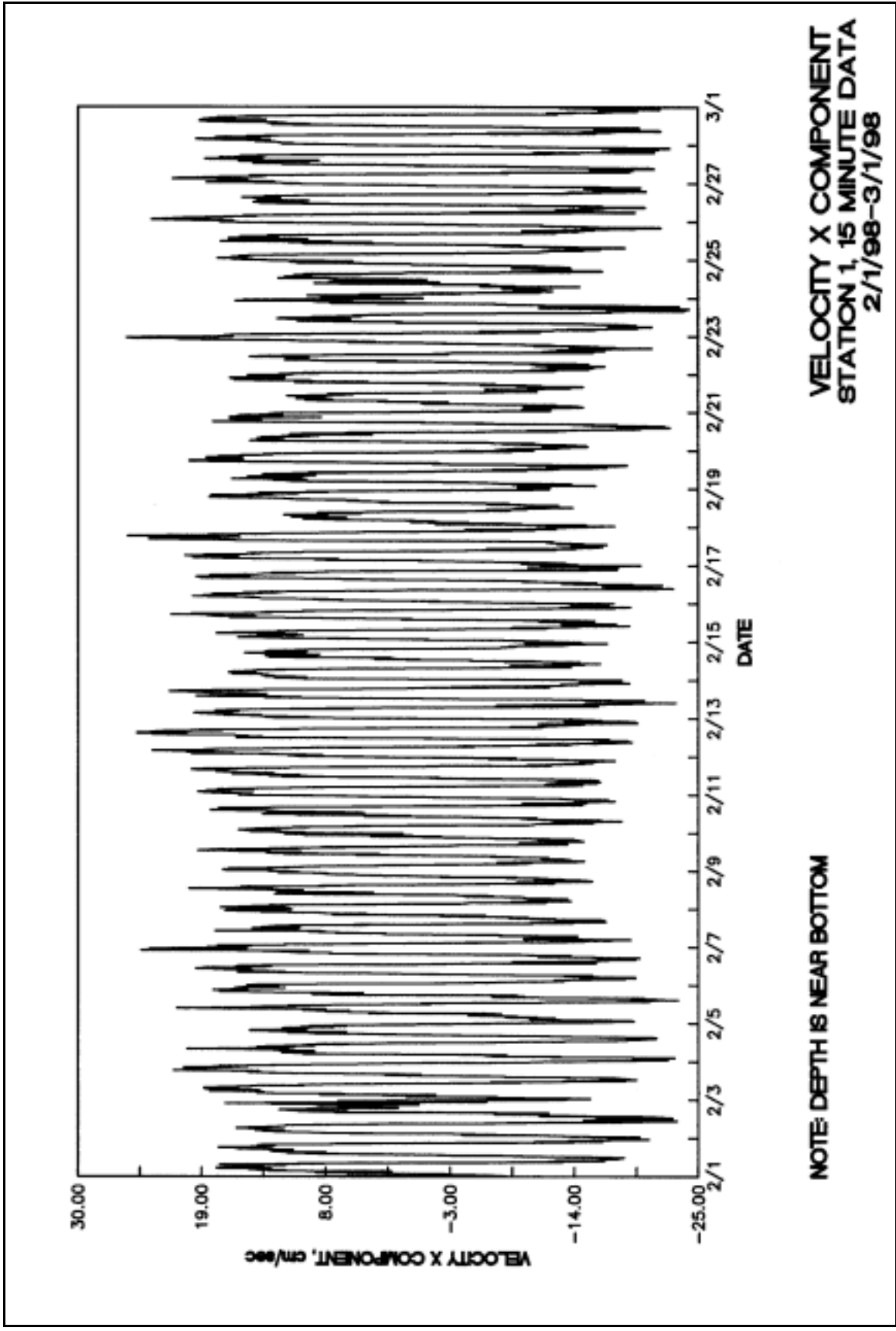
NOTE: DEPTH IS MIDDLE

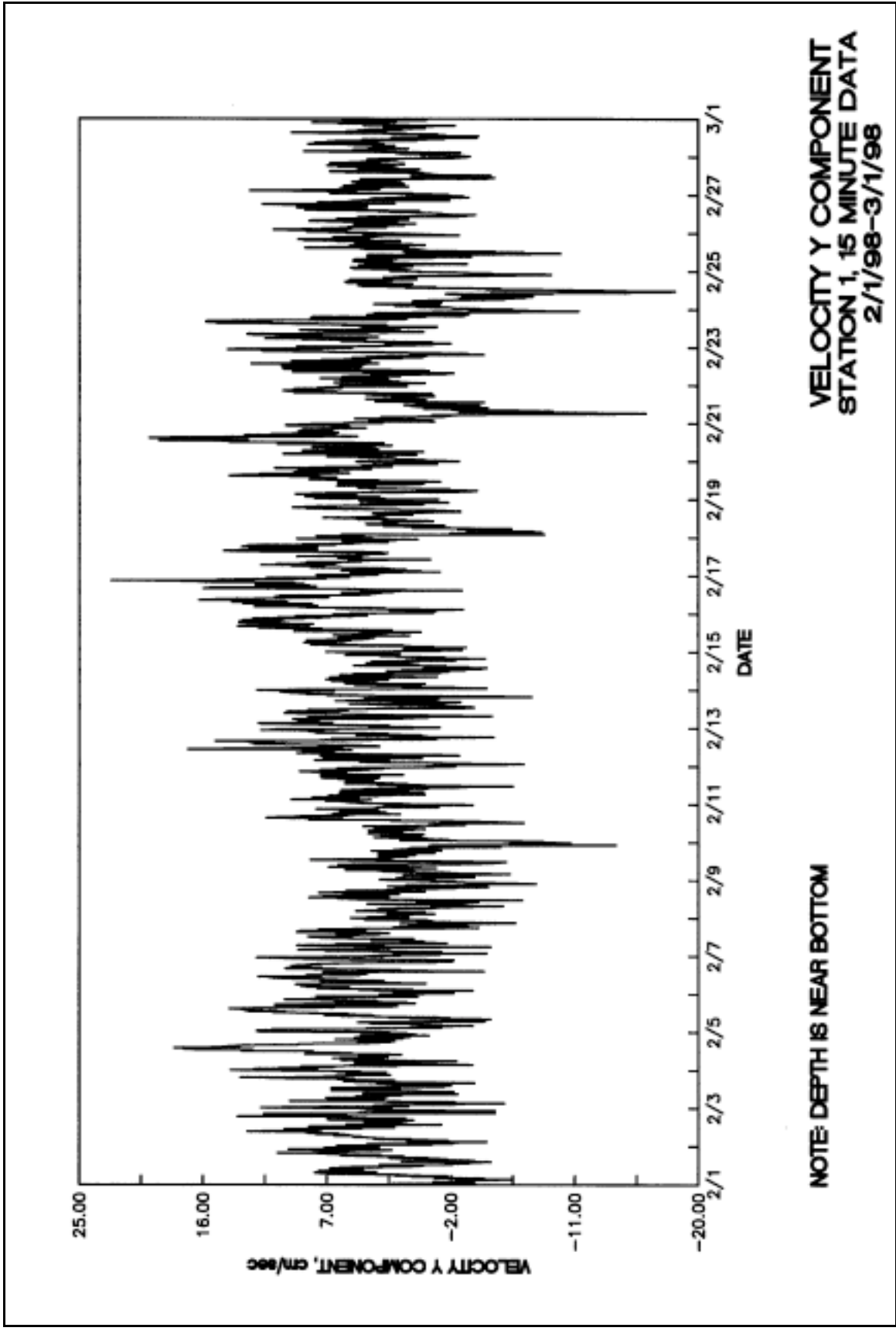


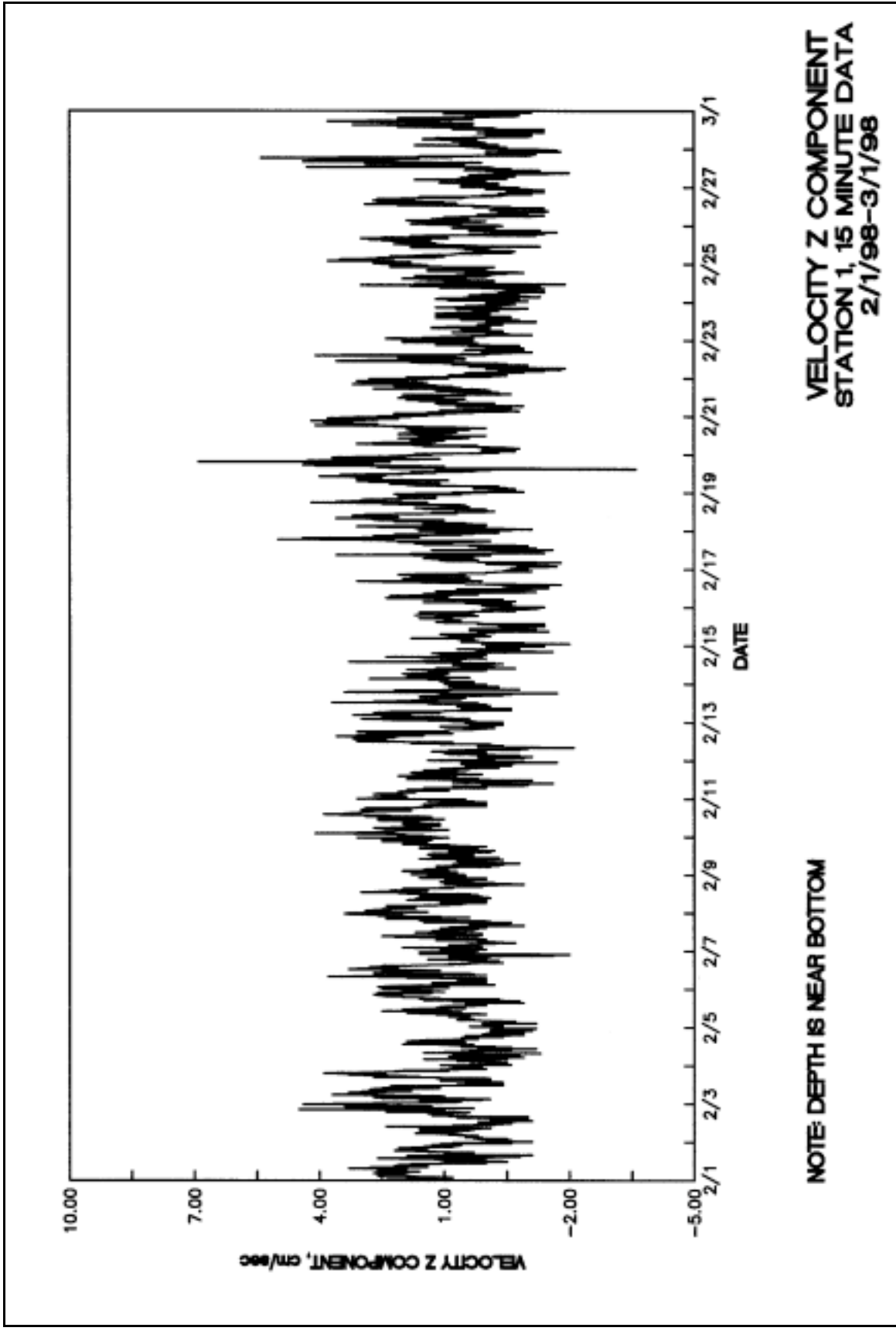


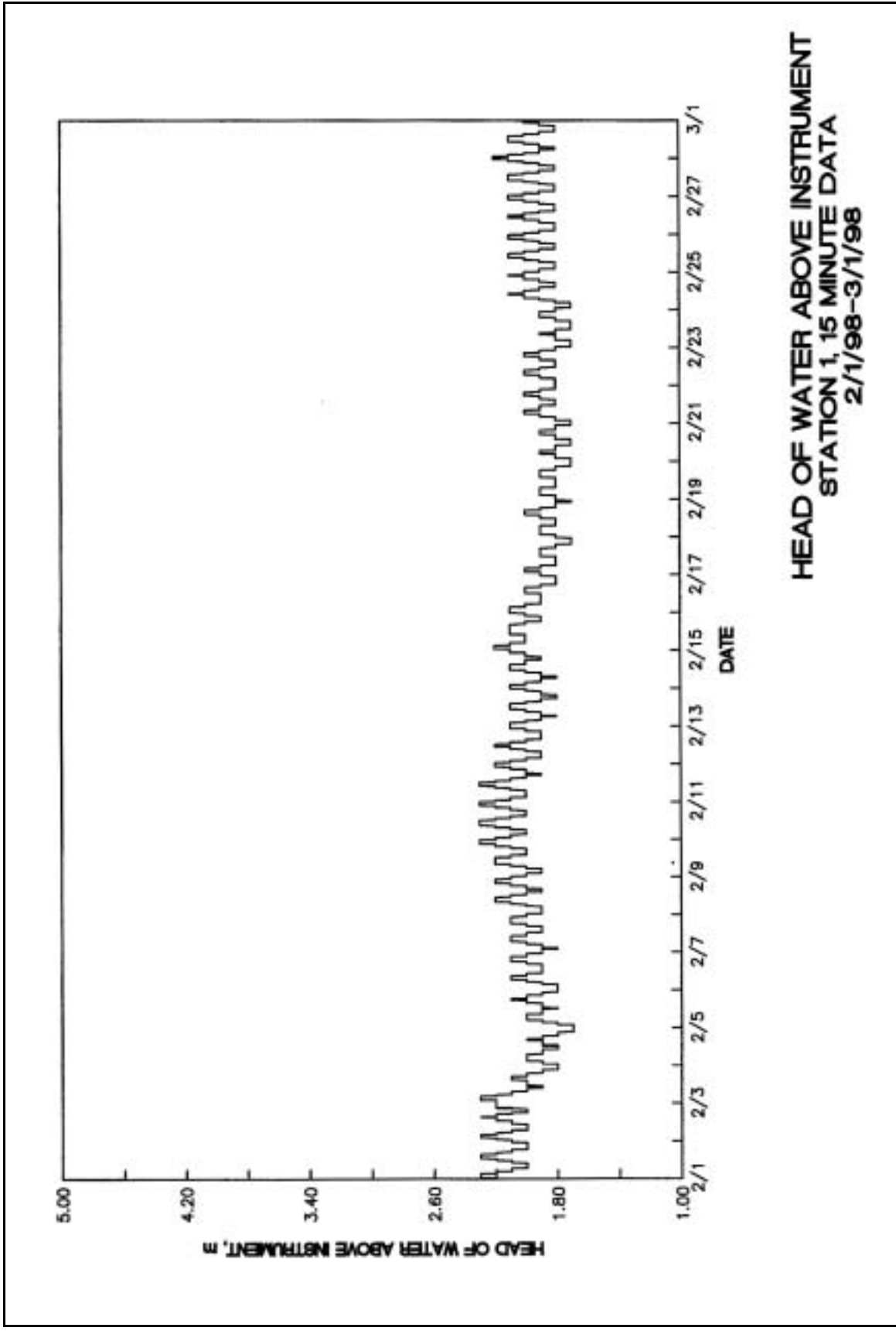
**VELOCITY DIRECTION
STATION 1, 15 MINUTE DATA
2/1/98-3/1/98**

NOTE: DEPTH IS NEAR BOTTOM

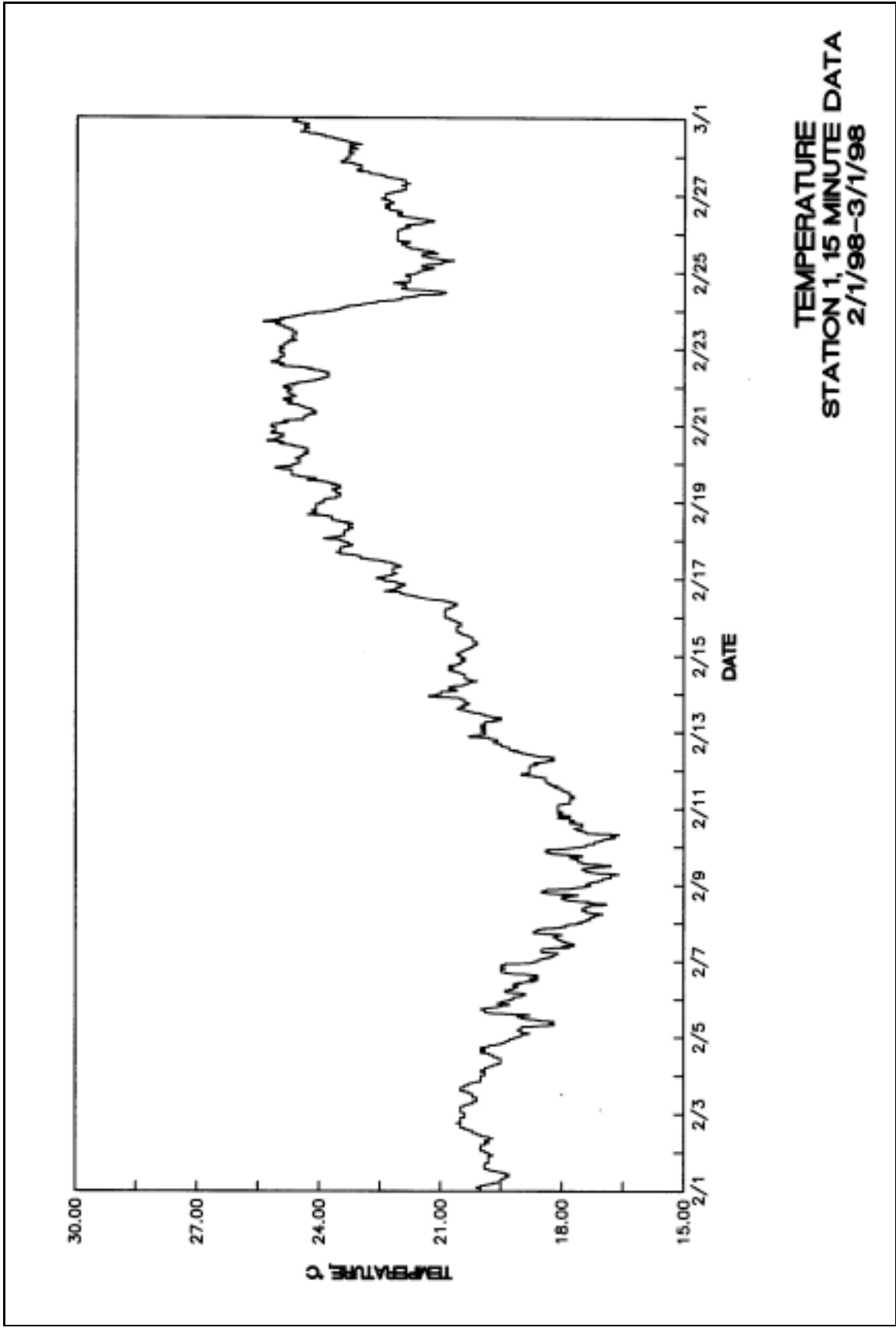


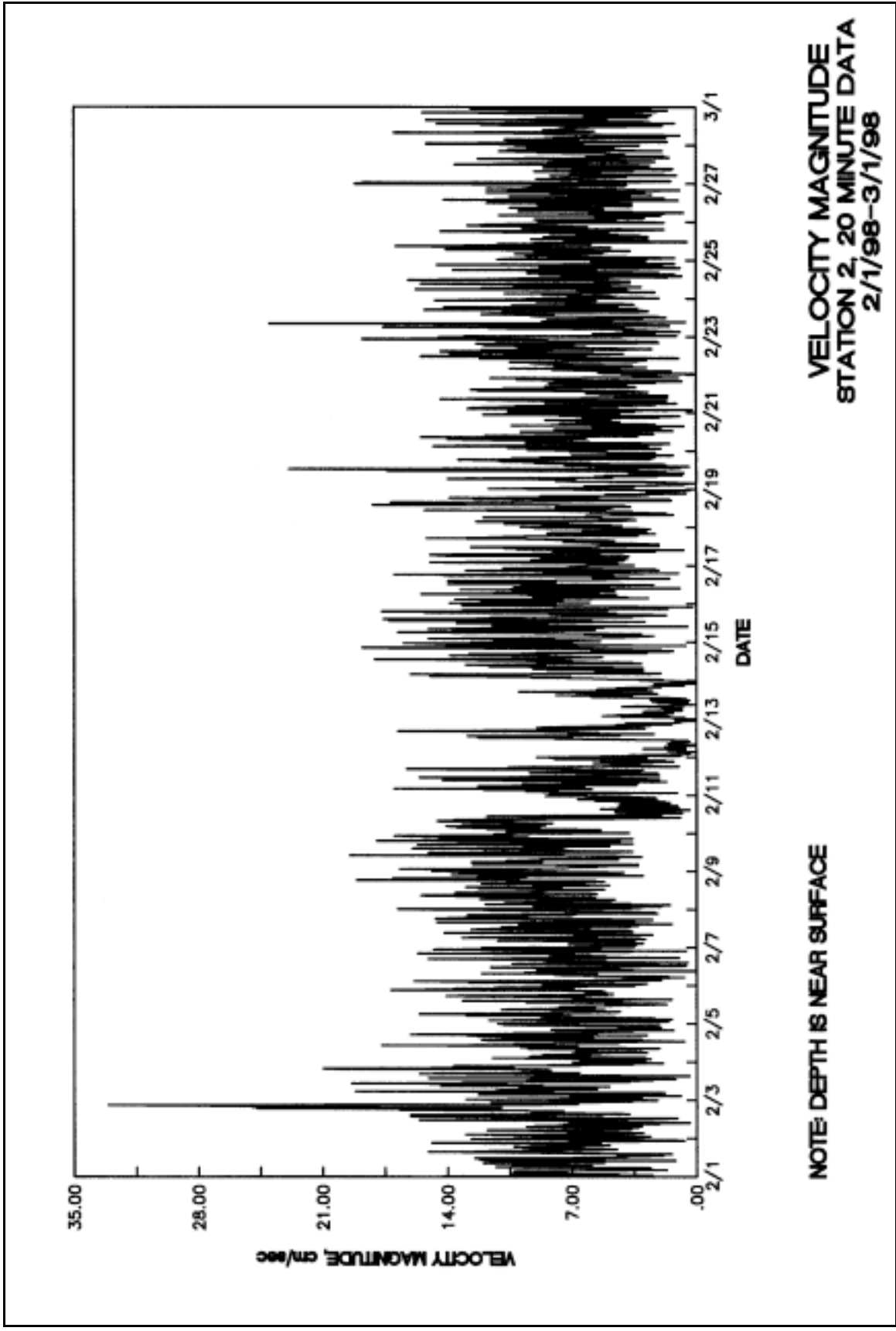


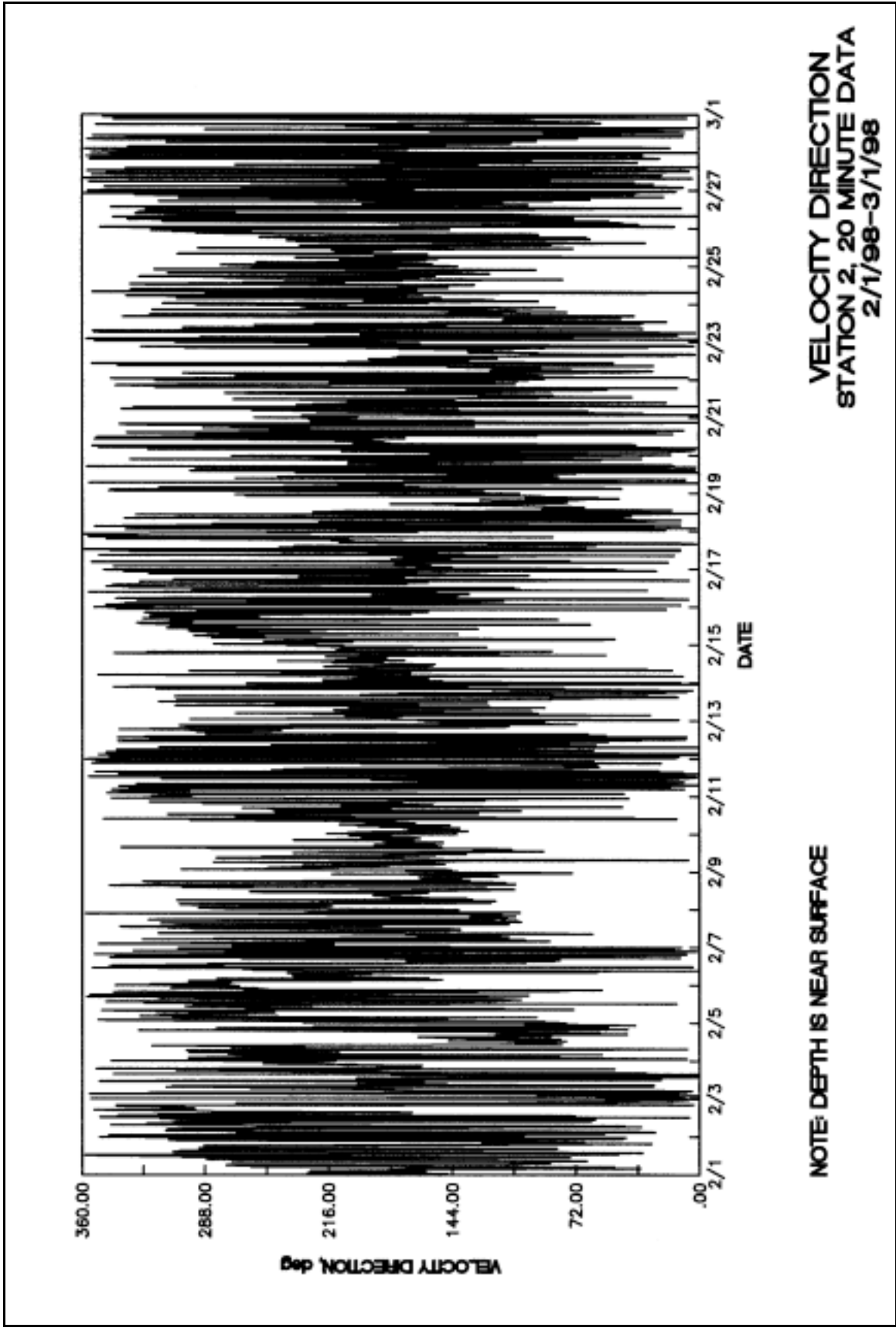


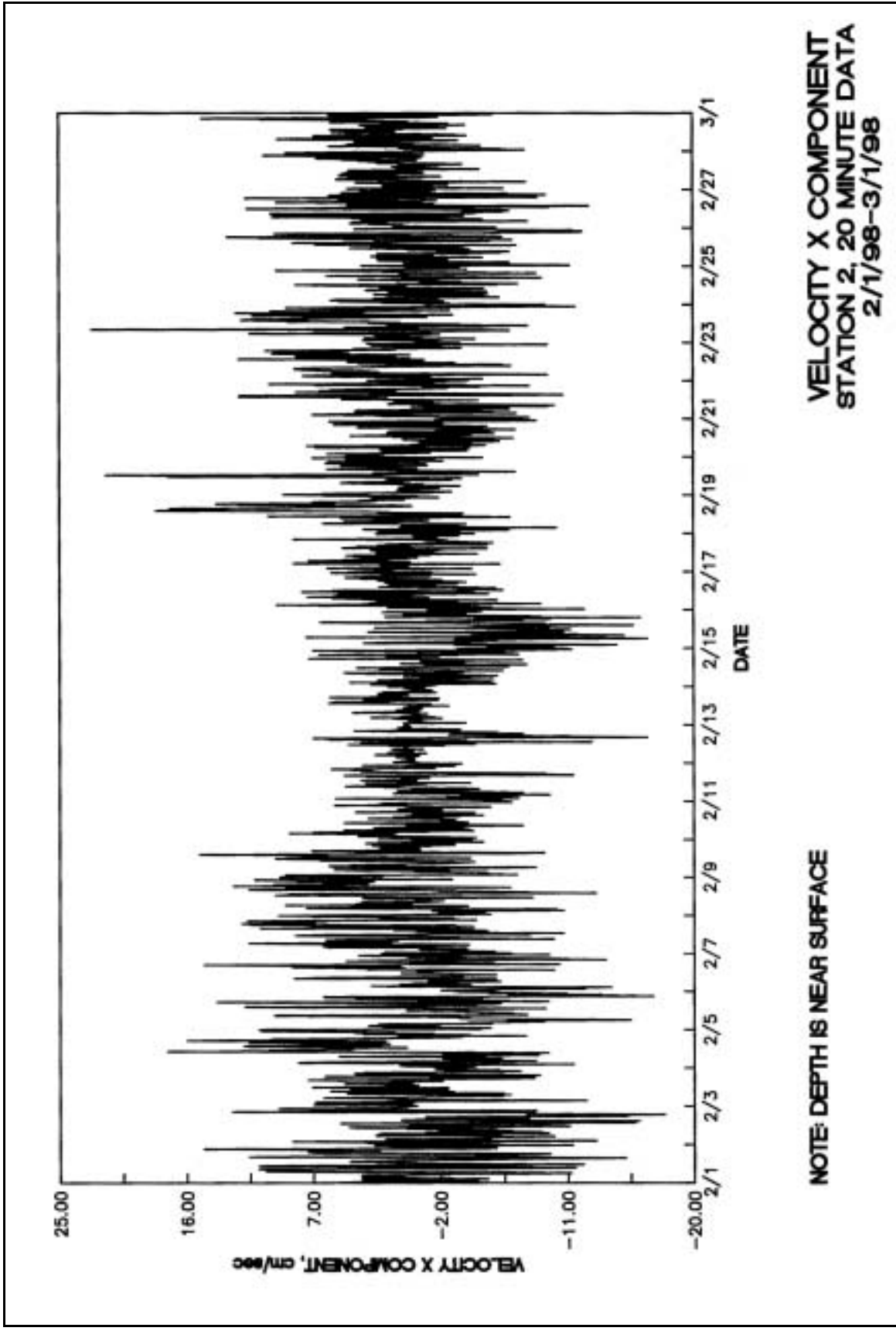


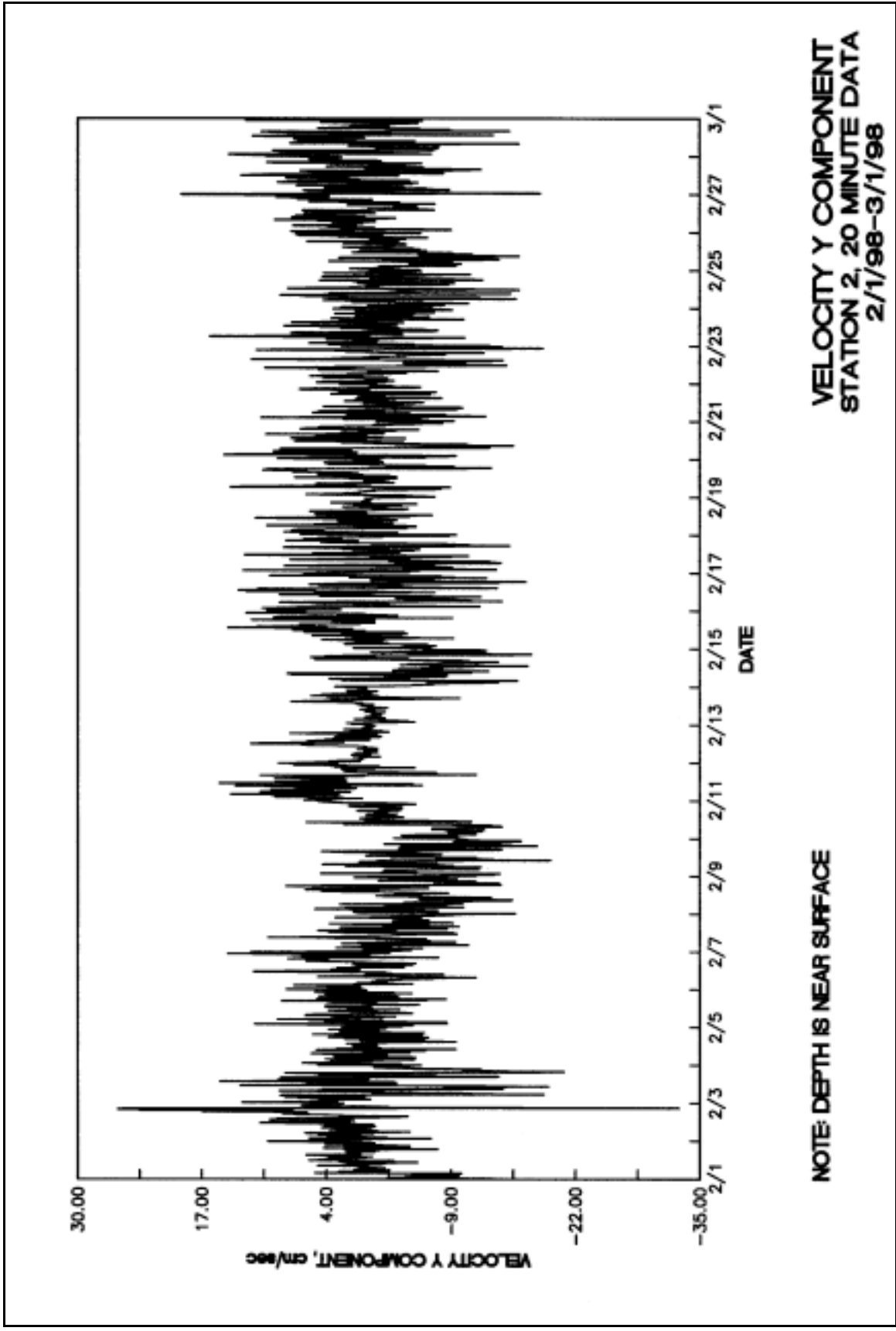
**HEAD OF WATER ABOVE INSTRUMENT
STATION 1, 15 MINUTE DATA
2/1/98-3/1/98**

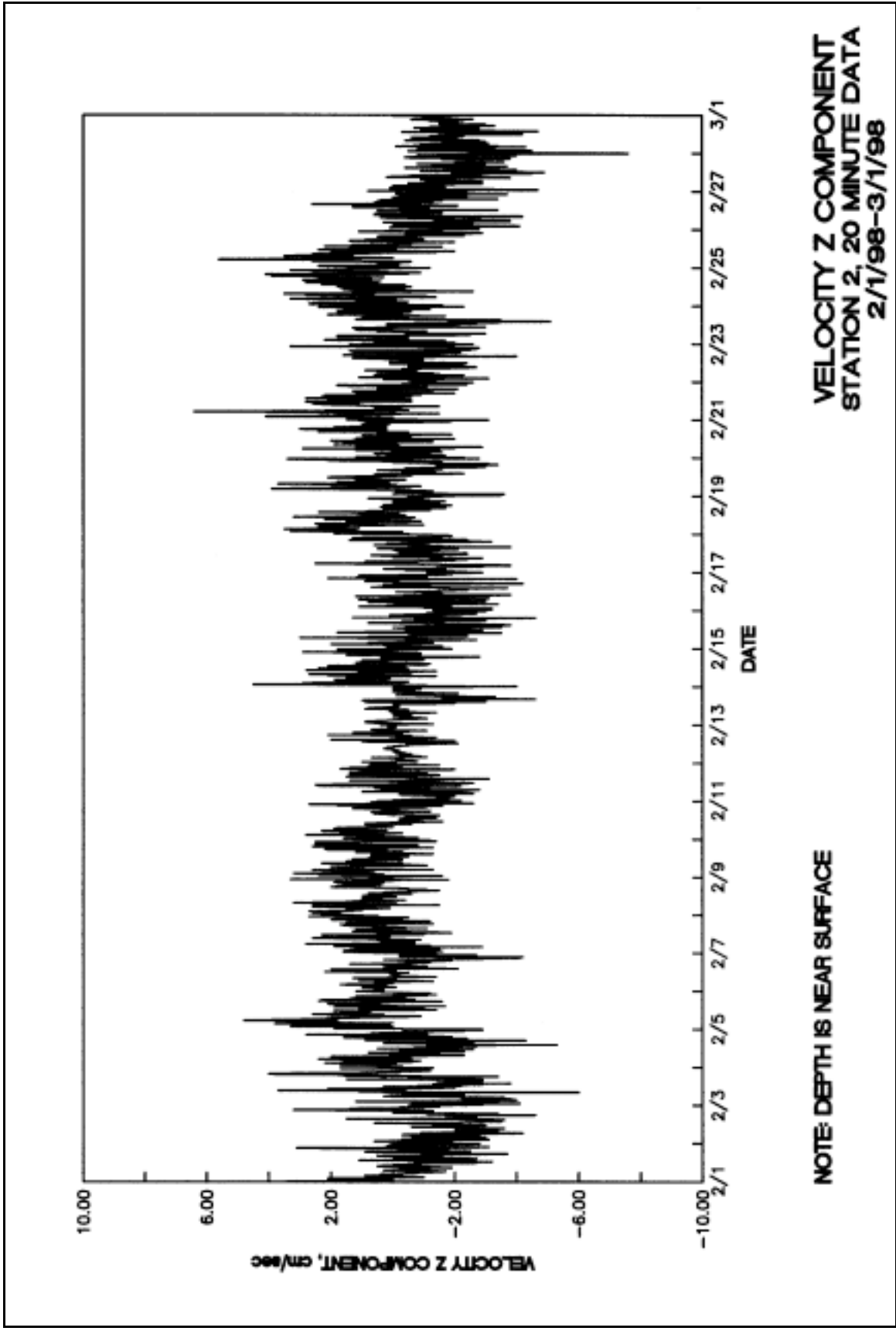


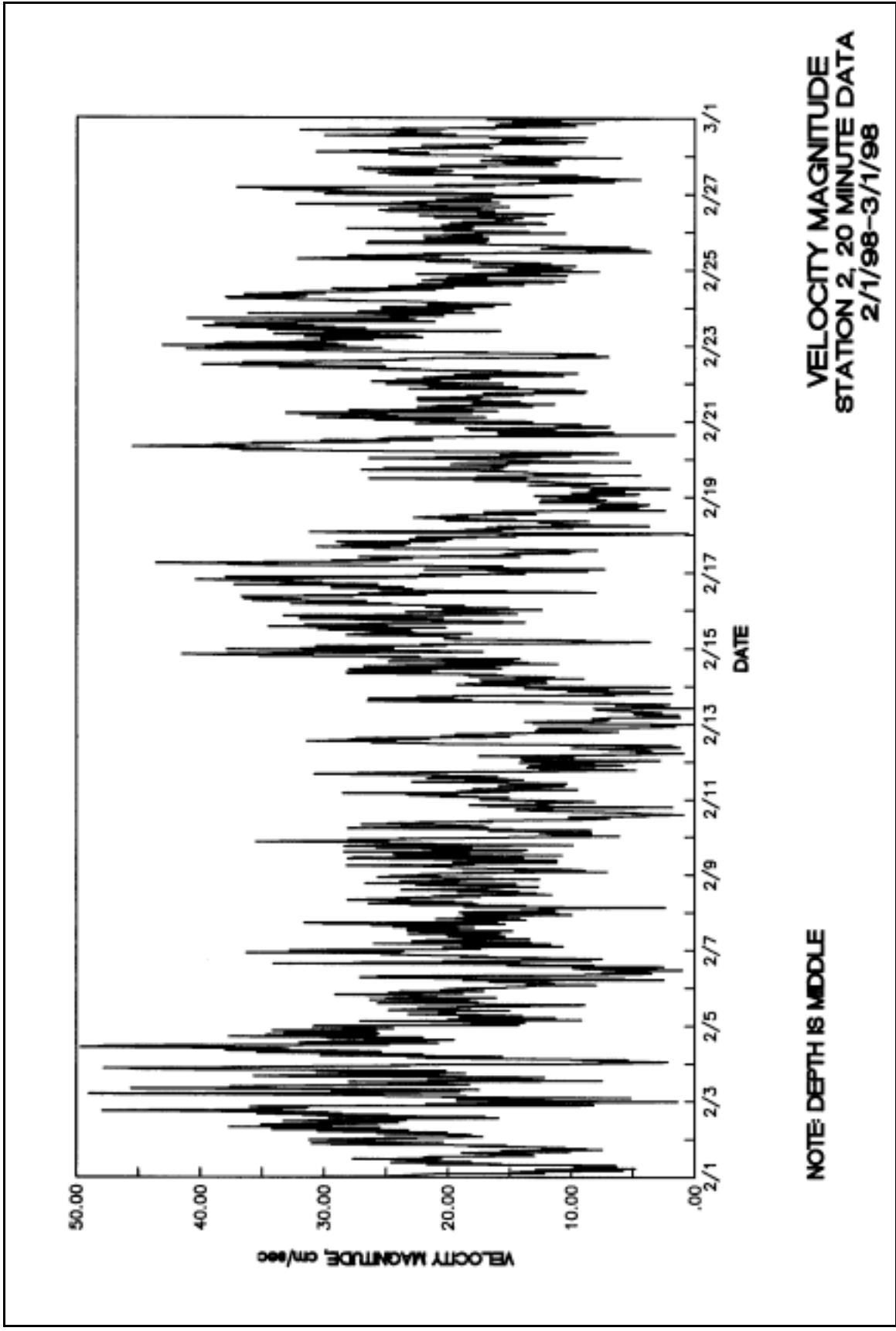


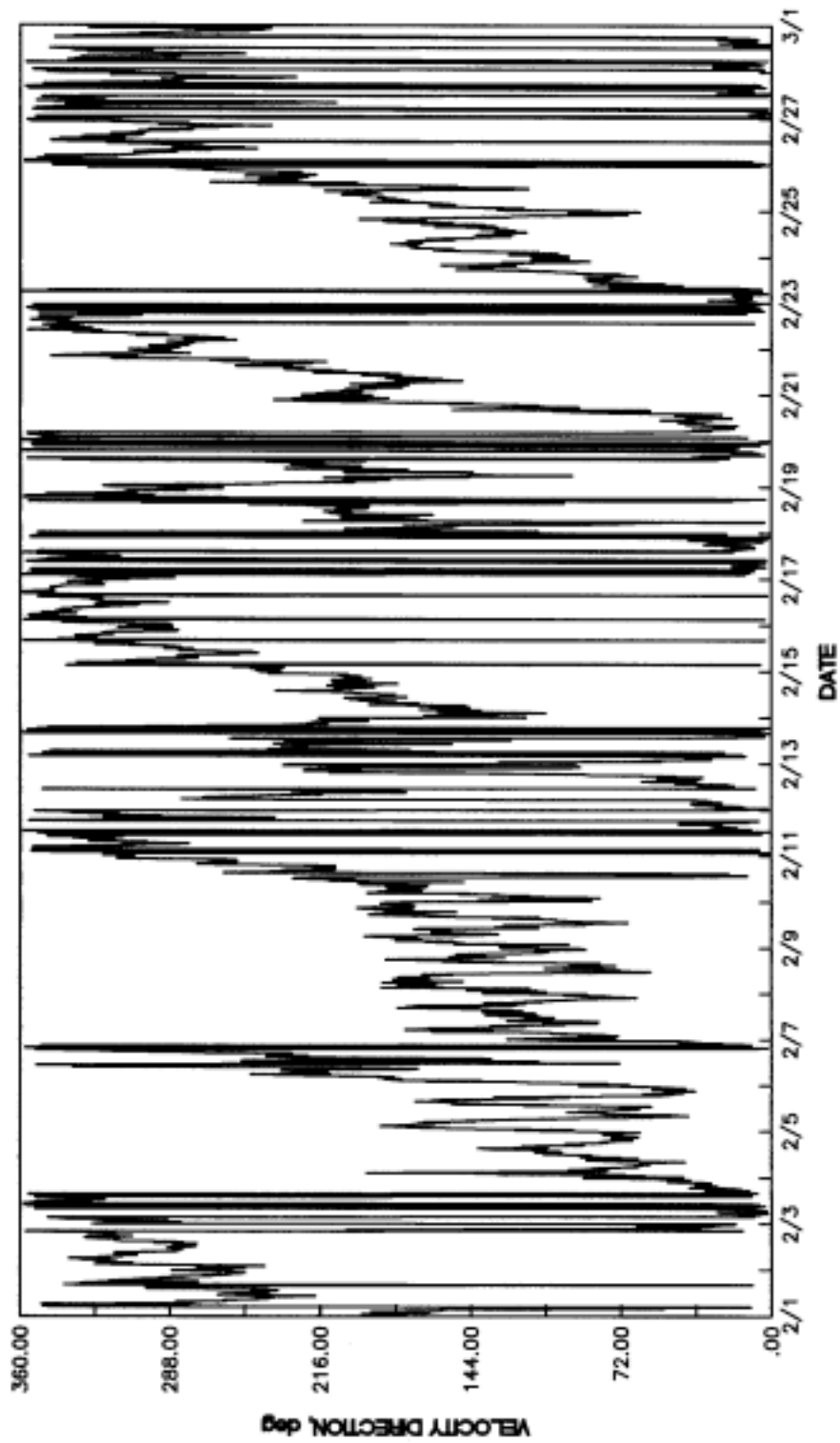






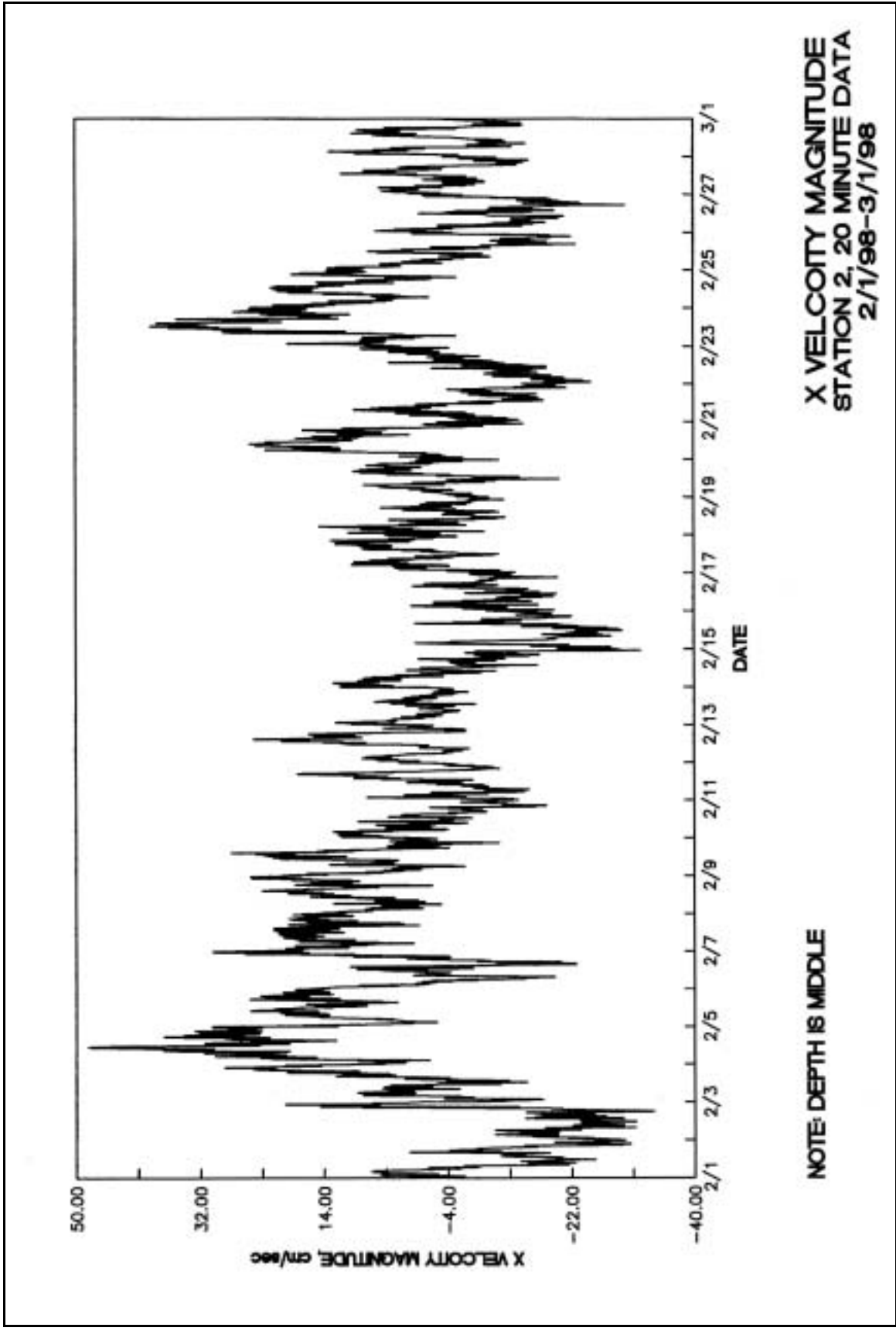


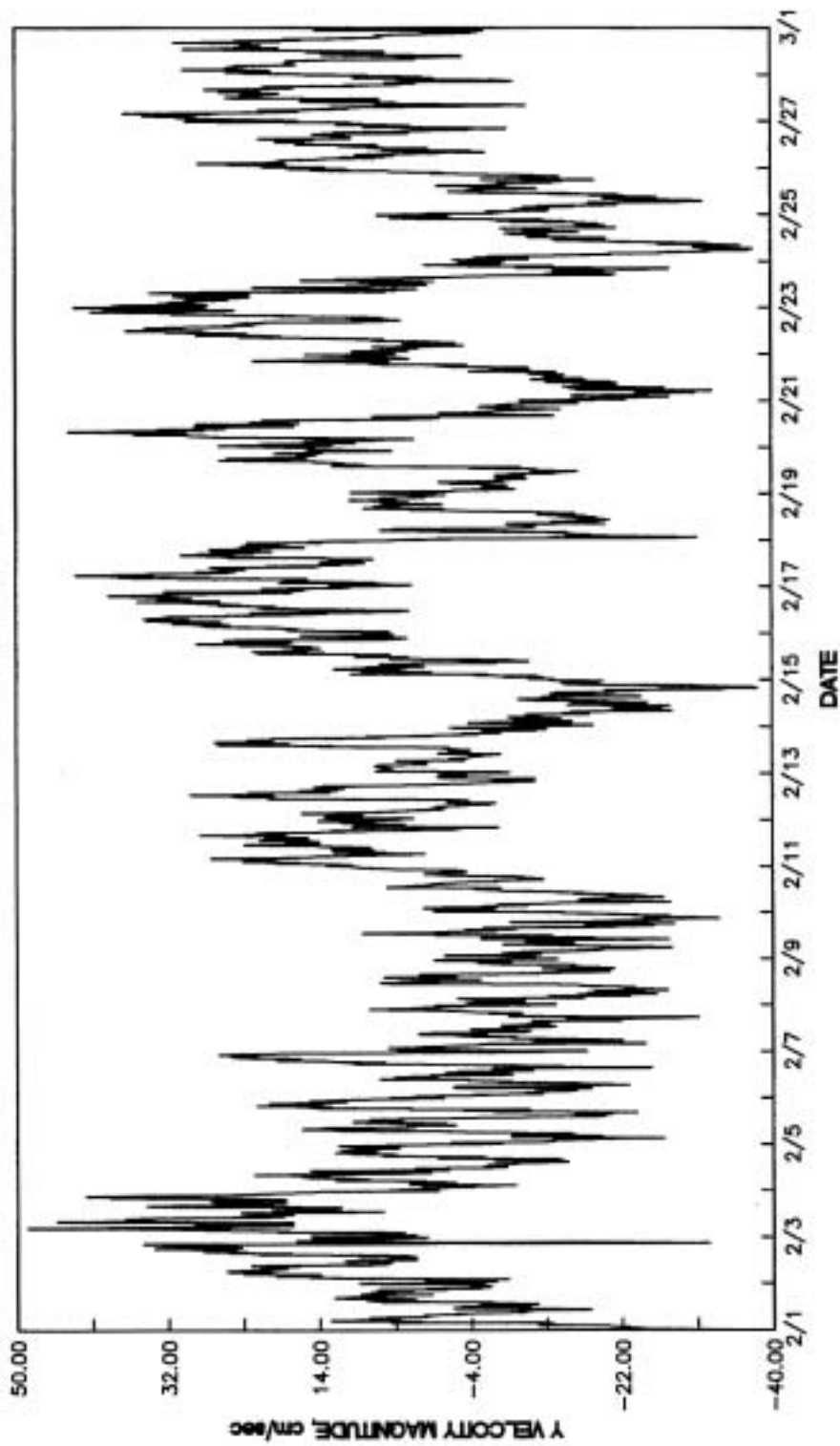




**VELOCITY DIRECTION
STATION 2, 20 MINUTE DATA
2/1/98-3/1/98**

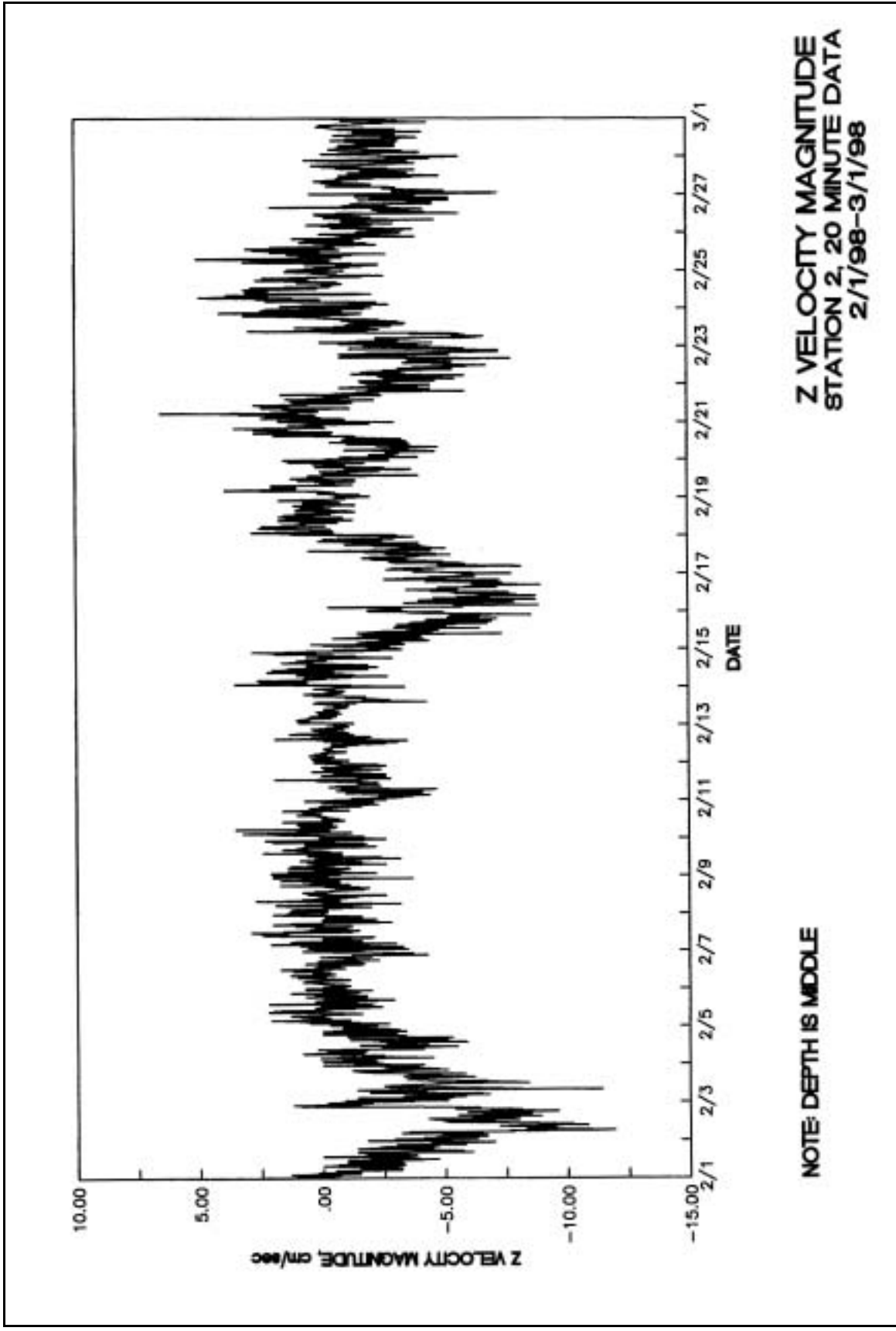
NOTE: DEPTH IS MIDDLE

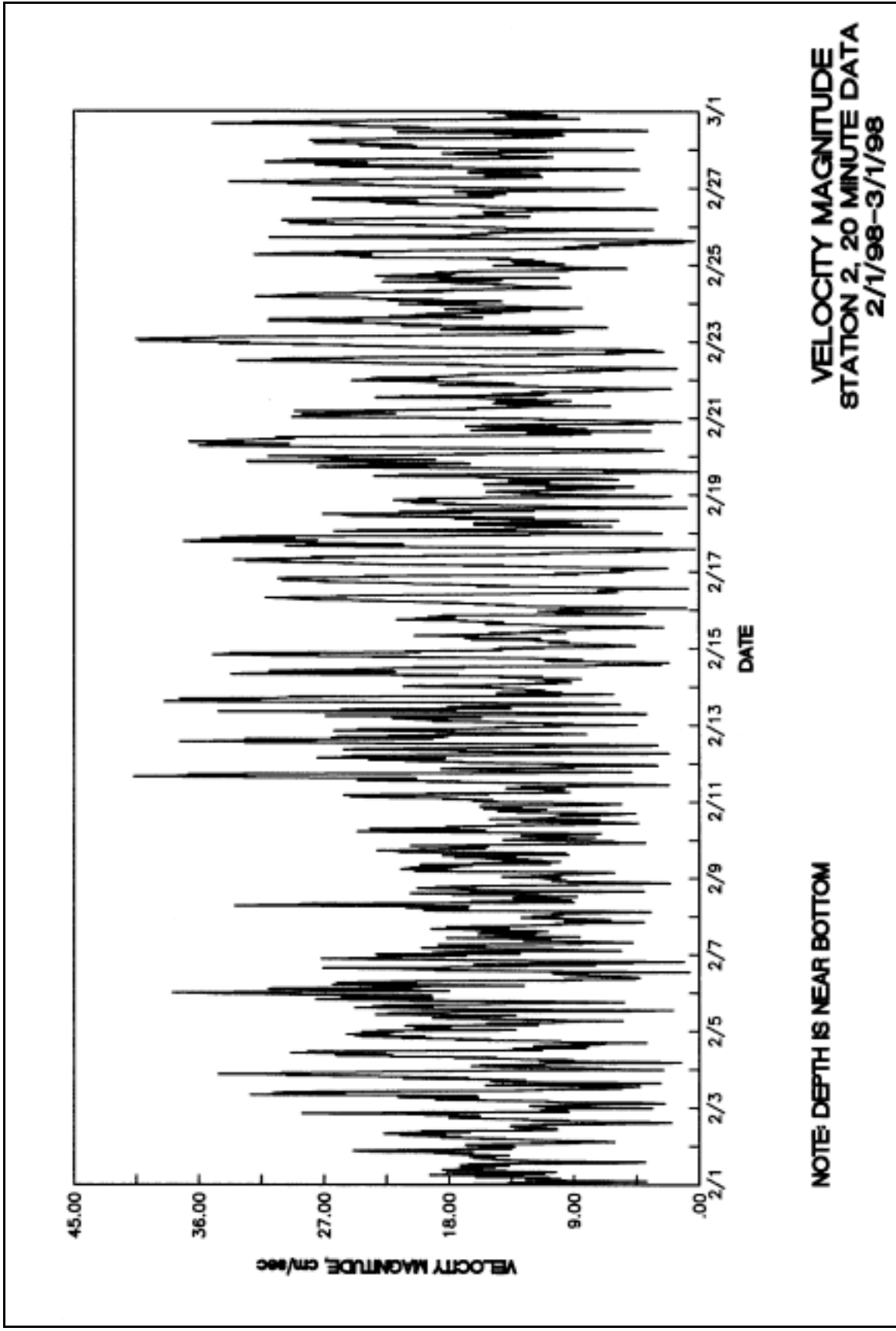


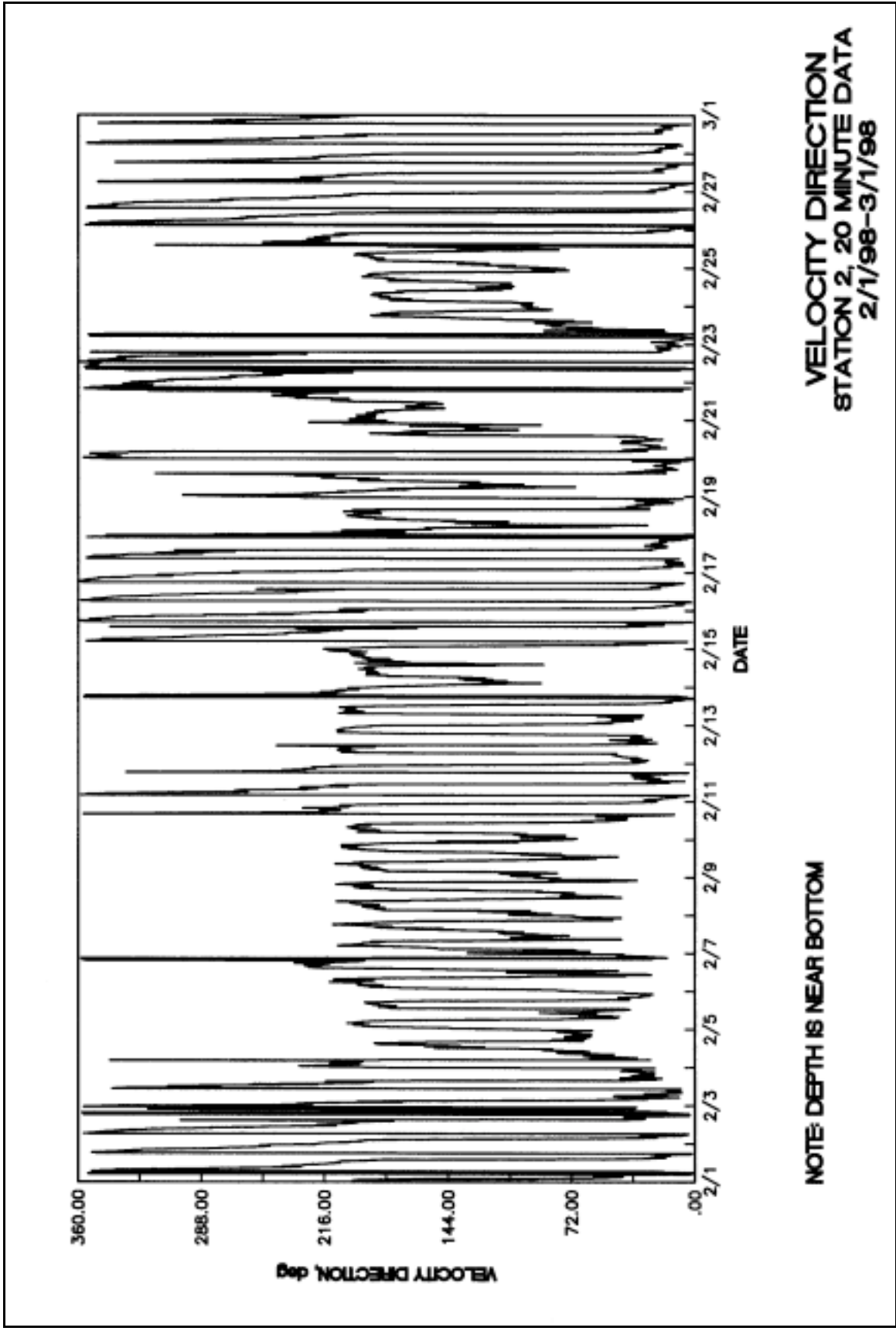


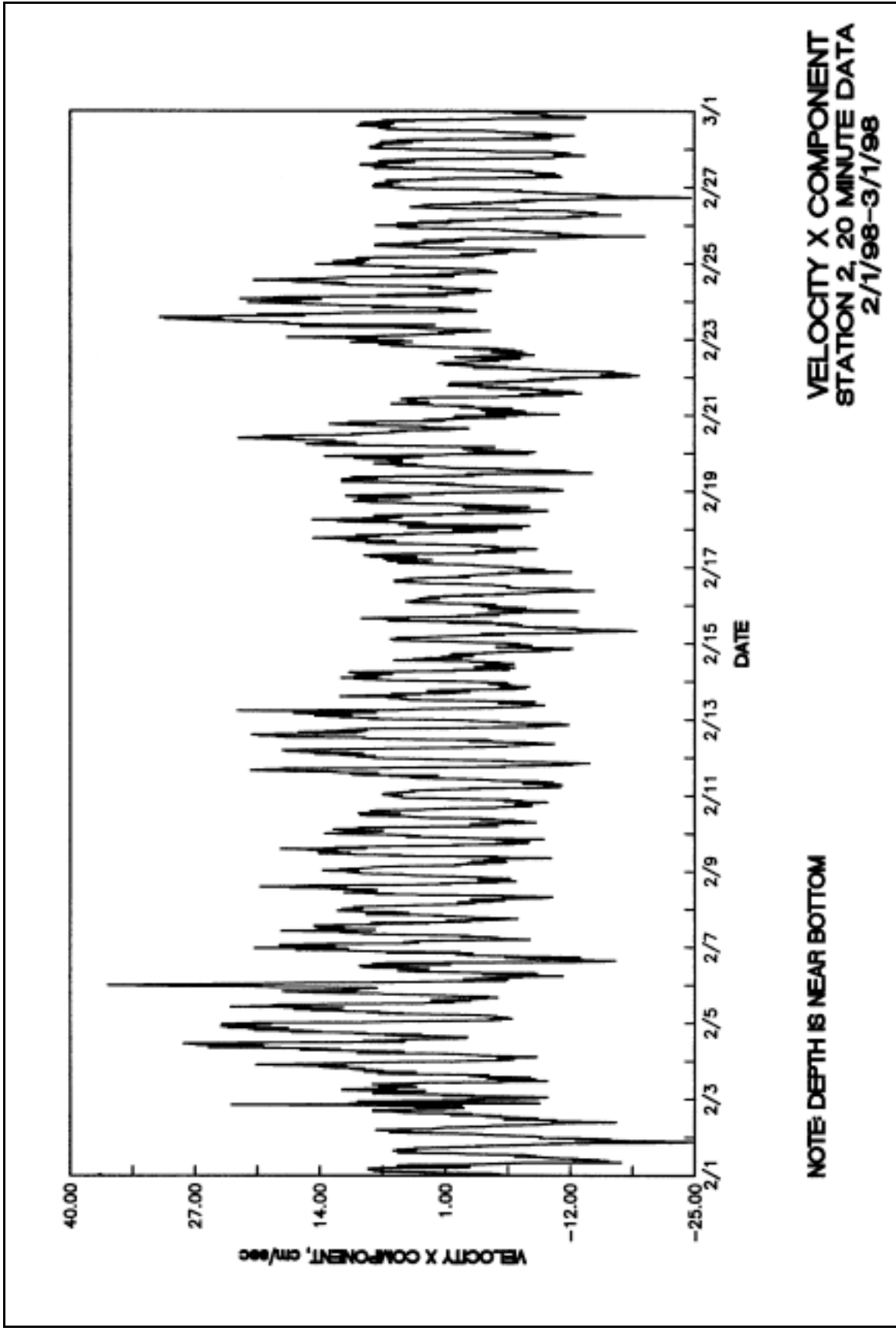
**Y VELOCITY MAGNITUDE
STATION 2, 20 MINUTE DATA
2/1/98-3/1/98**

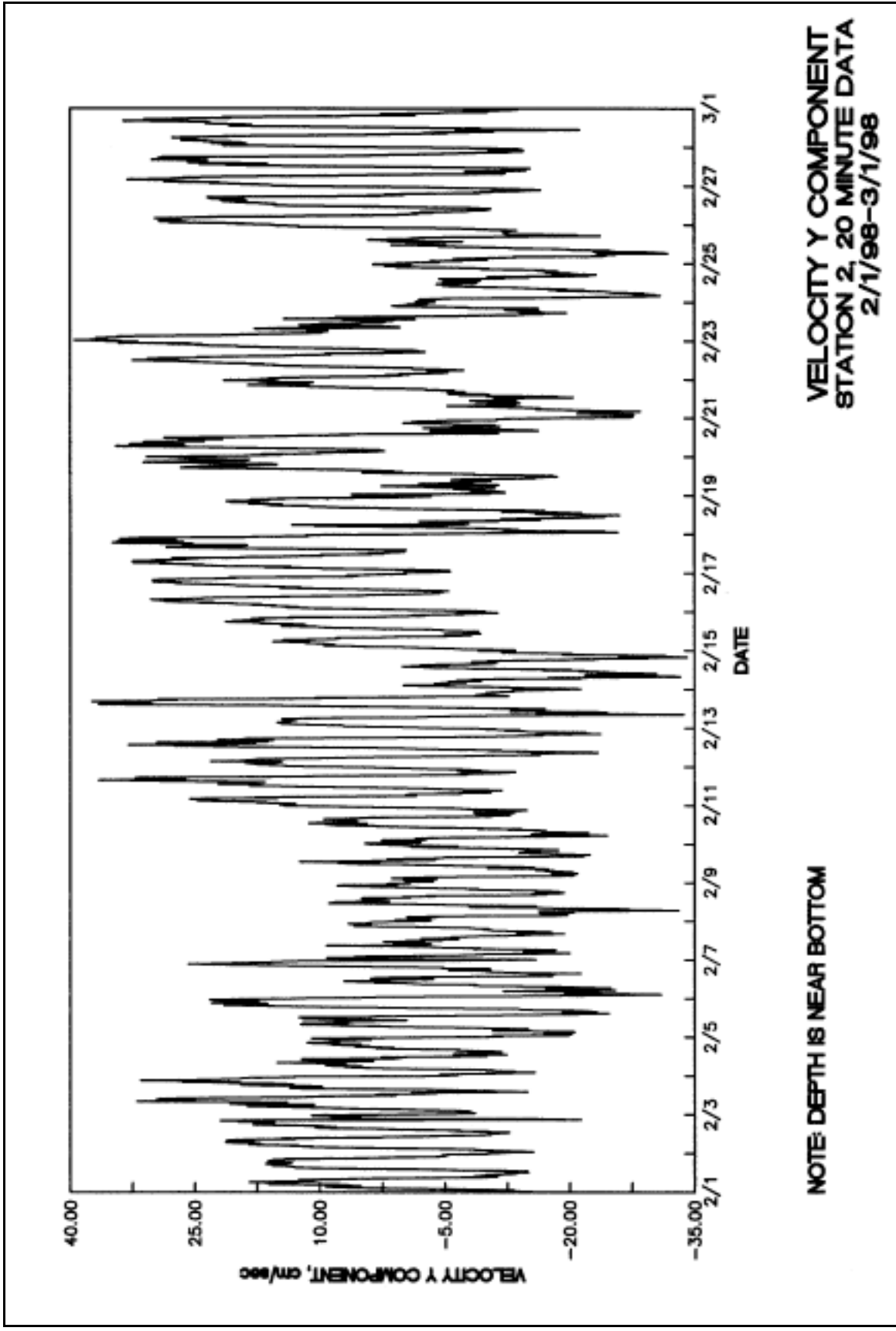
NOTE: DEPTH IS MIDDLE

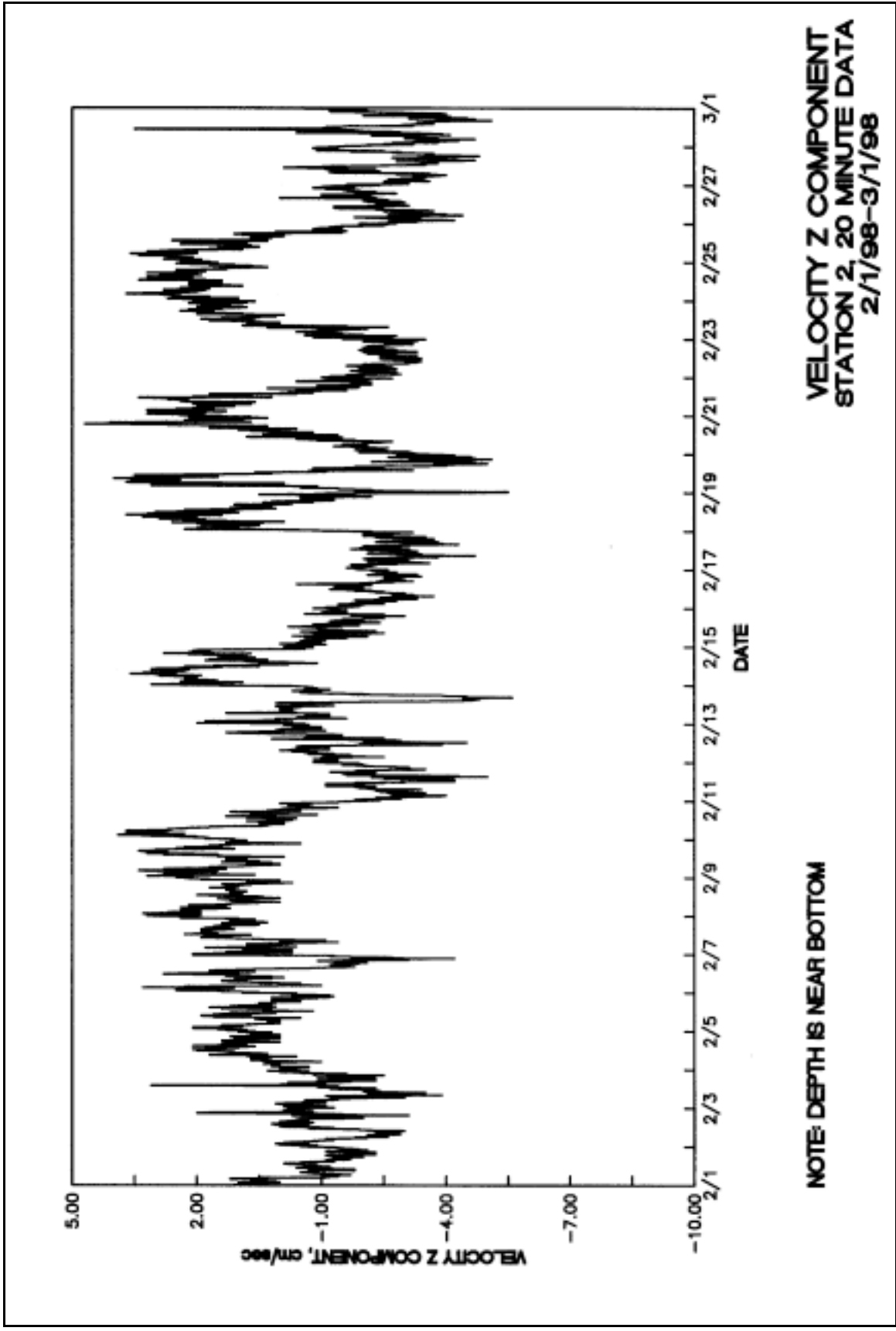


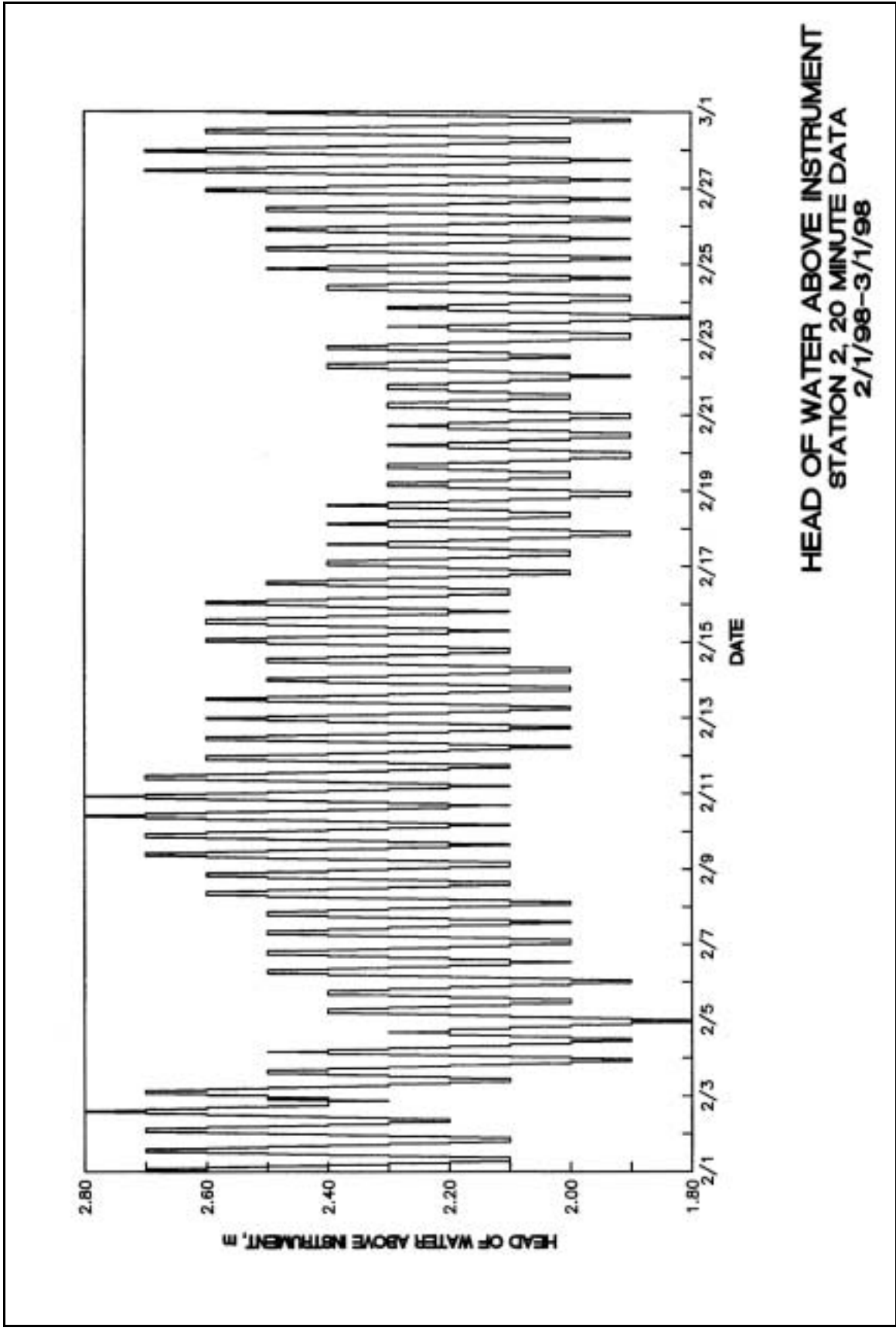




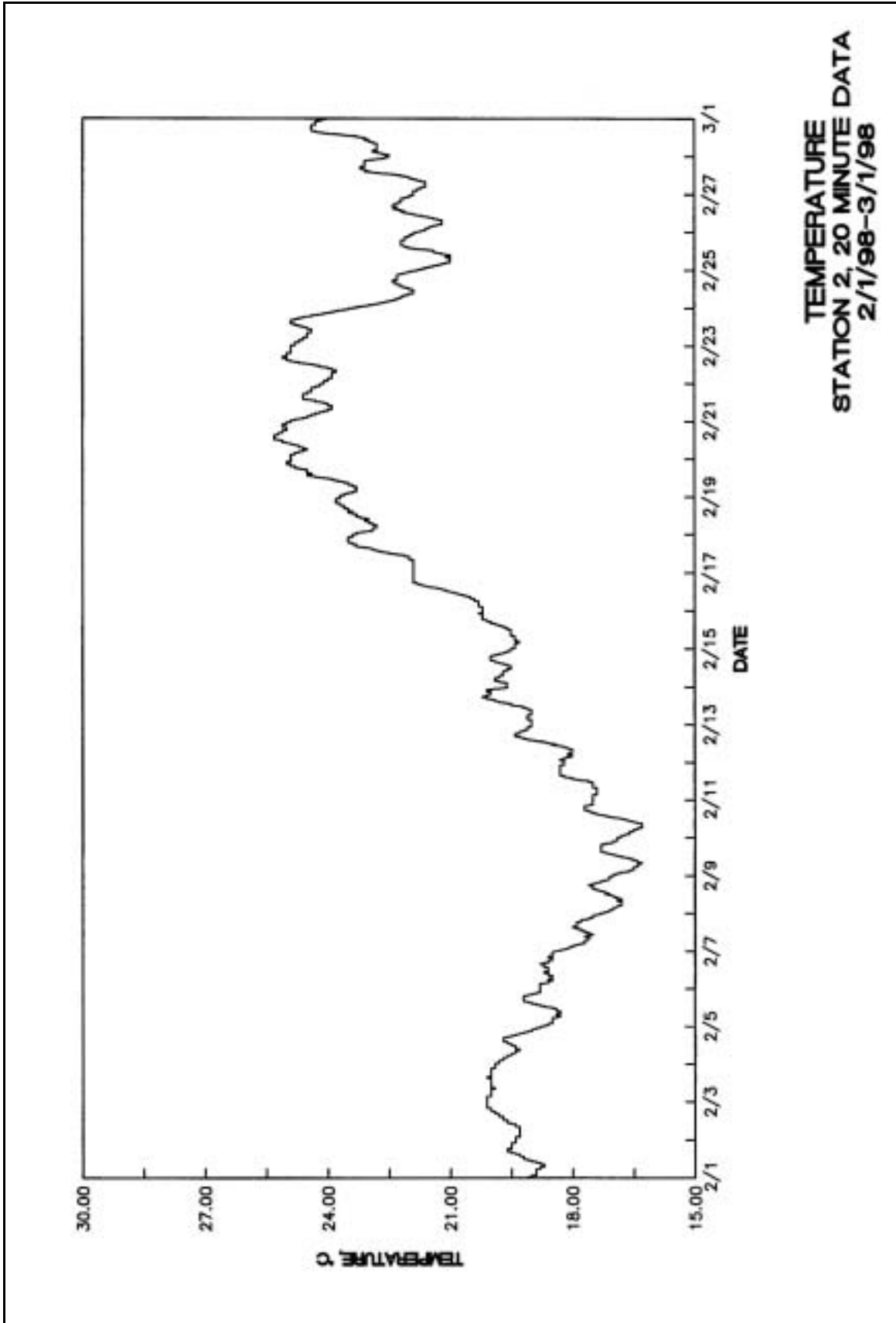


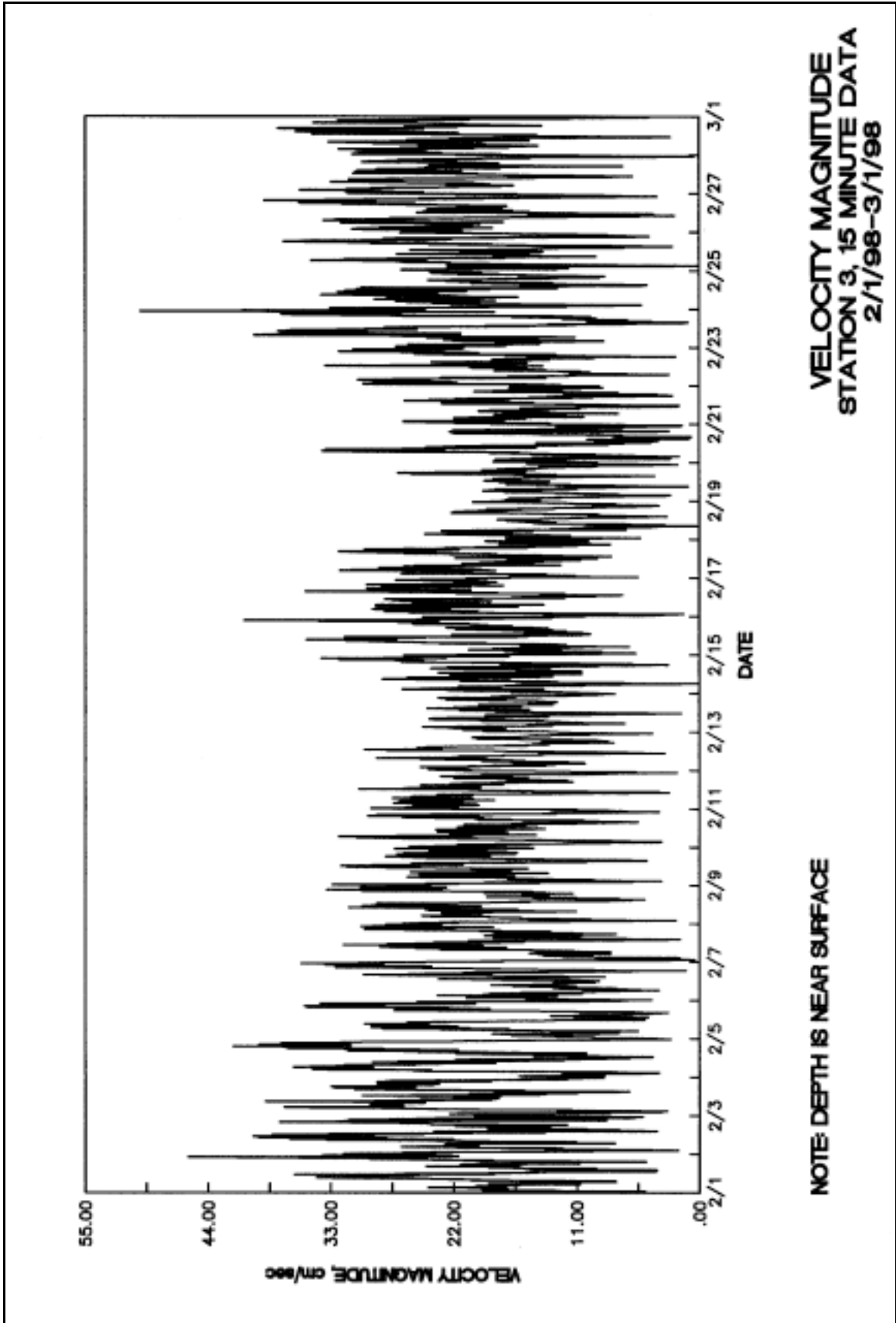


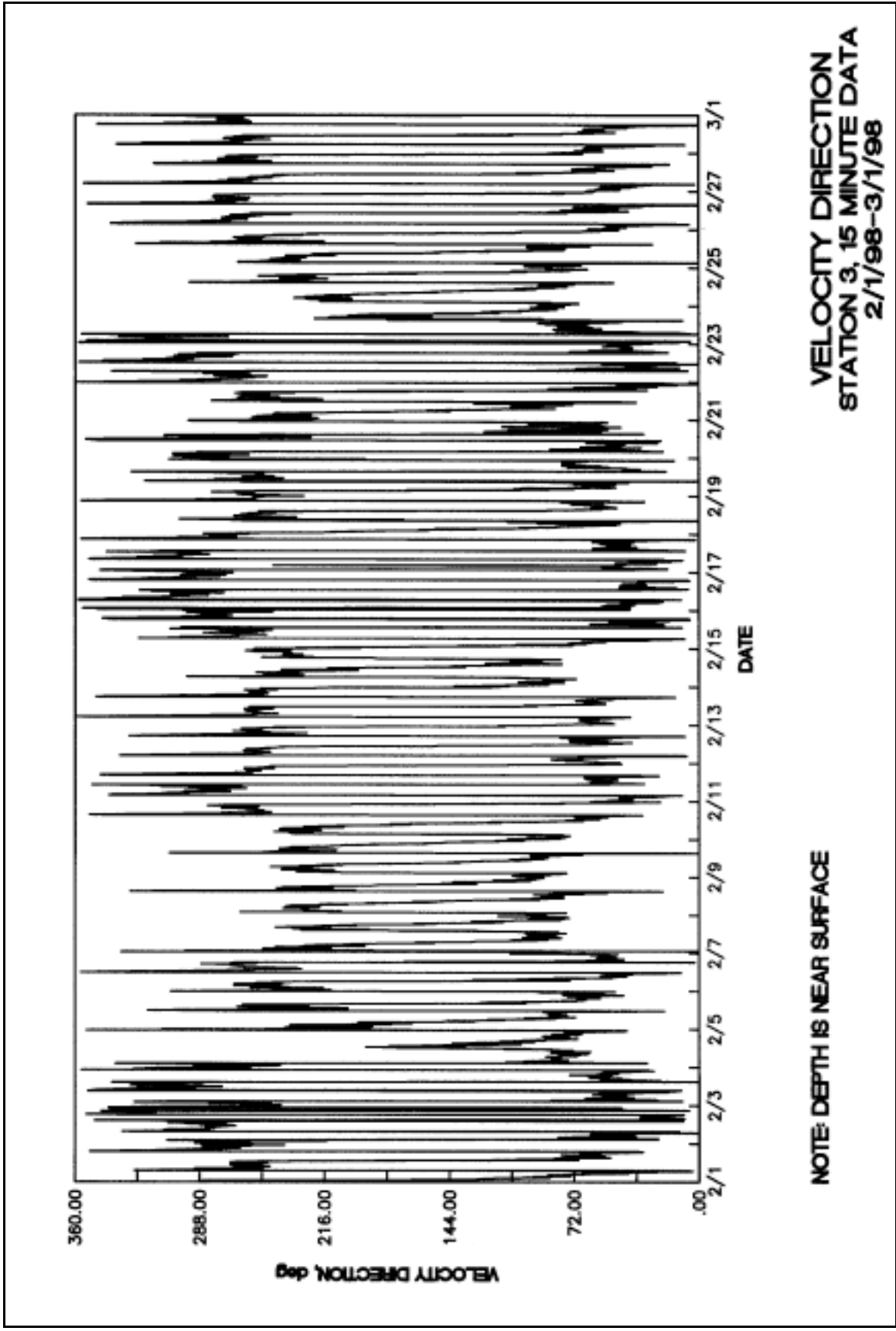


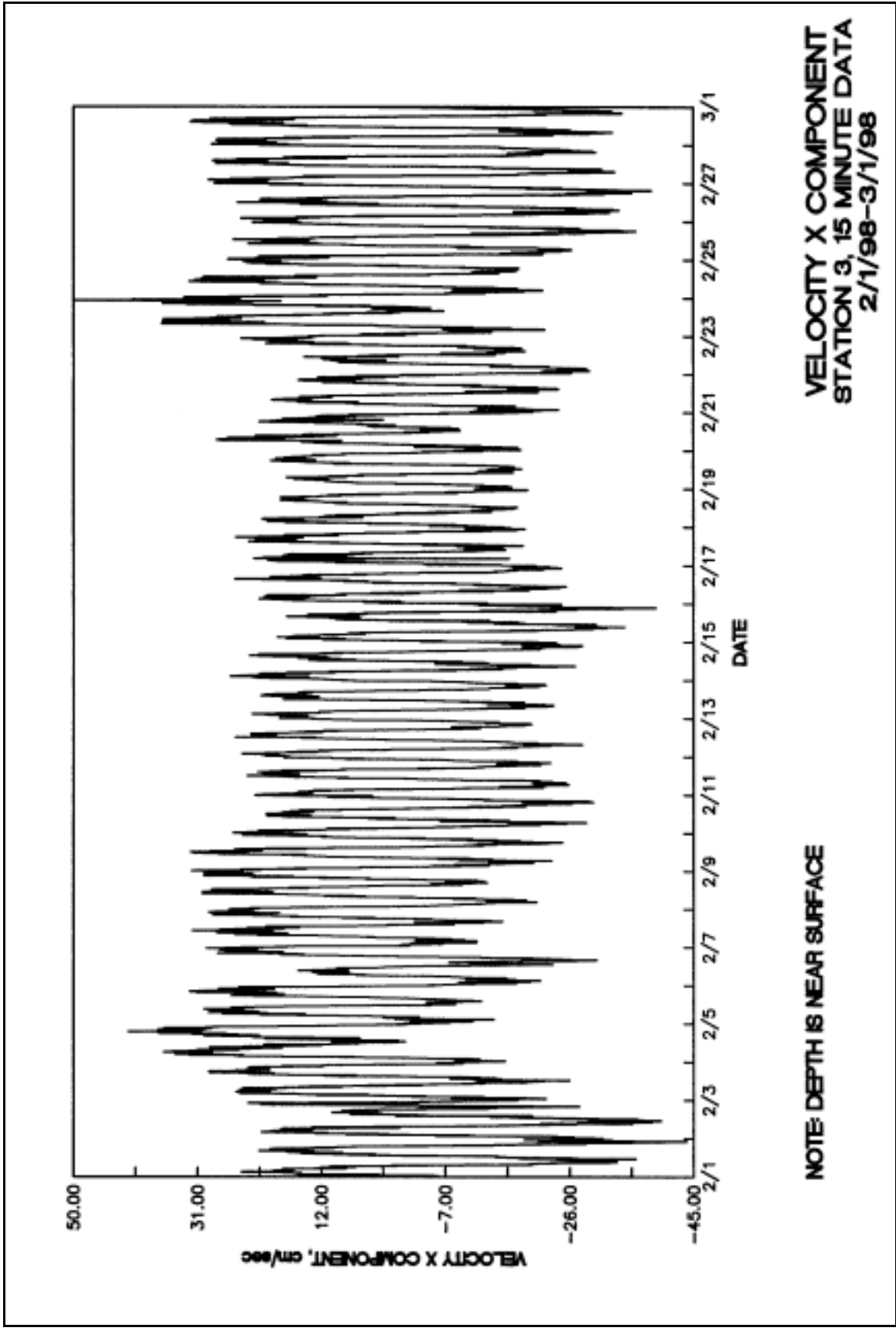


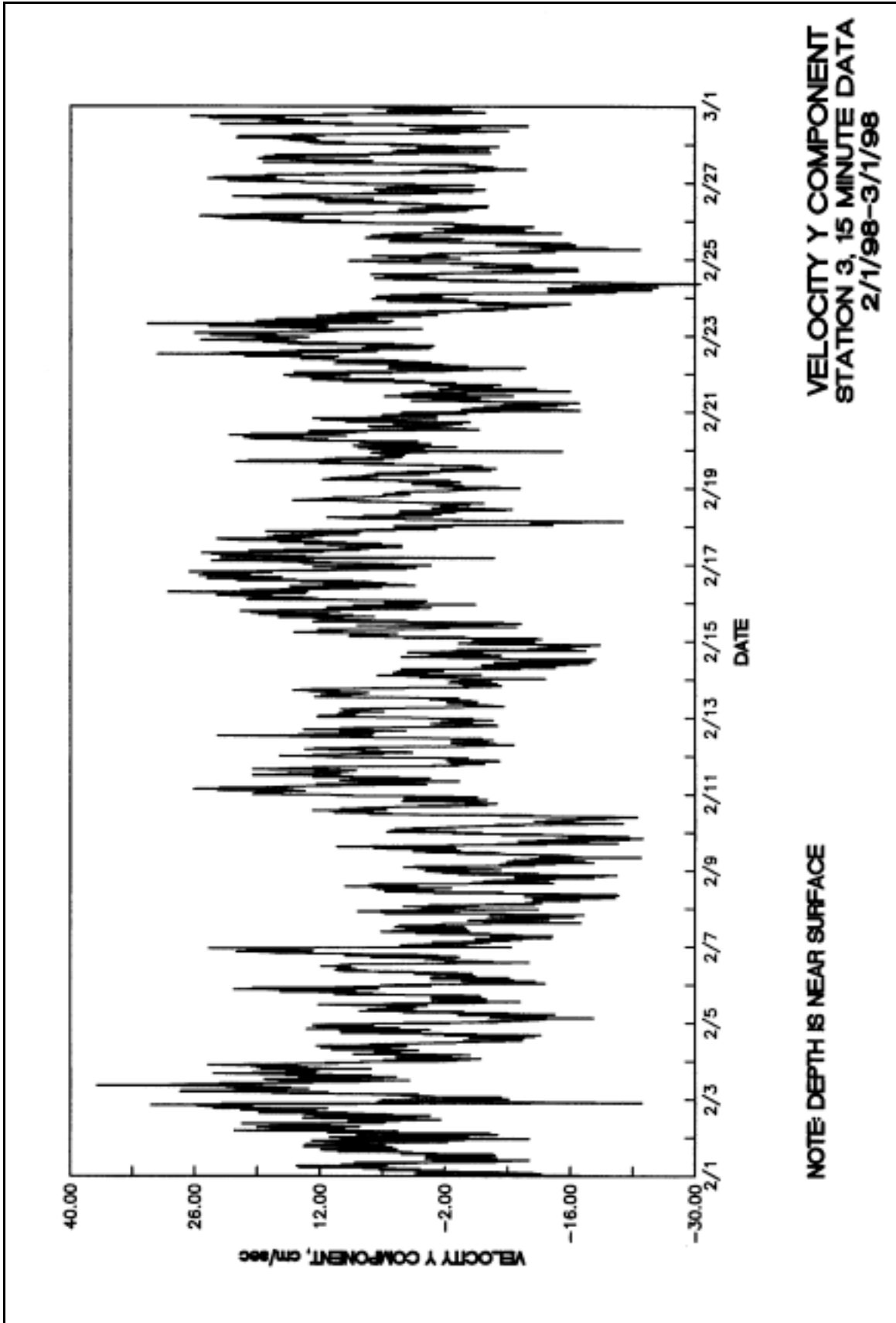
HEAD OF WATER ABOVE INSTRUMENT
STATION 2, 20 MINUTE DATA
2/1/98-3/1/98

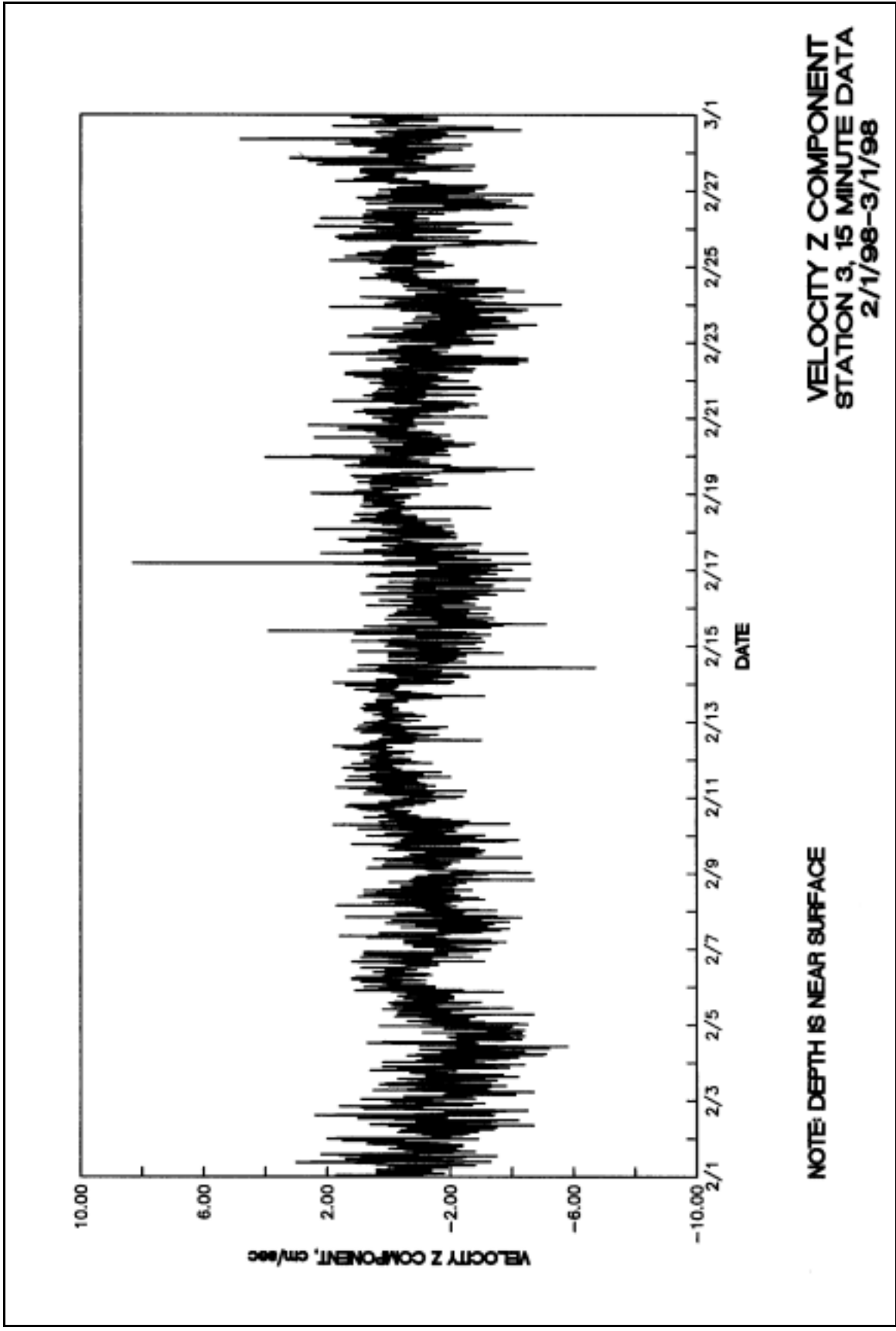


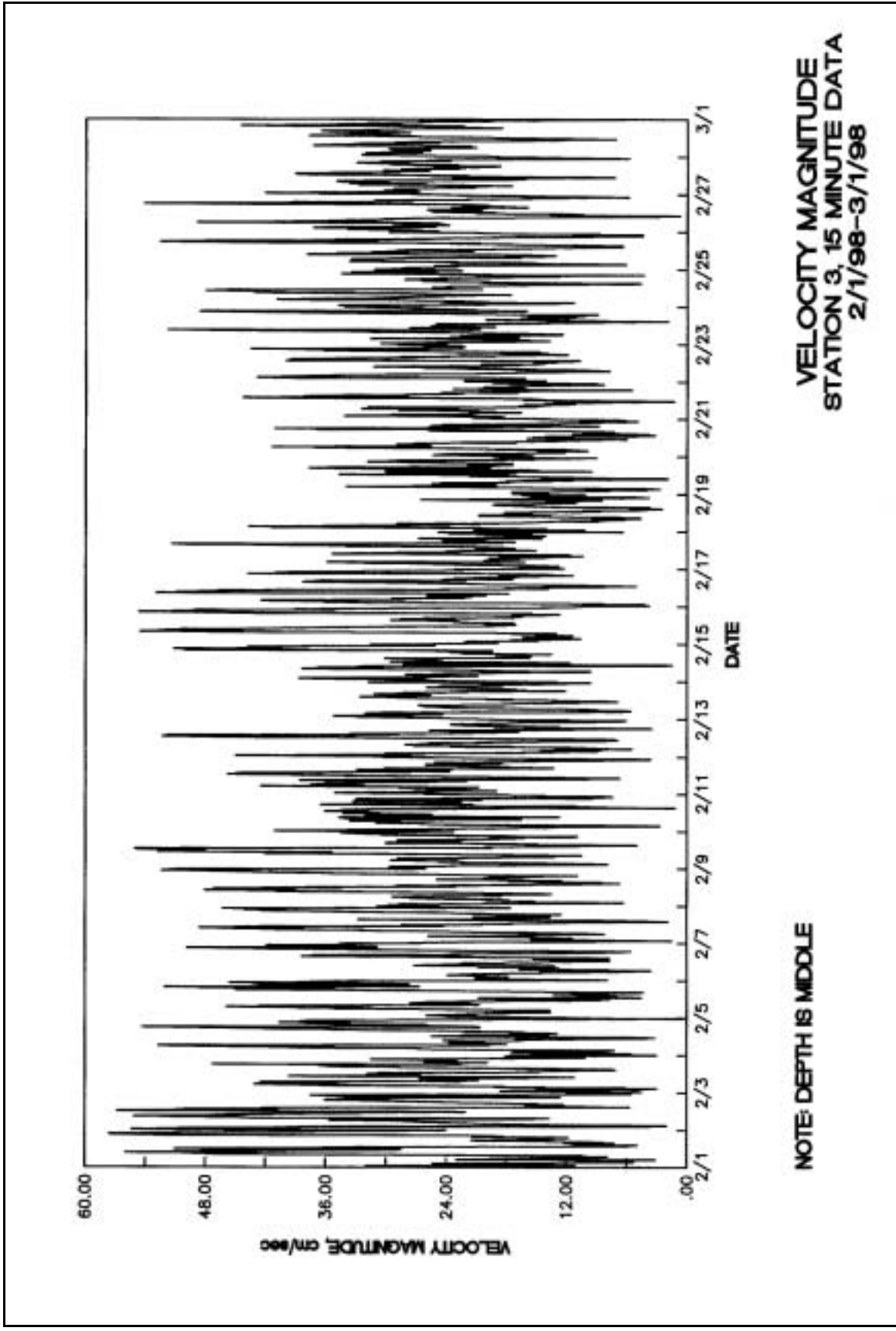


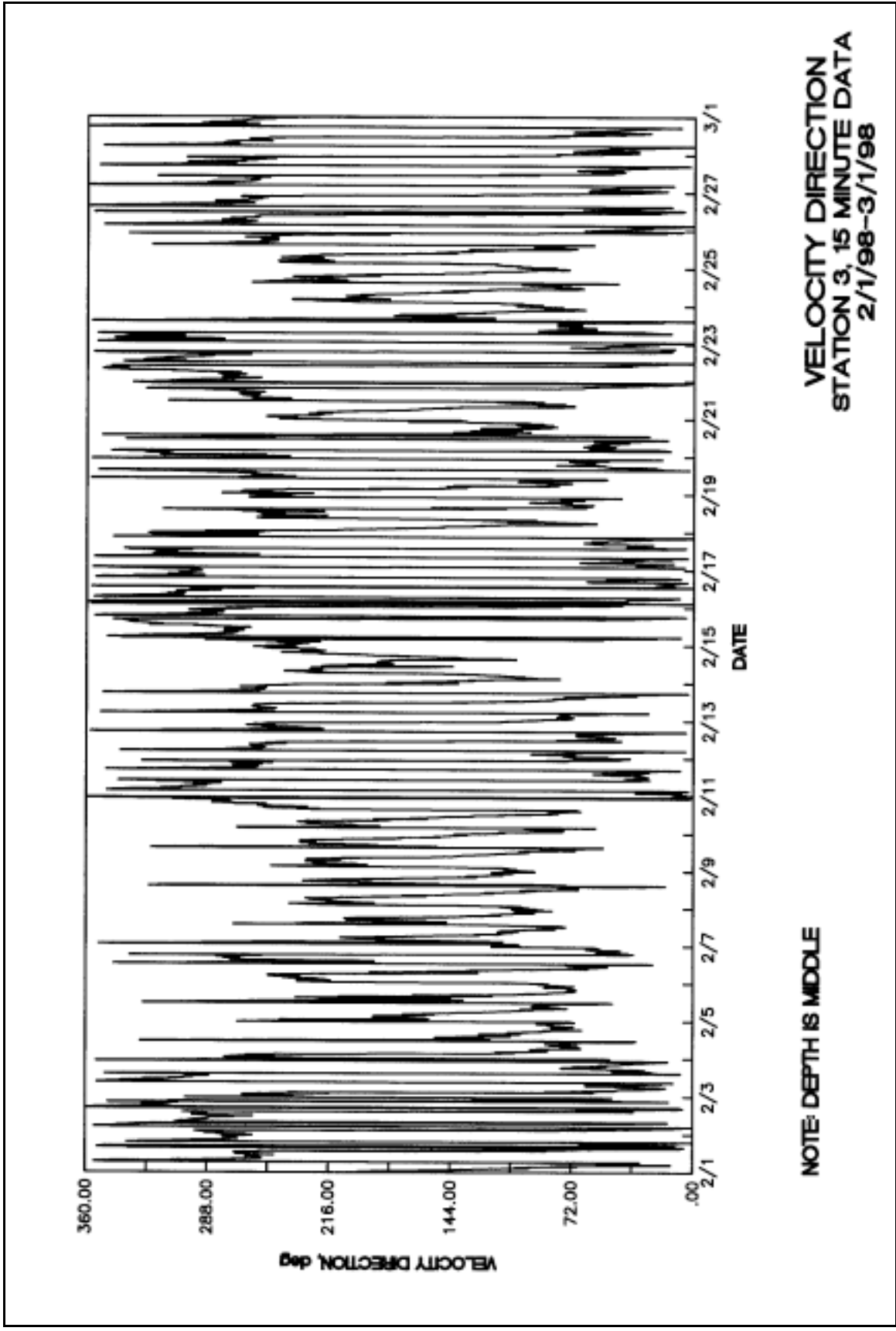


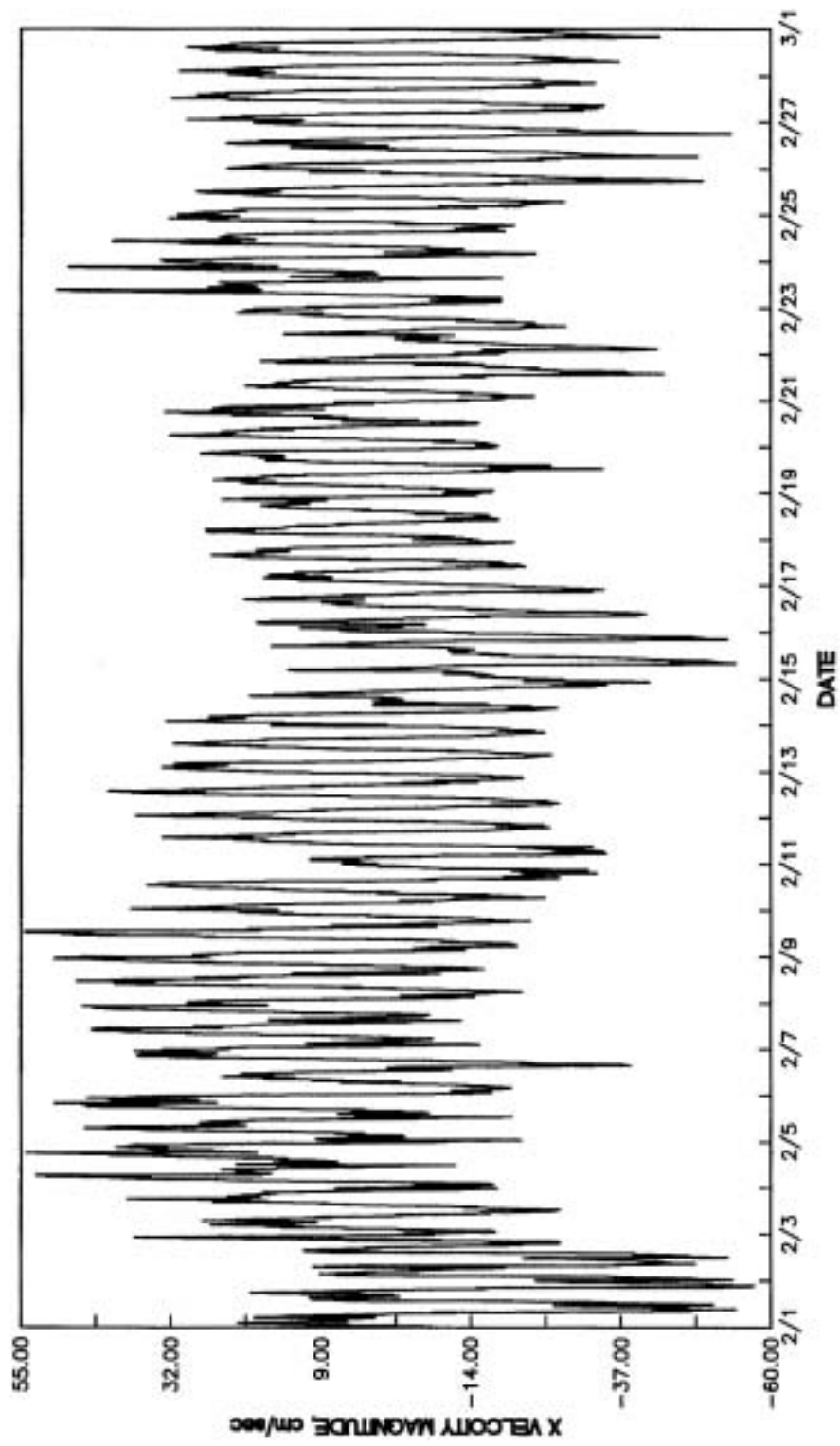






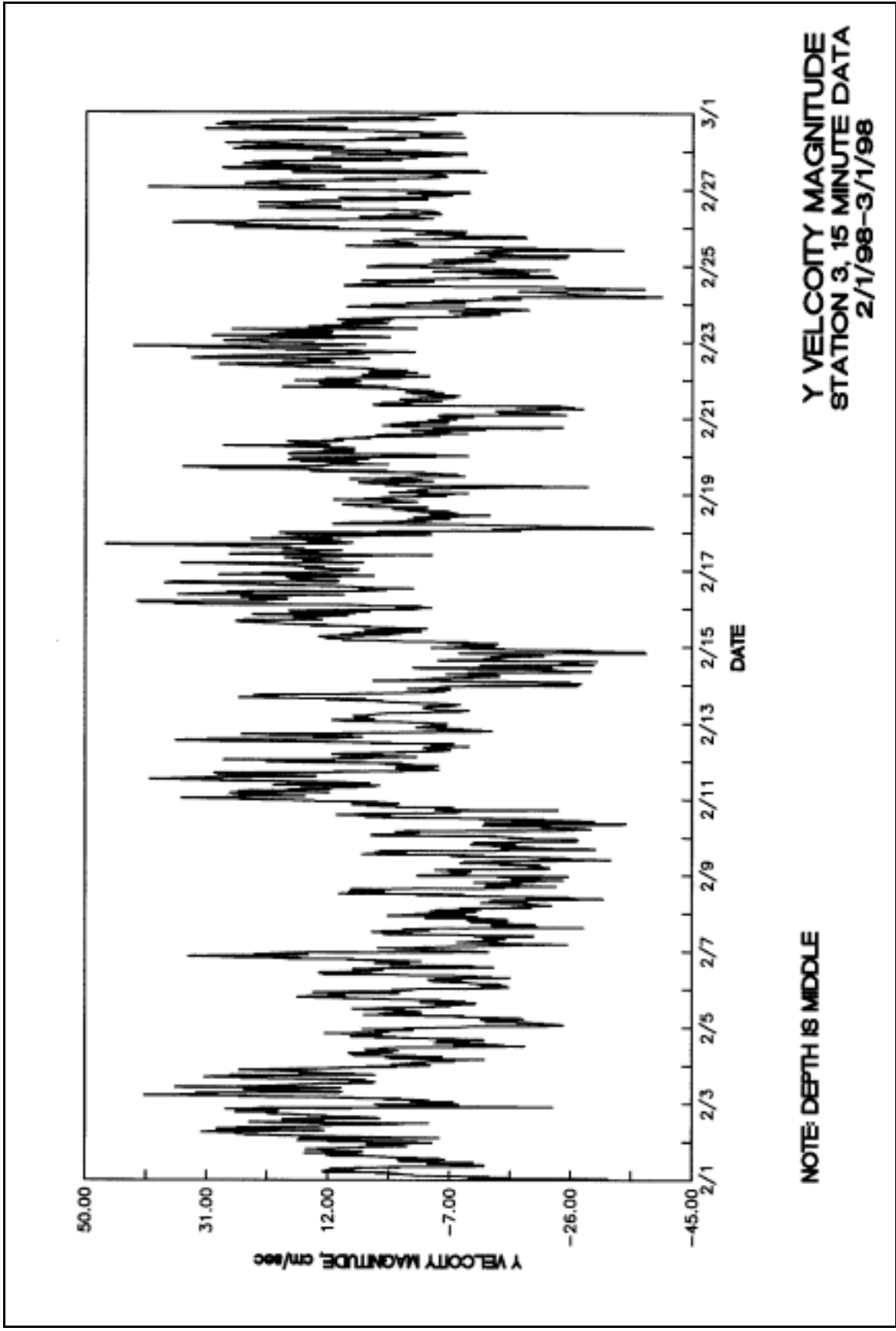


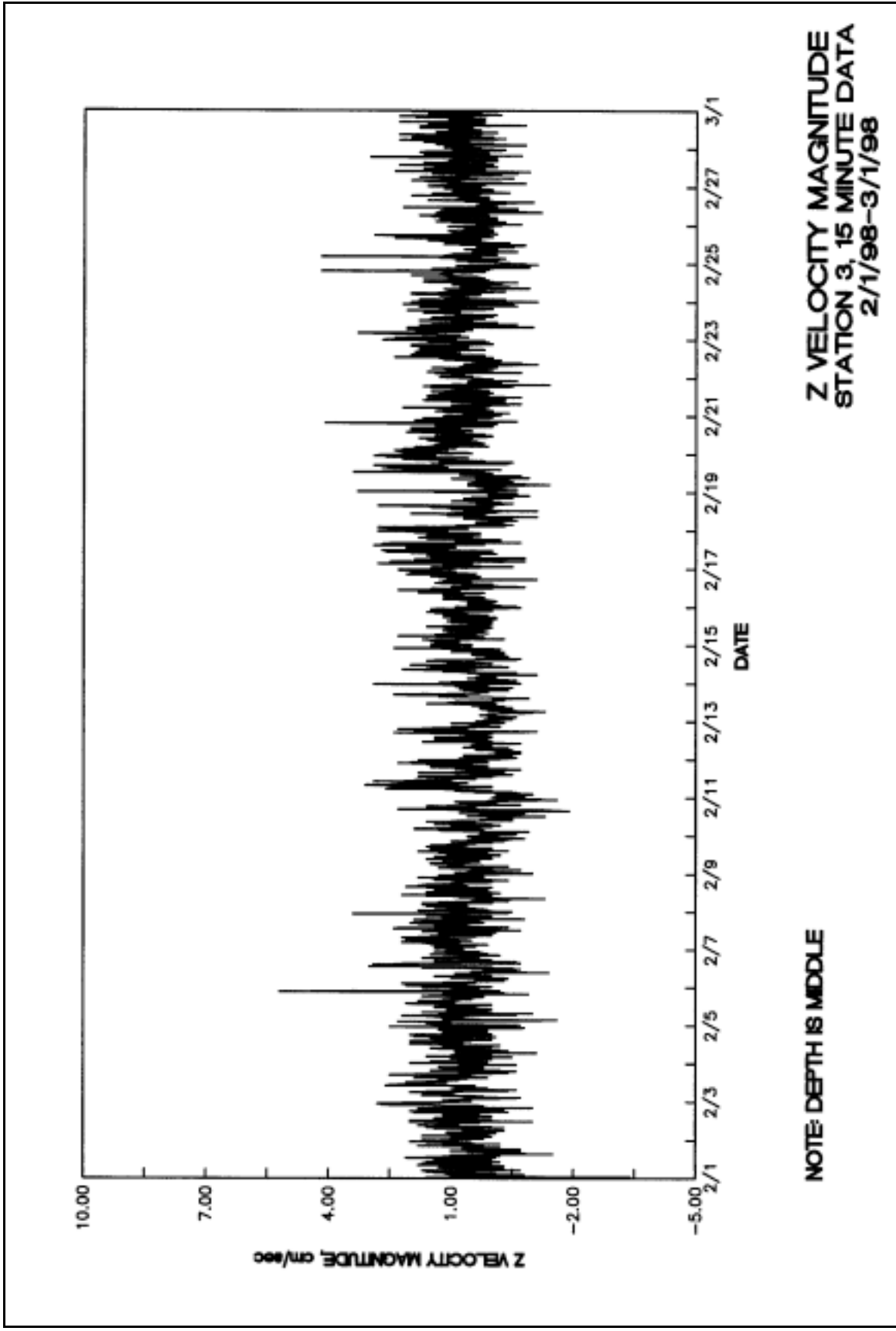


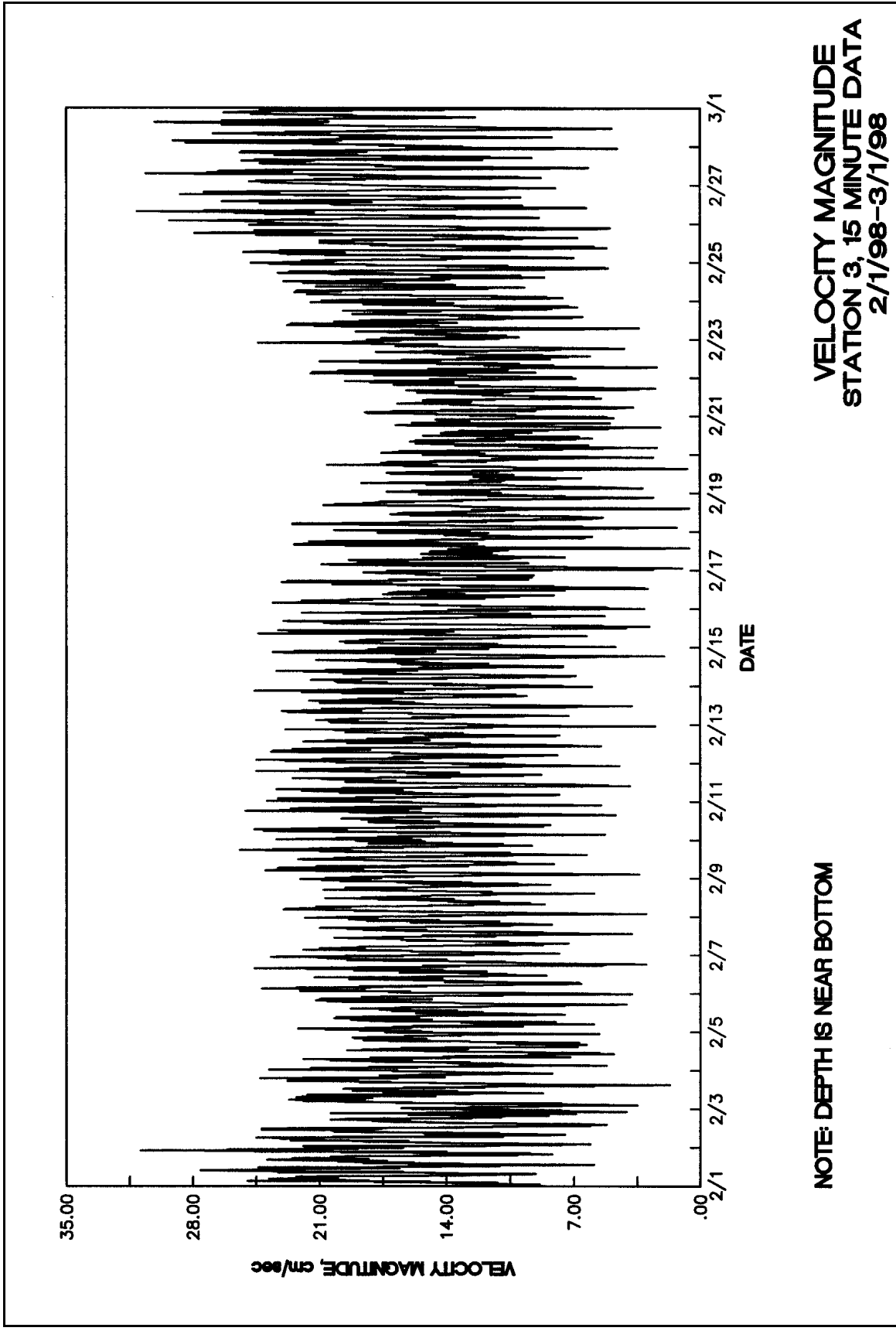


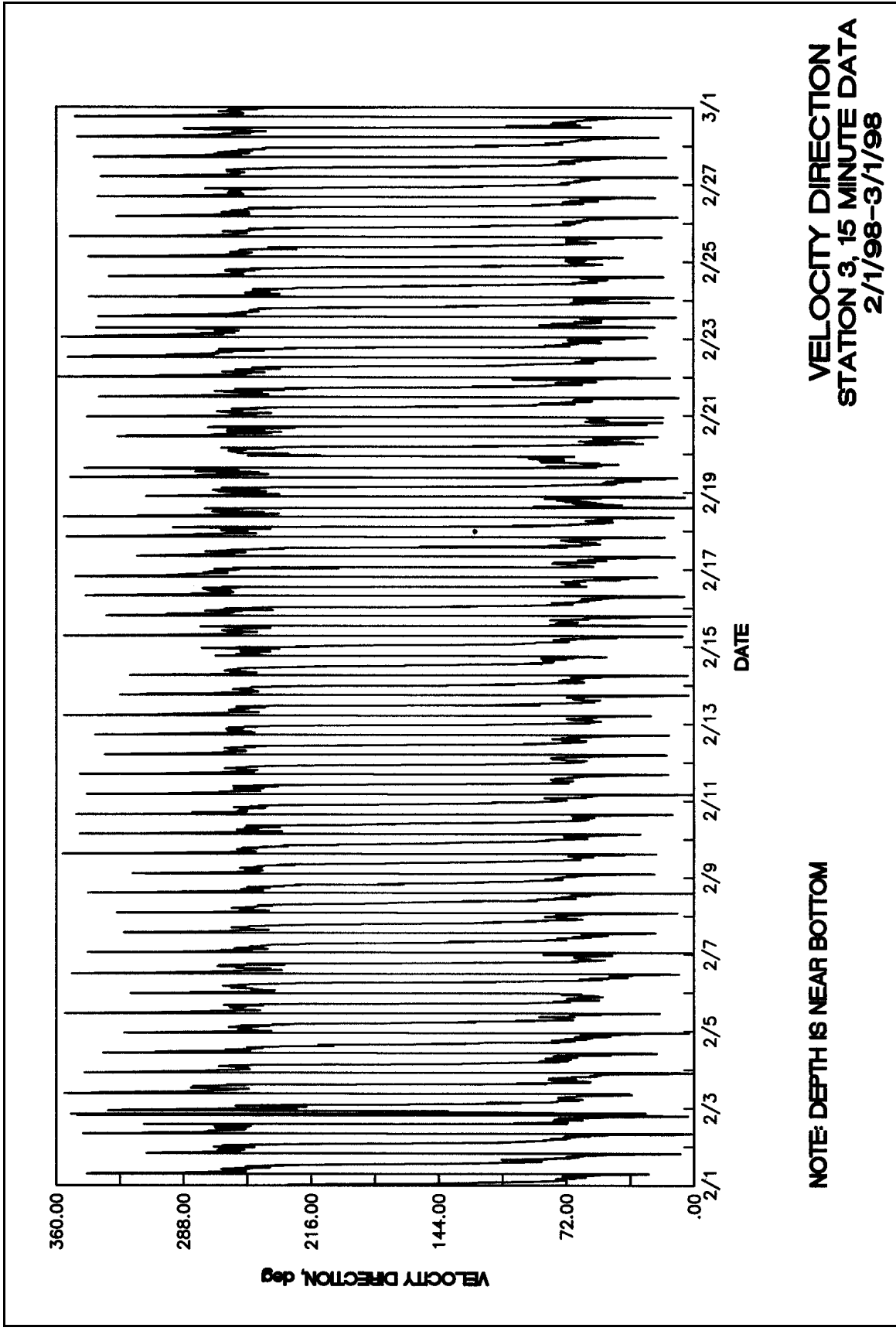
**X VELOCITY MAGNITUDE
STATION 3, 15 MINUTE DATA
2/1/98-3/1/98**

NOTE: DEPTH IS MIDDLE



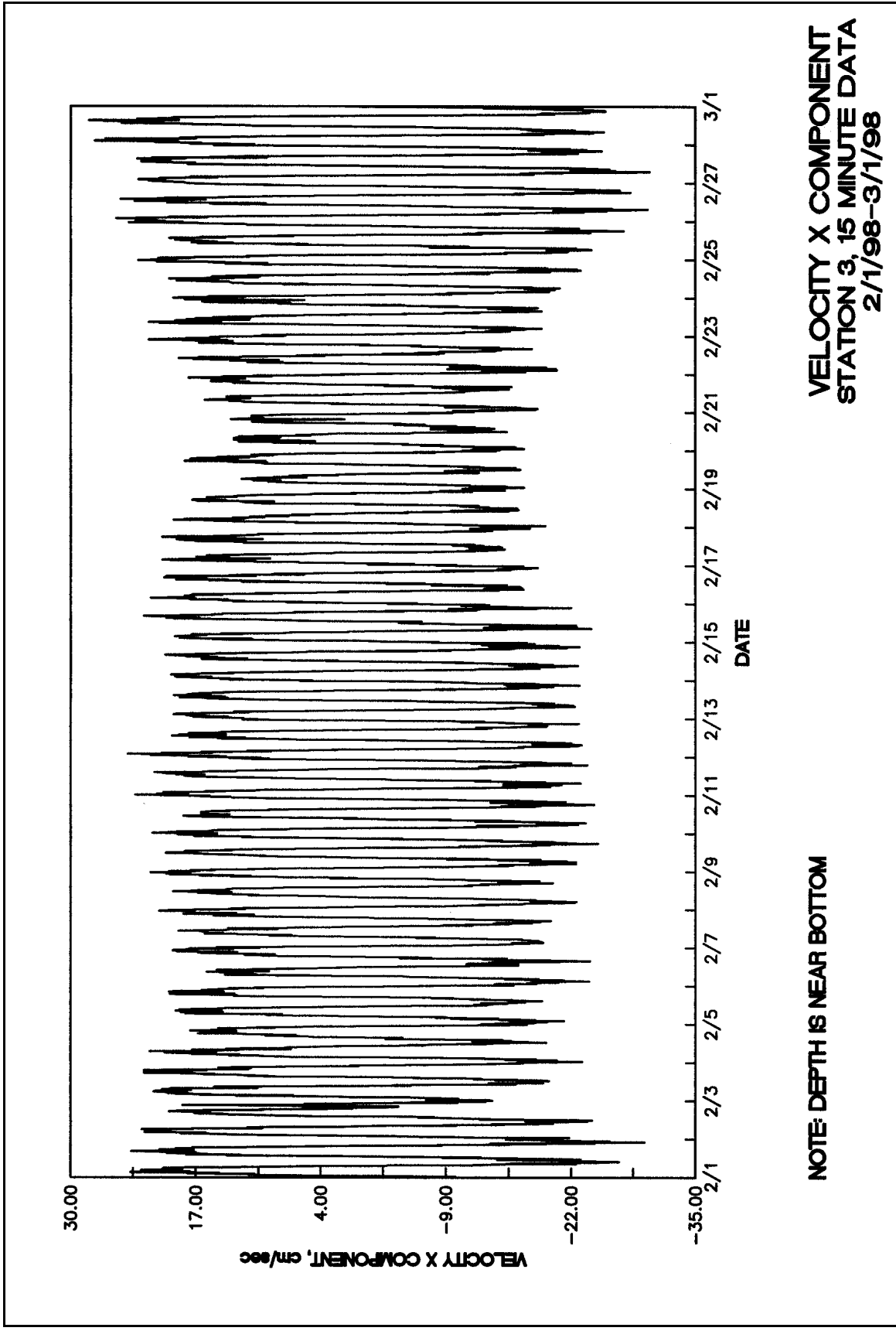


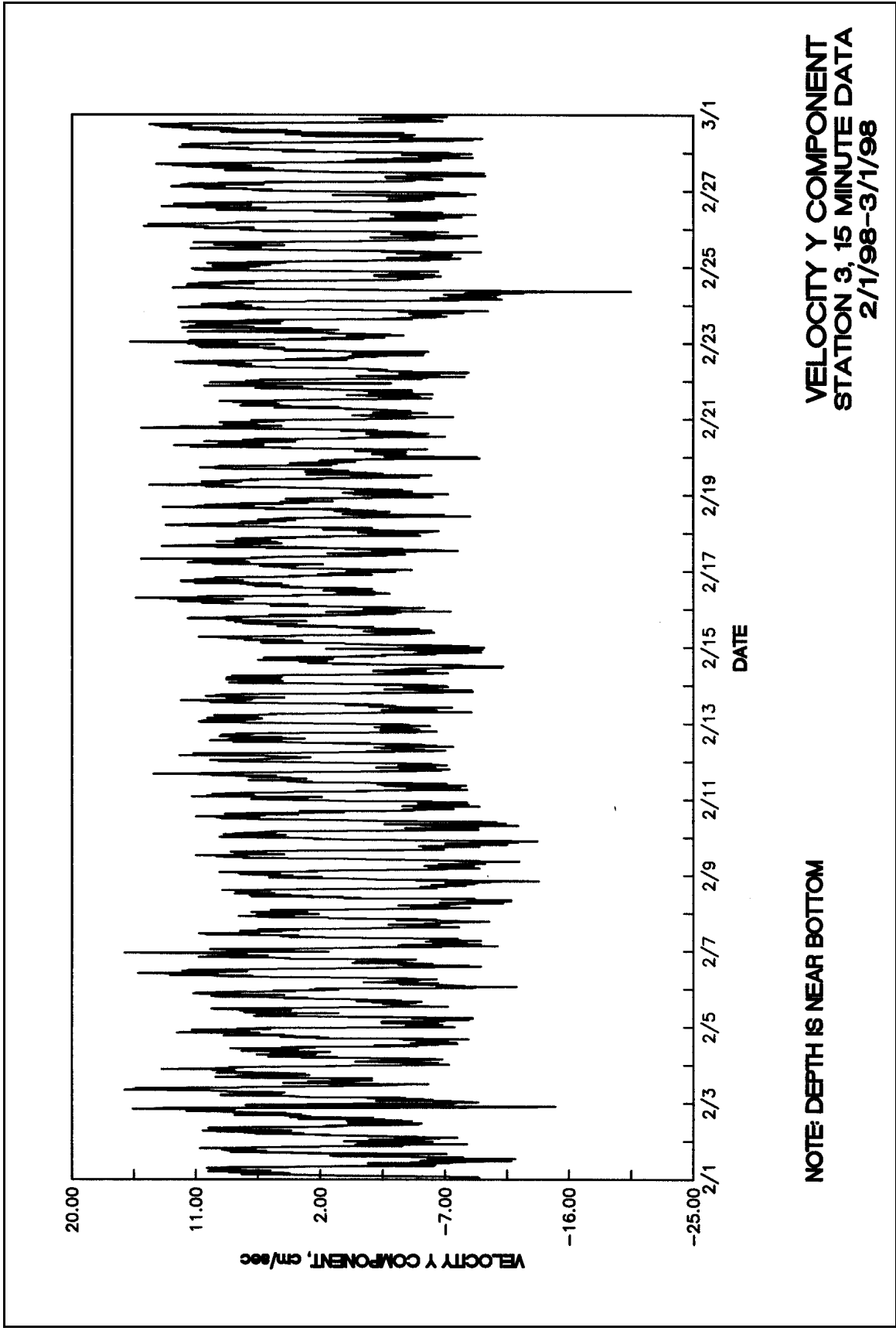


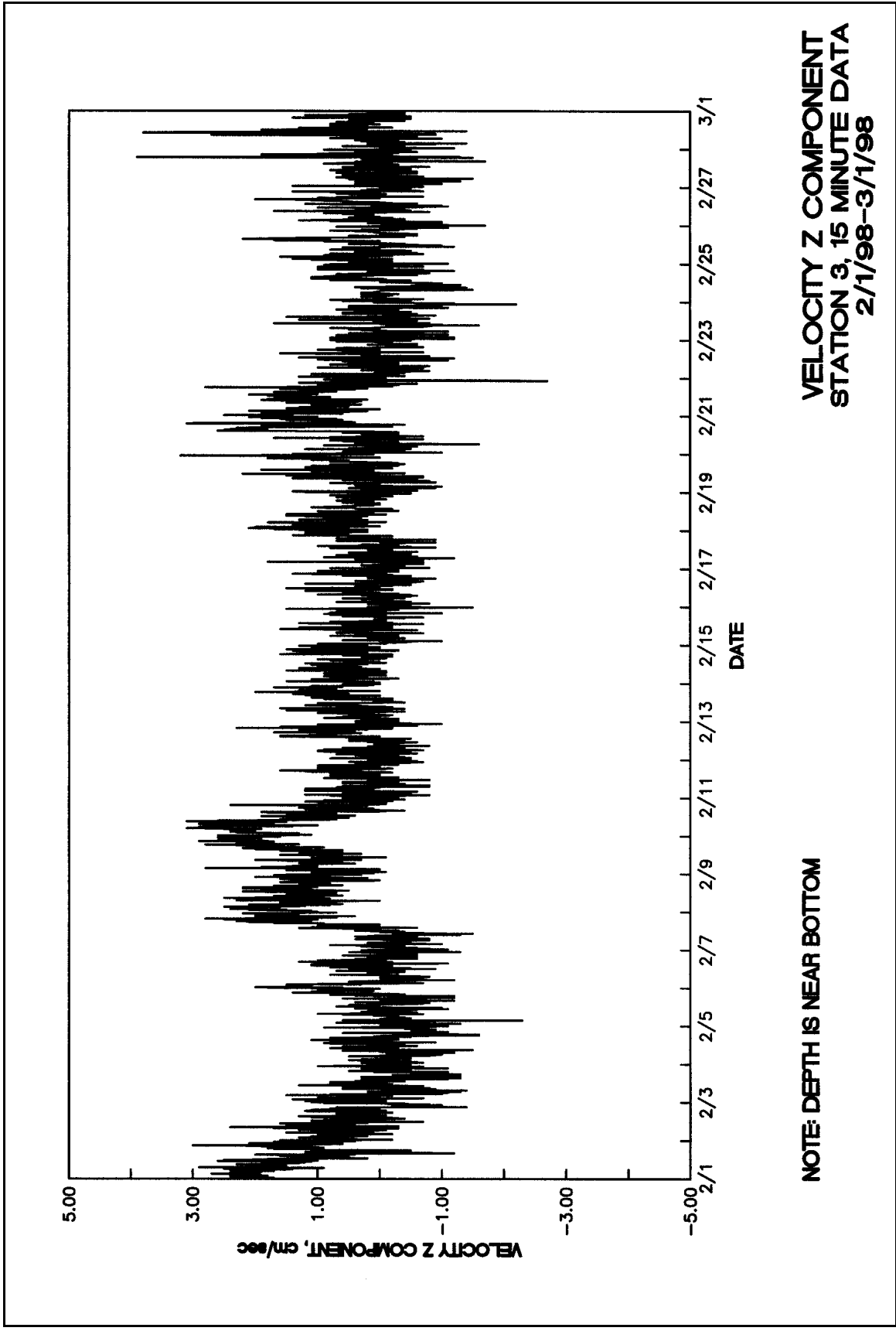


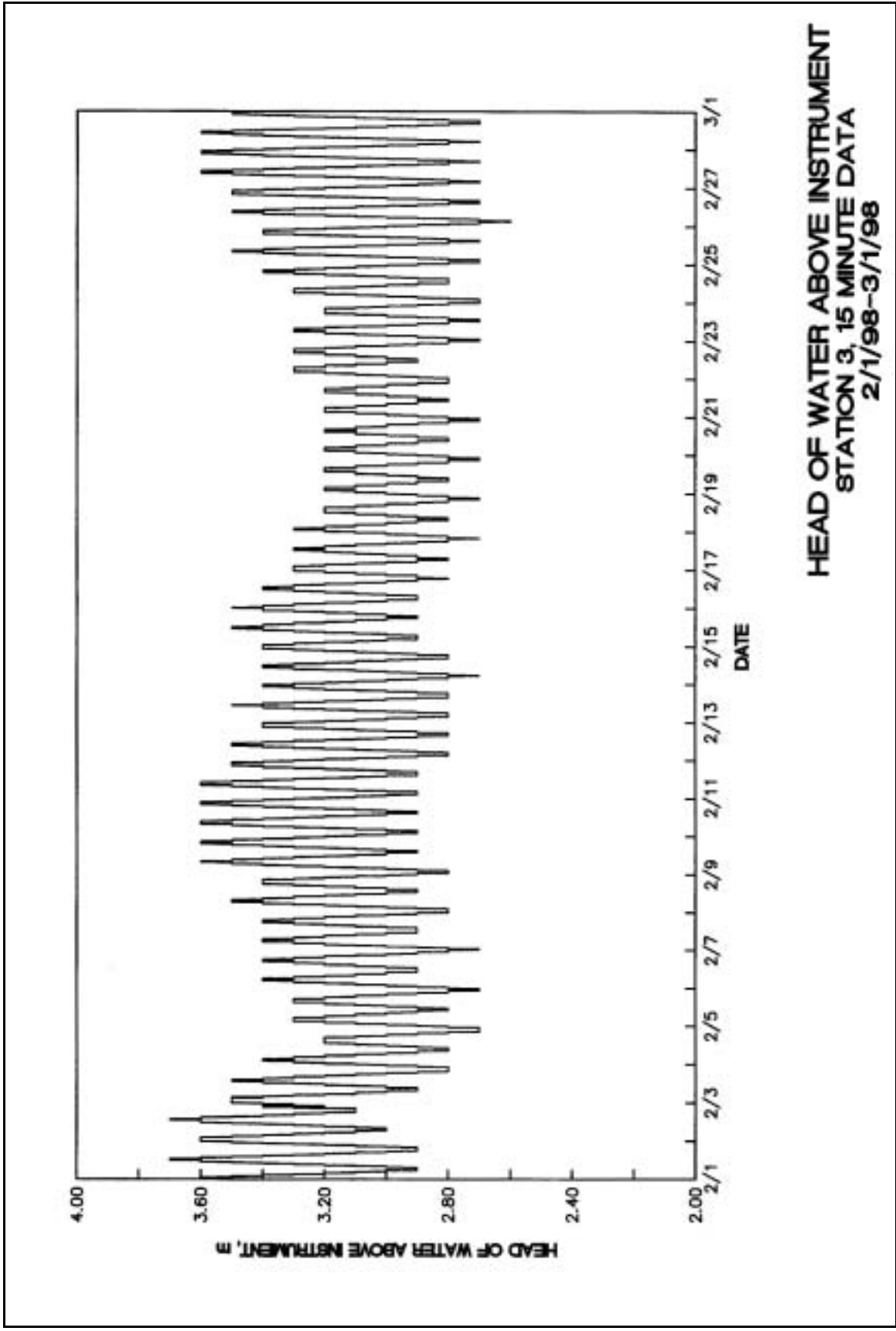
**VELOCITY DIRECTION
STATION 3, 15 MINUTE DATA
2/1/98-3/1/98**

NOTE: DEPTH IS NEAR BOTTOM









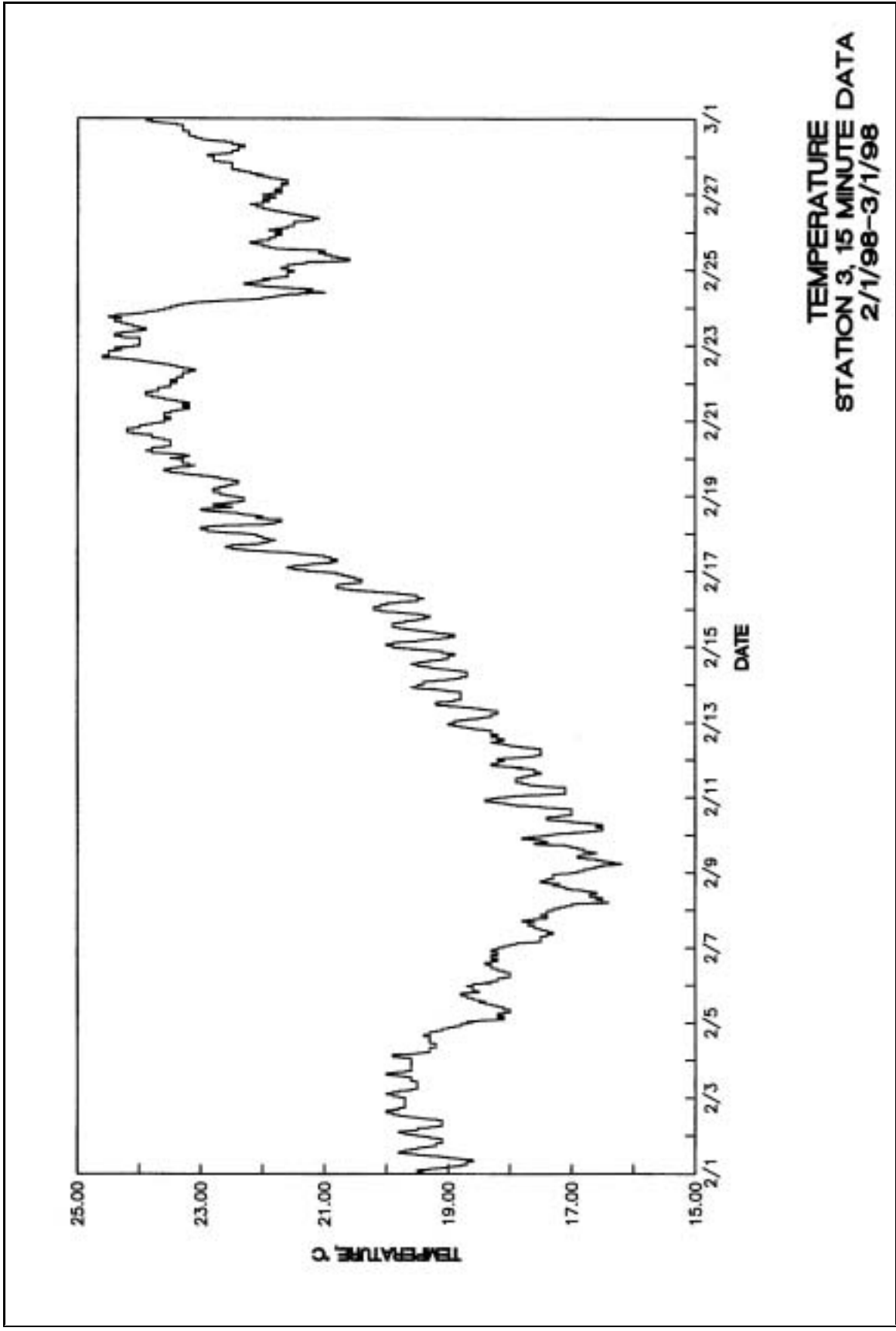
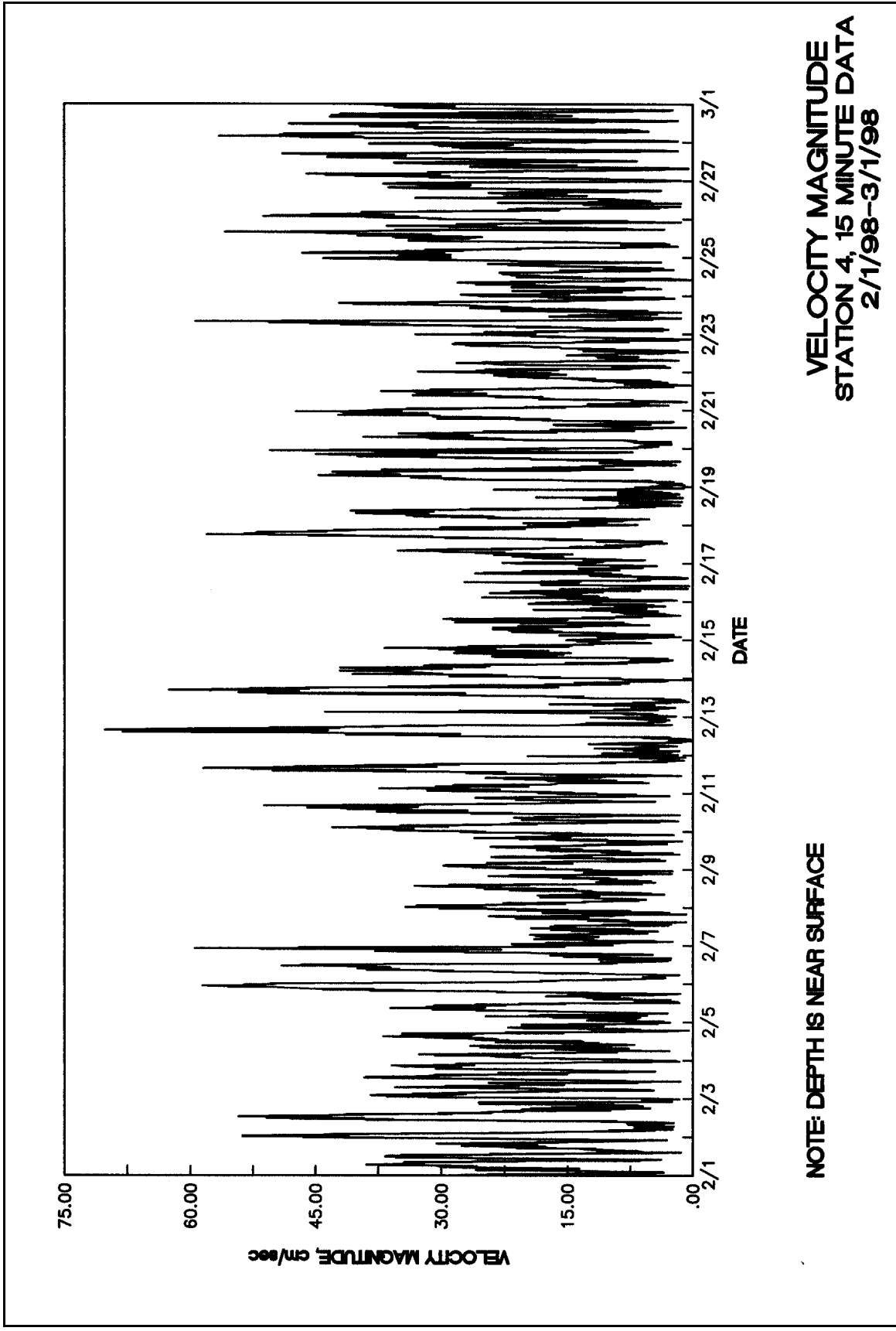
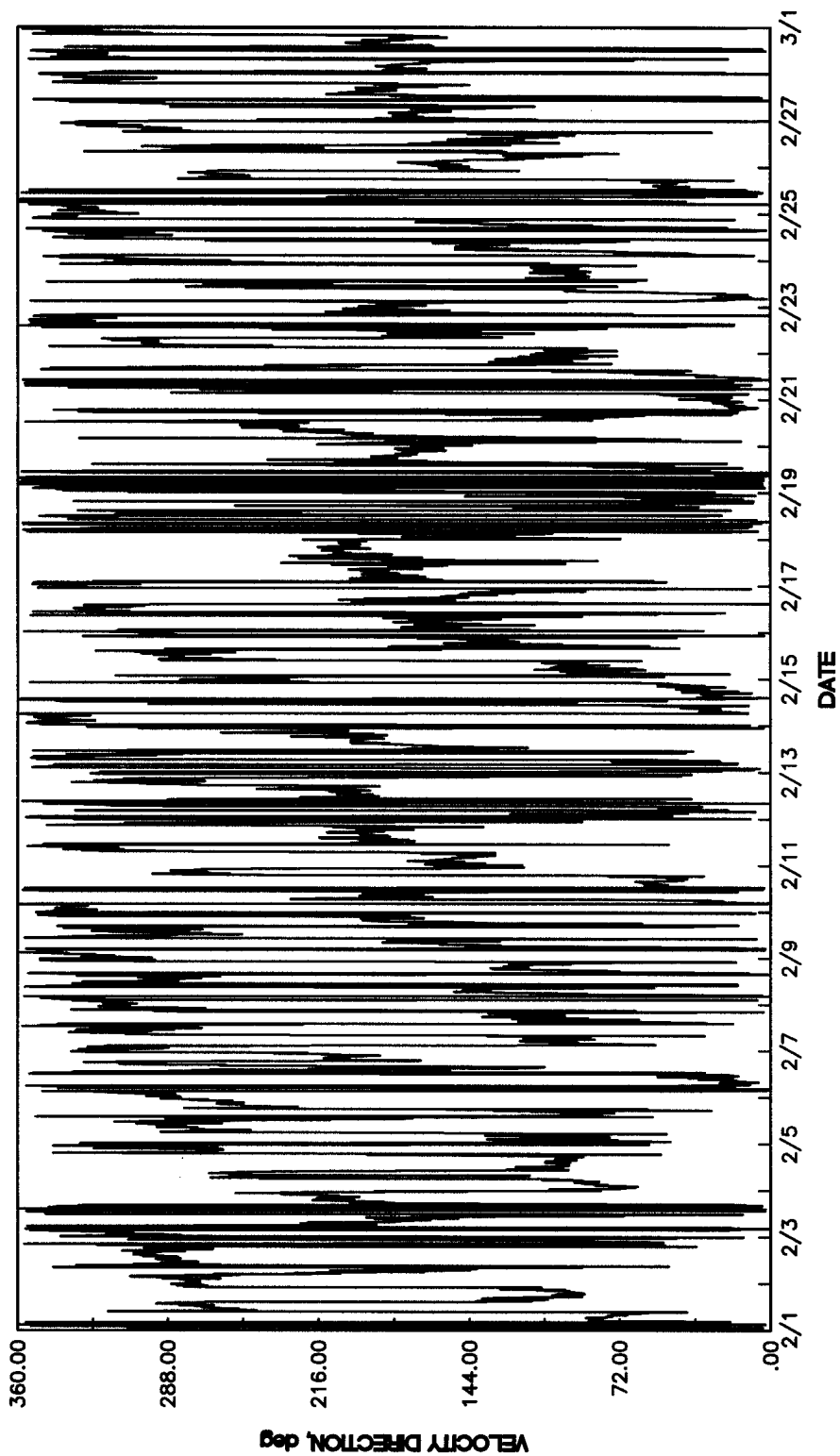


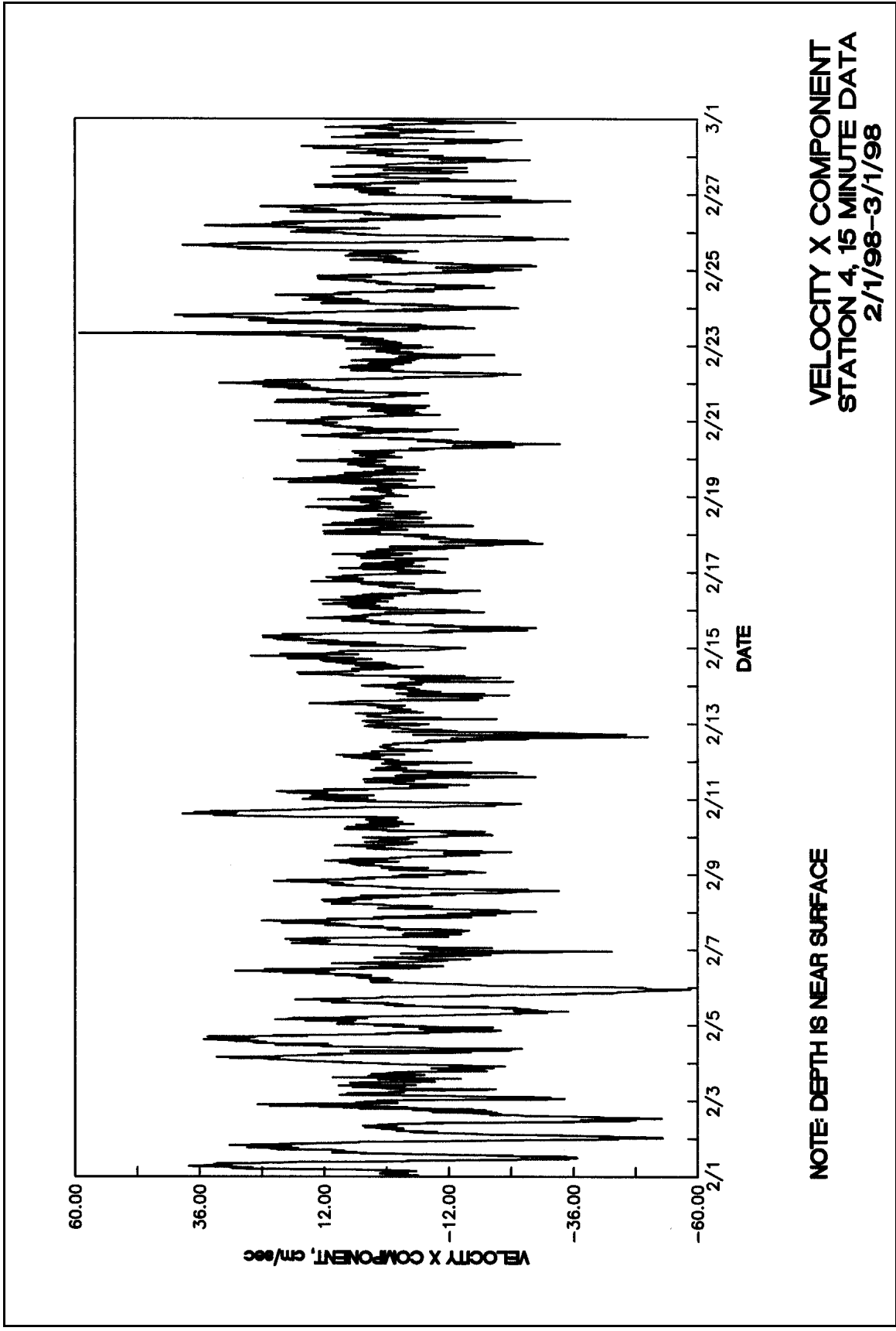
Plate 62





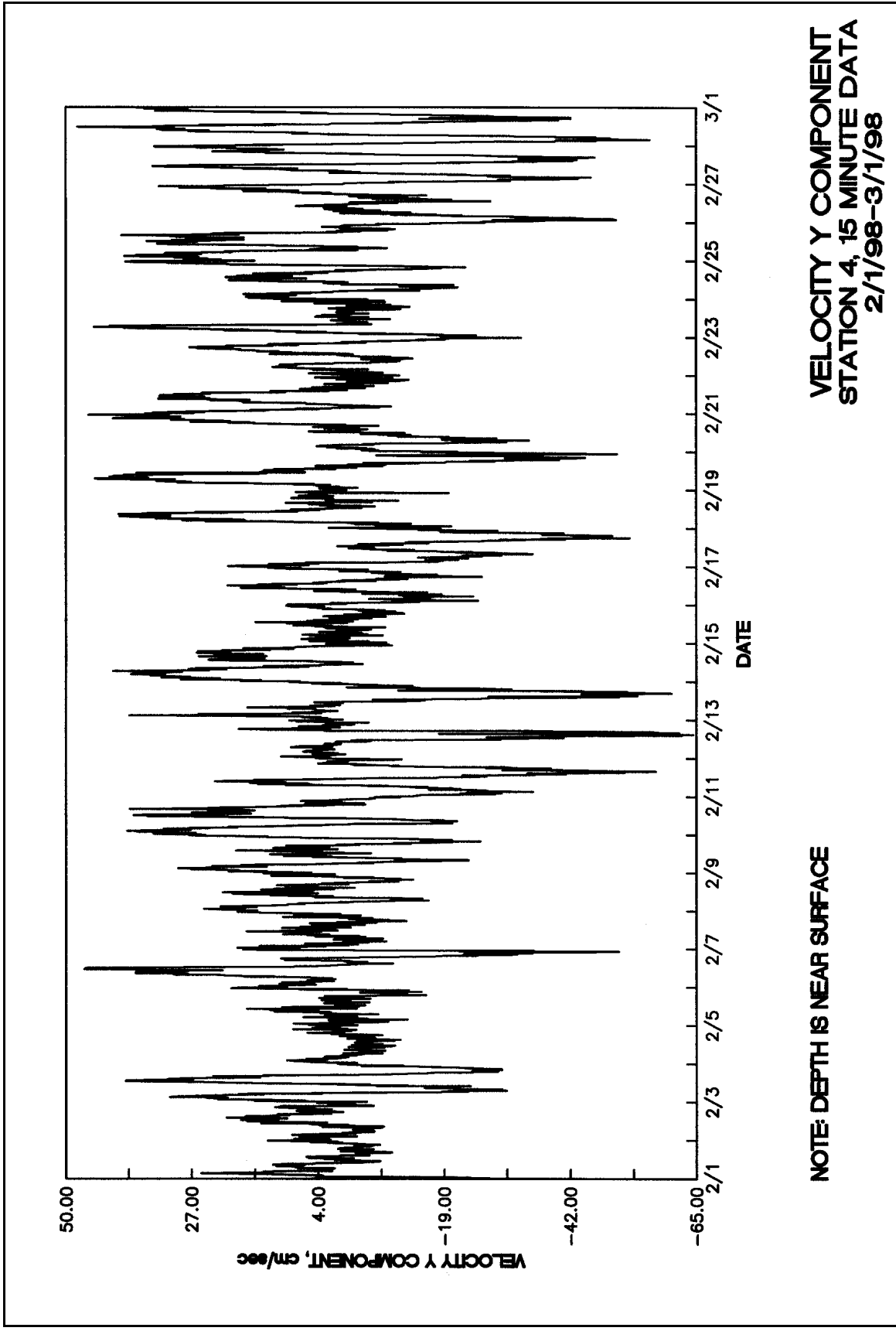
**VELOCITY DIRECTION
STATION 4, 15 MINUTE DATA
2/1/98-3/1/98**

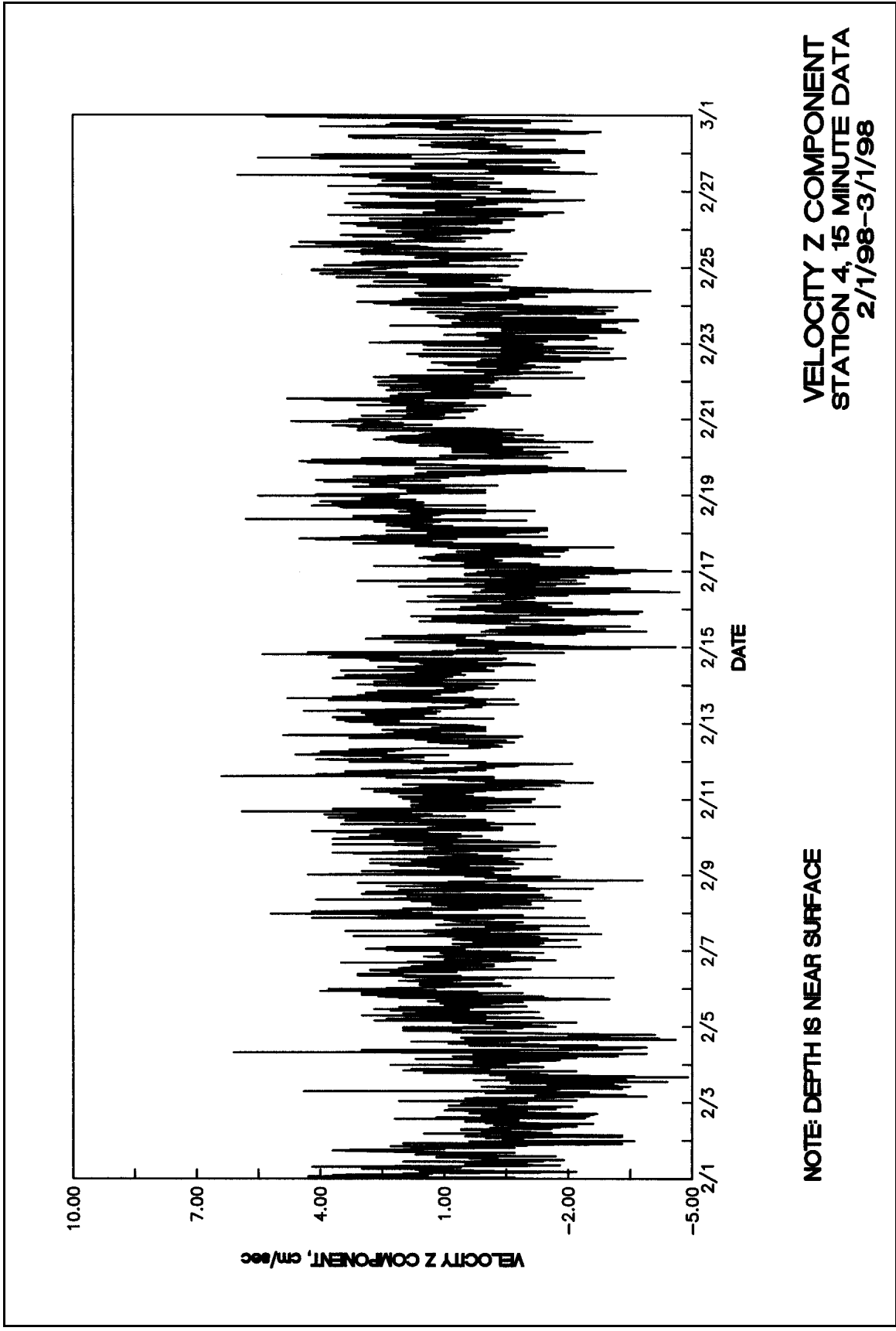
NOTE: DEPTH IS NEAR SURFACE

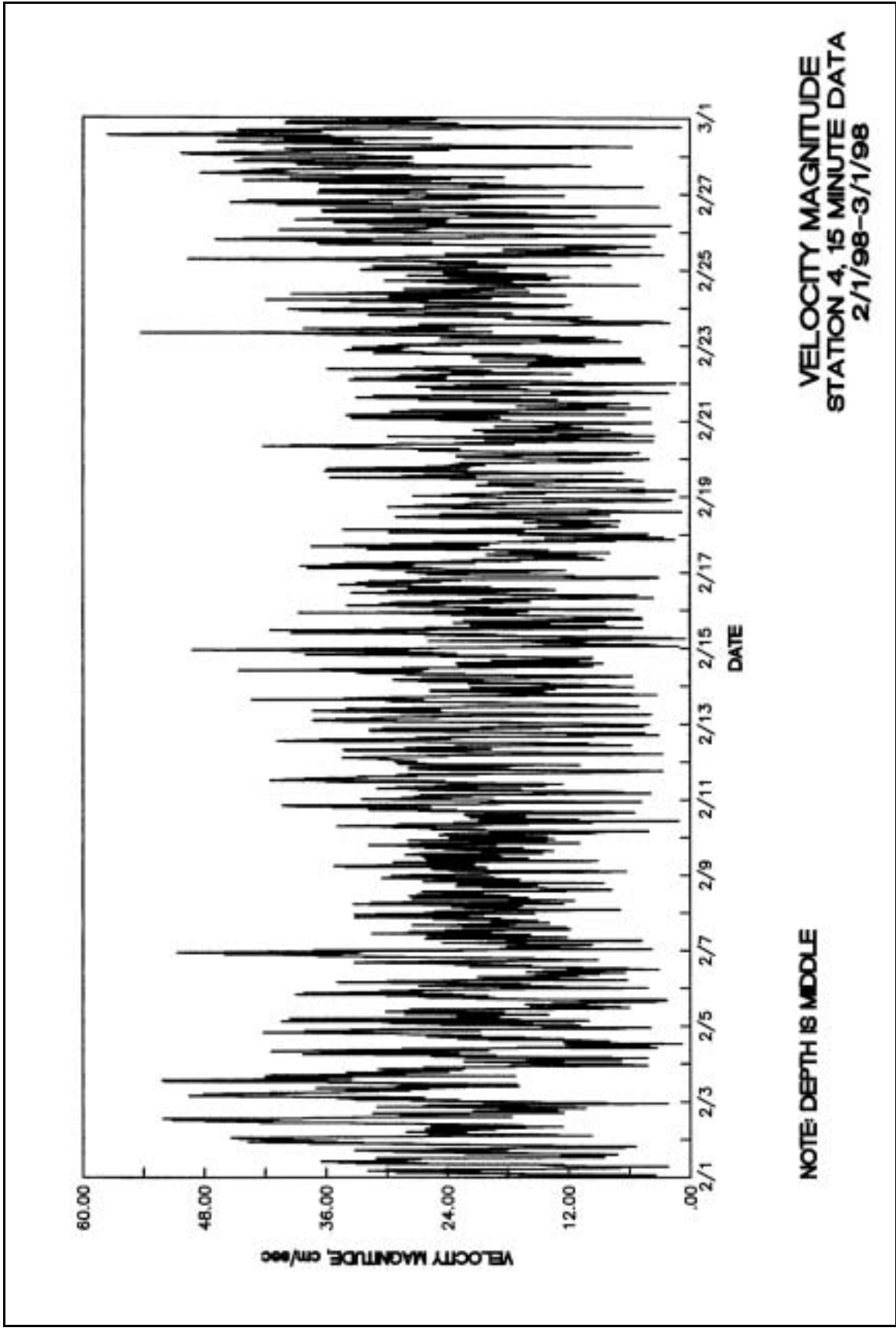


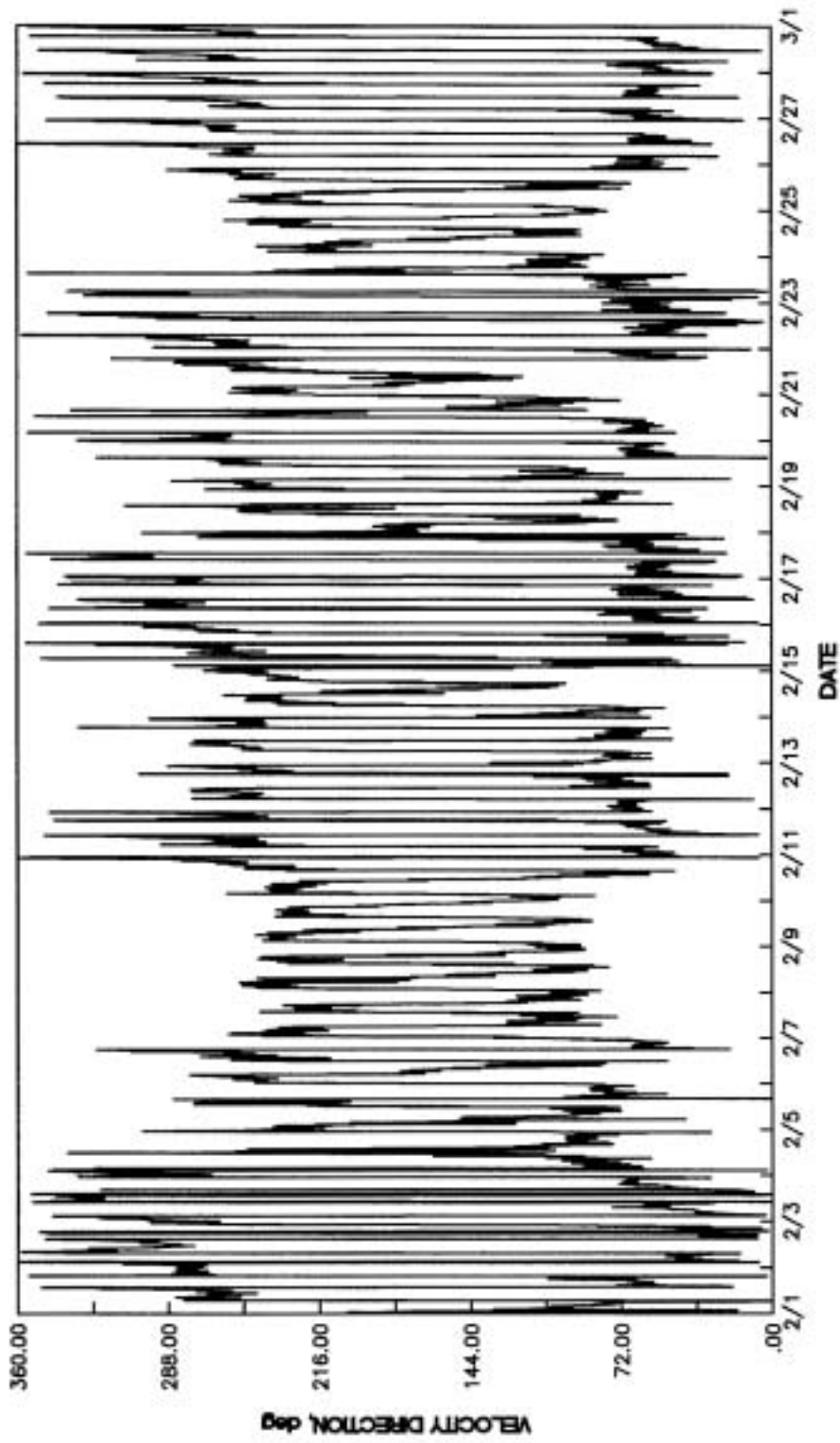
**VELOCITY X COMPONENT
STATION 4, 15 MINUTE DATA
2/1/98-3/1/98**

NOTE: DEPTH IS NEAR SURFACE



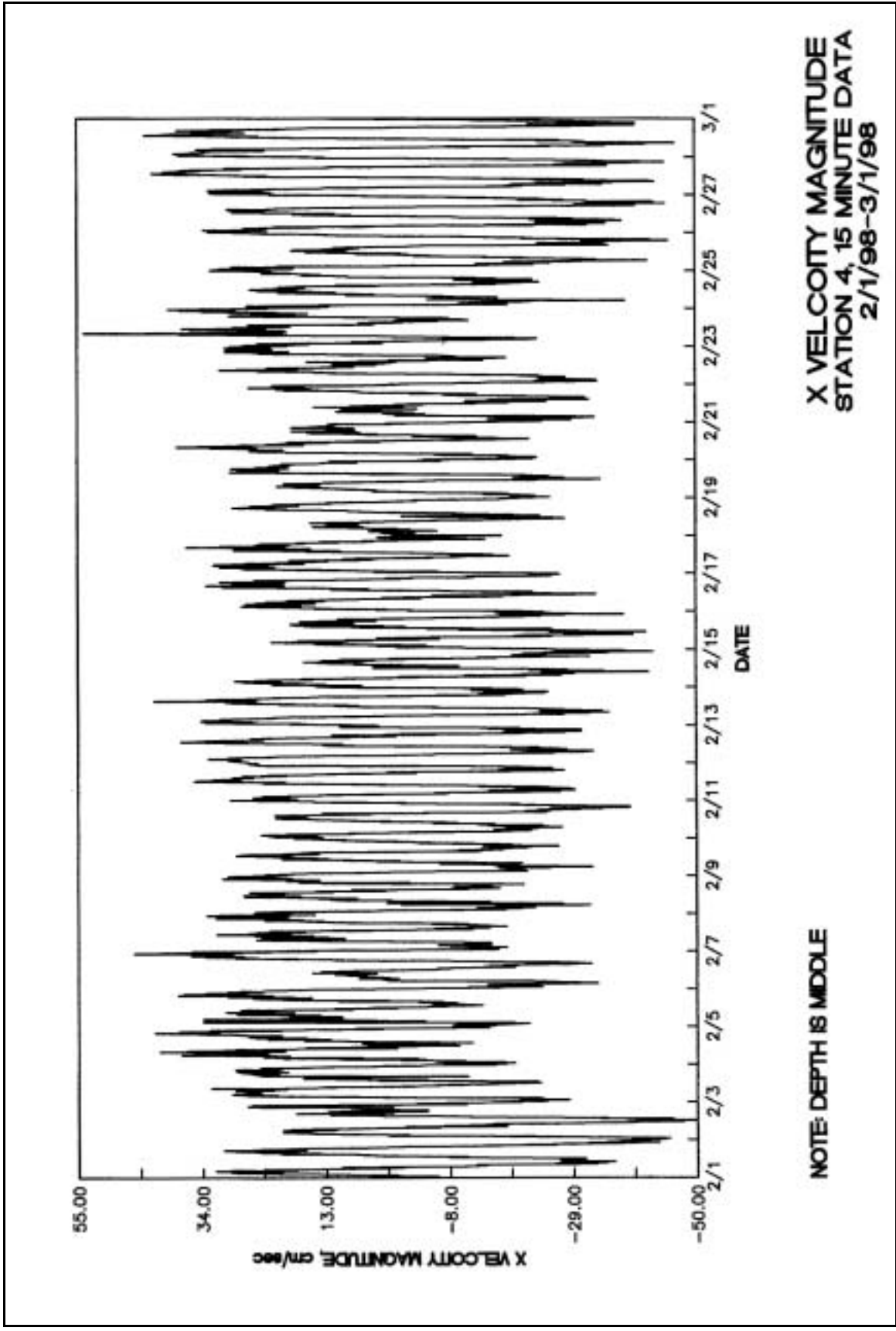


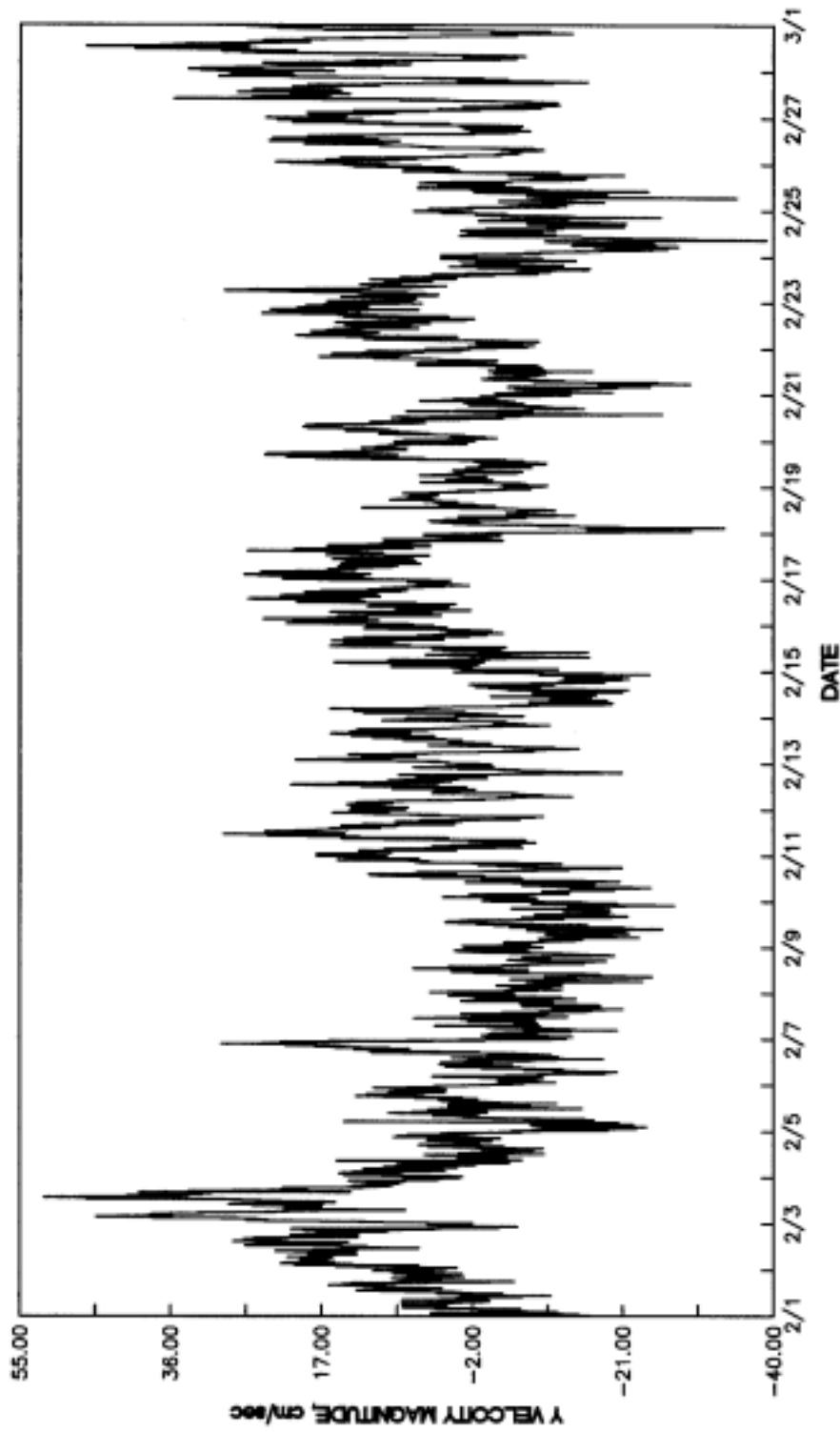




**VELOCITY DIRECTION
STATION 4, 15 MINUTE DATA
2/1/98-3/1/98**

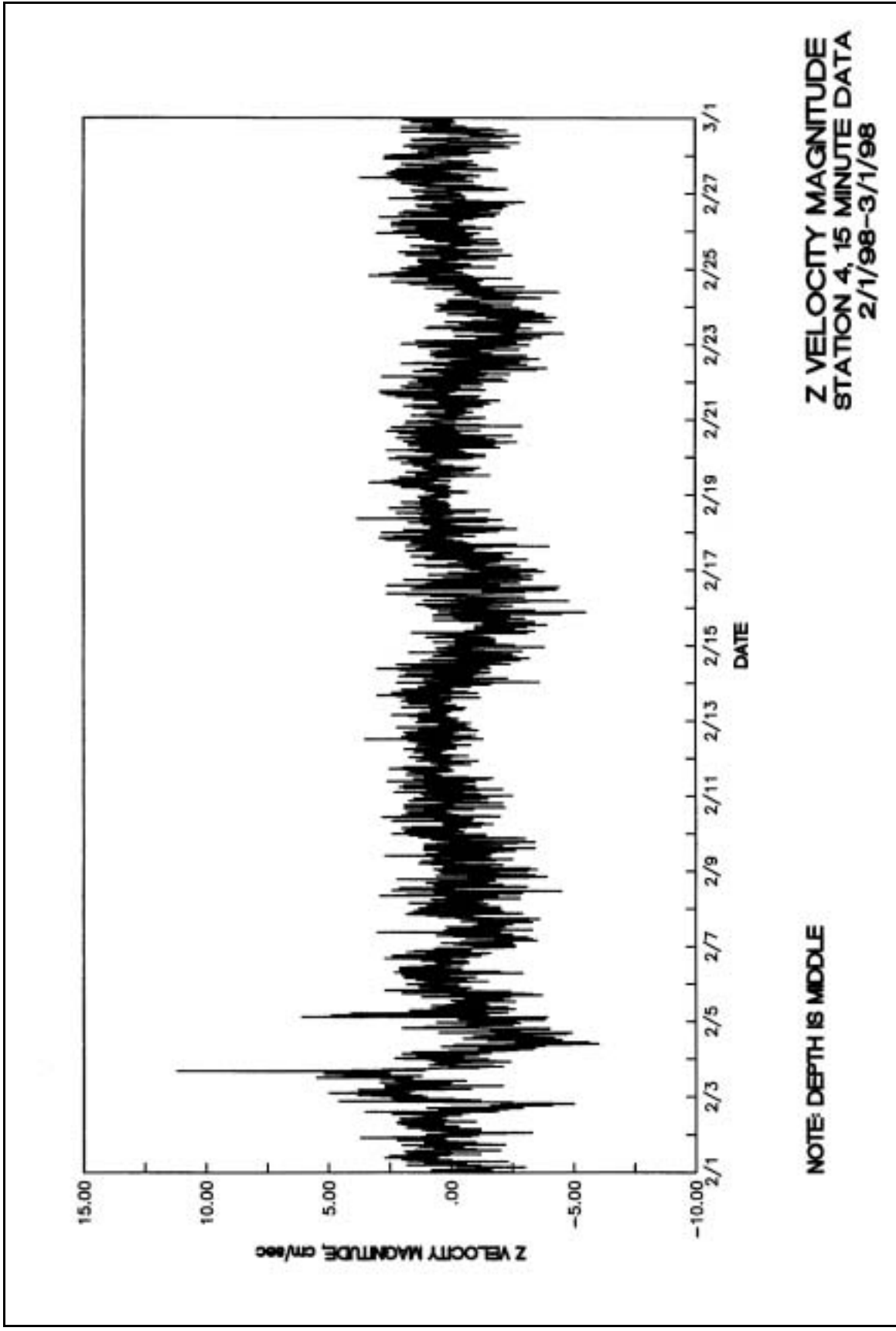
NOTE: DEPTH IS MIDDLE

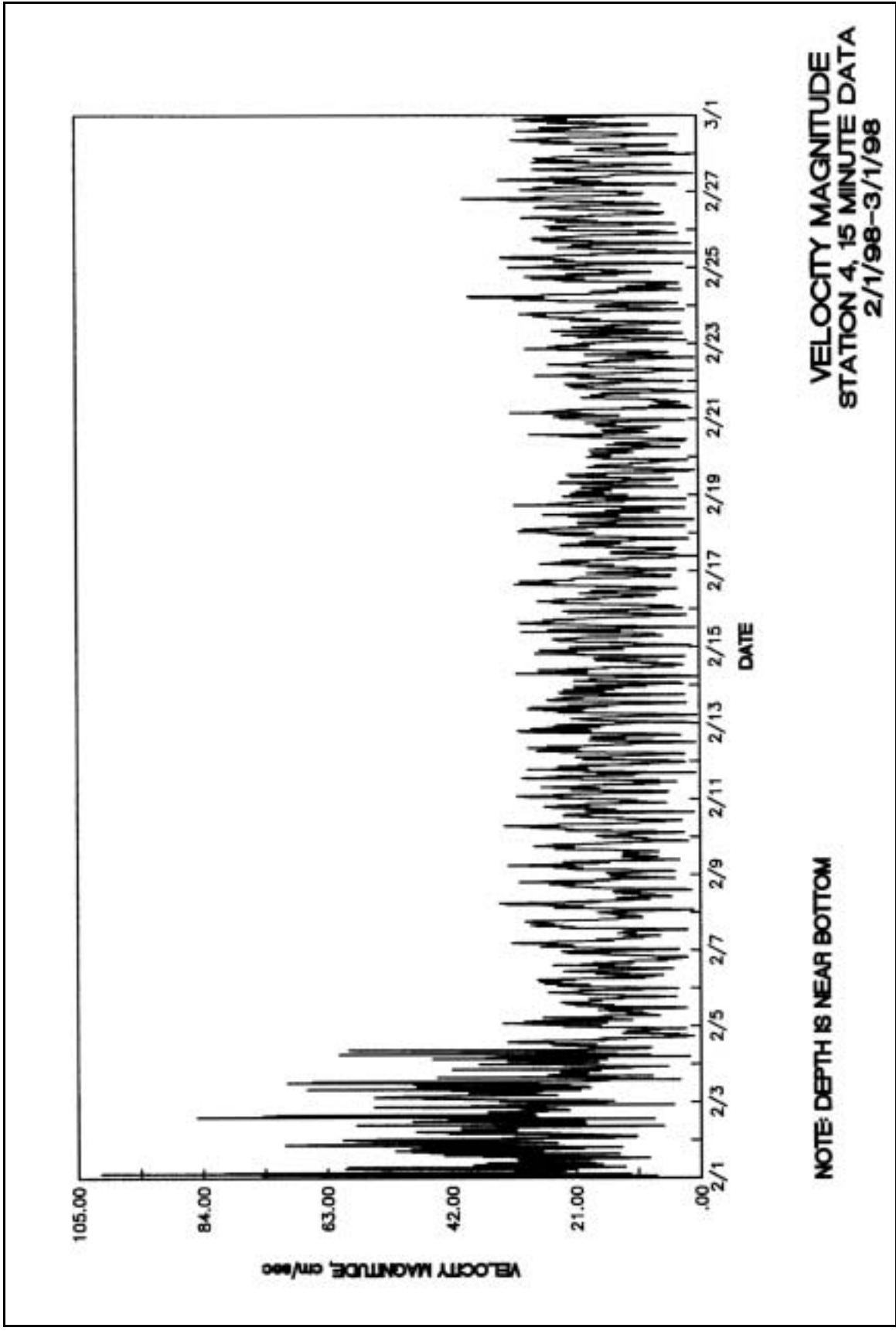


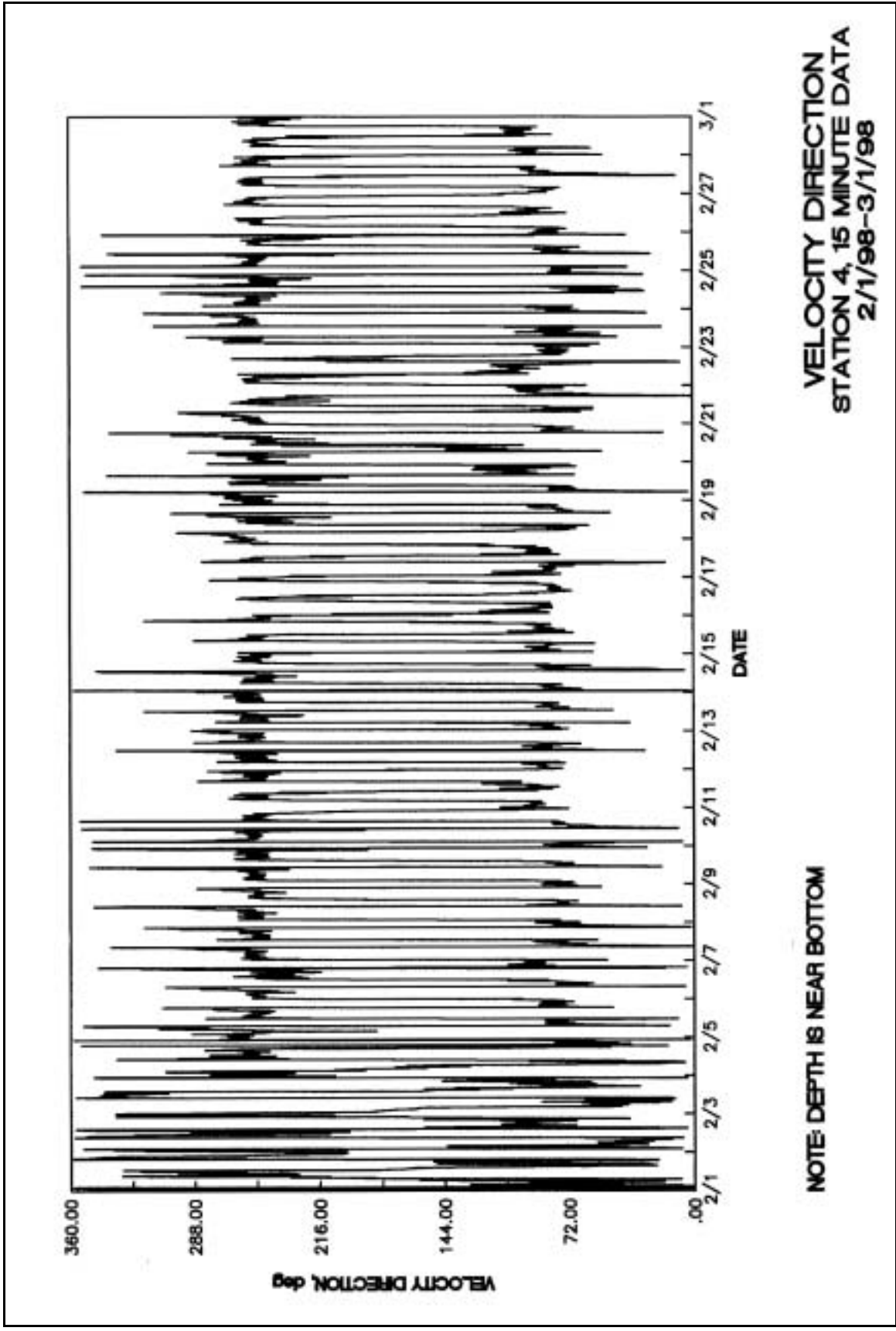


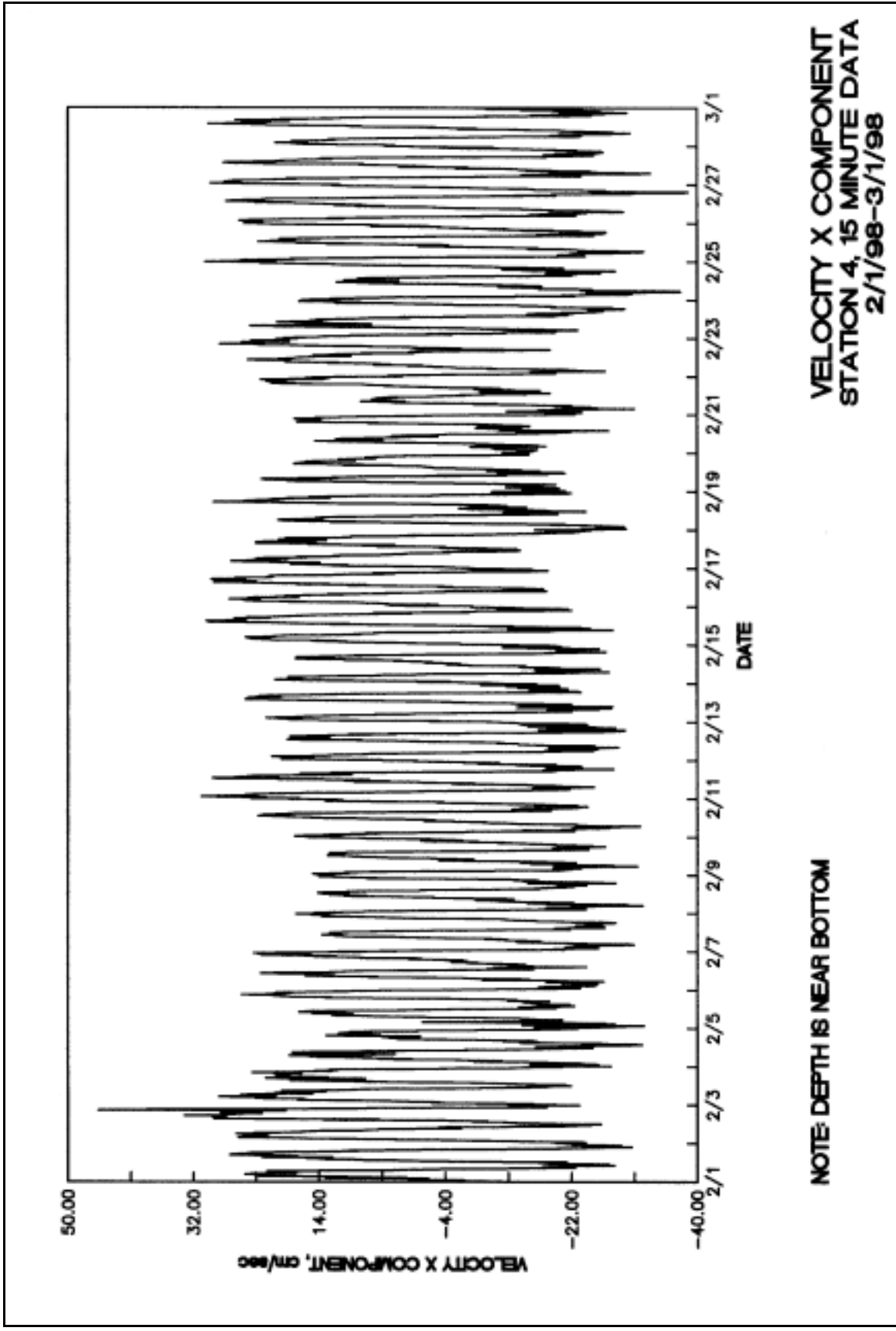
**Y VELOCITY MAGNITUDE
STATION 4, 15 MINUTE DATA
2/1/98-3/1/98**

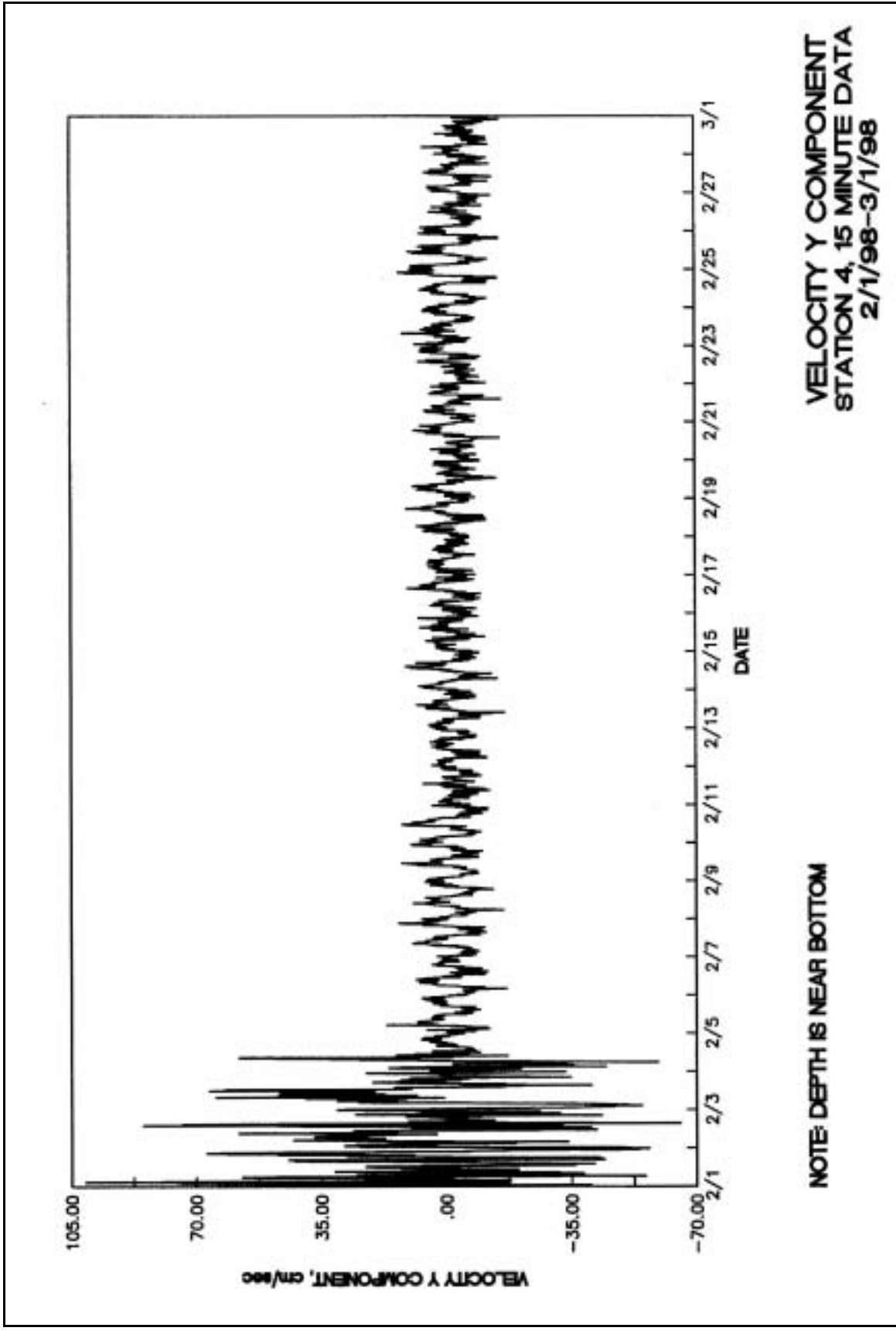
NOTE: DEPTH IS MIDDLE





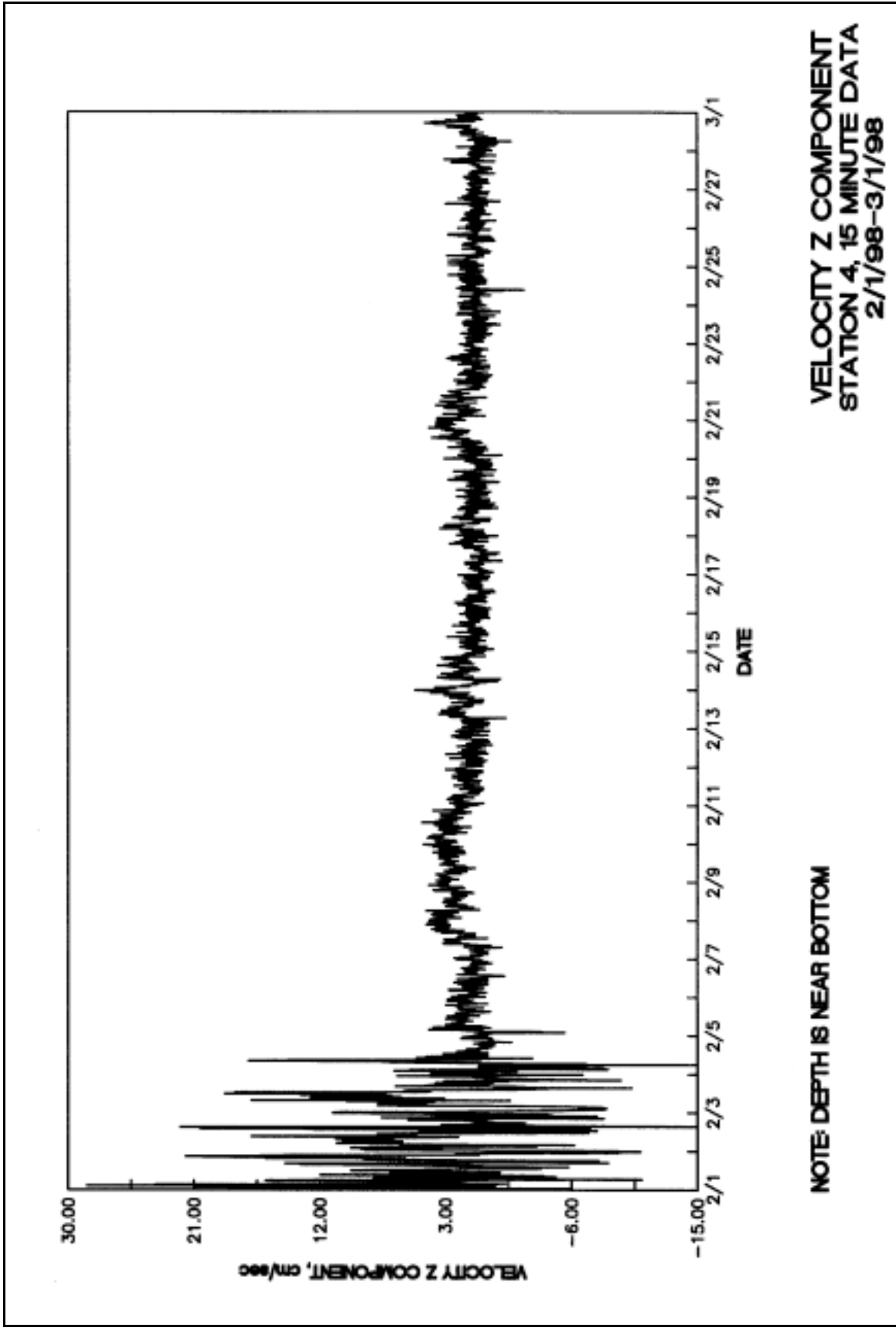


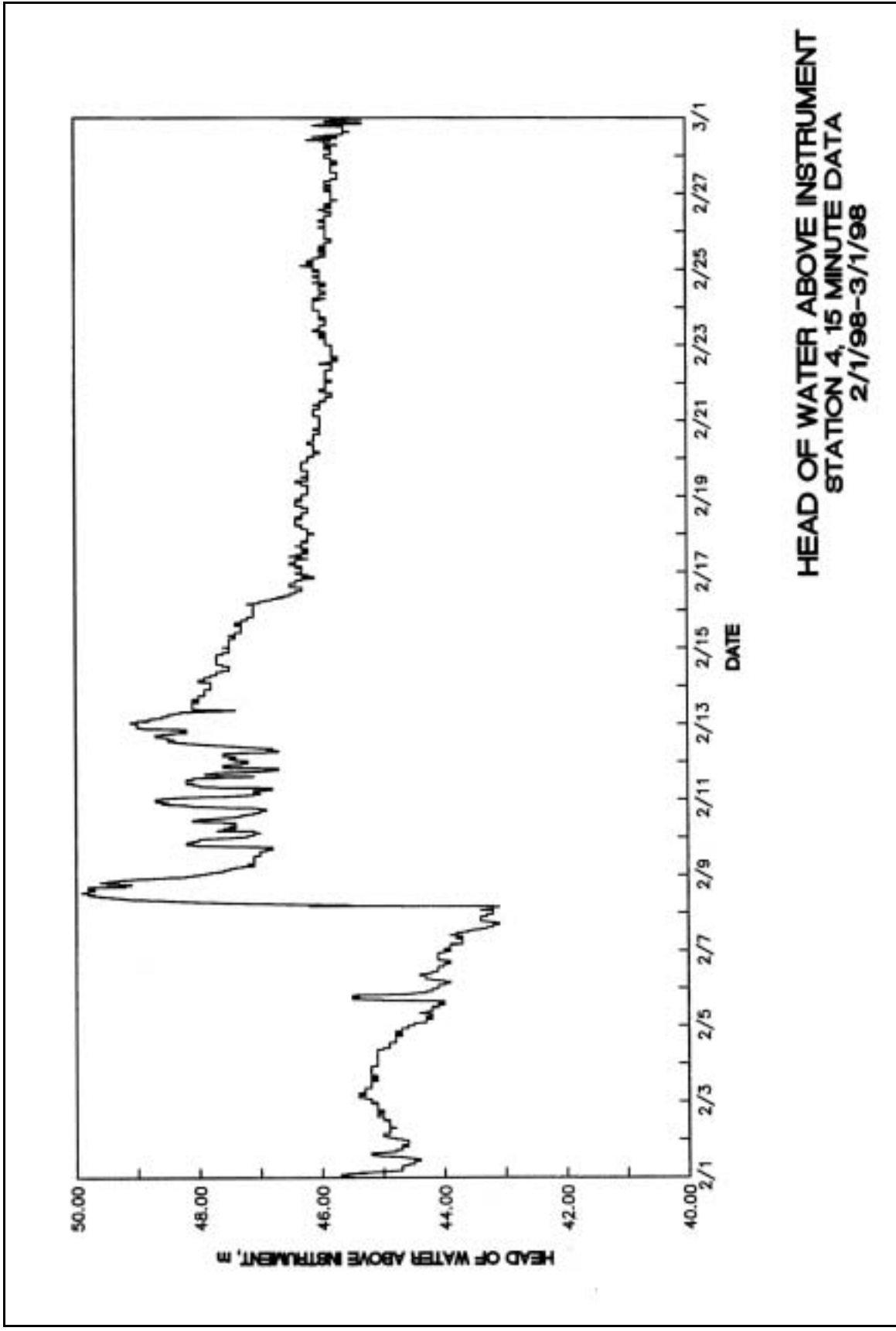




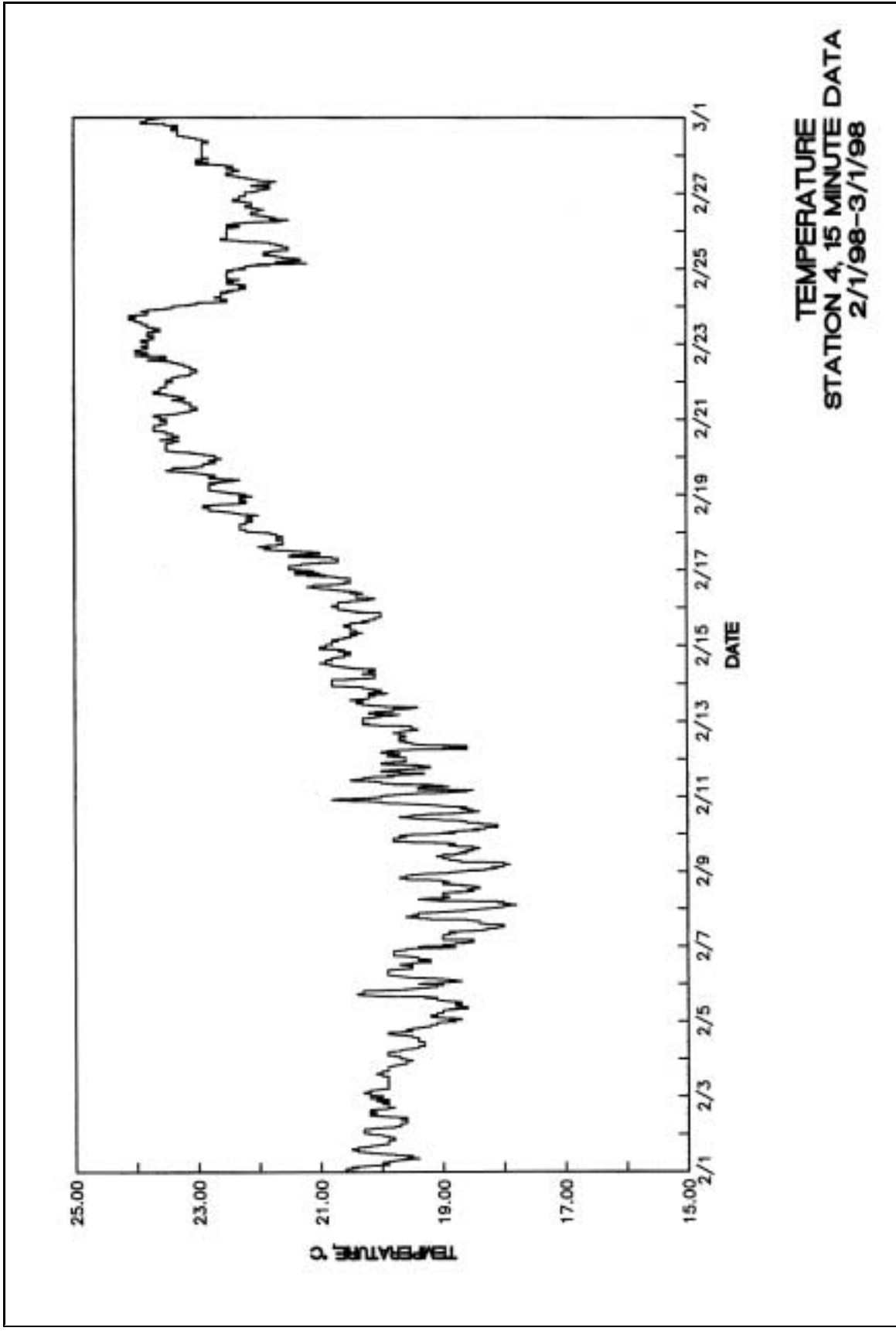
**VELOCITY Y COMPONENT
STATION 4, 15 MINUTE DATA
2/1/98-3/1/98**

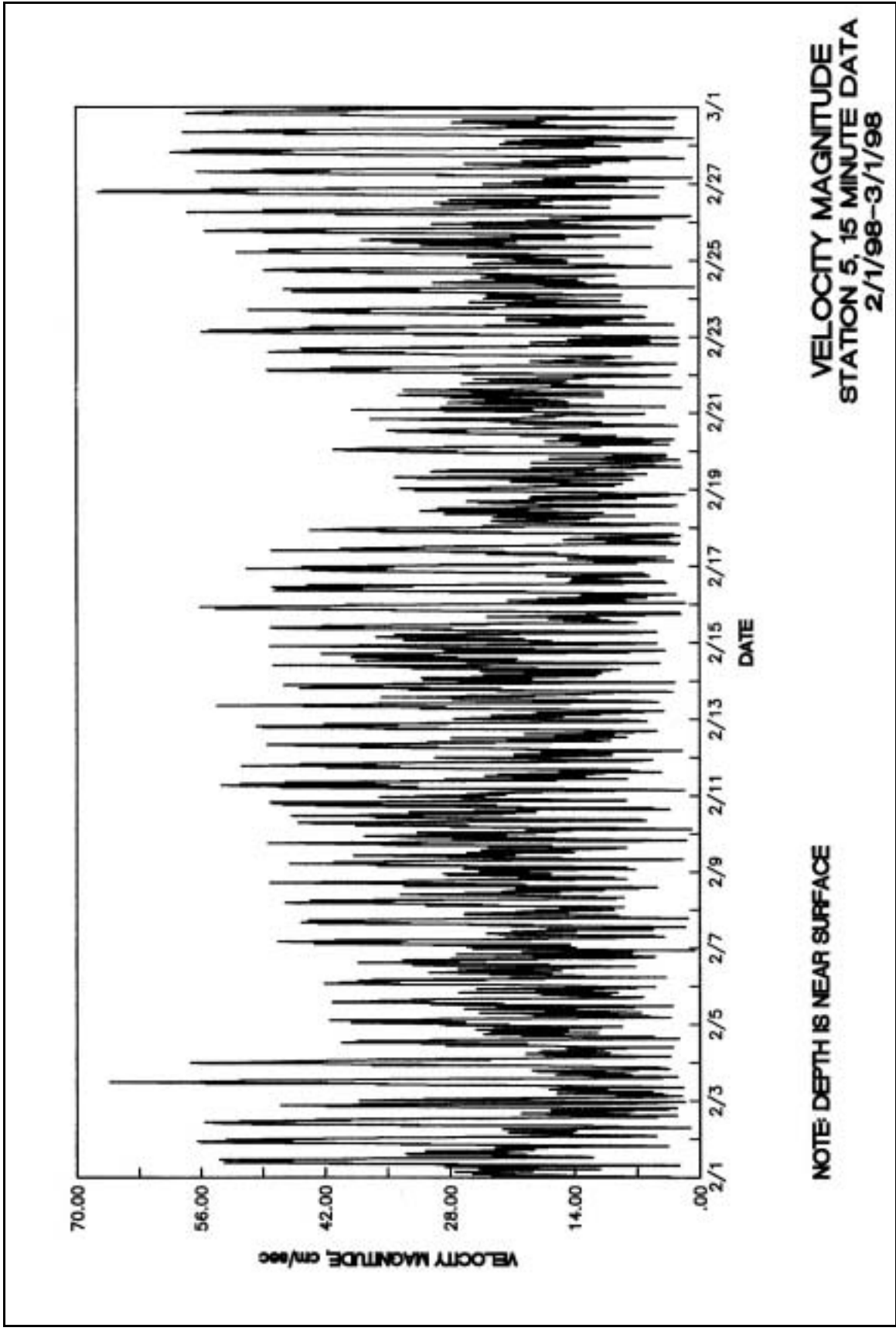
NOTE: DEPTH IS NEAR BOTTOM

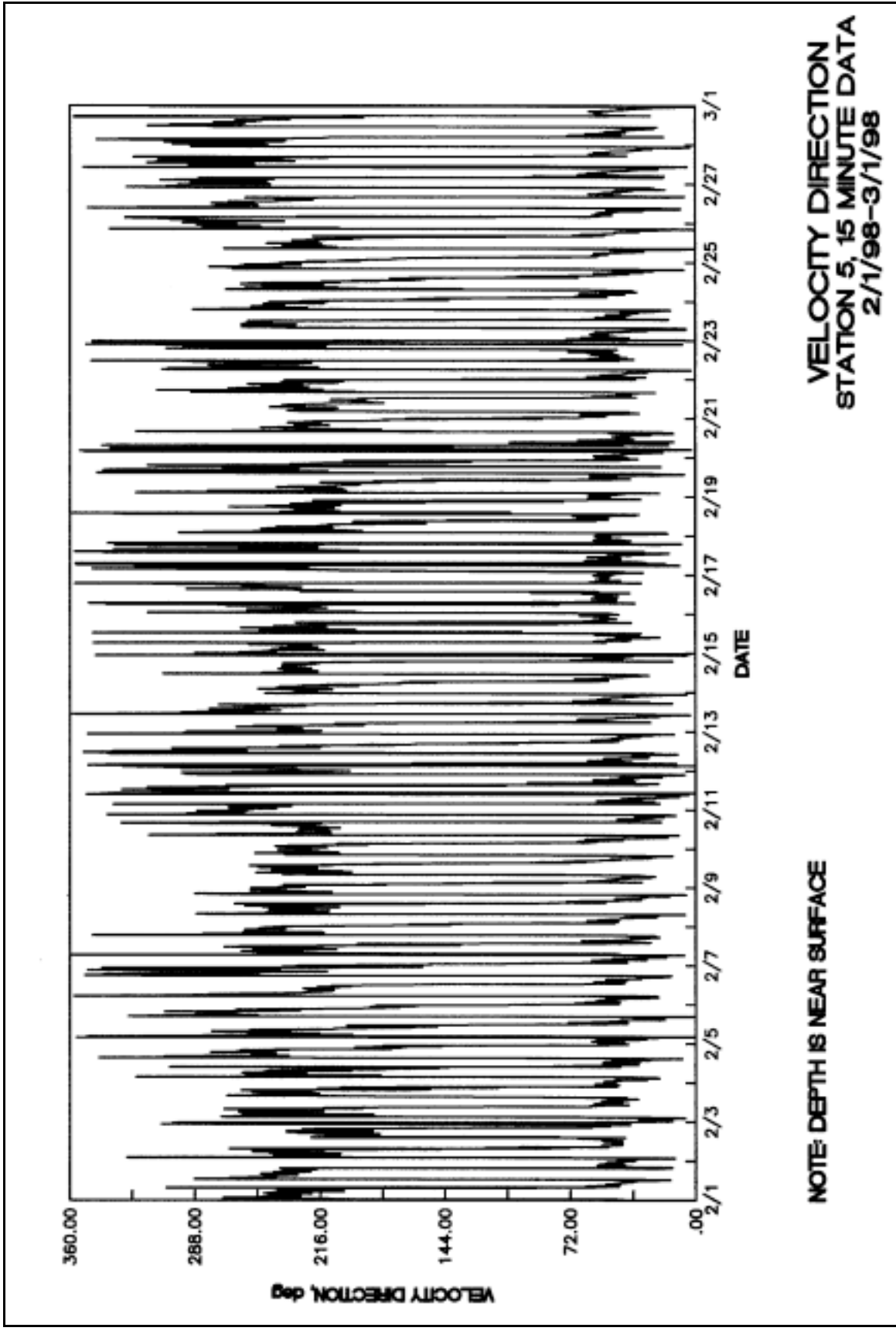


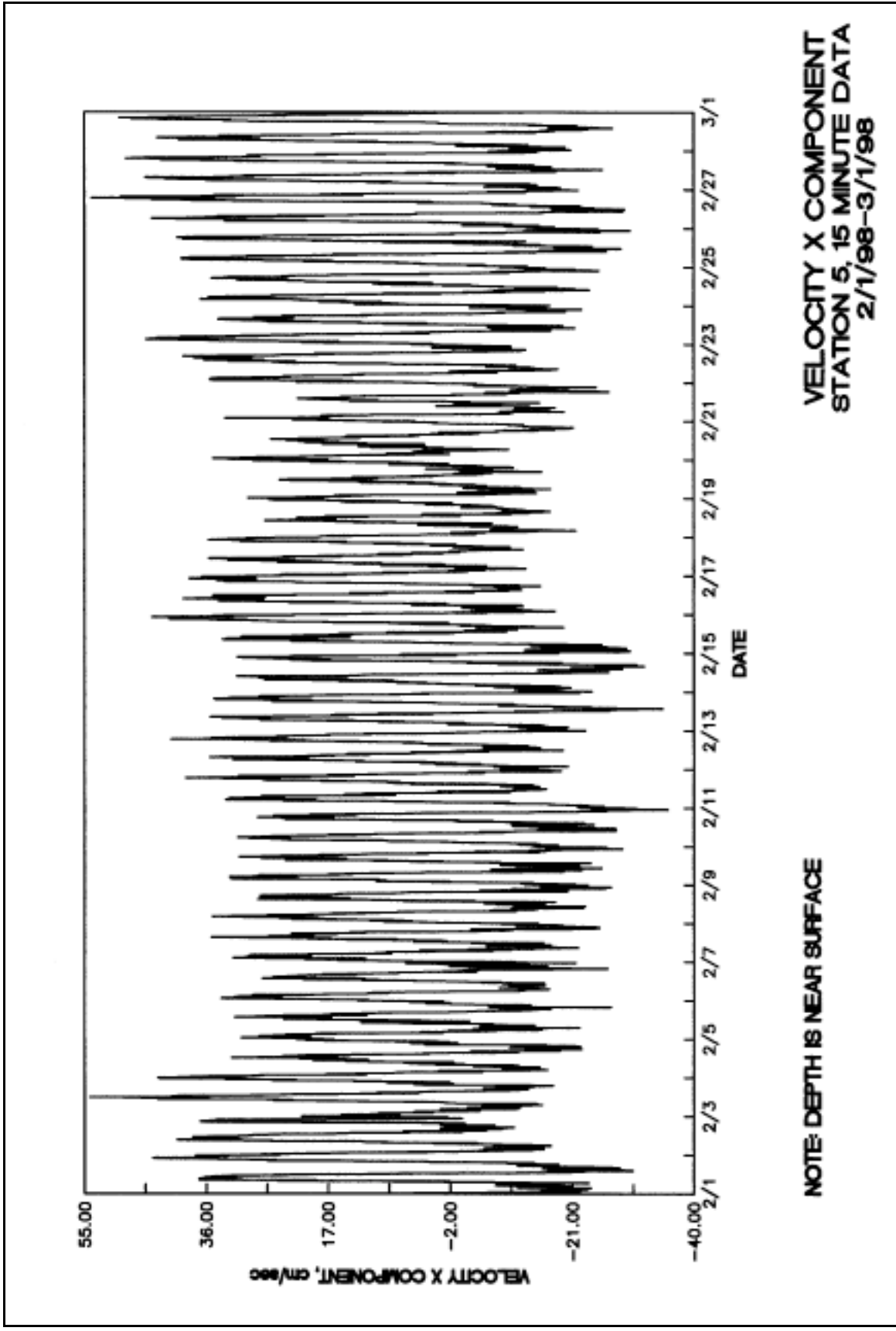


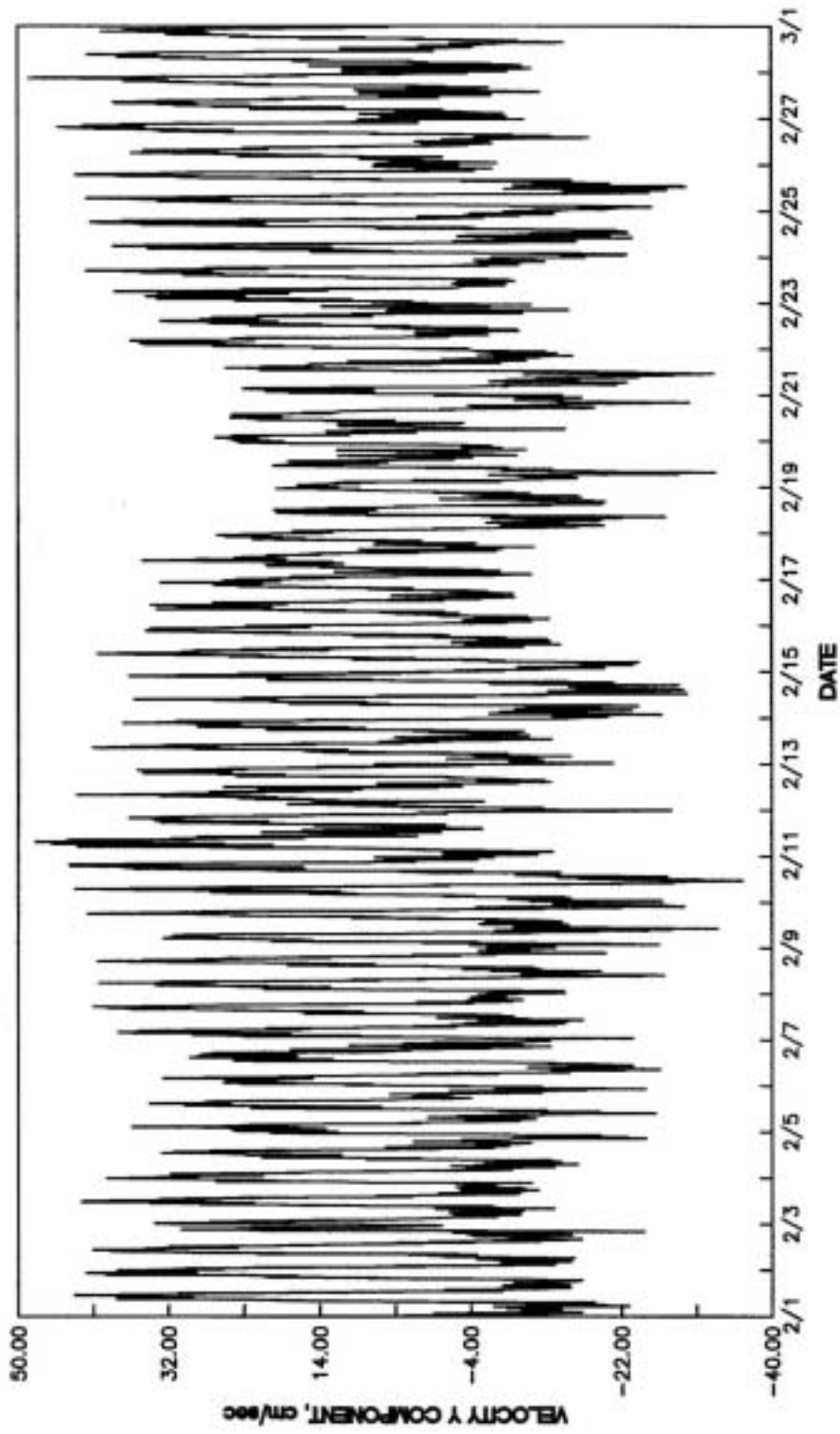
**HEAD OF WATER ABOVE INSTRUMENT
STATION 4, 15 MINUTE DATA
2/1/98-3/1/98**





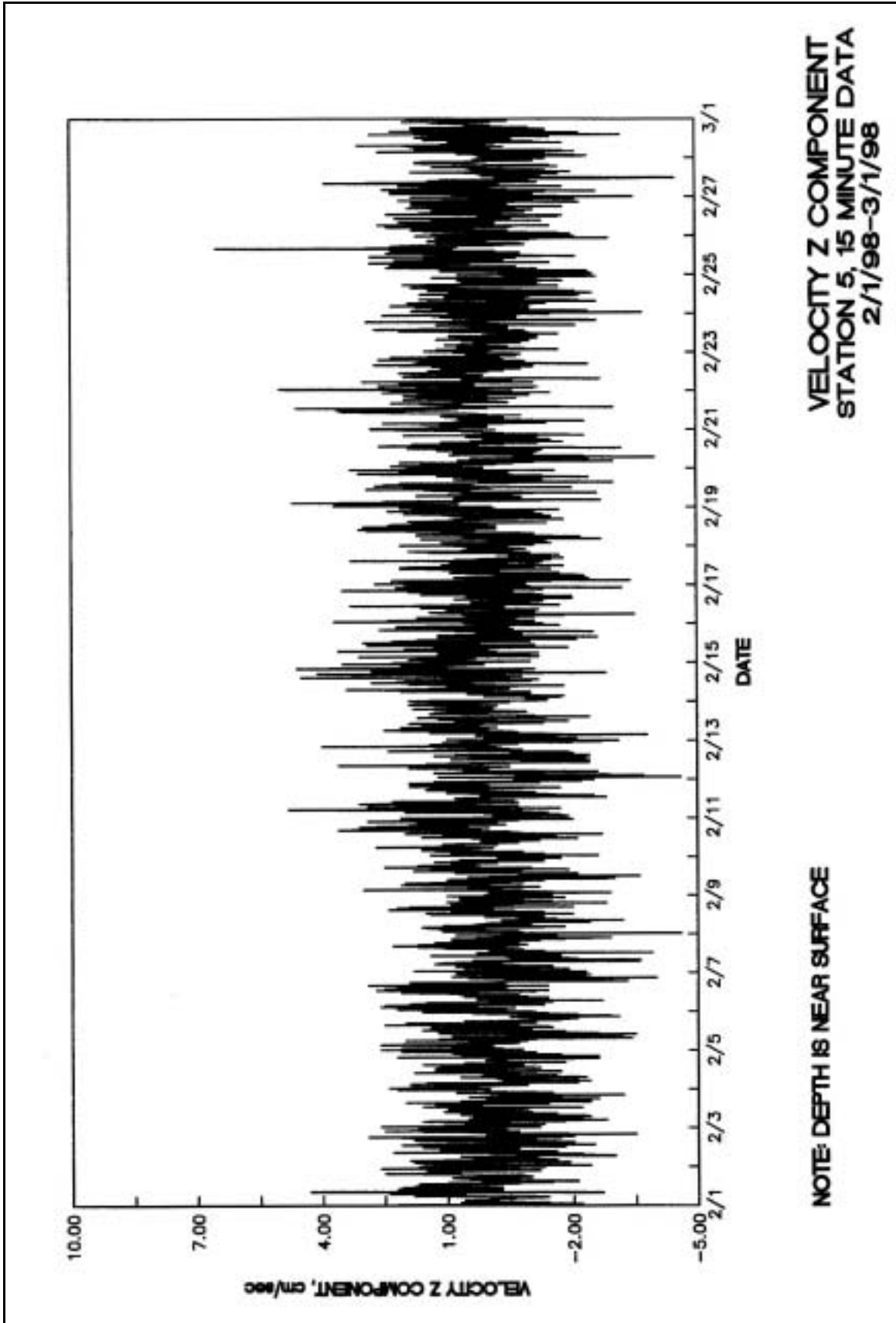


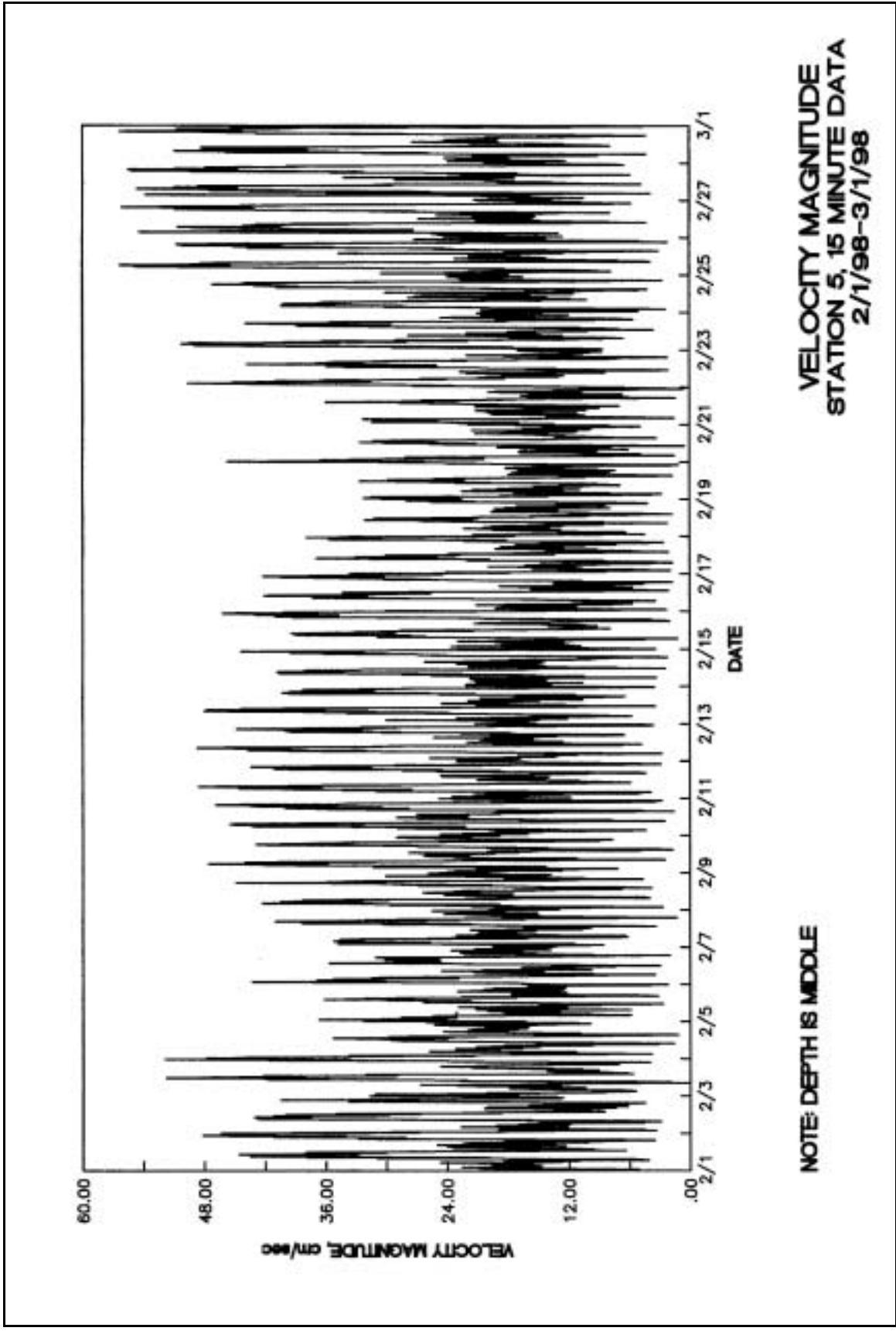


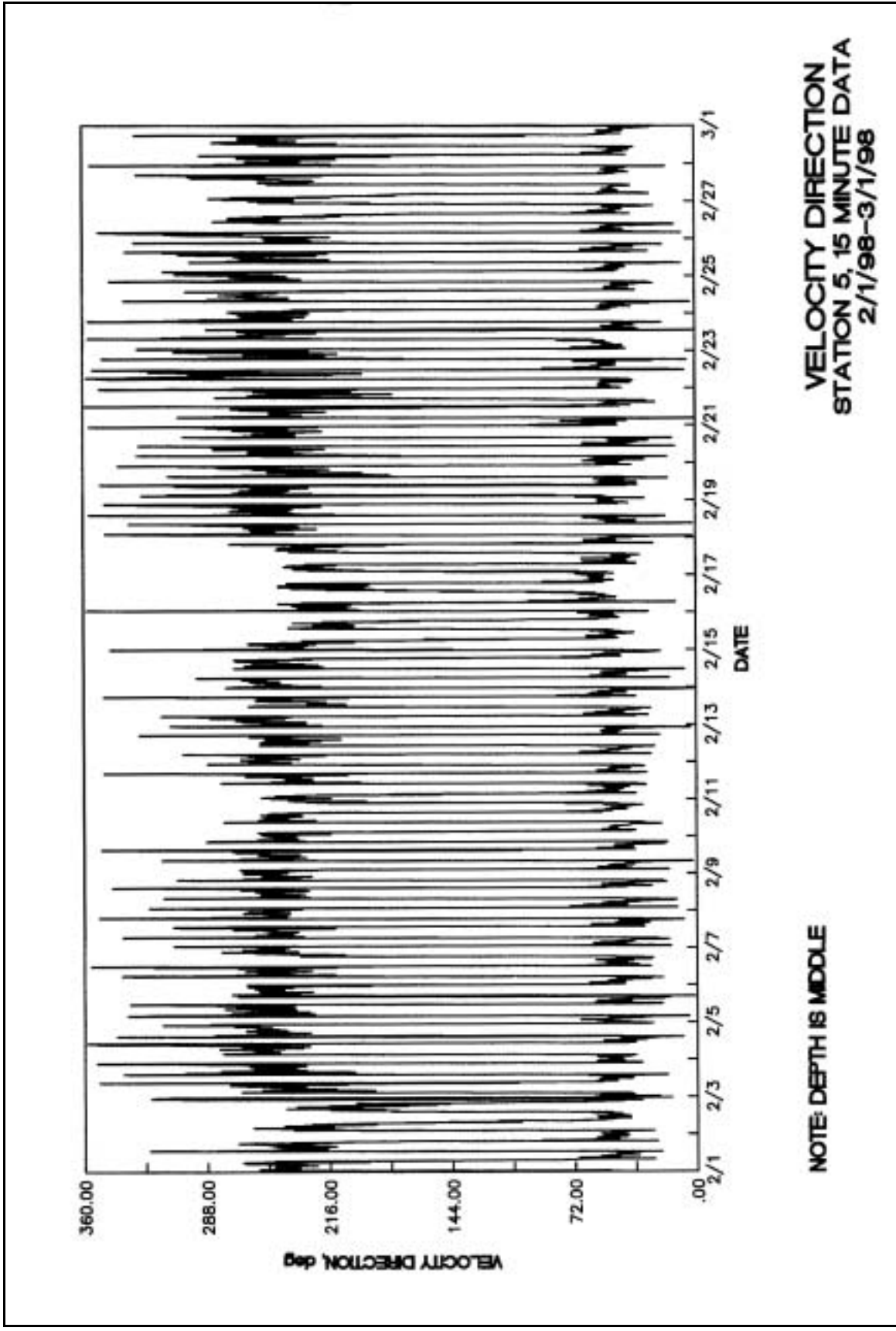


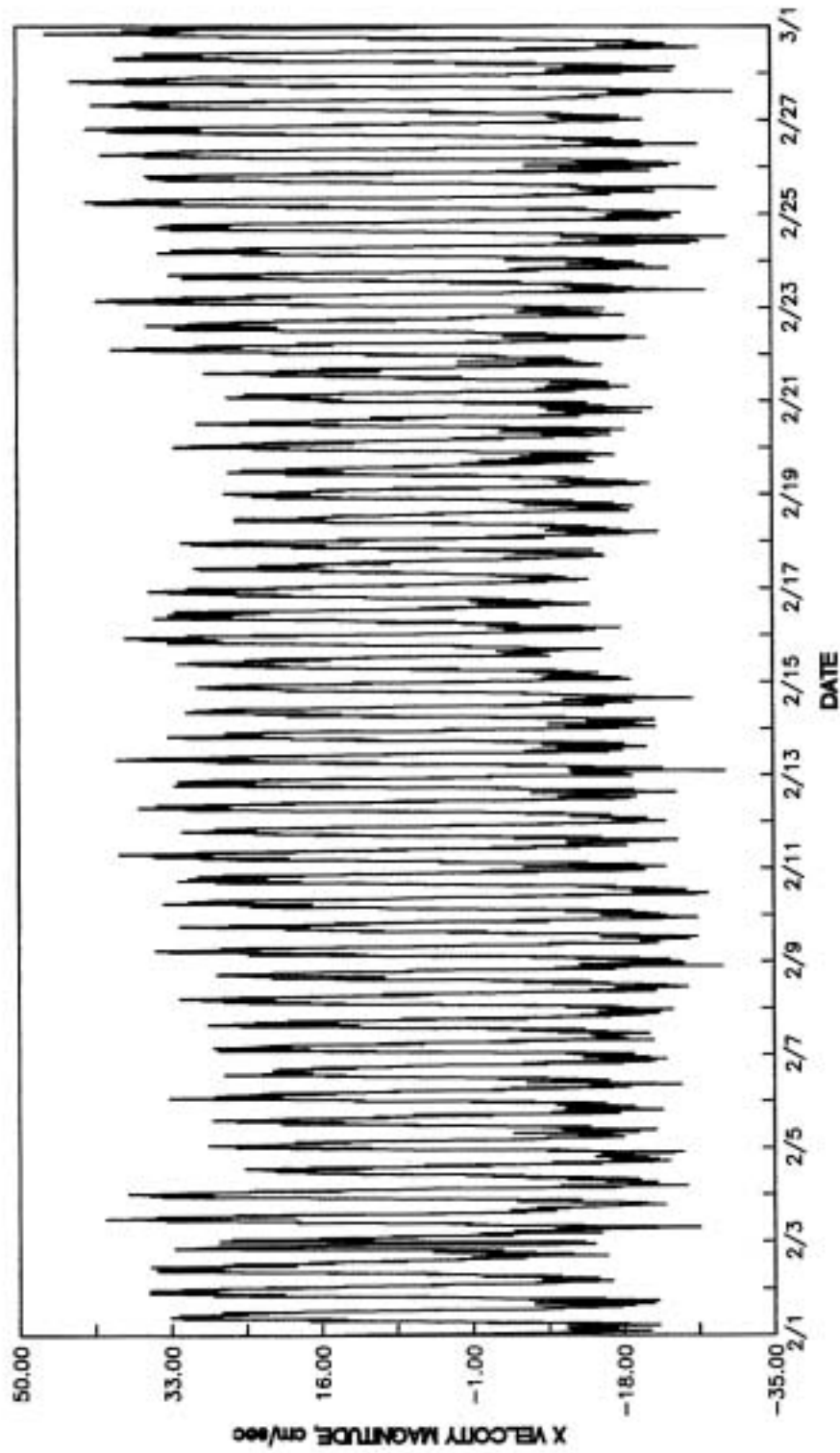
**VELOCITY Y COMPONENT
STATION 5, 15 MINUTE DATA
2/1/98-3/1/98**

NOTE: DEPTH IS NEAR SURFACE



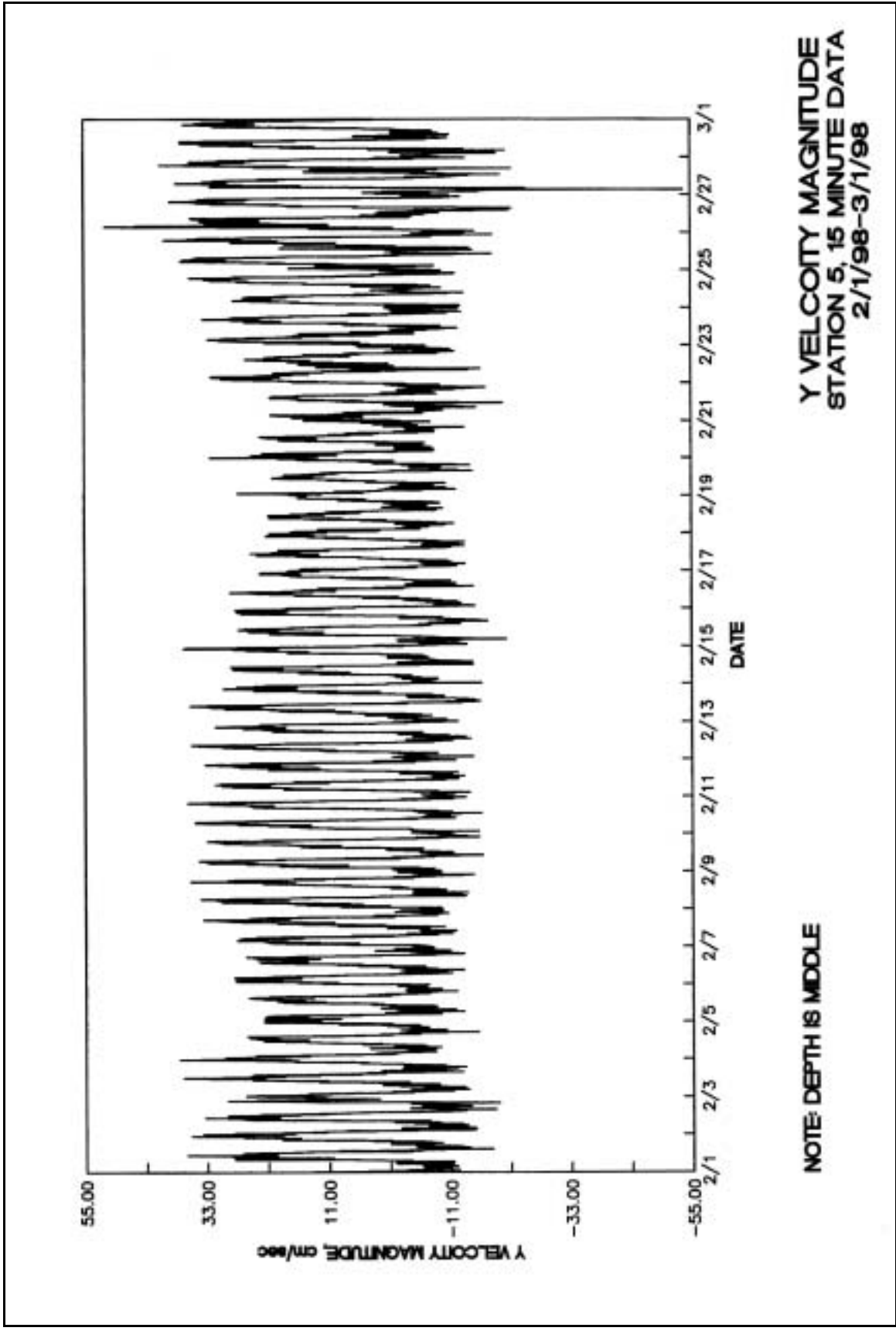


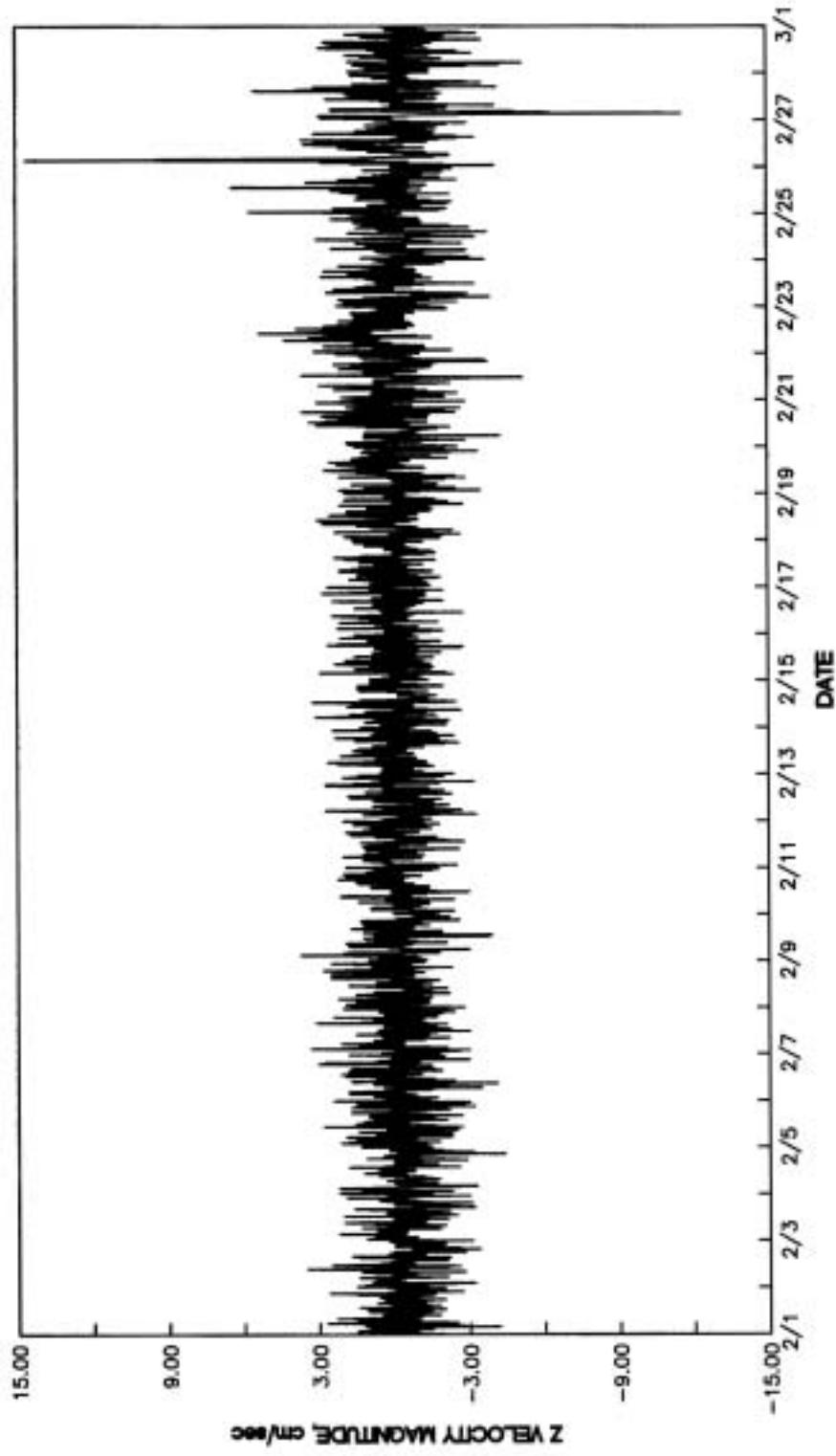




**X VELOCITY MAGNITUDE
STATION 5, 15 MINUTE DATA
2/1/98-3/1/98**

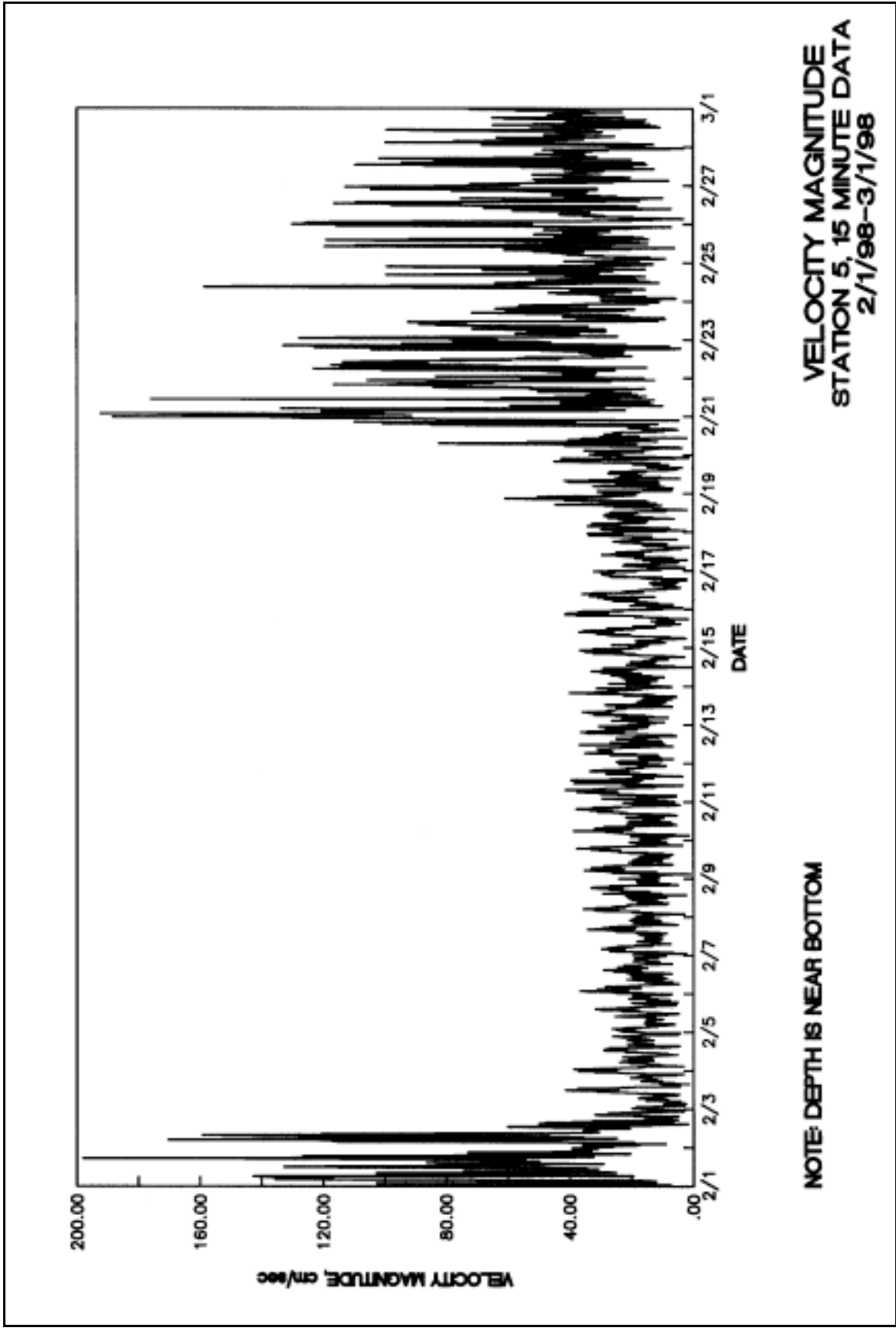
NOTE: DEPTH IS MIDDLE

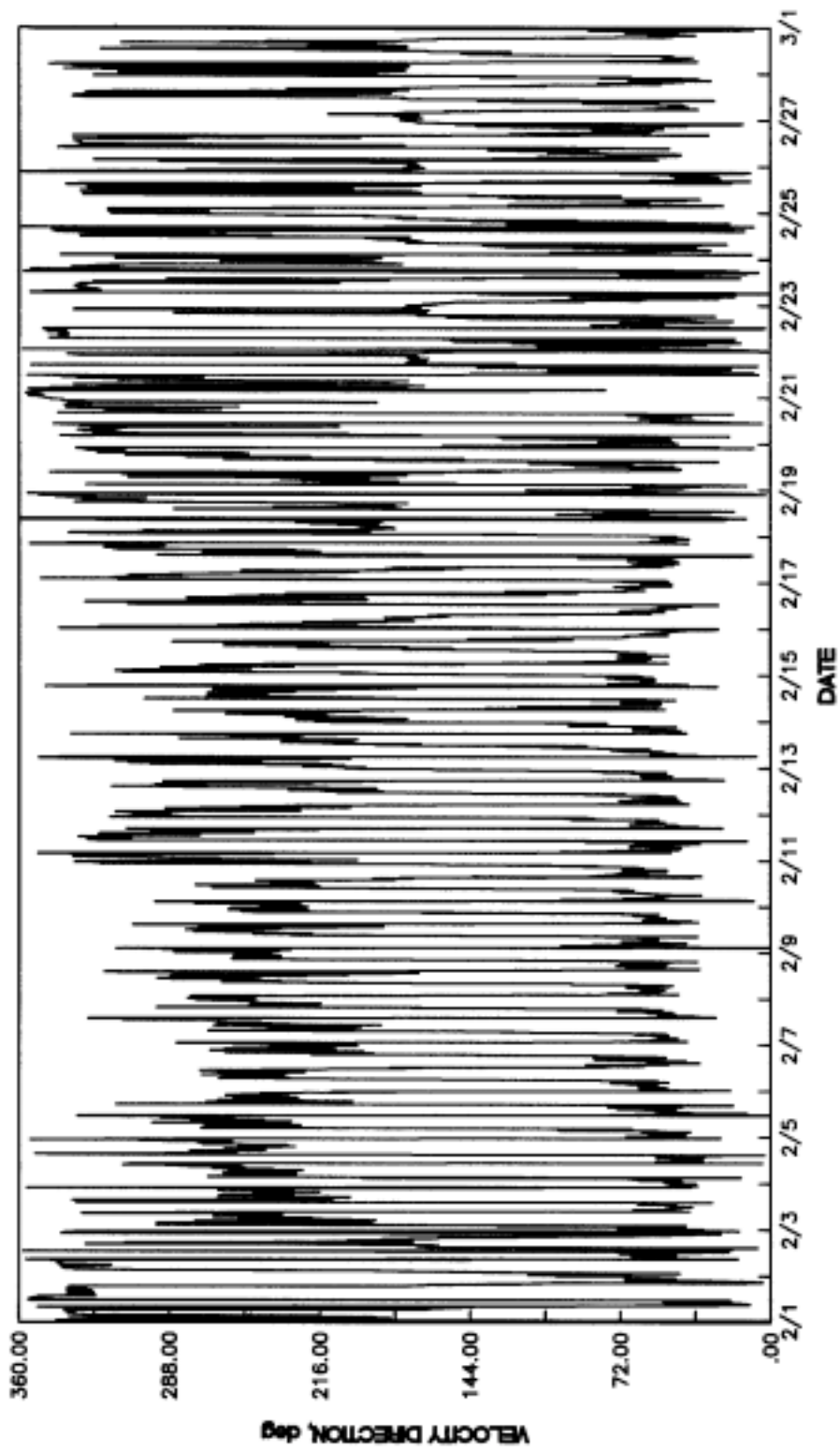




**Z VELOCITY MAGNITUDE
STATION 5, 15 MINUTE DATA
2/1/98-3/1/98**

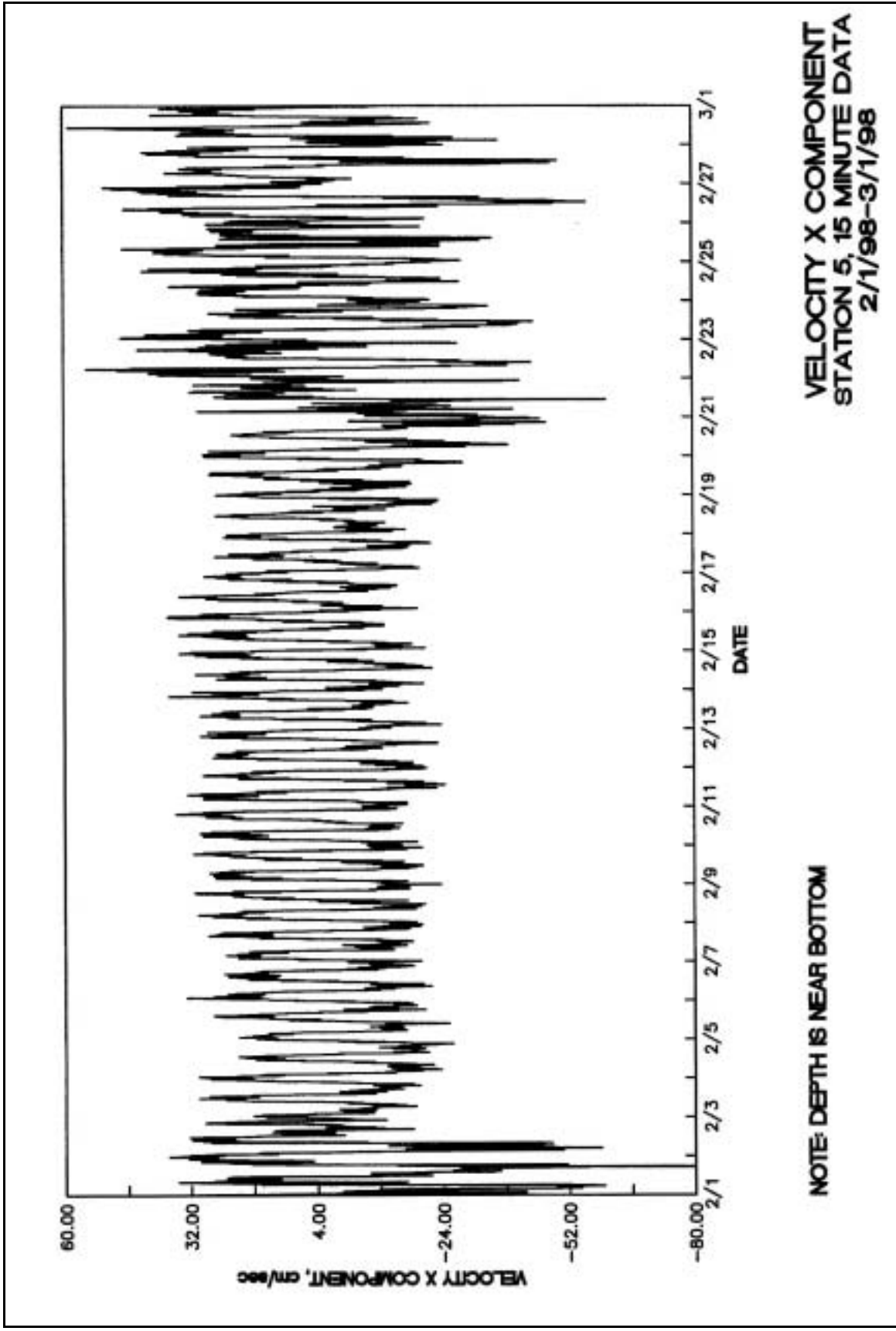
NOTE: DEPTH IS MIDDLE

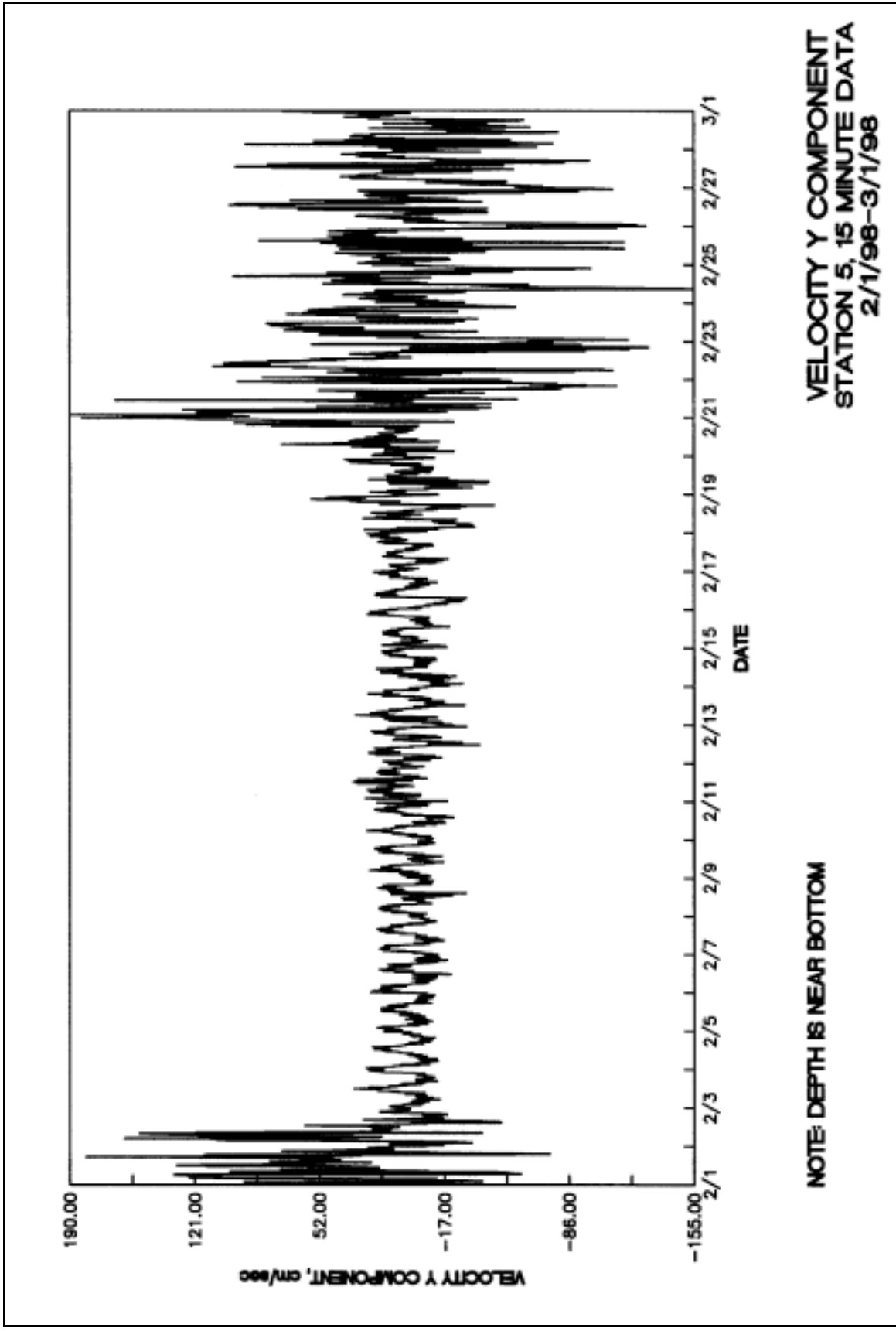


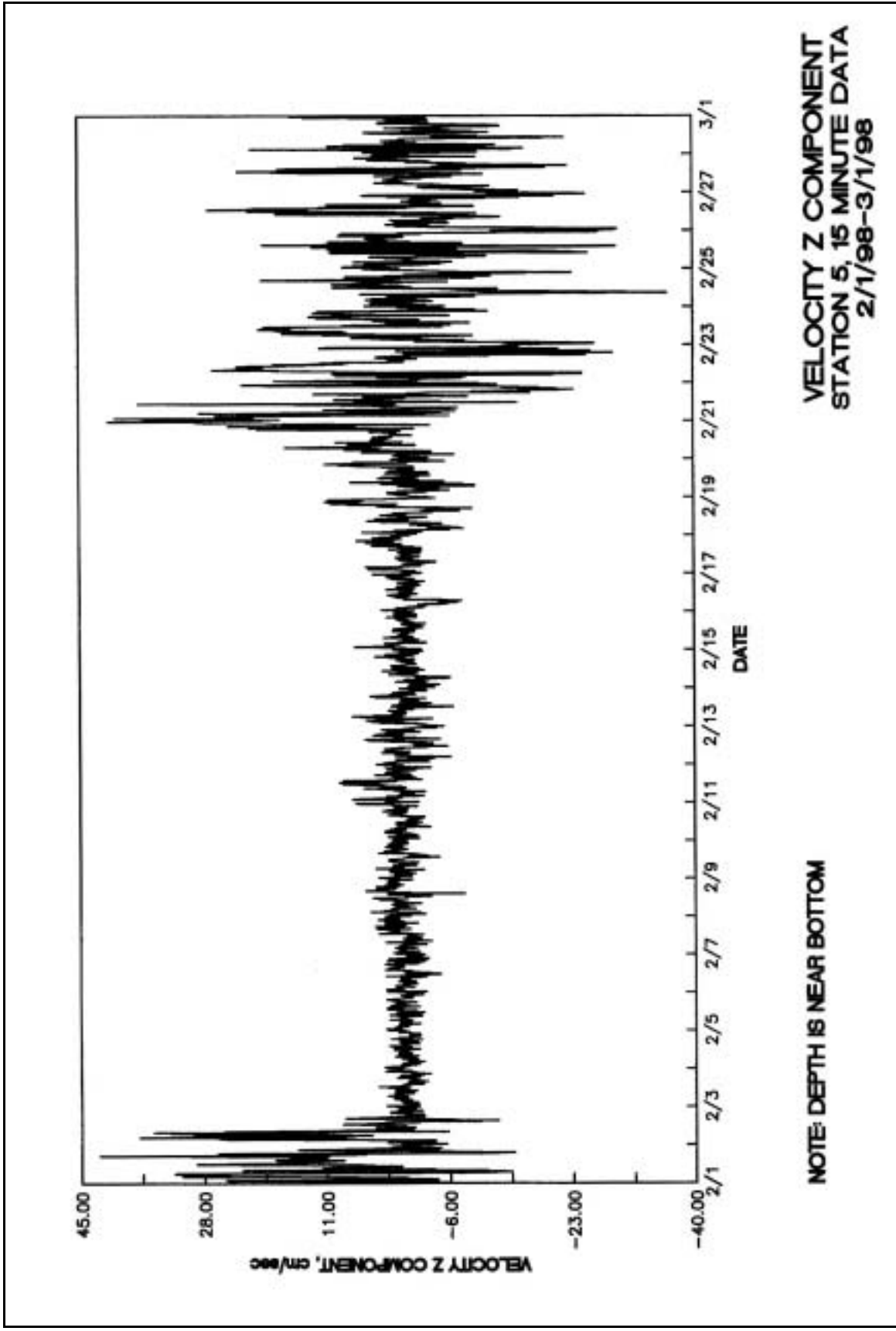


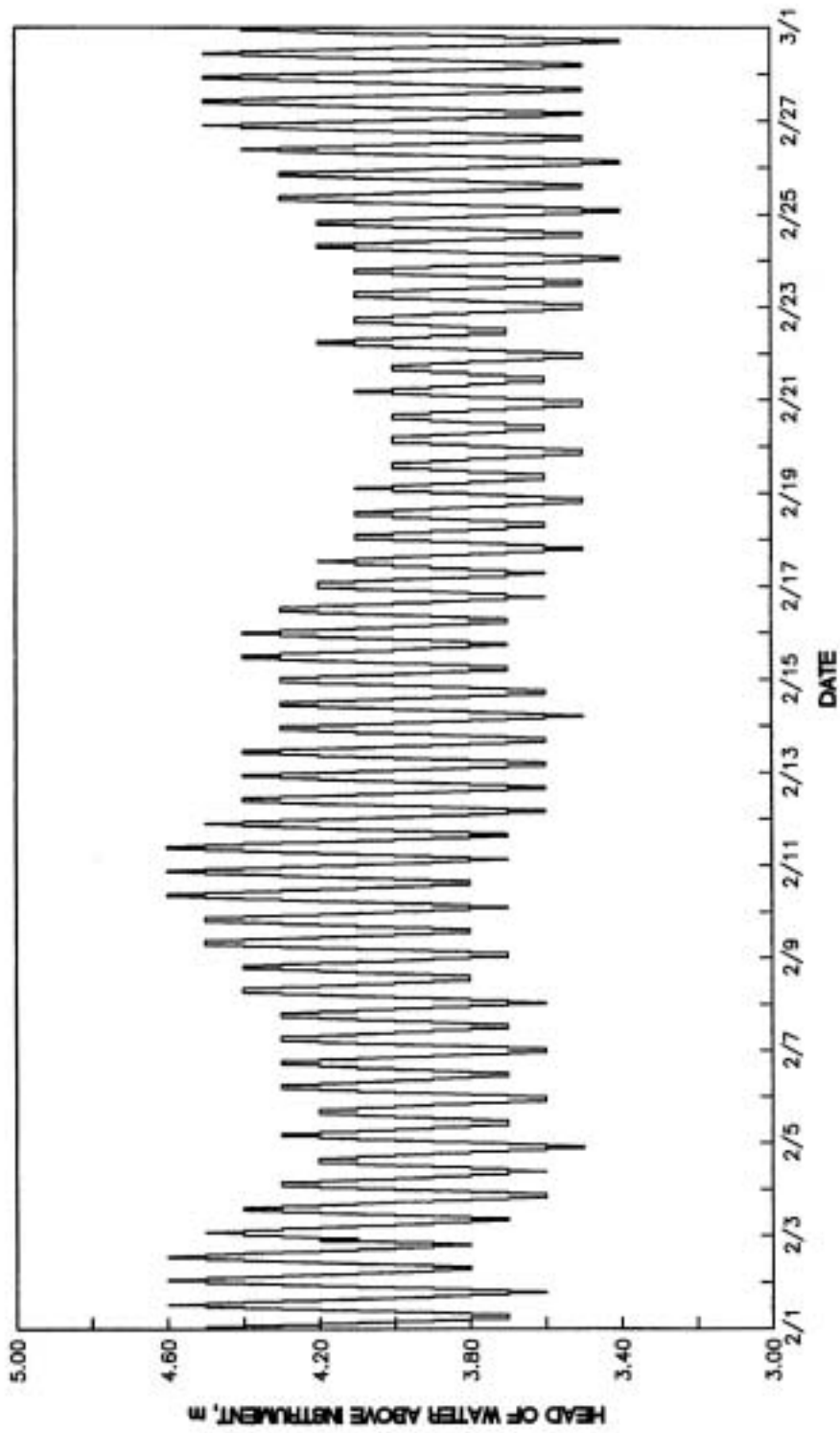
**VELOCITY DIRECTION
STATION 5, 15 MINUTE DATA
2/1/98-3/1/98**

NOTE: DEPTH IS NEAR BOTTOM

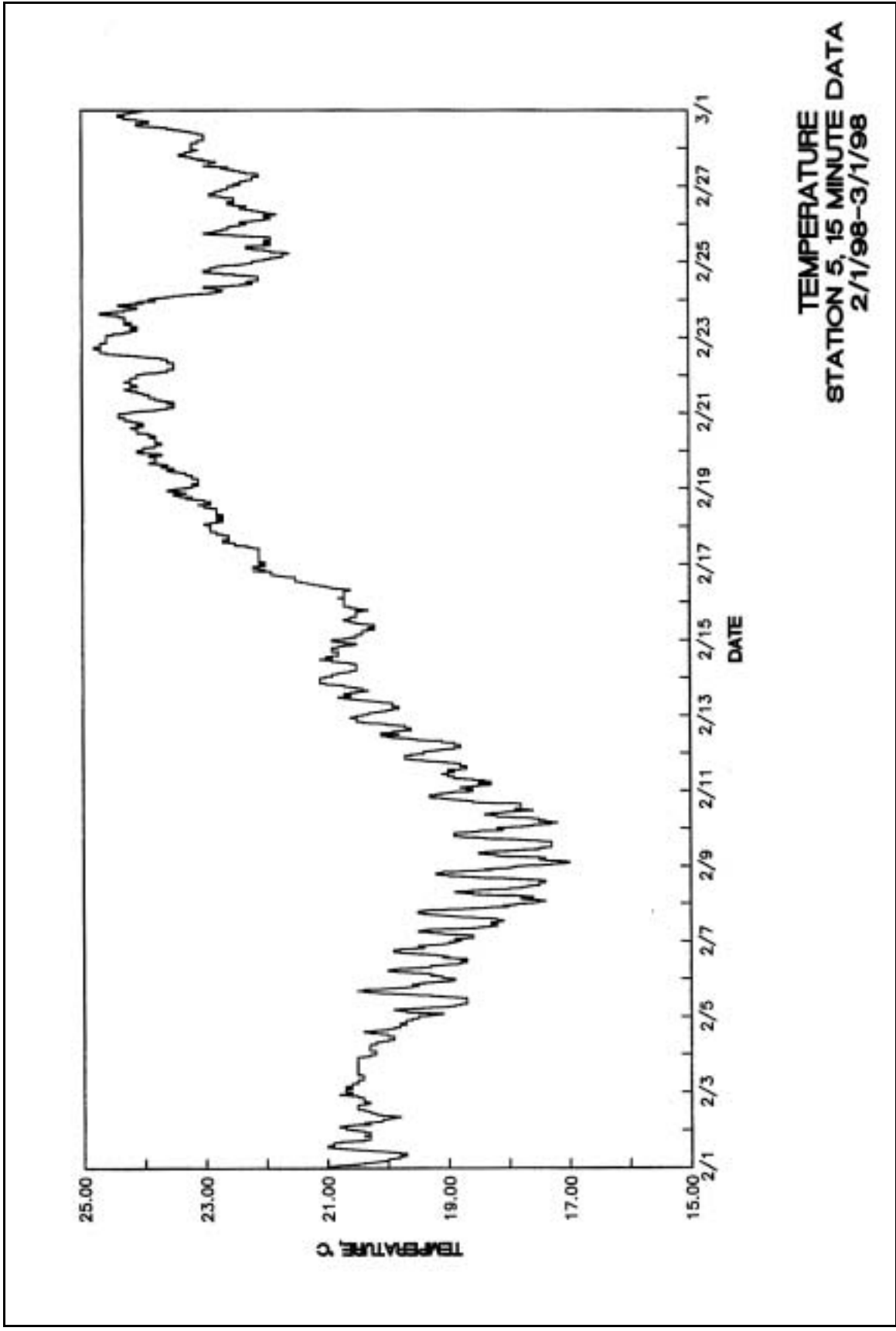


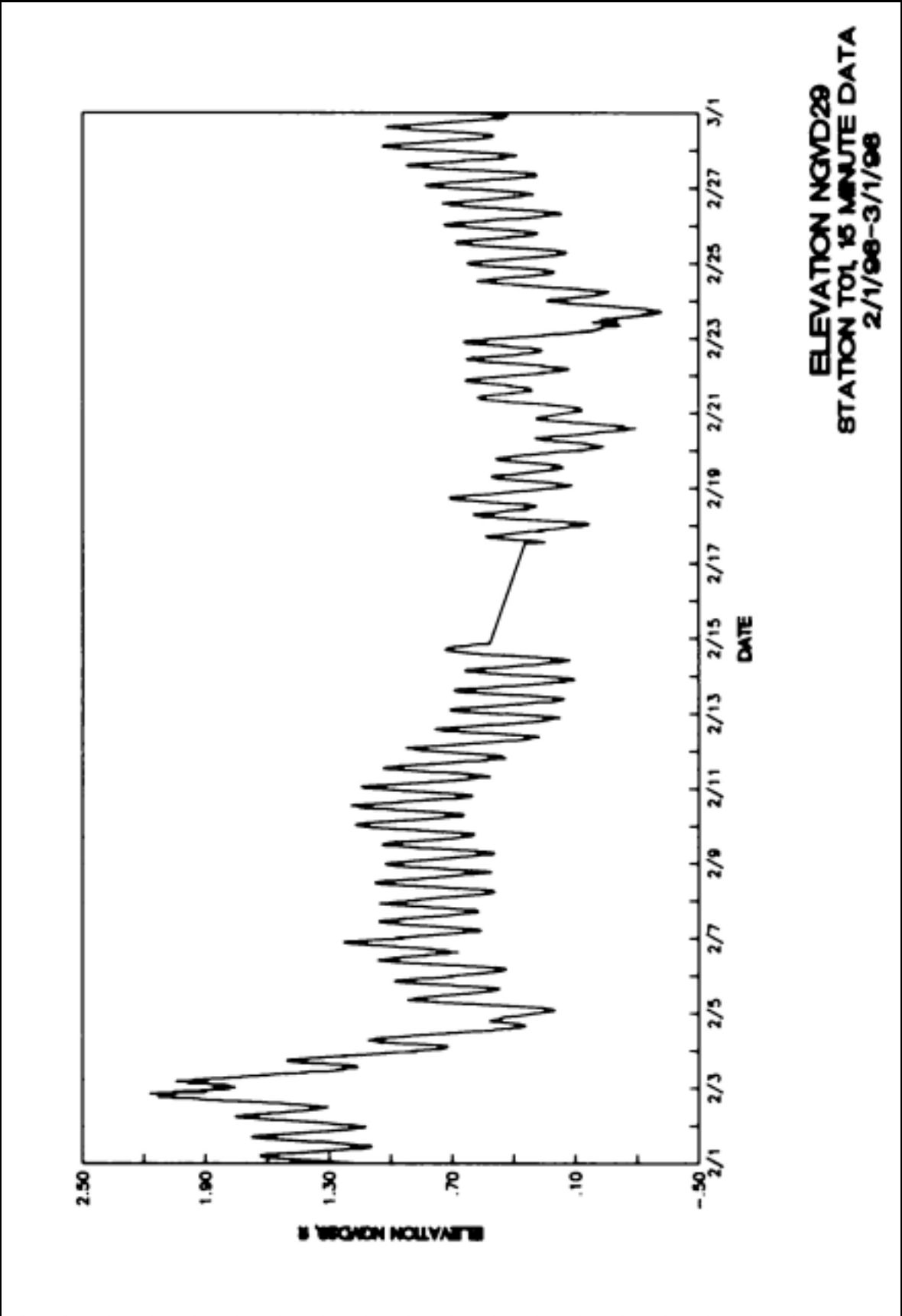


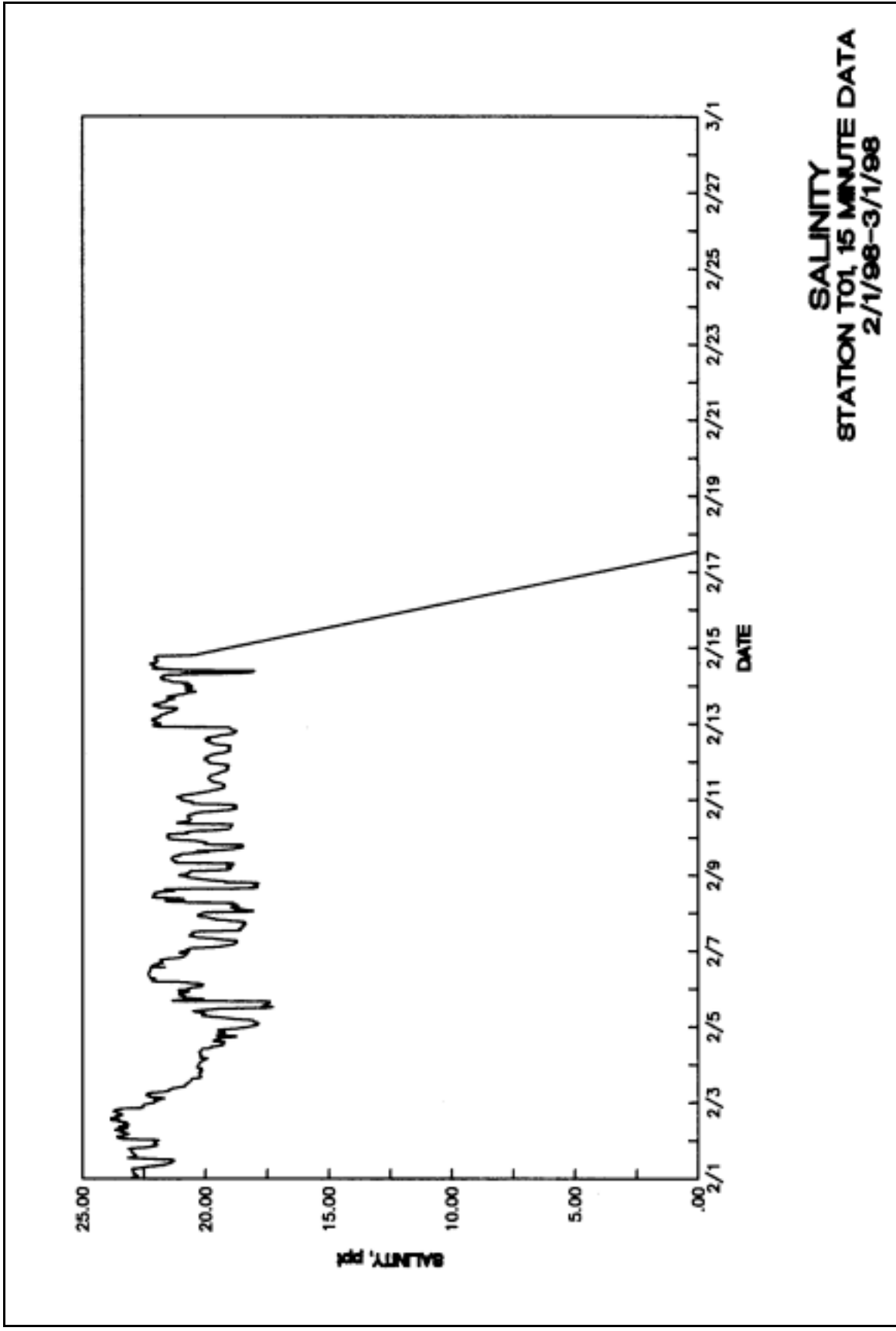


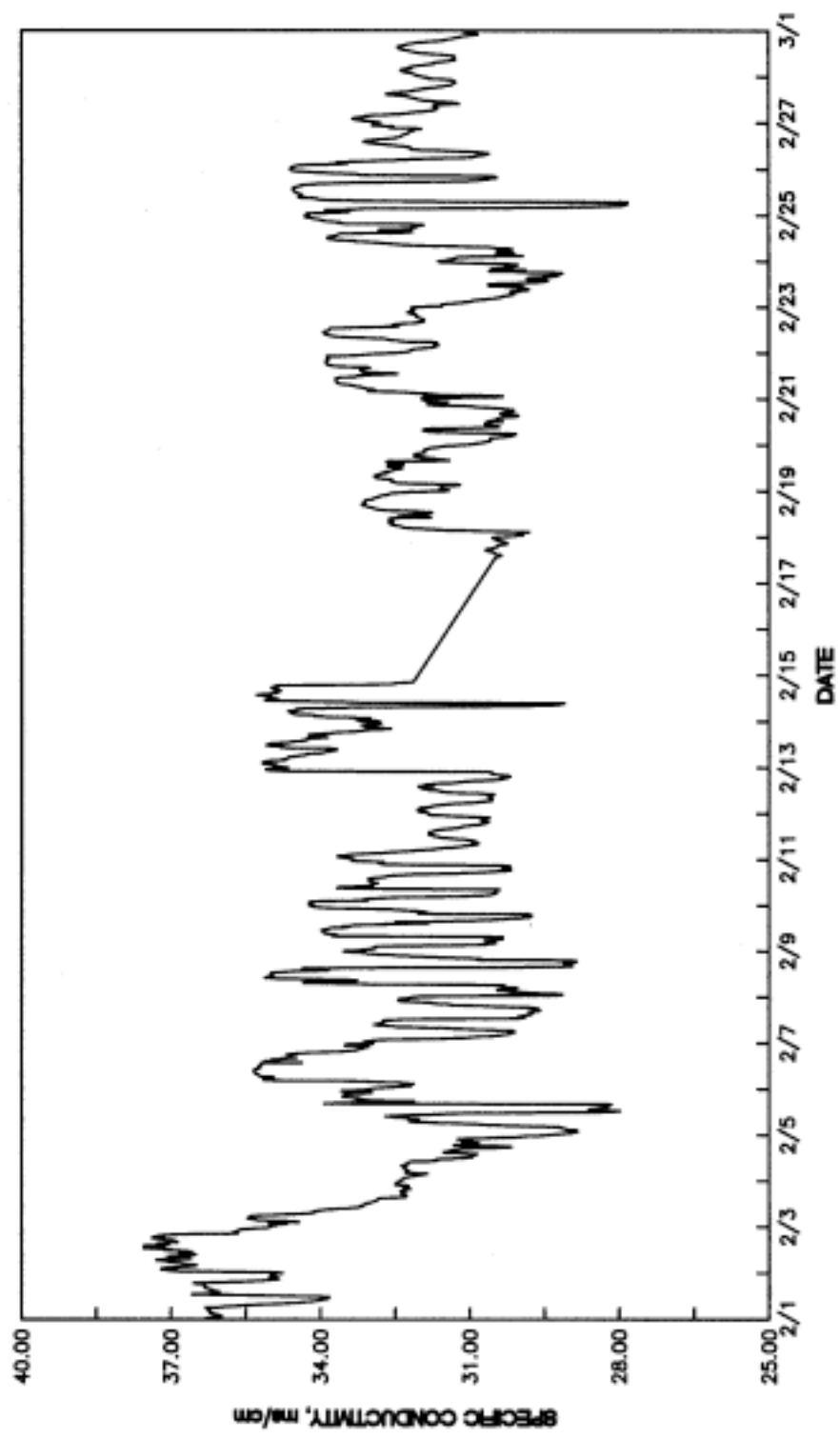


**HEAD OF WATER ABOVE INSTRUMENT
STATION 5, 15 MINUTE DATA
2/1/98-3/1/98**

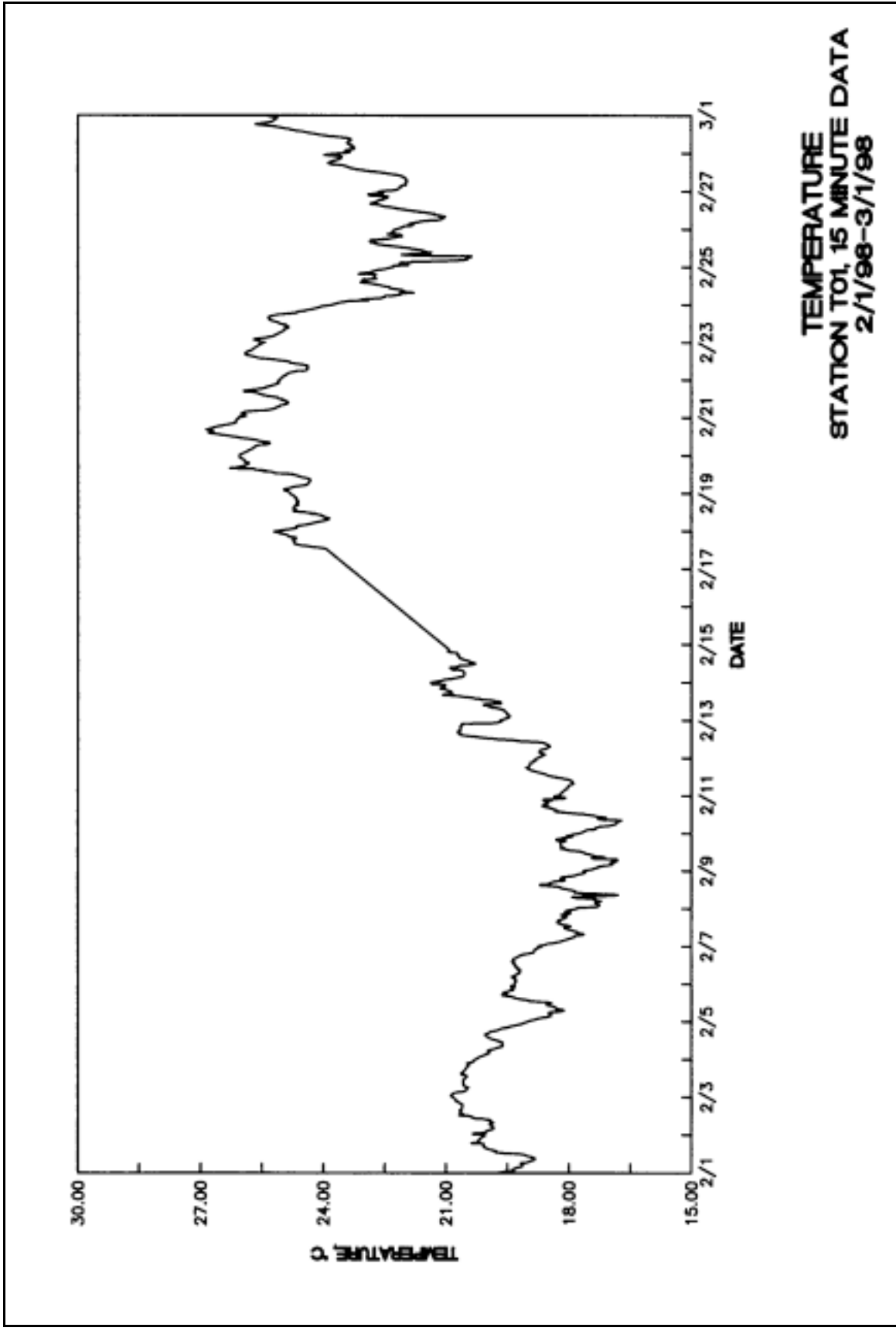


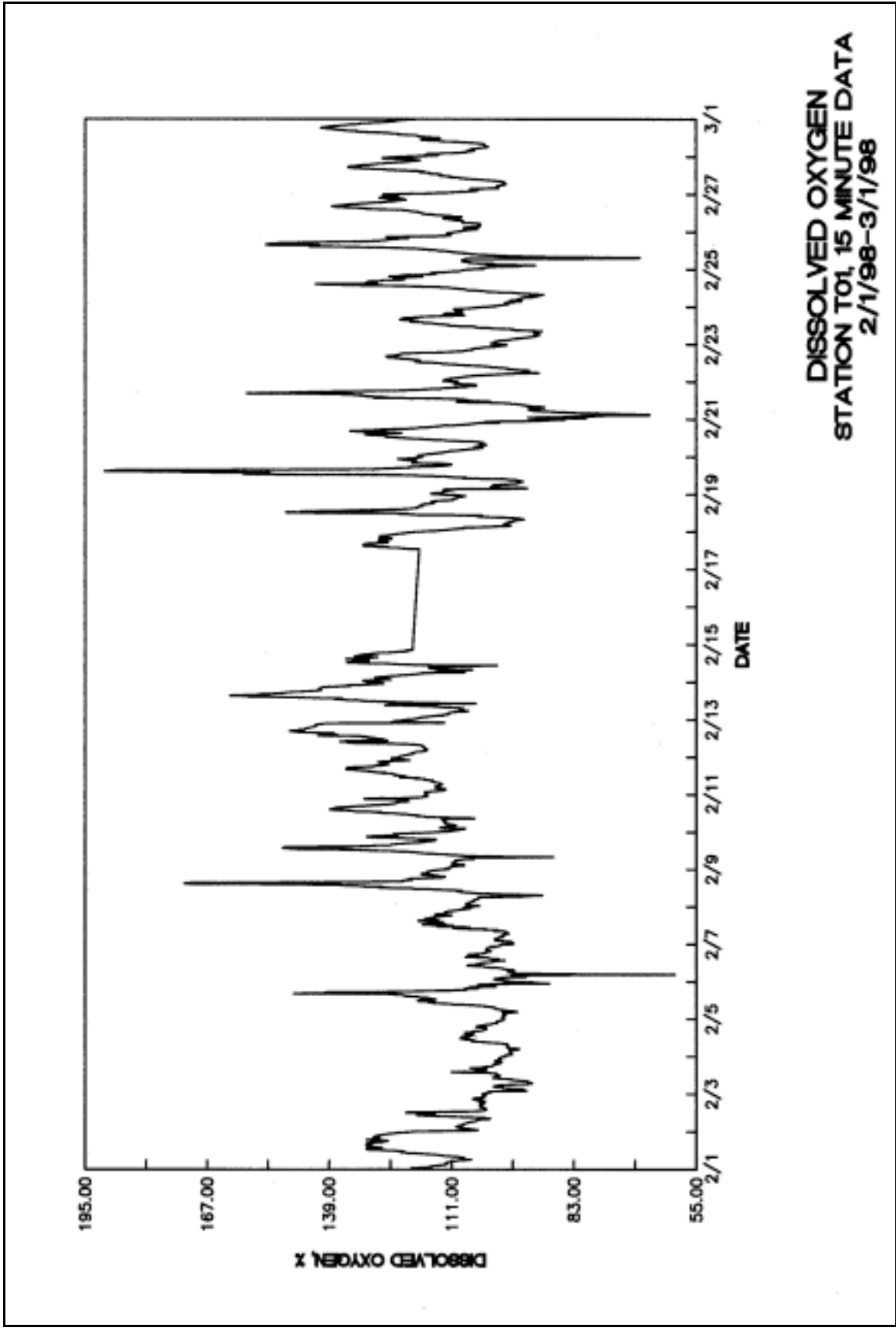


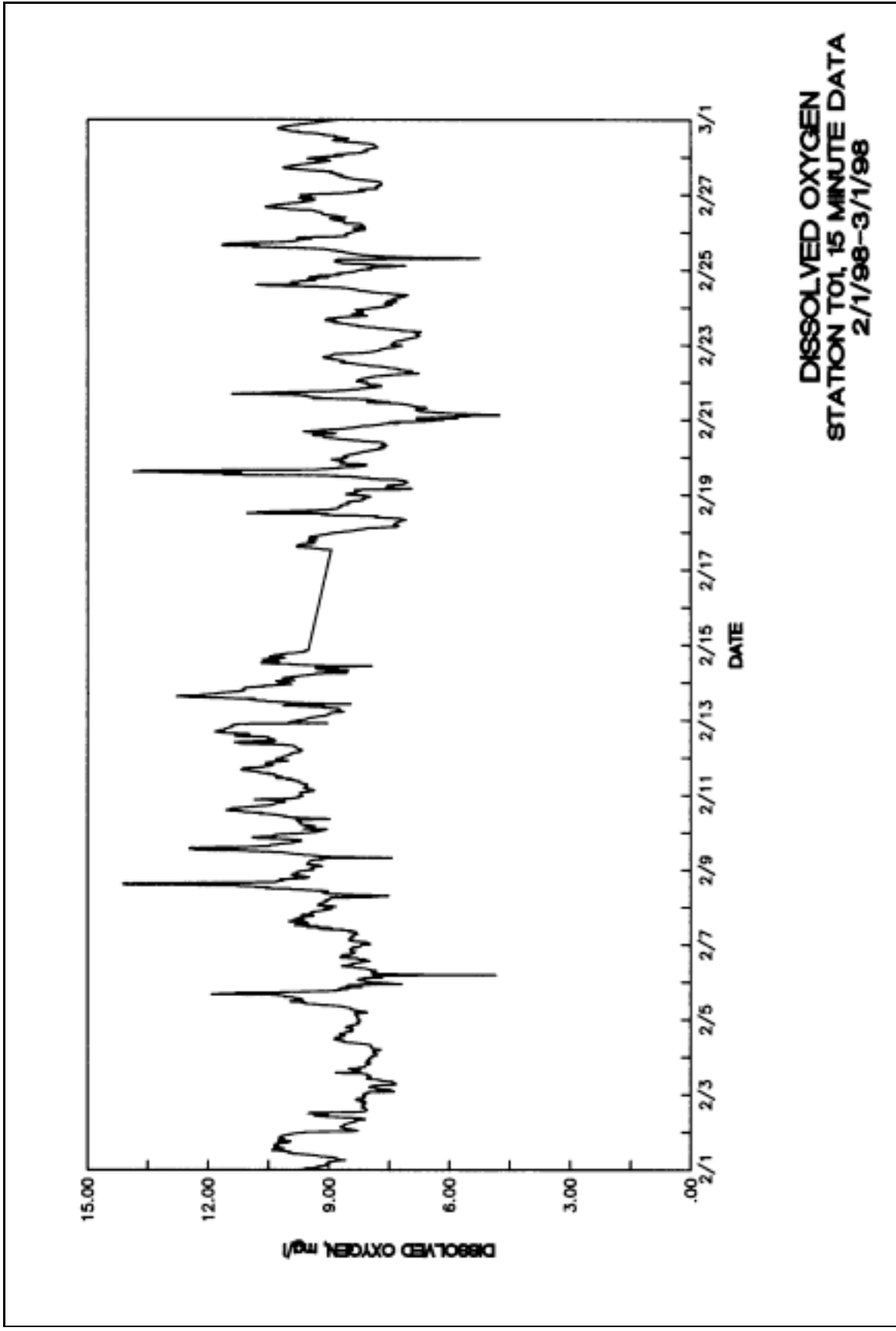


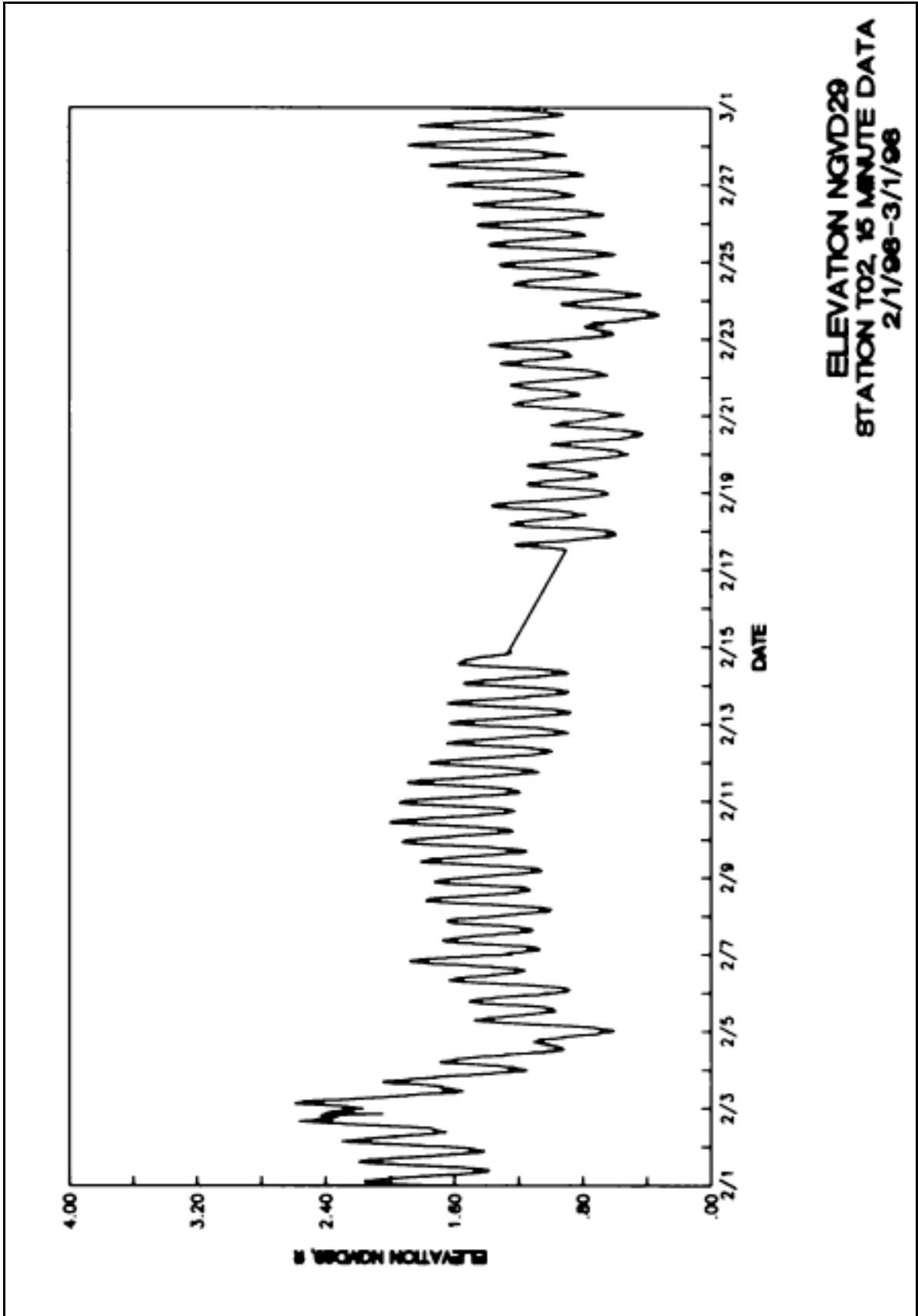


**SPECIFIC CONDUCTIVITY
STATION T01, 15 MINUTE DATA
2/1/98-3/1/98**









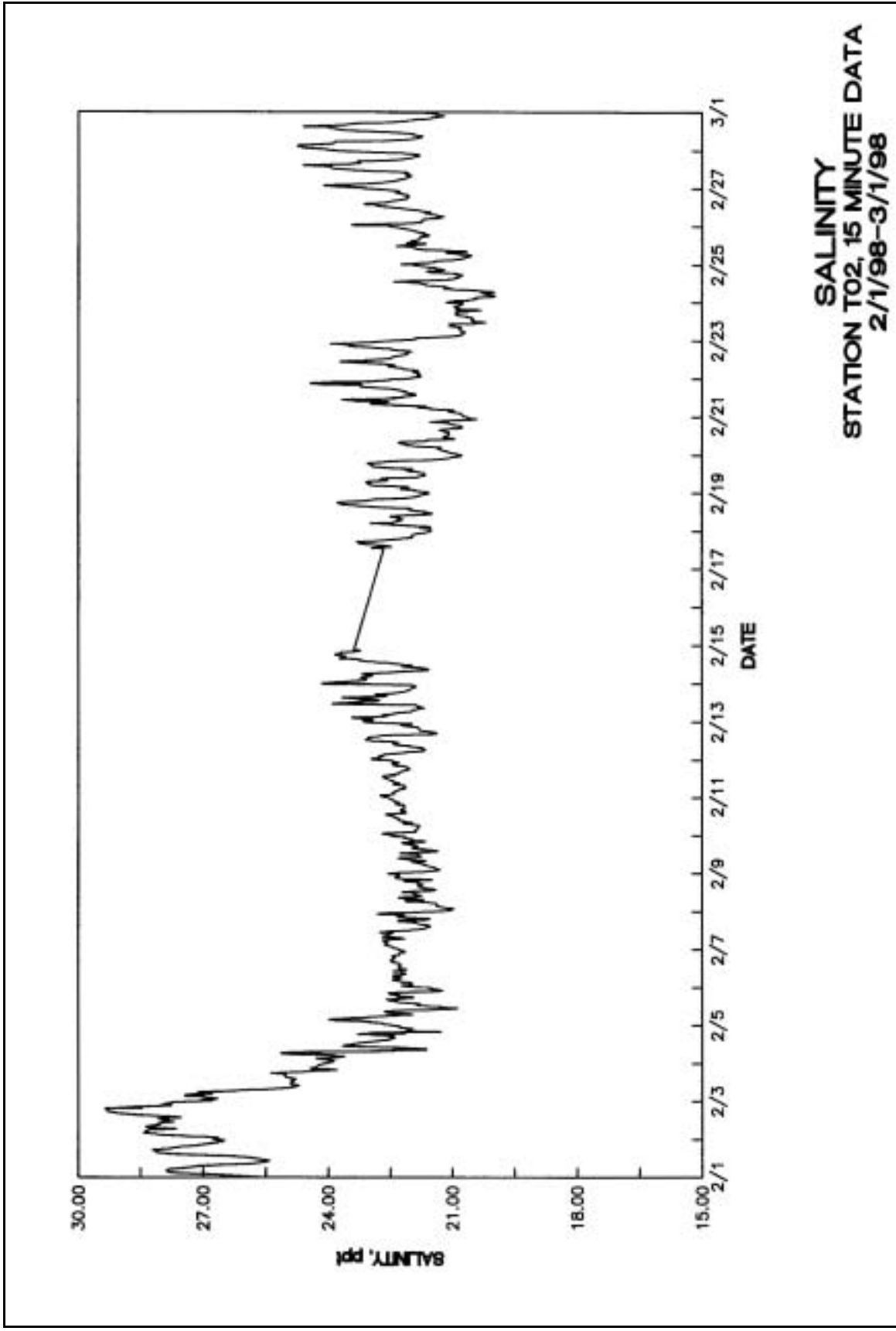
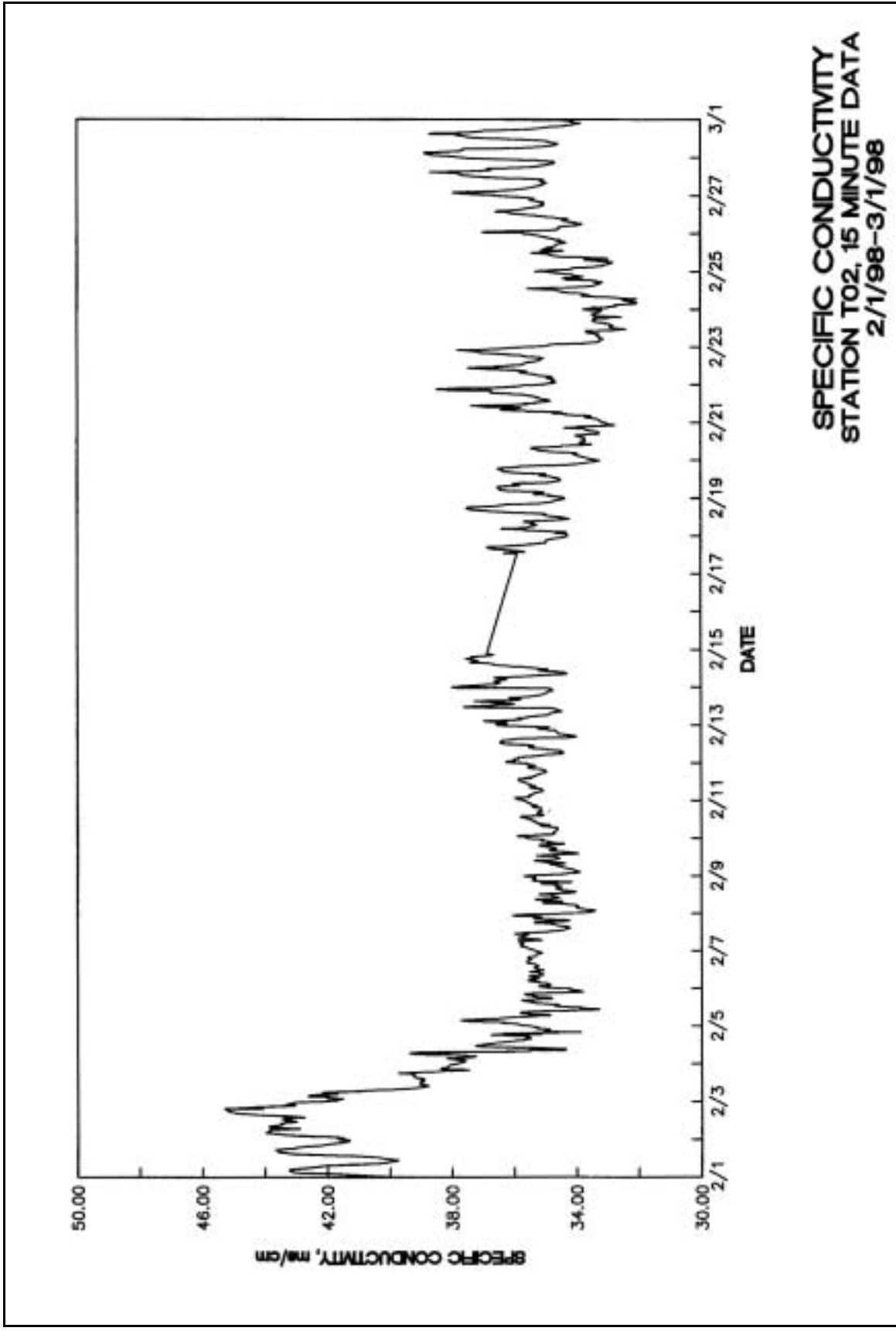
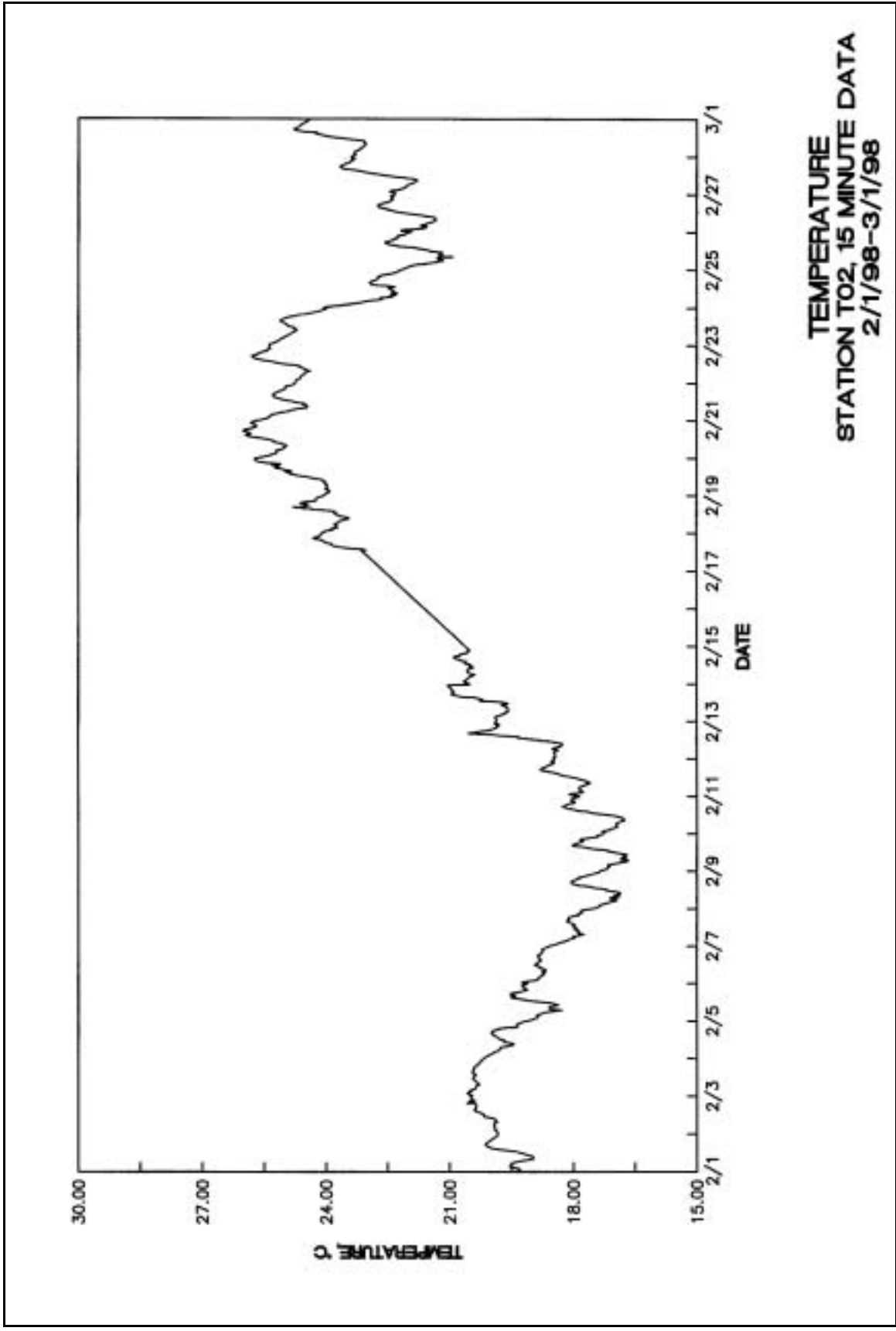
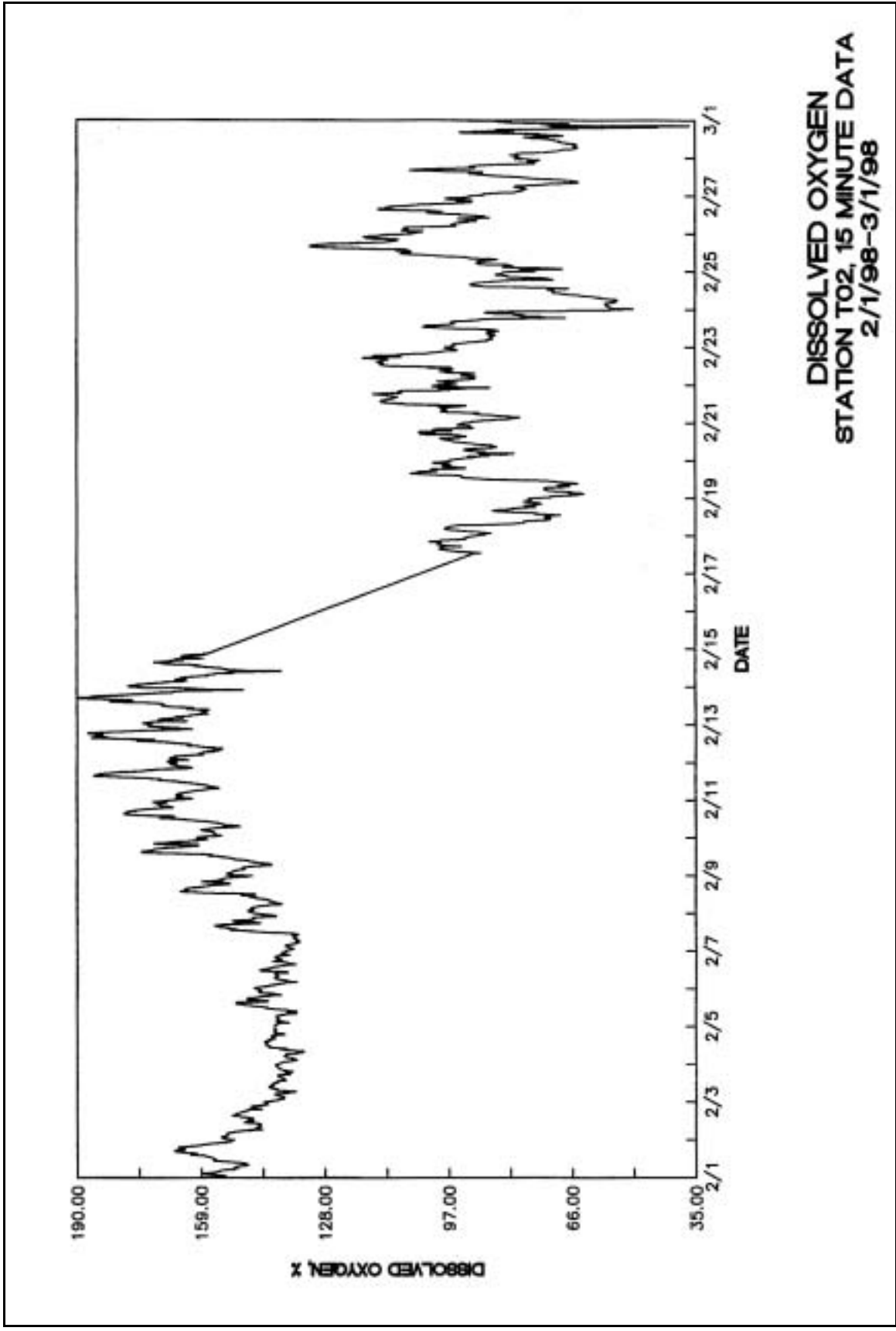


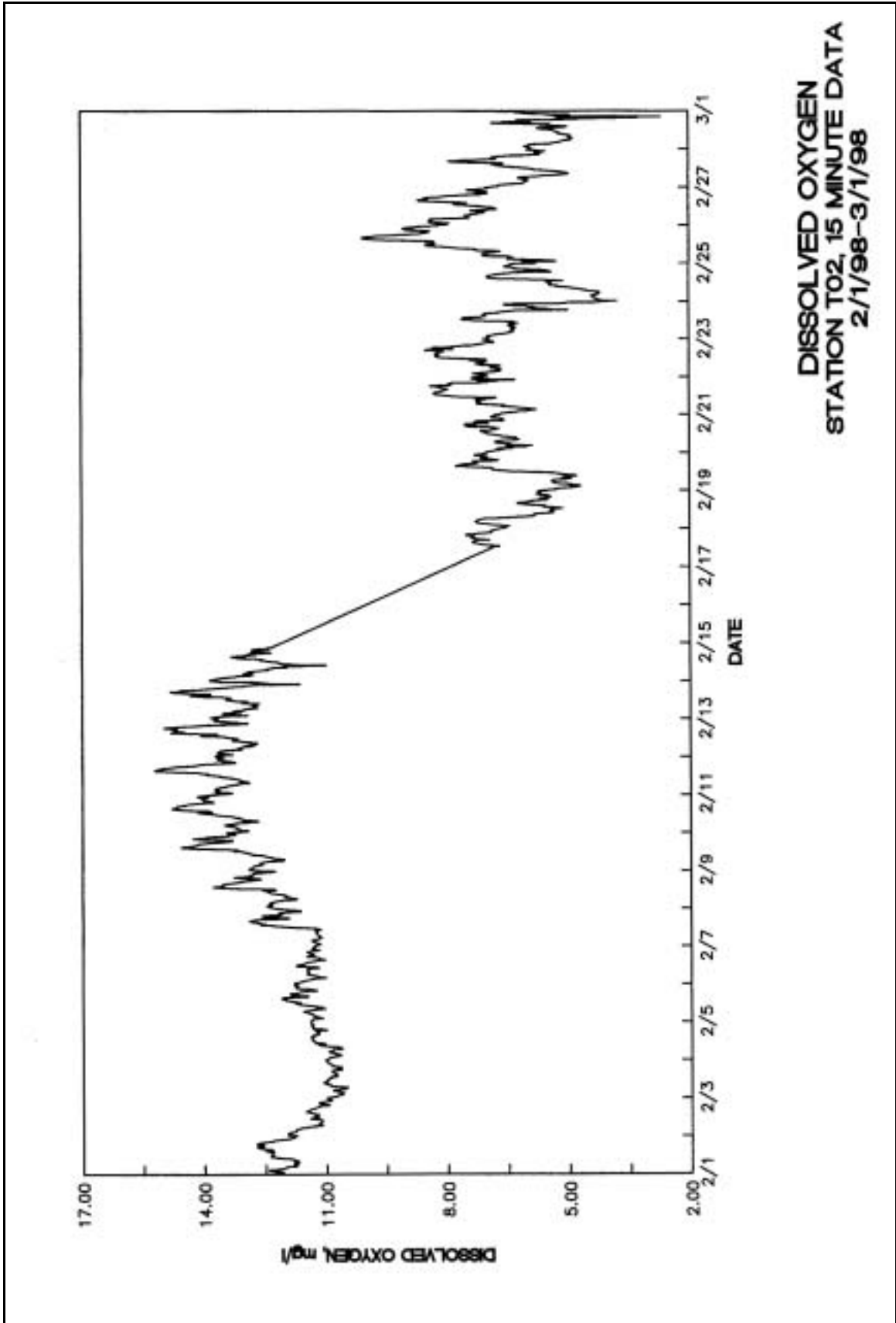
Plate 104

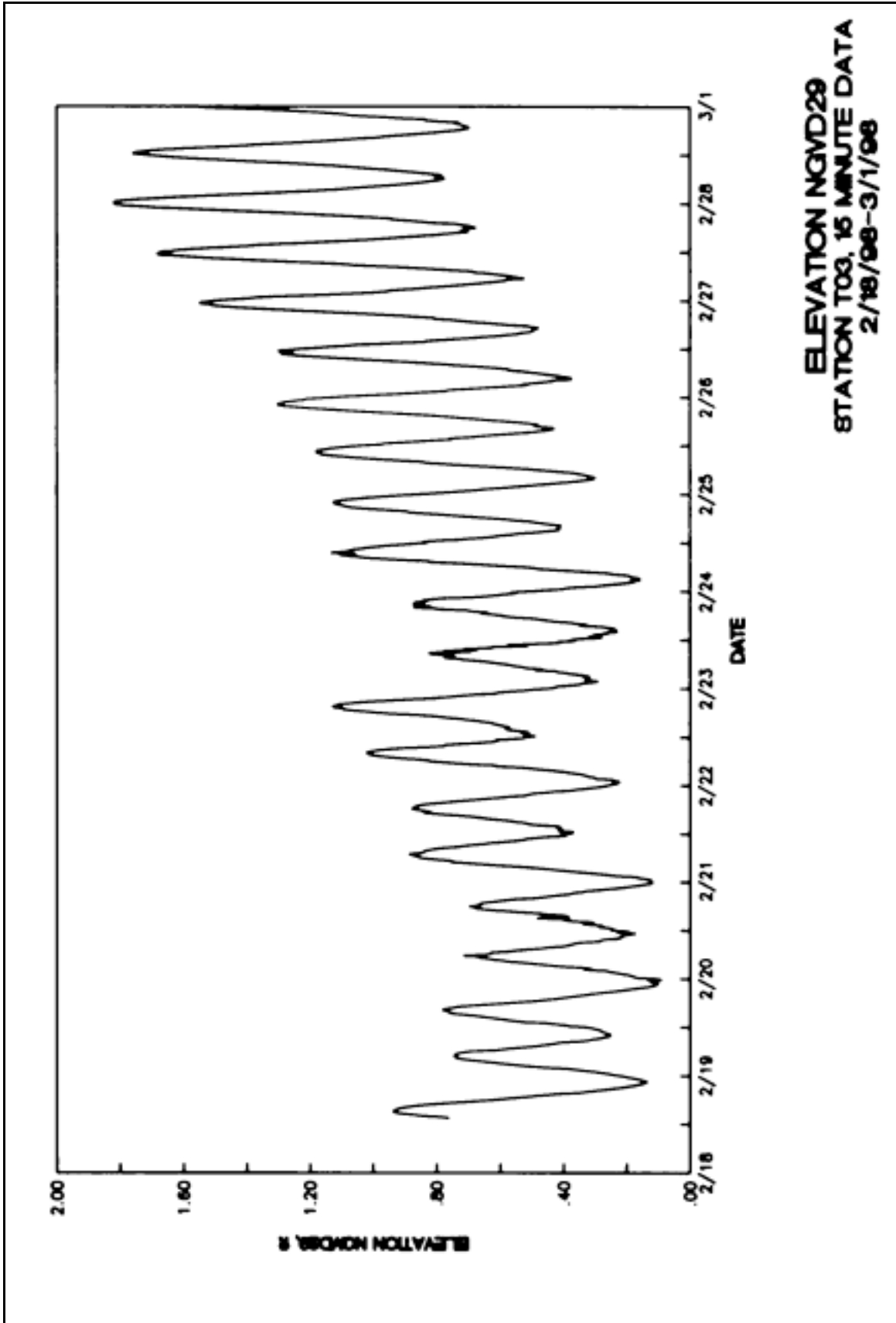


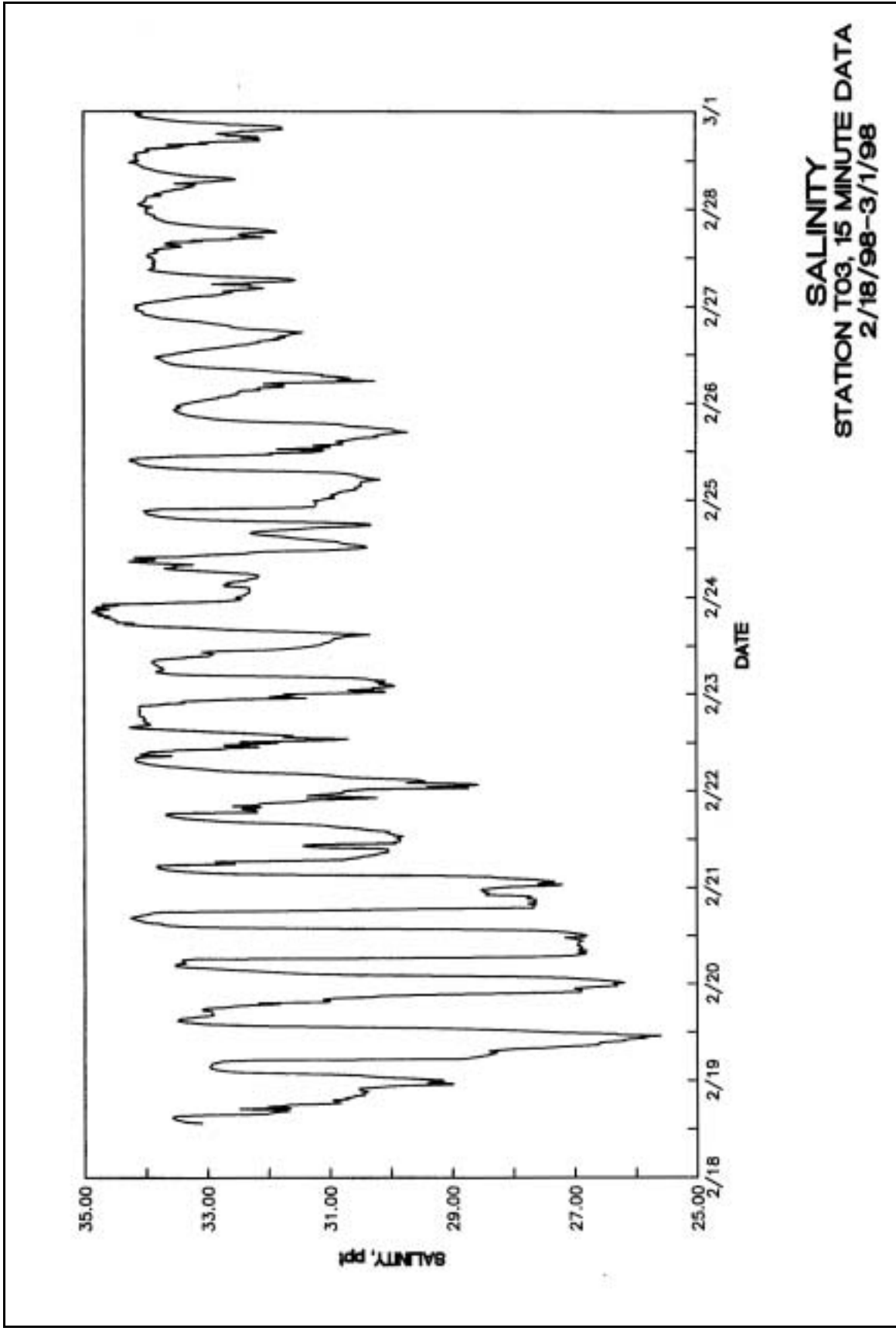


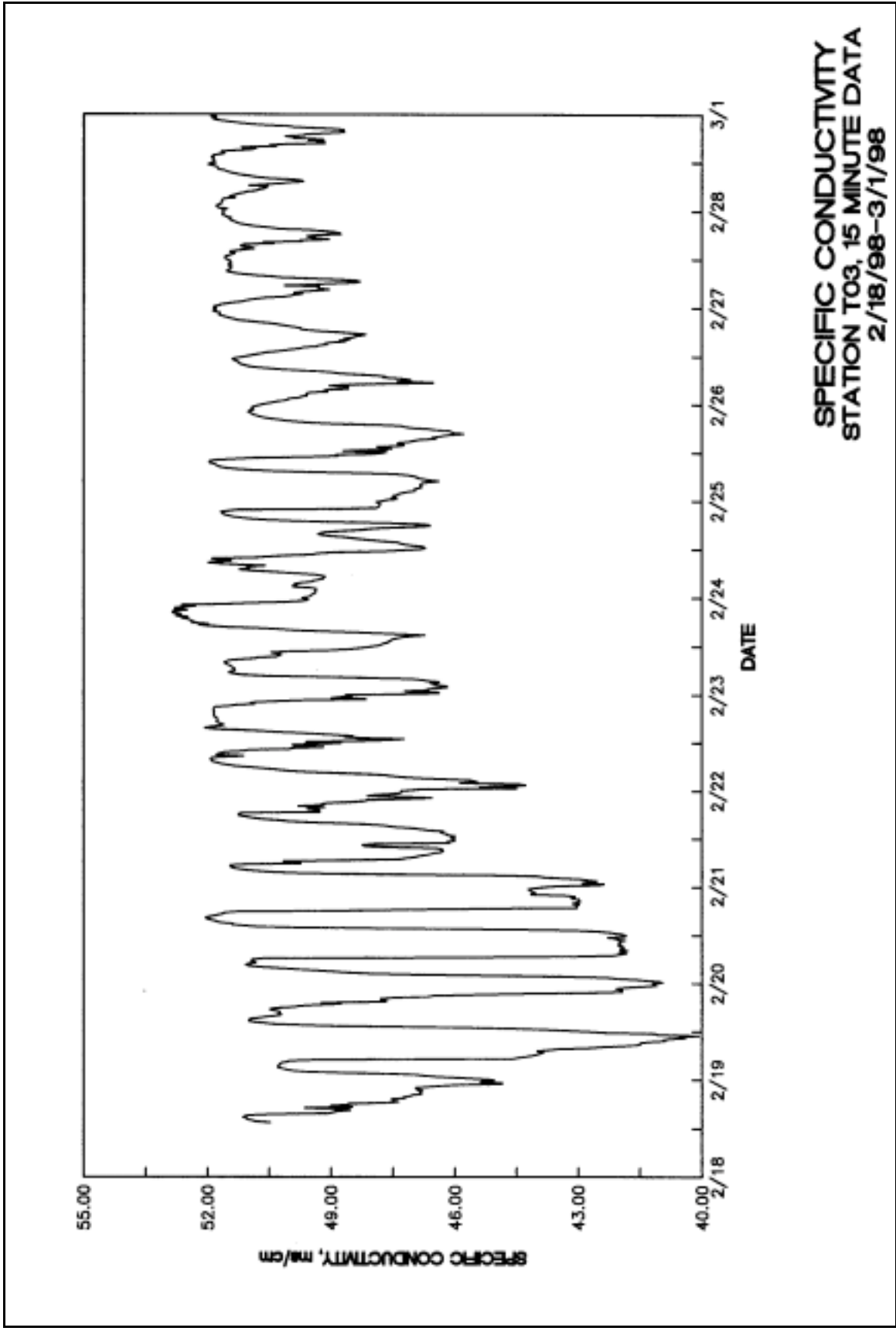


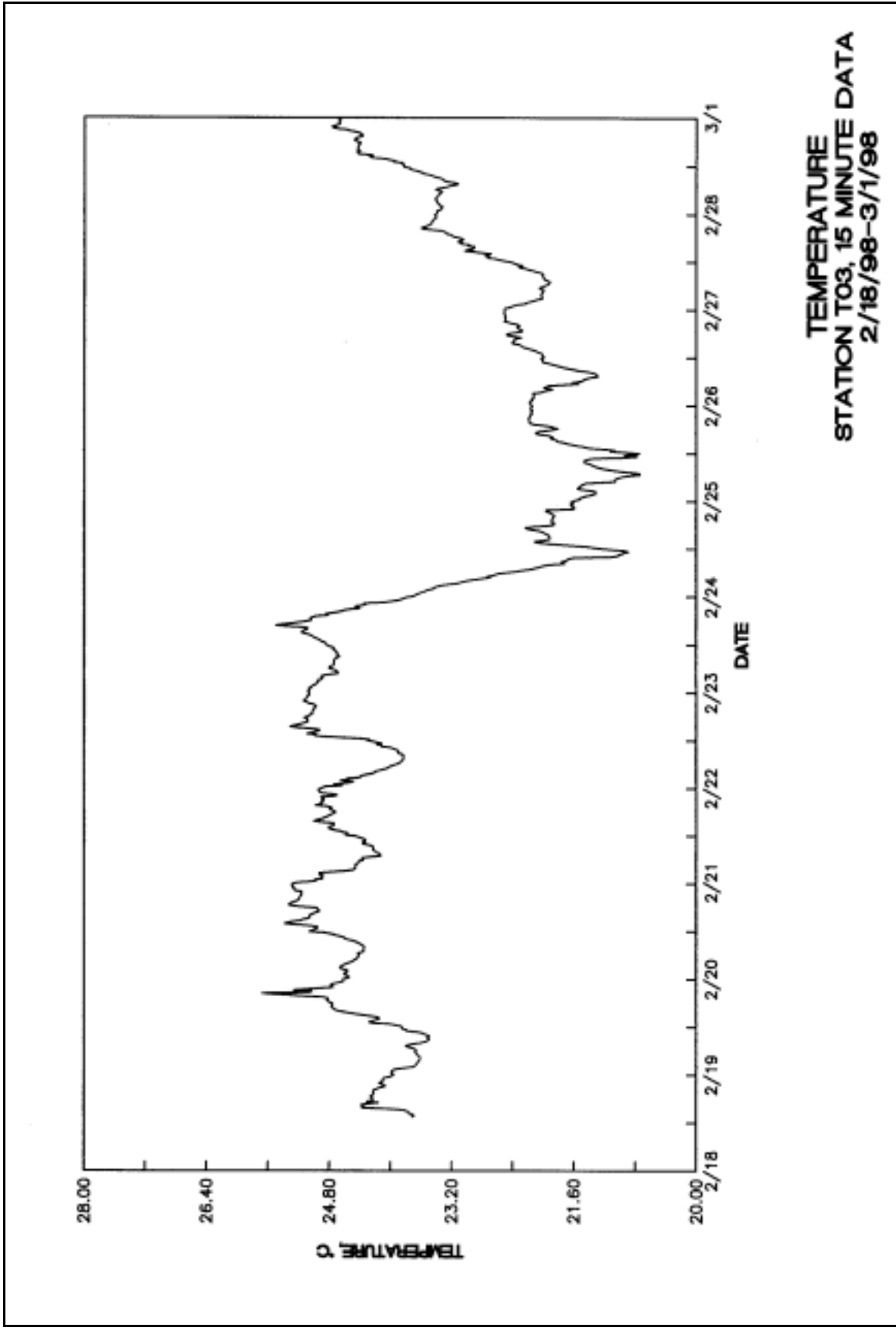
DISSOLVED OXYGEN
STATION T02, 15 MINUTE DATA
2/1/98-3/1/98



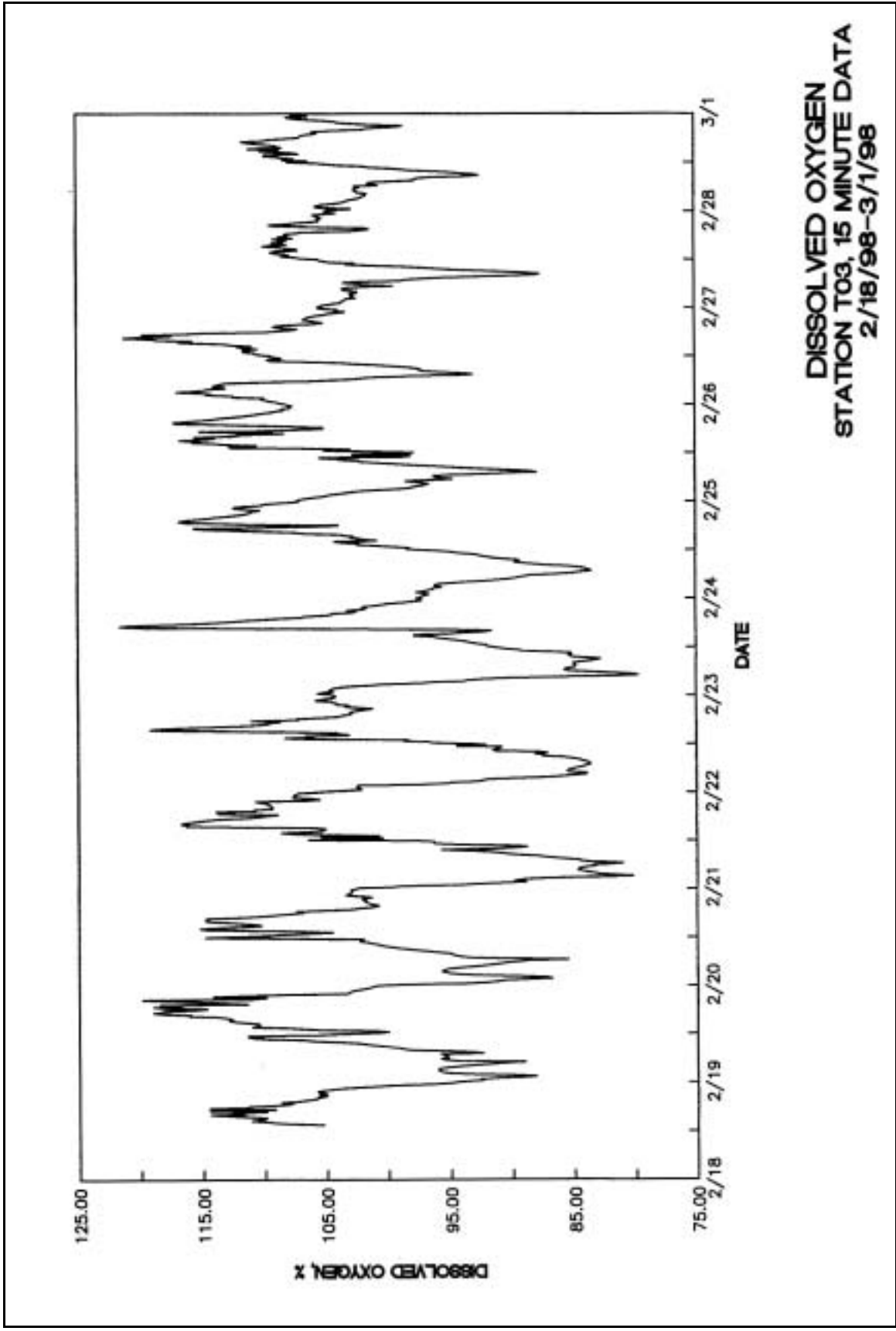


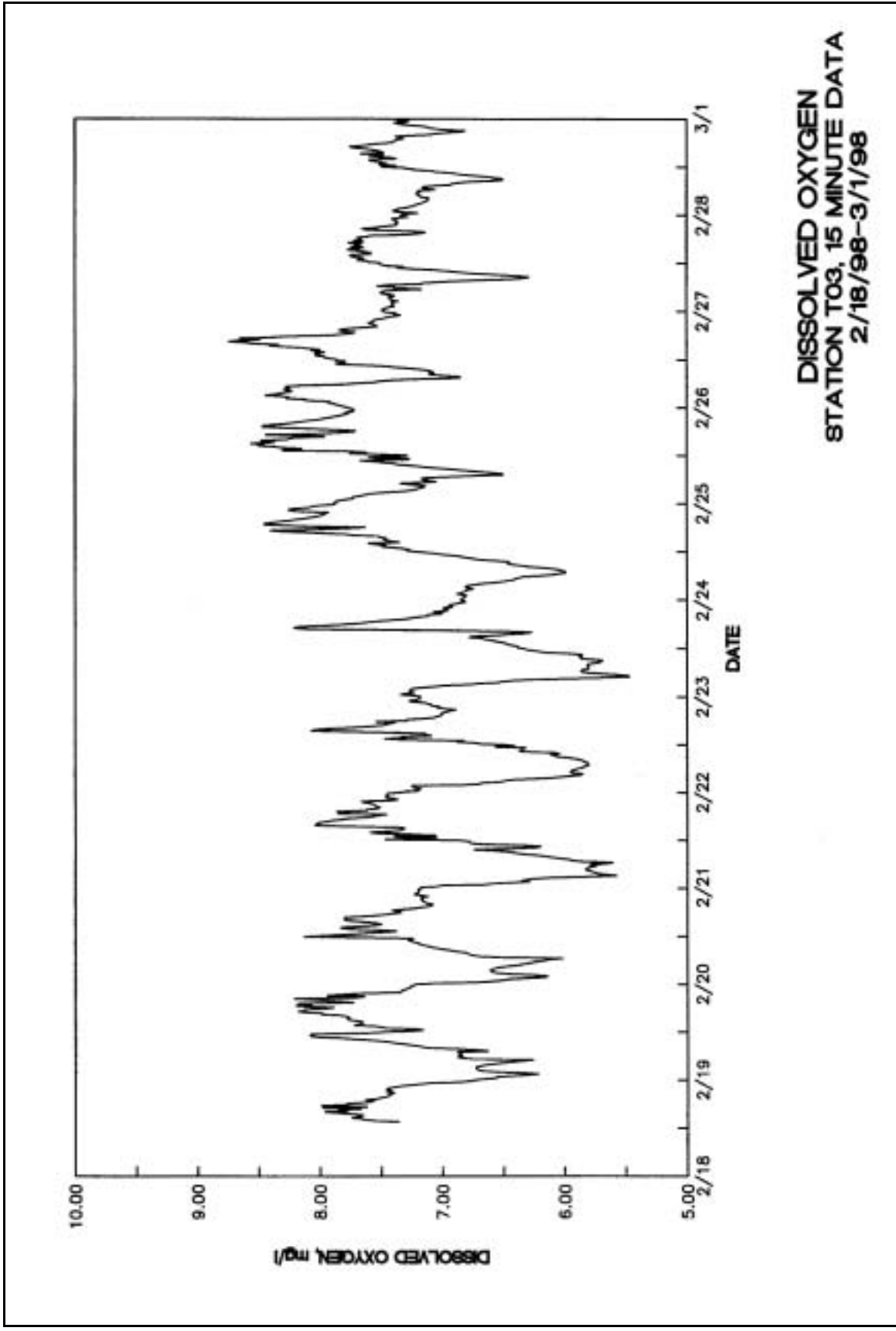




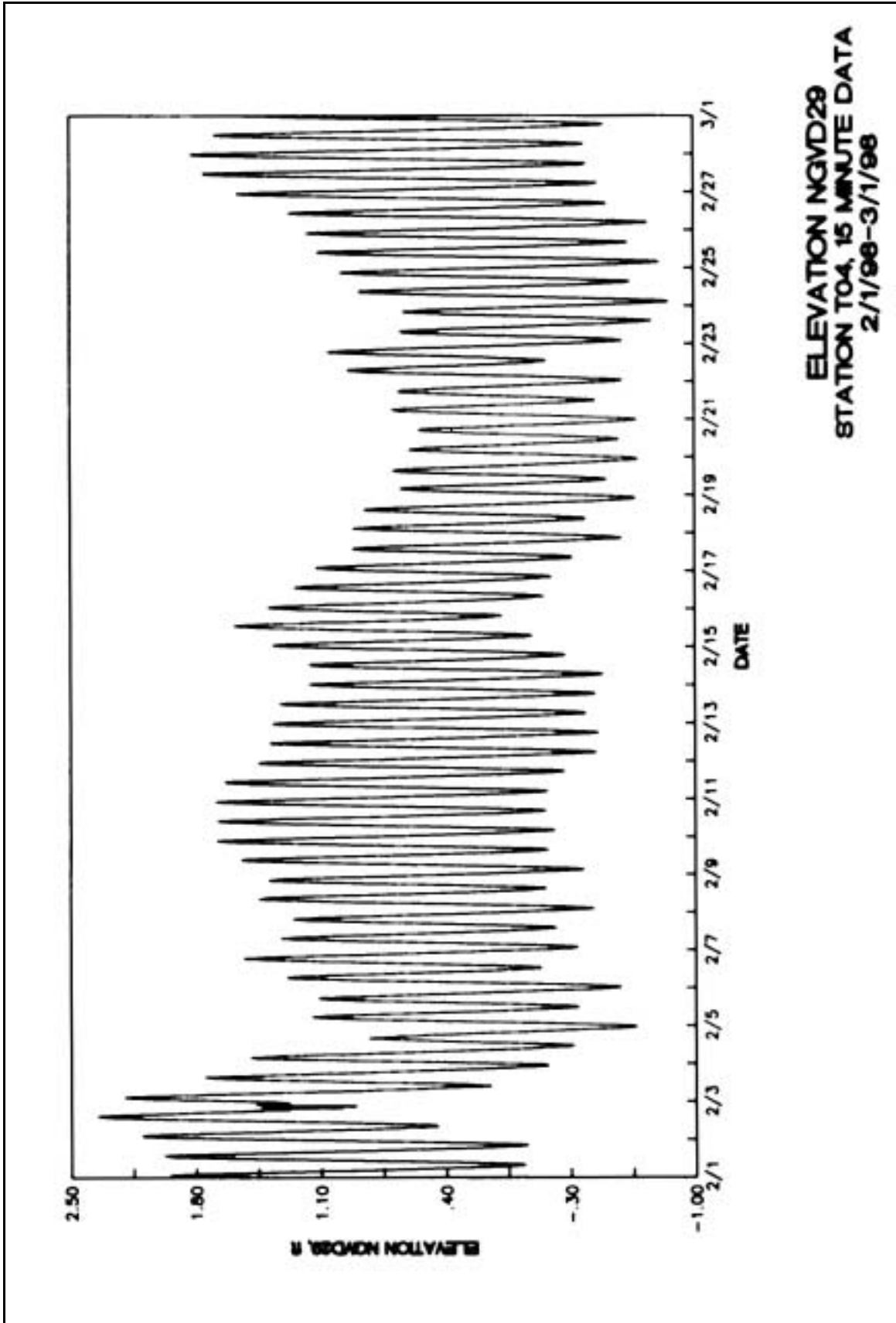


TEMPERATURE
STATION T03, 15 MINUTE DATA
2/18/98-3/1/98





**DISSOLVED OXYGEN
STATION T03, 15 MINUTE DATA
2/18/98-3/1/98**



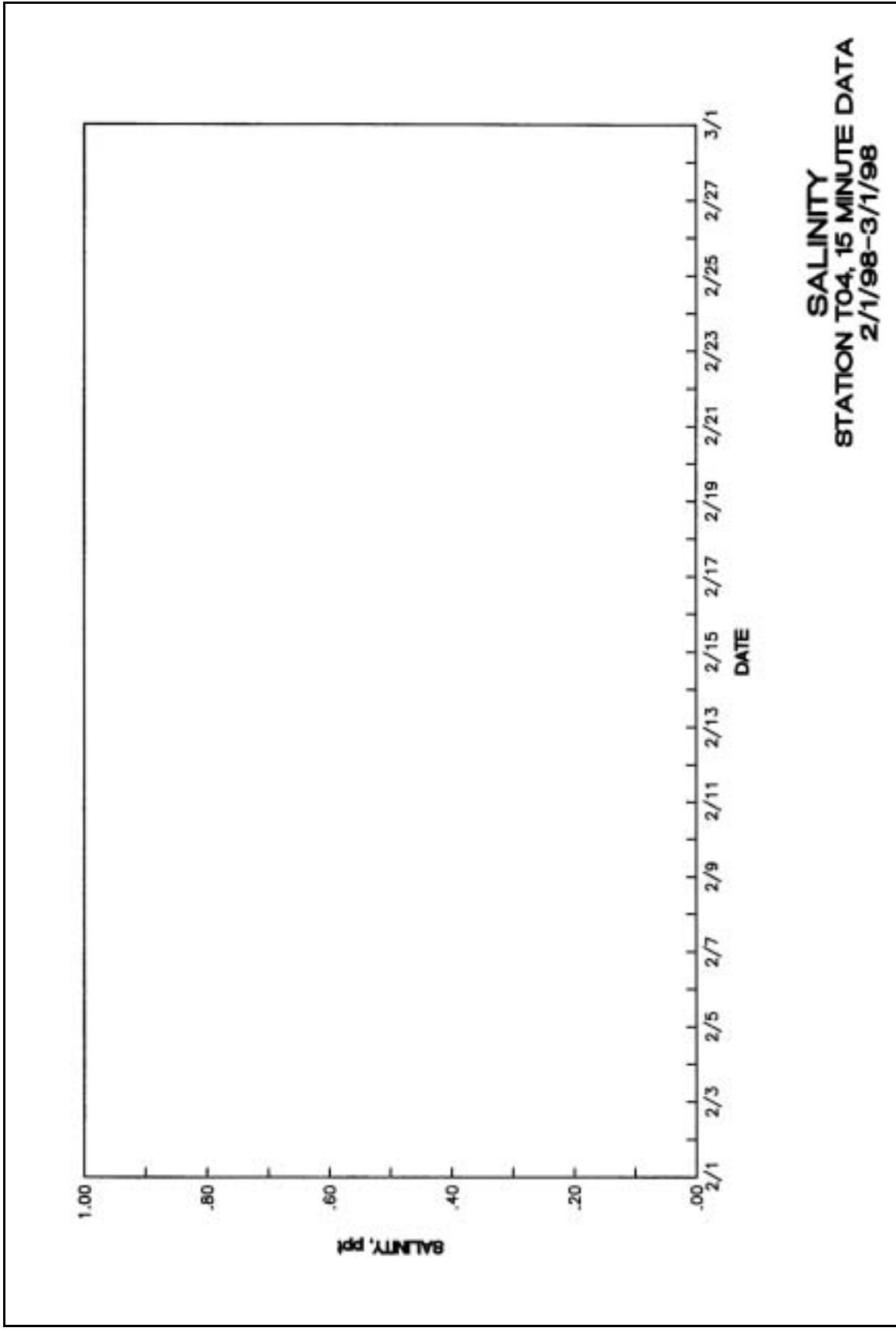
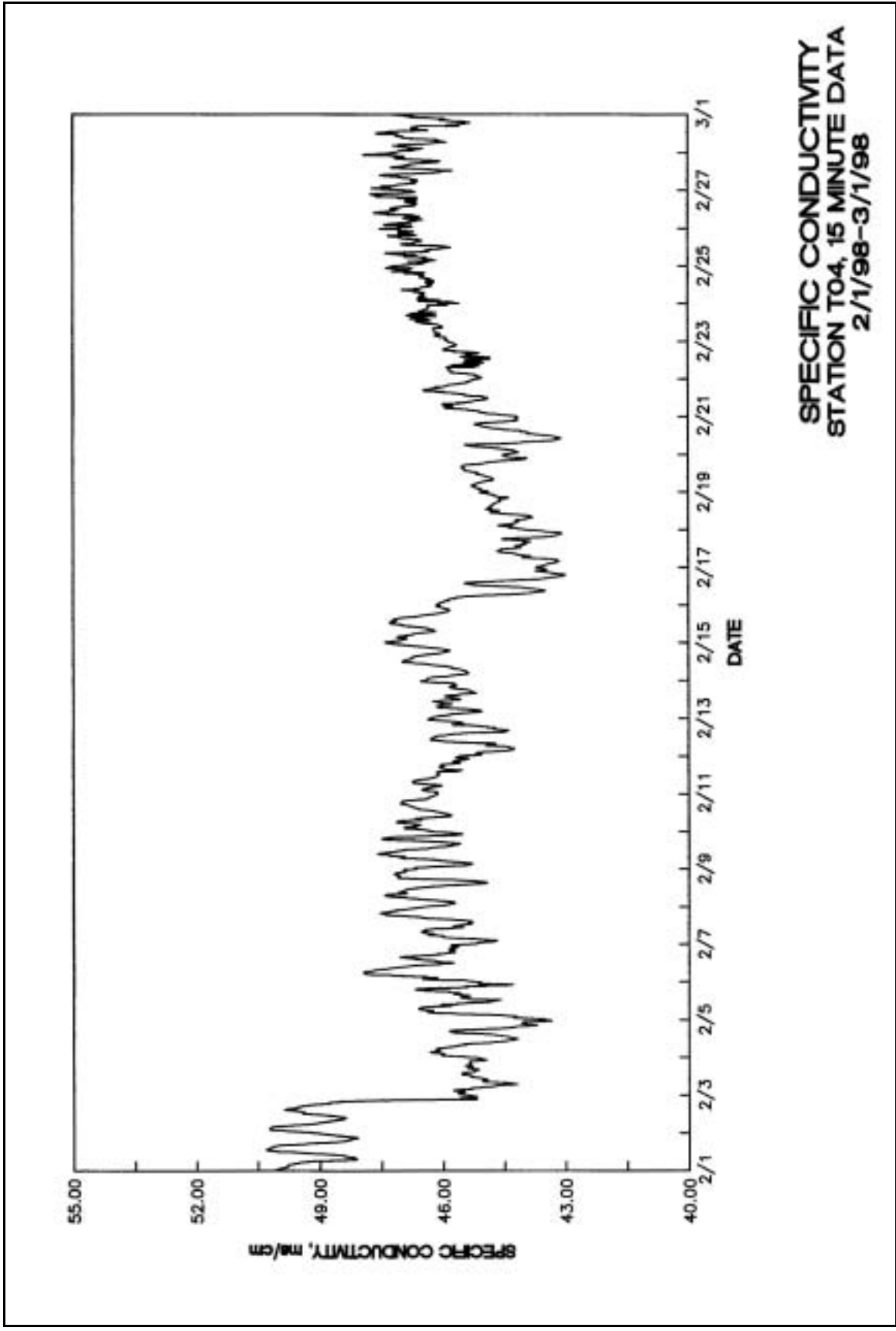
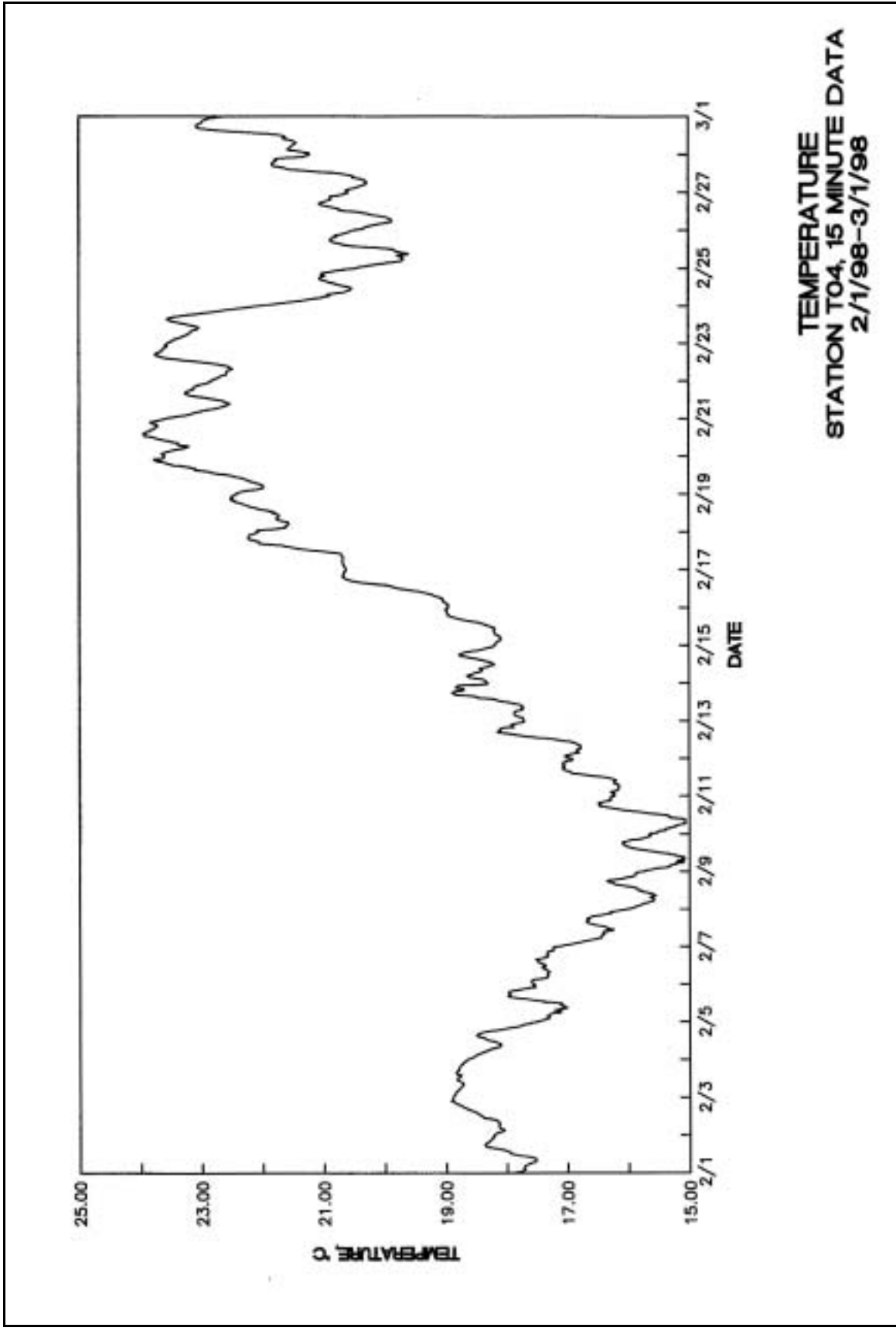
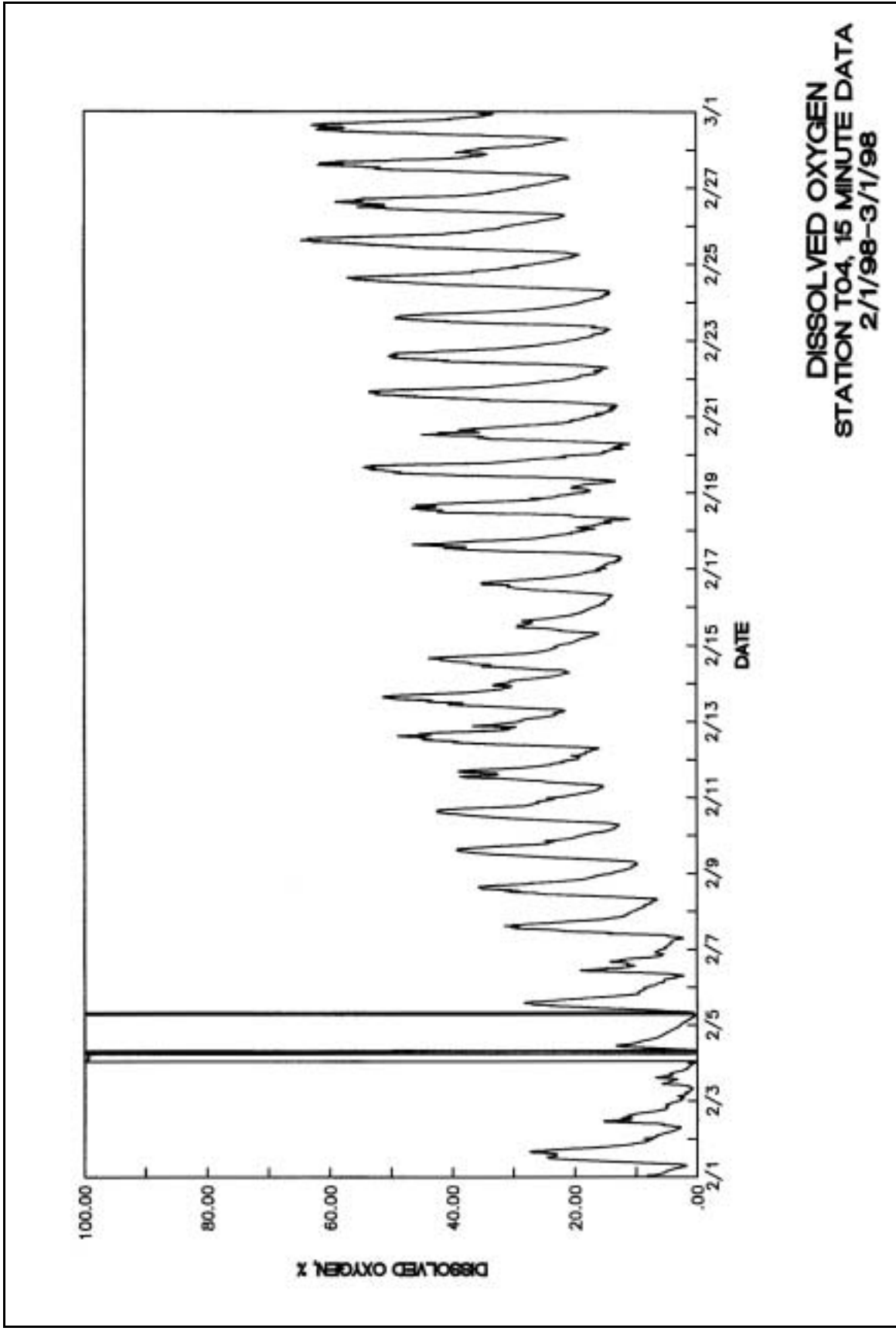


Plate 116







DISSOLVED OXYGEN
STATION TO4, 15 MINUTE DATA
2/1/98-3/1/98

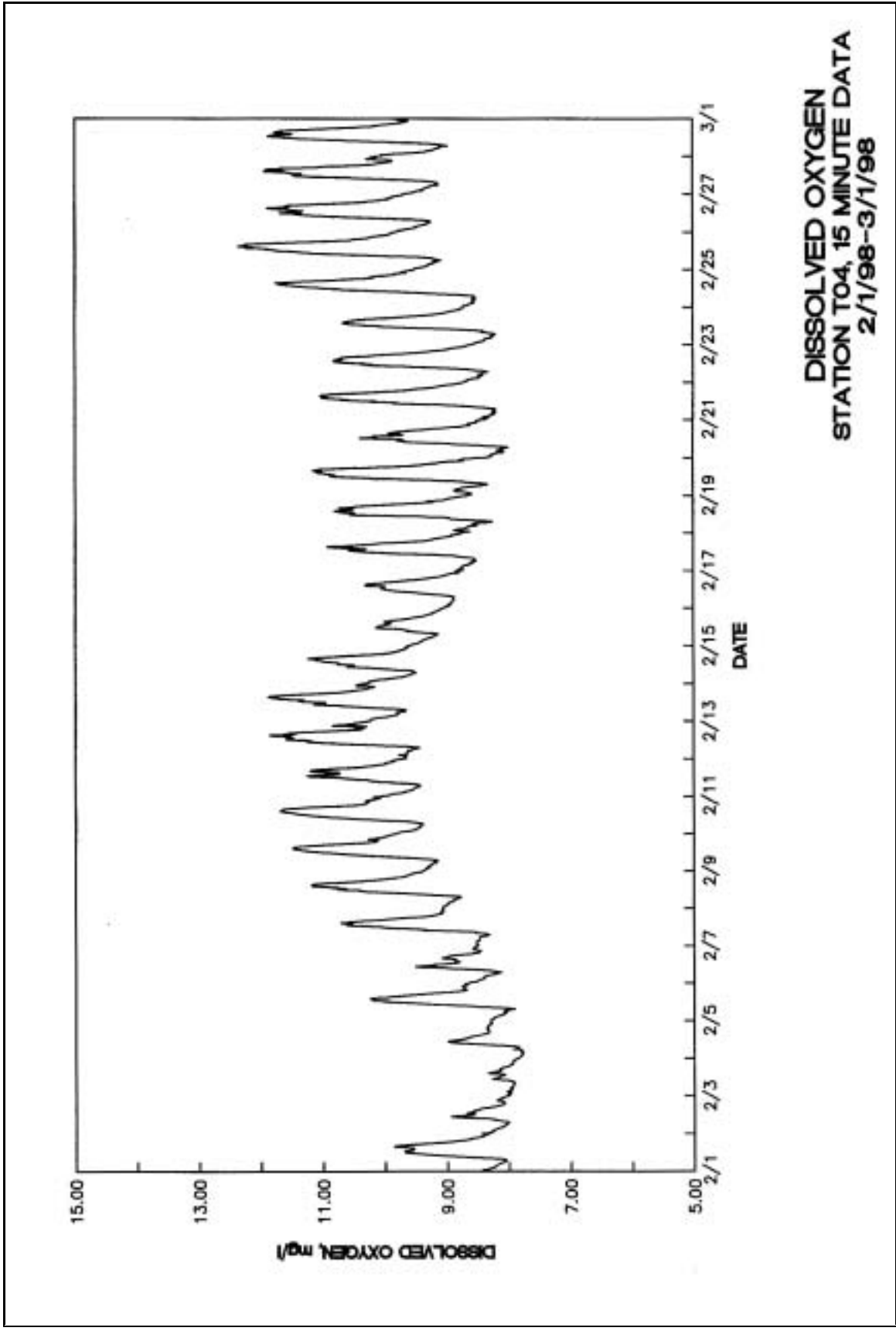
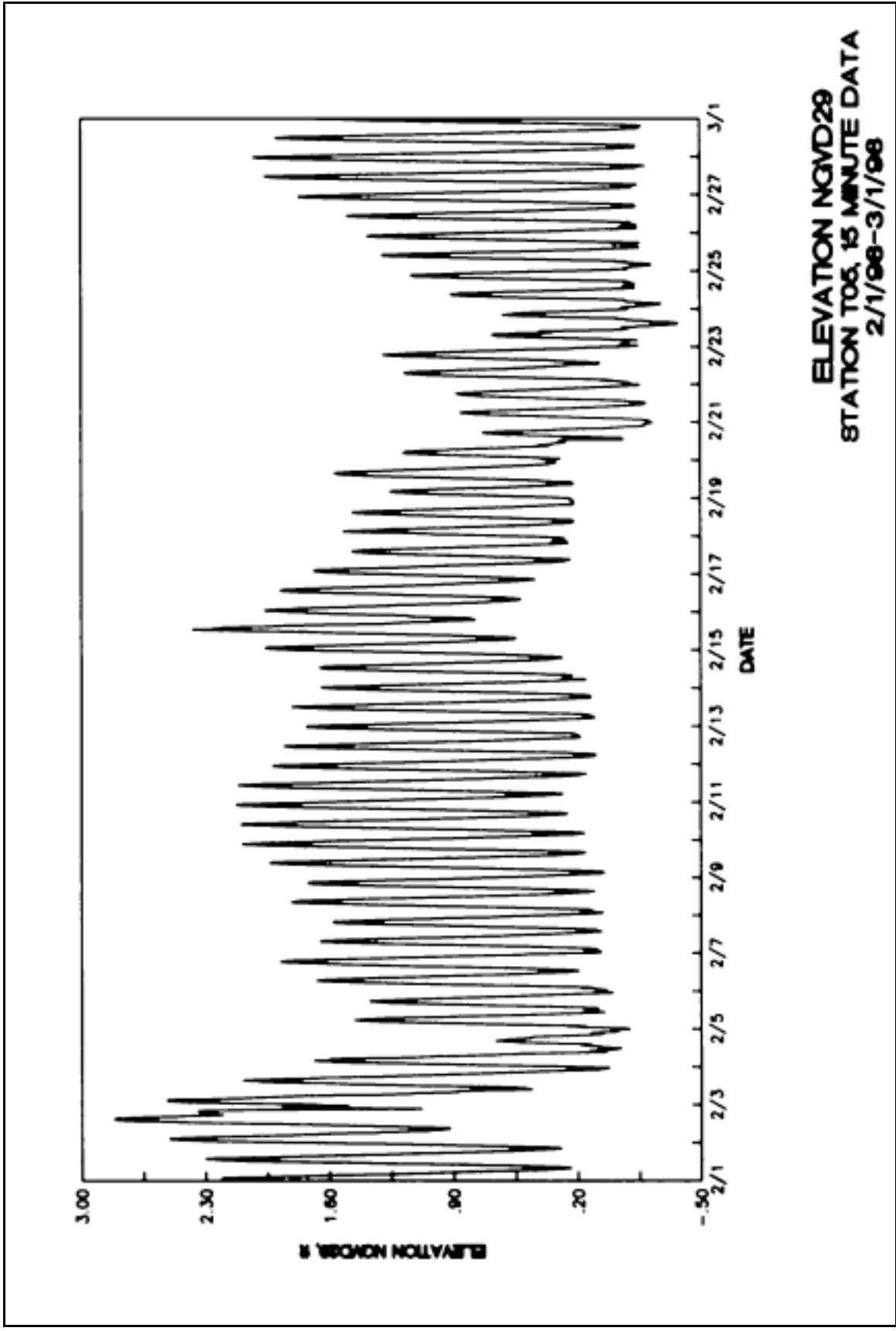
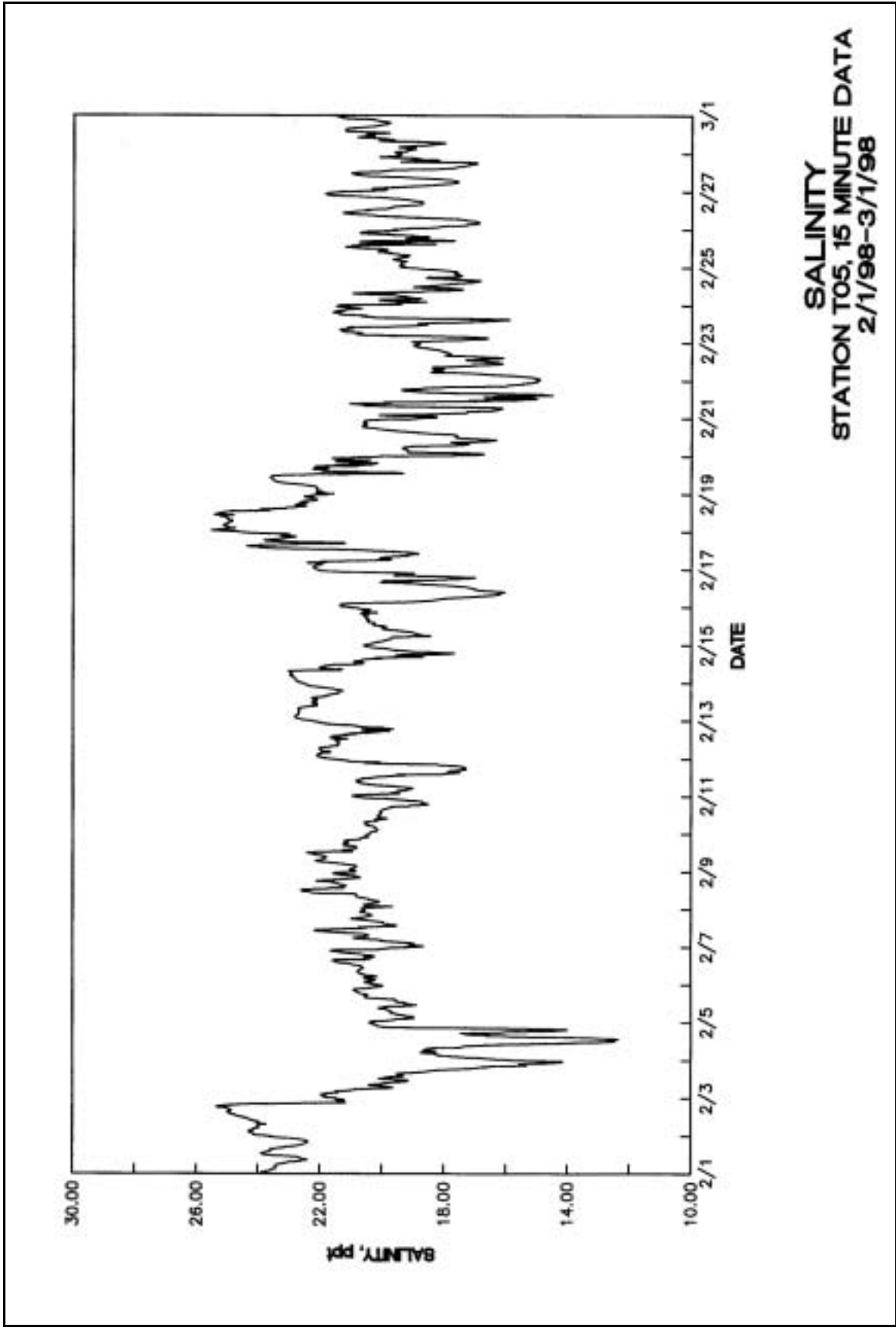
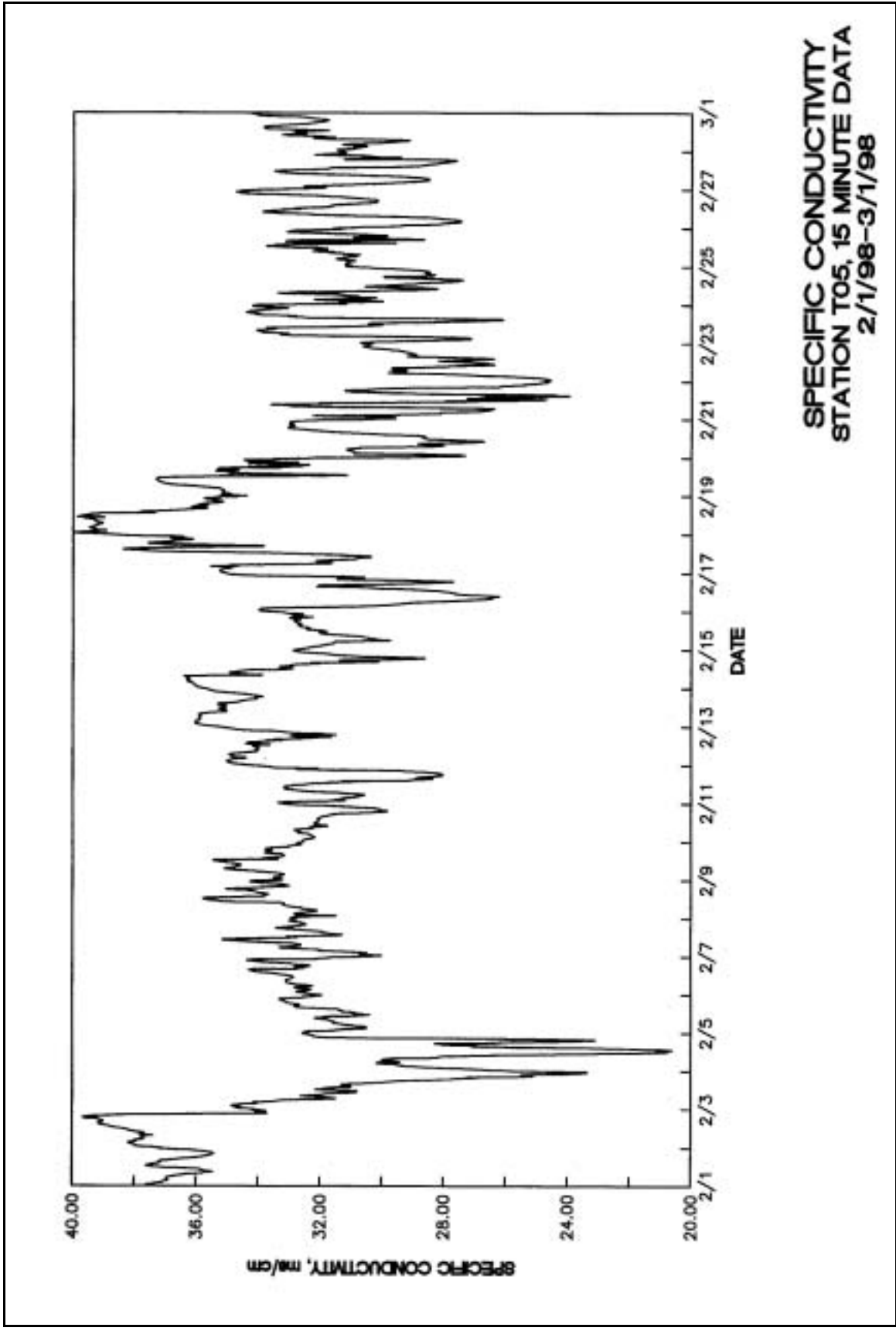


Plate 120







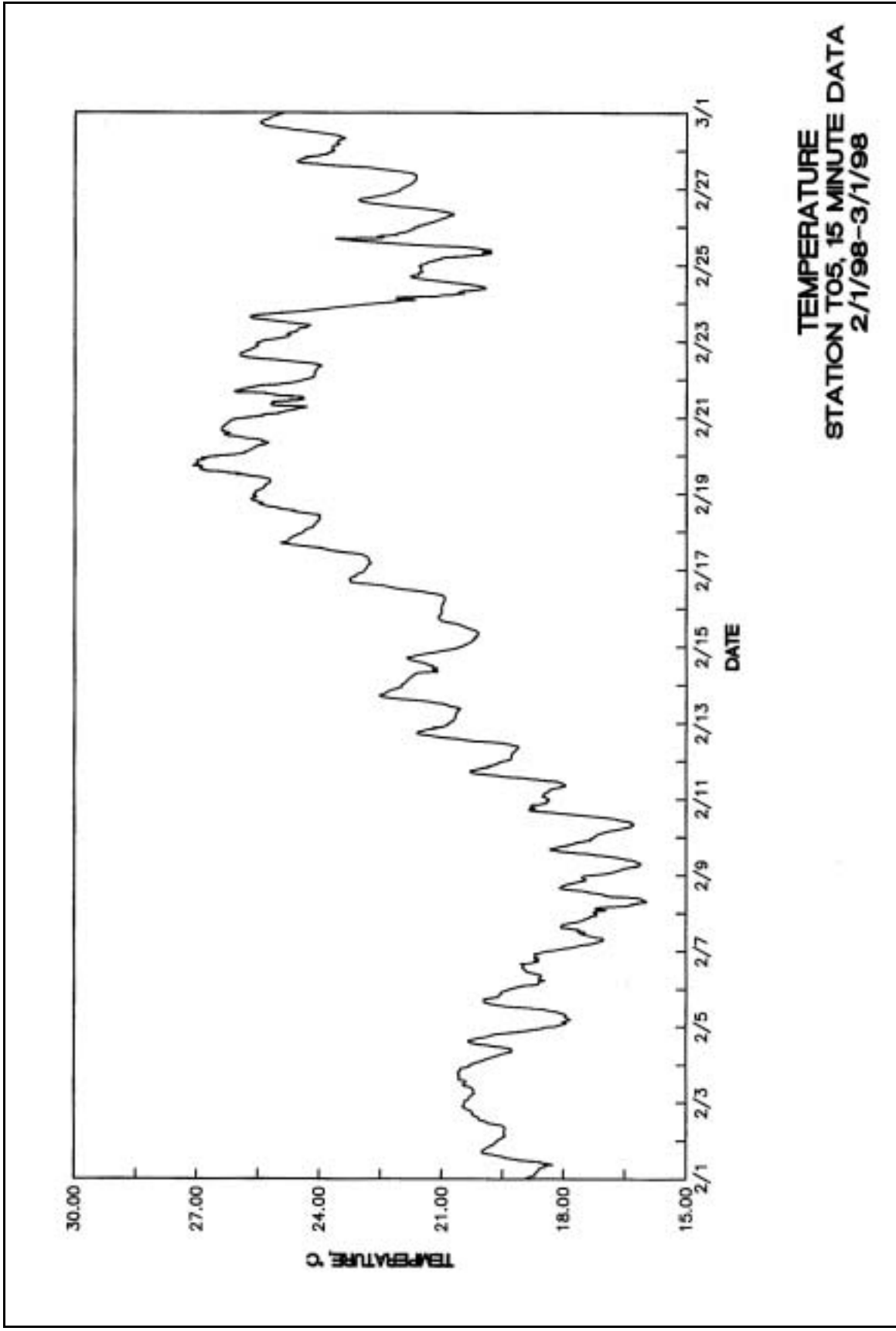
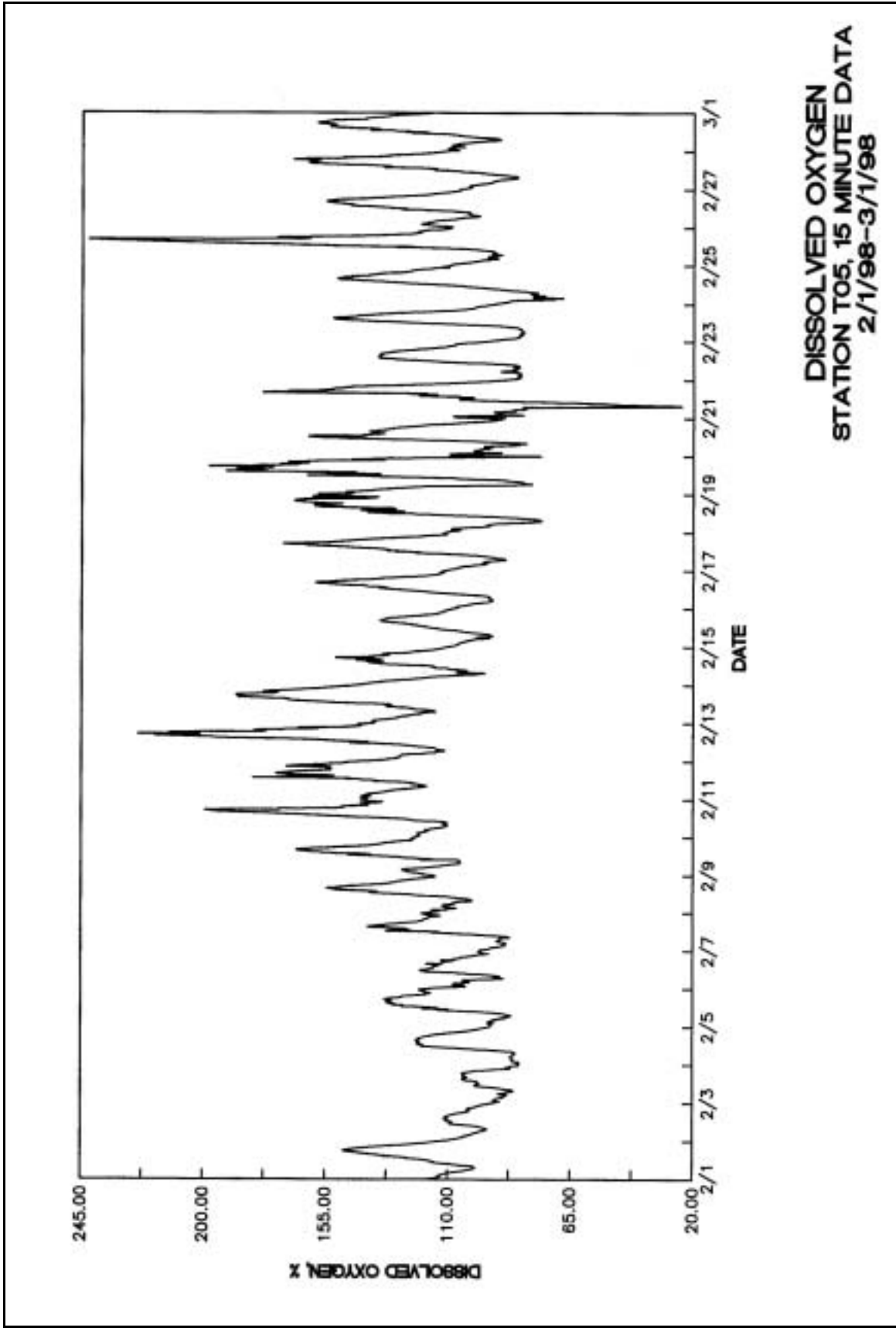
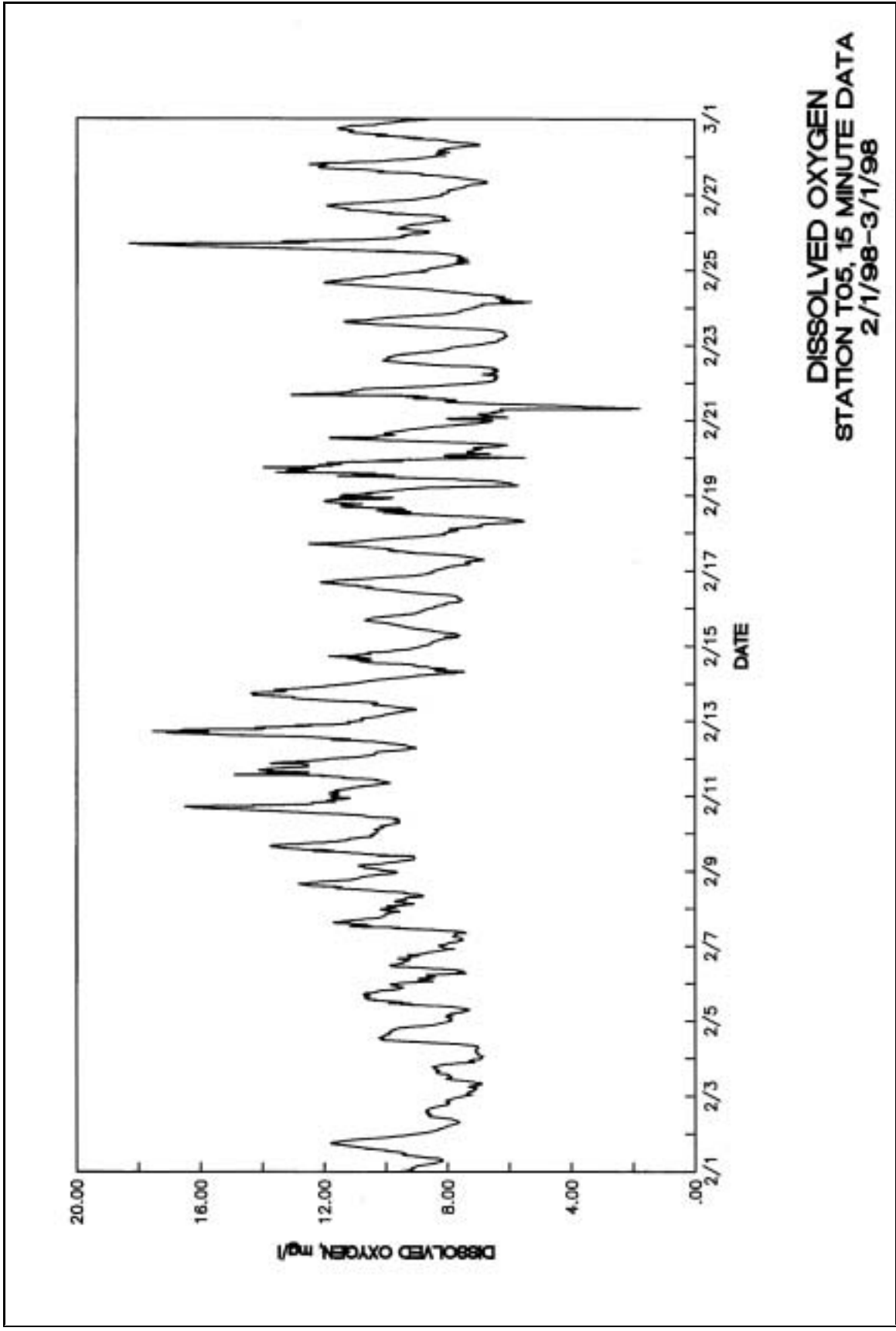
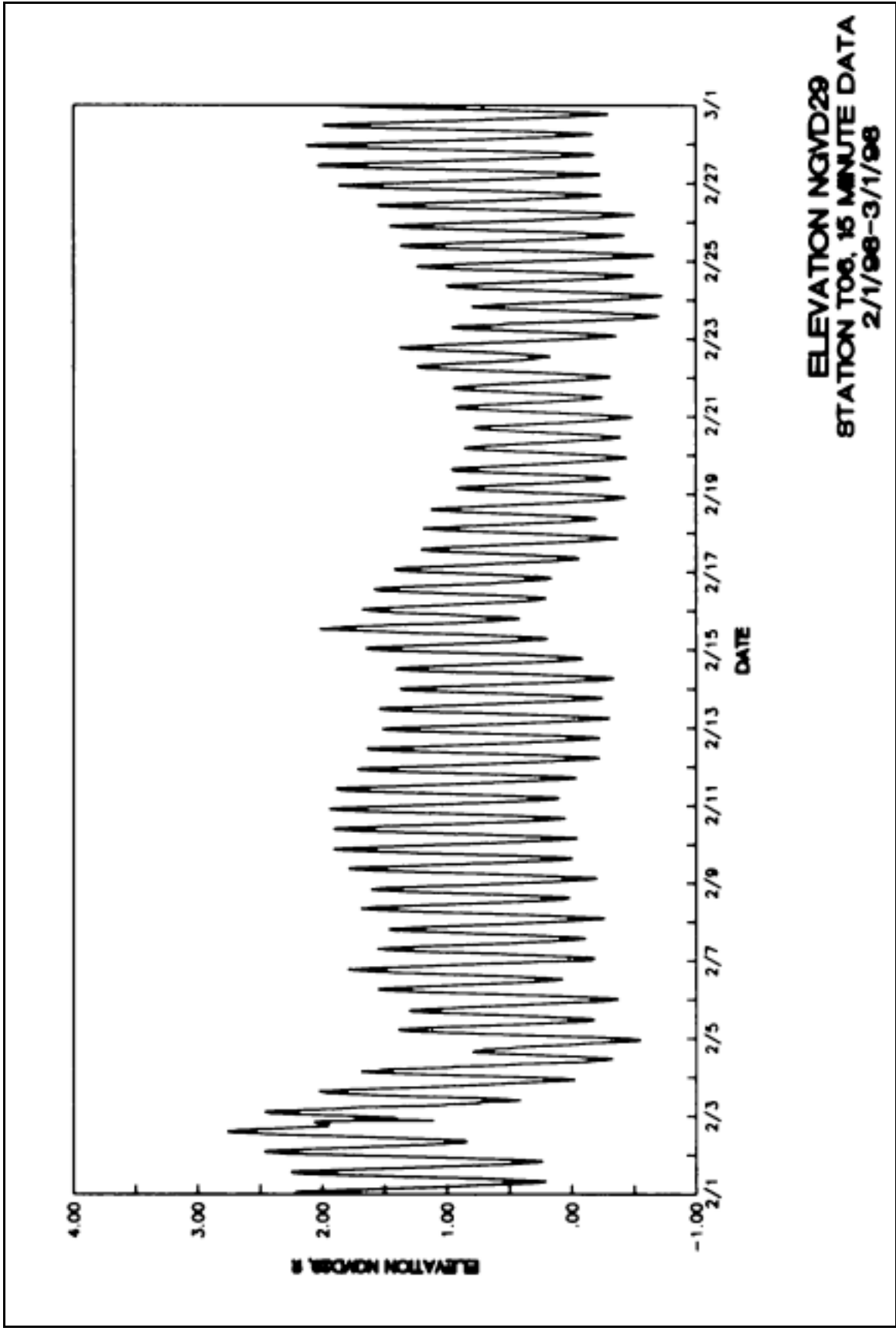


Plate 124





DISSOLVED OXYGEN
STATION T05, 15 MINUTE DATA
2/1/98-3/1/98



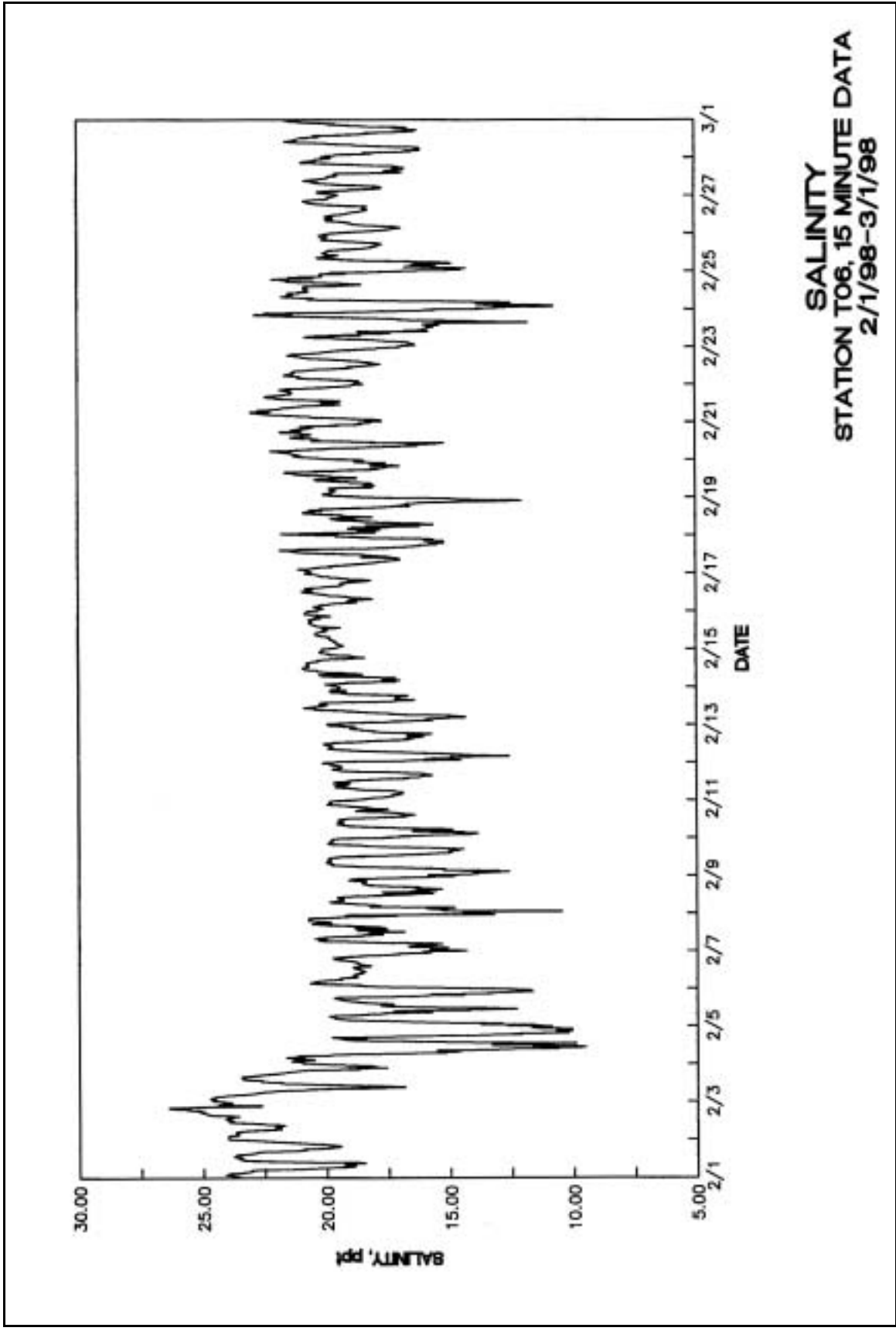
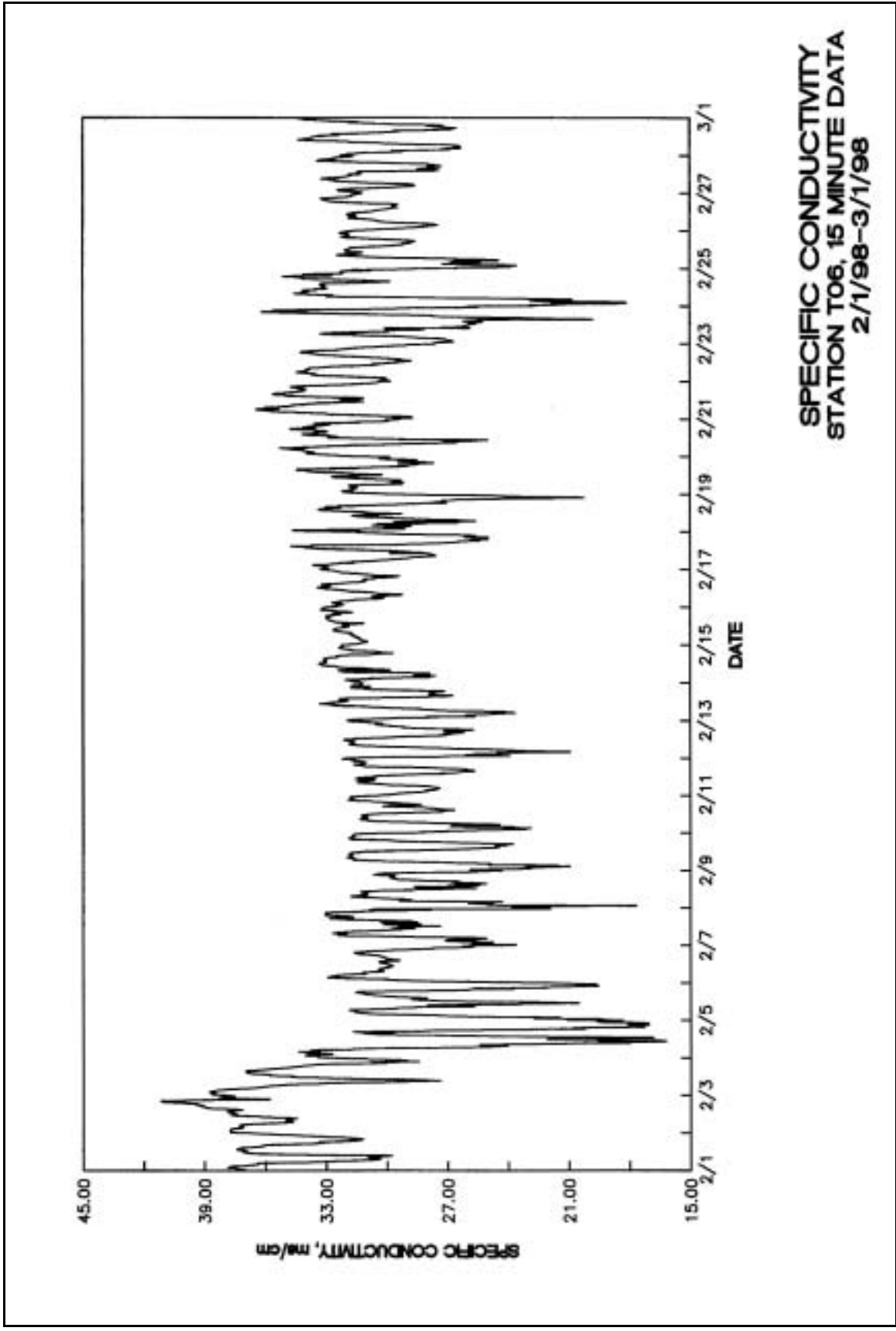


Plate 128



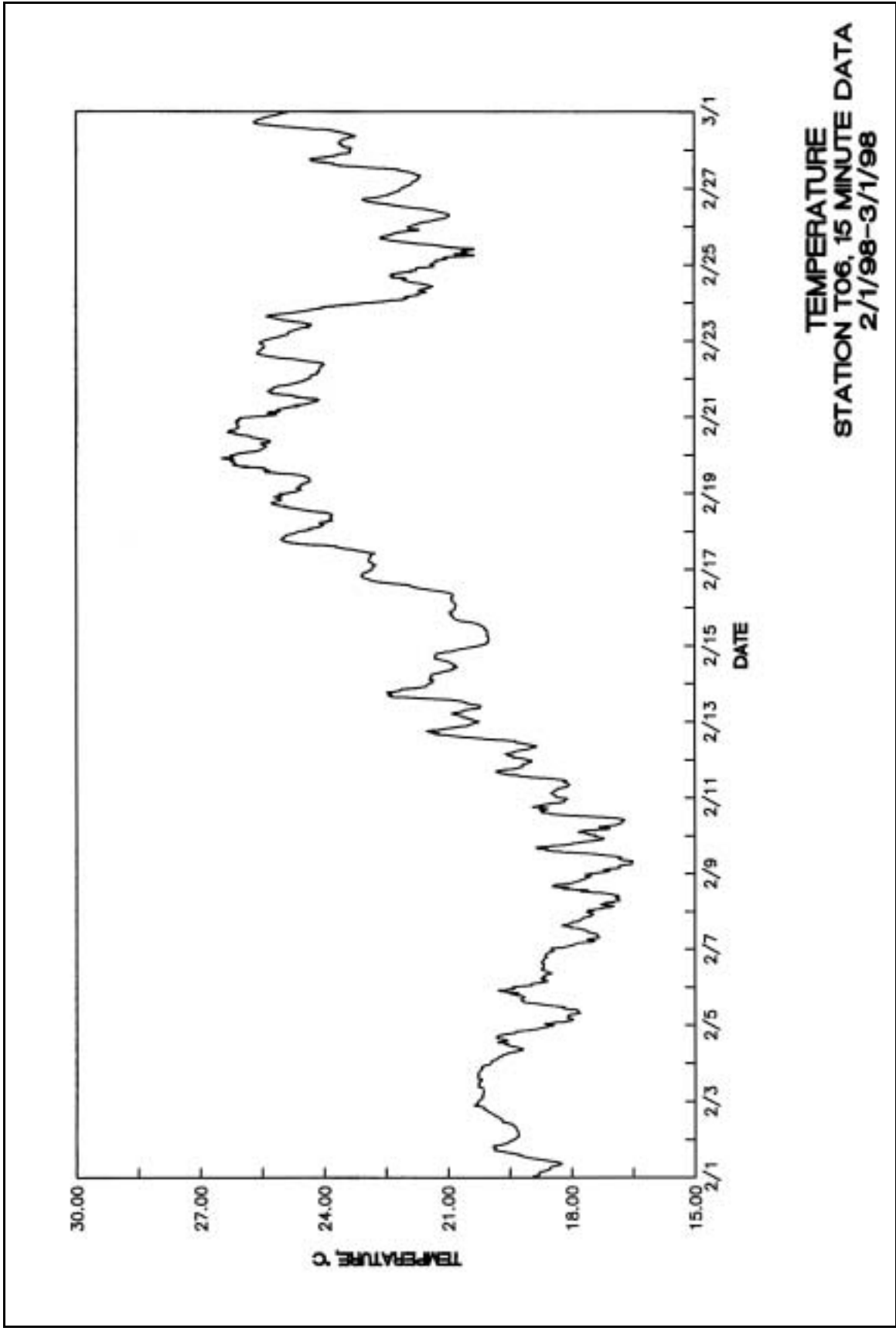
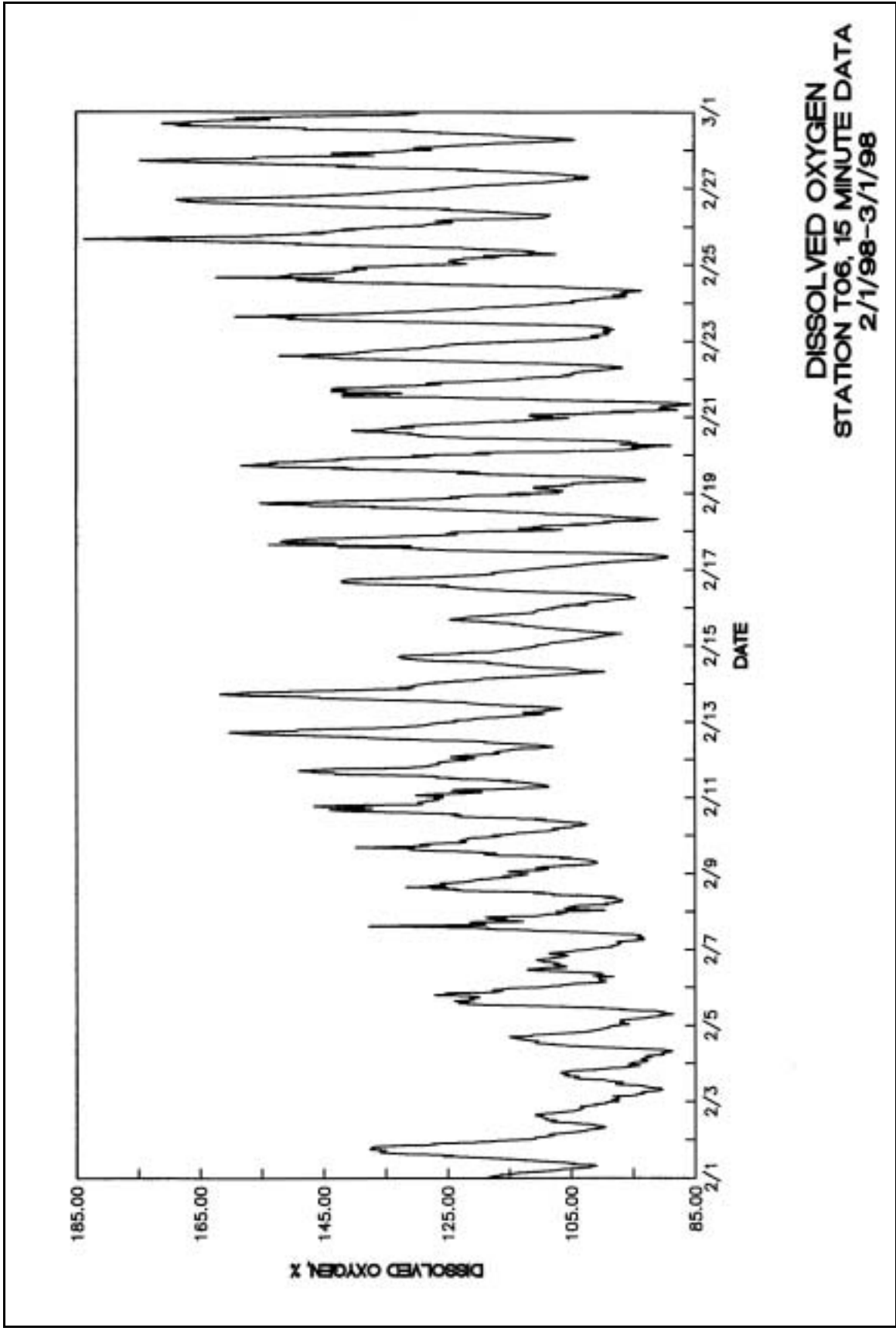
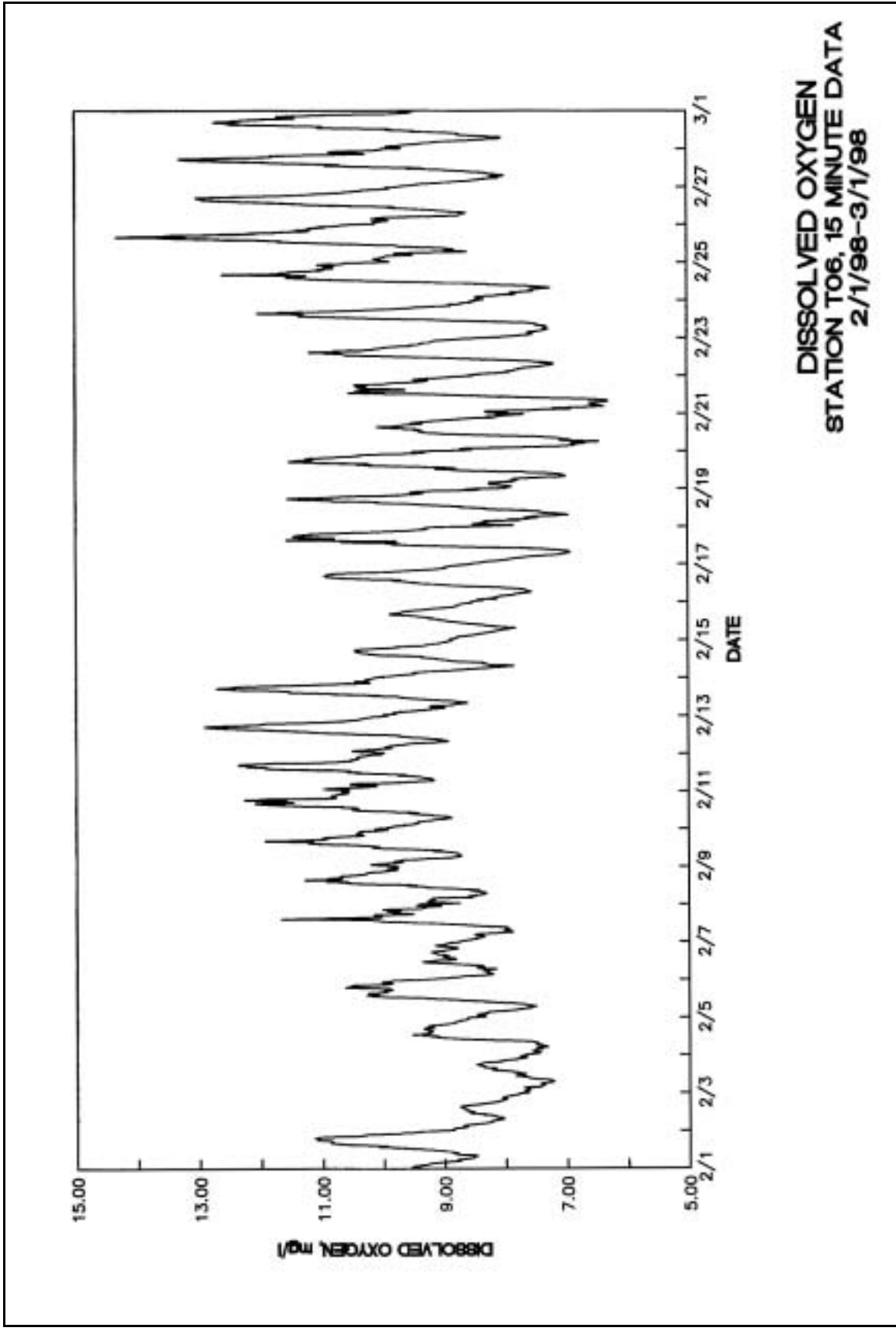
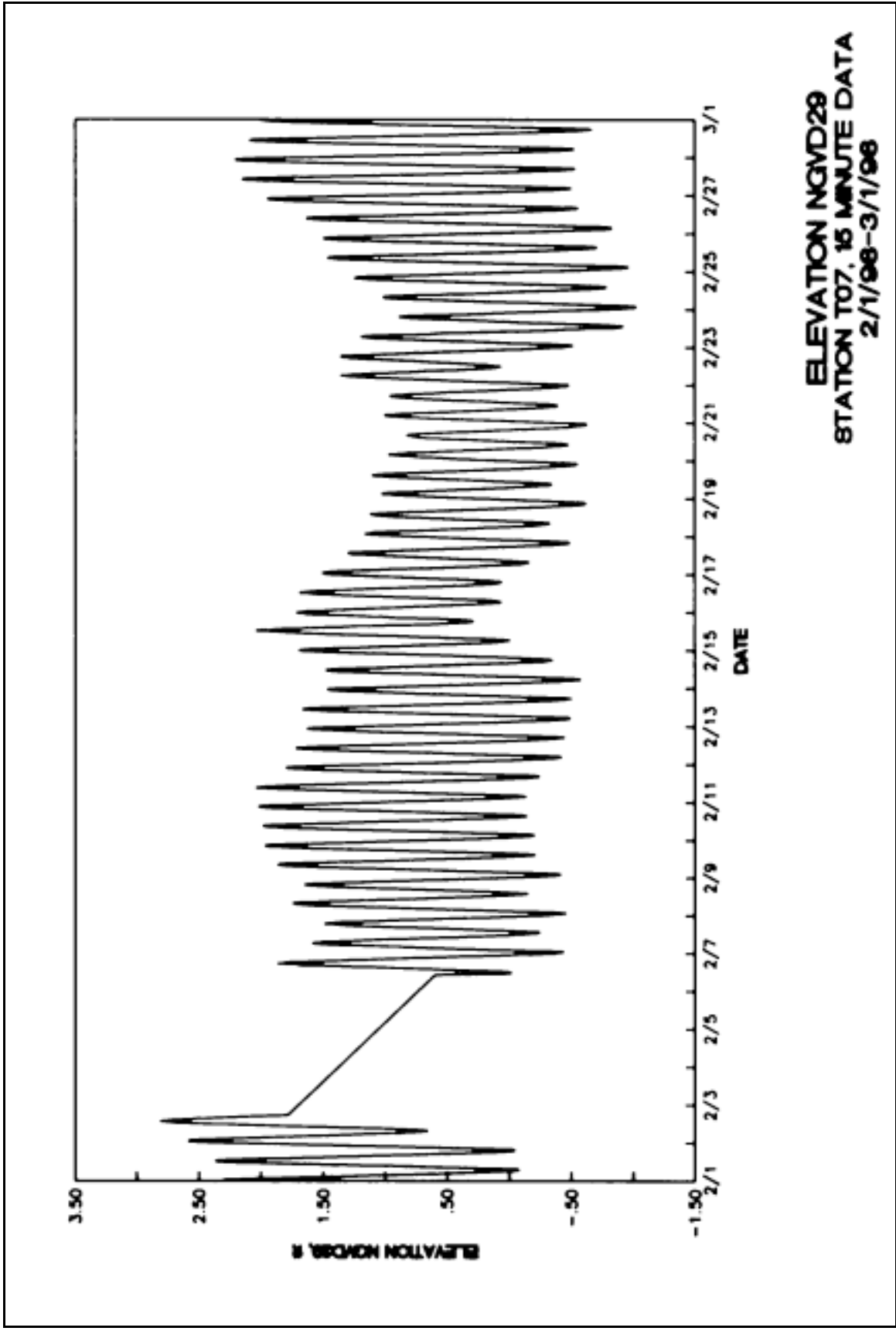


Plate 130



DISSOLVED OXYGEN
STATION T06, 15 MINUTE DATA
2/1/98-3/1/98





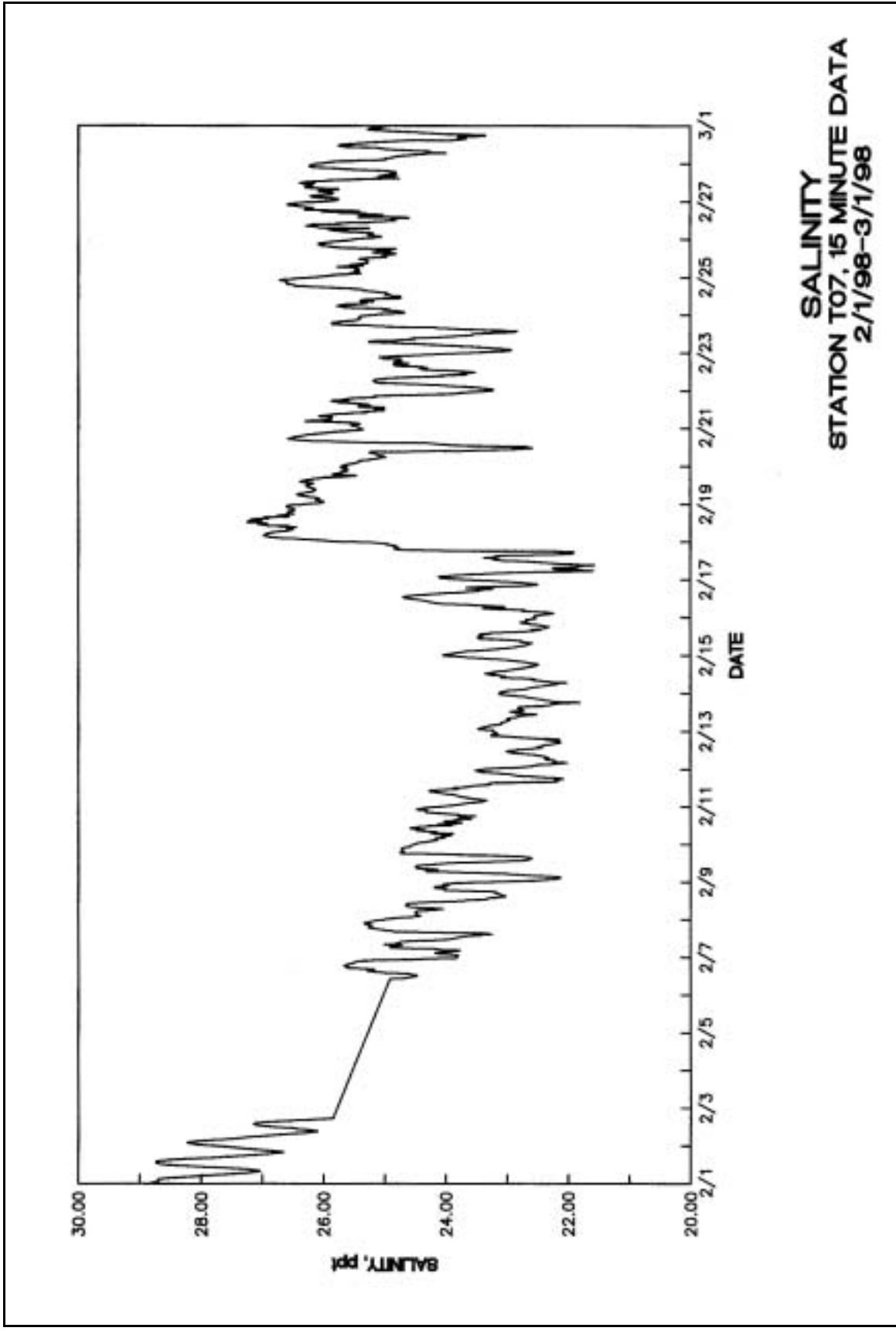
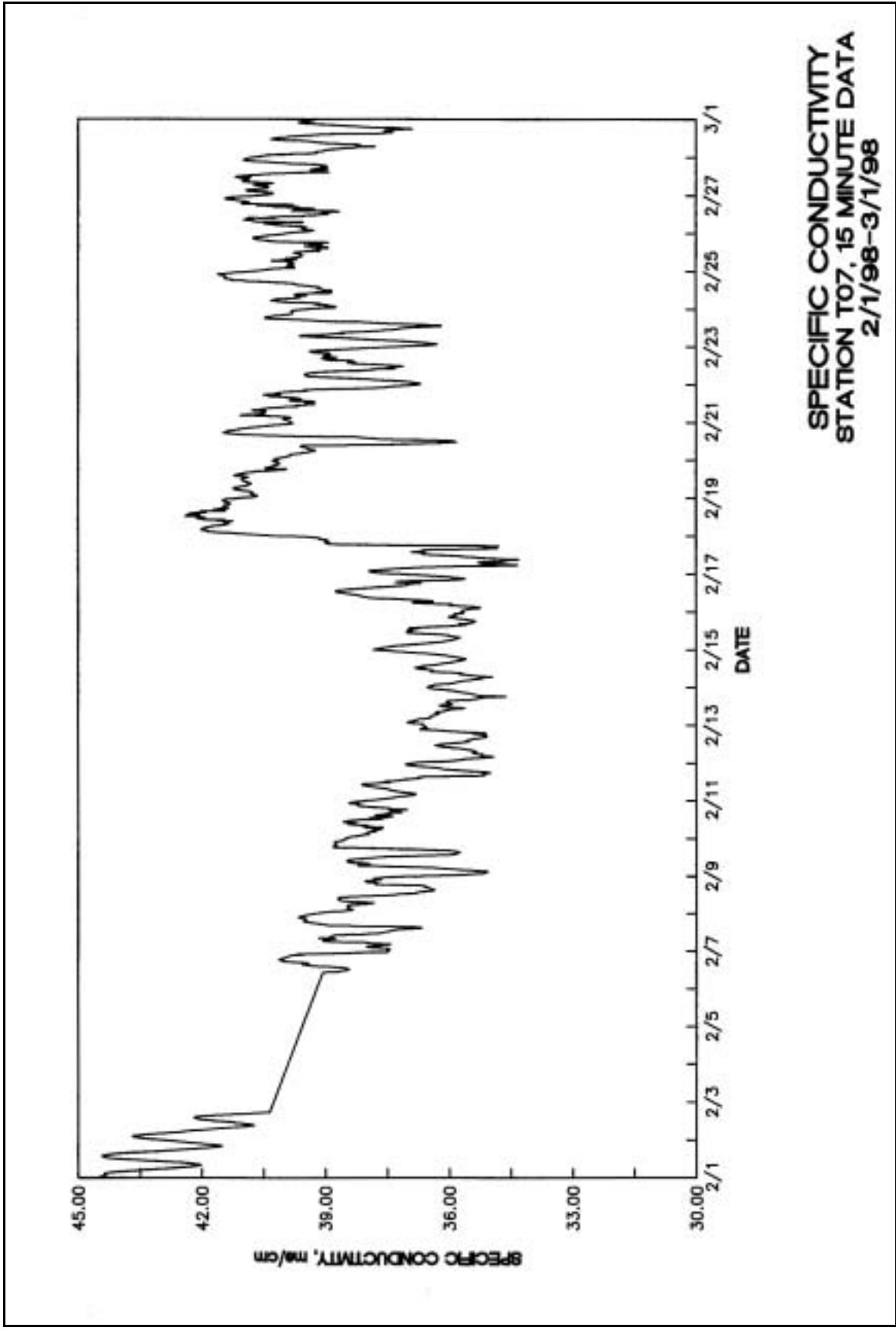
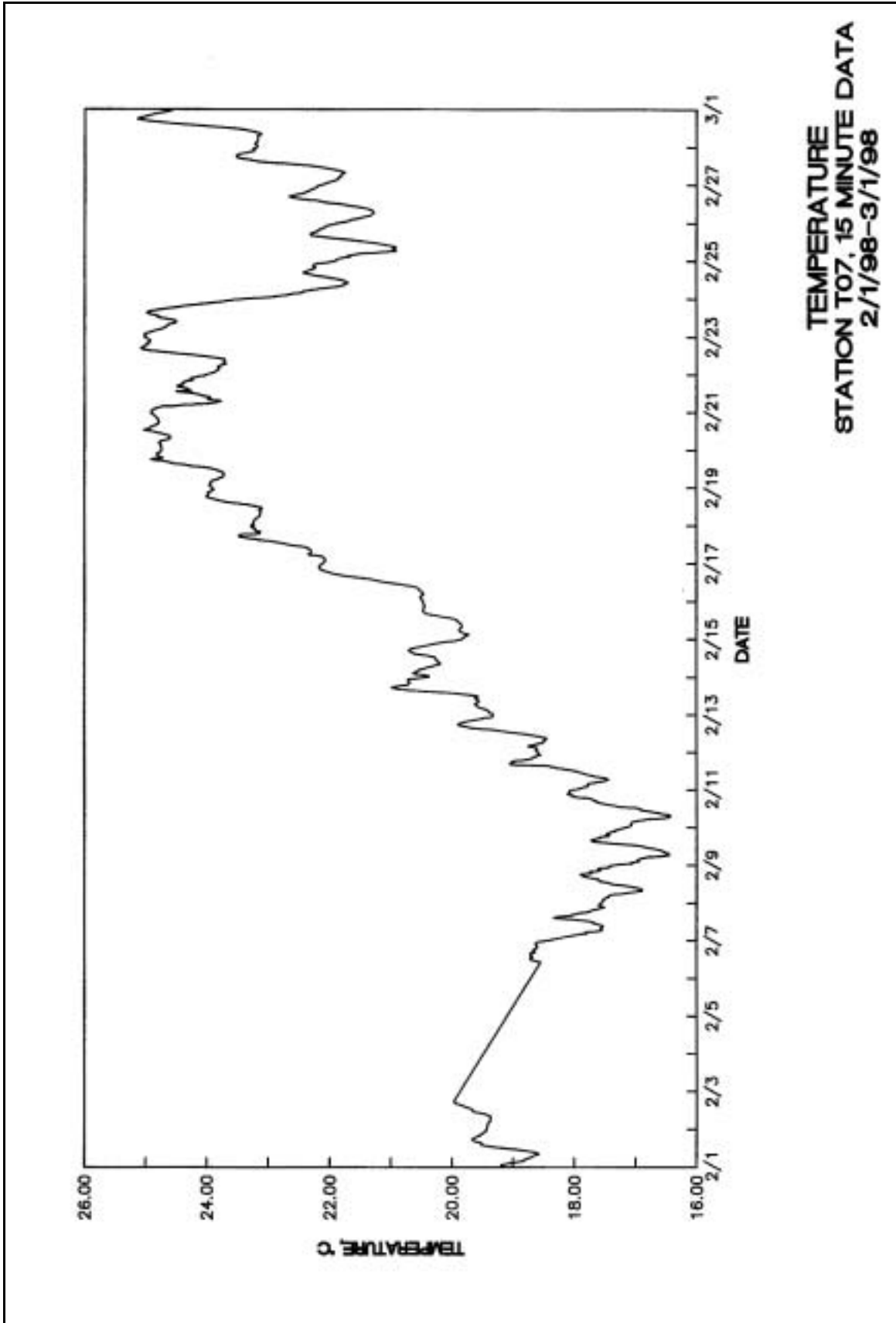
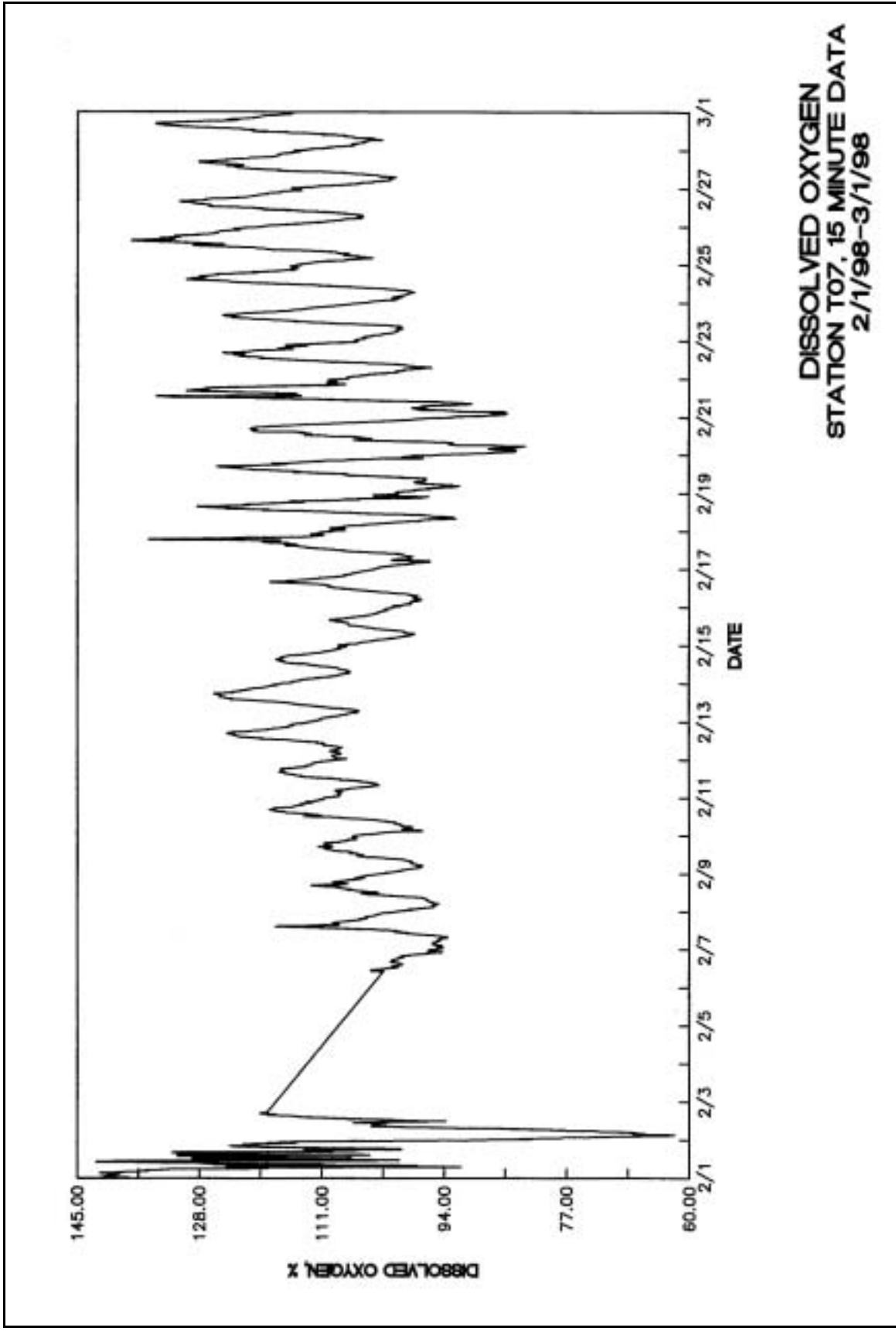


Plate 134

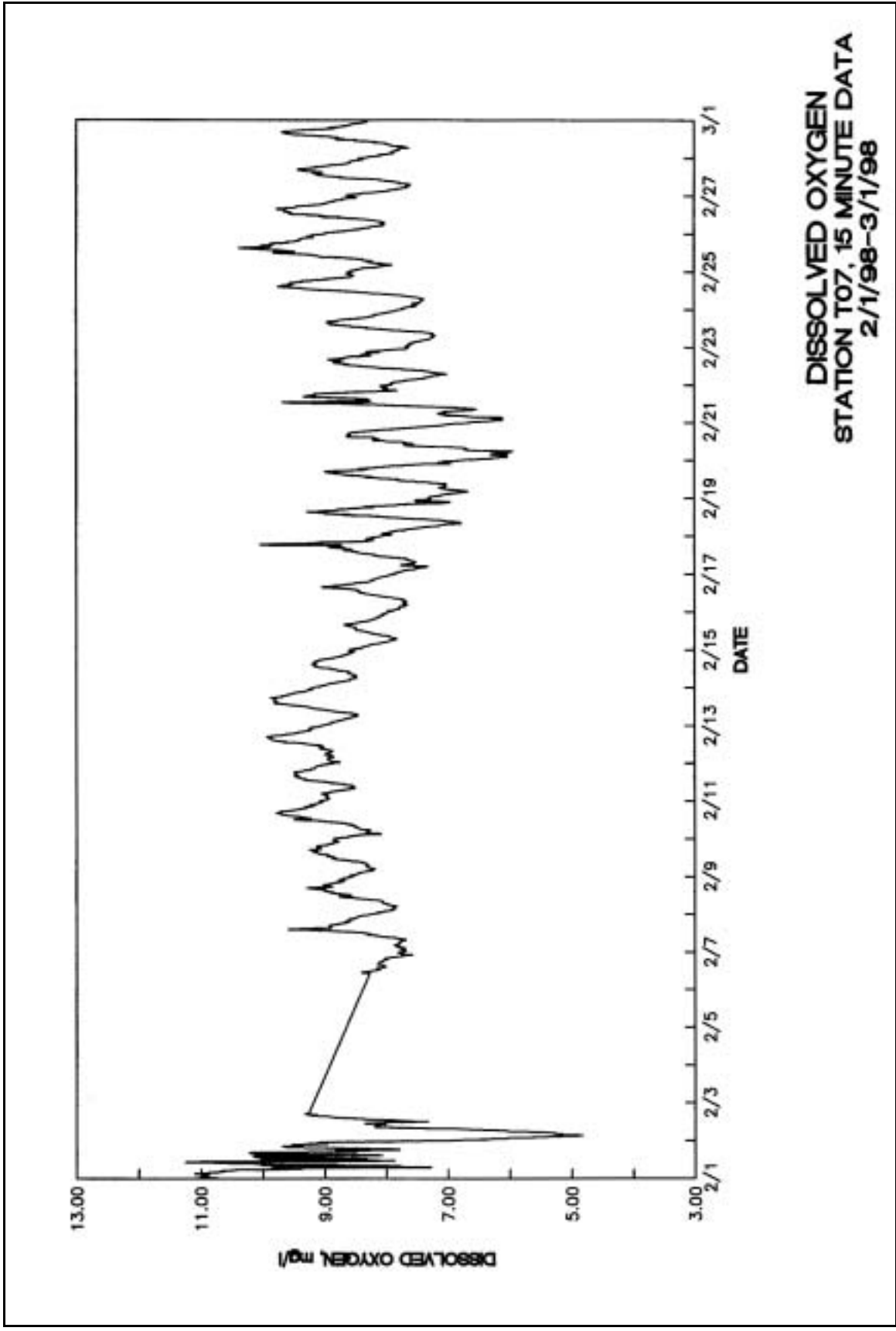


**SPECIFIC CONDUCTIVITY
STATION T07, 15 MINUTE DATA
2/1/98-3/1/98**

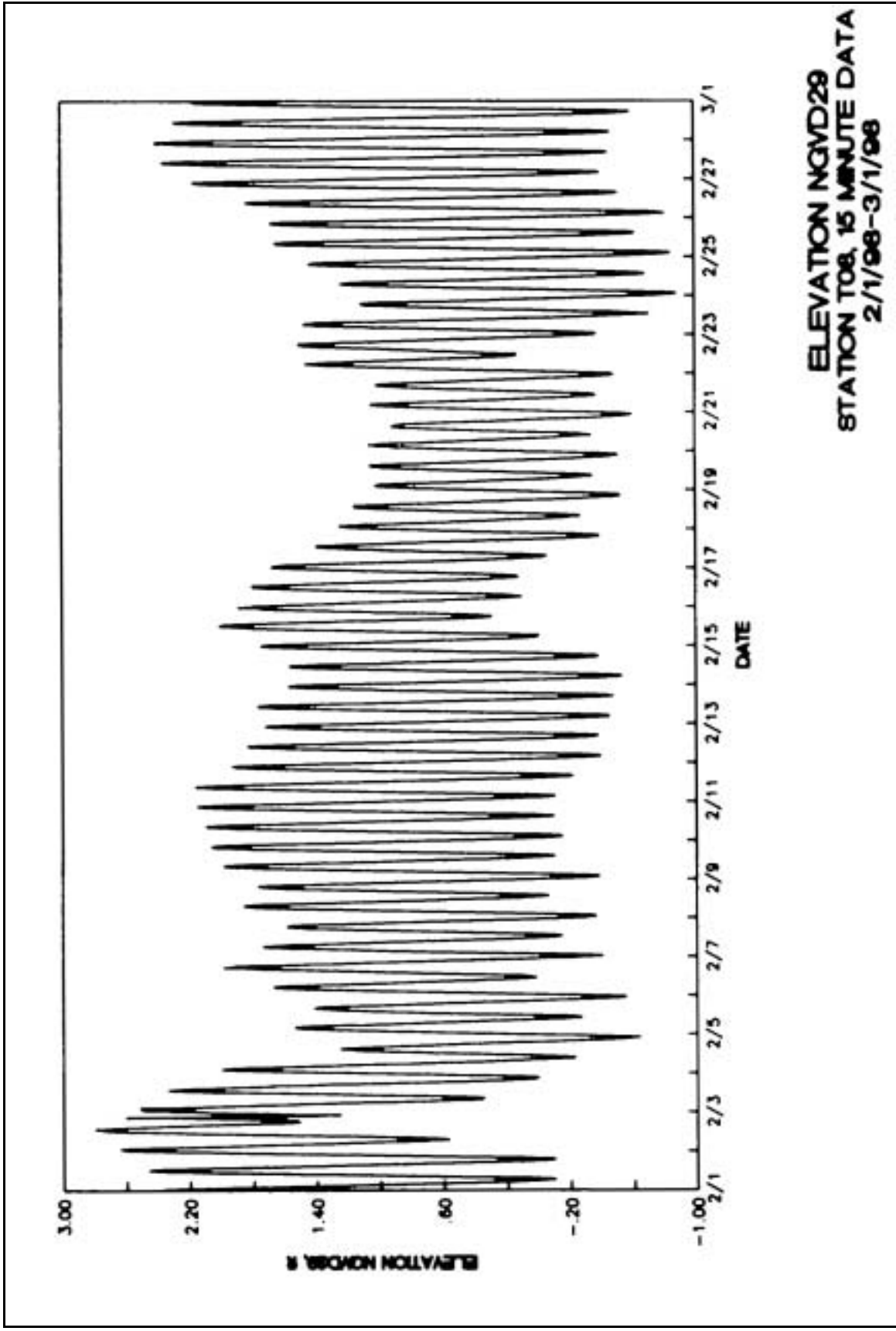




**DISSOLVED OXYGEN
STATION T07, 15 MINUTE DATA
2/1/98-3/1/98**



DISSOLVED OXYGEN
STATION T07, 15 MINUTE DATA
2/1/98-3/1/98



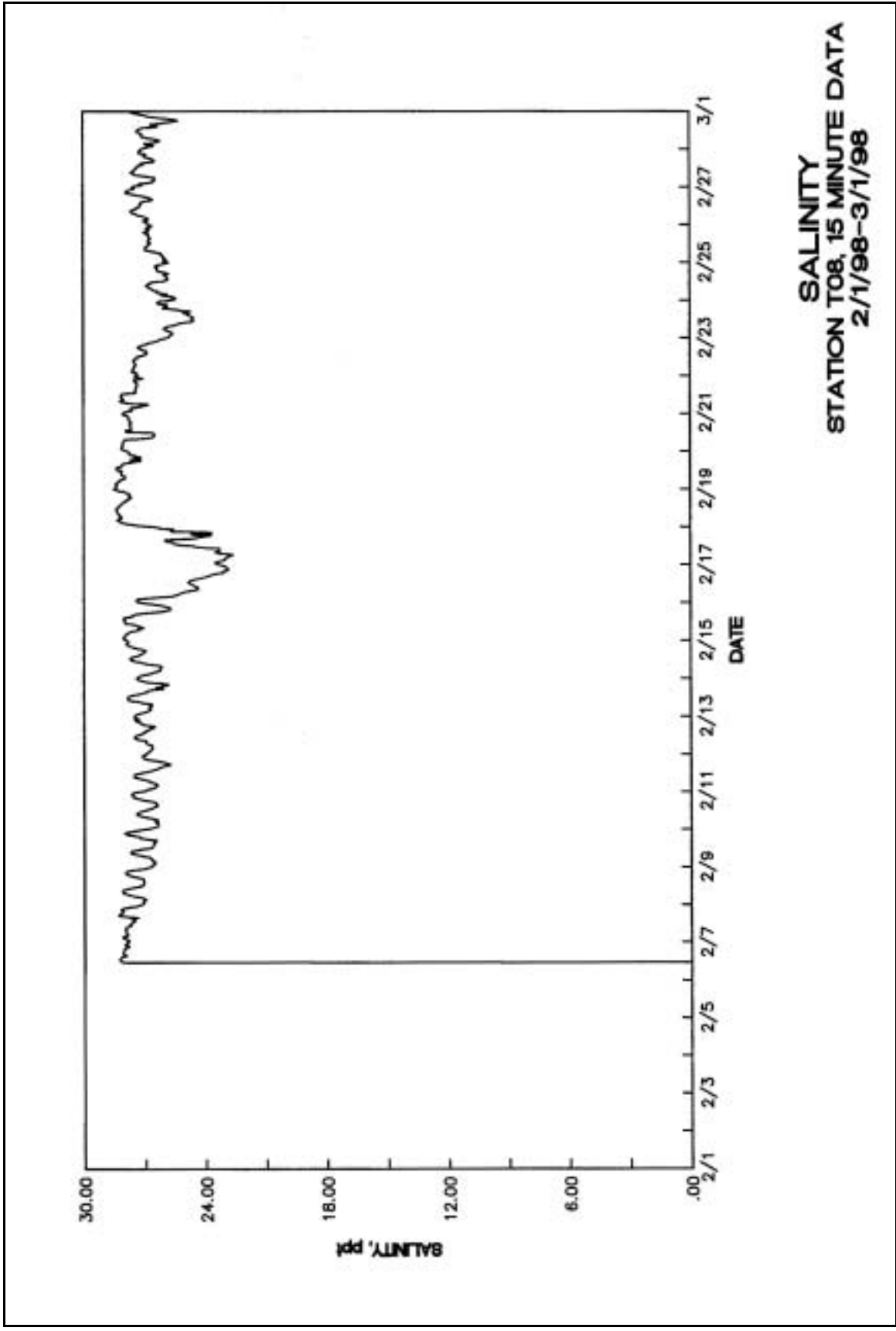
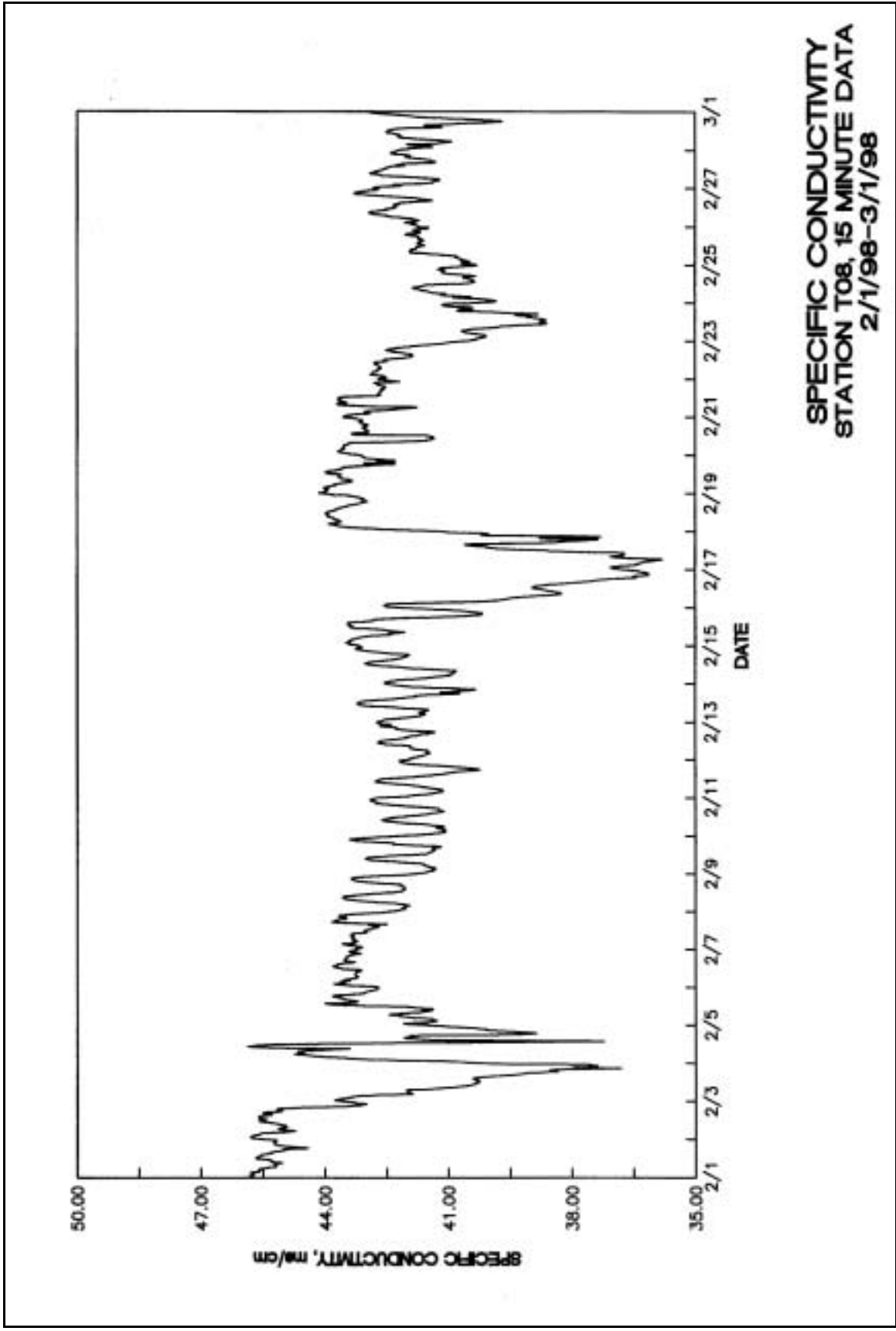


Plate 140



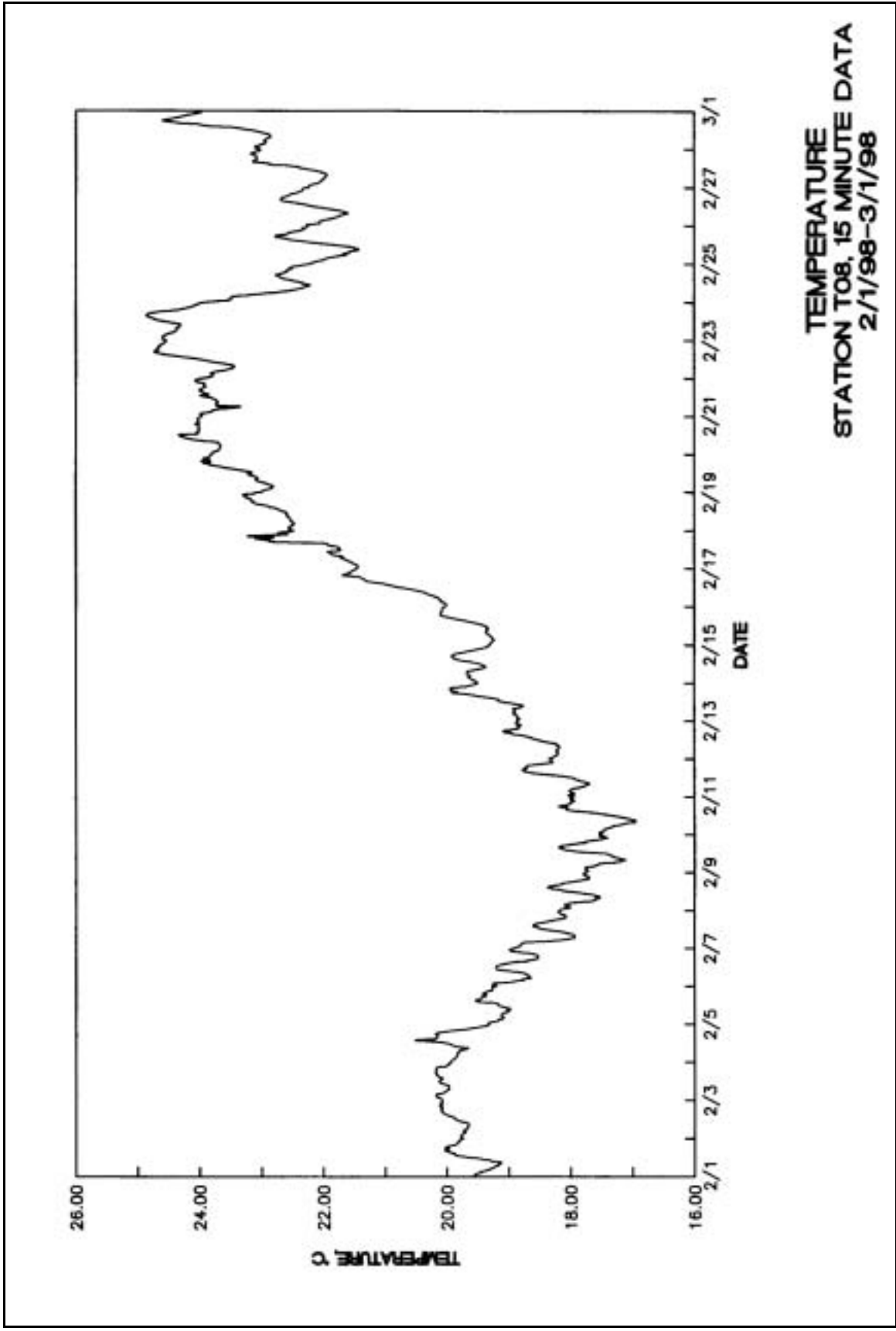
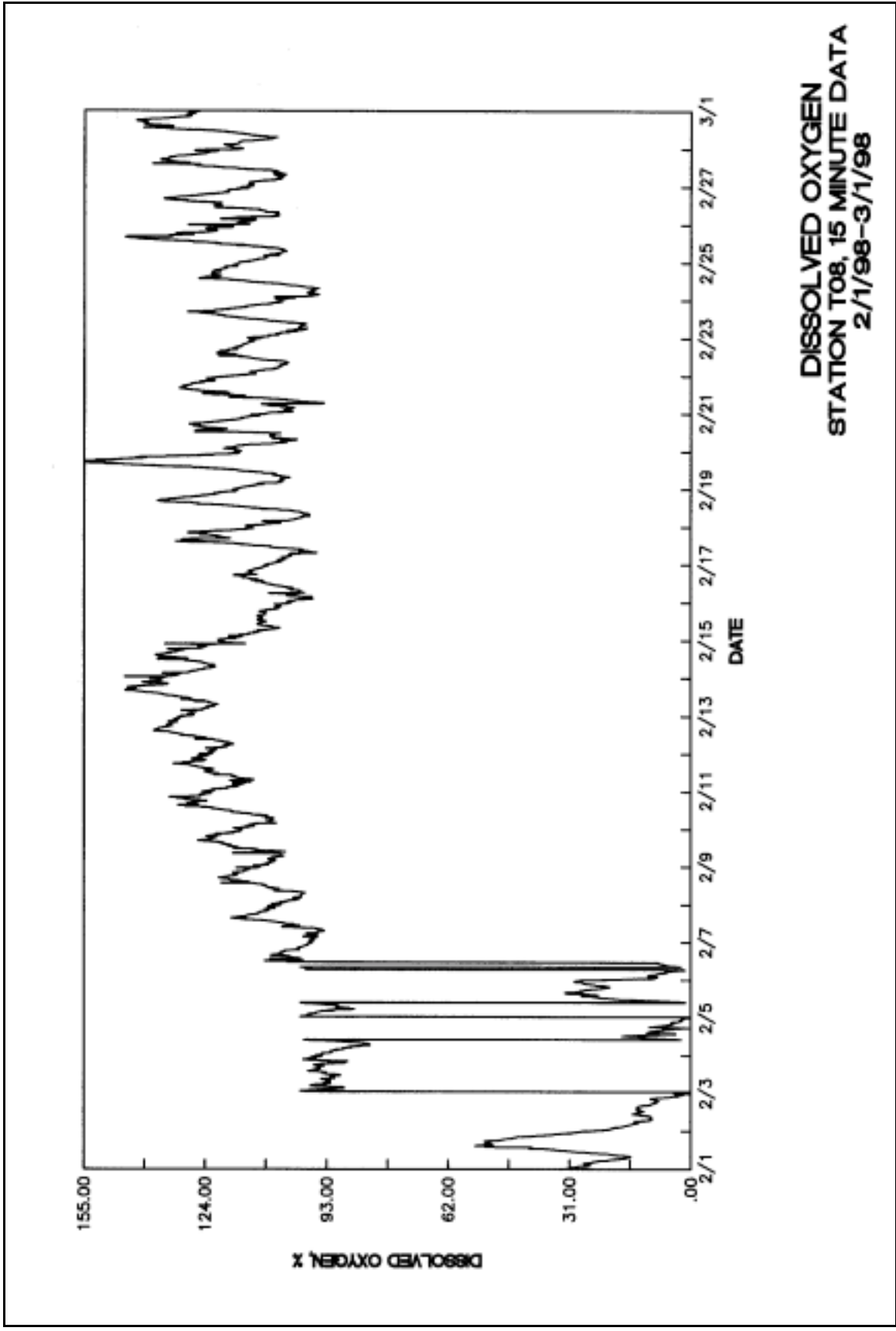
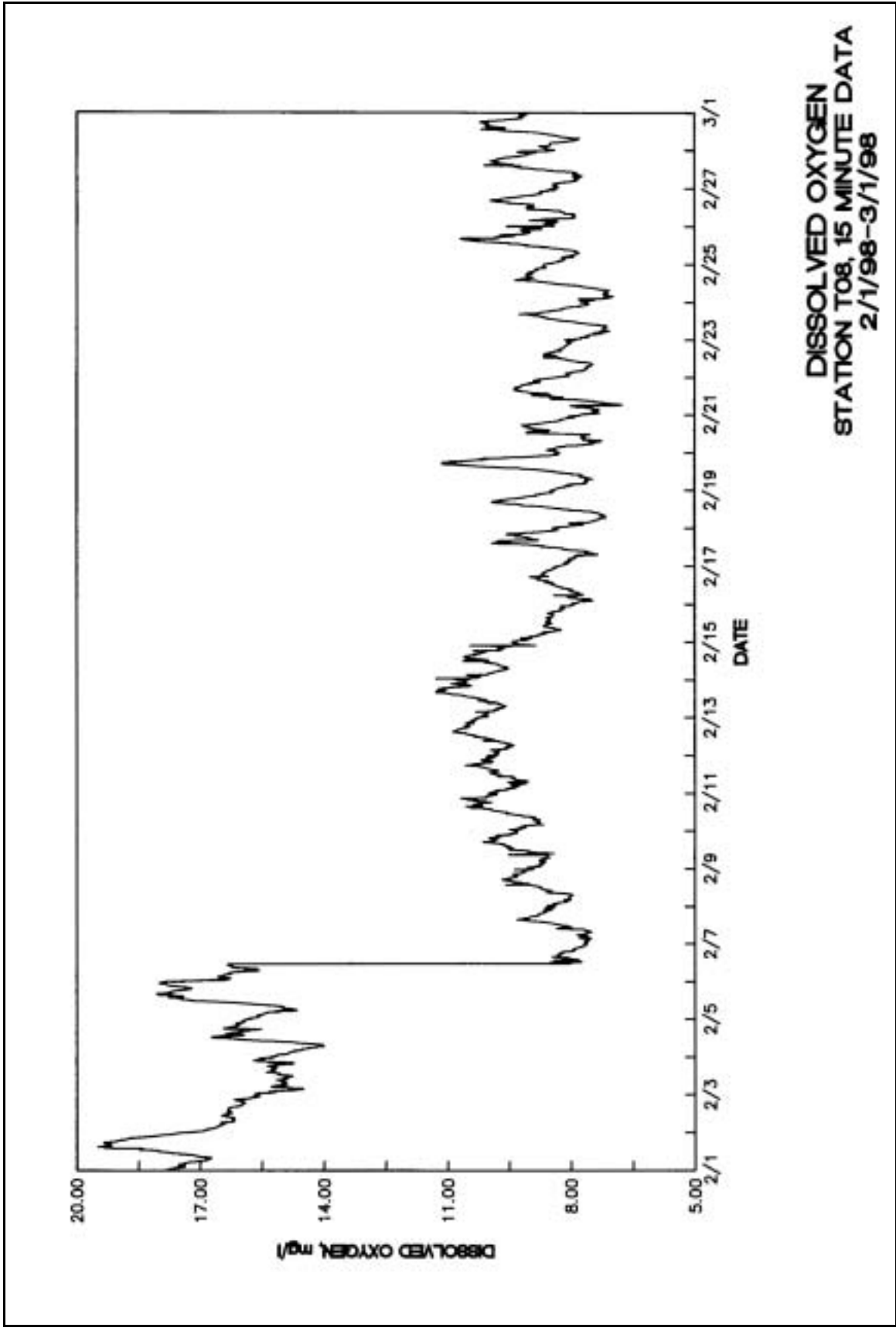


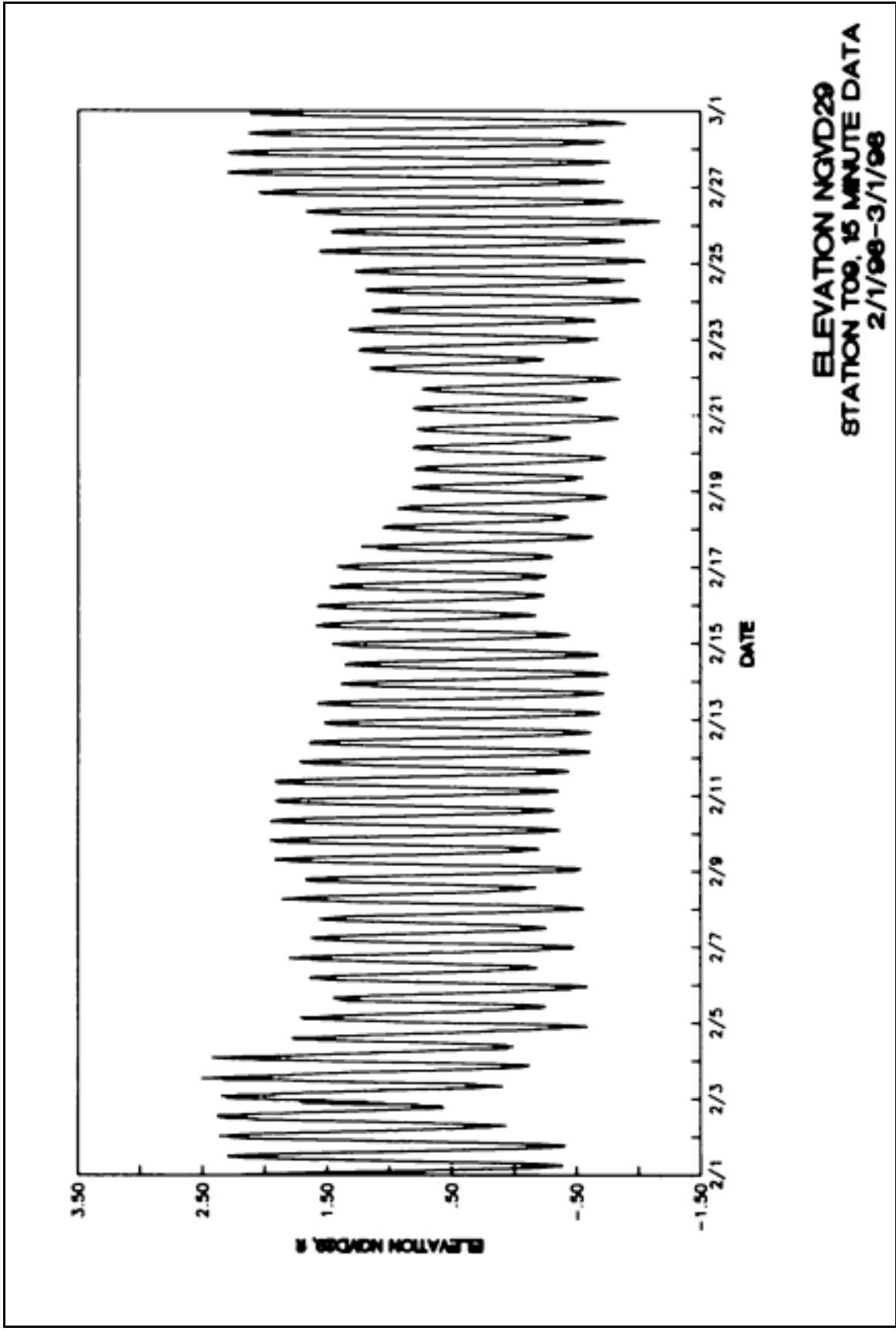
Plate 142

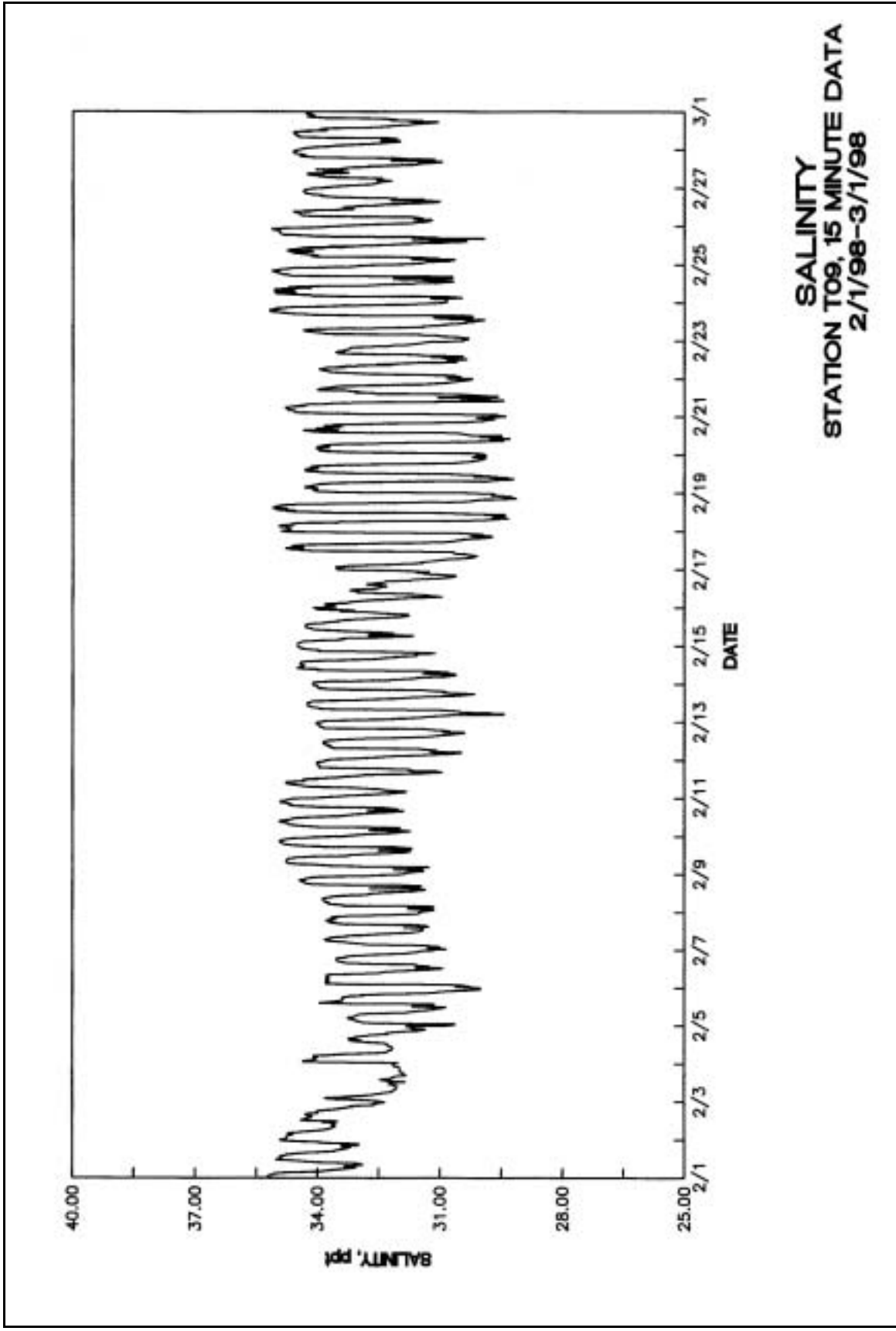


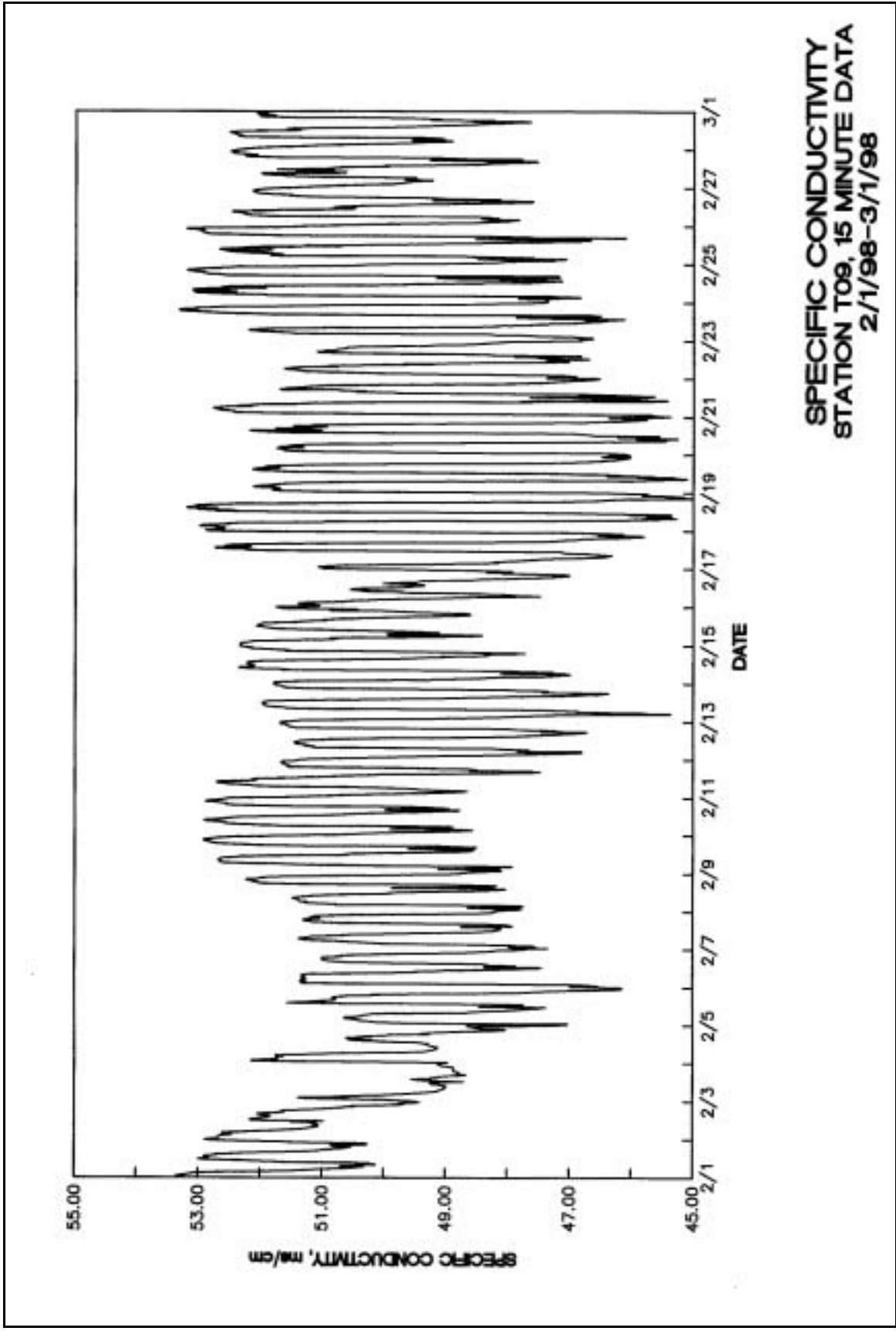
DISSOLVED OXYGEN
STATION T08, 15 MINUTE DATA
2/1/98-3/1/98



DISSOLVED OXYGEN
STATION T08, 15 MINUTE DATA
2/1/98-3/1/98







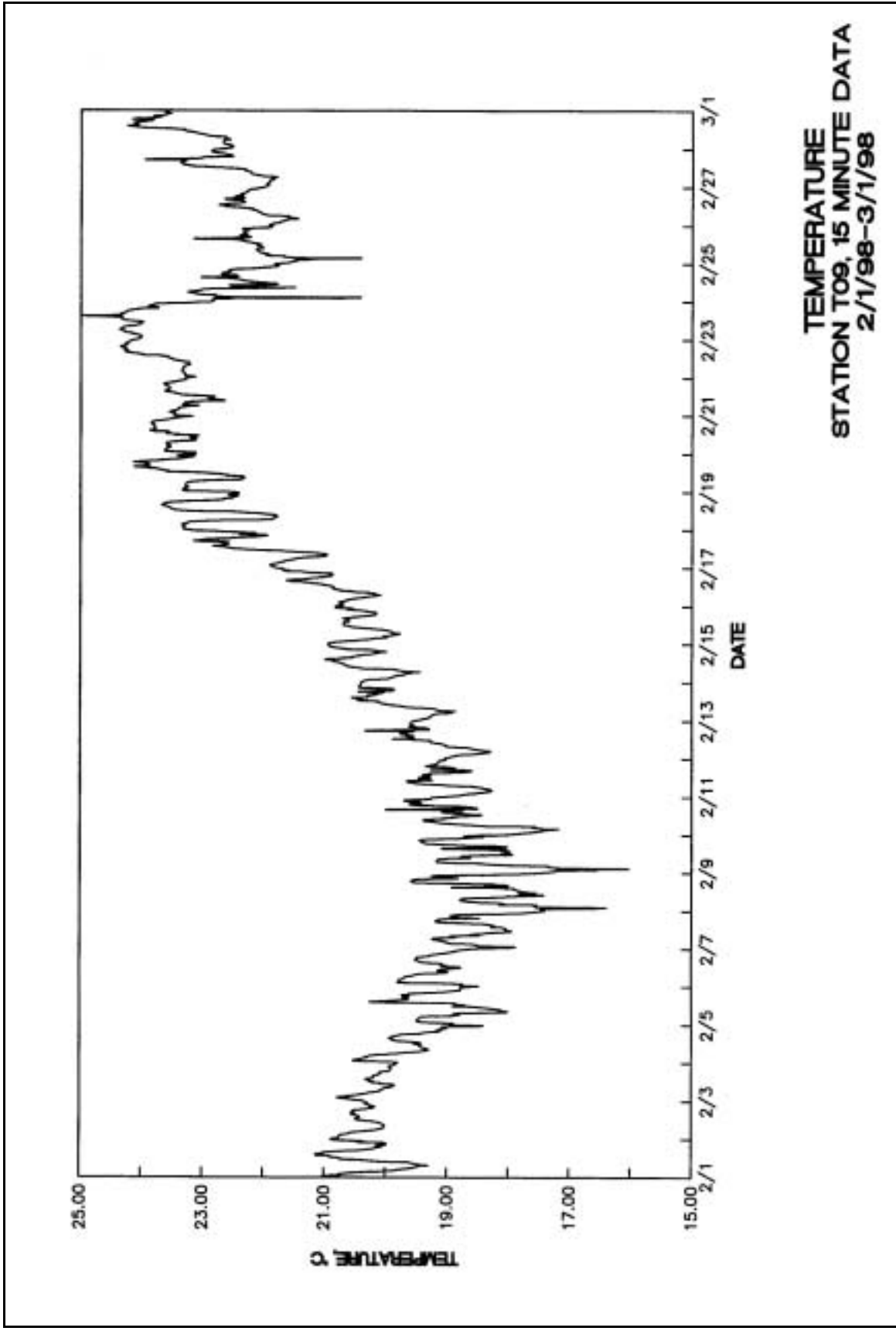
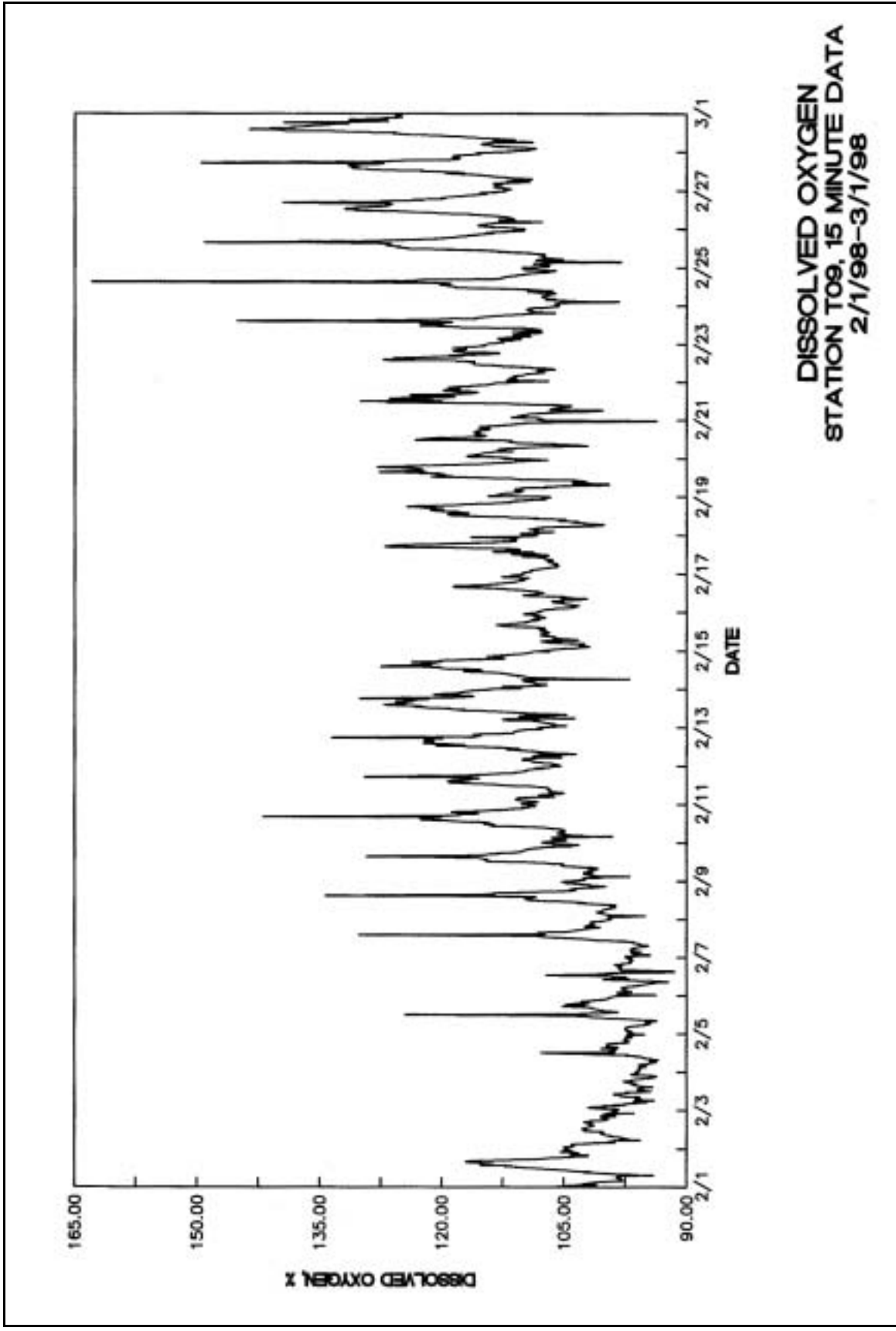


Plate 148



DISSOLVED OXYGEN
STATION T09, 15 MINUTE DATA
2/1/98-3/1/98

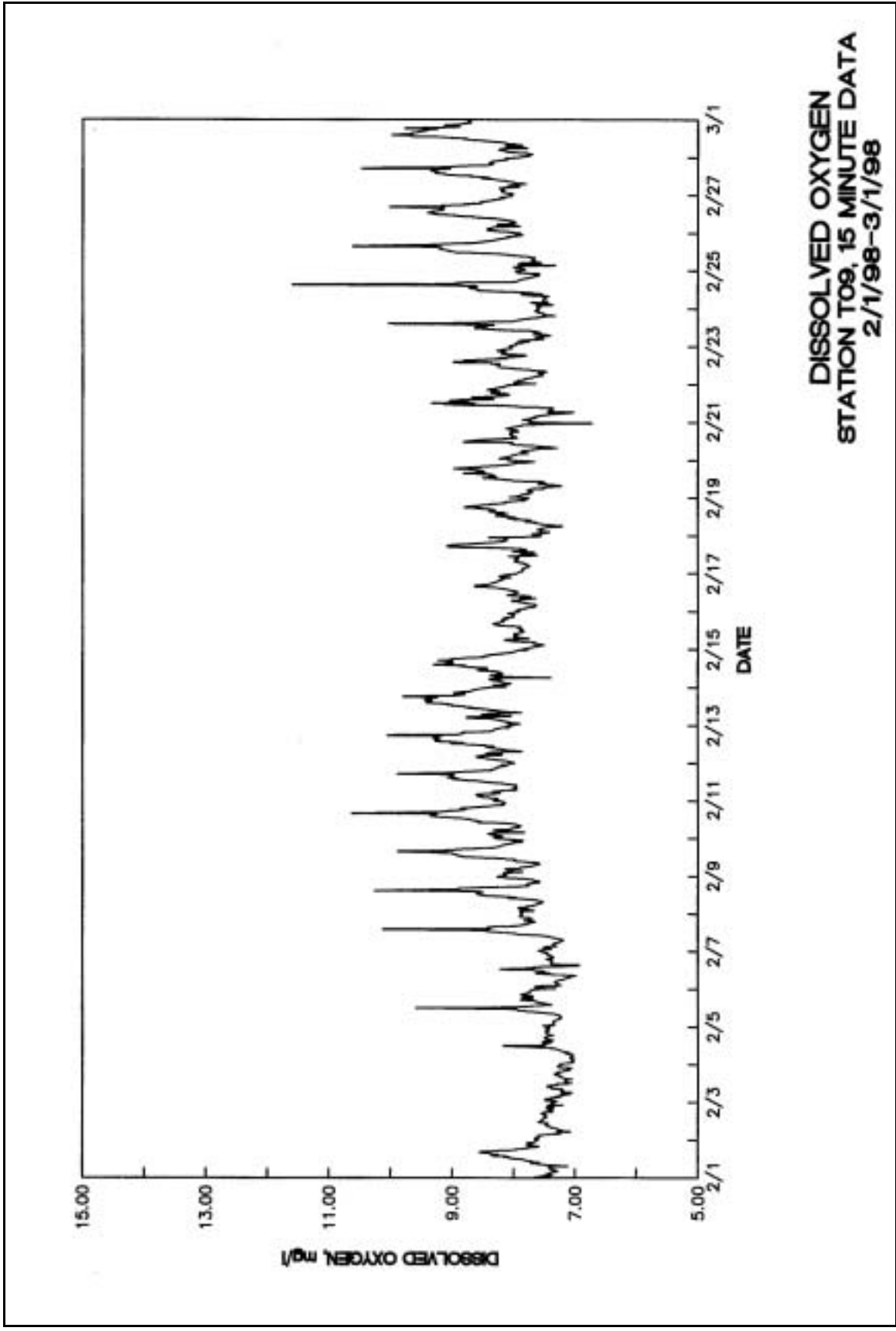
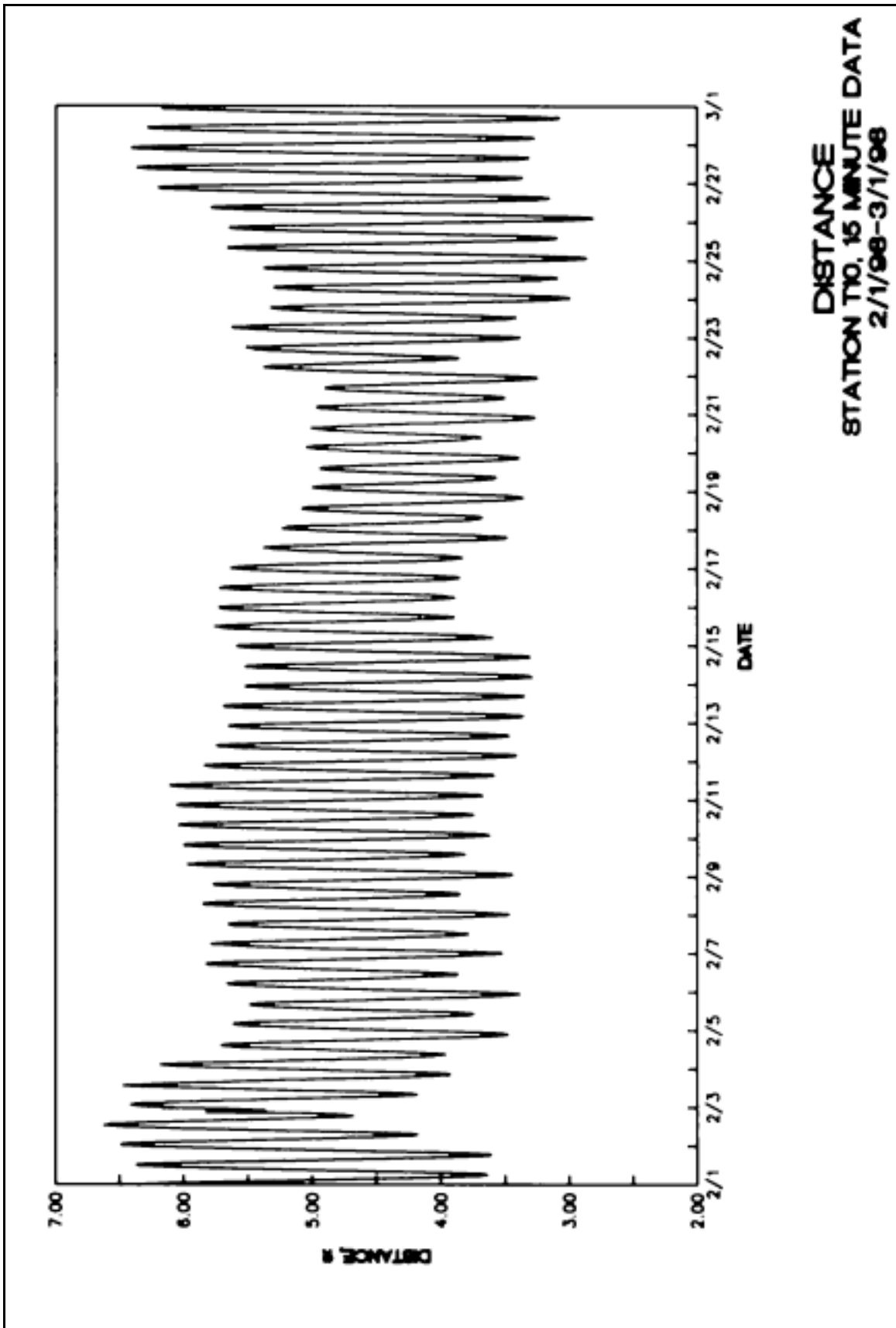
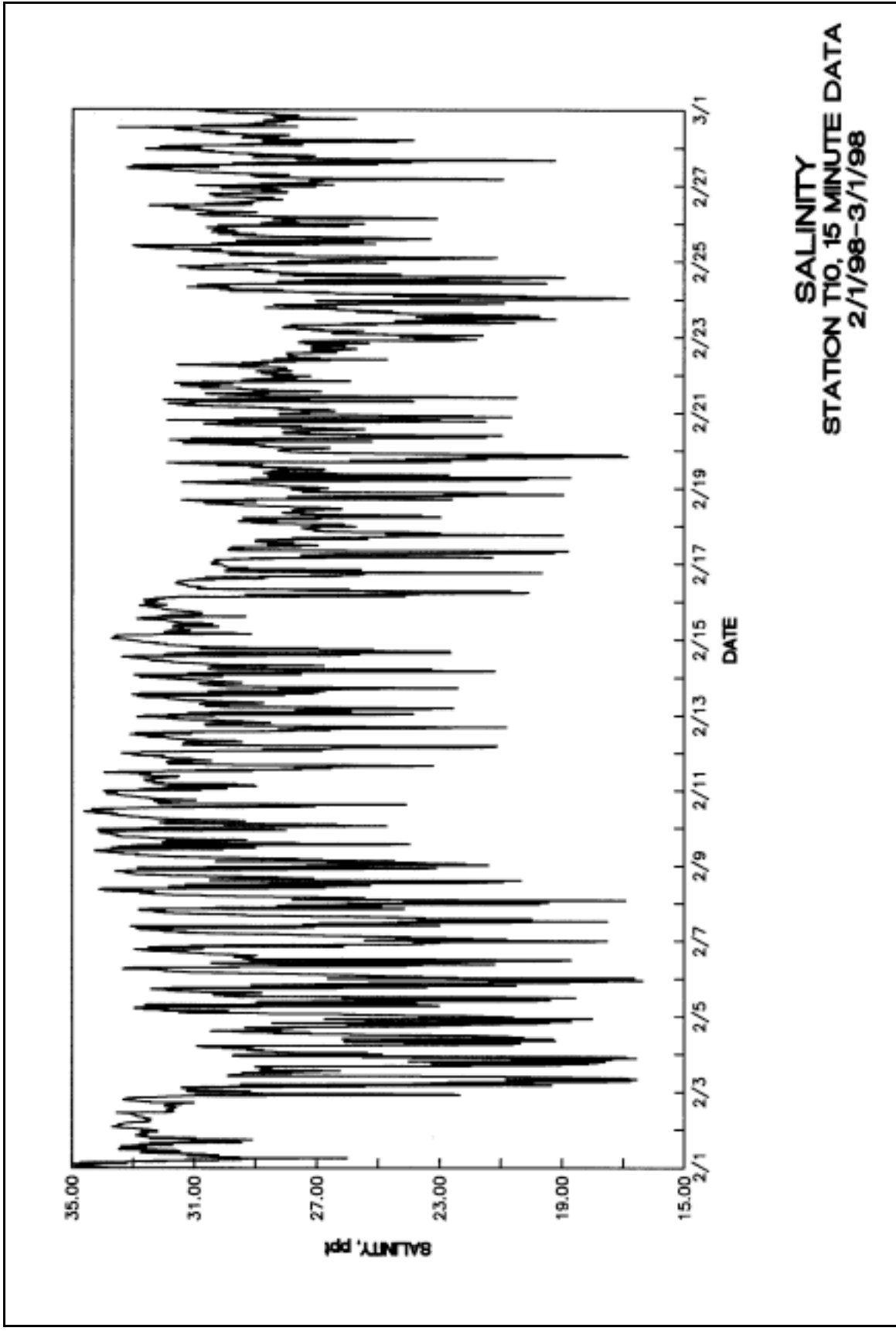
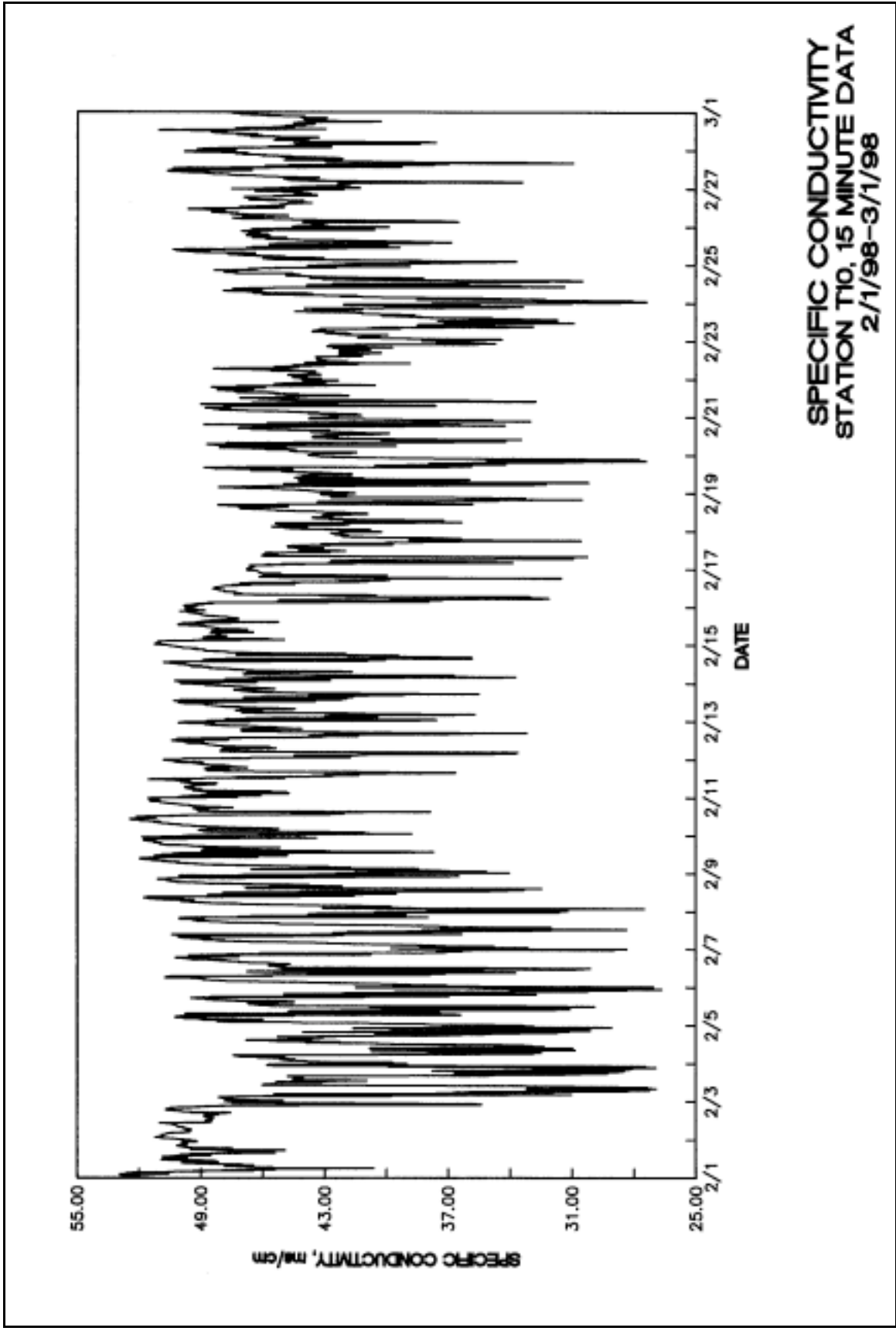


Plate 150







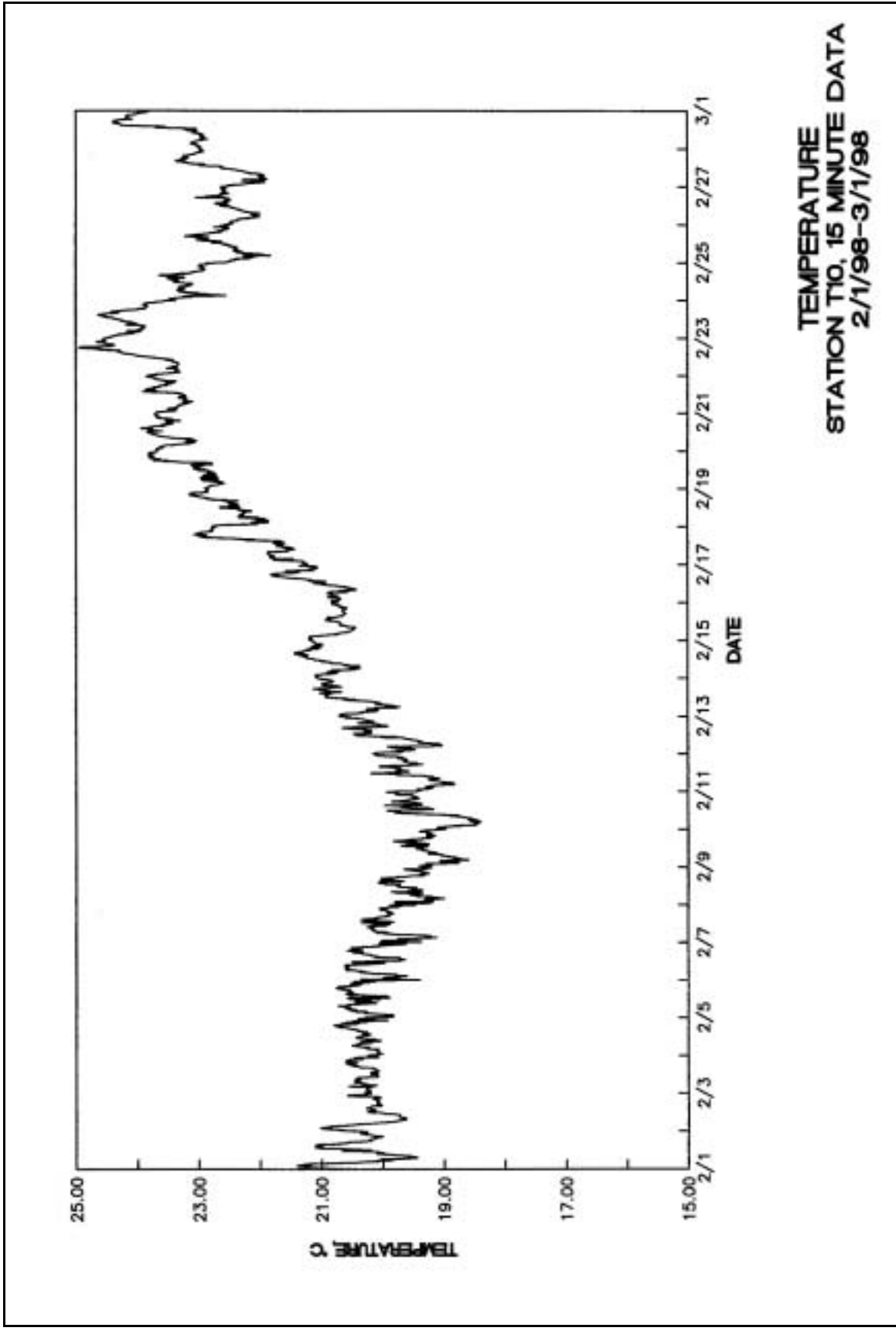
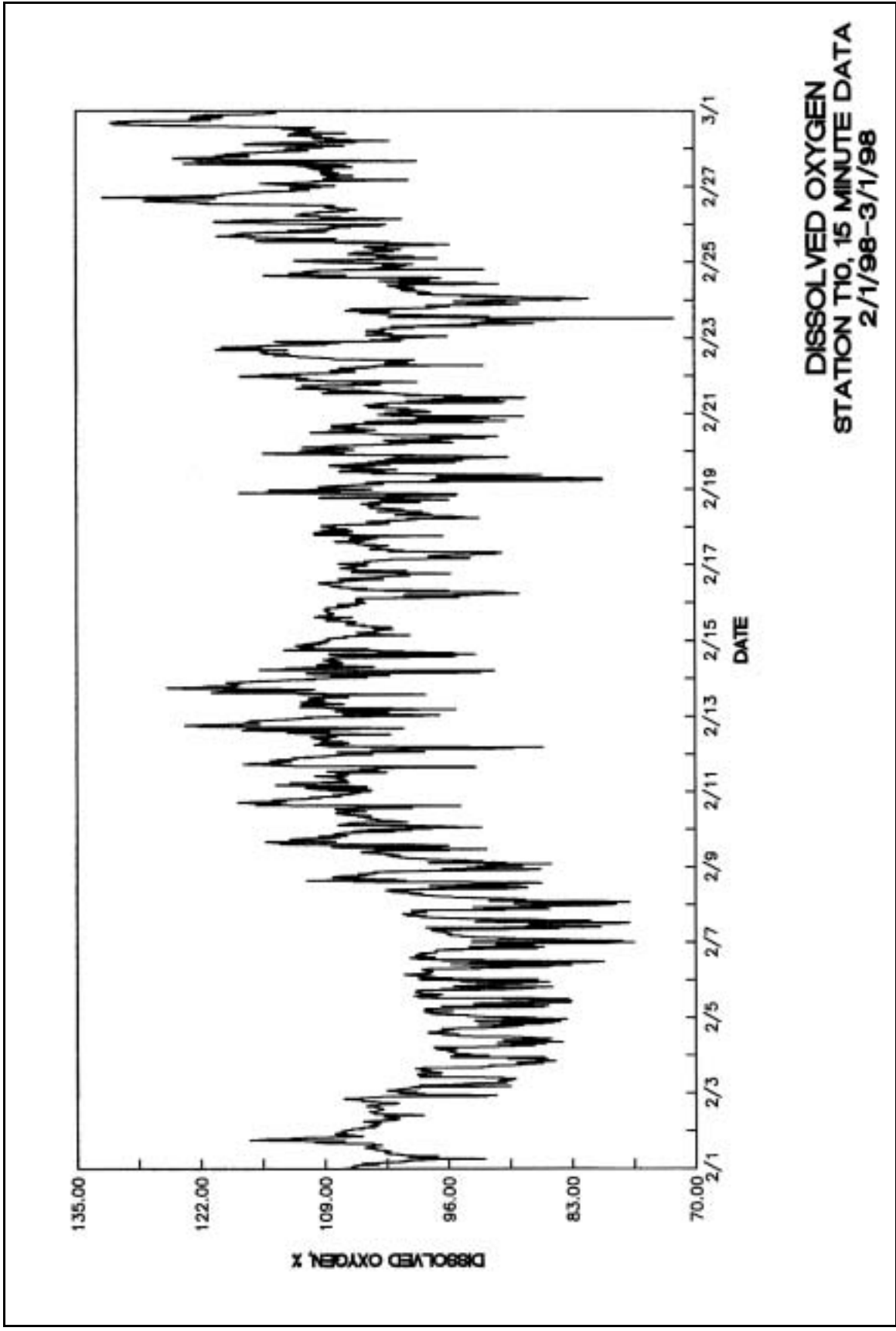


Plate 154



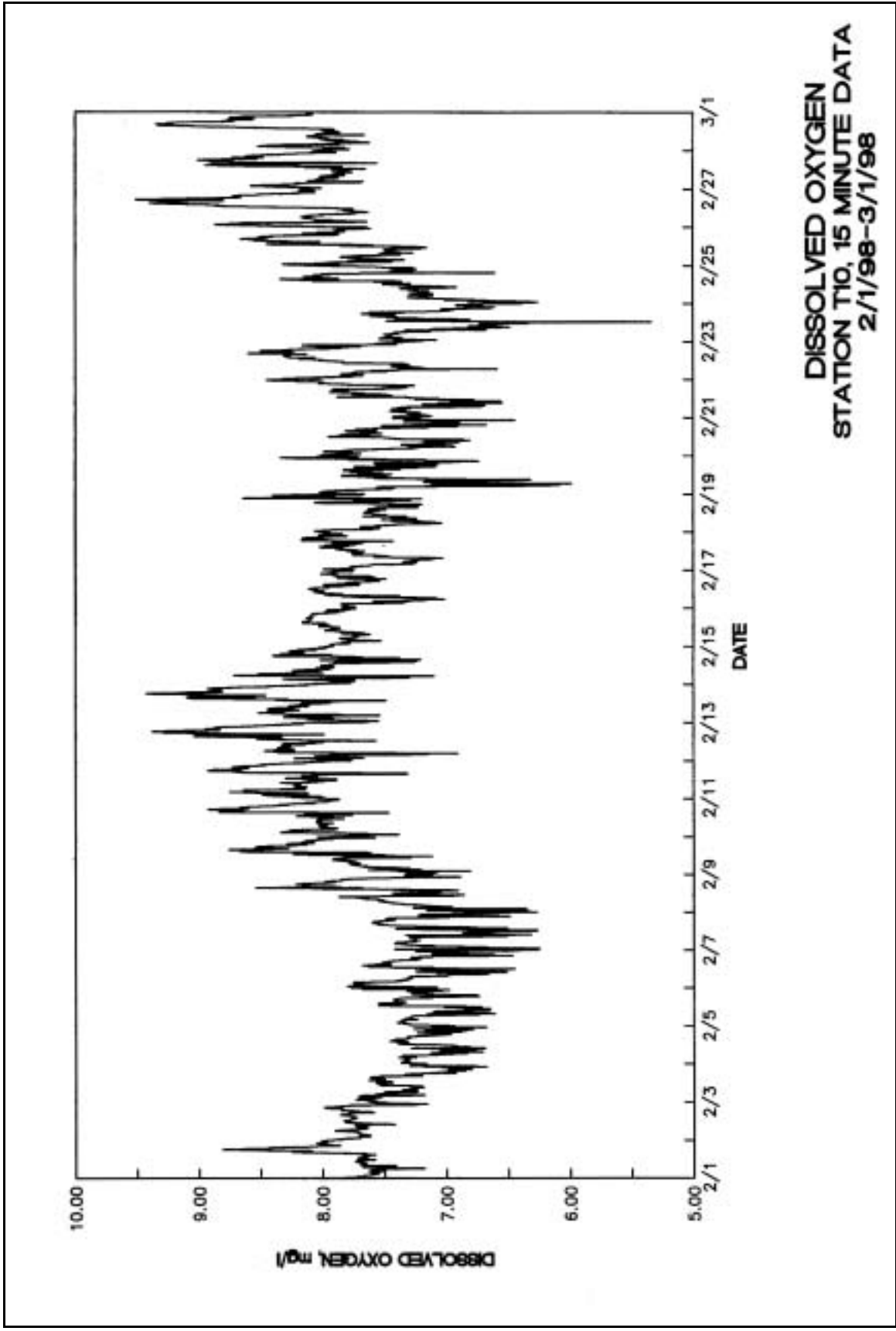
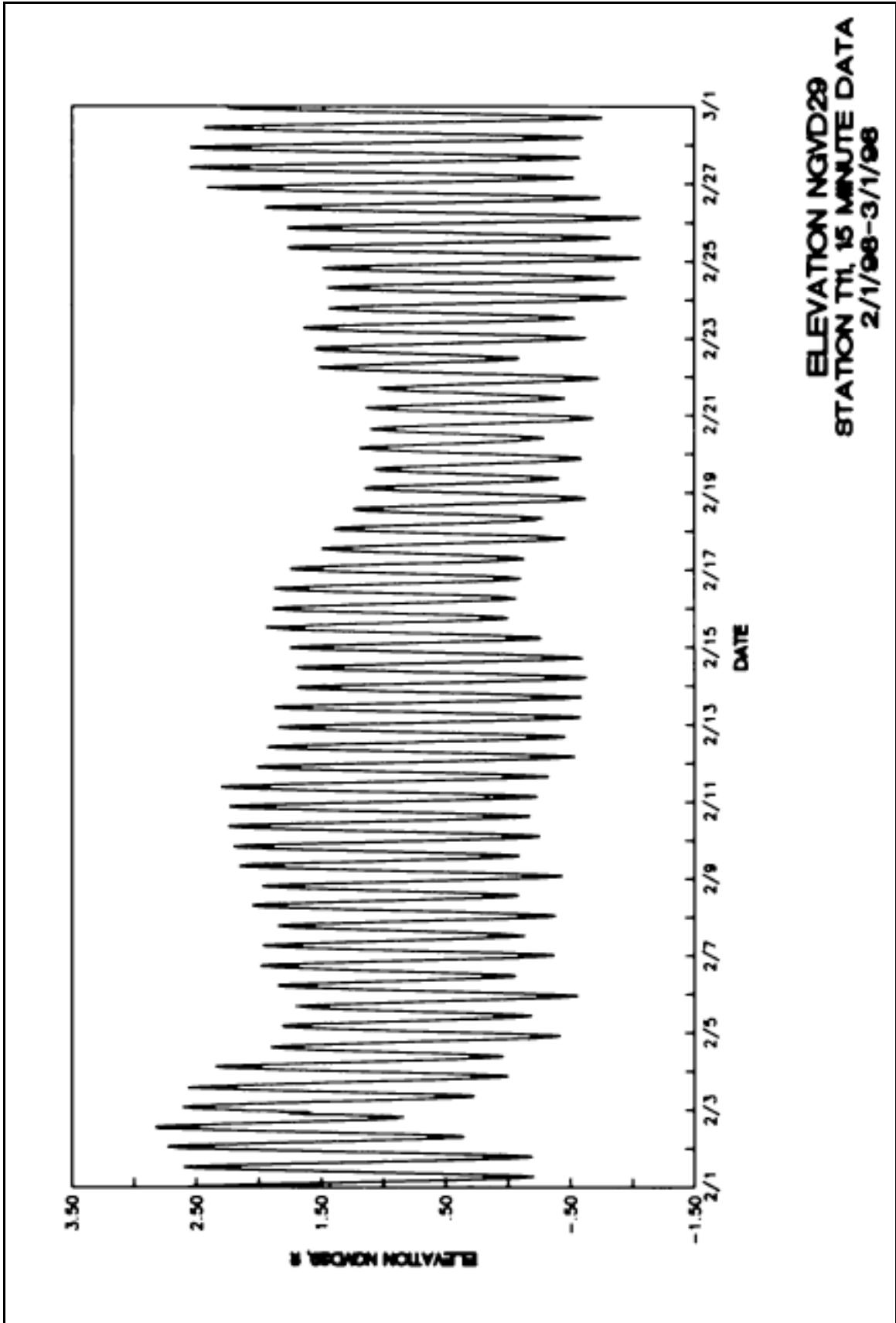
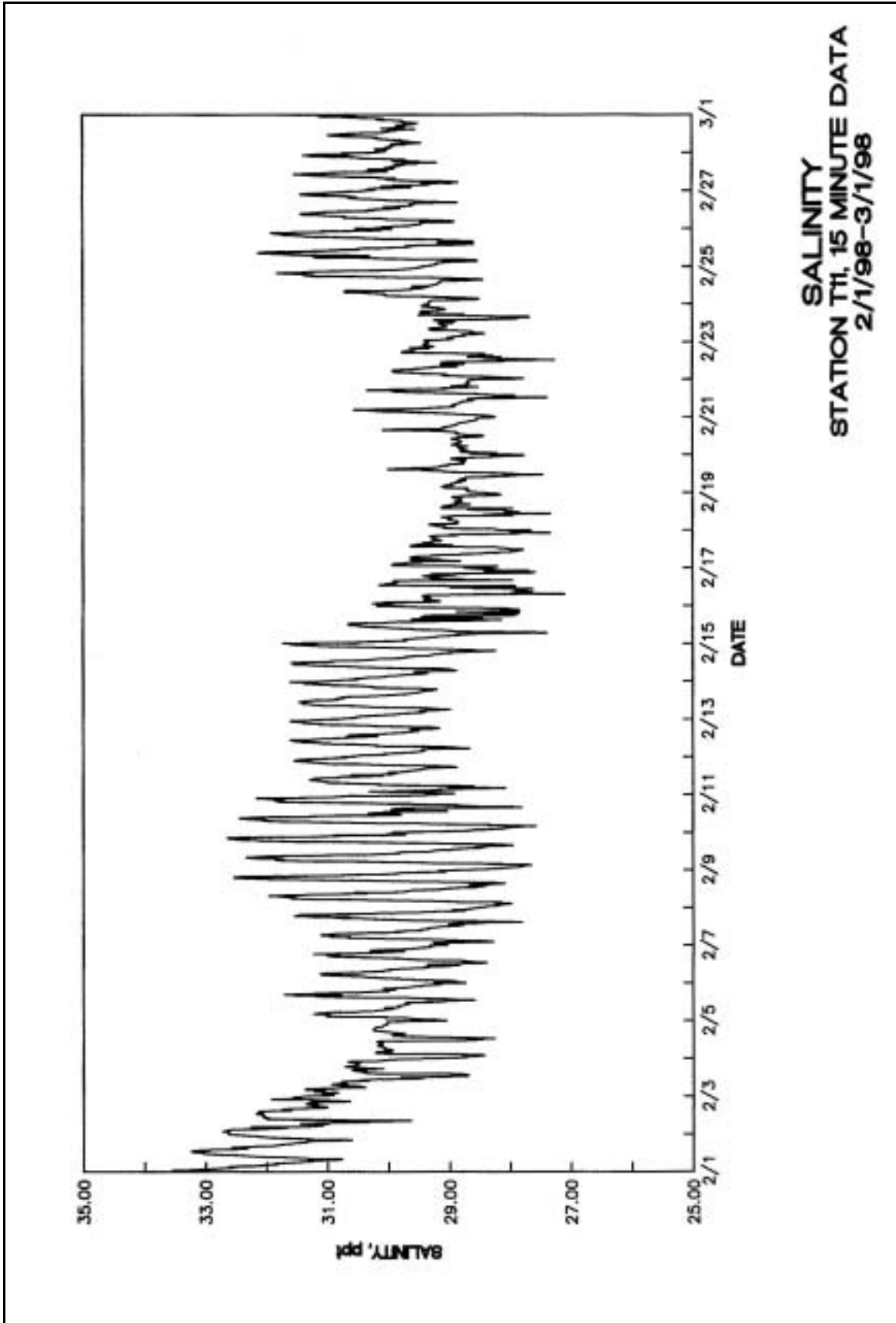
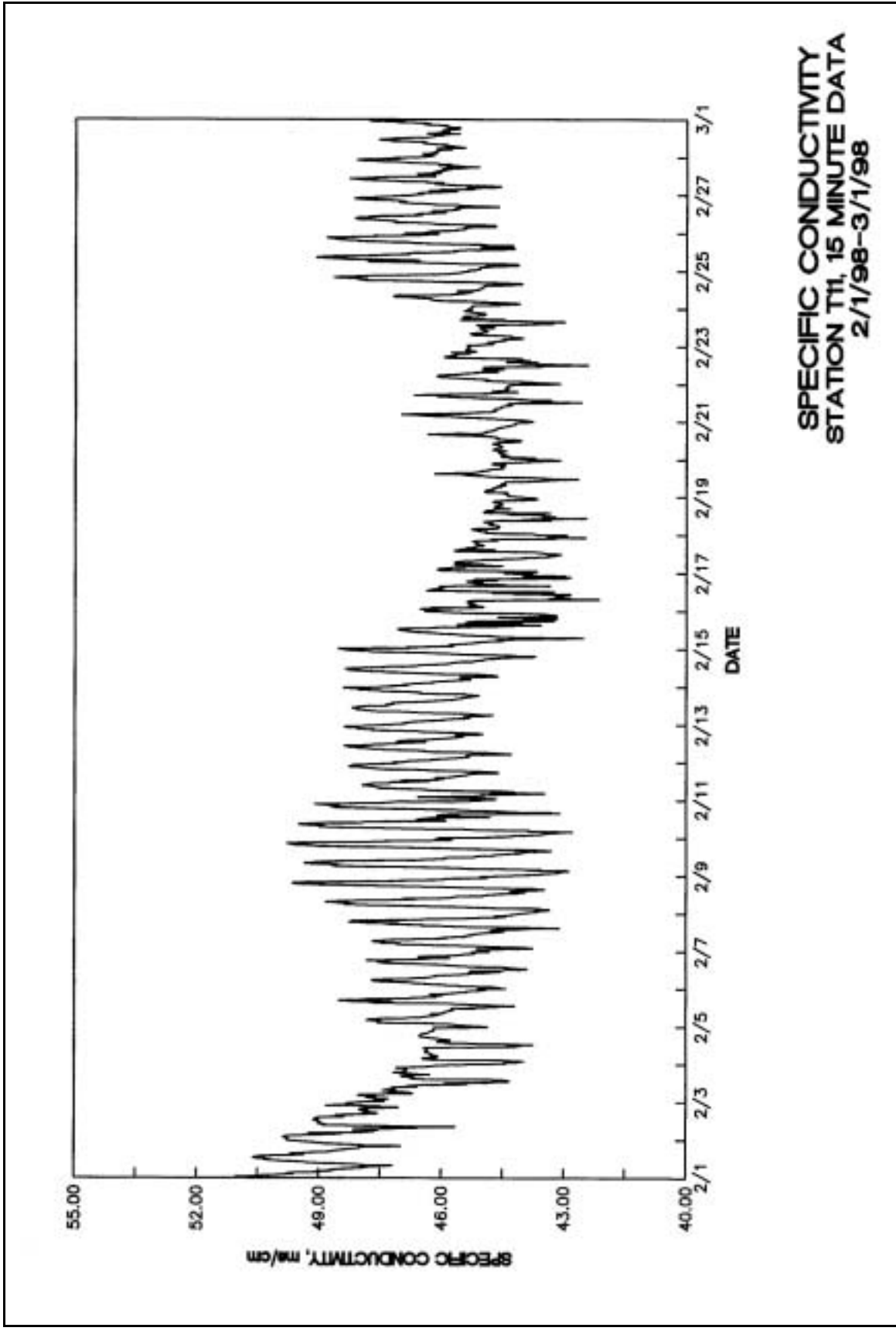


Plate 156







**SPECIFIC CONDUCTIVITY
STATION T11, 15 MINUTE DATA
2/1/98-3/1/98**

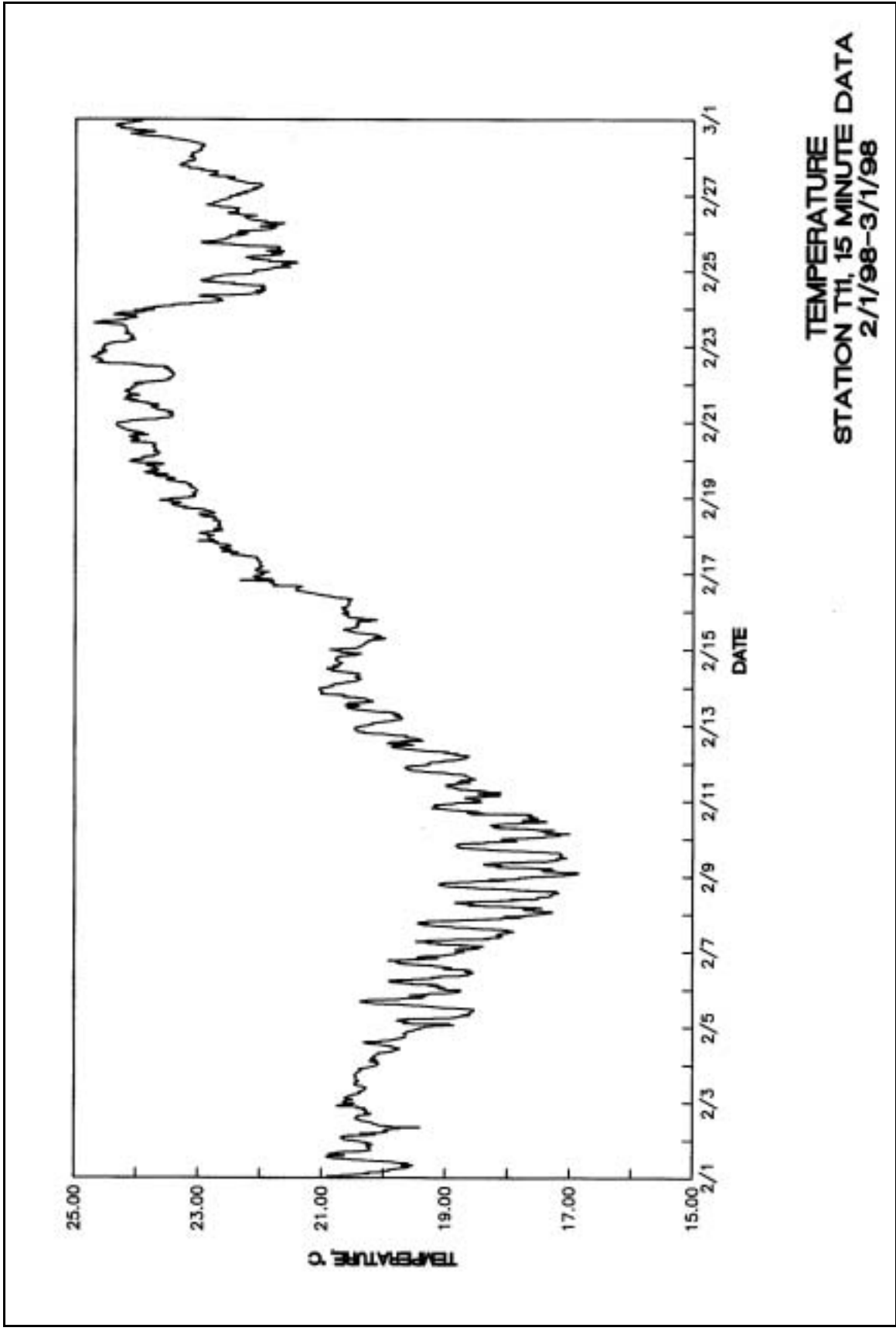
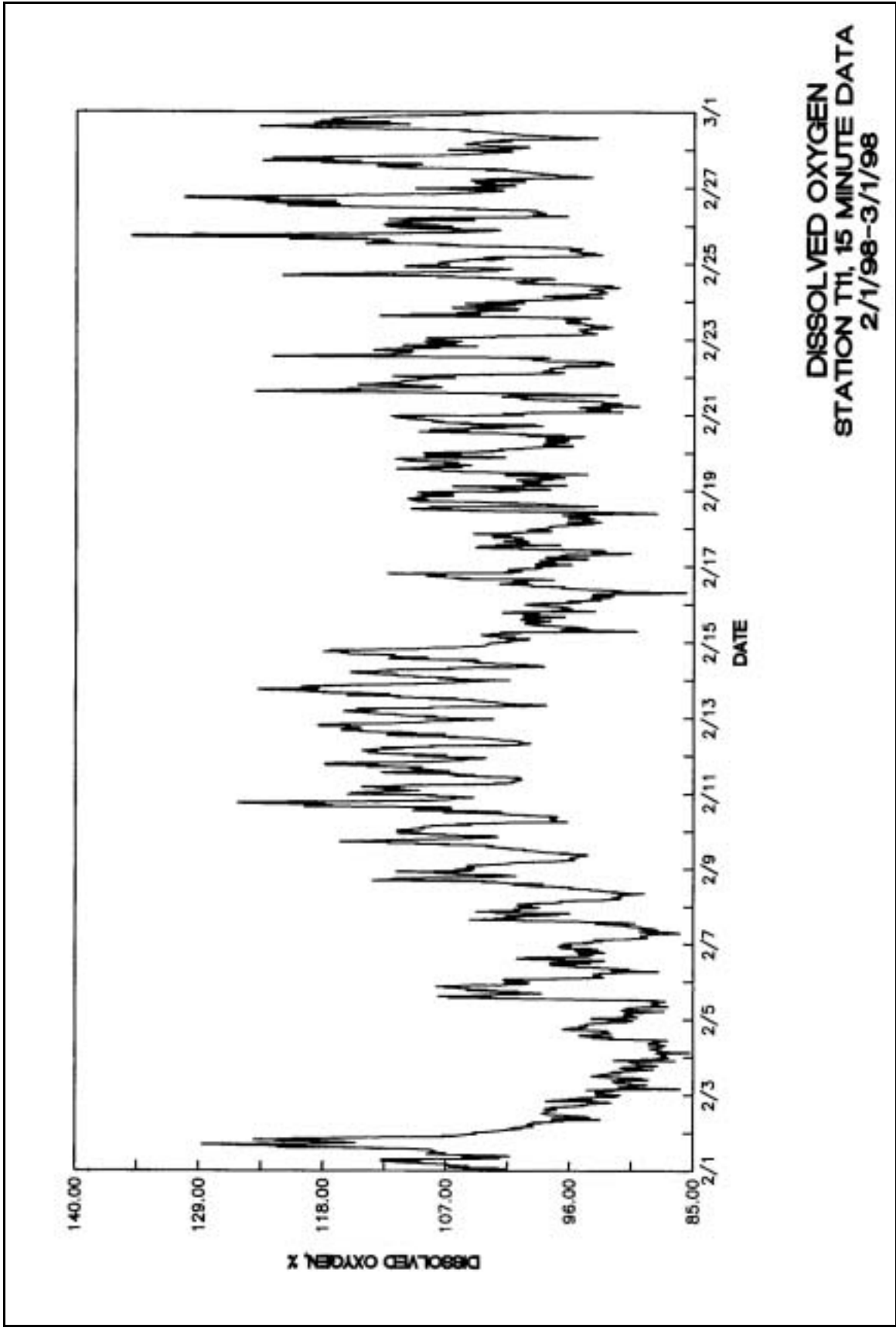
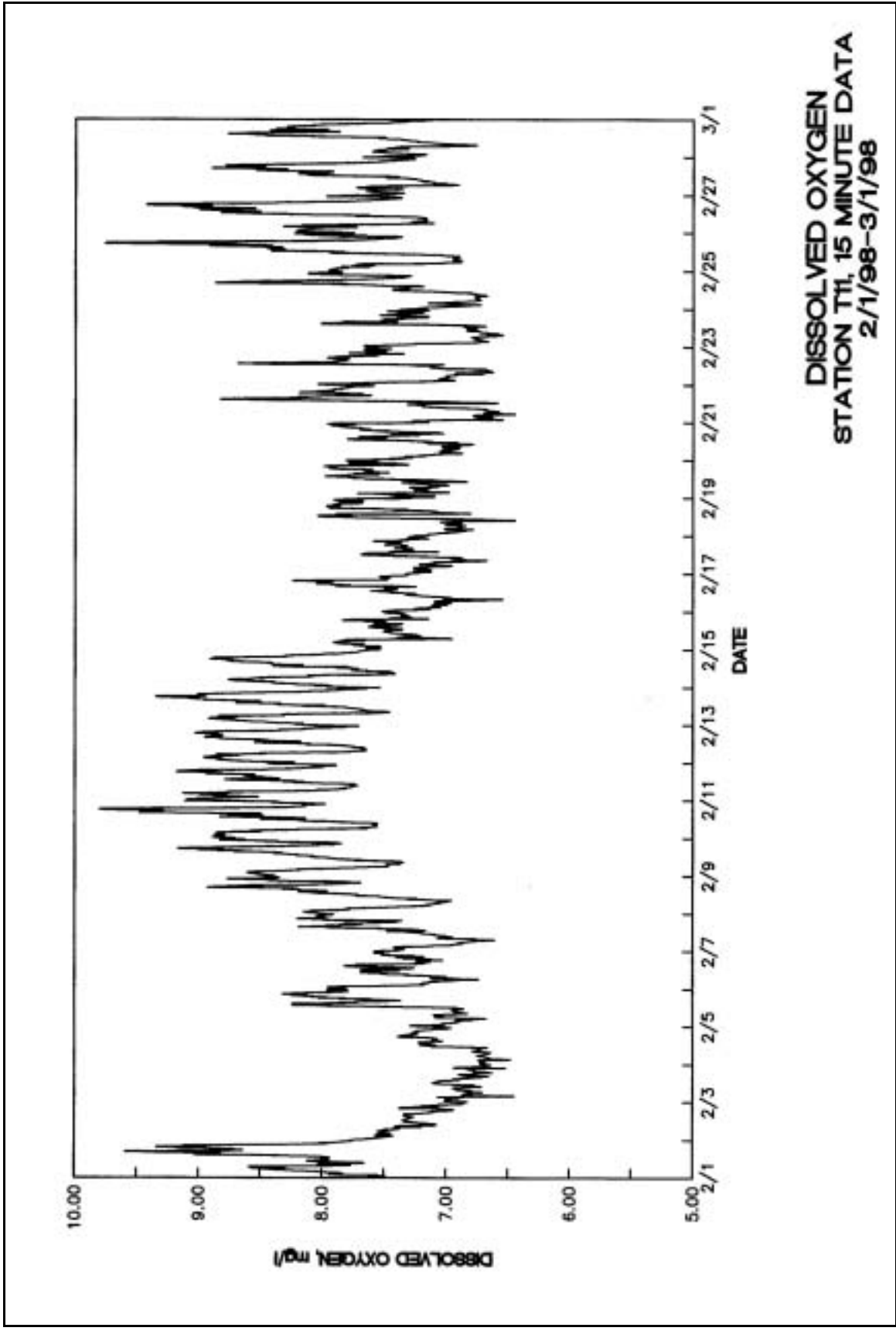
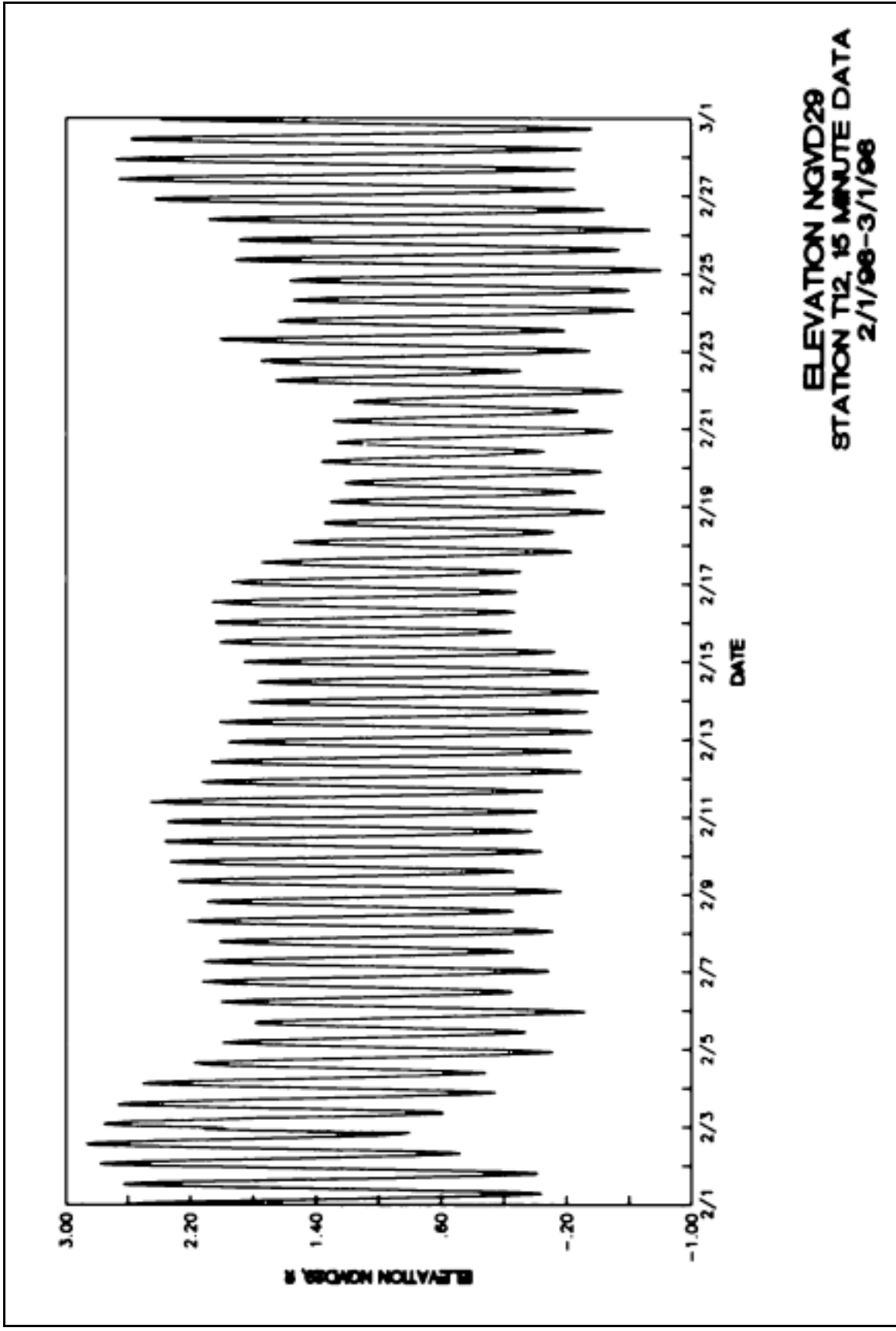
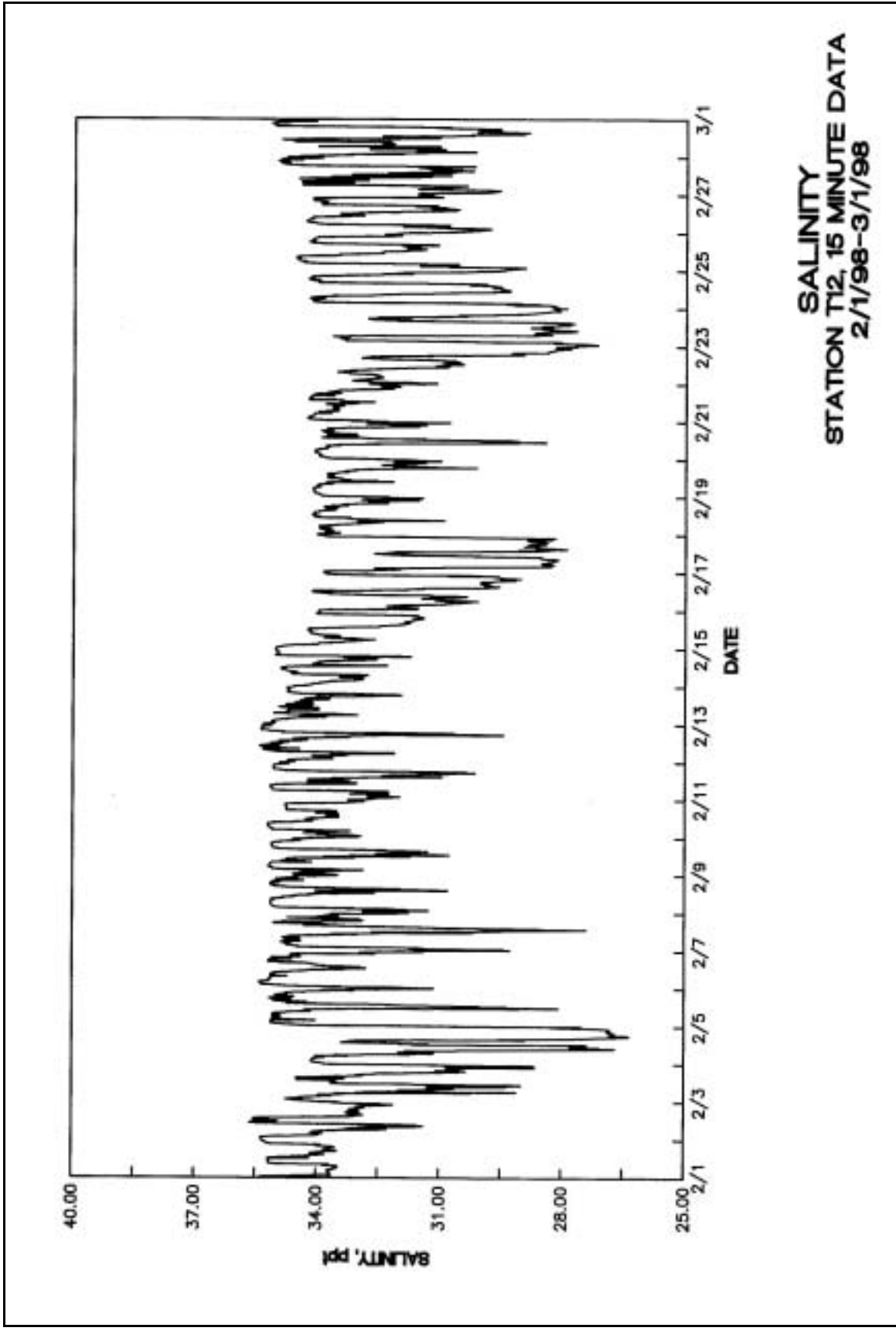


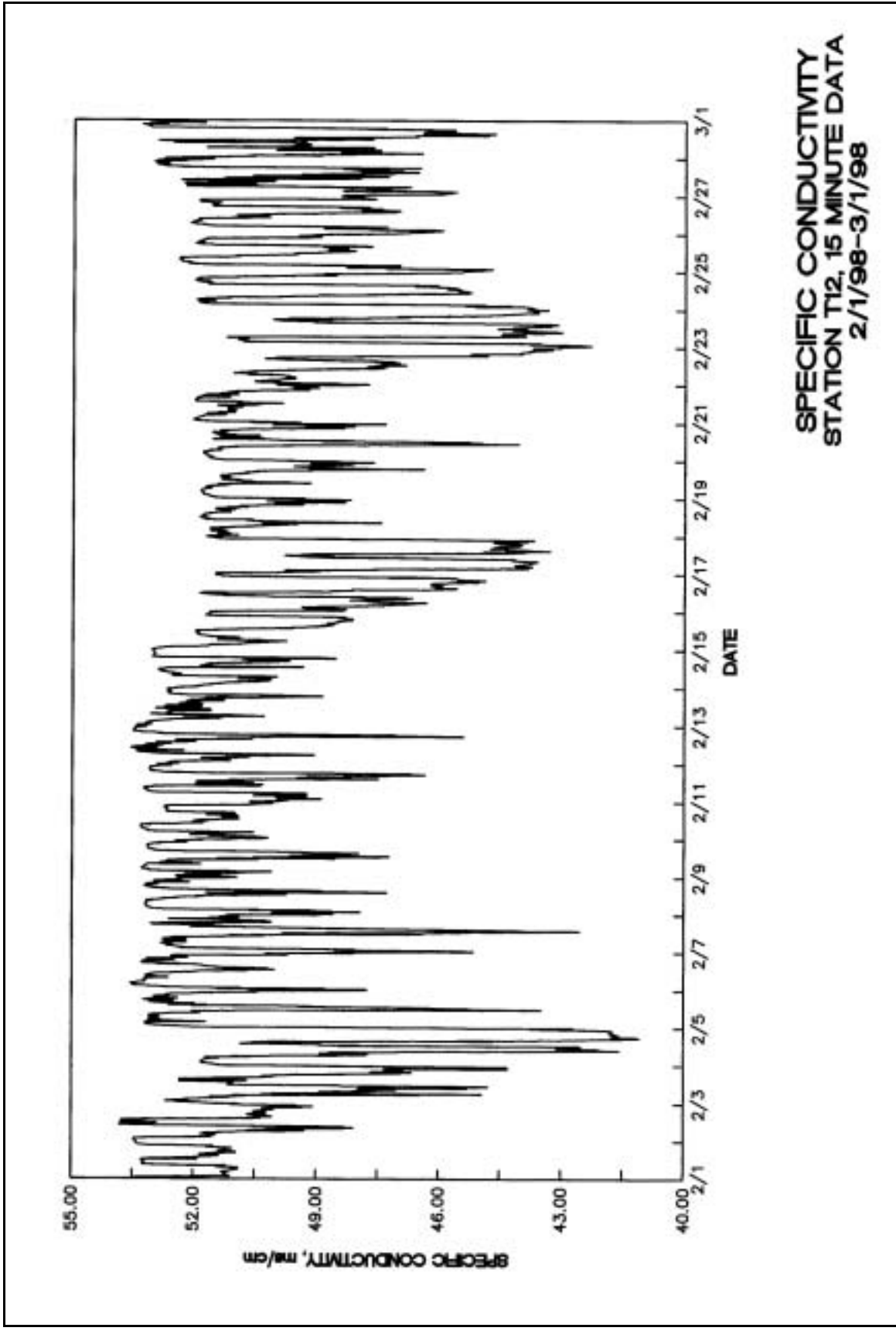
Plate 160

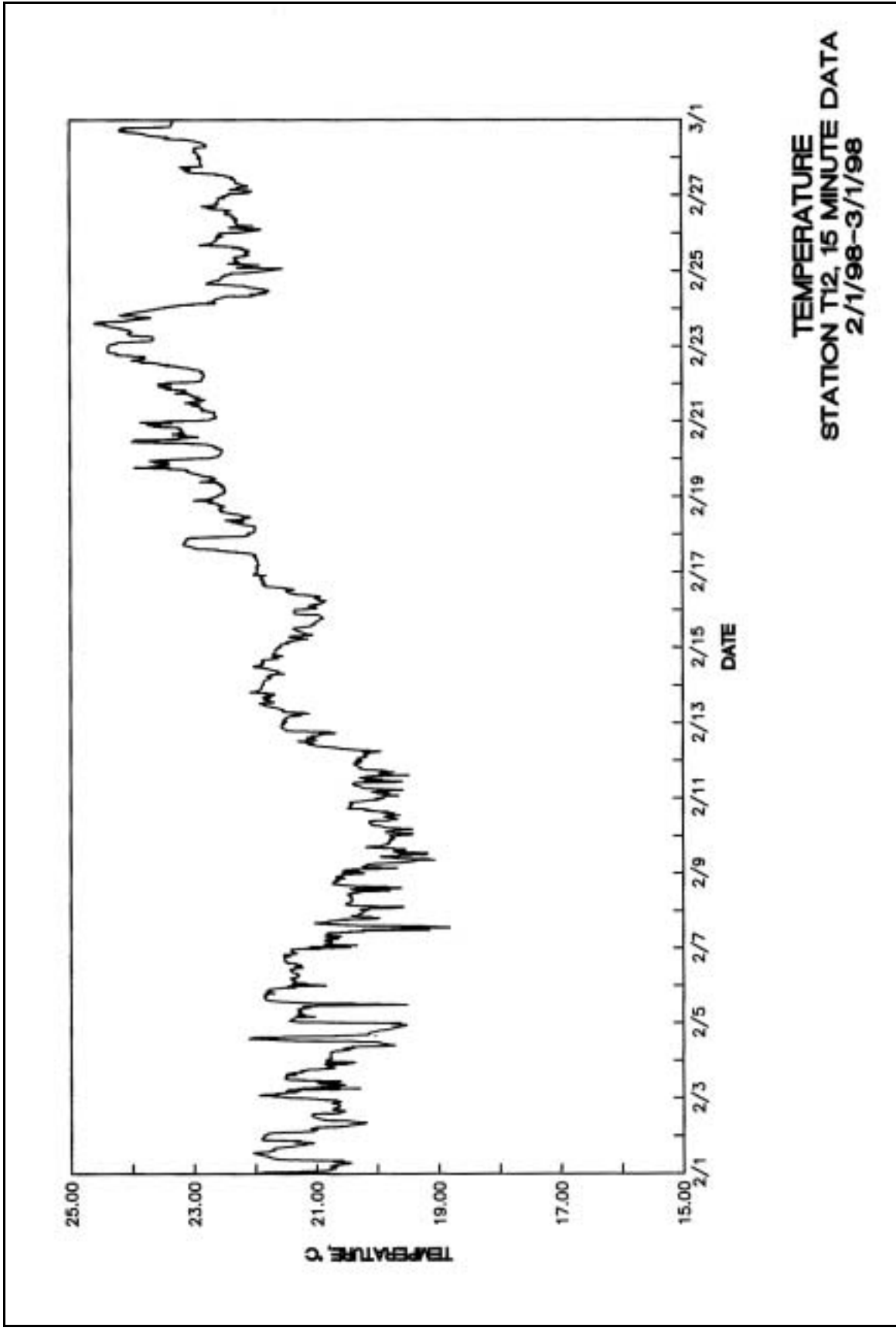


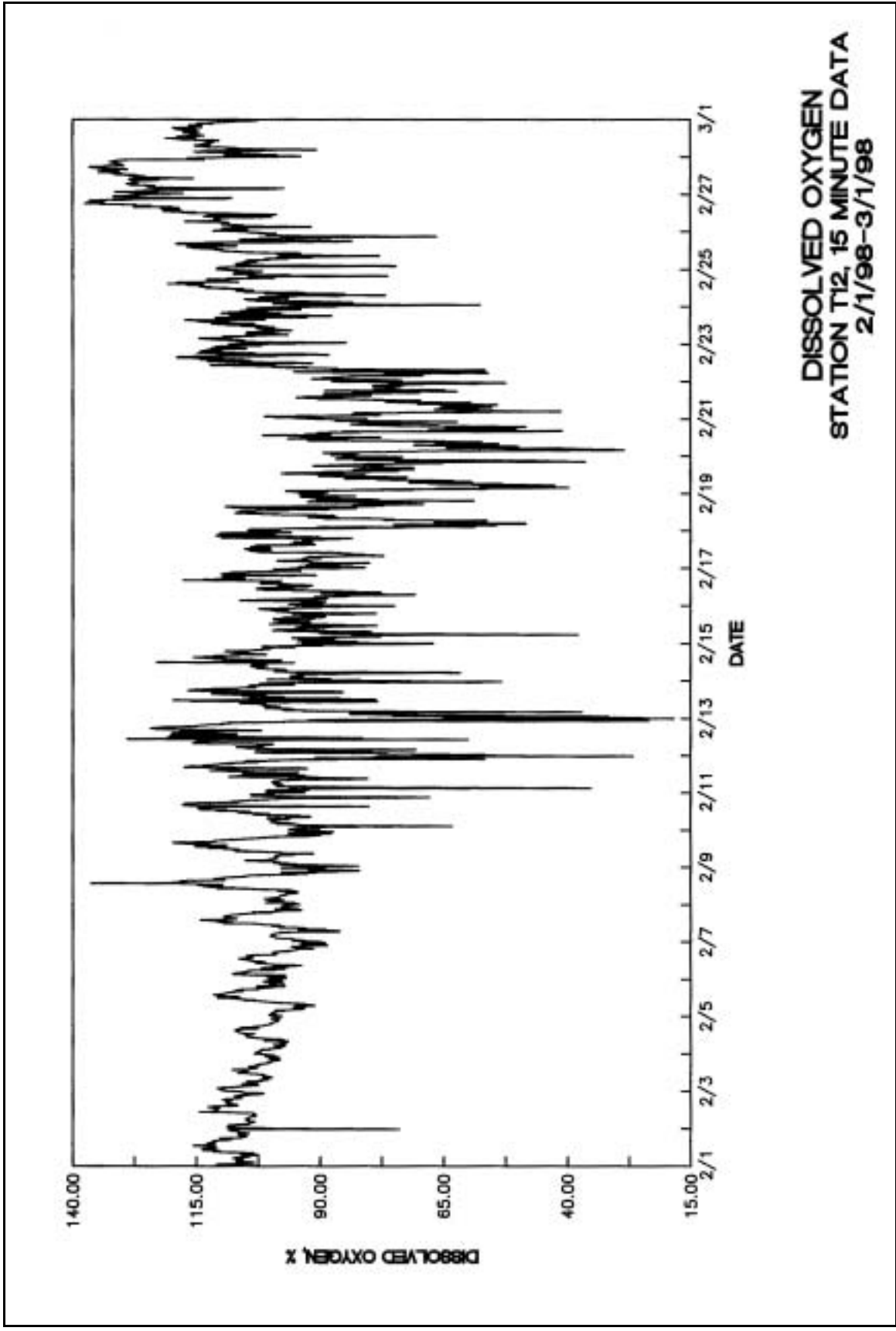


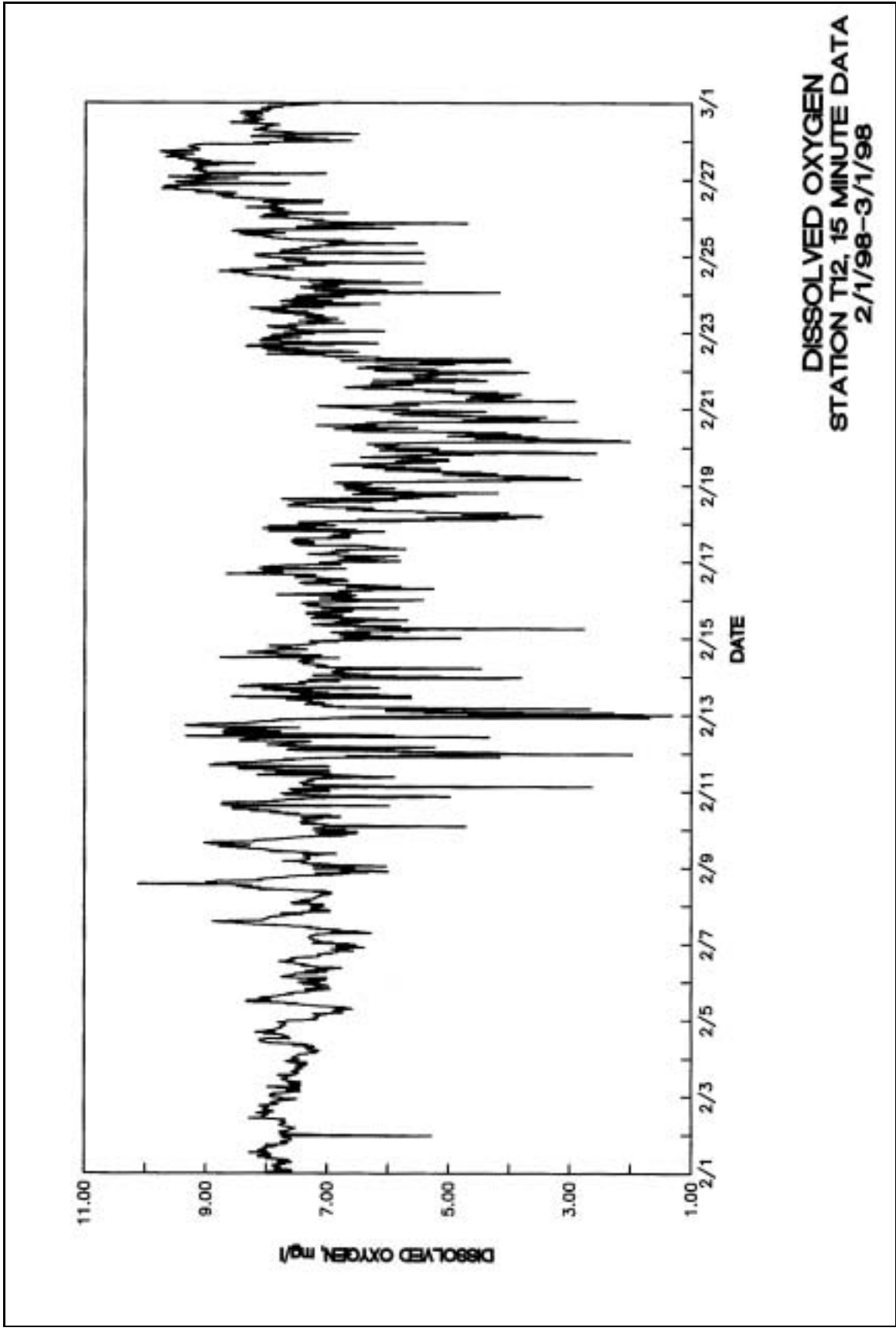


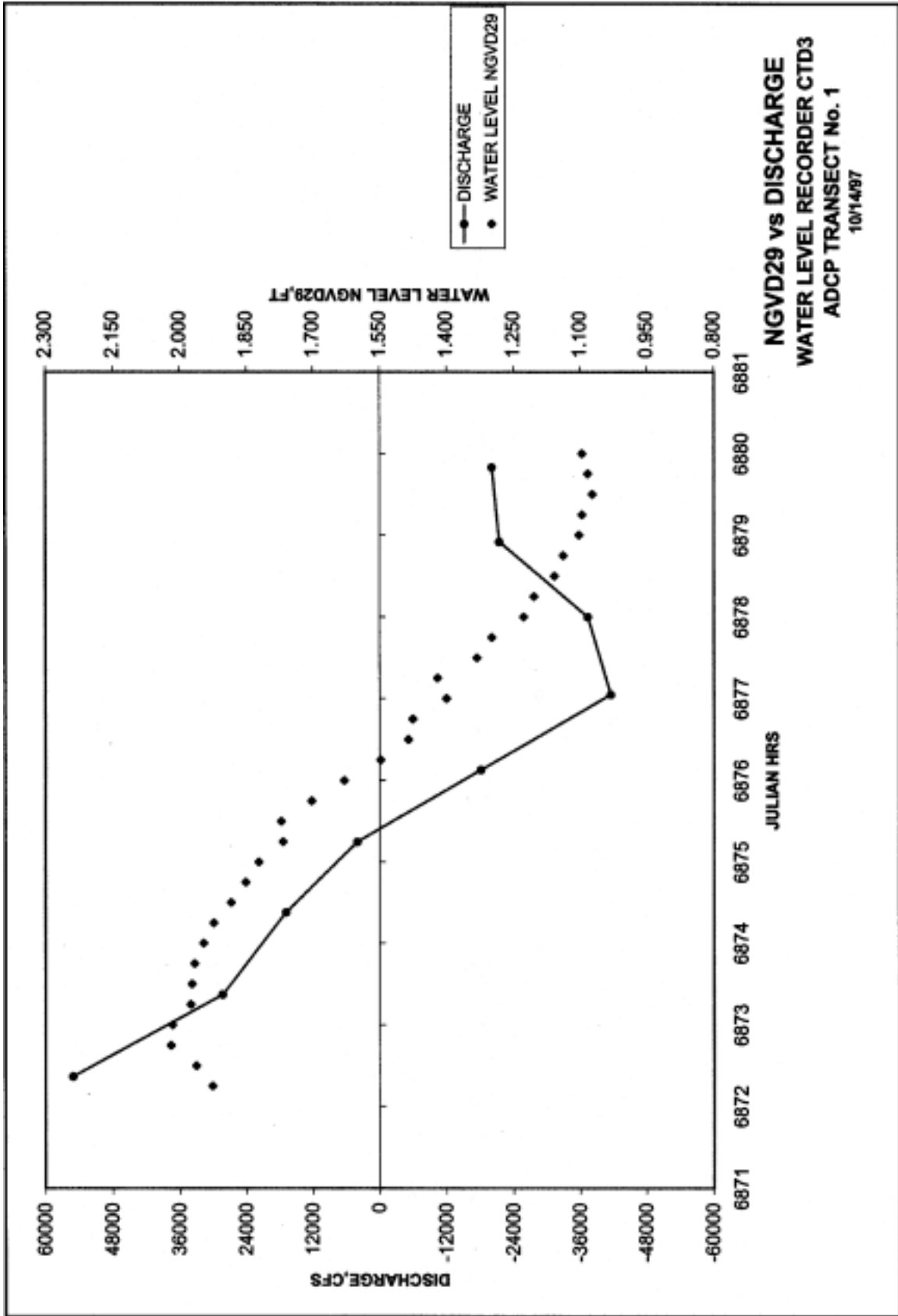


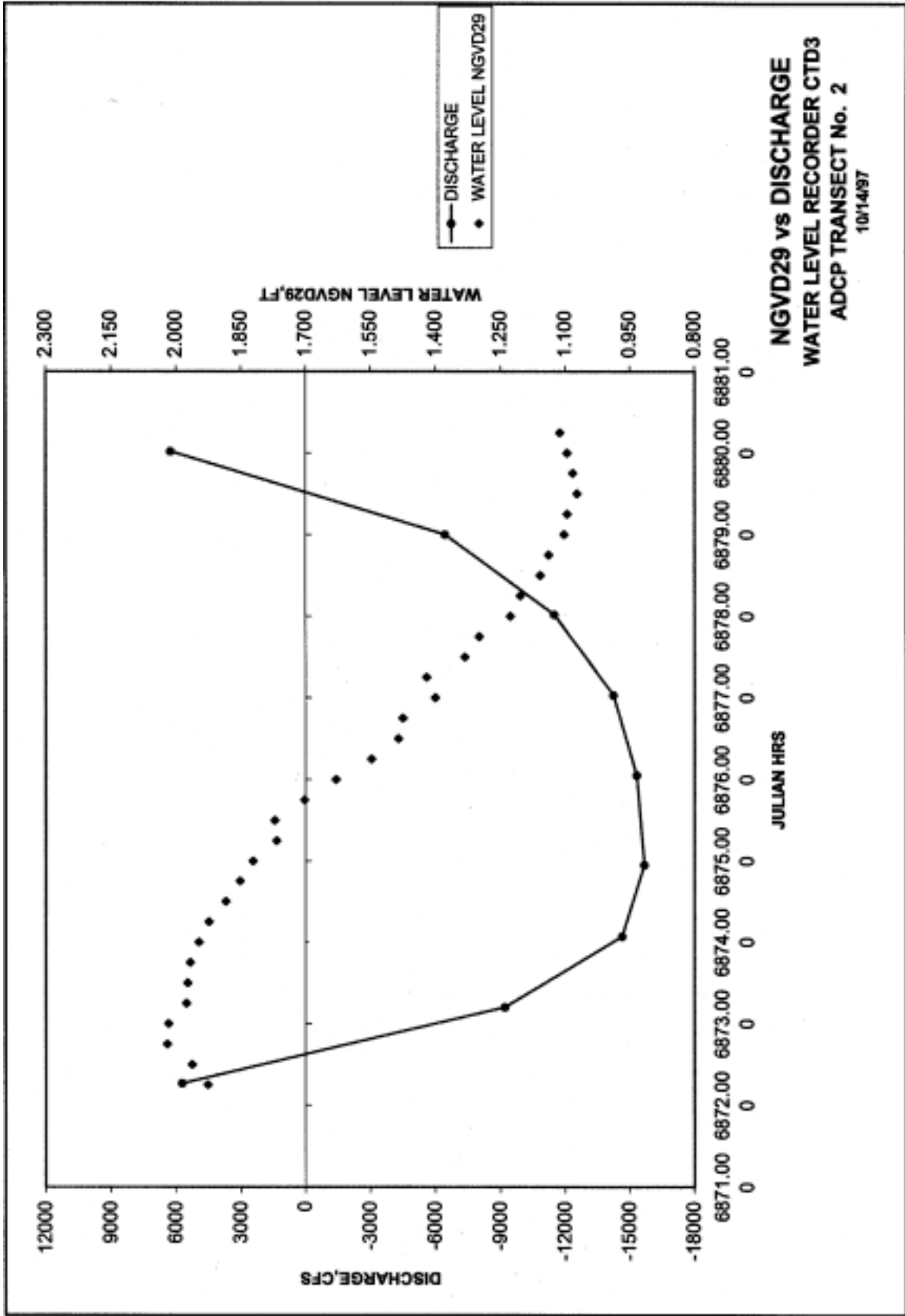


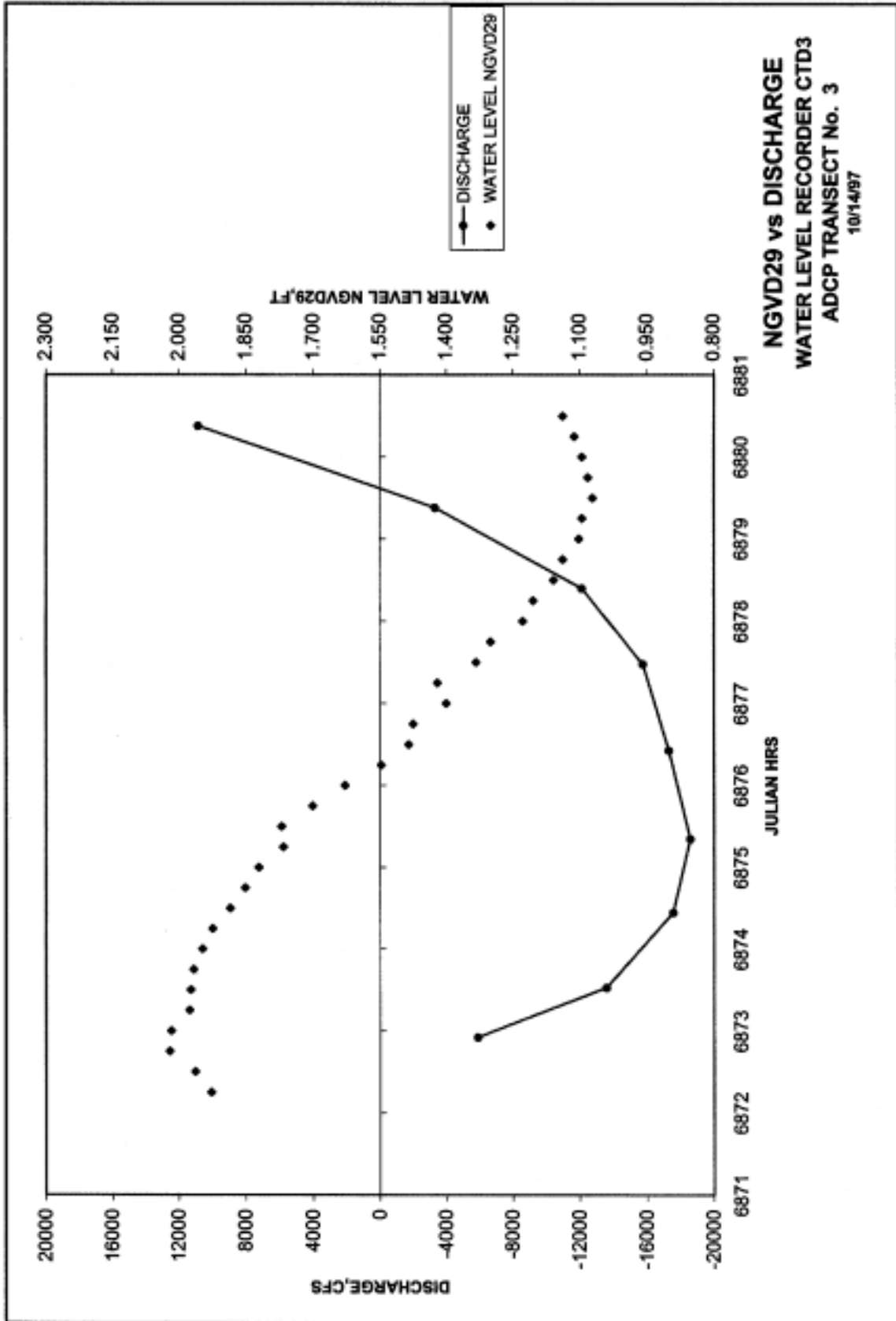


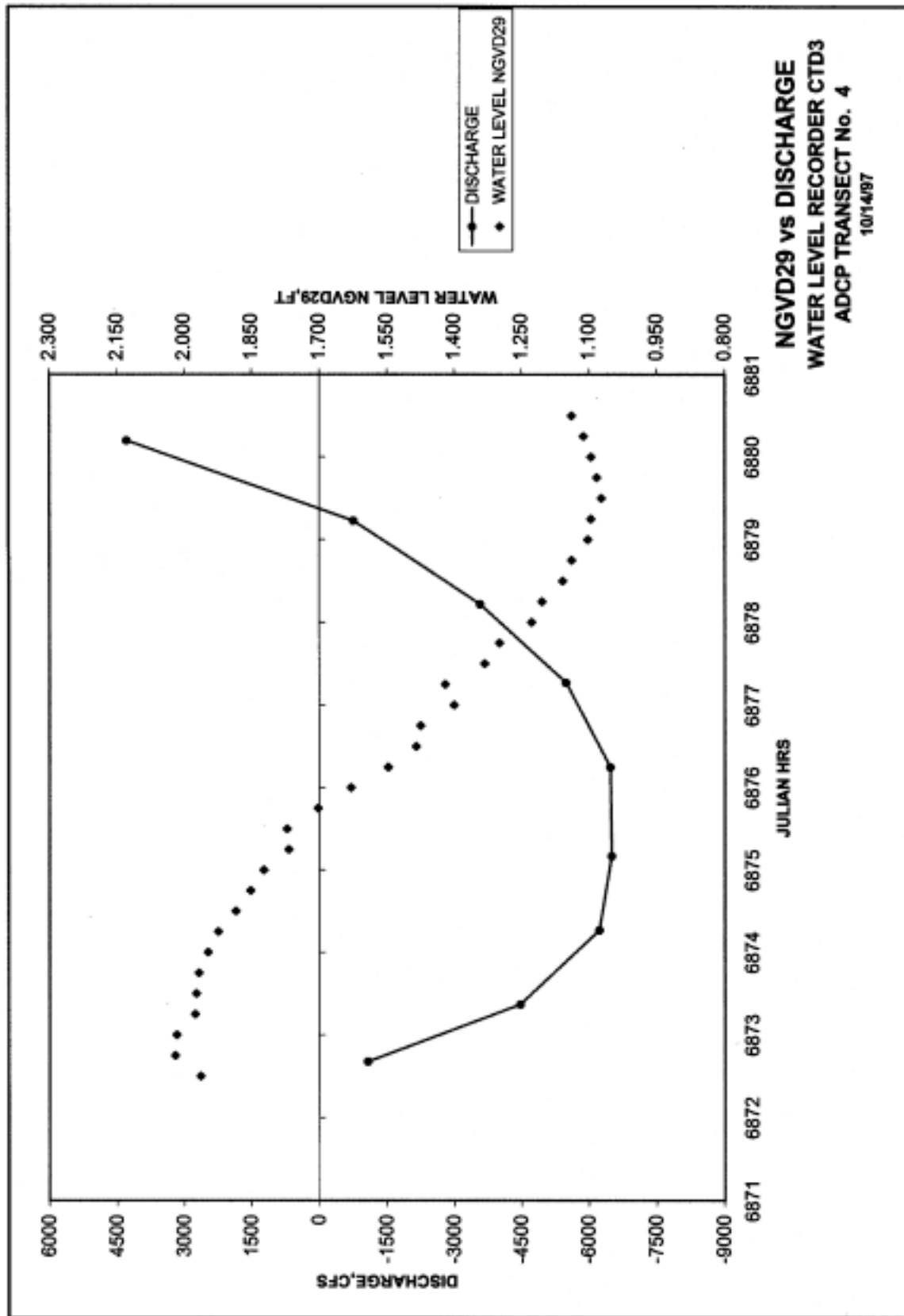


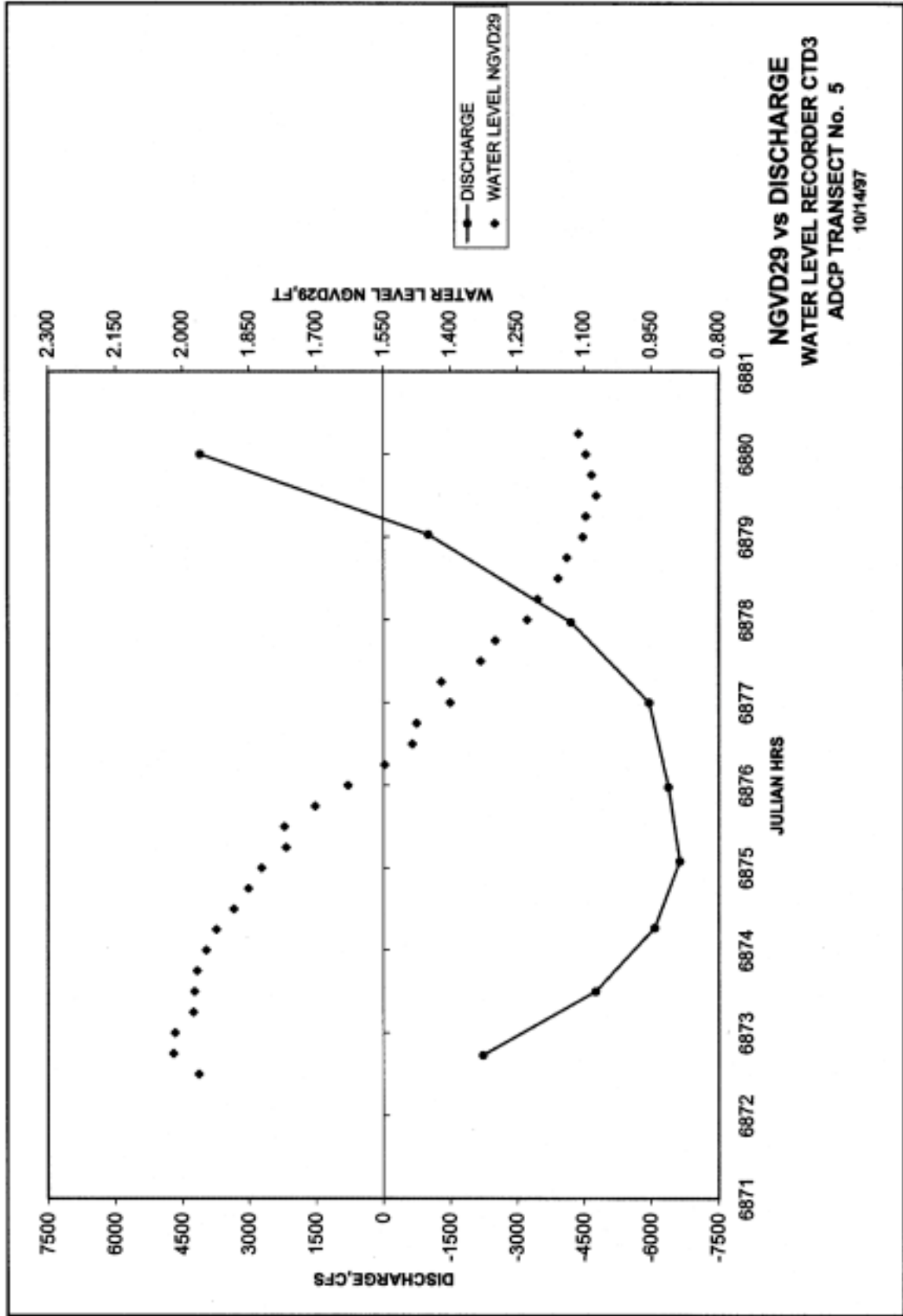












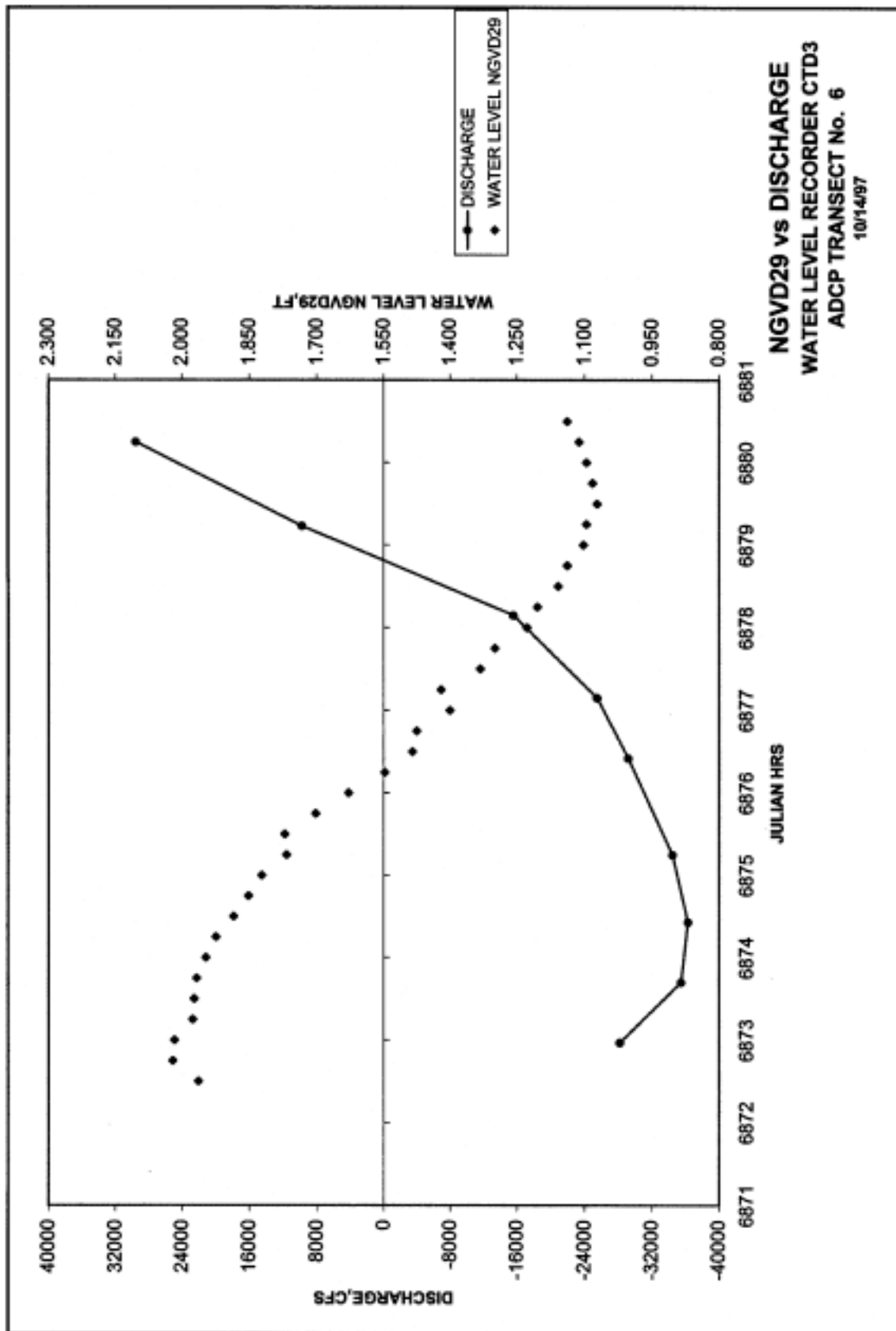
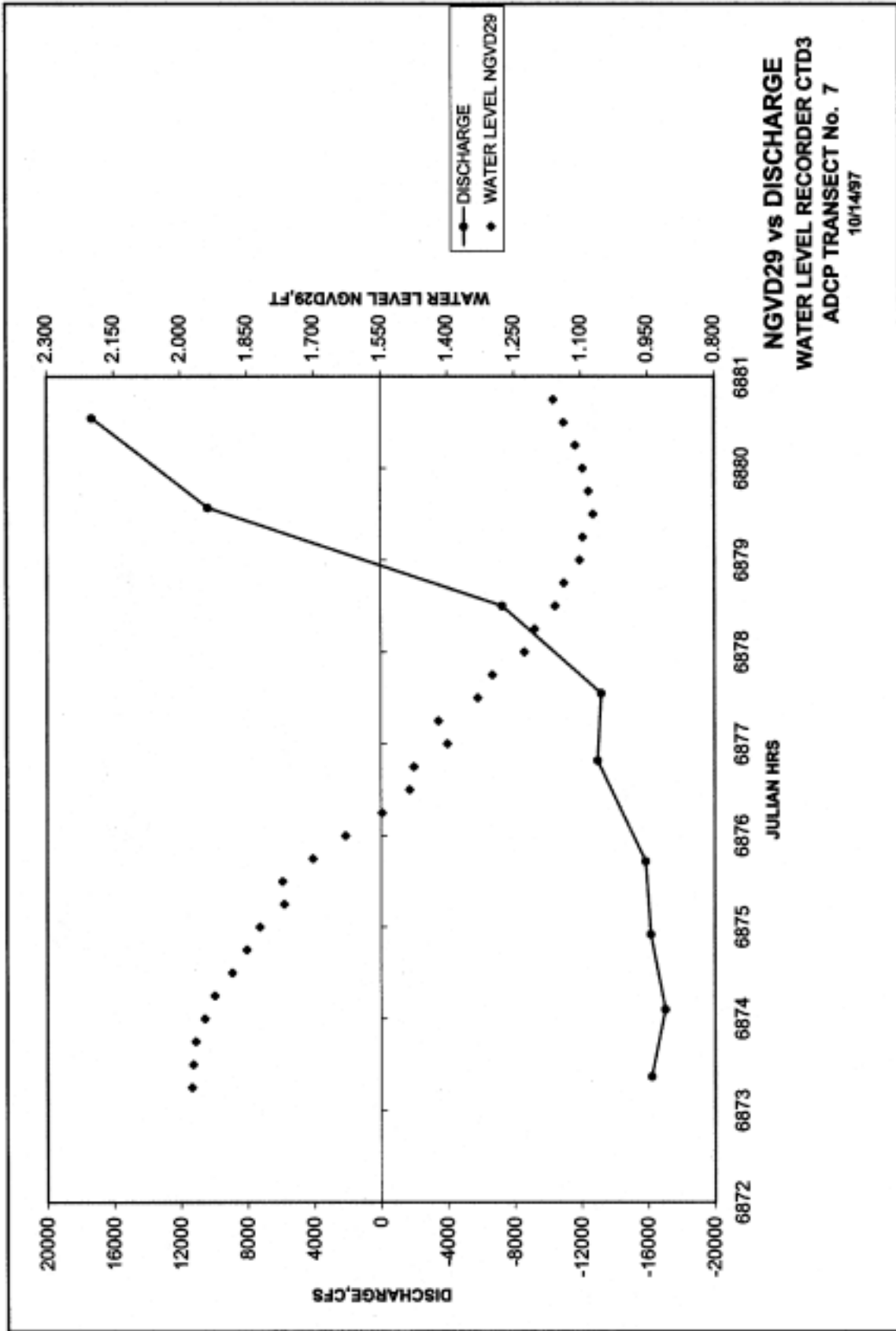


Plate 174



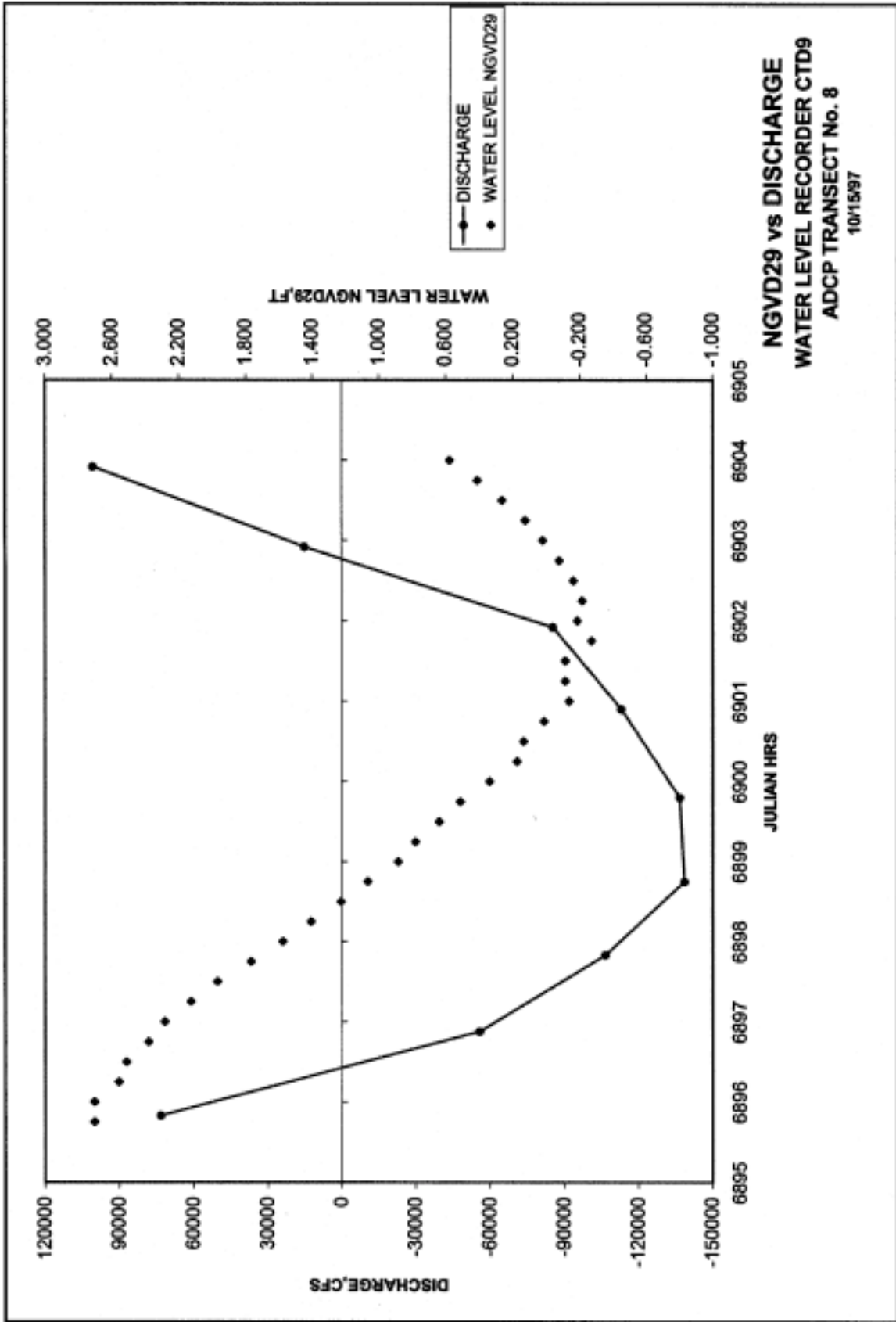
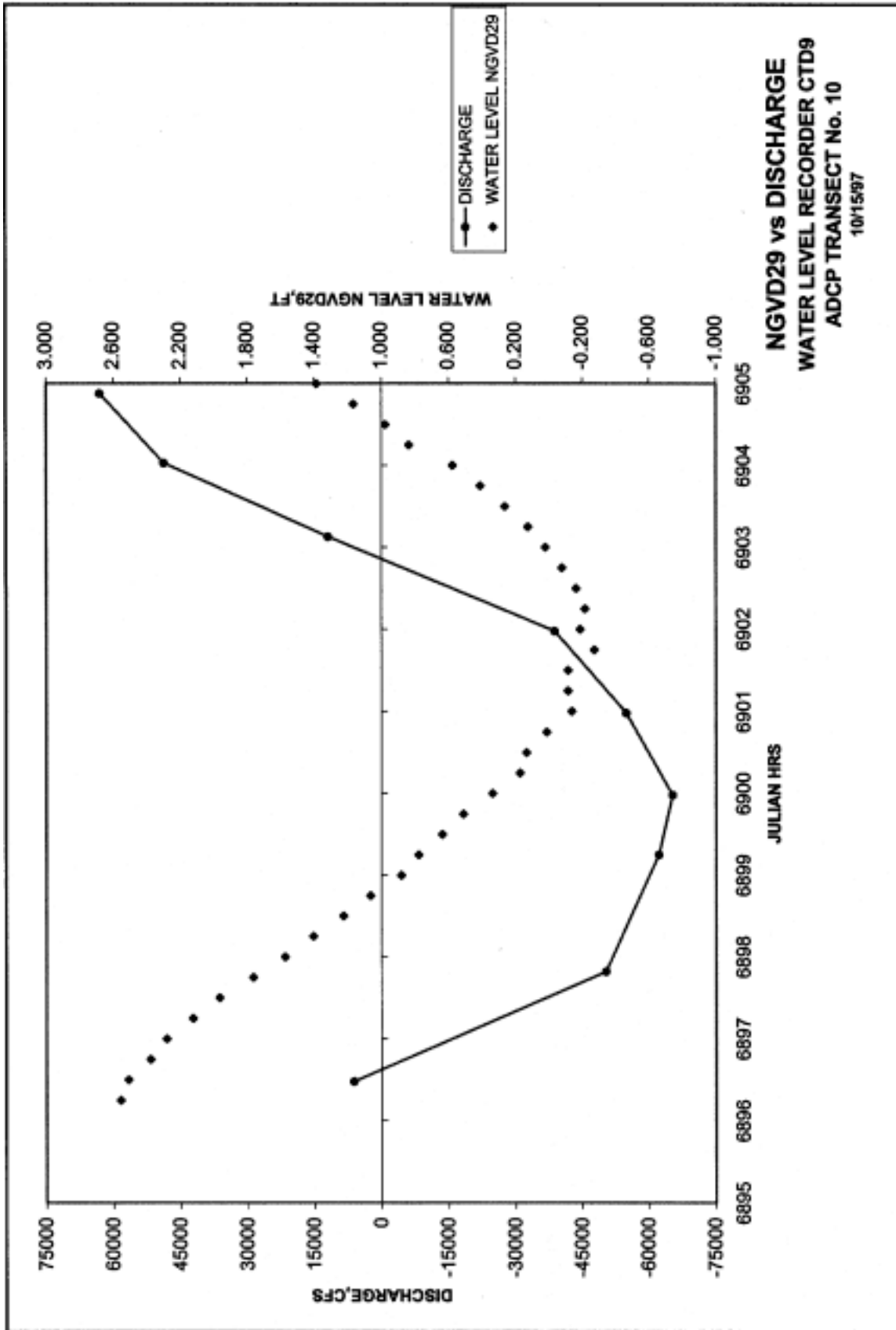
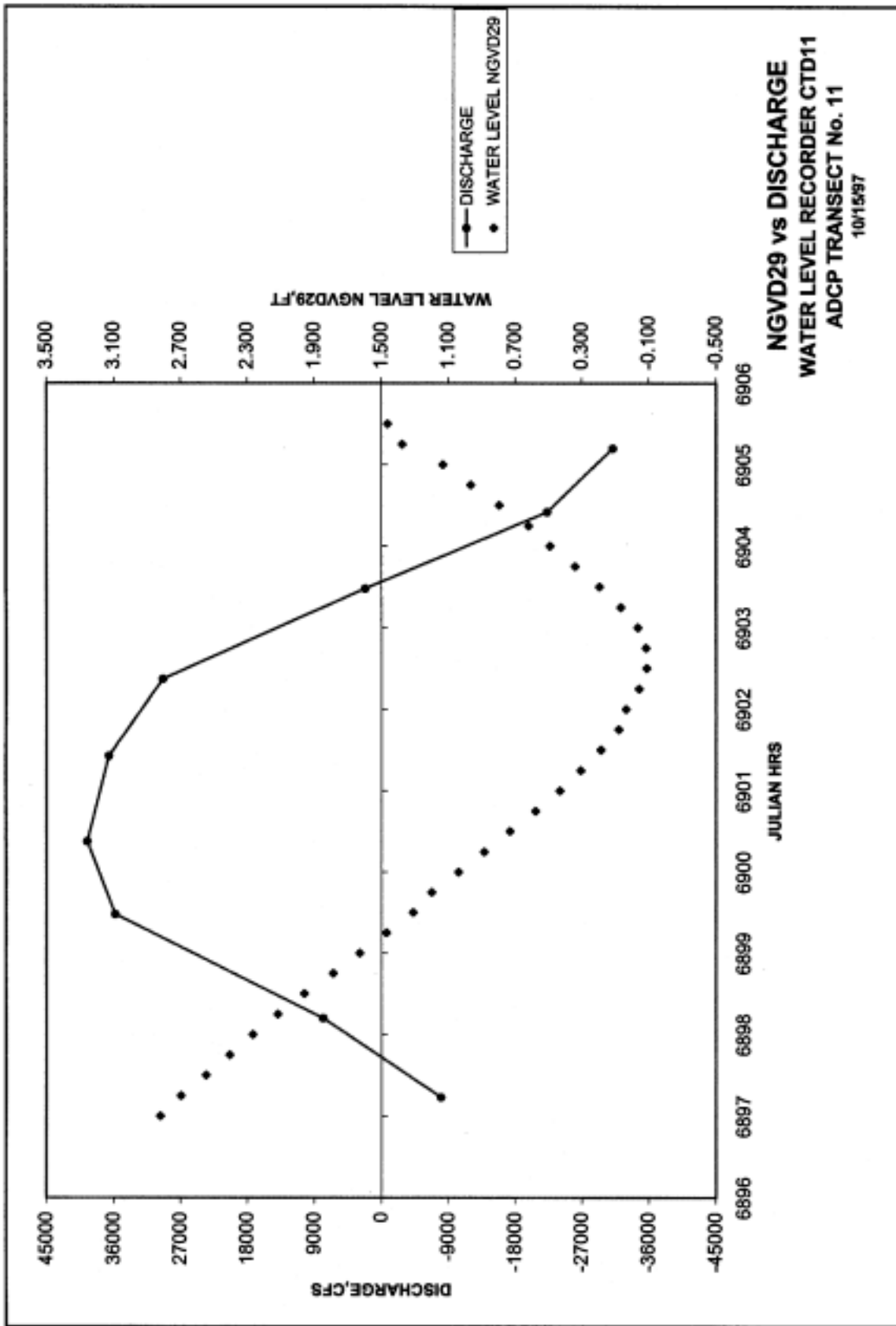
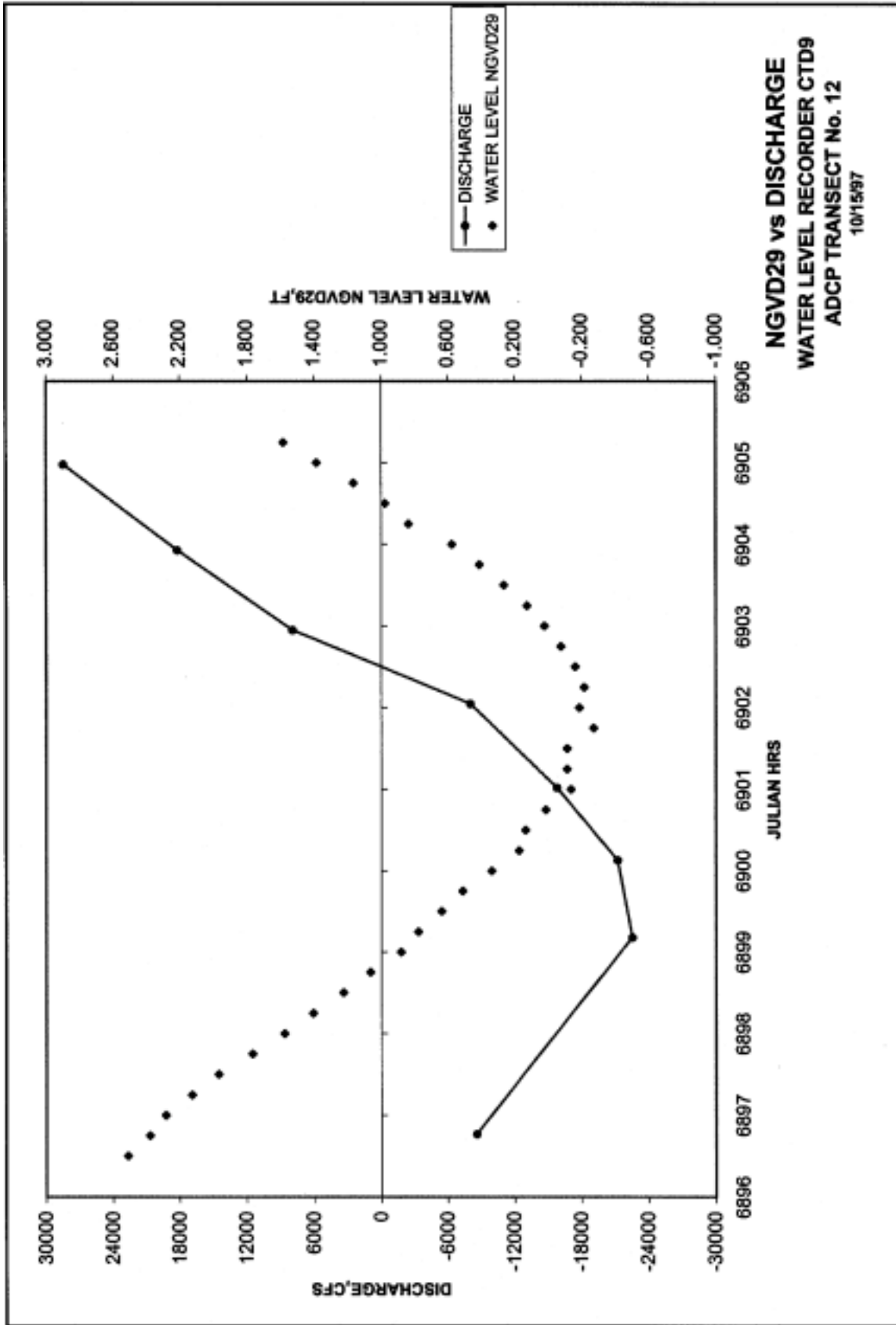


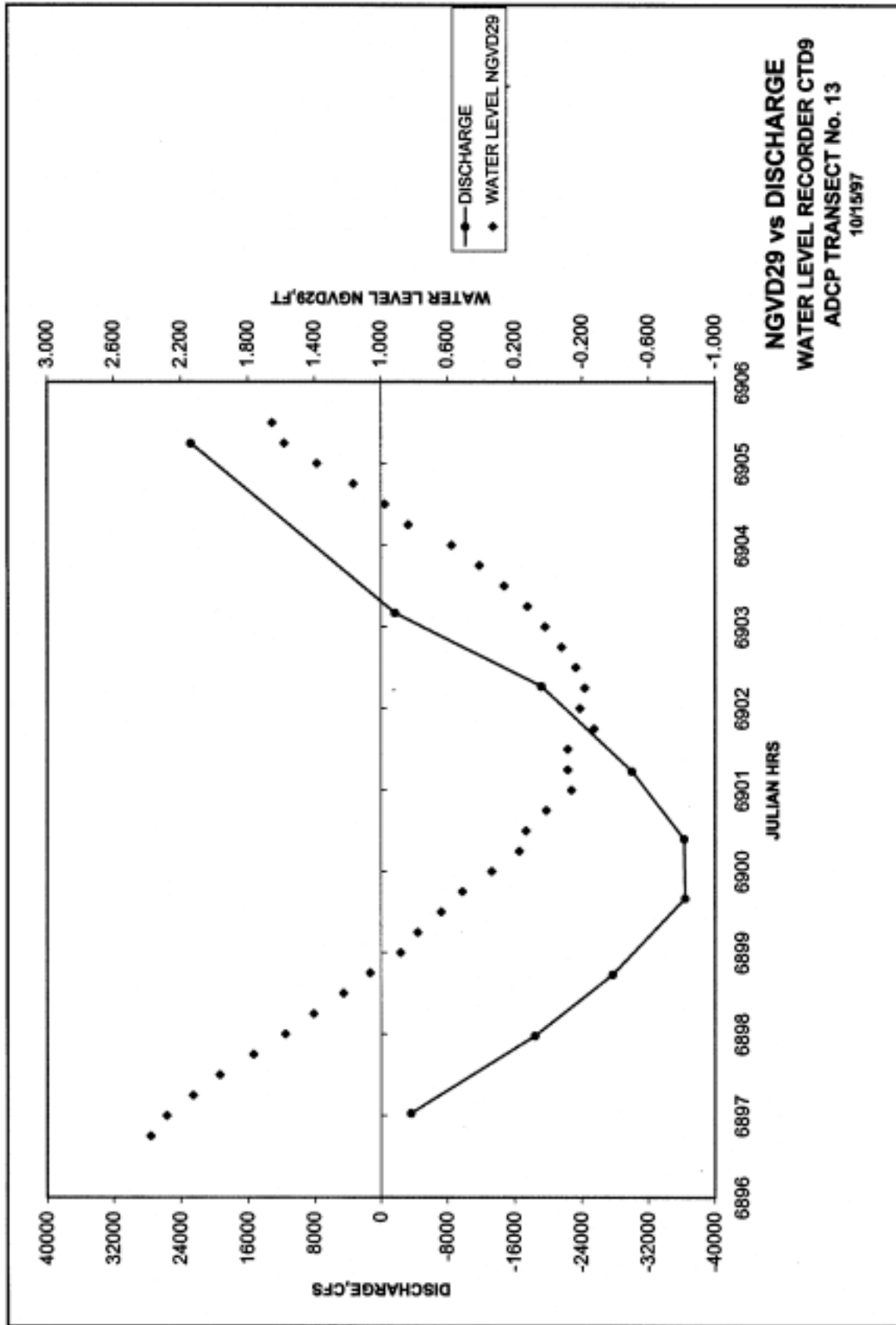
Plate 176

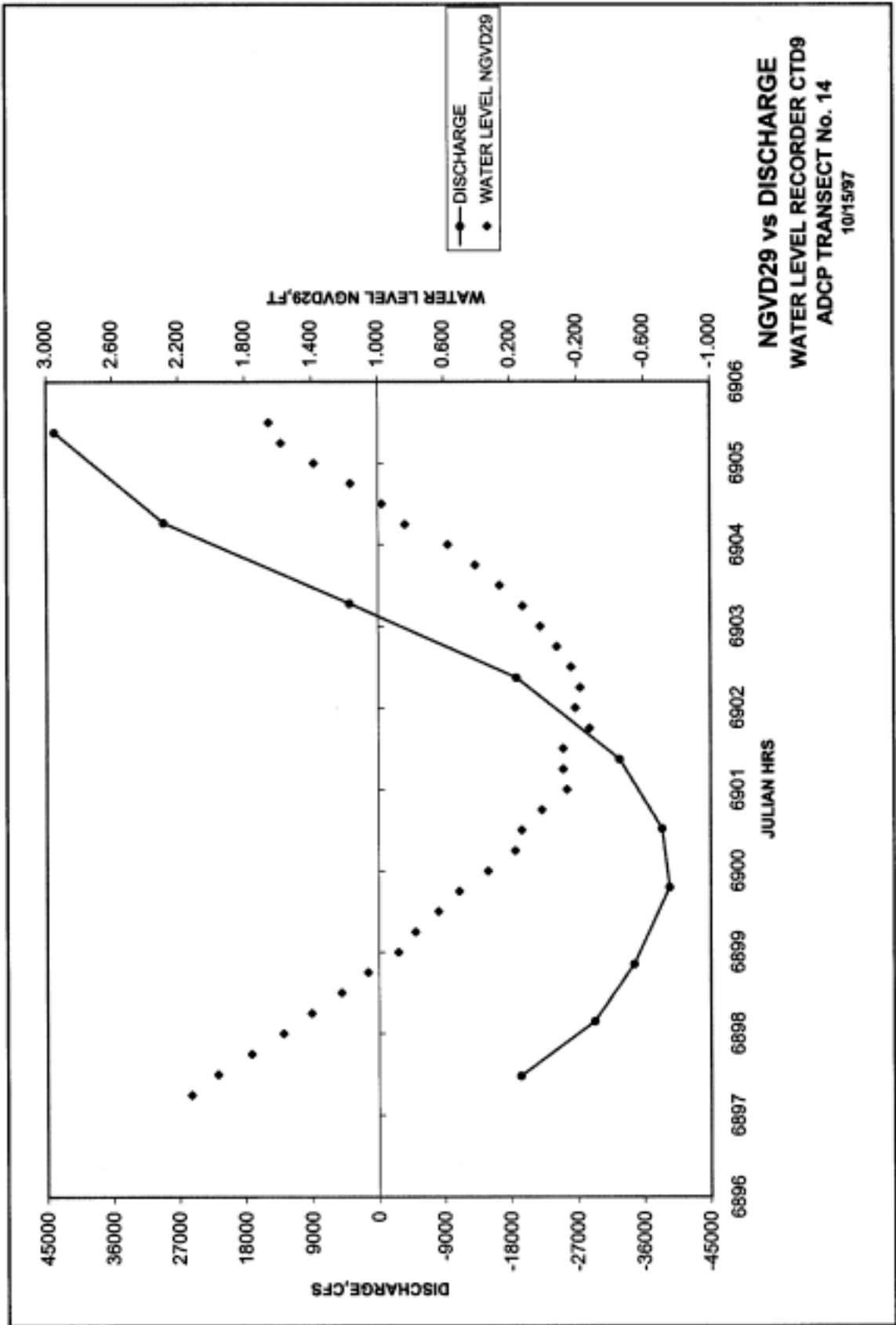


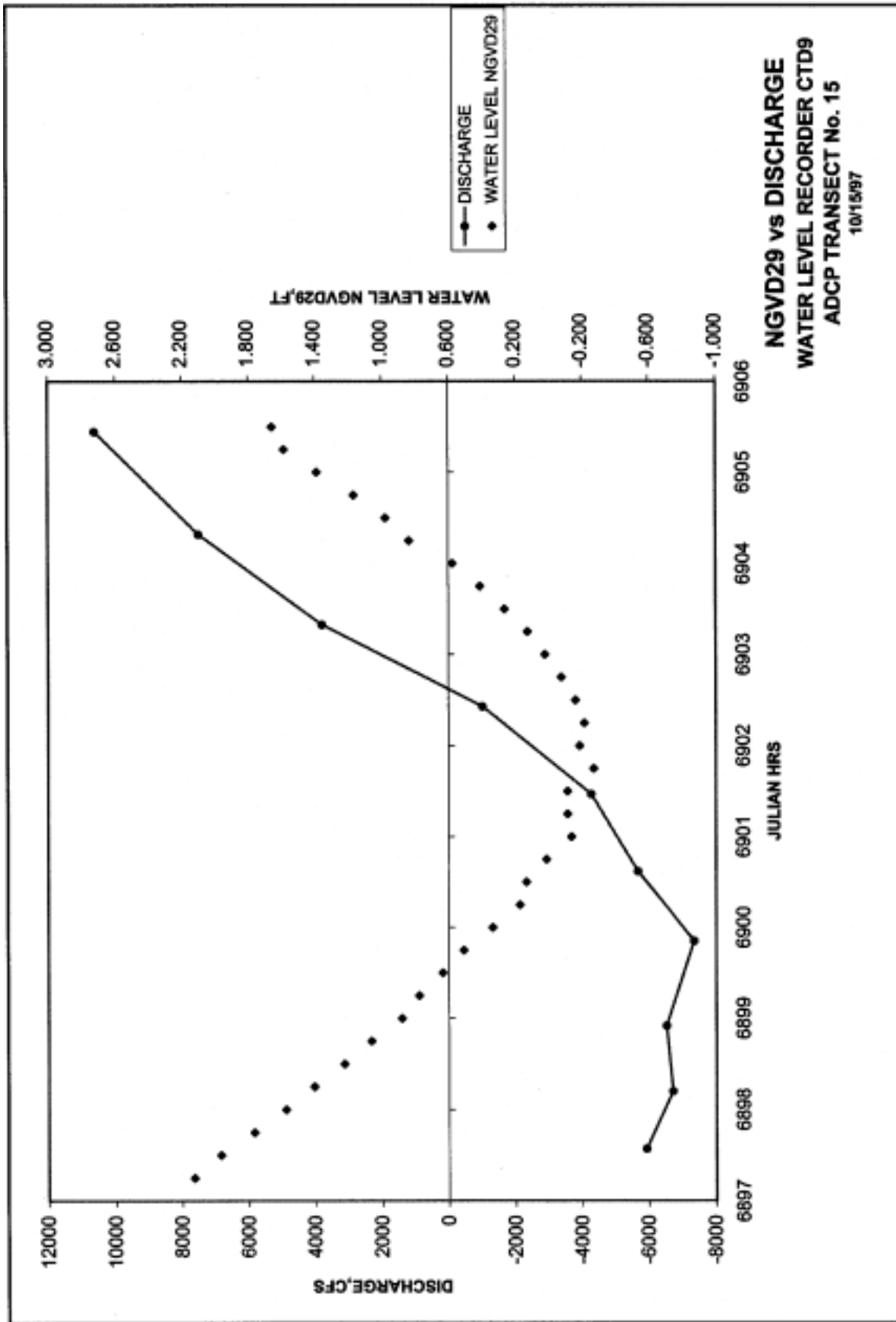


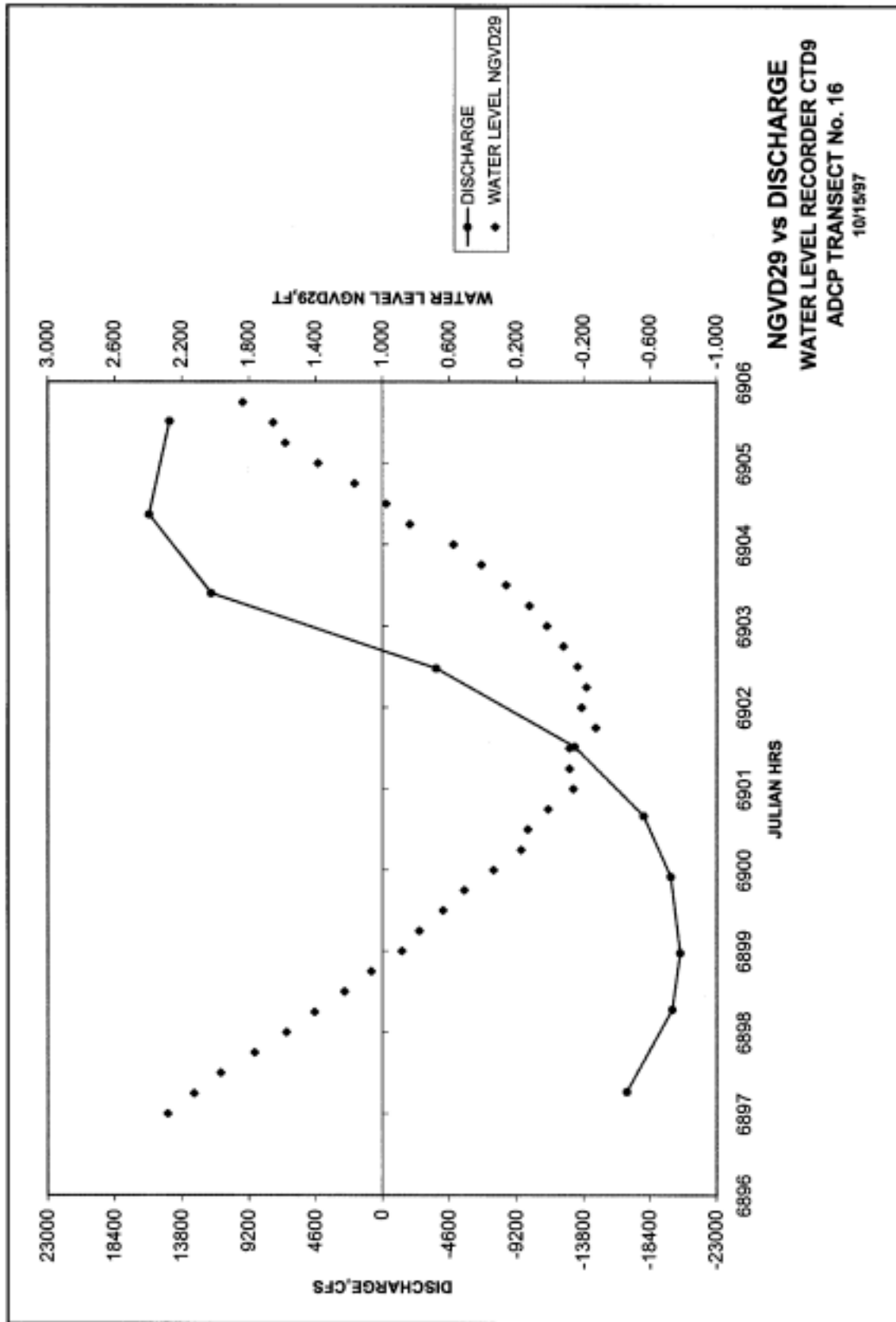


NGVD29 vs DISCHARGE
WATER LEVEL RECORDER CTD9
ADCP TRANSECT No. 12
 10/15/97









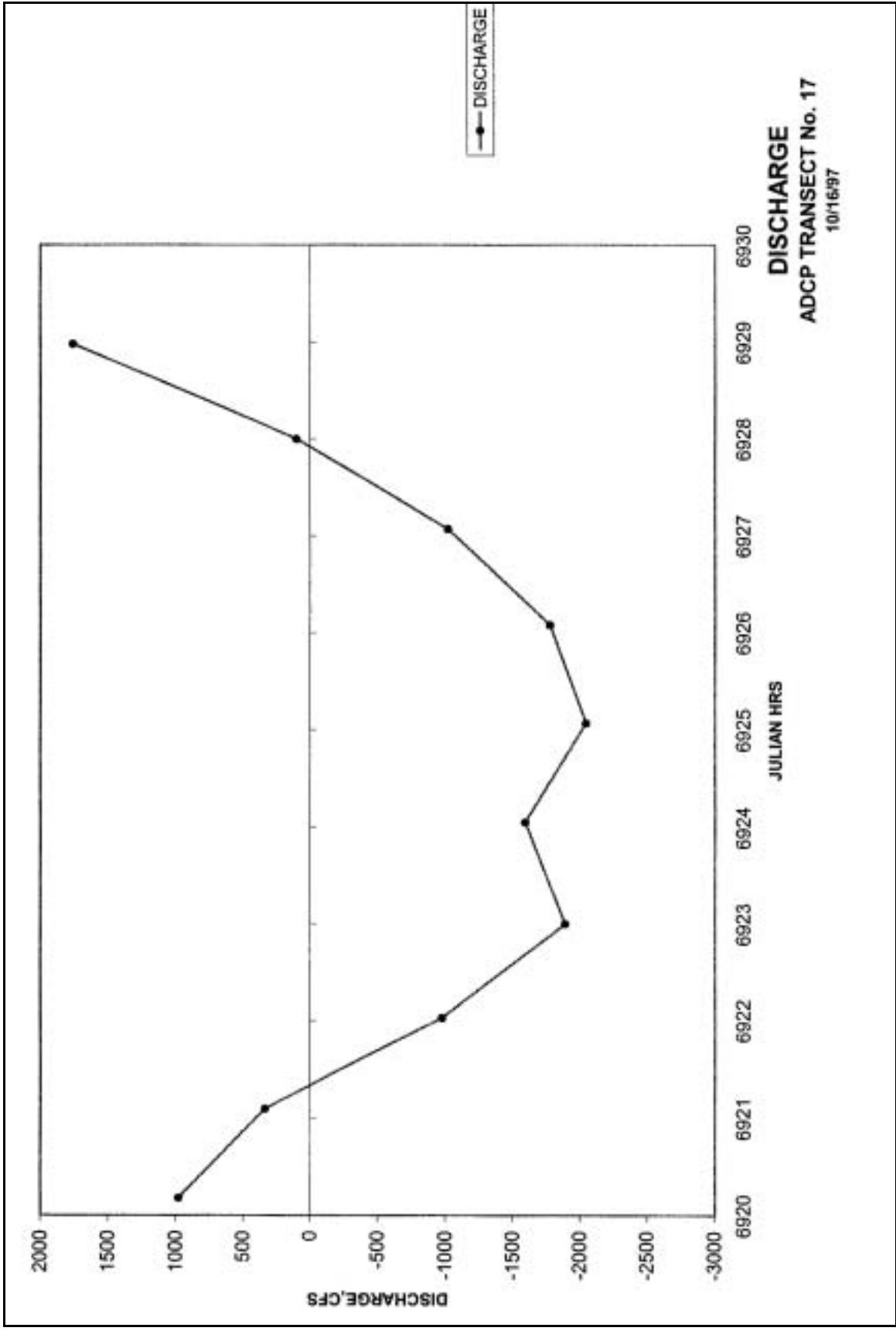
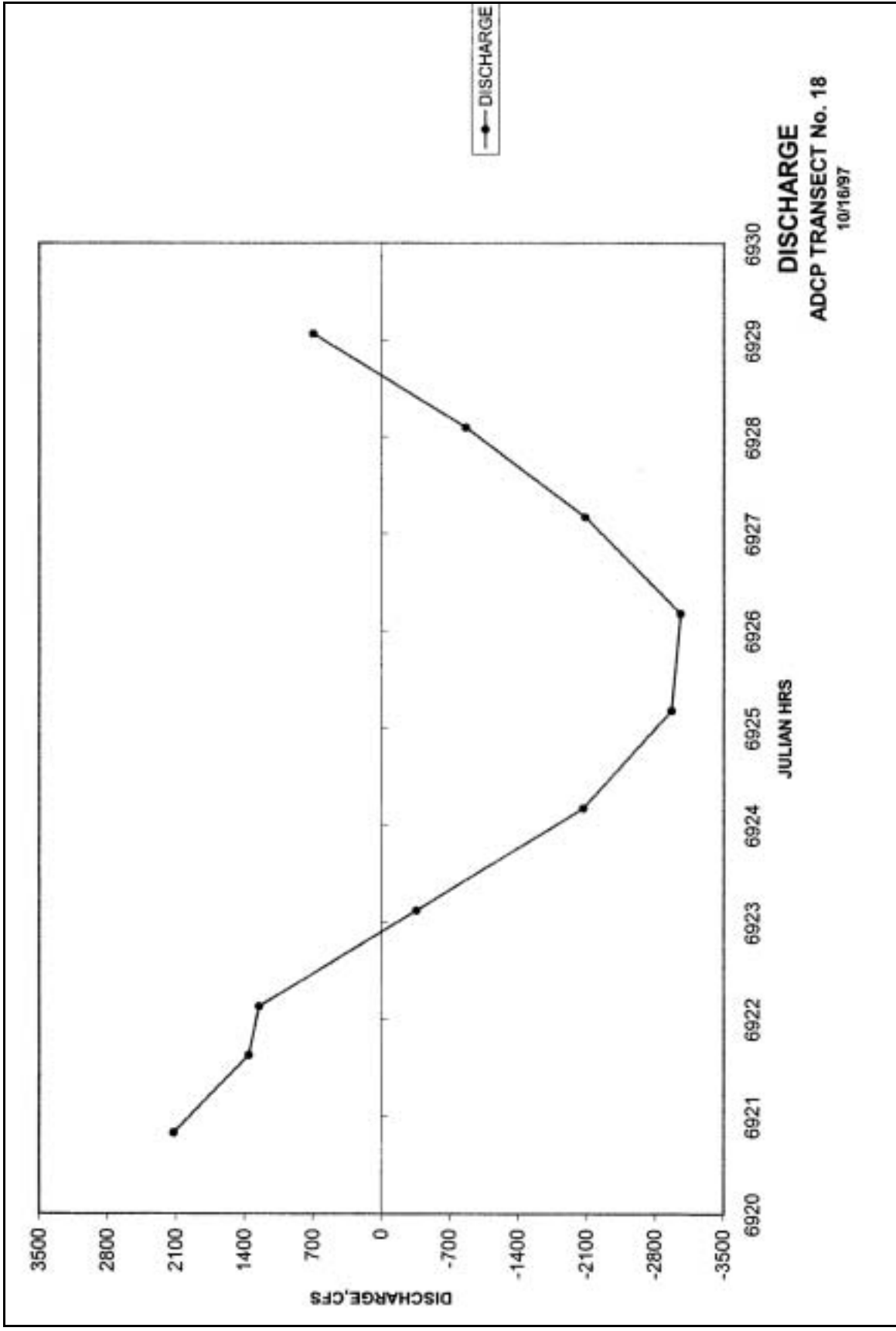


Plate 184



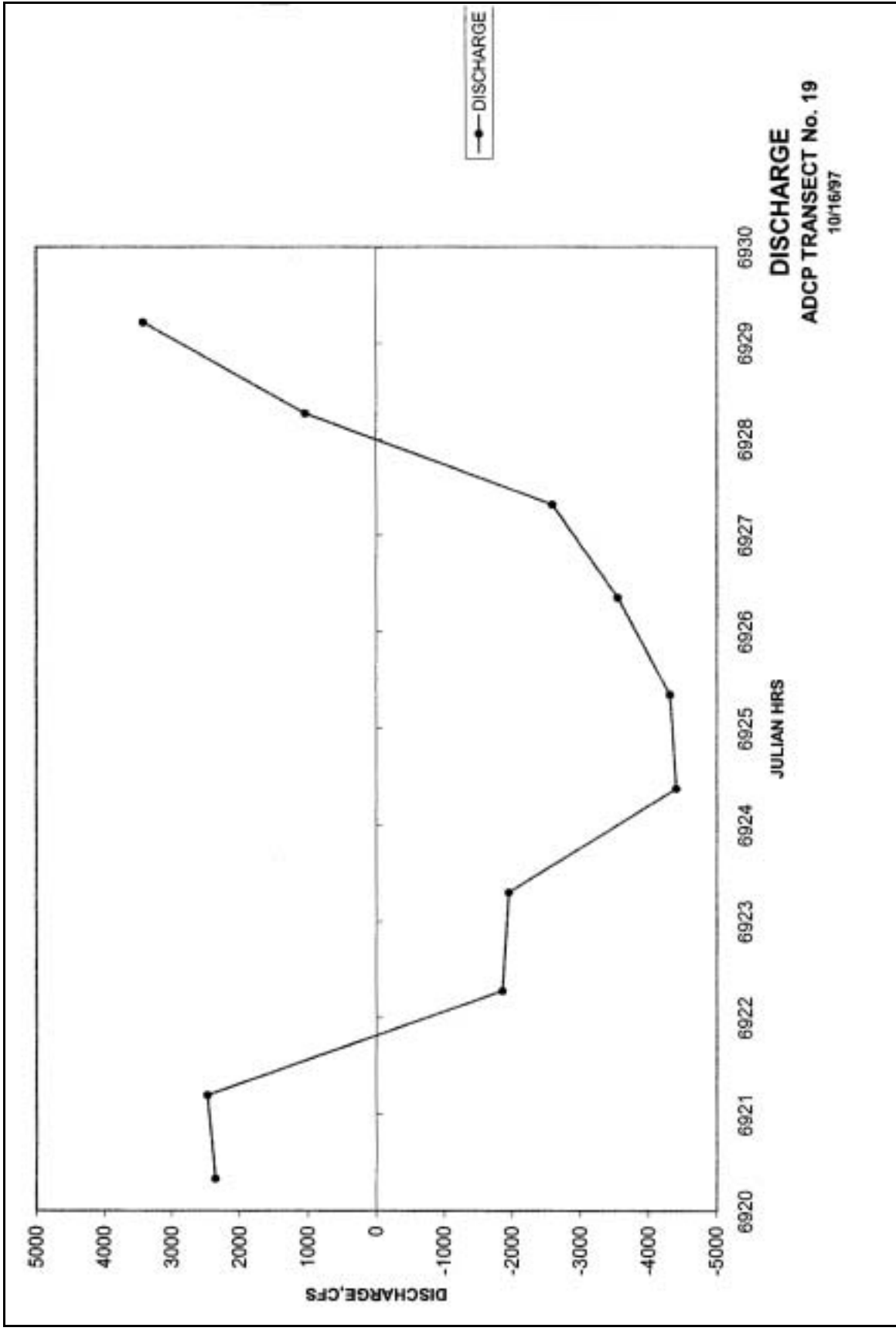
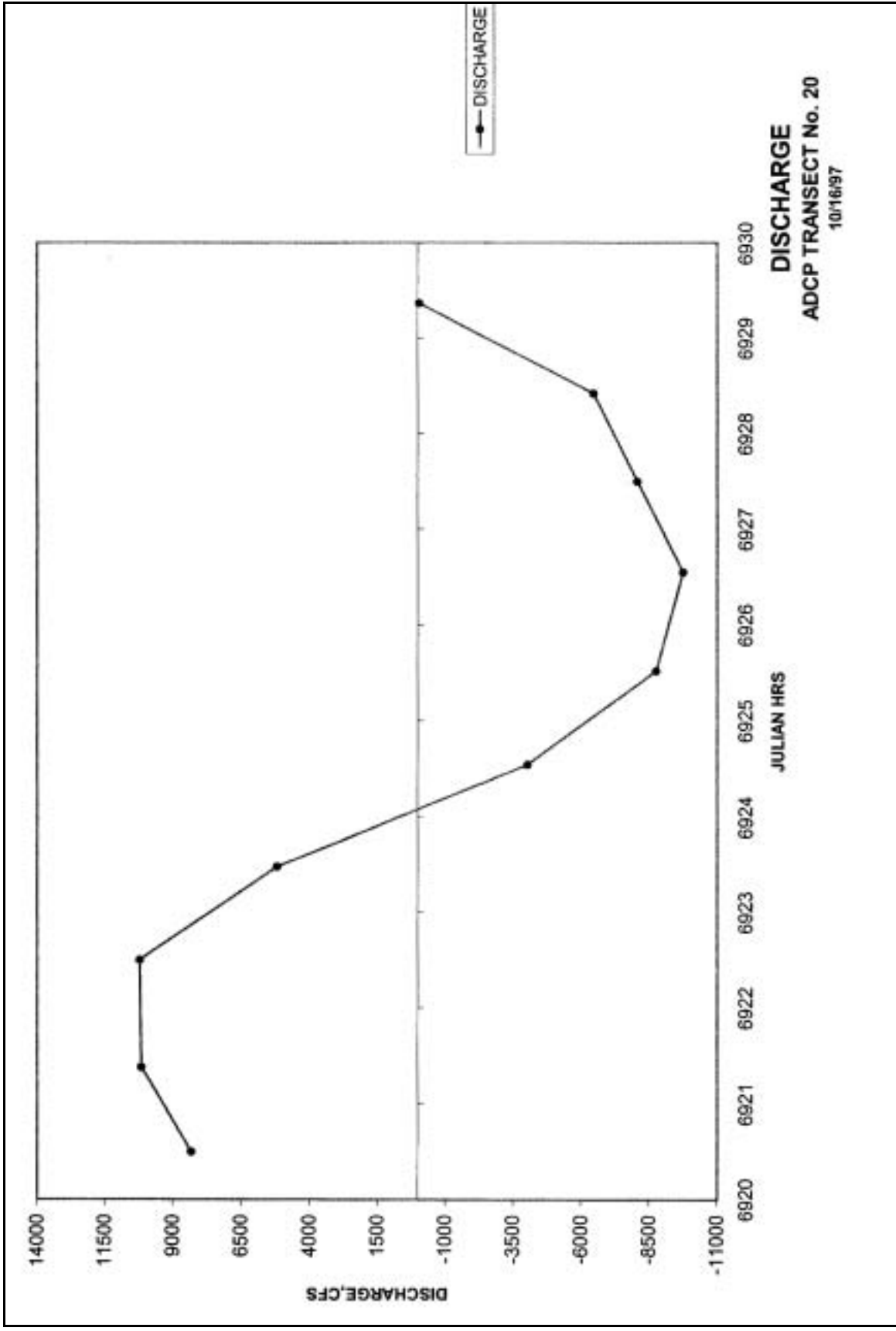
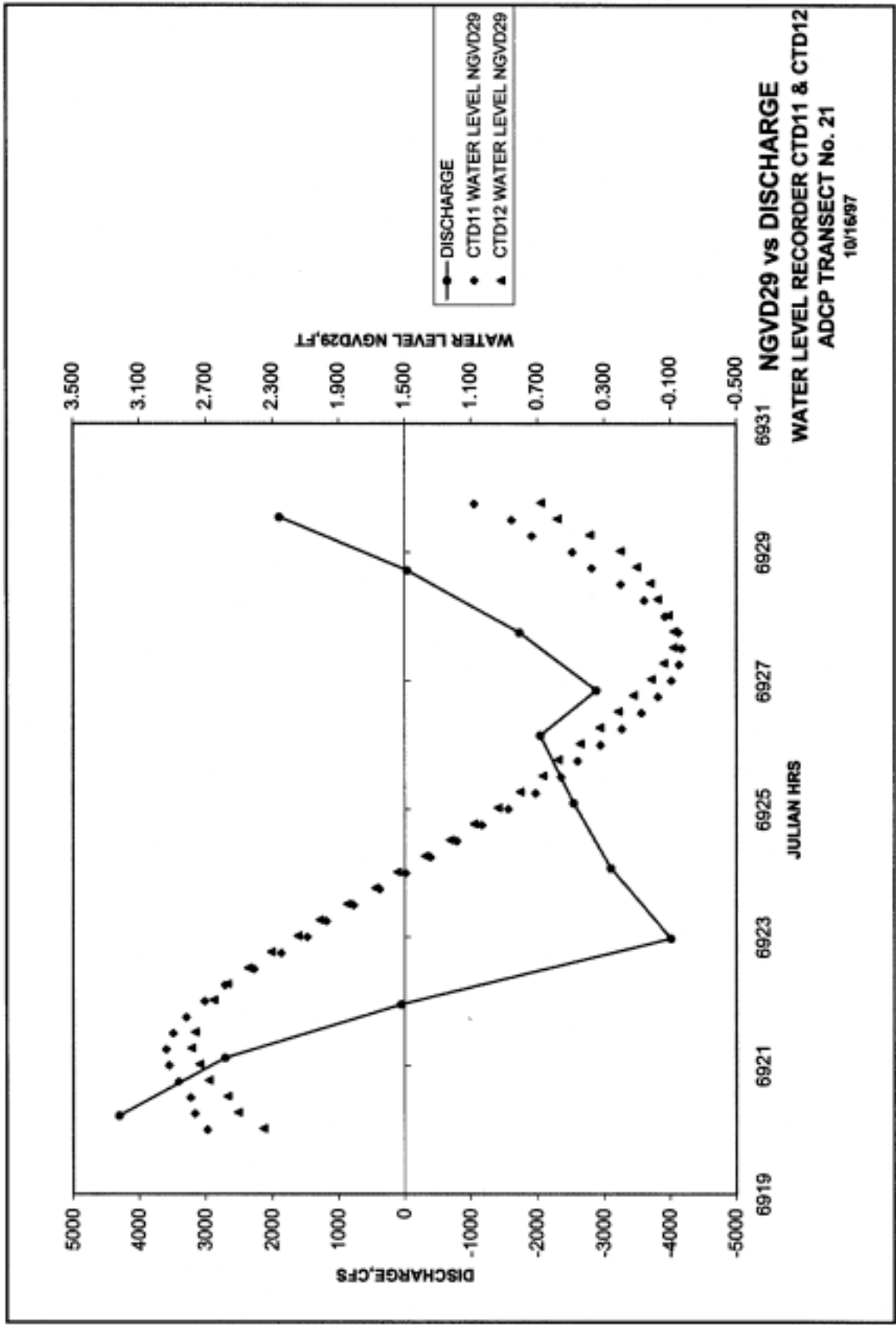
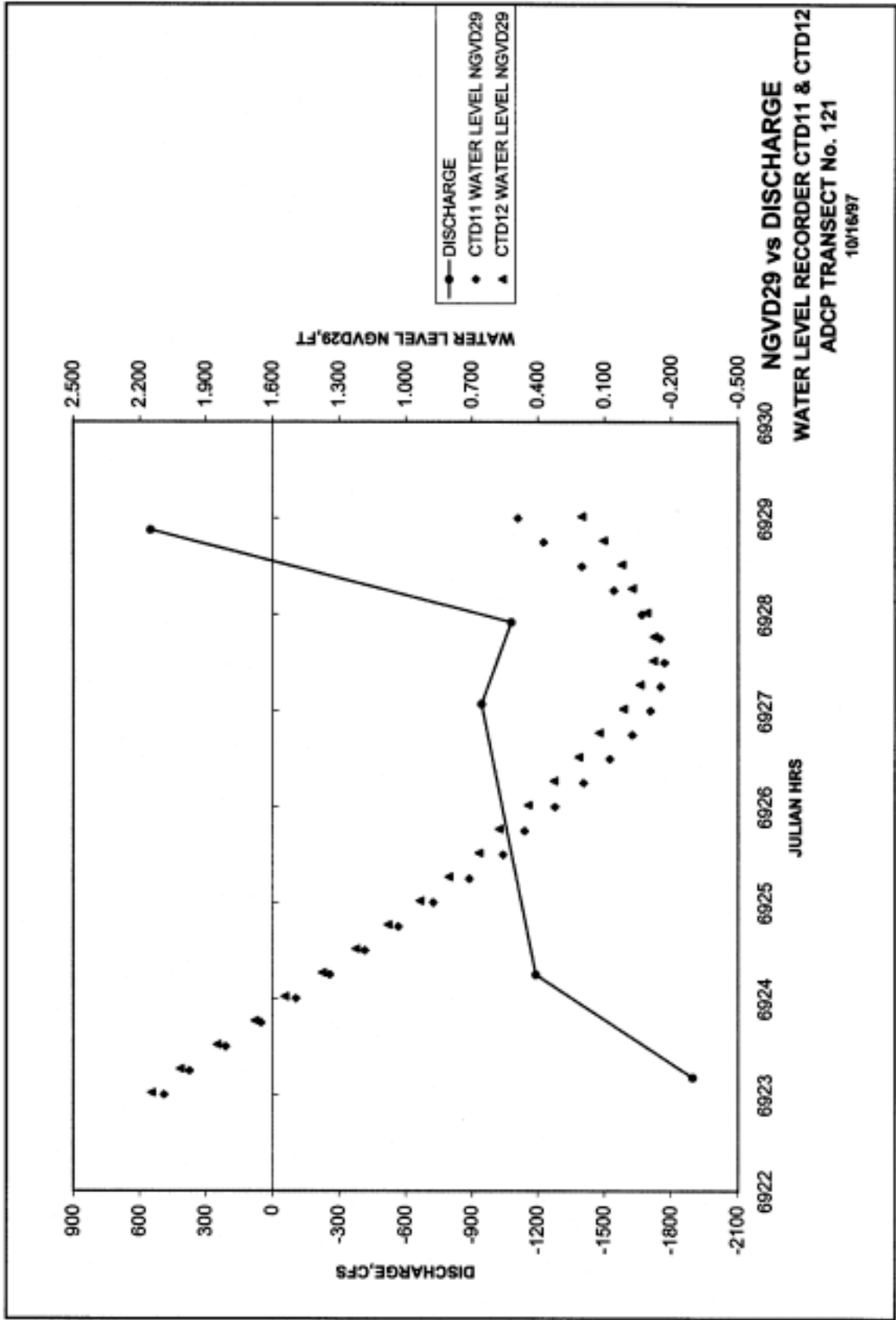
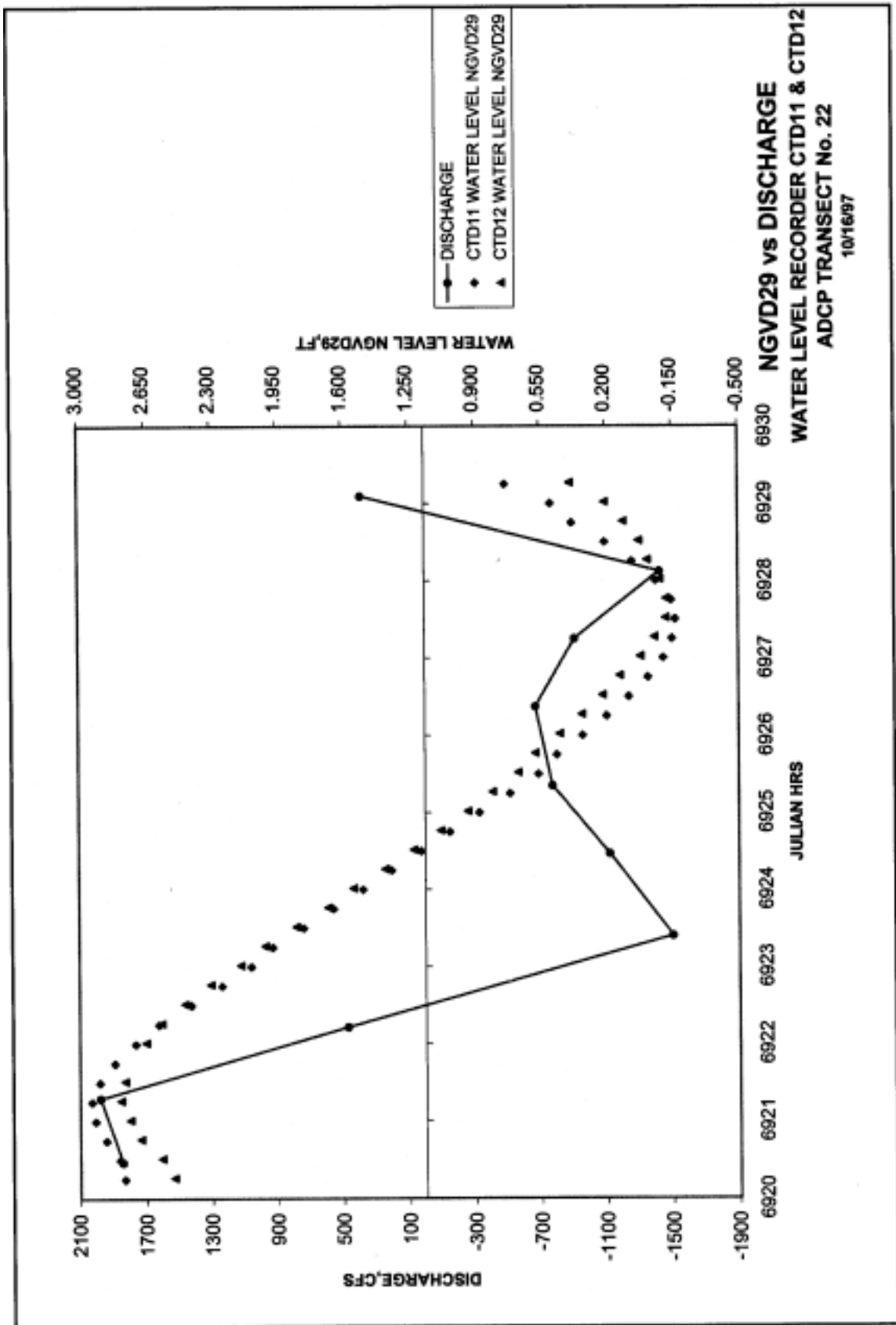


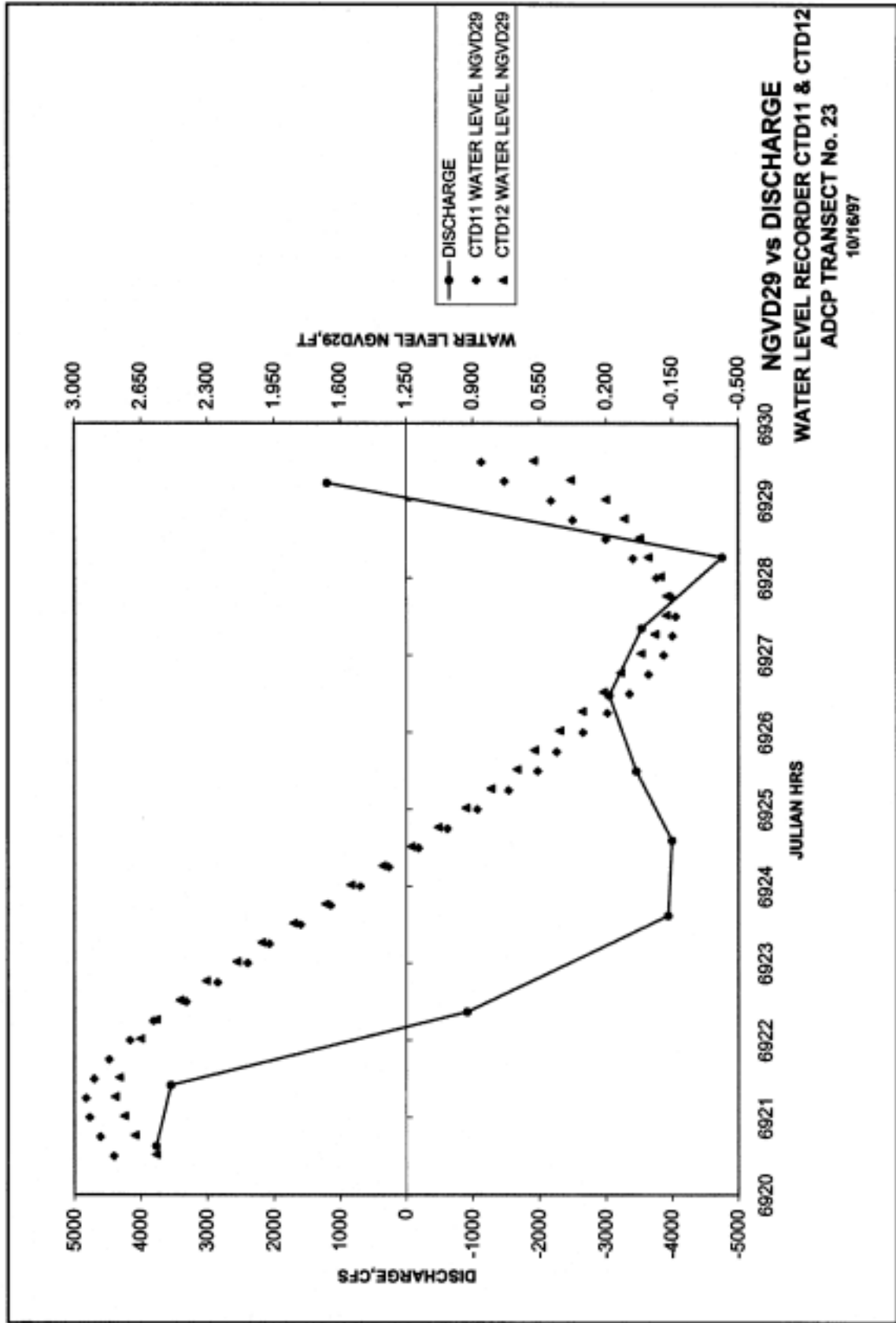
Plate 186

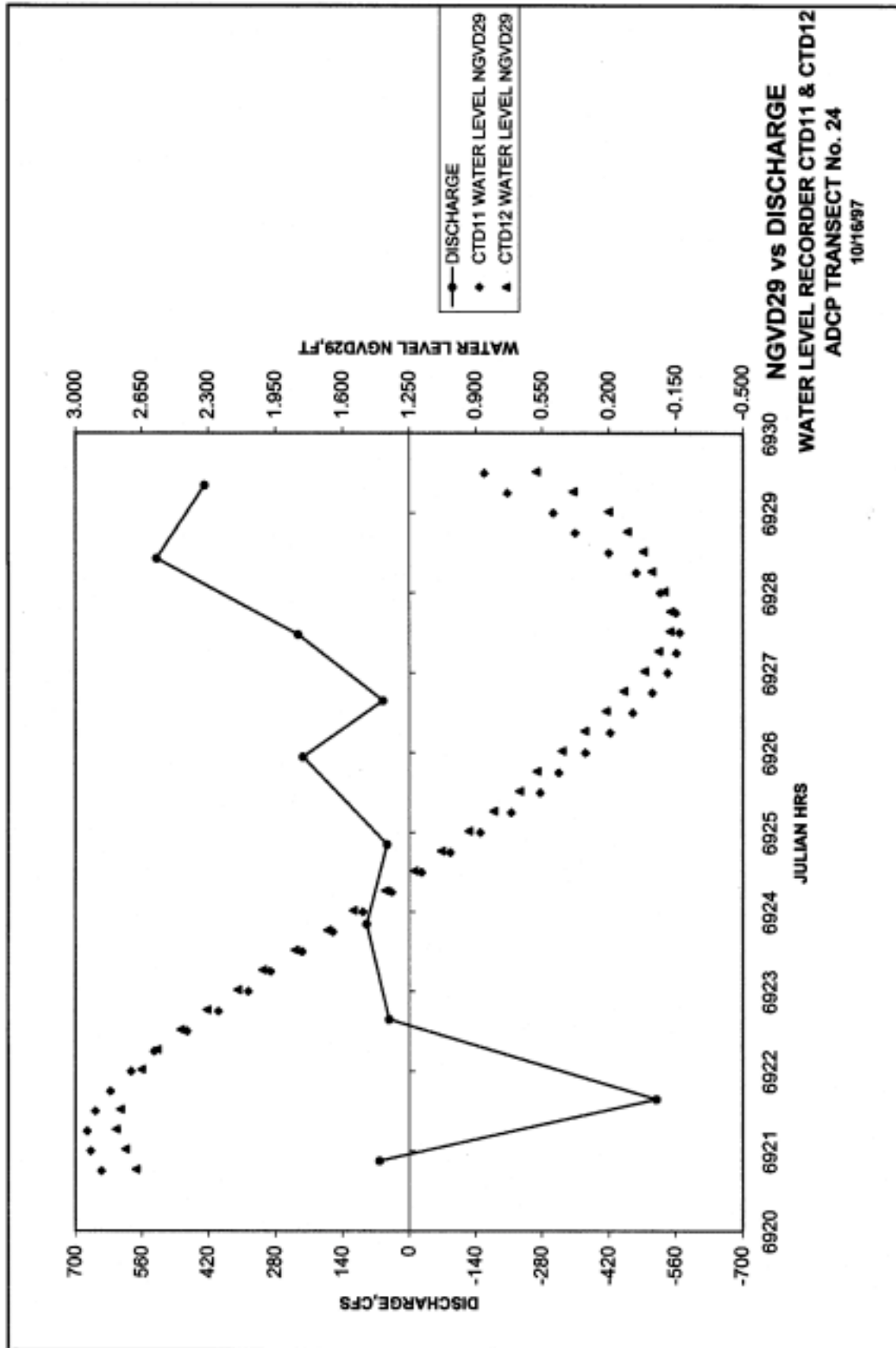


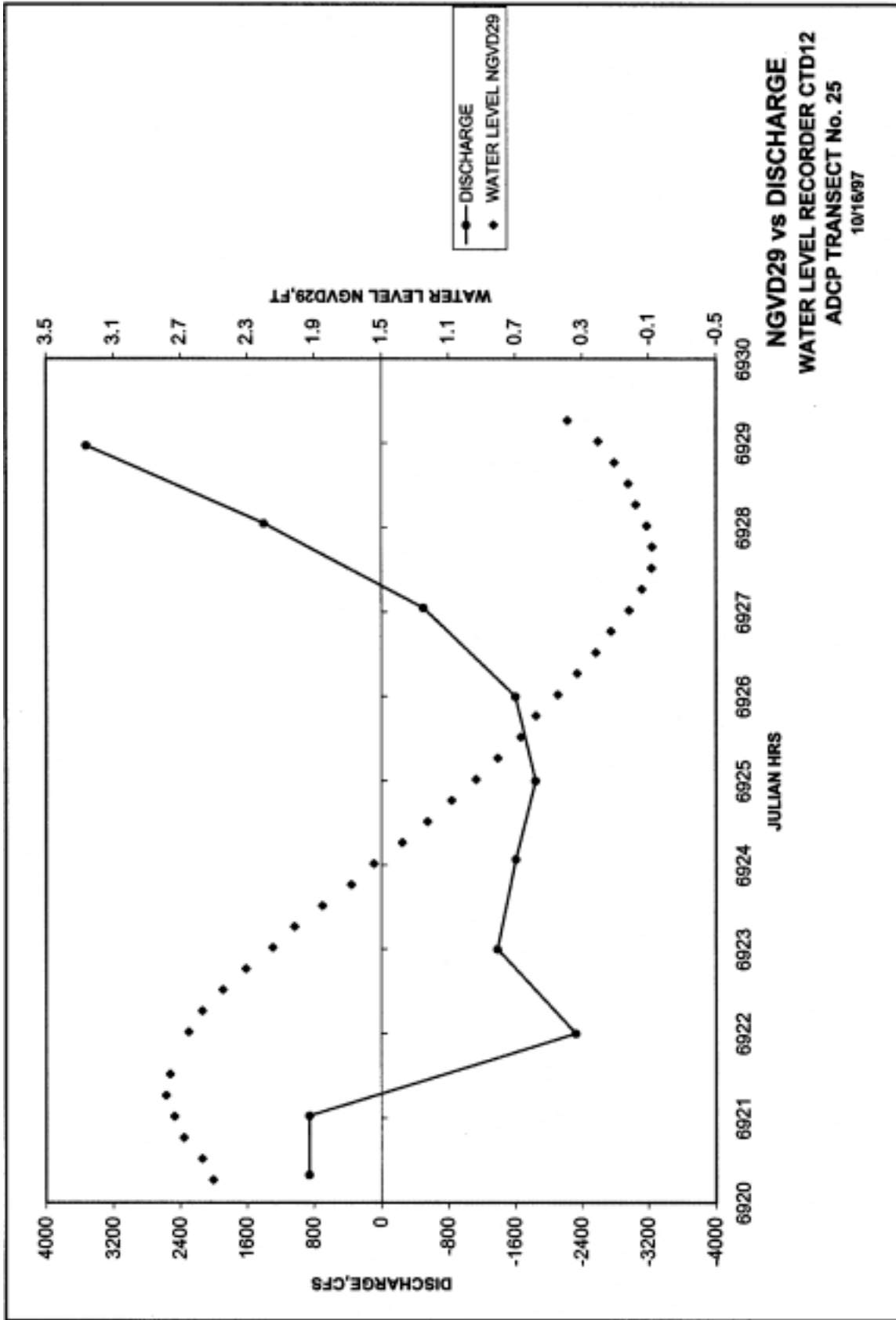


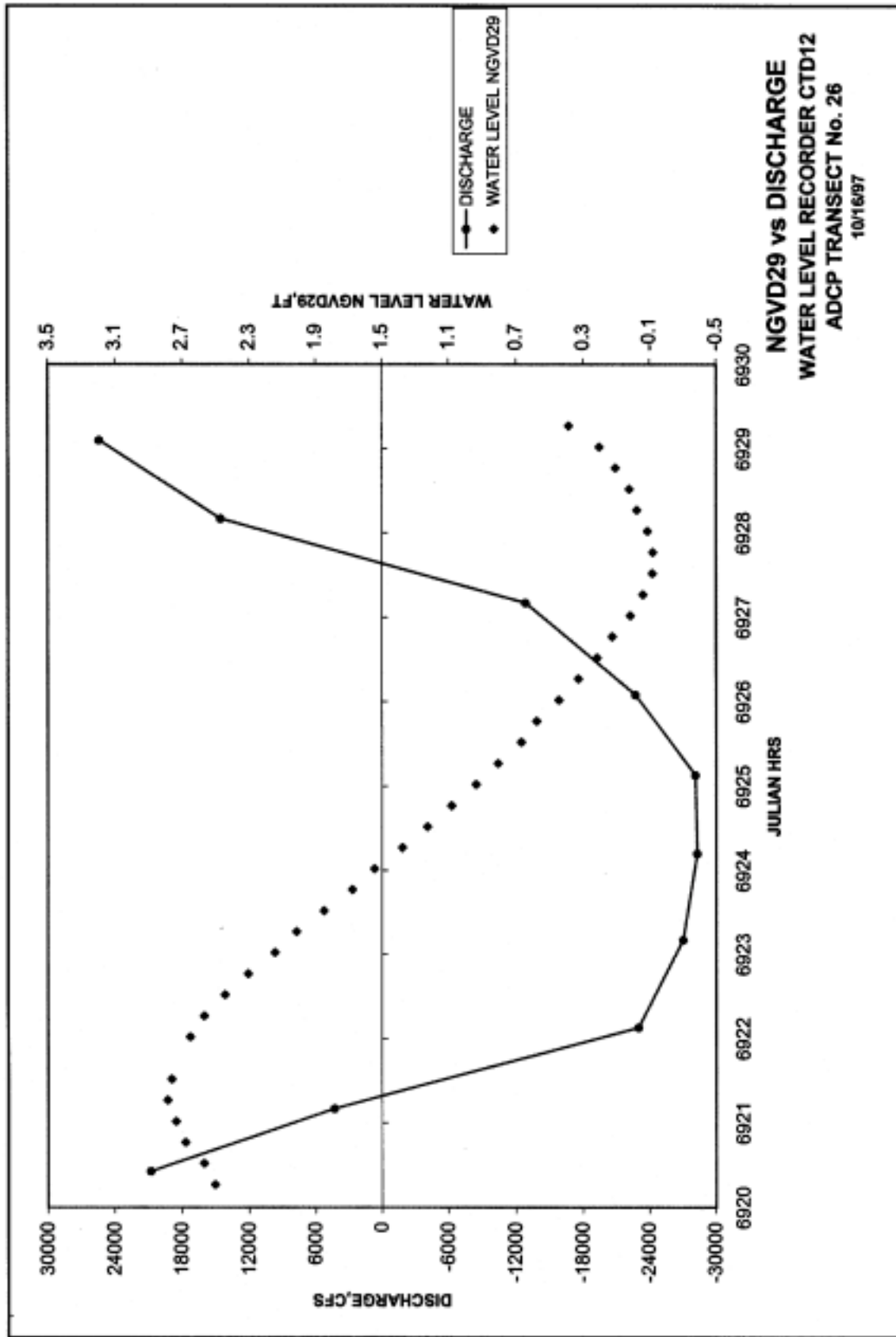


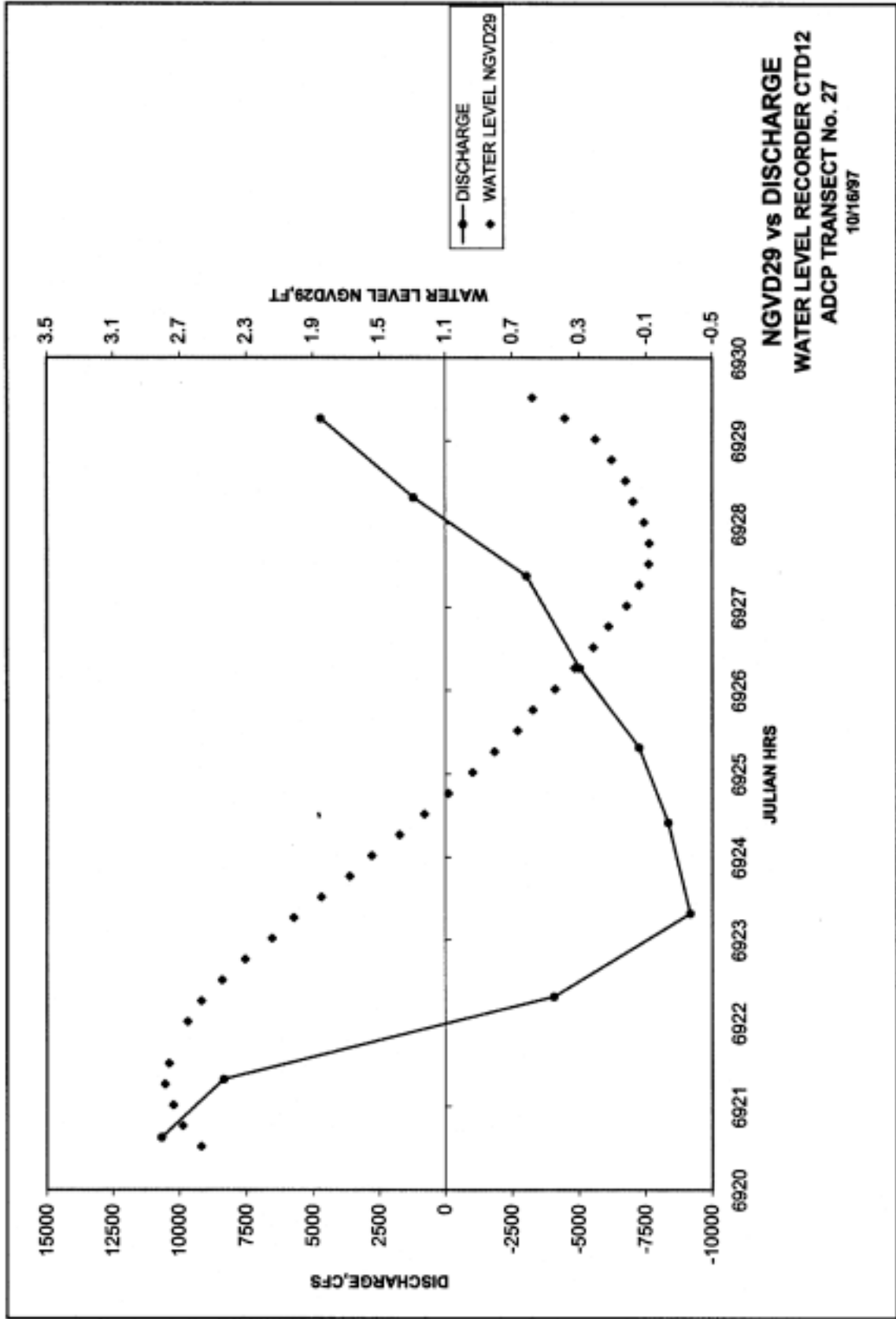


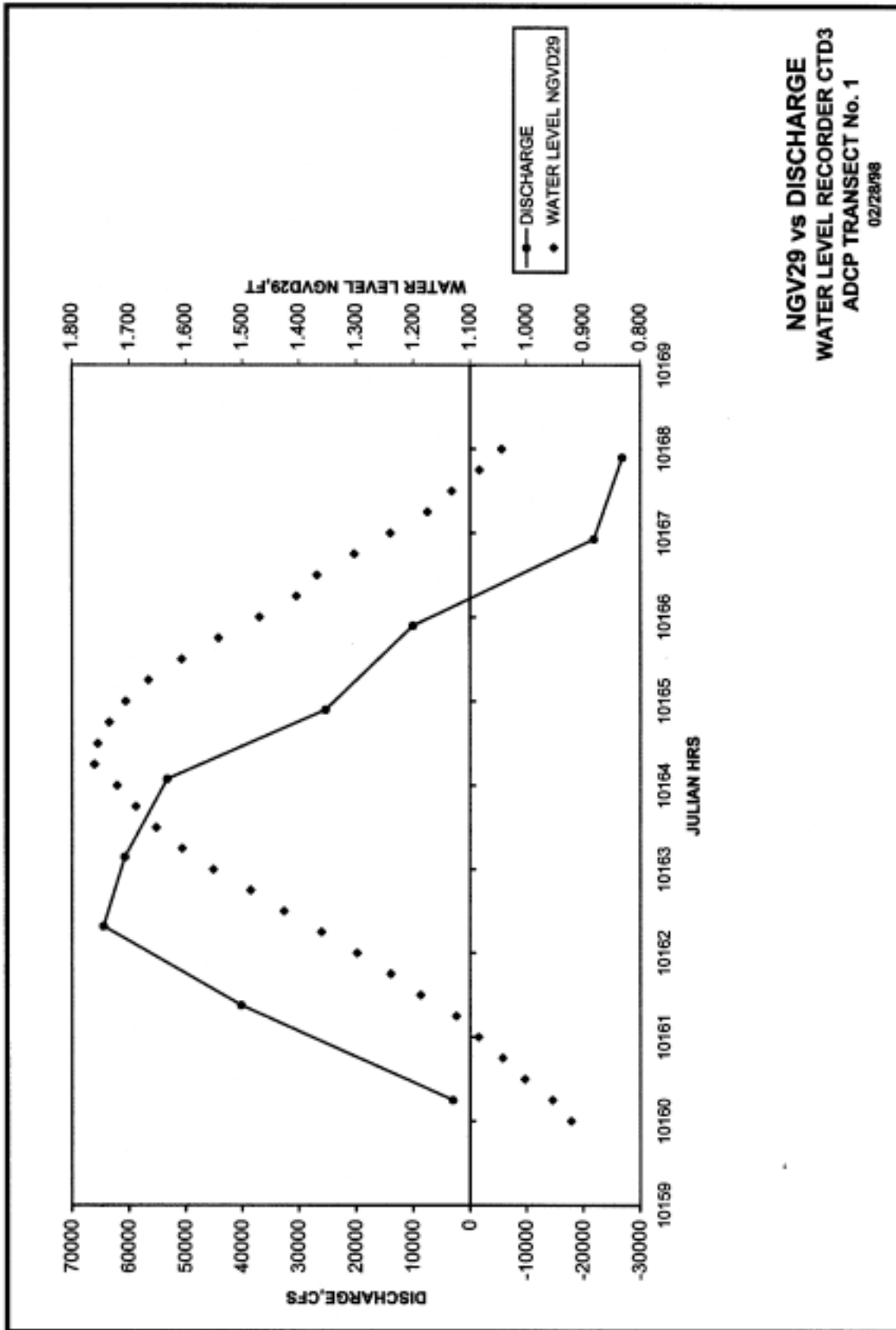


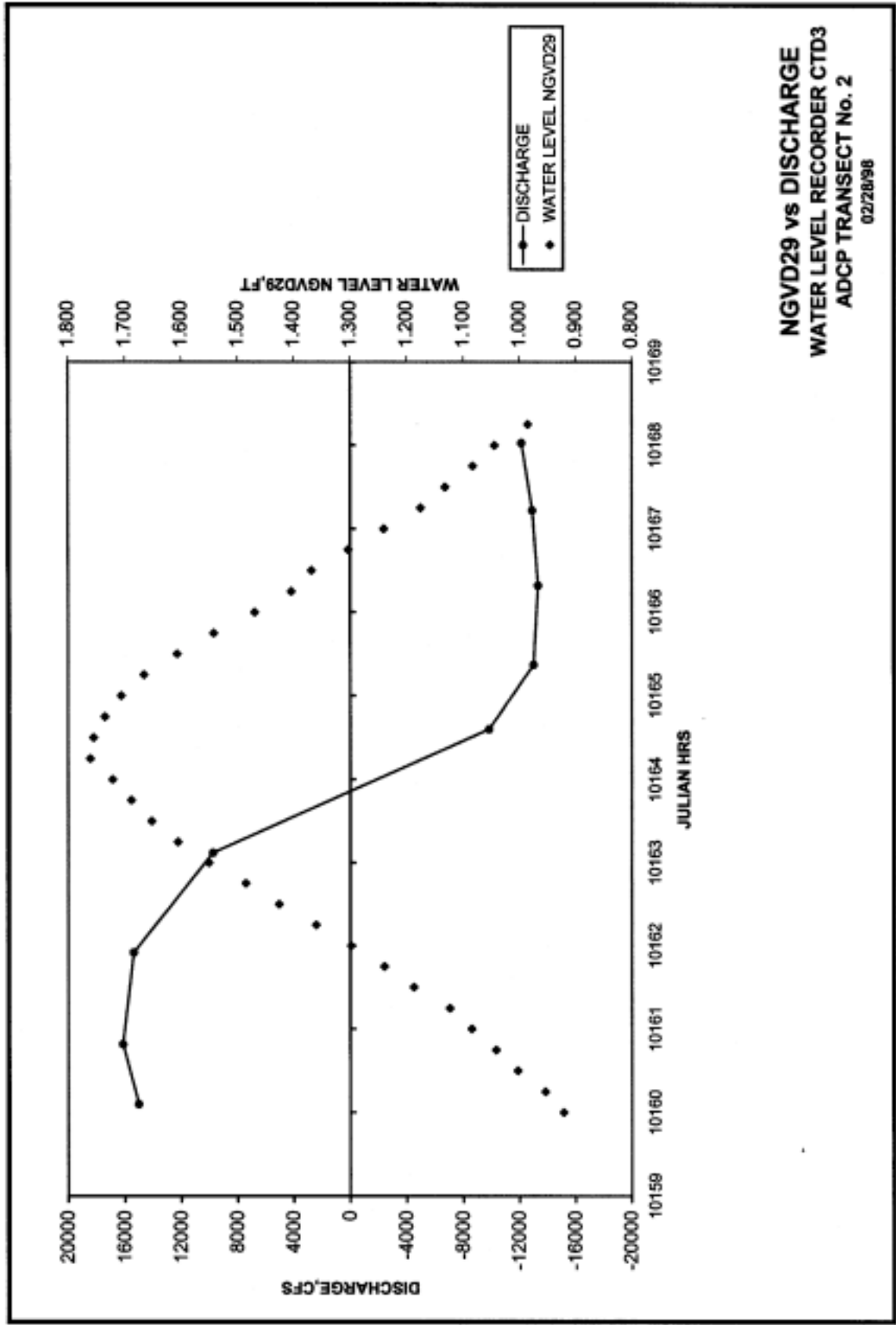


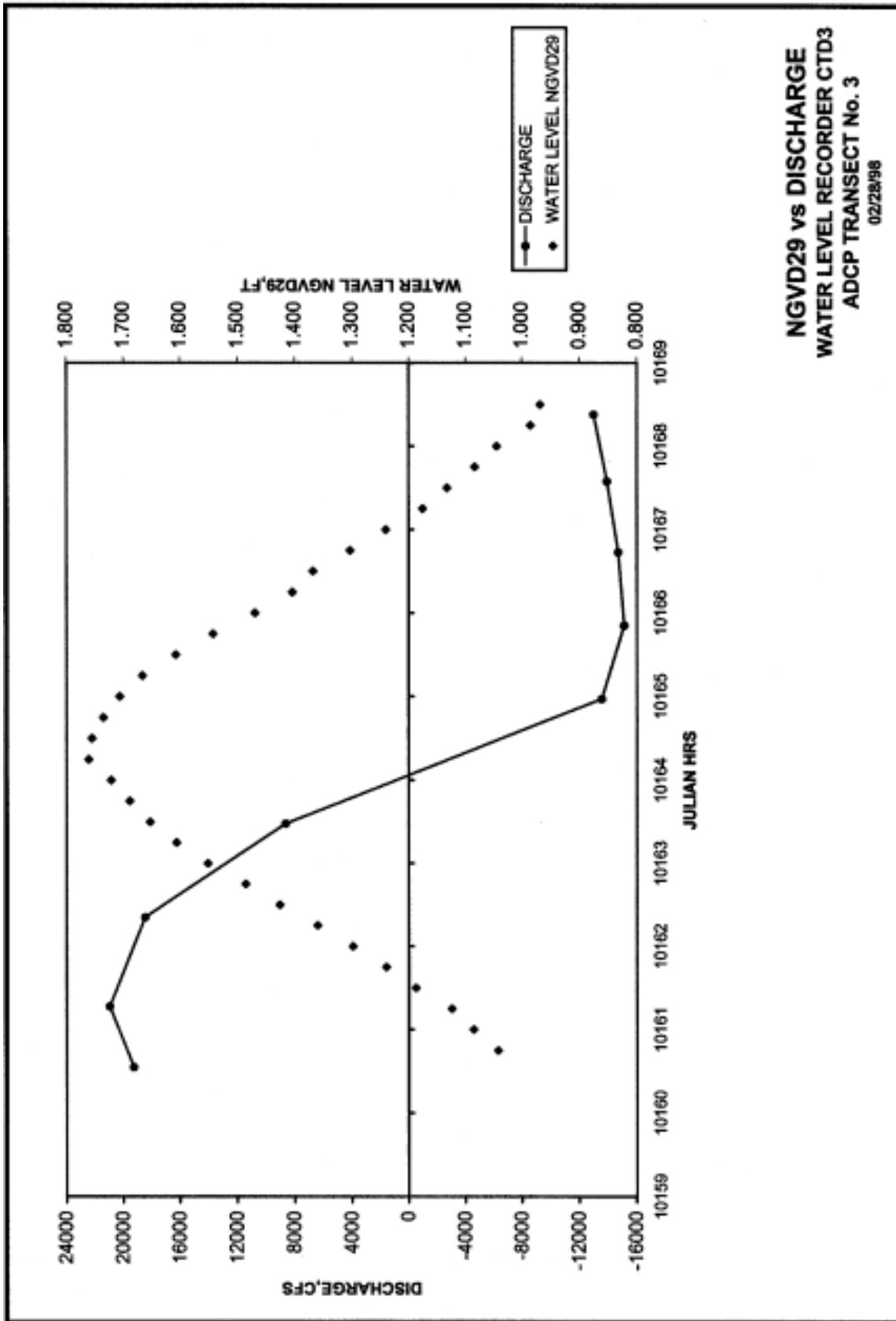




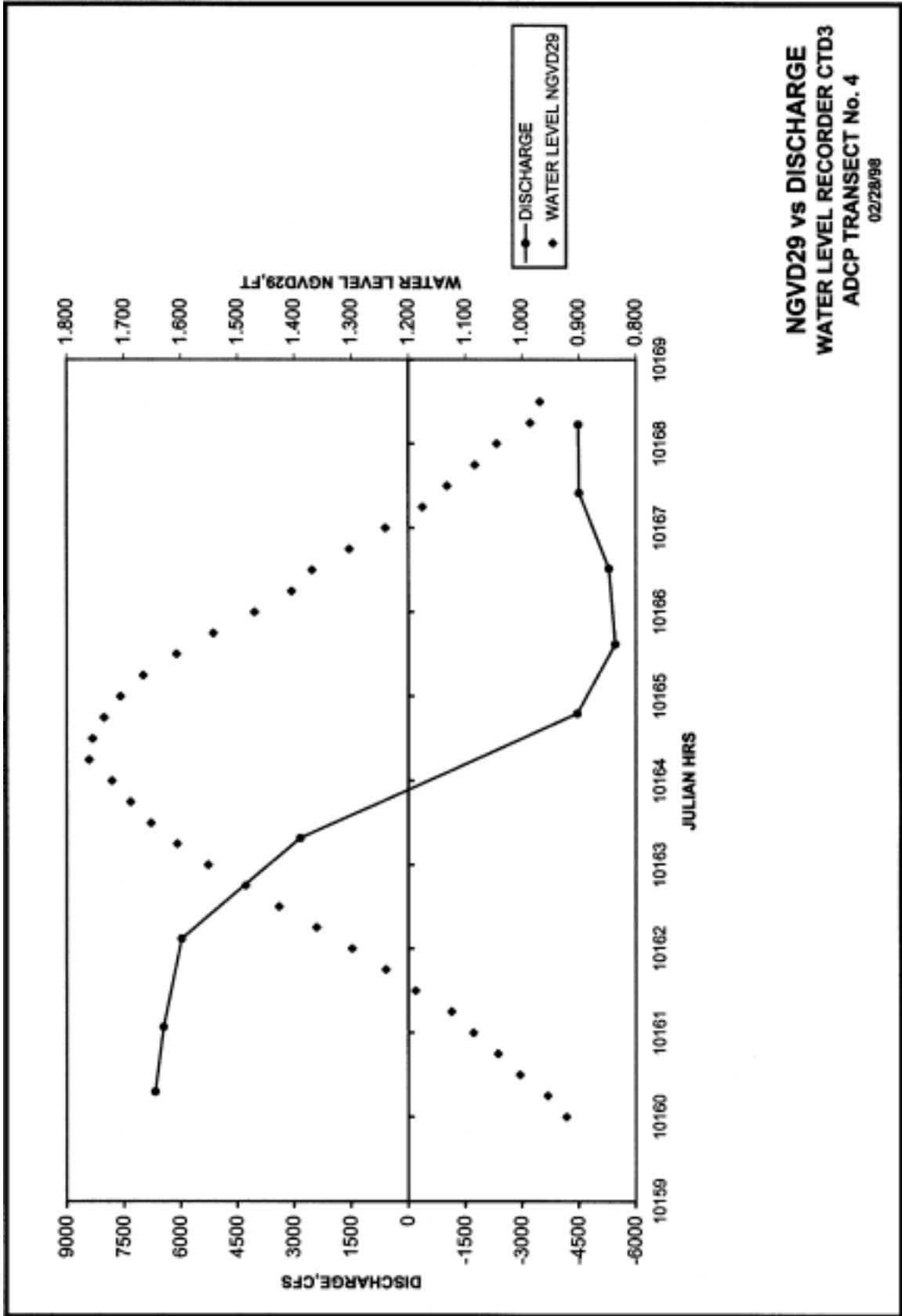


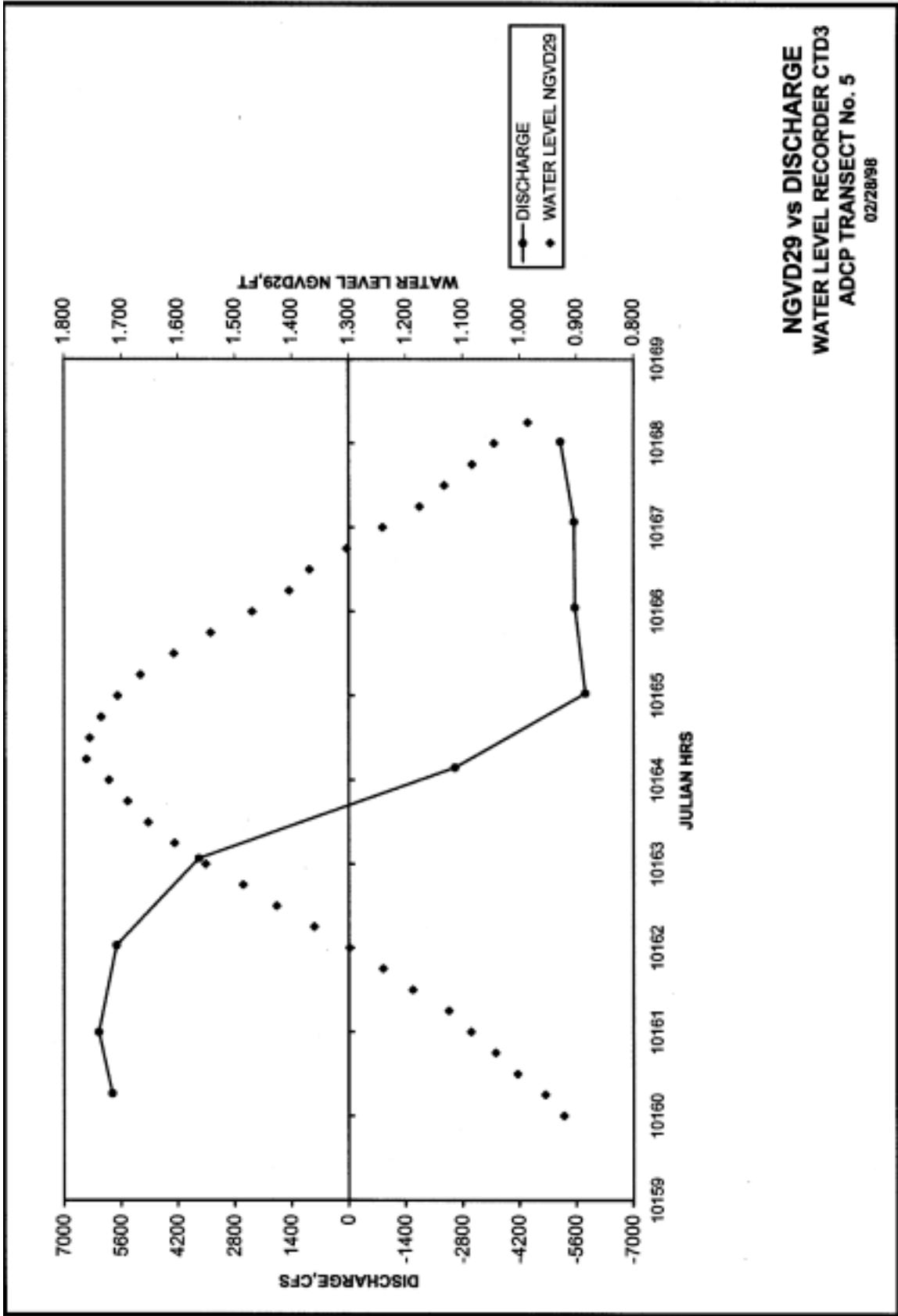




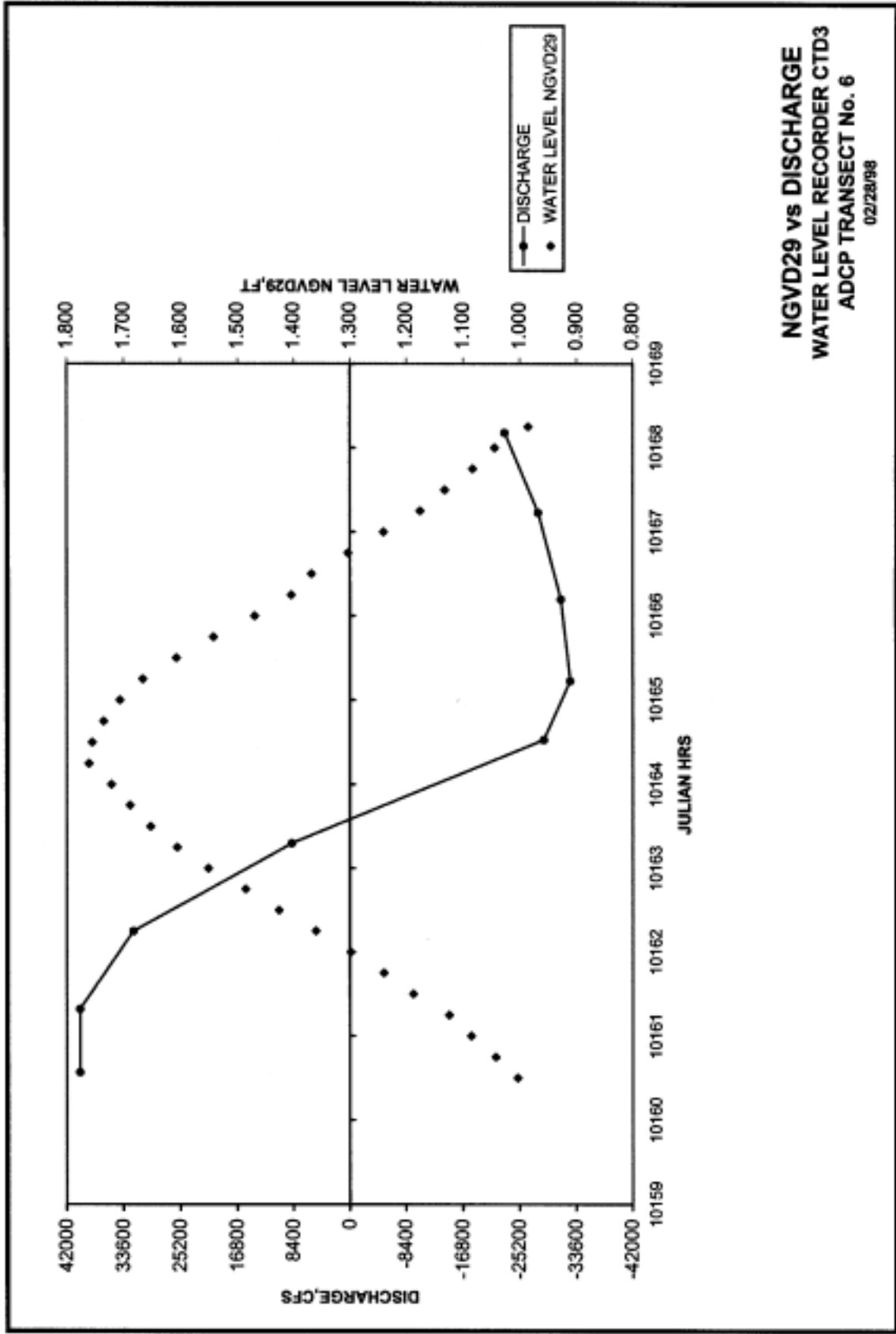


NGVD29 vs DISCHARGE
WATER LEVEL RECORDER CTD3
ADCP TRANSECT No. 3
 02/28/98

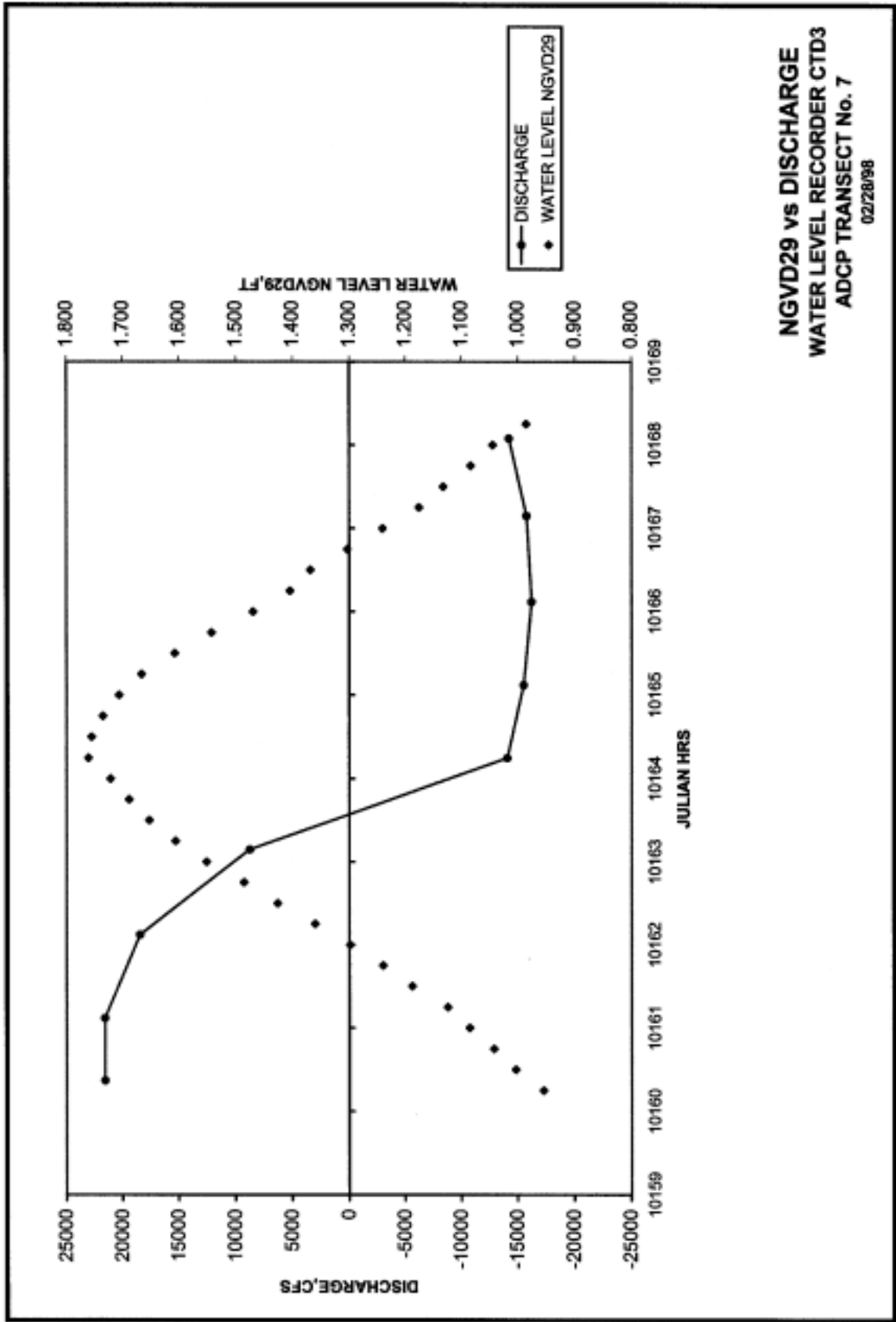


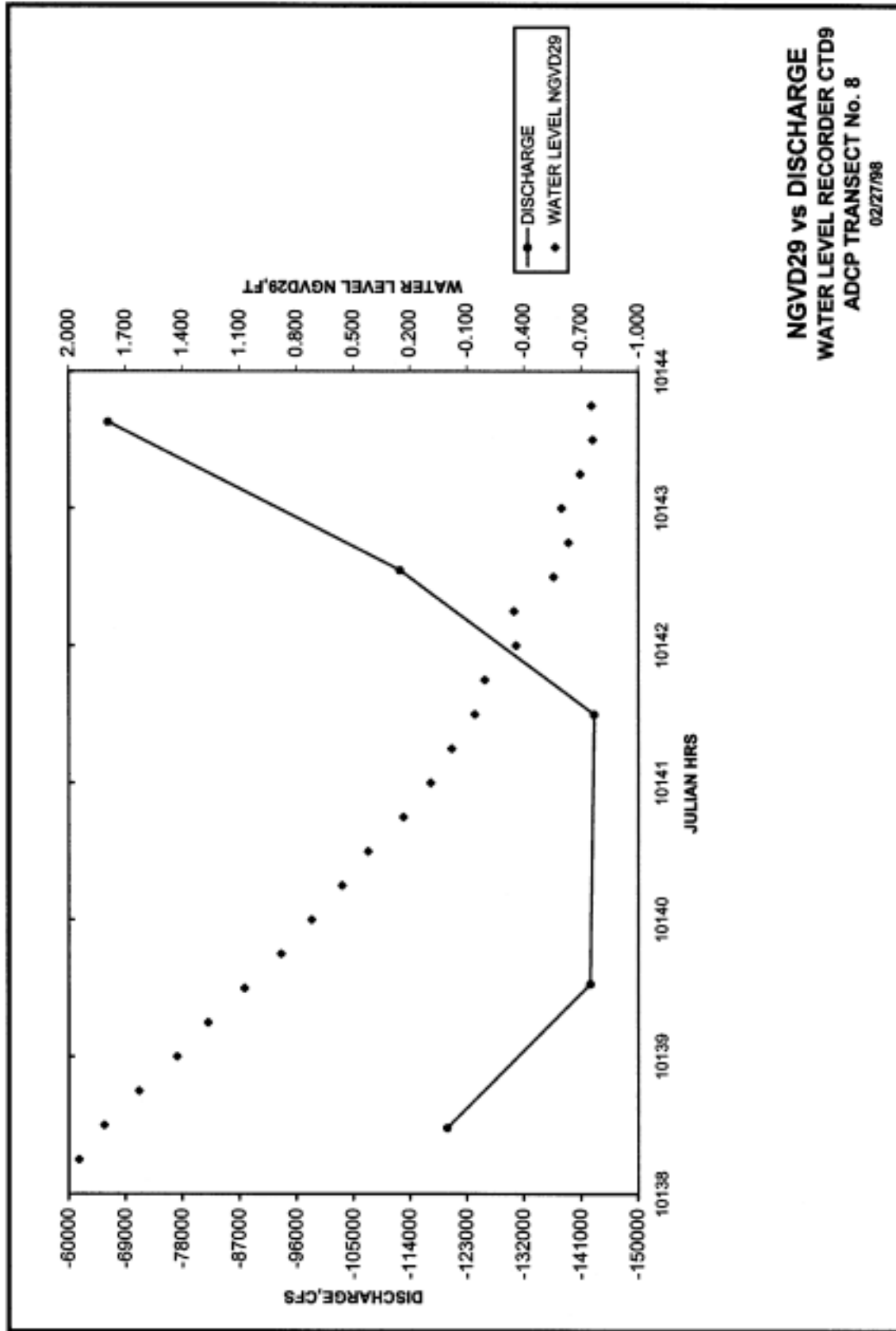


NGVD29 vs DISCHARGE
WATER LEVEL RECORDER CTD3
ADCP TRANSECT No. 5
 02/28/98

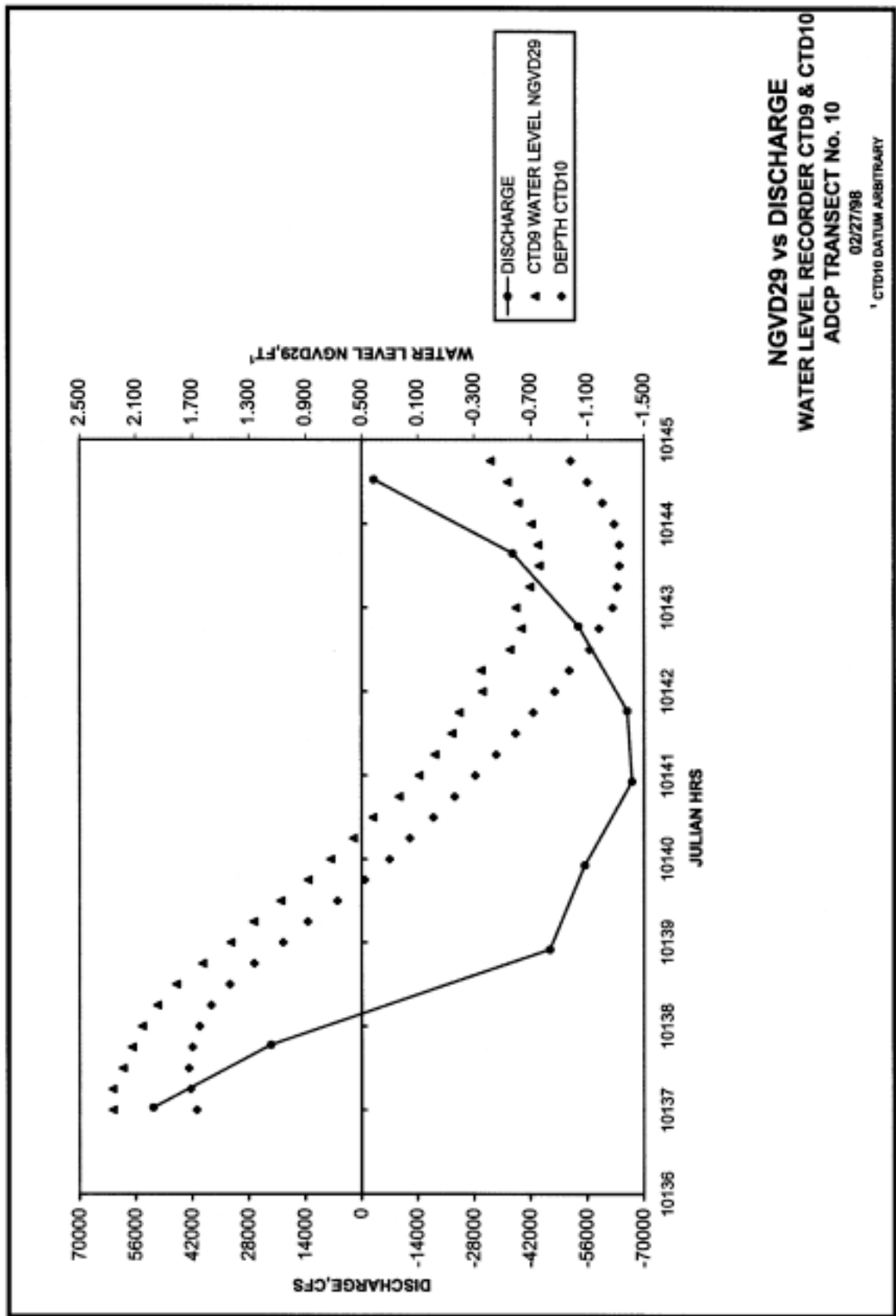


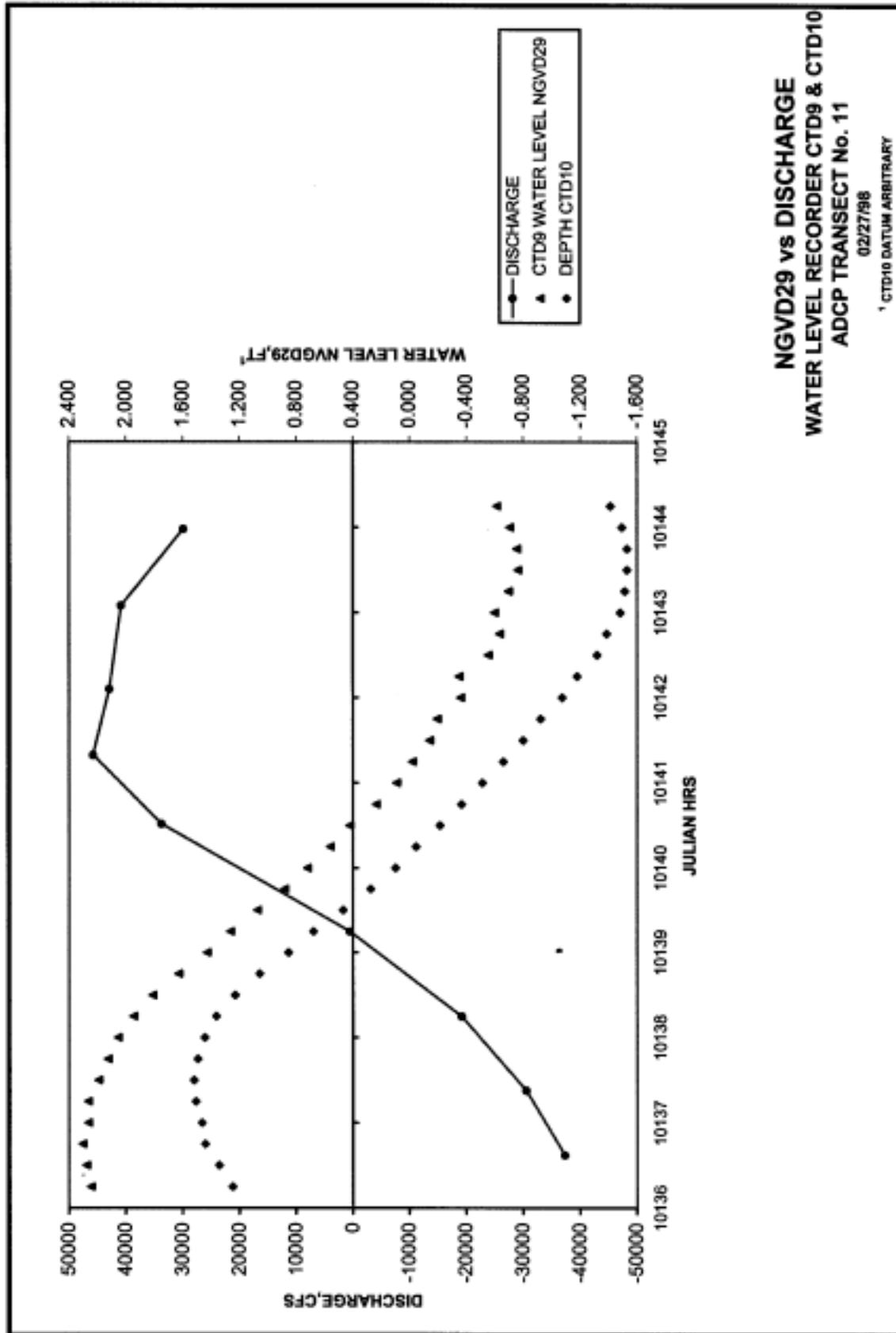
NGVD29 vs DISCHARGE
WATER LEVEL RECORDER CTD3
ADCP TRANSECT No. 6
 02/28/98

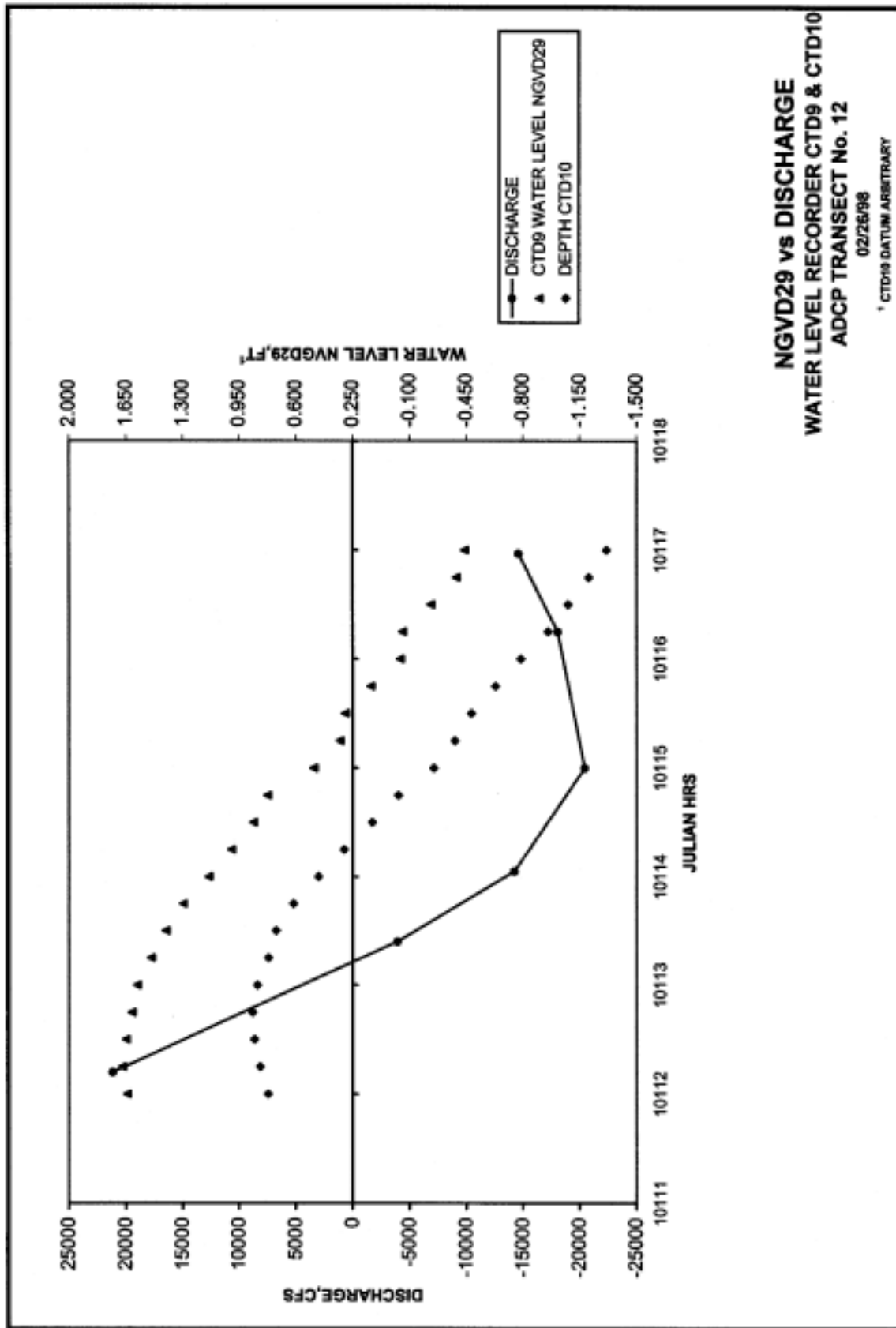


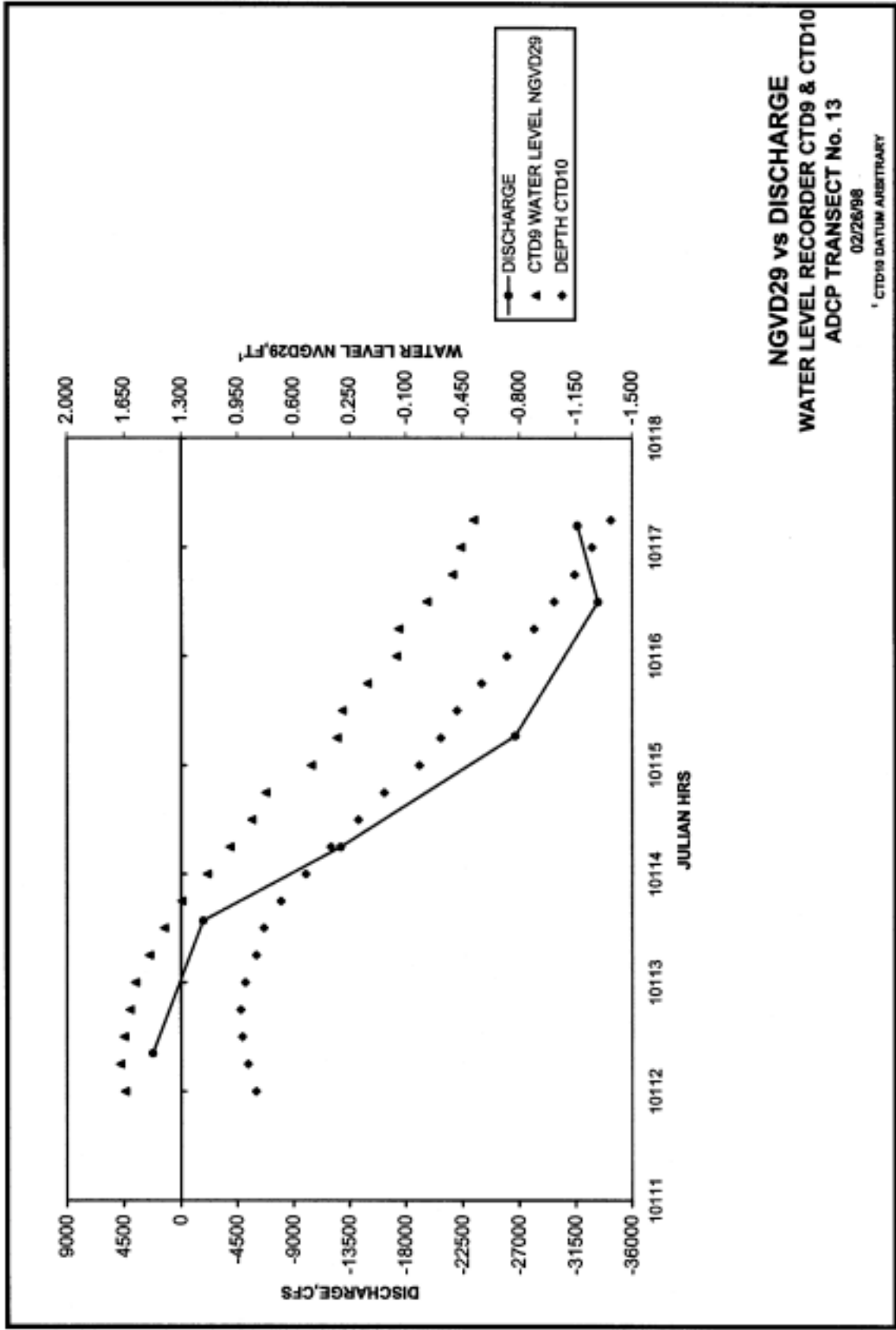


NGVD29 vs DISCHARGE
WATER LEVEL RECORDER CTD9
ADCP TRANSECT No. 8
 02/27/98

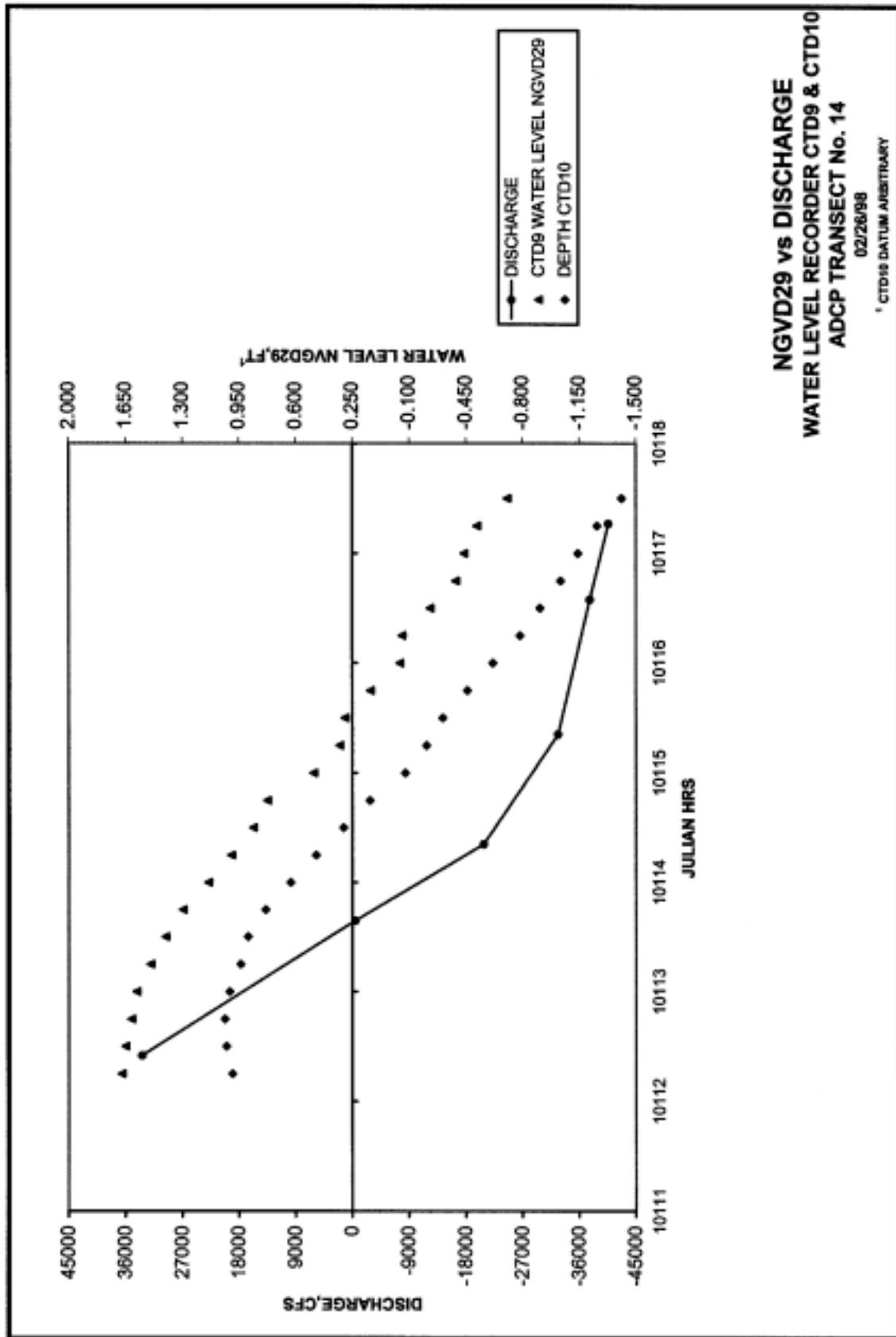




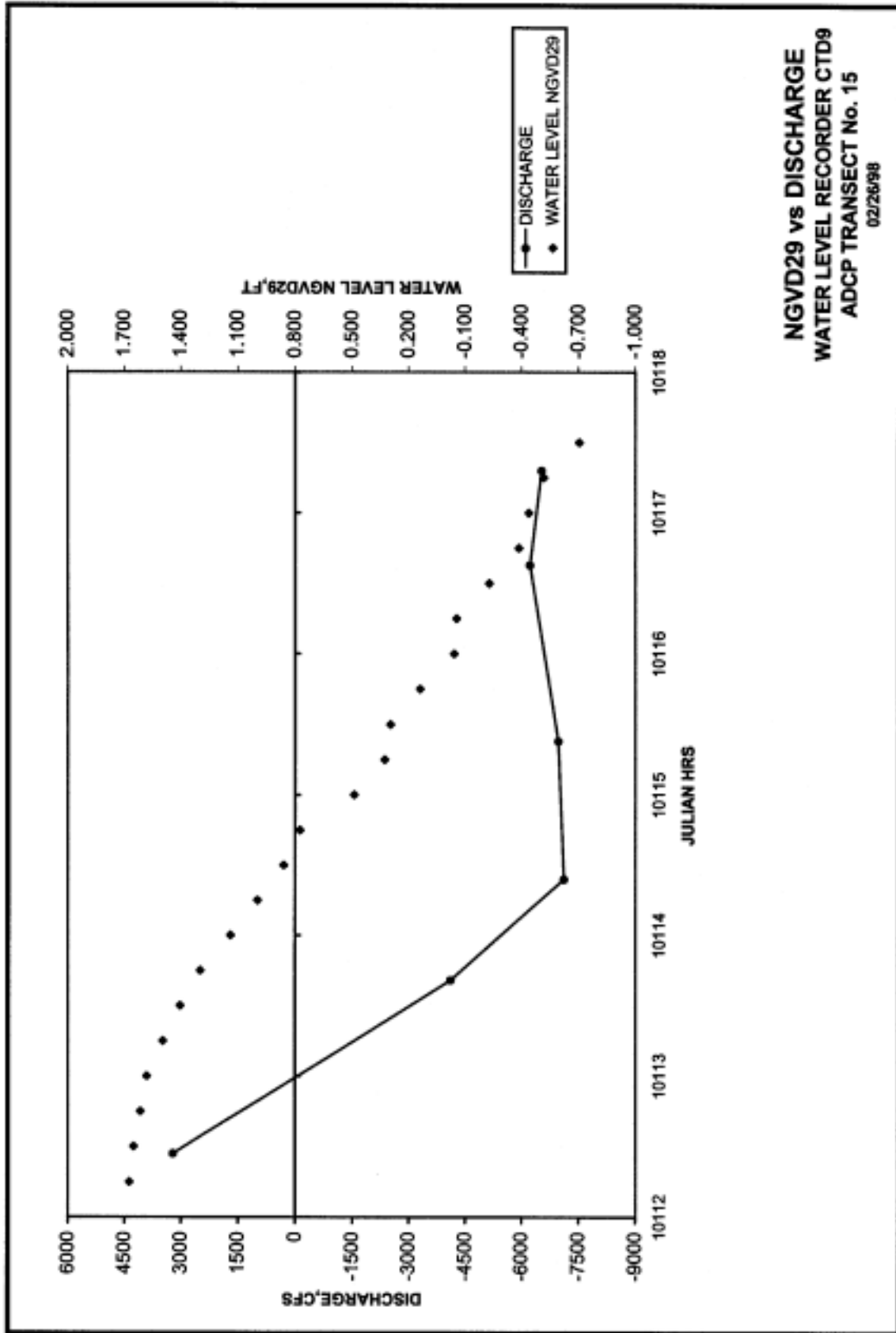




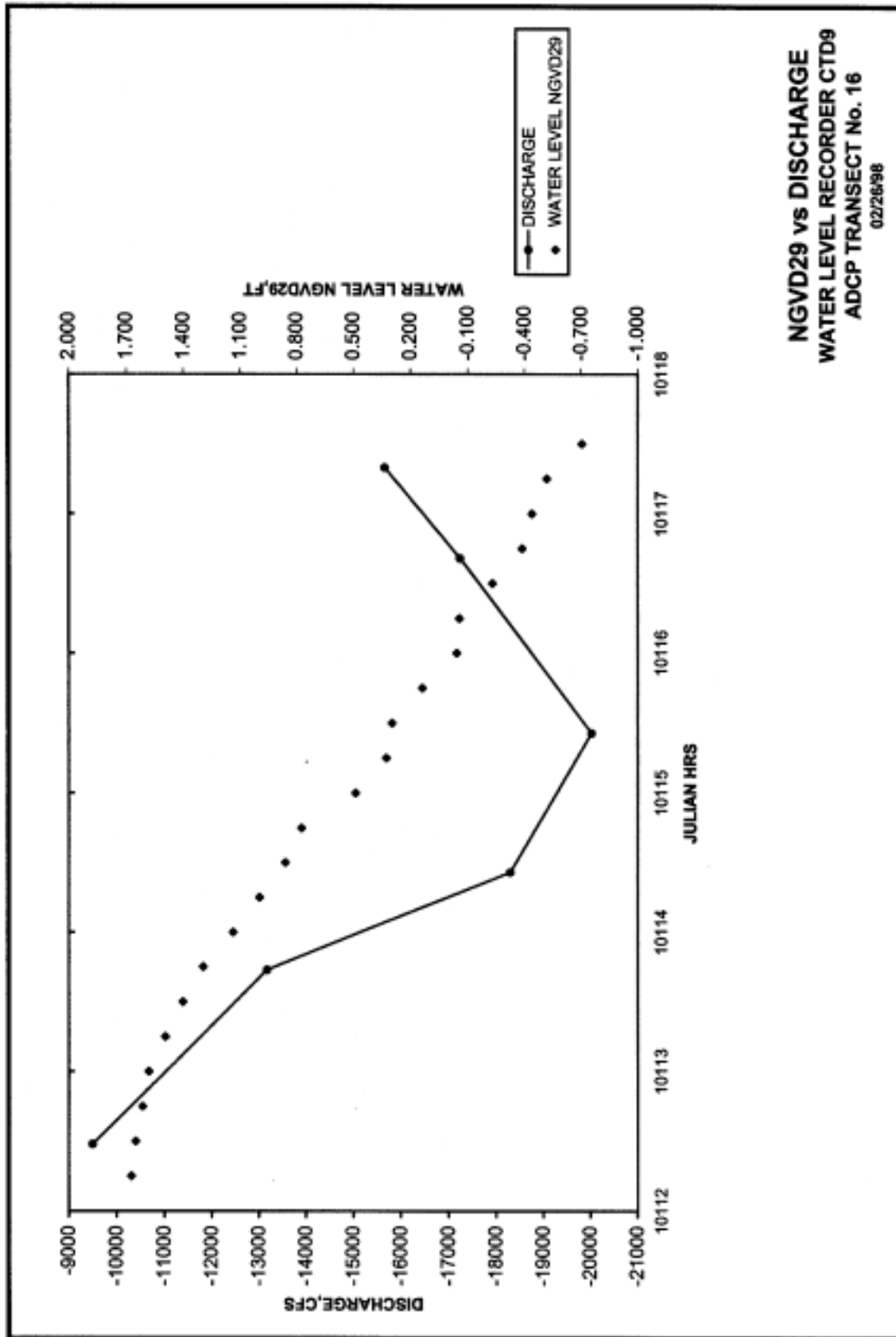
NGVD29 vs DISCHARGE
WATER LEVEL RECORDER CTD9 & CTD10
ADCP TRANSECT No. 13
 02/26/98
 * CTD9 DATUM ARBITRARY

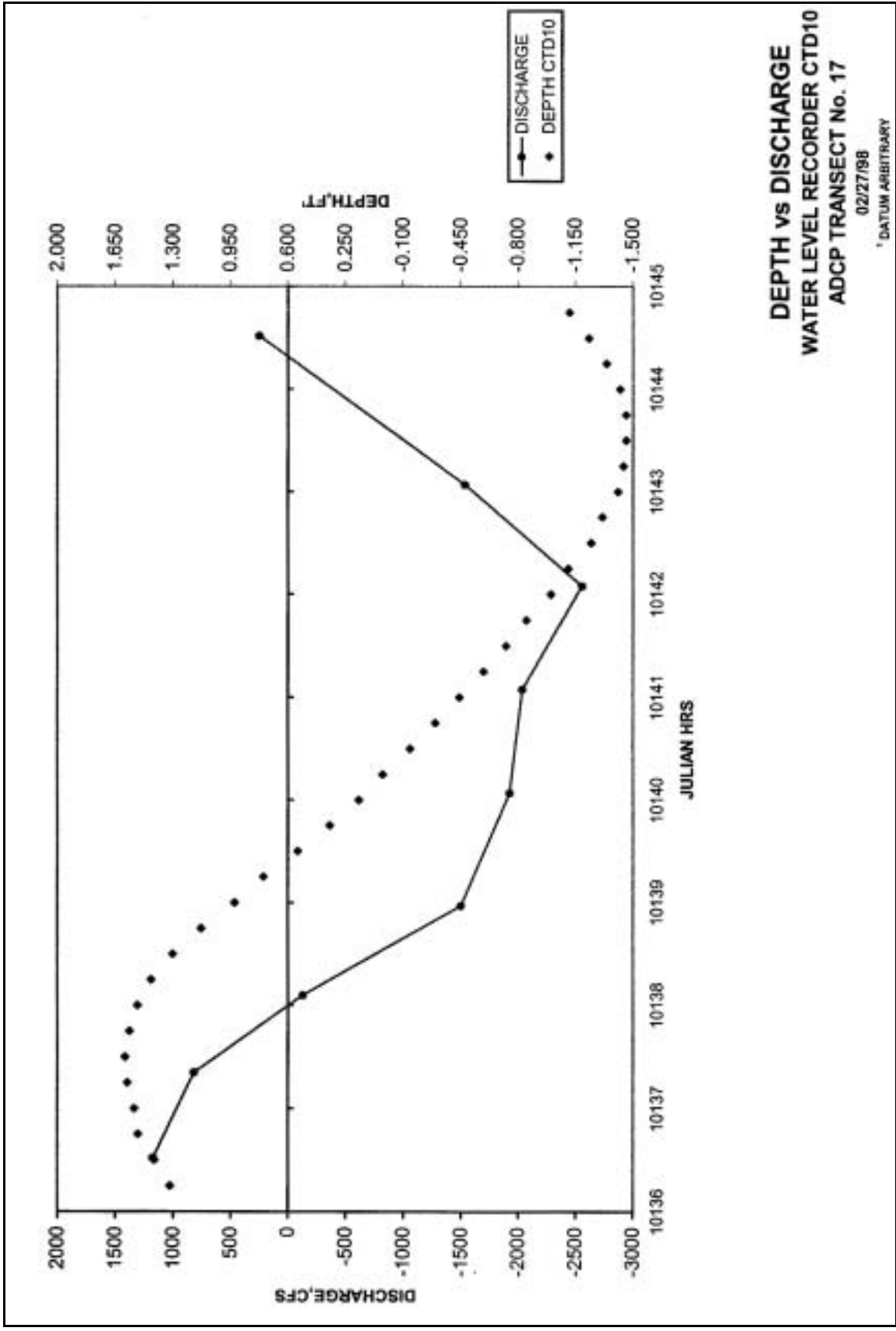


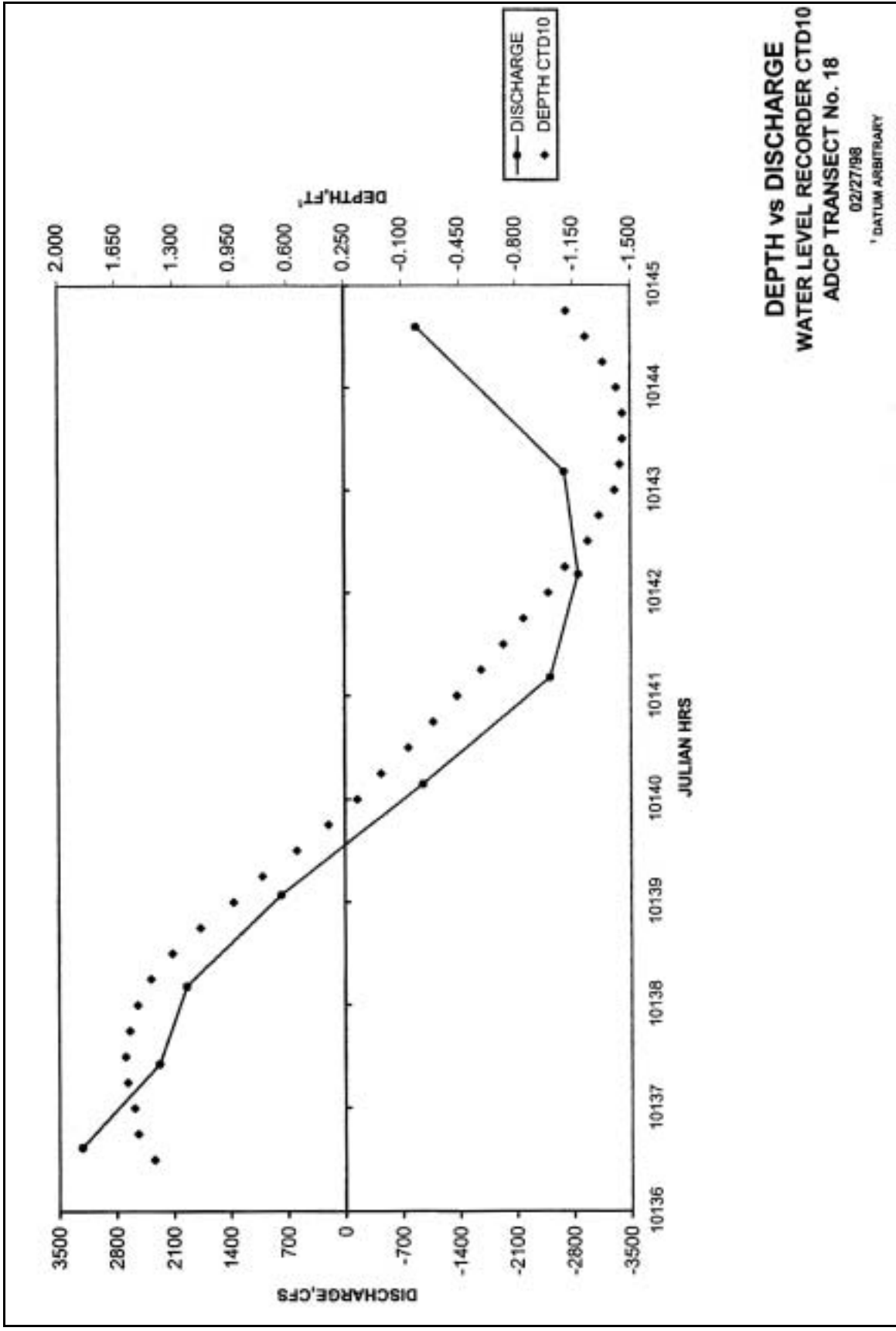
NGVD29 vs DISCHARGE
WATER LEVEL RECORDER CTD9 & CTD10
ADCP TRANSECT No. 14
 02/28/98
 * CTD9 DATUM ARBITRARY



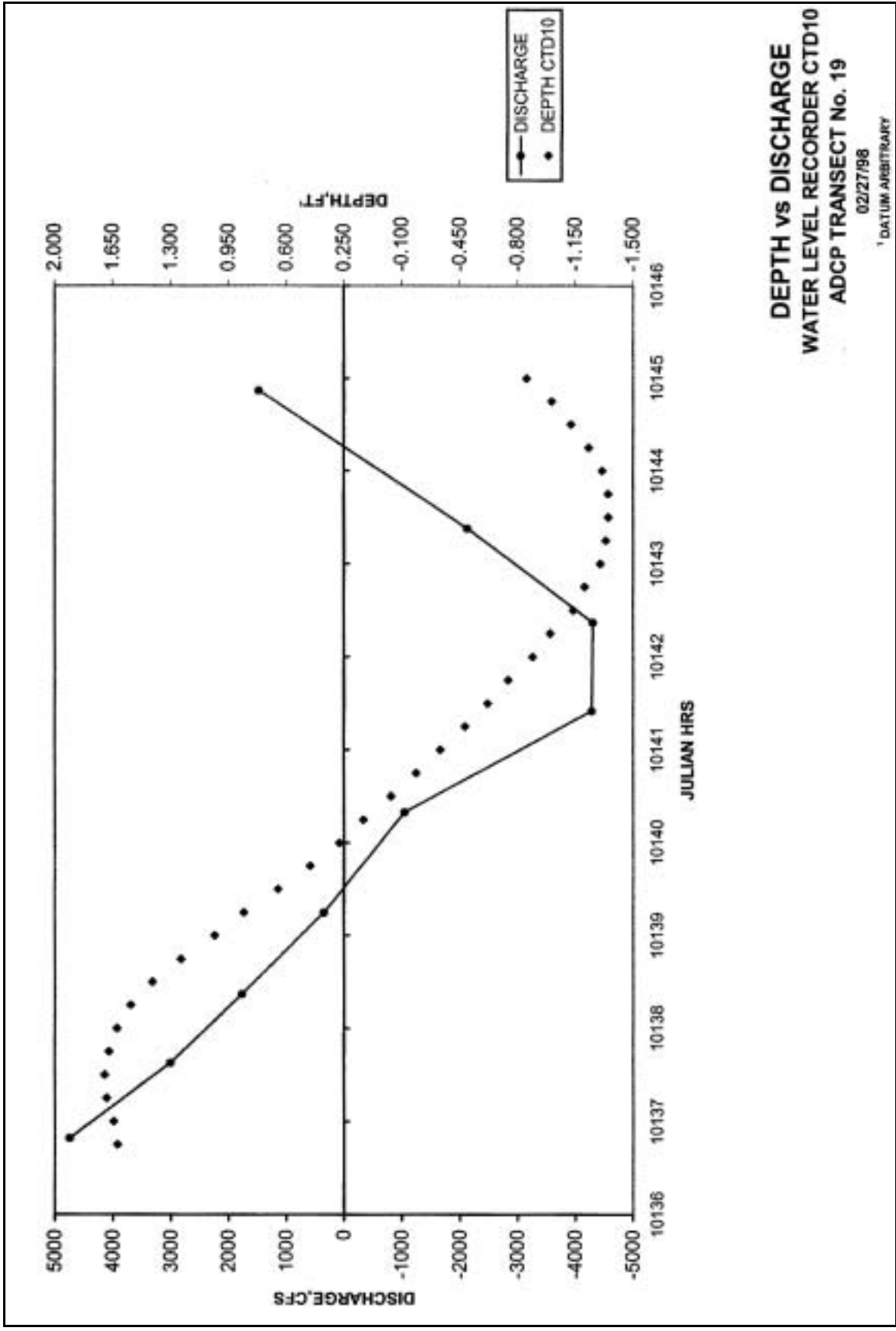
NGVD29 vs DISCHARGE
WATER LEVEL RECORDER CTD9
ADCP TRANSECT No. 15
 02/26/98







DEPTH vs DISCHARGE
WATER LEVEL RECORDER CTD10
ADCP TRANSECT No. 18
 02/27/98
 ' DATUM ARBITRARY



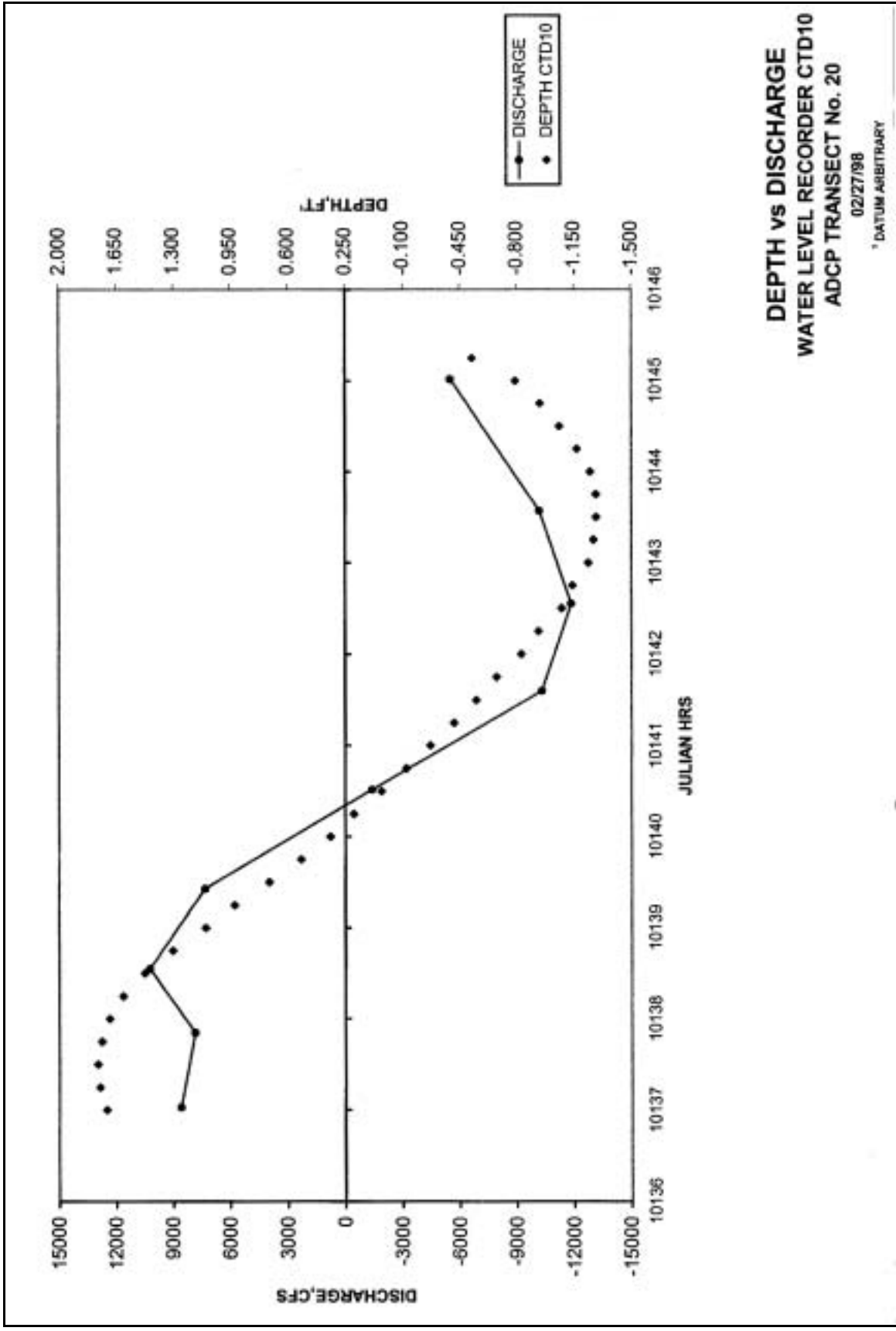
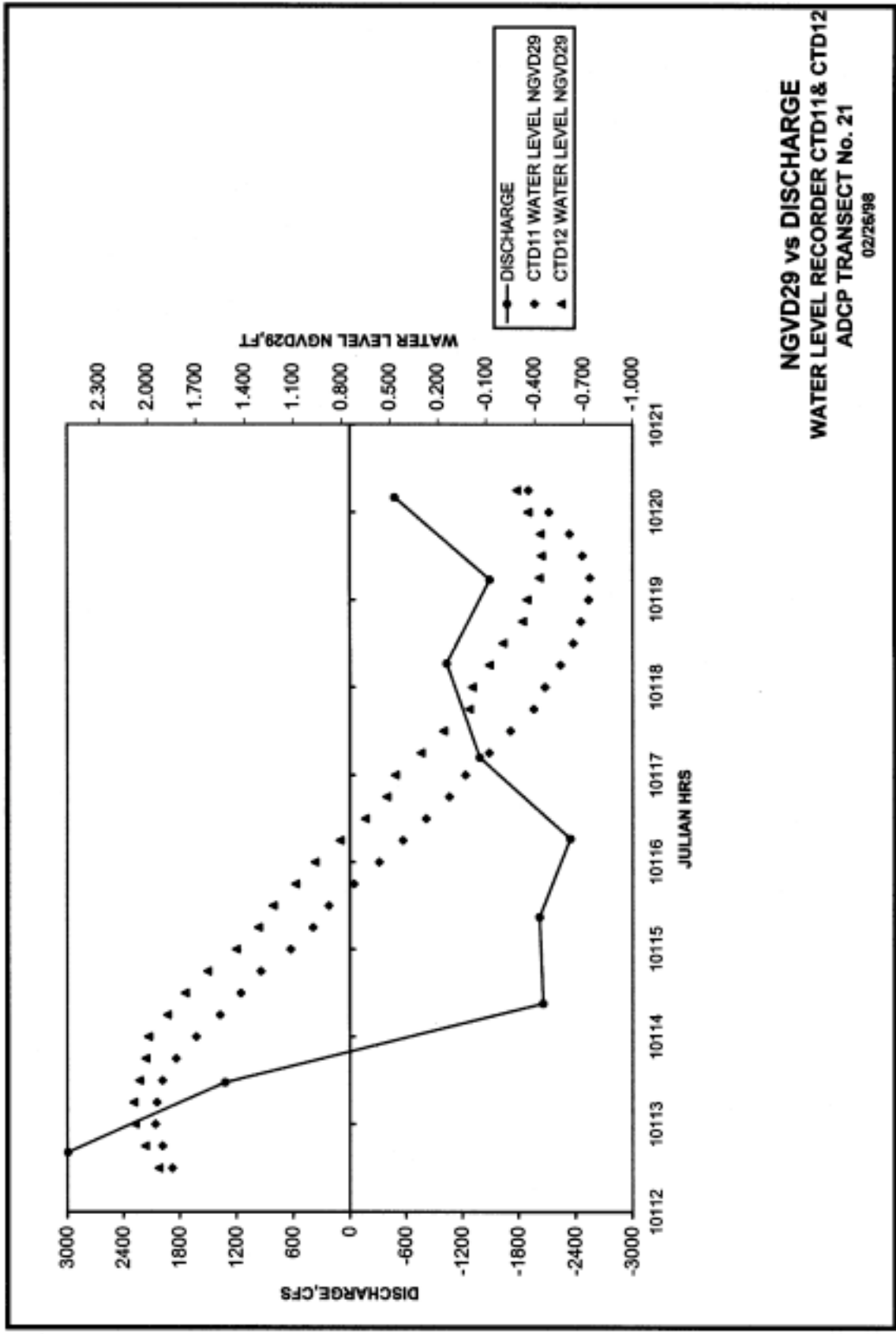
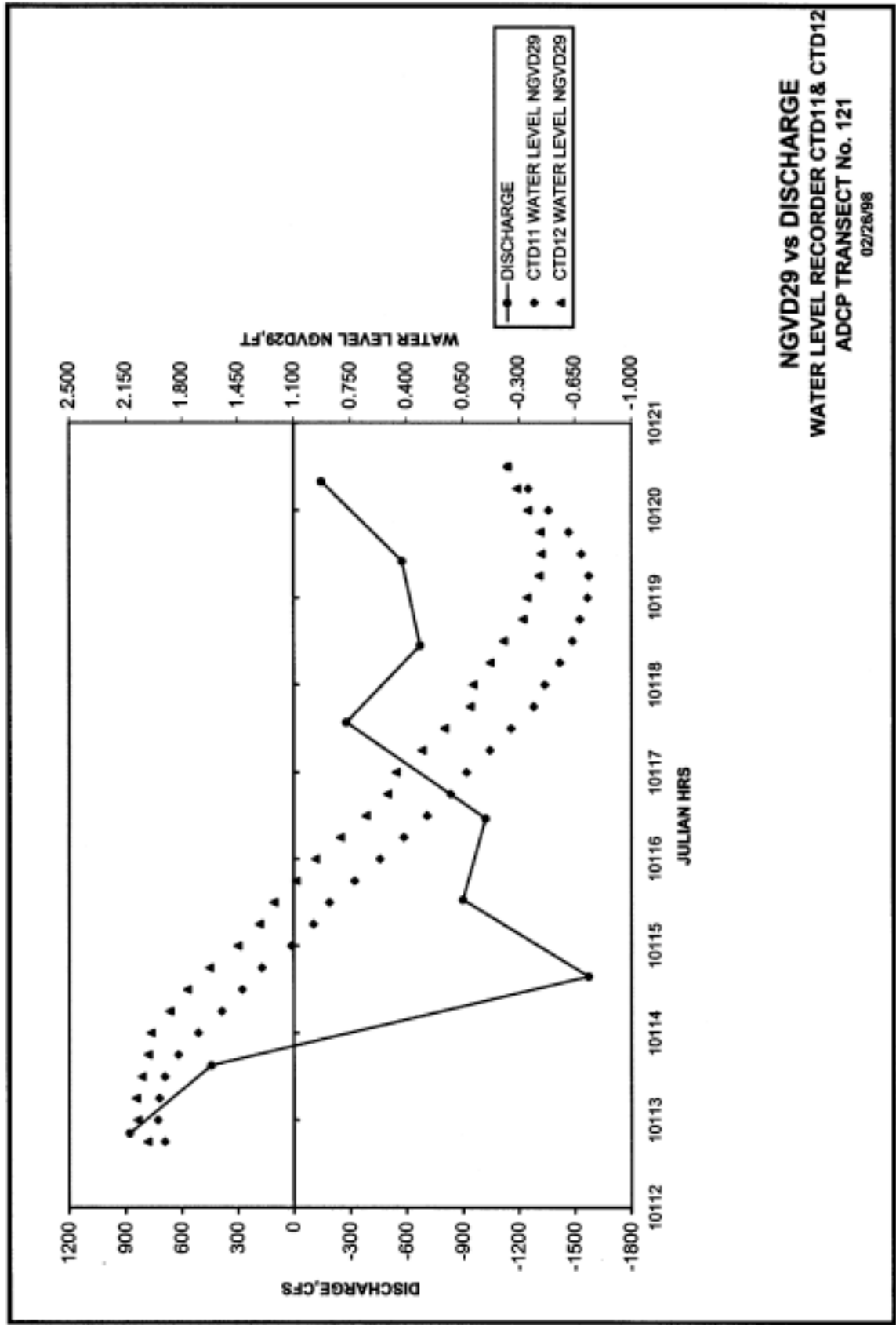


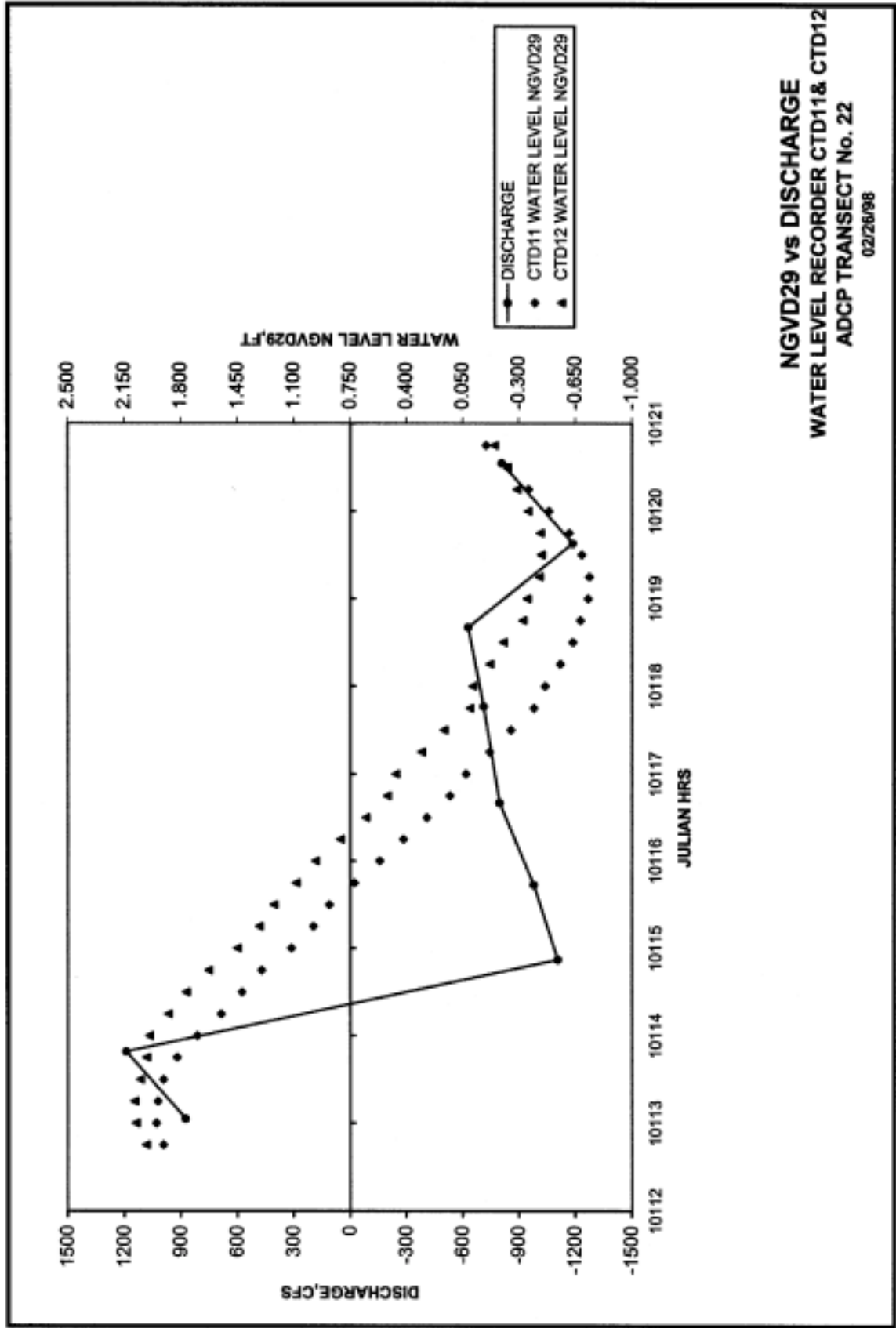
Plate 214

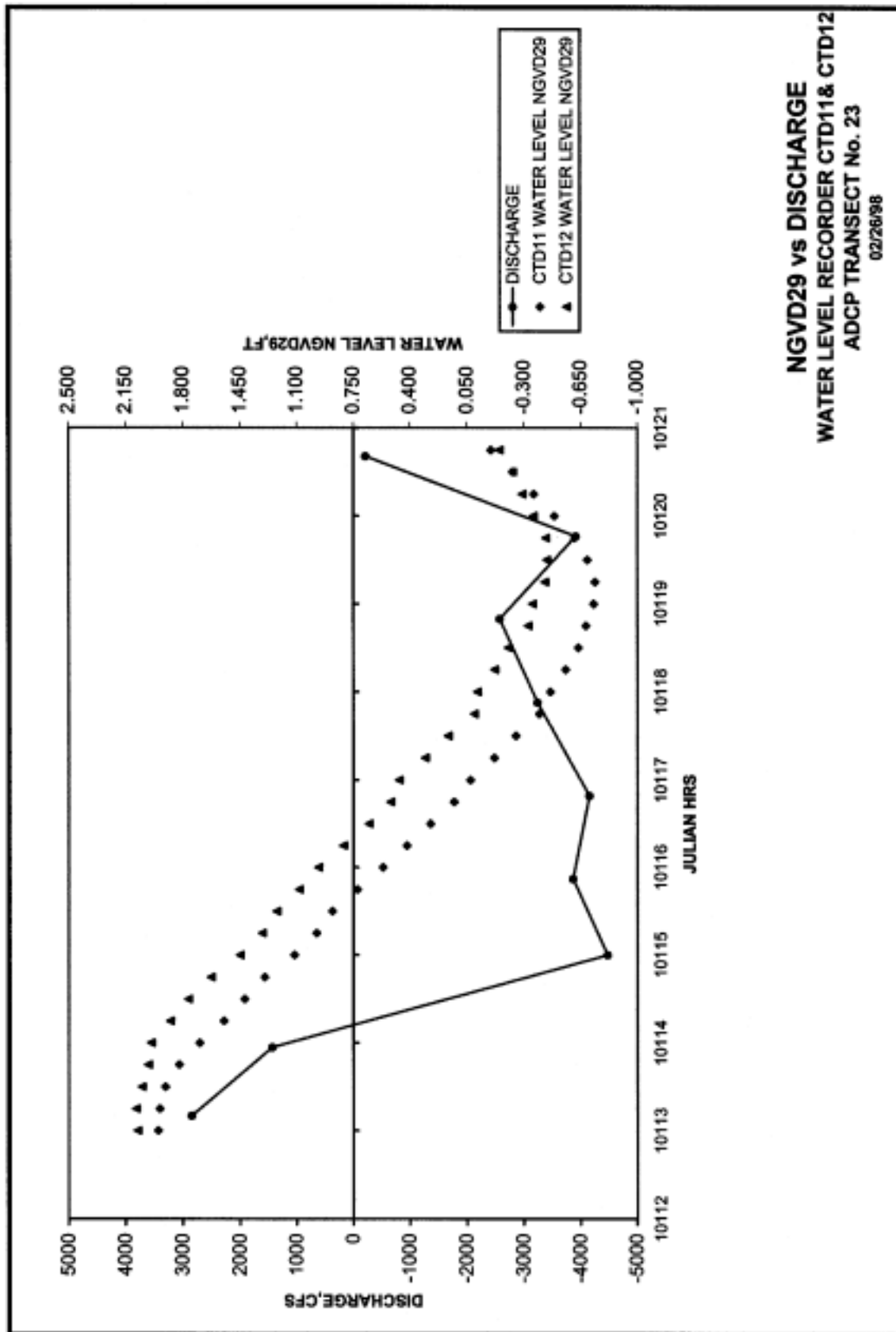


NGVD29 vs DISCHARGE
WATER LEVEL RECORDER CTD11& CTD12
ADCP TRANSECT No. 21
 02/25/98

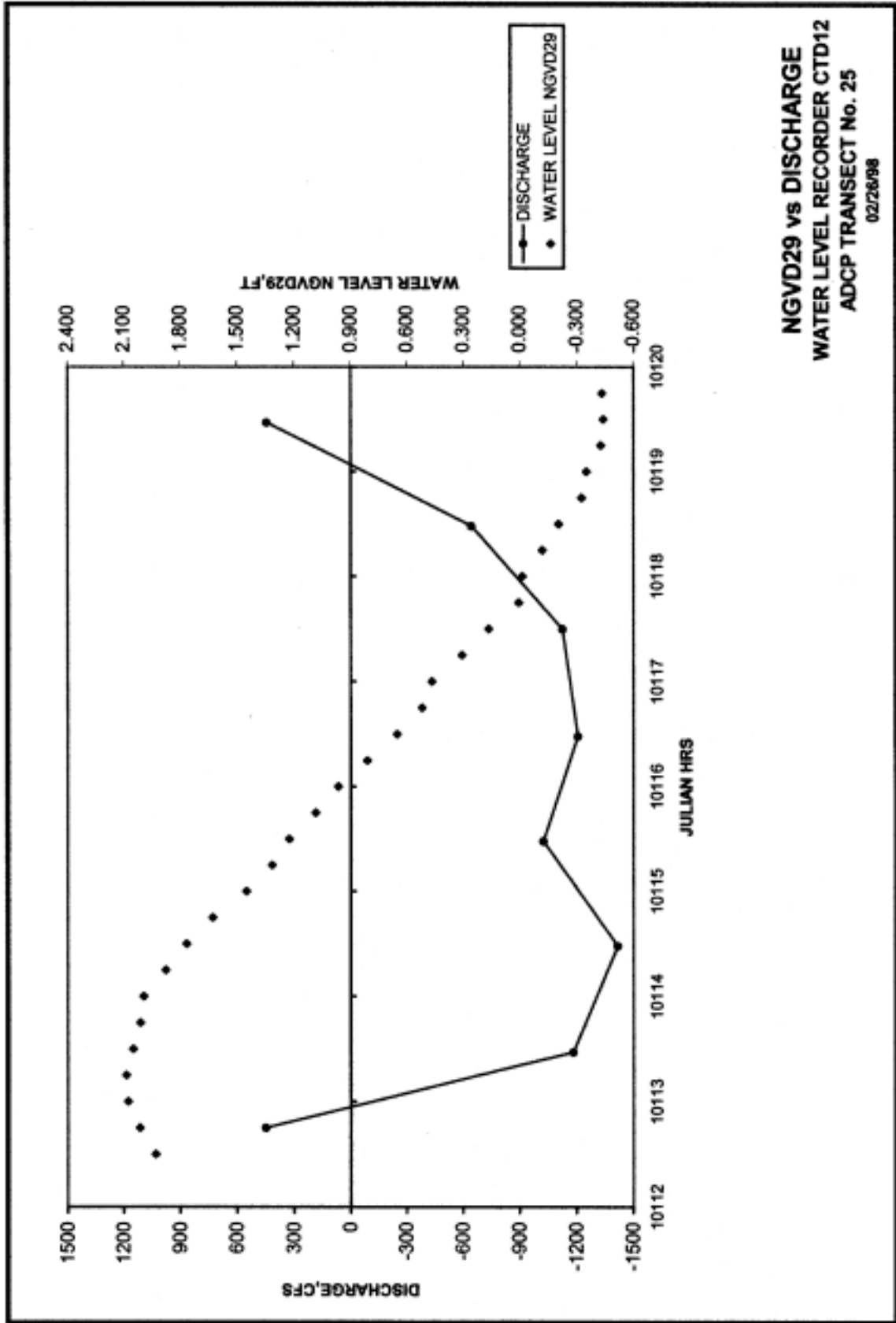


NGVD29 vs DISCHARGE
WATER LEVEL RECORDER CTD11& CTD12
ADCP TRANSECT No. 121
 02/26/98

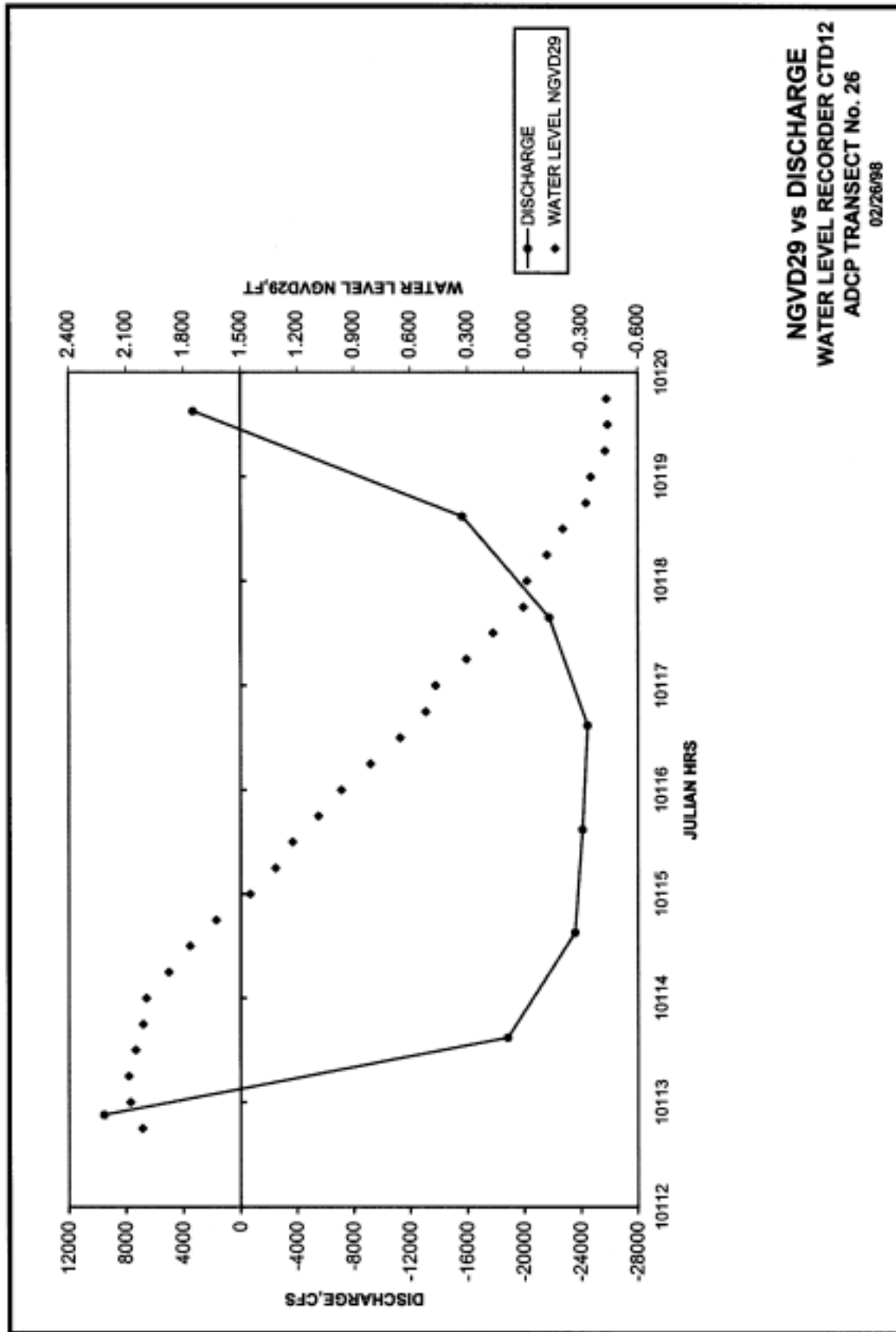




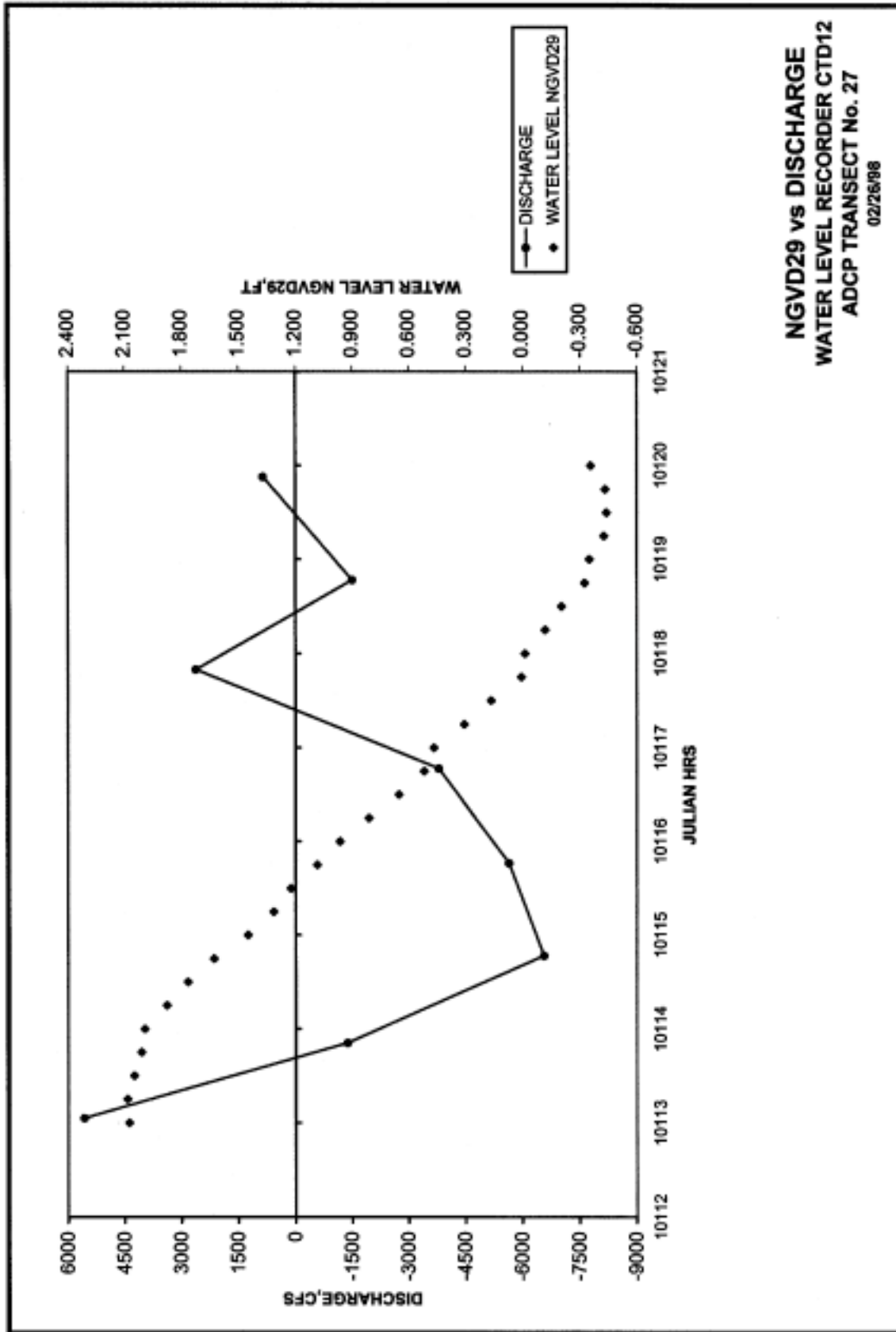
NGVD29 vs DISCHARGE
WATER LEVEL RECORDER CTD11& CTD12
ADCP TRANSECT No. 23
 02/26/98

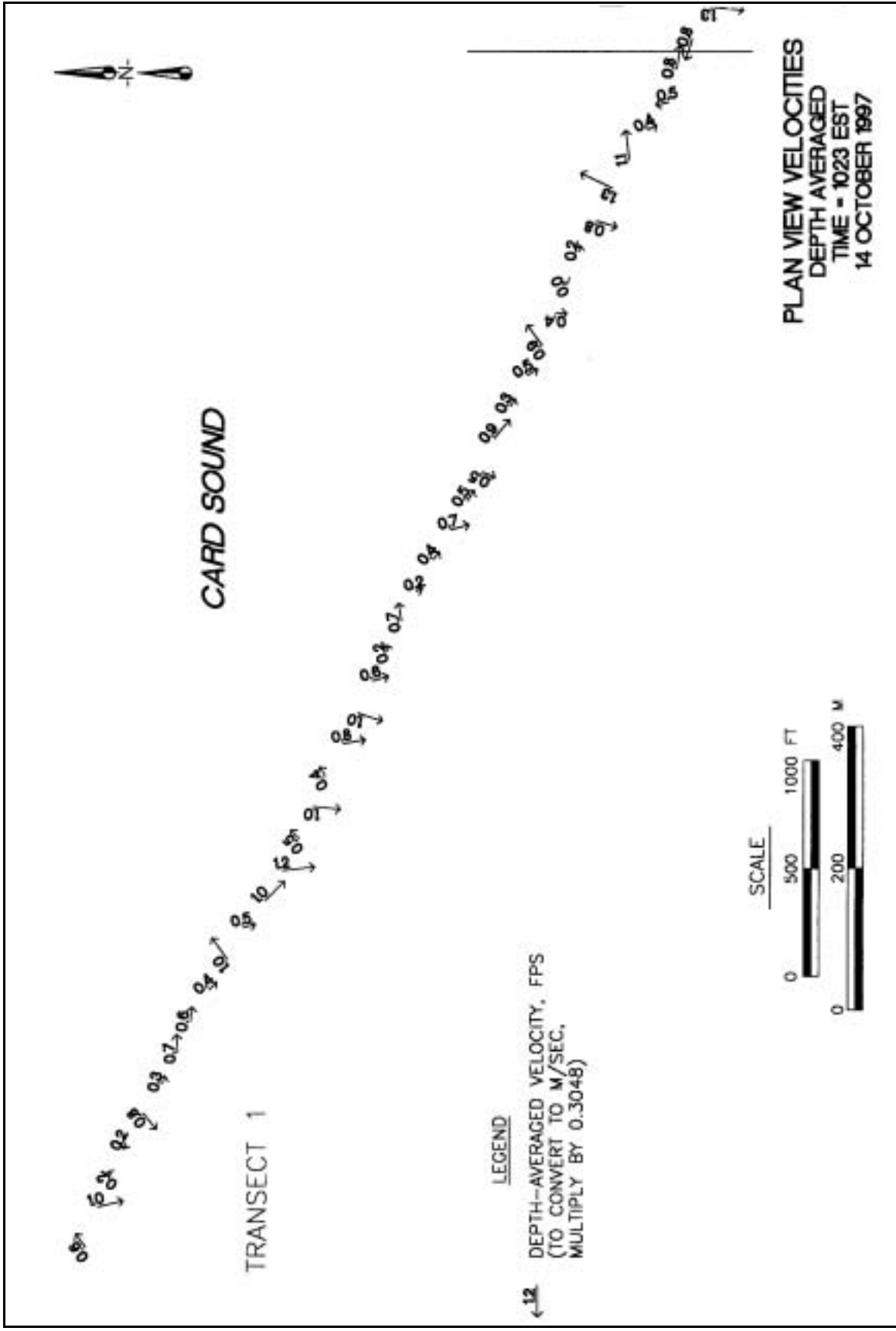


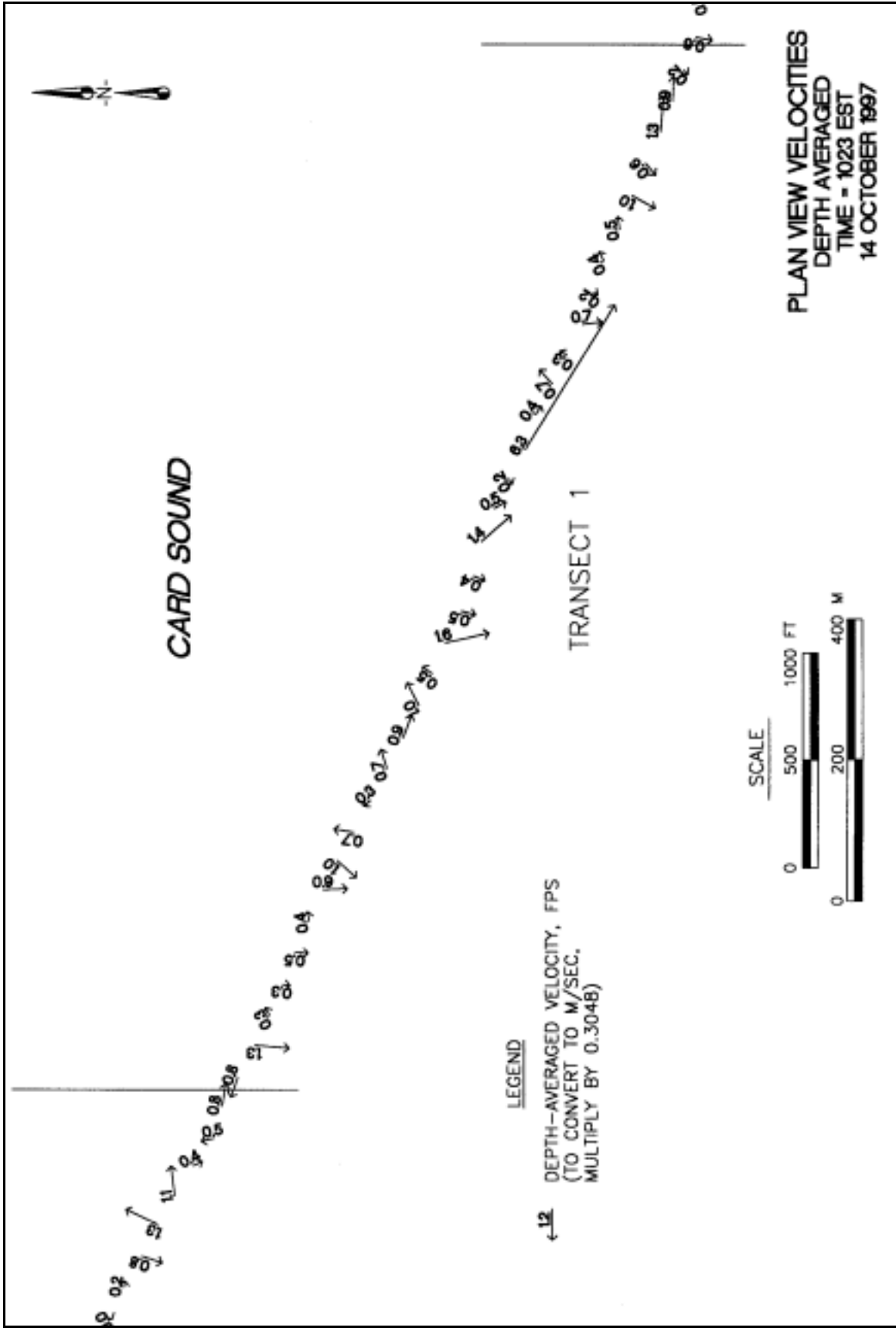
NGVD29 vs DISCHARGE
WATER LEVEL RECORDER CTD12
ADCP TRANSECT No. 25
 02/26/98



NGVD29 vs DISCHARGE
WATER LEVEL RECORDER CTD12
ADCP TRANSECT No. 26
 02/26/98







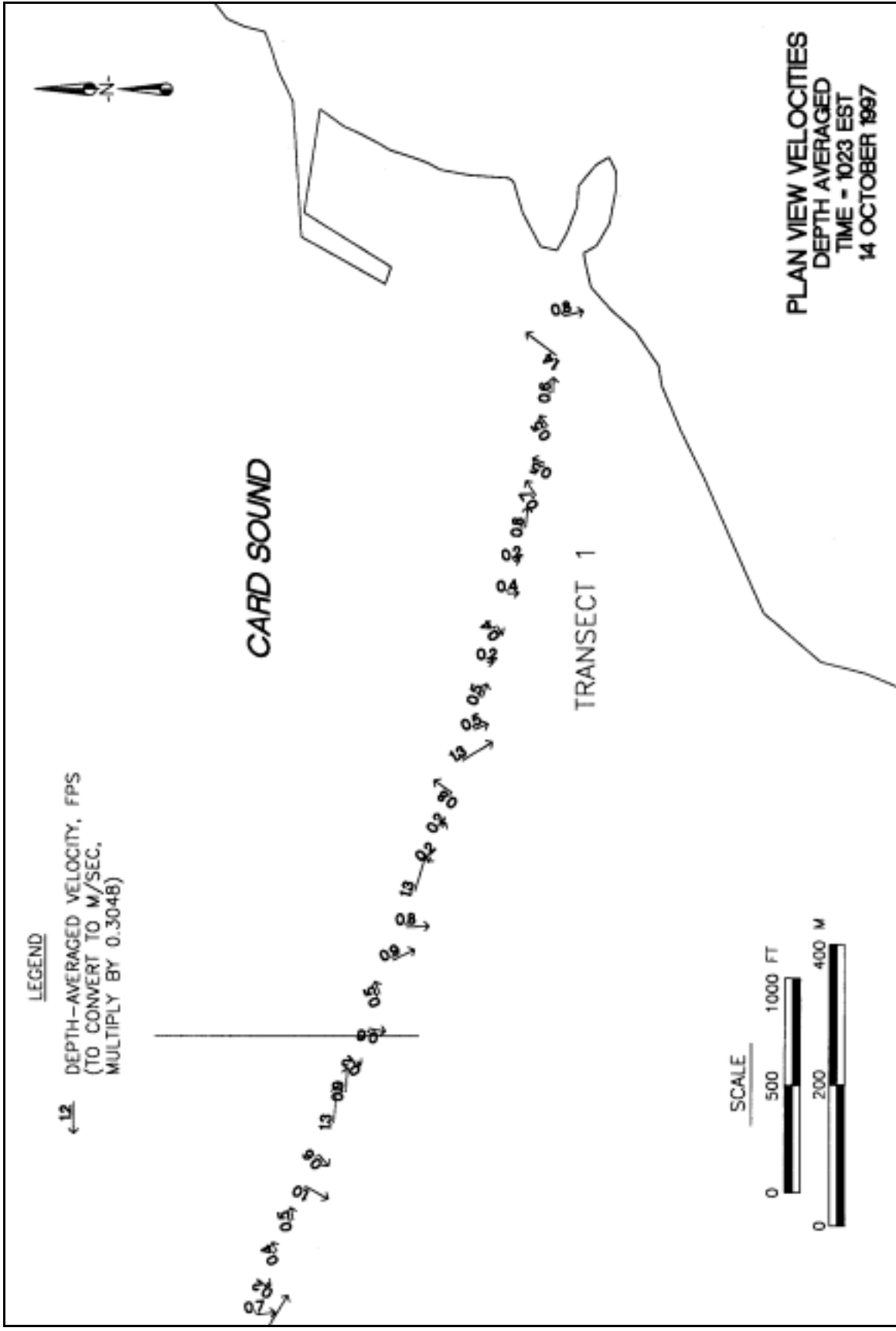
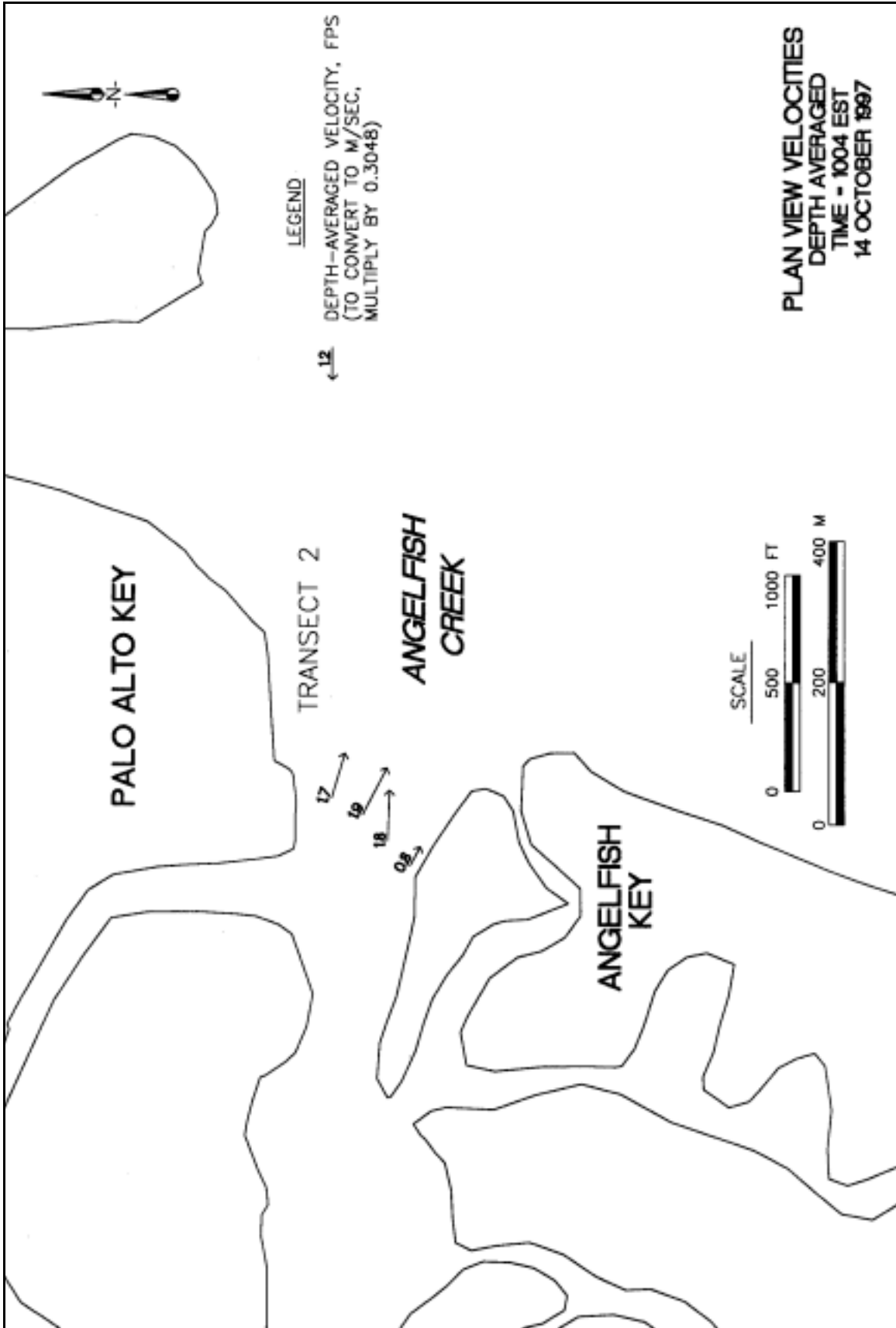


Plate 224



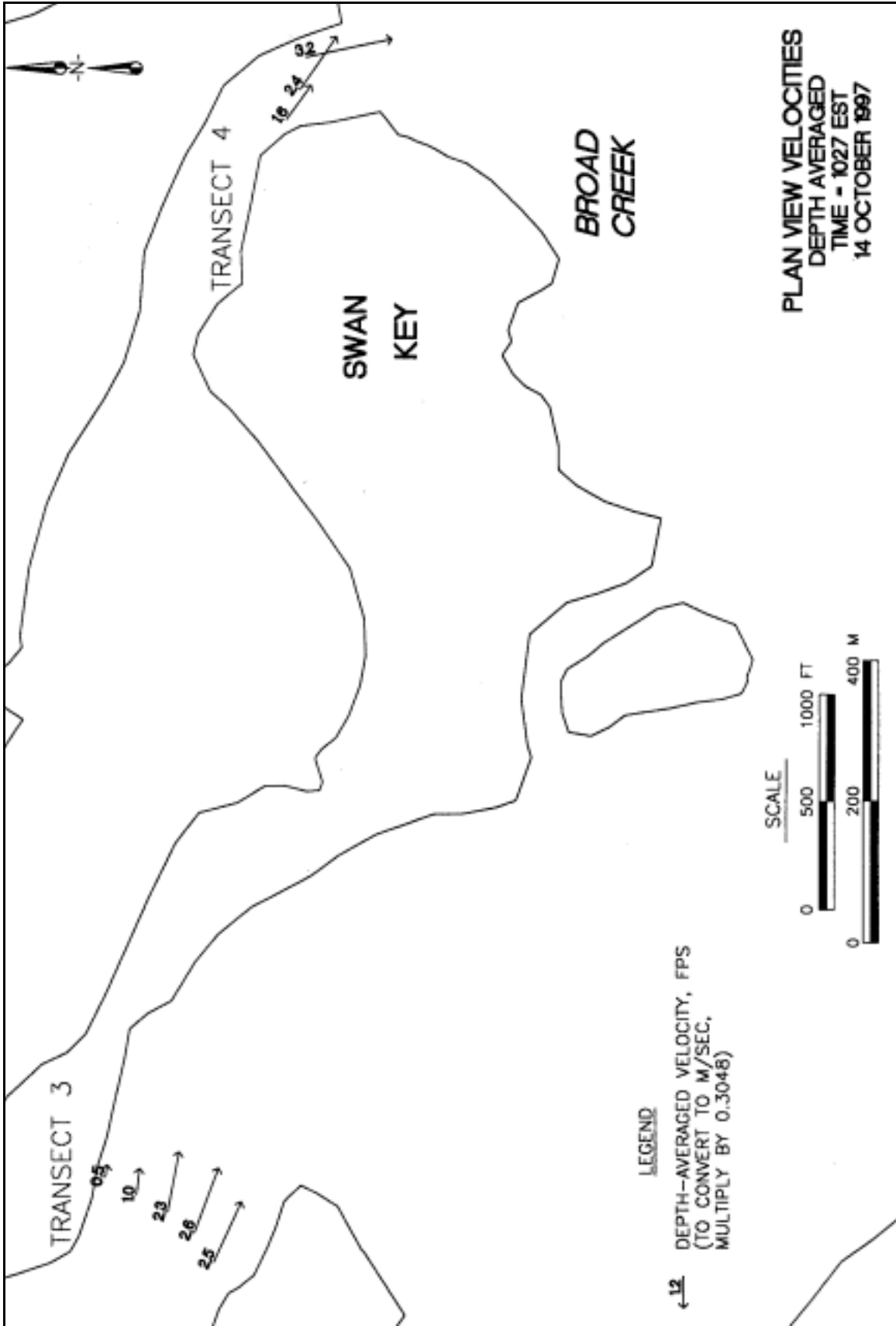


Plate 226

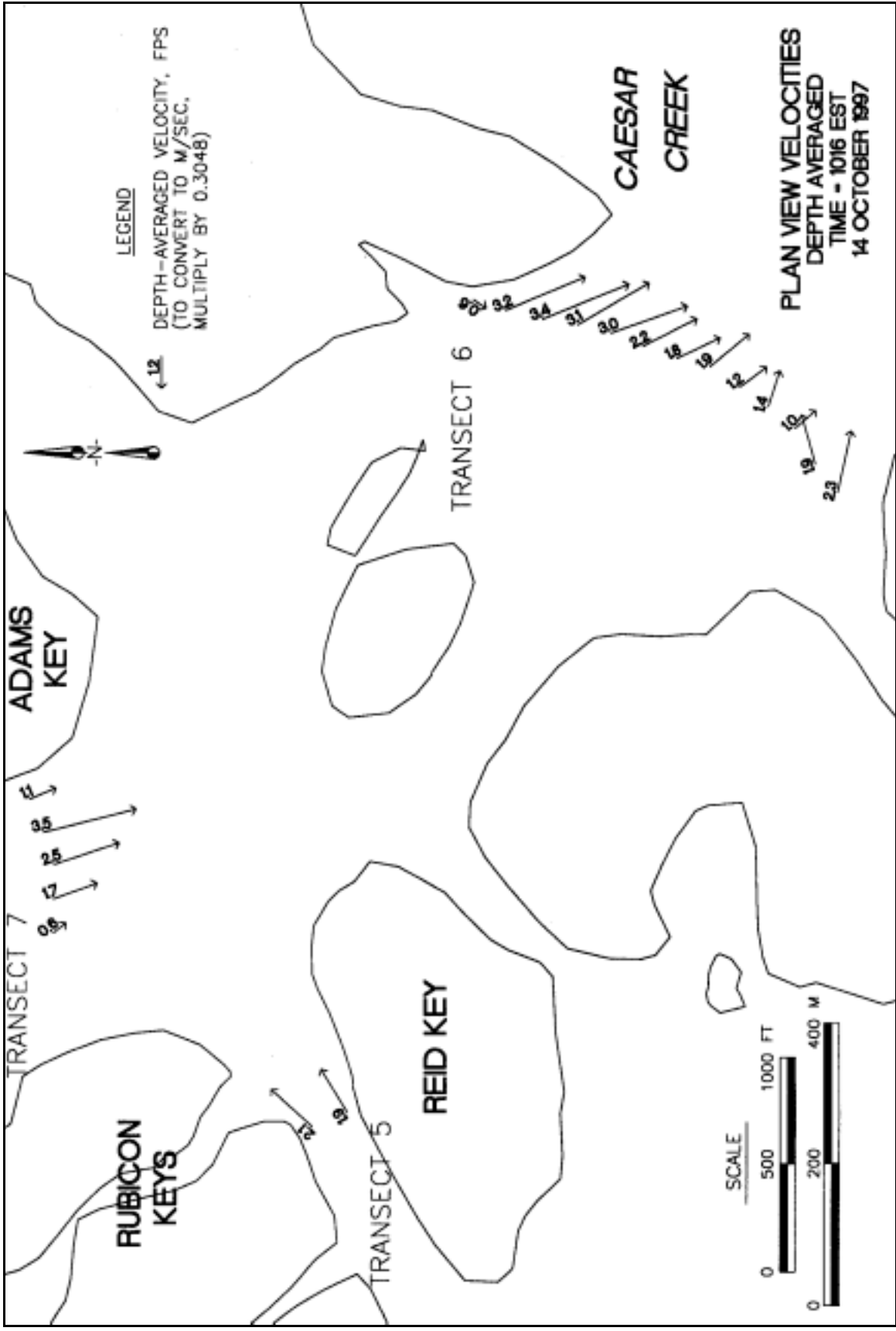


Plate 227

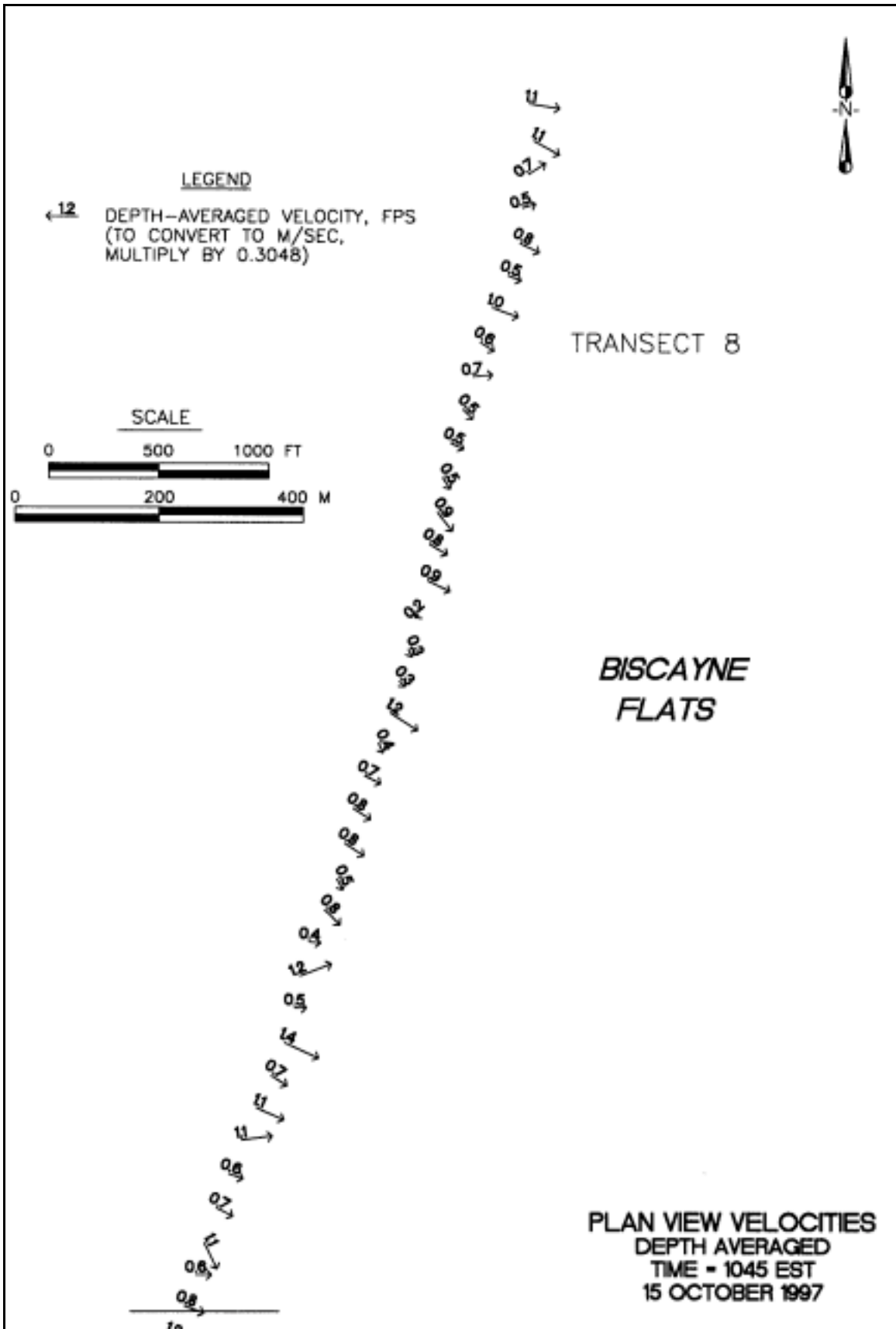
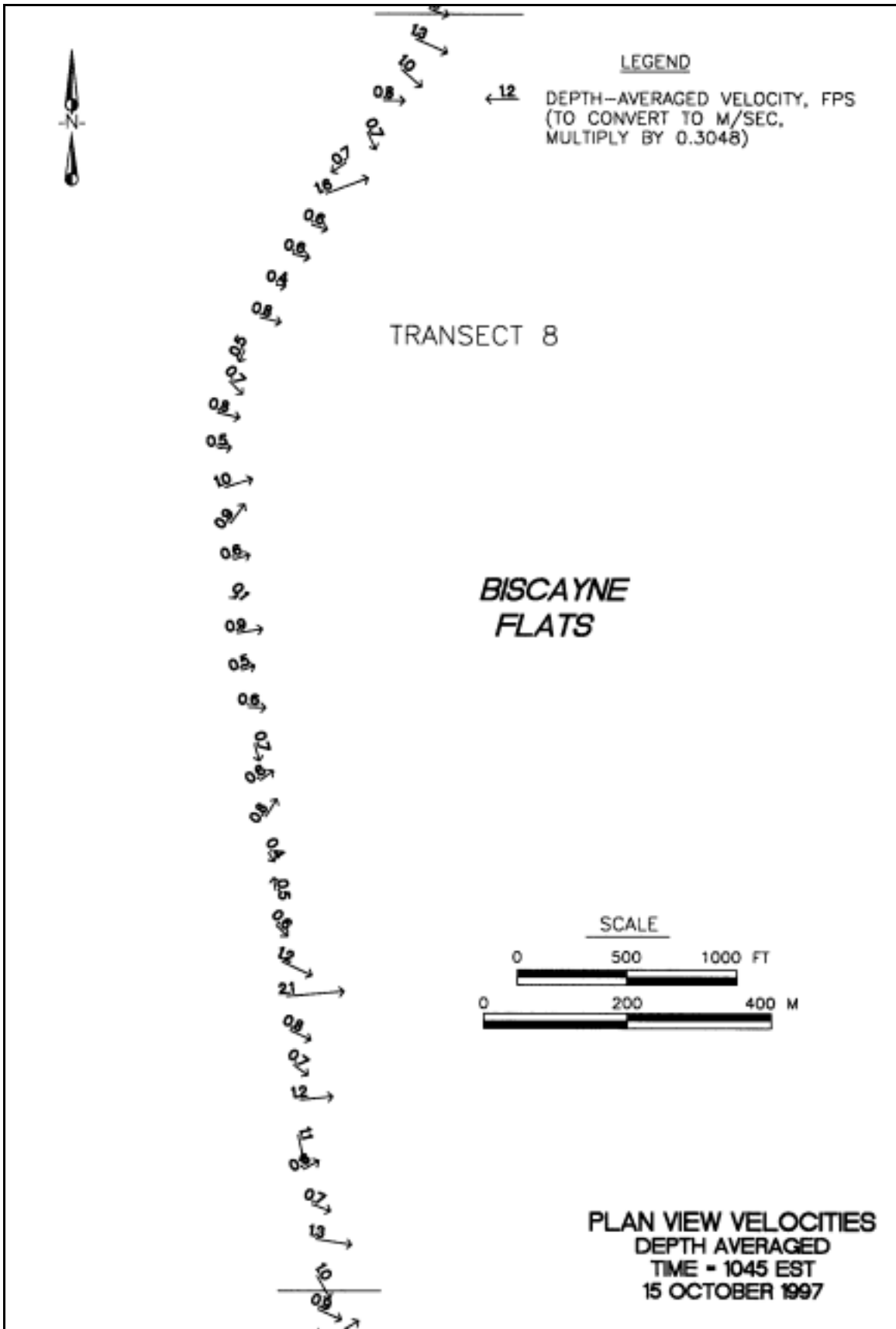
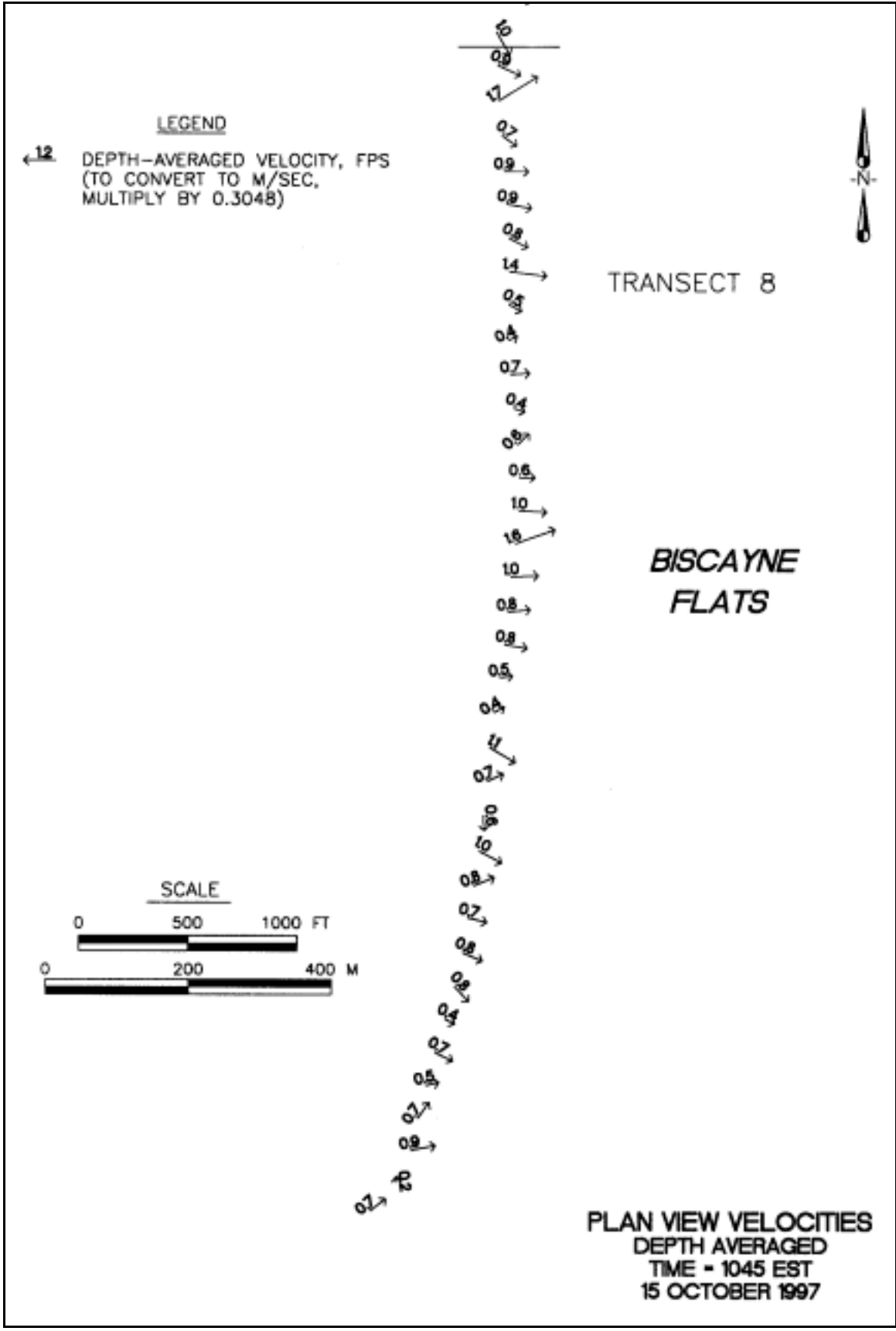


Plate 228





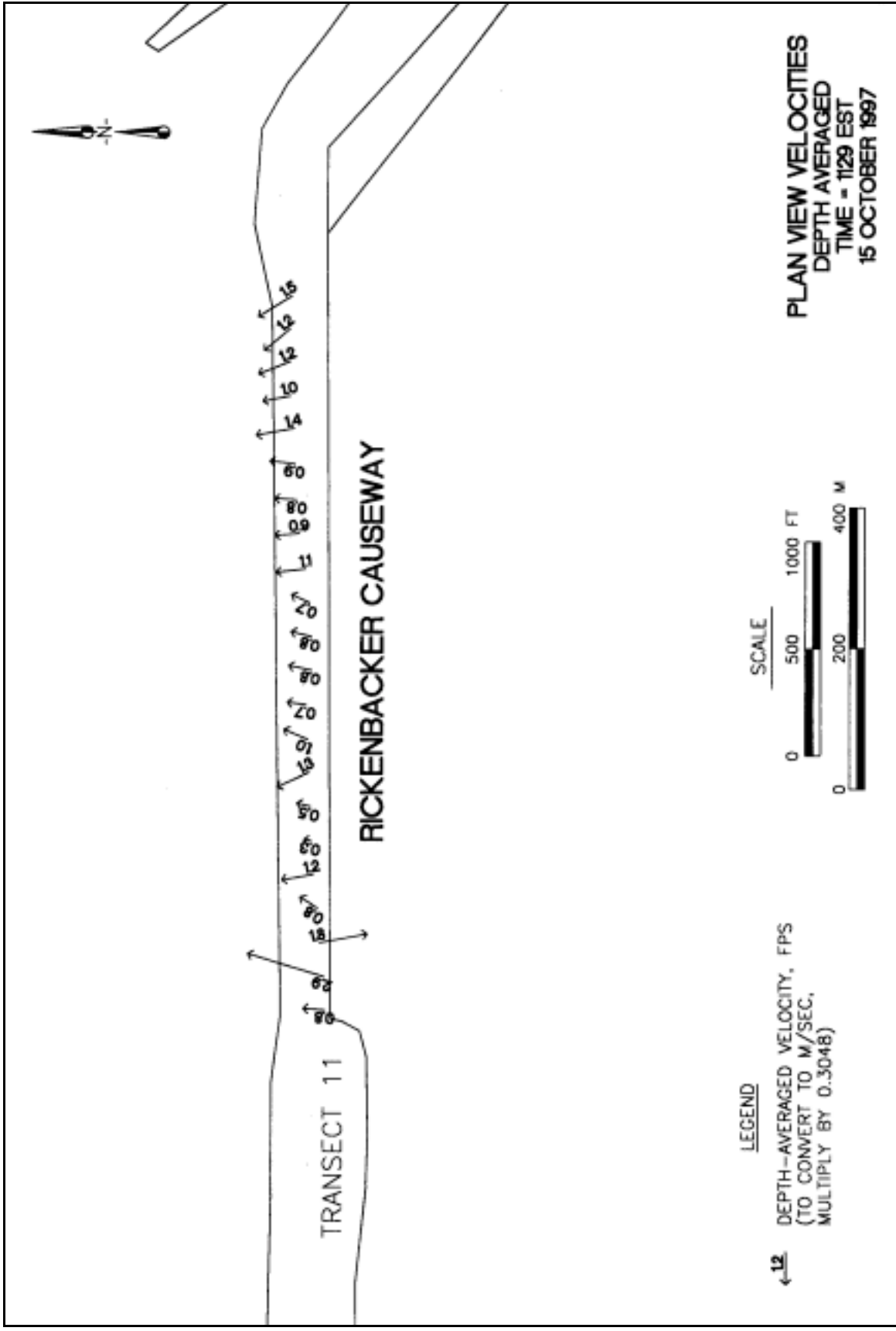


Plate 232

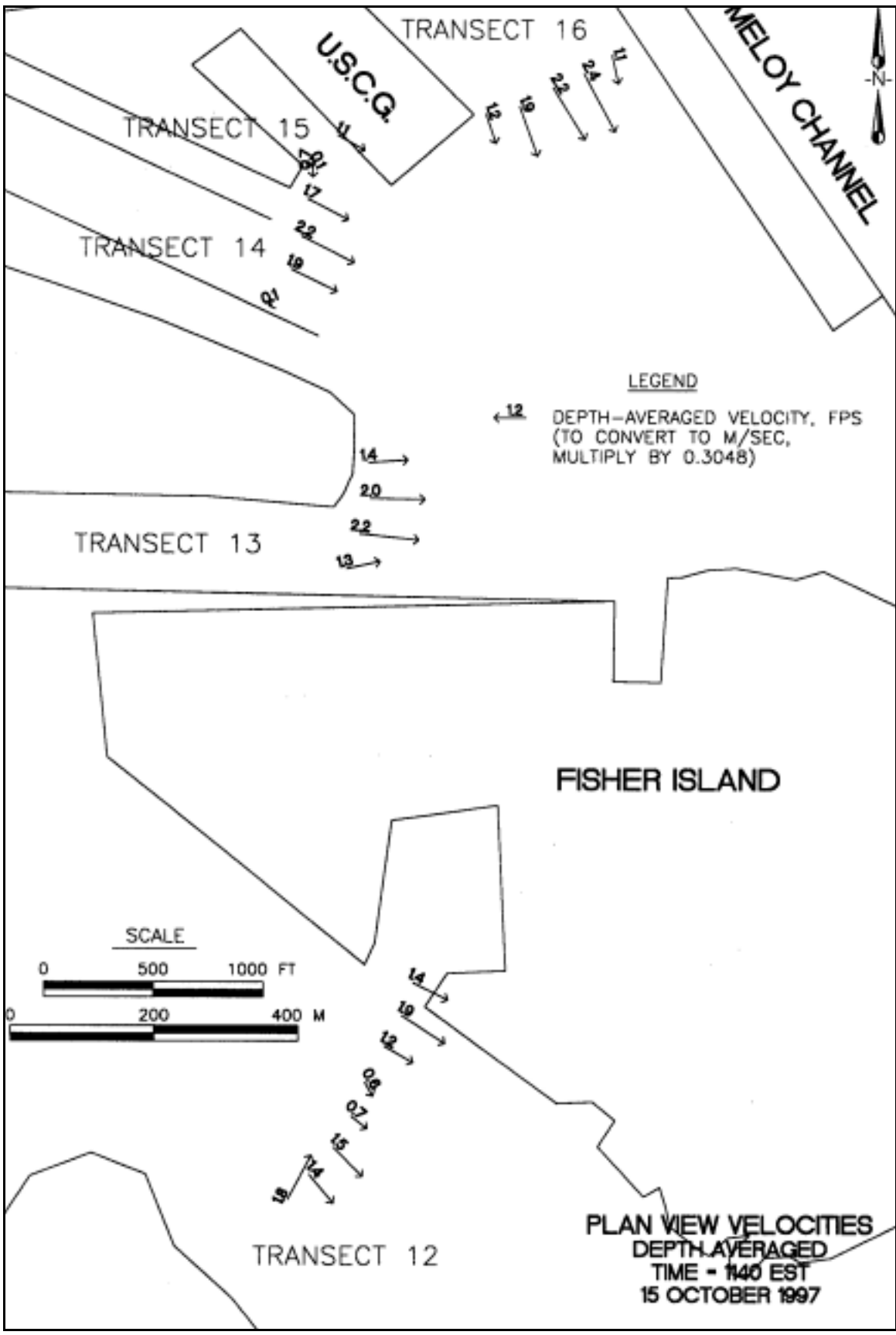


Plate 233

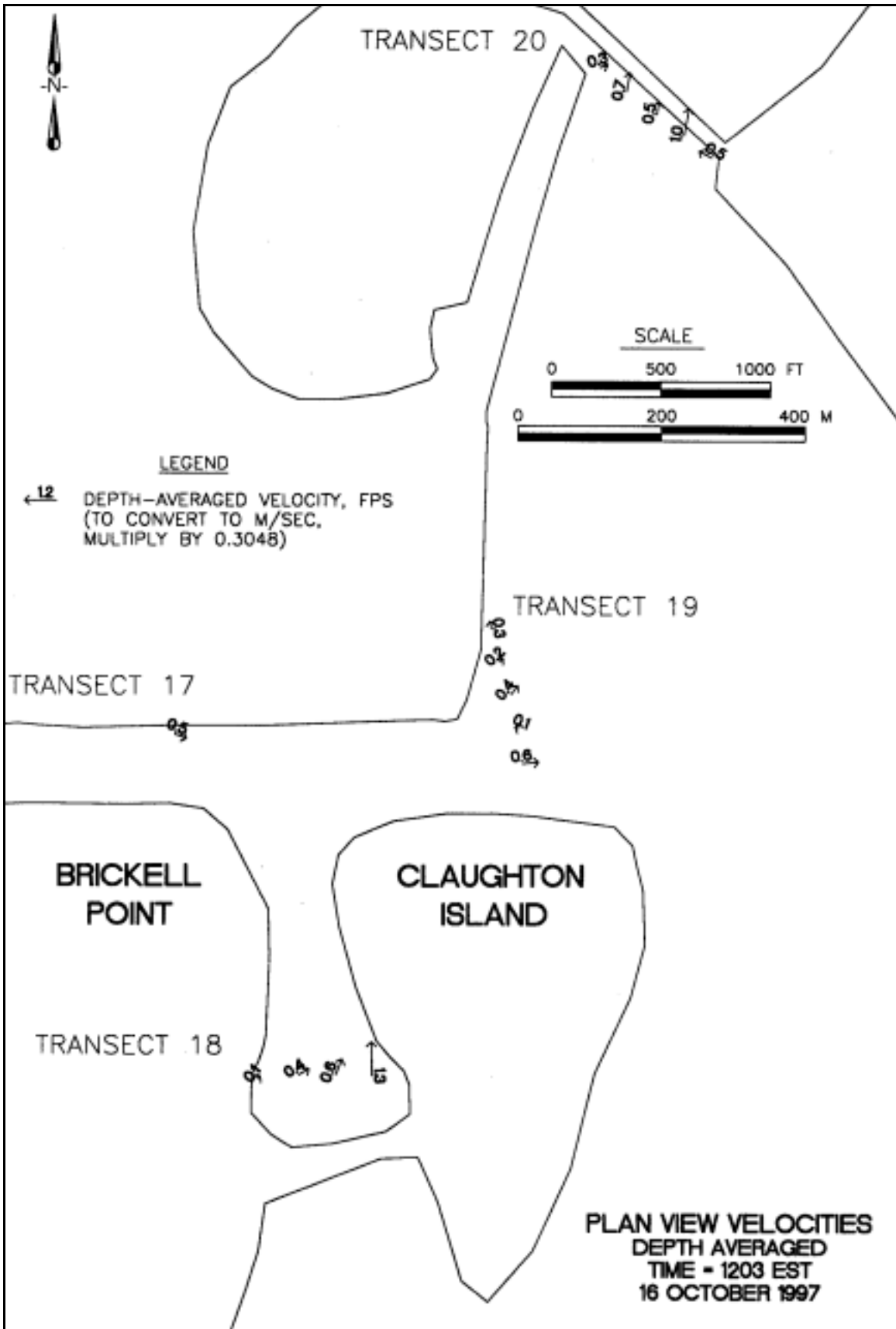


Plate 234

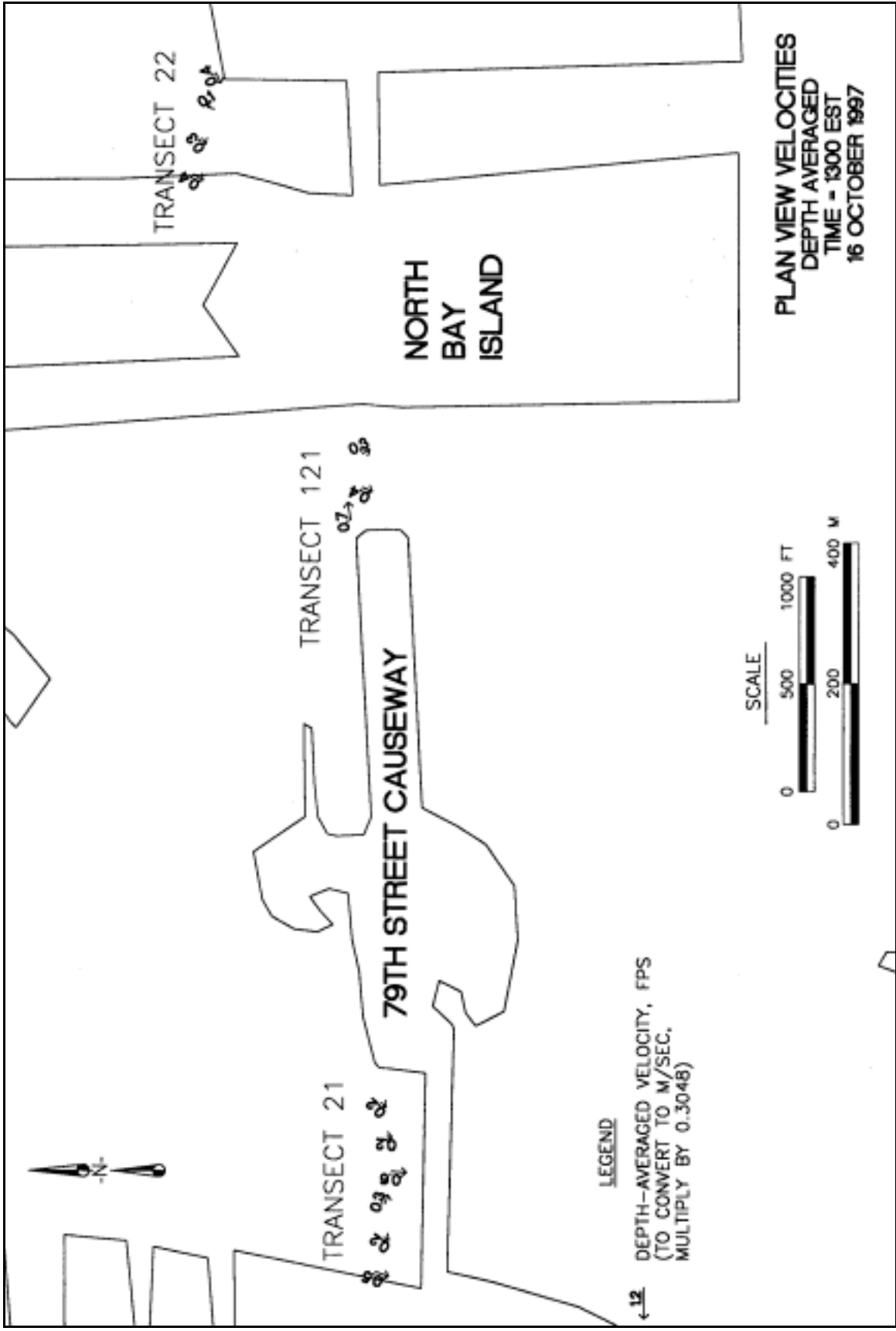


Plate 235

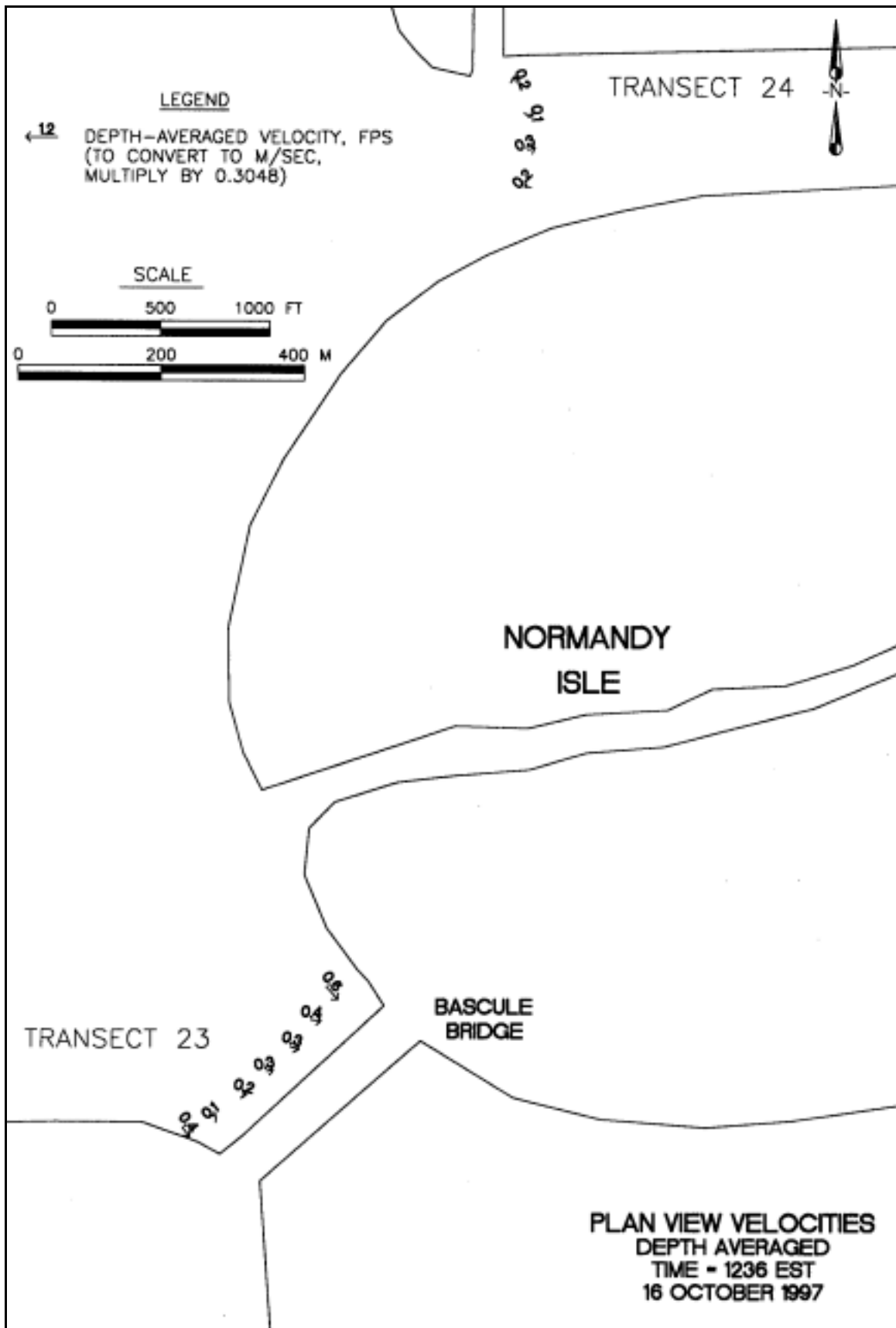


Plate 236

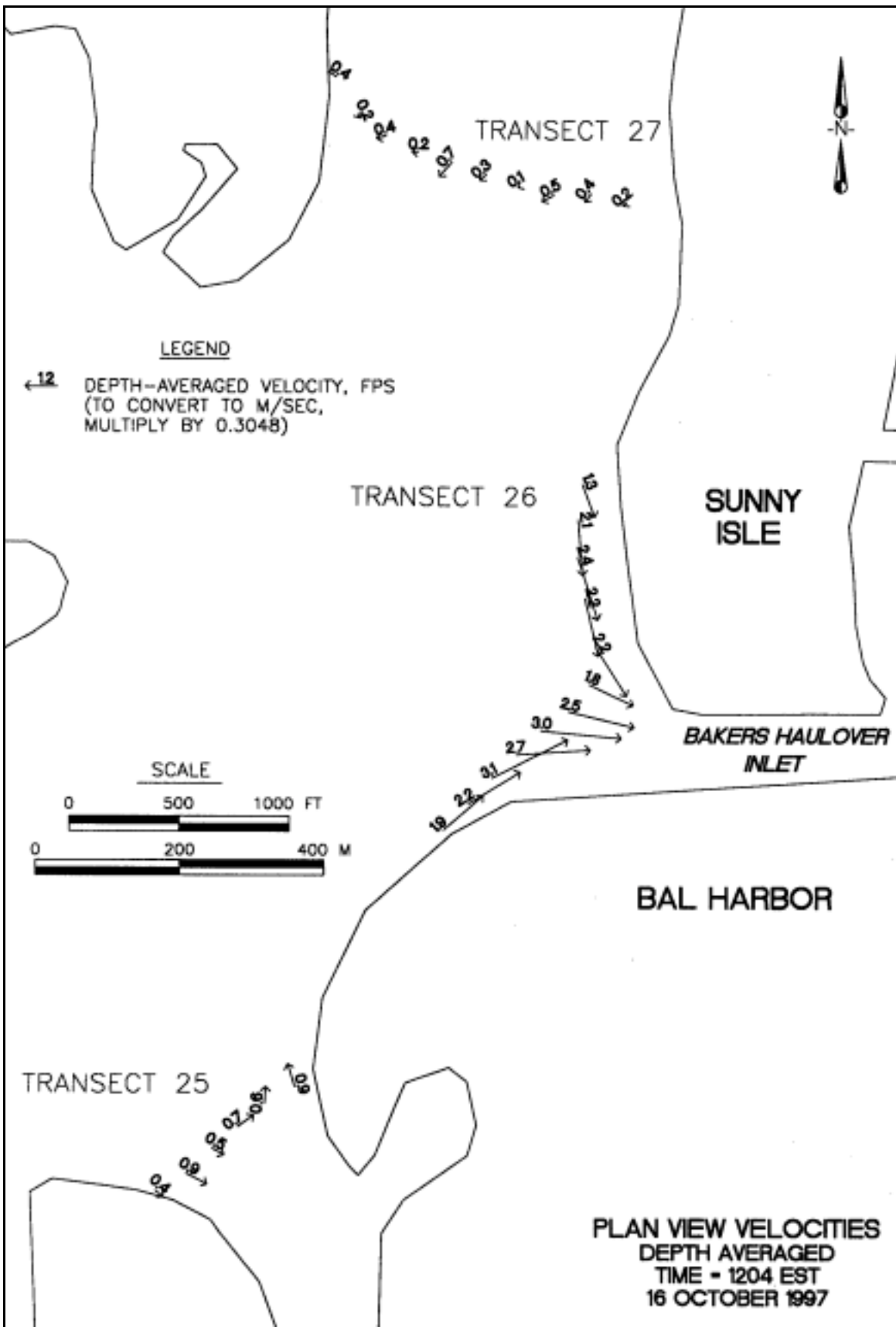


Plate 237

Appendix A Hydraulic Analysis Group Data Collection Equipment and Laboratory Analysis Procedures

by Timothy Fagerburg, Coastal and Hydraulics Laboratory

Appendix A

Hydraulic Analysis Group Data Collection Equipment and Laboratory Analysis Procedures

The contents of this appendix are to provide detailed information on the types of data collection and laboratory equipment used in a majority of the field investigations performed by the Hydraulic Analysis Group (HAG), Coastal and Hydraulics Laboratory (CHL), of the US Army Engineer Waterways Experiment Station (USAEWES). The following tabulation is provided to identify the parameters most commonly measured and the types of instruments which can provide these measurements.

	Page No.
Current Velocity and Direction Measurements	
Acoustic Doppler current meters	A4
Fixed-depth recording current meters	A7
Suspended Sediment Sampling	
Pumped water samples	A10
Automatic water samplers.....	A10
Optical backscatterance (OBS) sensors	A11
Salinity Measurements	
Hydrolab DataSonde 3 water quality data logger	A12
Wave Height Measurements	
Electronic wave height recorders.....	A13

Water Level Measurements

Electronic water level recorders.....	A14
---------------------------------------	-----

Bottom Sediment Sampling

Push-core samplers	A16
Box-core samplers	A17
Petite ponar samplers	A18
Tethered drag samplers.....	A18

Meteorological Measurements

Digital data acquisition of meteorological data.....	A19
--	-----

Laboratory Equipment and Sample Analysis

Laboratory analysis for salinity concentrations.....	A20
Laboratory analysis for total suspended materials.....	A21
Density analysis	A21

Current Velocity and Direction Measurements

Acoustic Doppler current meters

Acoustic techniques are used to obtain current velocity and direction measurements for fast and accurate profiling in the field. The equipment used is RD Instruments BroadBand Acoustic Doppler Current Profilers (ADCPs) and SonTek Acoustic Doppler Profilers (ADPs), as shown in Figures A1 and A2, respectively. The RDI instruments vary in operating frequency ranges from 150 to 1,200 kHz, whereas the SonTek instruments have frequency ranges from 75 to 3,000 kHz. The equipment can be mounted over the side of a boat with the acoustic transducers submerged, and data are collected while the vessel is underway as shown in Figure A3. It can also be mounted on a stable platform and placed on the riverbed or seabed as shown in Figure A4.

The ADCP and ADP transmit sound bursts into the water column. The sound bursts are scattered back to the instrument by particulate matter suspended in the flowing water. The ADCP and ADP sensors listen for the returning signal and assign depth and velocity to the received signal based on the change in the frequency caused by the moving particles. This change in frequency is referred to as a Doppler shift. The ADCP is also capable of measuring vessel direction, current direction, water temperature, and bottom depth. Communication with the instrument for setup and data recording is performed with a portable computer using manufacturer-supplied software, hardware, and communication cables. The manufacturer-stated accuracies are ± 0.2 cm/sec for current speed measurement; ± 2 deg for vessel direction; and ± 5 °F for temperature.

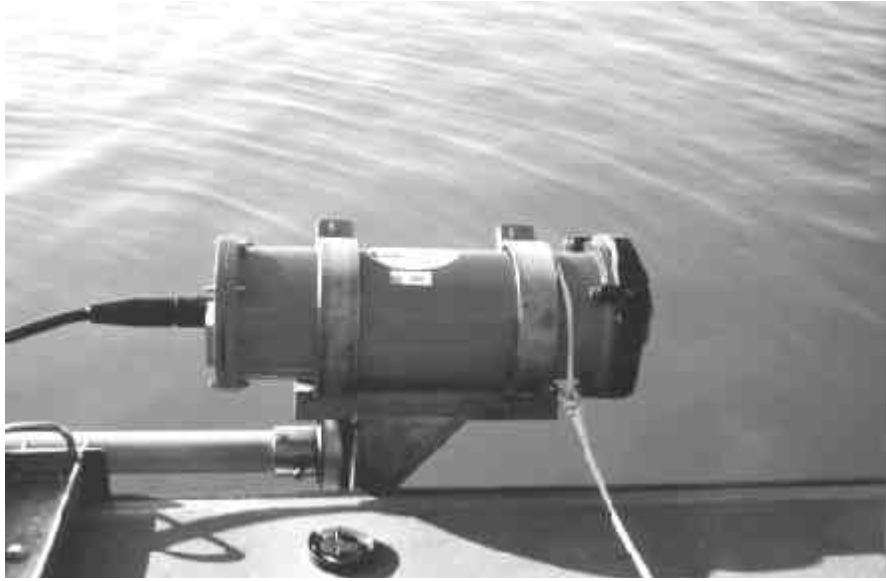


Figure A1. Acoustic Doppler Current Profiler (ADCP)



Figure A2. Acoustic Doppler Profiler (ADP)



Figure A3. Vessel-mounted ADCP



Figure A4. Bottom-mounted ADP unit

Fixed-depth recording current meters

Self-contained recording current meters are used to obtain current velocity and direction measurements for both profiling and for long-term fixed-depth deployment. The Environmental Device Corporation (ENDECO) Type 174 SSM current meter, shown in Figure A5, is tethered to a stationary line or structure and floats in a horizontal position at the end of the tether (as shown in Figure A6). It measures current speed with a ducted impeller and current direction with an internal compass. It also measures temperature with a thermilinear thermistor and conductivity with an induction-type probe. Data are recorded on an internal solid-state memory data logger. Data are off-loaded from the meter data logger by means of a communication cable connected between the meter and a computer. The threshold speed is less than 2.5 cm/sec, maximum speed of the unit is about 2.5 m/sec (10 knots), and stated speed accuracy is ± 2 percent of full scale. The manufacturer states that direction accuracy is ± 7.2 deg above 2.5 cm/sec. Time accuracy is ± 4 sec/day.



Figure A5. ENDECO Type 174 SSM current meter

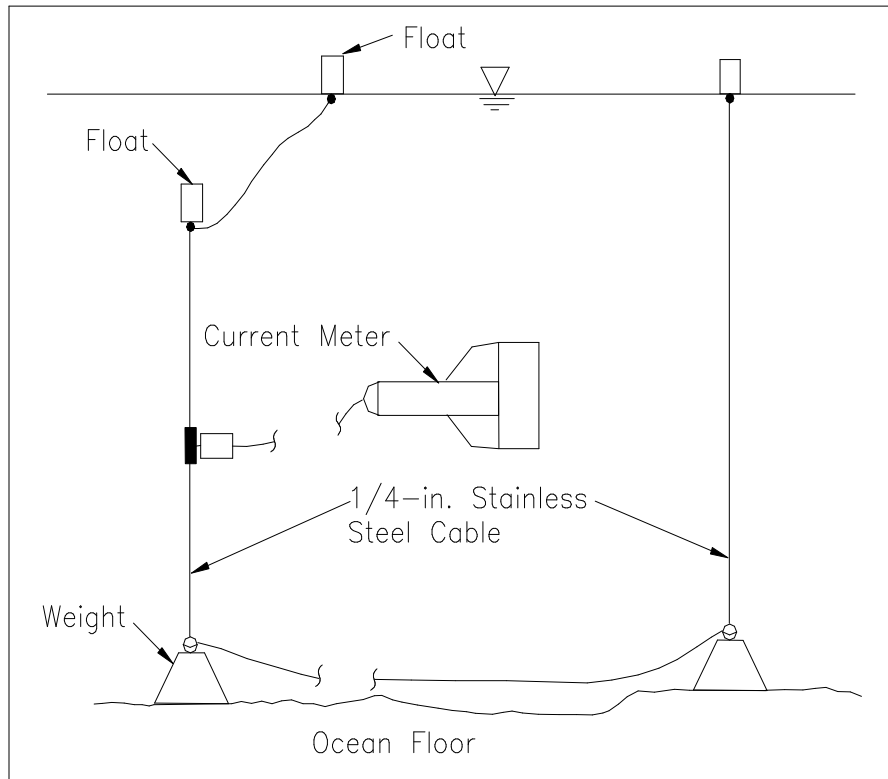


Figure A6. ENDECO 174 SSM current meter as deployed in the field

The InterOcean Model S4 electromagnetic current meter, shown in Figure A7, can continuously record current velocity and direction at fixed depths or can be used to profile the water column for current velocity and direction. The S4 meter is a 10-in.-diameter sphere that is suspended vertically in the water column with a submerged flotation device and anchored to the bottom by a heavy block-and-anchor arrangement. This deployment technique is illustrated in Figure A8. The S4 meter measures the current velocity using an electromagnetic microprocessor coupled with an internal flux-gate compass and computes the velocity vectors, which are then stored in the solid-state memory. The accuracy of the S4 meter current speed is ± 0.2 cm/sec.



Figure A7. InterOcean S4 electromagnetic current meter

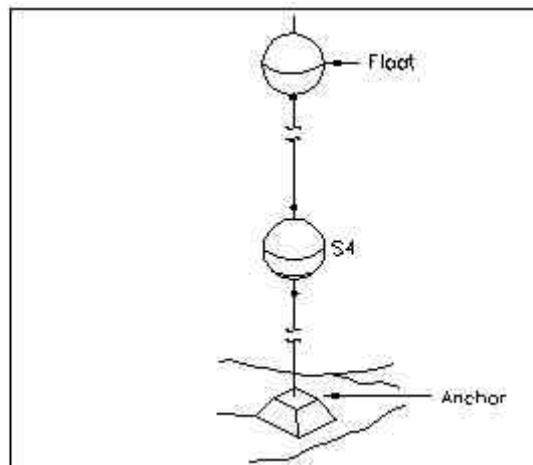


Figure A8. Electromagnetic current meter deployment technique

Suspended Sediment Sampling

Pumped water samples

In combination with the over-the-side velocity measuring equipment, water samples for analysis of suspended sediment concentrations and total suspended solids are obtained by pumping the sample from the desired depth to the surface collection point. The pumping system consists of a 1/4-in.-ID plastic tubing attached to the current meter signal cables for support. The opening of the sampling tubing is attached to the solid suspension bar at the same elevation as the current meter and is pointed into the flow. A 12-V dc pump is used to pump the water through the tubing to the deck of the boat where each sample is then collected in individual 8-oz. plastic bottles. The pump and tubing are flushed for approximately 1 min at each depth before collecting the sample.

Automatic water samplers

The ISCO Model 6700 automatic water sampler, shown in Figure A9, and the American Sigma Models 700 and 2000 are employed to provide unattended sampling. A typical field installation of these water samplers is shown in Figure A10. Discrete water samples are collected in 1-l. plastic bottles located



Figure A9. ISCO Model 6700 automatic water sampler

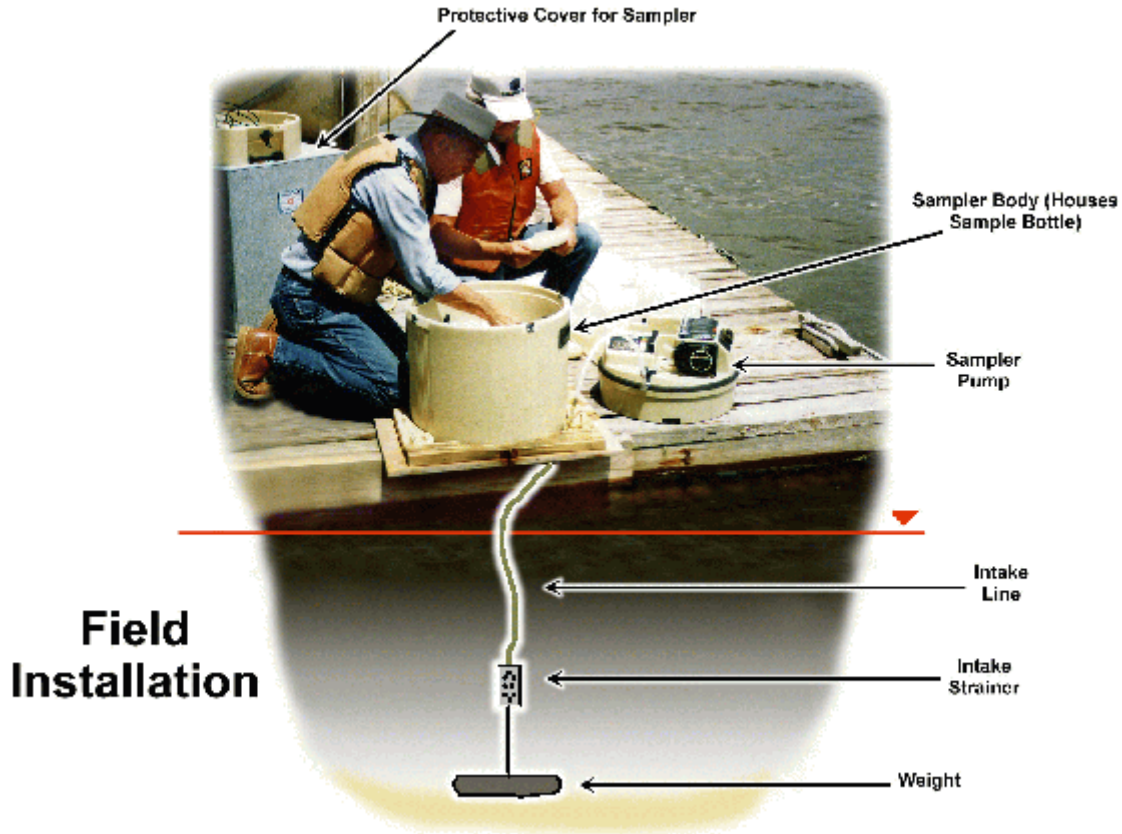


Figure A10. Typical field installation of automatic water samplers

inside the sampler. The samplers are fully programmable, operating from a 12-V dc power source, for obtaining any volume of sample desired up to the maximum size of the bottle, for obtaining composite samples, for setting different intervals between samples, and for setting times to begin the sampling routine. During servicing, the sample bottles are replaced with empty bottles to begin a new sampling period.

Optical backscatterance (OBS) sensors

The OBS sensor, a product of D&A Instruments and Engineering, is a type of nephelometer for measuring turbidity and solids concentrations by detecting scattered infrared light from suspended matter. It consists of a high-intensity infrared emitting diode (IRED), a series of silicon photodiodes as detectors, and a linear solid-state temperature transducer. The IRED emits a beam, at angles 50 deg in the axial plane and 30 deg in the radial plane, to detect suspended particles by sensing the radiation they scatter, as shown in Figure A11. Scattering by particles is a strong function of the angle between the path of radiation from the sensor through the water and the signal return to the detector. OBS sensors detect only radiation scattered at angles greater than 140 deg. As with other optical turbidity sensors, the response of the OBS sensor depends on the size distribution, composition, and shape of particles suspended in the medium being monitored. For this reason, sensors must be calibrated with suspended solids from the waters

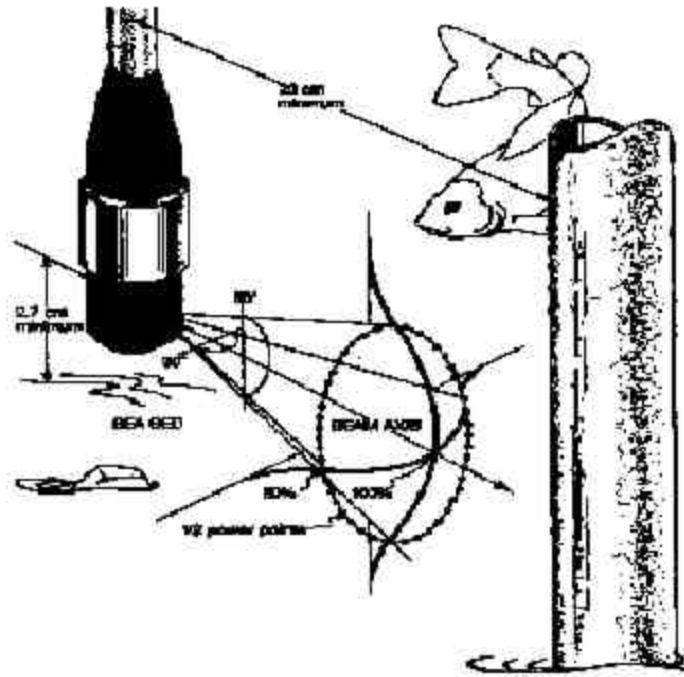


Figure A11. OBS sensor beam pattern

being monitored. The OBS sensor can be interfaced with “smart” data loggers that are capable of powering the sensor during sampling intervals.

Salinity Measurements

Hydrolab DataSonde 3 water quality data loggers

The Hydrolab Datasonde 3 water quality data logger, shown in Figure A12, provides conductivity and temperature with a computed salinity concentrations measurement corrected to a known calibration standard at 25 °C. The recorder housing is a high-density PVC case with a specific conductance cell and temperature sensor. The specific conductance probe is a six-electrode cell having a measurement range of 0.0 to 100 mS/cm with an accuracy of ± 1 mS/cm. The salinity concentration range is from 0.0 to 40 ppt with an accuracy of ± 0.2 ppt (calculated from the conductivity). The temperature probe is a thermistor-type sensor with a measurement range of -5 ° to 50 °C with an accuracy of ± 0.15 °C. The data sampling intervals range from 1 to 59 sec, 1 to 59 min, or 1 to 23 hr. Data are stored on nonvolatile EPROM chips. Internal or external batteries provide the power requirements for sensor operation and data storage. Data are off-loaded from the instrument via an industry standard RS-232 port to a portable computer using standard communication software.



Figure A12. Hydrolab Datasonde 3 water quality data logger

Wave Height Measurements

Electronic wave height recorders

The Microtide water level recorder, shown in Figure A13, contains a strain-gauge-type pressure transducer in a subsurface case which records the absolute pressure of the column of water above the case. The pressure transducer is not vented to the atmosphere; therefore, an extra unit is positioned in the study area to record atmospheric pressure changes. Water pressure is measured for the desired sample interval and an average value is computed and stored on the internal RAM data logger. The stated accuracy is ± 0.6 cm. The sampling time interval can be set from 0.25 sec to 24 hr. The Microtide also measures temperature by means of a Yellow Springs Instruments (YSI) thermilinear thermistor built into the water level recorder. The thermistor has a range of -5° to $+45^{\circ}$ C, with a stated accuracy of $\pm 0.1^{\circ}$ C. The data from each recorder are stored on an accessible RAM located in the waterproof subsurface unit which also contains the d-c power supply.



Figure A13. Microtide electronic wave height recorder

Water Level Measurements

Electronic water level recorders

Water level elevation measurements can also be recorded using solid-state electronic recorders, such as Microtide, YSI, and ENDECO water level recorders. Water level elevations, temperature, conductivity, salinity, and dissolved oxygen (DO) concentration measurements are recorded using YSI Model 6000 water level recorders and ENDECO Models 1152 and 1029 SSM (solid-state measurement) water level recorders (excluding the DO measurements).

The ENDECO Model 1152 SSM, shown in Figure A14, and Model 1029 SSM recorders contain a strain-gauge-type pressure transducer located in a subsurface case which records the absolute pressure of the column of water above the case. The pressure transducer is vented to the atmosphere by a small tube in the signal cable to compensate for atmospheric pressure. The pressure is measured for 49 sec of each minute of the recording interval with a frequency of 5-55 kHz to filter out surface waves, therefore eliminating the need for a stilling well. The accuracy is ± 1.5 cm. The sampling time interval can be set from 1 min to 1 hr. The Models 1152 and 1029 also measure temperatures by means of a thermilinear thermistor built into the recorders. The thermistor has a range of -5° to $+45^{\circ}$ C, with an accuracy of $\pm 0.2^{\circ}$ C. The Model 1152 measures conductivity by an inductively coupled probe installed on the meter. These measurements and the measurements of temperature are used to calculate salinity concentrations in units of parts per thousand (ppt). The salinity concentrations are computed with an accuracy of ± 0.2 ppt.



Figure A14. ENDECO Model 1152 SSM

The sampling time interval for conductivity and temperature cannot be set independently from the water level measurements. The data from each recorder are stored on a removable EPROM solid-state memory cartridge located in a waterproof surface unit which also contains the d-c power supply.

The YSI/ENDECO Model 6000 recorder also uses a strain-gauge type pressure transducer located in a subsurface case and records the absolute pressure of the water column above the case. The Model 6000 is not vented to compensate for atmospheric pressure; therefore, after the sensor is initially calibrated, any changes in barometric pressure will appear as changes in depth. This is particularly significant in shallow water. For example, a change of 1 mm of Hg in barometric pressure will change the apparent depth by approximately 1.37 cm. The range of 0 to 9.14 m of water has an accuracy of ± 1.83 cm and a resolution of 0.03 cm. The Model 6000 utilizes a thermistor of sintered metallic oxide which changes predictably in resistance with temperature variations. The thermistor has a range of -5° to $+45^{\circ}$ C, with an accuracy of $\pm 0.15^{\circ}$ C and a resolution of 0.01° C. The Model 6000 measures conductivity using a four nickel electrode cell in the range of 0 to 100 mS/cm with an accuracy of ± 0.5 percent and a four-digit resolution. Salinity is calculated based on the conductivity and temperature measurements in the range of 0 to 70 ppt with an accuracy of ± 0.1 ppt and a resolution of 0.01 ppt. The Model 6000 uses a dissolved oxygen (DO) sensor that employs a patented "Rapid-Pulse" measuring technique. Its range is 0-20 mg/l with an accuracy of ± 0.2 mg/l and 0 to 200 percent saturation with an accuracy of ± 2 percent.



Figure A15. YSI/ENDECO Model 6000 water level recorder

Bottom Sediment Sampling

Push-core sampler

Bottom sediments are obtained using a push-core type sampler. The sampler consists of a 1.5-in.-diam PVC pipe, 18 in. in length. Attached to this is a smaller section of pipe with a valve attached at the upper end. The purpose of the valve is to create a reduced pressure holding the sample in the larger-diameter pipe. The samples are then brought to the surface and classified by visual inspection or transported back to WES for more detailed analysis. The push-core sampler is displayed in Figure A16.



Figure A16. Push-core sampler

Box-core samplers

The box-core sampler is very similar to the petite ponar in its triggering mechanism and sampling technique. The main difference in the two samplers is where the sample is trapped. The box-core has clam-shell jaws that scoop the sediment into a clear plastic square tube. When the sampler is opened at the surface, the sample is visible from a top door on the sampler. From this top door, the trapped sample can be sub-sampled for more detailed analysis. Figure A17 is a picture of the box-core sampler.

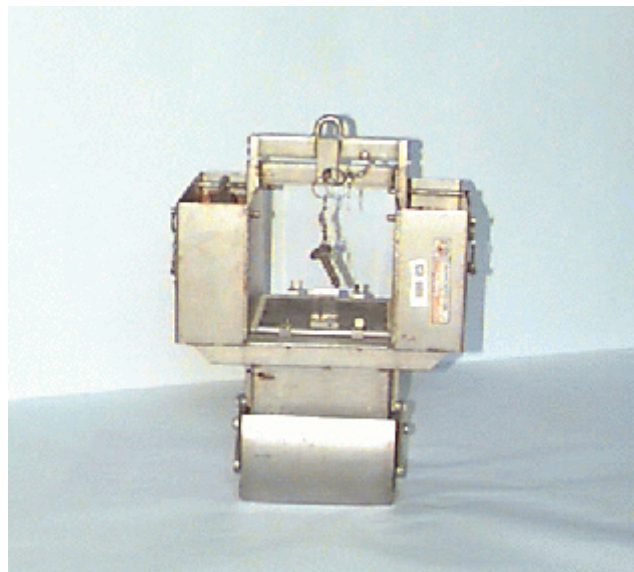


Figure A17. Box-core sampler

Petite ponar samplers

The petite ponar sampler is basically a clam-shell-type sampler. The sampler is cocked on the surface before lowering to the bottom. When the sampler makes contact with the bottom, the trigger pin releases allowing the sampler to close. As the sampler is raised to the surface, it closes around the captured sediment until it is opened at the surface. Samples are removed, inspected, and packaged in plastic bags or jars for further analysis once returned to WES. The petite Ponar is displayed in Figure A18.



Figure A18. Petite ponar sampler

Tethered-drag sampler

The tethered-drag sampler is basically a 3-in.-diam pipe cut on a 45-deg angle with a shackle mounted on one side. The sampler is thrown over the side and dragged along the bottom. The sample accumulates inside the pipe. Samples are removed, inspected, and packaged in plastic bags or jars for further analysis once returned to WES. The tethered-drag sampler is displayed in Figure A19.



Figure A19. Tethered-drag sampler

Meteorological Measurements

Digital data acquisition of meteorological data

Continuous wind speed and direction measurements are recorded using a Campbell Scientific Model W2000 Data Acquisition system (see Figure A20). The data collection platform is typically located at some central location in the study area and mounted approximately 5 m above the water. The data acquisition system is a battery-powered microcomputer with a real-time clock, a serial data interface, and programmable analog-to-digital converter.

The battery is constantly charged using a solar panel charging system located near the system. Various programming options are available for setting the sampling interval of the system for the input signals from the wind speed and direction sensors. The system can be programmed to sample the input signals each second over a set period of time to determine the mean wind speed, mean direction, maximum wind gust speed, and maximum wind gust direction.

The data are processed internally and stored in formats specified in a user-entered output table. The accuracy of the analog input of the wind speed and direction sensors is ± 1.0 mph and ± 3.0 deg, respectively. The barometric pressure sensor, Model CS105, has an accuracy of ± 0.5 mb for a range from 600 to 1,060 mb. The tipping bucket rain gauge has a resolution of 0.01 in. for each tip. The calibrated accuracy is ± 1 tip or 1 percent at 2 in./hr or less. The relative humidity sensor has an accuracy of ± 2 percent RH within the range of 0 to 90 percent and ± 3 percent RH within the range of 90 to 100 percent.



Figure A20. Weather Station Model W2000

Laboratory Equipment and Sample Analysis

Laboratory analysis for salinity concentrations

An AGE Instruments Incorporated Model 2100 MINISAL salinometer (Figure A21) with automatic temperature compensation is used for the determination of suspended sediment concentrations in the individual samples. The salinometer is a fully automated system, calibrated with standard seawater, and the manufacturer's stated accuracy is ± 0.003 ppt on samples ranging from 2 to 42 ppt.



Figure A21. AGE MINISAL salinometer

Laboratory analysis for total suspended materials

Total suspended materials (TSM) are determined by filtration of samples. Nuclepore (Registered Trademark) polycarbonate filters with 0.40 micron pore size are used. They are desiccated and preweighed, then a vacuum system (8-lb vacuum maximum) is used to draw the sample through the filter. After the filters and holders are washed with distilled water, the filters are dried at 105 °C for 1 hr and reweighed. The TSM are calculated based on the weight of the filter and the volume of the filtered sample.

Density analysis

A density analysis is done using wide-mouth, 25-cm constant-volume pycnometers. They are calibrated for tare weight and volume. A pycnometer is partially filled with sediment and weighed, then topped off with distilled water. Care is taken to remove any bubbles before the pycnometer is reweighed. The bulk density (BSG) of the sediment is then calculated by the equation:

$$BSG \cdot \frac{(\bullet)(sedwt \cdot tarewt)}{(\bullet)(volpy) \cdot (sedwt) \cdot (sed \cdot waterwt)} \quad (A1)$$

where

ρ = density of water at temperature of analysis

$sedwt$ = total weight of pycnometer and sediment

$tarewt$ = tare weight of pycnometer

vol_{pyc} = volume of pycnometer

$sed + waterwt$ = total weight of pycnometer, sediment, and water

Appendix B

Analysis of Water Level, Weather, and Acoustic Doppler Profiler Data from Biscayne Bay, Card Sound, and Barnes Sound

by Ned P. Smith and Patrick A. Pitts, Harbor Branch Oceanographic Institution

Contents

Introduction	B4
Data	
a. Weather data	B6
b. Water level data.....	B6
c. Acoustic Doppler profiler data	B6
Methodology	
a. Weather data	B9
b. Water level data.....	B9
c. Acoustic Doppler profiler data	B11
Results	
a. Weather data	B11
b. Water level data.....	B17
c. Acoustic Doppler profiler data	B55
Discussion and Summary	B70
References	B71

Introduction

In early June 1997, the U.S. Army Corps of Engineers Waterways Experiment Station (WES) initiated a field study of Biscayne Bay and adjacent waters, including Card Sound, Barnes Sound, and Manatee Bay. The field study included the collection of water level data from 12 stations (see Figure B1), Acoustic Doppler Profiler (ADP) data from five stations, and weather data from Convoy Point, along the western shore of Biscayne Bay. Recording instrumentation was in place for an approximately one-year period. Station coordinates and starting and ending times are listed in Table B1. The objective of the field study was to collect data that could be used to verify a hydrodynamic model of the Biscayne Bay system.

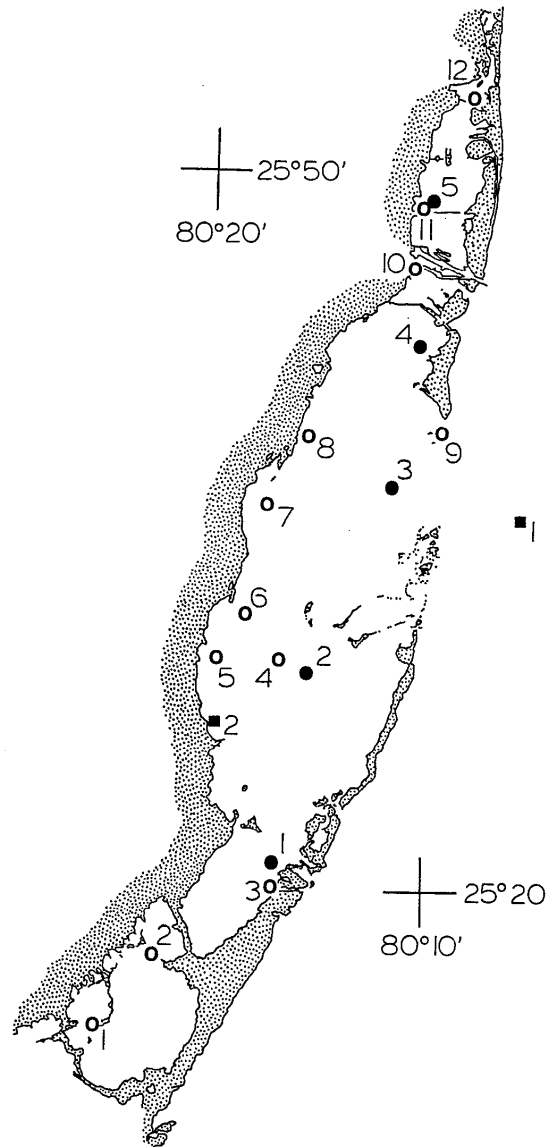


Figure B1. Map of the study area, including Biscayne Bay, Card Sound, Little Card Sound, Barnes Sound, and Manatee Bay. Solid squares show locations of the weather stations at (1) Fowey Rocks and (2) Convoy Point; open circles show locations of water level stations 1-12; solid circles show locations of ADP stations 1-5

In a June 7, 1999 letter to the National Park Service, Harbor Branch offered to analyze the water level, ADP, and weather data within the restricted context of model verification. Following a period of negotiation, Harbor Branch offered a Scope of Work that included screening, editing, analyzing, and plotting the data. Specifically, data would be inspected for outliers and gaps. Gaps longer than 12 hours would be considered breaks in the record, and data collected before and after a break would be treated as separate time series. Data would be plotted as time series and presented with expanded captions to aid in the interpretation. Data would be subjected to time series analyses to characterize tidal conditions, and to establish statistically significant associations between wind stress and both water levels and ADP transport. Two reports would be provided. The first would be a Quality Assurance Report that would address the suitability of the data for model verification purposes. The second would be a Final Report to summarize findings directly related to validating model simulations.

The Quality Assurance (QA) Report was submitted on September 9, 1999 and again in amended form on February 3, 2000. The QA Report included plots of north-south and east-west wind stress components from the C-MAN Station at Fowey Rocks and from the WES weather station at Convoy Point, plots of the water level data in analog form from each of the twelve stations, plots of the north-south and east-west components of ADP current speed from each of the five stations, a table of the harmonic constants (amplitudes and local phase angles) of the principal tidal constituents, and co-amplitude and co-phase charts of the M_2 and N_2 tidal constituents. Except for the table of harmonic constants and the co-amplitude and co-phase charts, the emphasis was on analog plots. While analog plots are useful for model validation, the QA Report did little more than repeat what had appeared earlier in the Biscayne Bay Field Data Report (Pratt 1999). The analog plots of current component speed and water level that appear in the Field Data Report provide information that can be compared with model results simulated for the same location and under the same environmental conditions. Such comparisons are qualitative, however, and the acceptance or rejection of the model's ability to reproduce variations in water level and circulation is subjective.

In this Final Report, we include analog plots, but we carry the analysis an important step further by presenting results that can be used for a digital approach to model validation. The Final Report focuses on results of harmonic analyses and spectral analyses. Amplitudes and local phase angles resulting from a harmonic analysis of field data can be compared with amplitudes and local phase angles obtained using simulated data from the corresponding part of the model domain. This quantifies the model's ability to reproduce tidal conditions in Biscayne Bay, and it permits comparisons of individual tidal constituents. Similarly, the gain resulting from spectral analyses of field data can be compared with the gain calculated from model input and output. For example, a spectral analysis of observations of winds and water levels will quantify the response to low-frequency variations in east-west wind stress. If the model is then forced specifically with east-west wind stress varying at the same periodicity, results can be compared directly. One sees immediately if the model is under- or over-estimating wind-forced variations in water level. The primary contribution that this report makes to the Biscayne Bay Field Study is the opportunity to take model verification beyond a subjective comparison of analog plots.

Data

a. Weather Data

Weather data are available from the WES study site at Convoy Point and from the Coastal-Meteorological Automated Network (C-MAN) station on the Fowey Rocks tower (Figure B1). The Convoy Point record covers the time period from July 17, 1997, to July 8, 1998, and data were collected quarter-hourly. The Fowey Rocks record covers the time period from June 6, 1997, to June 29, 1998, and data were collected hourly. Six gaps of as long as one day were found in the Fowey Rocks record. Because of the better exposure of the Fowey Rocks study site, however, and because the C-MAN station is a permanent weather station that can provide historical data, as well as data for future studies, the Fowey Rocks weather record was used for comparison with the water level and ADP records.

b. Water Level Data

Water level data were collected at twelve locations in Biscayne Bay, Card Sound, and Barnes Sound (see Table B1, Figure B1). Most records start in June 1997 and continue through late June 1998. Water level was recorded at 15-minute intervals, but for comparison with wind records the data were sub-sampled at hourly intervals.

Gaps were expected, and major gaps were found in nine of the twelve records. Data from Station TG-10 did not start until December 15, 1997, but the remainder of the record was continuous. Minor gaps occurred when water level recorders were being downloaded. Gaps of twelve hours or less were filled by linear interpolation.

Timing errors of two kinds were found in the water level records. All records starting before approximately mid-July are apparently annotated in Eastern Daylight Time; those records starting after mid-July are apparently annotated in Eastern Standard Time. The one-hour time shift that occurs when EDT is being used becomes apparent when local phase angles are calculated for the principal tidal constituents and compared with phase angles from nearby NOS study sites. The second kind of timing error in the water level records resulted from missing observations. Several records included a missing observation in early to mid-July 1997 that was not indicated by the time stamps. Again, harmonic analyses for tidal amplitudes and phase angles suggested approximately where data were missing, and analog plots were used to determine the missing hour.

c. Acoustic Doppler Profiler Data

Acoustic Doppler Profiler data were collected at five locations (see Table B1). Records began in late June 1997 at four of the five locations and on December 21 at Station ADP-1. End times vary from March 21 to July 31, 1998. Four of the five ADP records are fragmented with one or more gaps. Station ADP-3 contains five gaps, but two of the partial records are sufficiently long for characterizing wind forcing. Station ADP-4 has only two gaps, but the available partial records are short and suspect in appearance. Neither transport nor vertically averaged current speed could be calculated for Station ADP-4 because of a malfunction of the pressure sensor used to determine water depth. ADP data were recorded at 15- or 20-minute intervals, but all records have been sub-sampled and time-shifted when necessary to provide top-of-the-hour readings for comparison with wind records.

Table B1. Locations, start and end times (MM/DD/YY) of time series from WES study sites in Biscayne Bay, Card Sound, Barnes Sound, and Manatee Bay. Also included is the NOAA C-MAN station at Fowey Rocks. The analog plot of instrument vs. time that follows the table shows when gaps appeared in the time series.

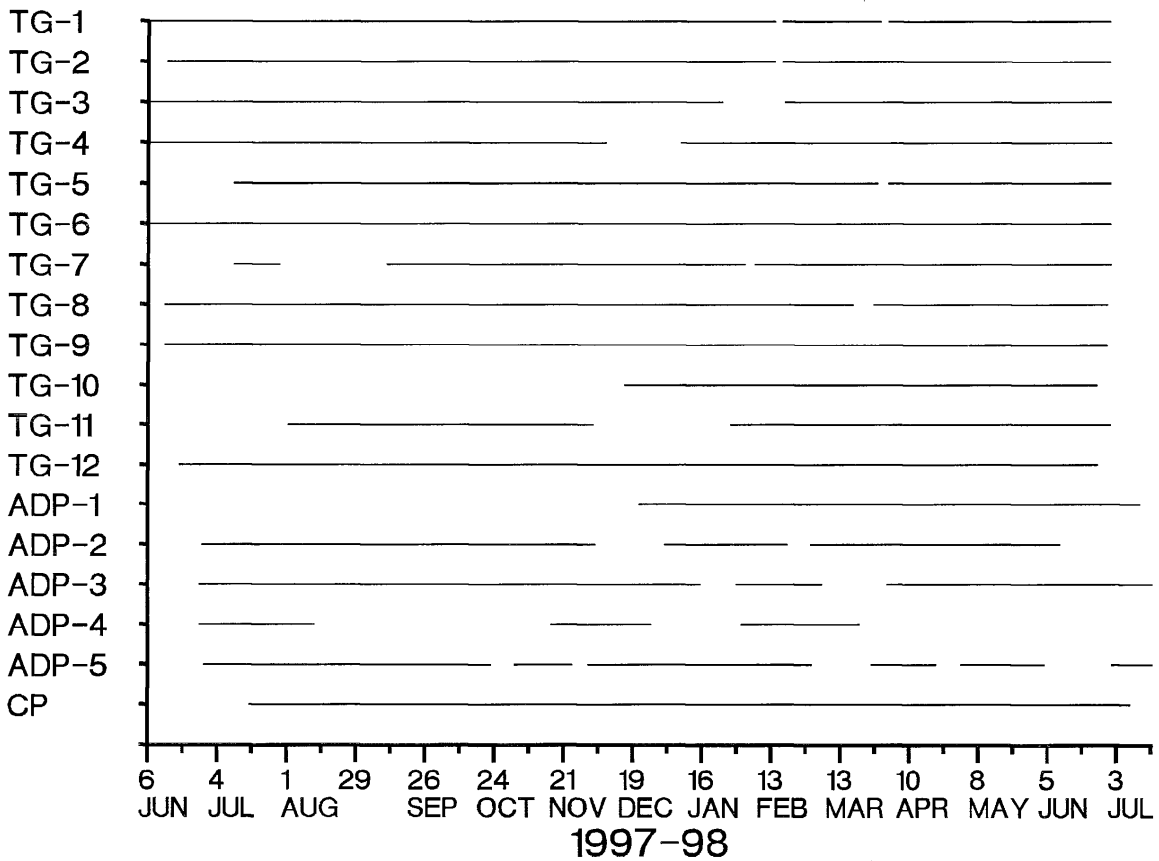
	Lat. (N)	Lon. (W)	Start	End
A. Water Level Data				
TG-1, Manatee Bay	25° 14.208'	80° 24.671'	06/06/97 02/17/98 04/01/98	02/14/98 03/29/98 06/30/98
TG-2, Card Sound Bridge	25° 17.304'	80° 22.122'	06/13/97 01/17/98	01/14/98 06/30/98
TG-3, Angelfish Creek	25° 20.164'	80° 16.817'	06/06/97 02/18/98	01/24/98 06/30/98
TG-4, Military Canal, East	25° 29.681'	80° 16.698'	06/06/97 01/07/98	12/08/97 06/30/98
TG-5, Military Canal, West	25° 29.788'	80° 19.526'	07/10/97 04/04/98	03/28/98 06/30/98
TG-6, Black Point, Marker 8	25° 31.638'	80° 18.244'	06/06/97	06/30/98
TG-7, Snapper Creek	25° 36.244'	80° 17.359'	07/10/97 09/10/97 02/06/98	07/29/97 02/02/98 06/30/98
TG-8, Gables by the Sea	25° 39.076'	80° 15.570'	06/12/97 03/26/98	03/18/98 06/29/98
TG-9, Biscayne Channel	25° 39.269'	80° 09.567'	06/12/97	06/29/98
TG-10, Miami River	25° 46.224'	80° 10.902'	12/15/97	06/25/98
TG-11, Julia Tuttle Causeway	25° 48.823'	80° 10.489'	08/01/97 01/27/98	12/03/97 06/30/98
TG-12, Broad Causeway	25° 53.413	80° 08.384'	06/18/97	06/25/98
B. Acoustic Doppler Profiler Data				
ADP-1, Angelfish Creek	25° 20.167'	80° 16.816'	12/21/97	07/12/98
ADP-2, Srn Biscayne Bay	25° 29.091'	80° 15.424'	06/27/97 01/01/98 03/01/98	12/03/97 02/19/98 06/10/98
ADP-3, Ern Biscayne Bay	25° 37.013'	80° 11.550'	06/26/97 01/30/98 04/01/98	01/15/98 03/05/98 07/31/98
ADP-4, Nrn Biscayne Bay	25° 42.886'	80° 10.630'	06/26/97 11/15/97 02/01/98	08/12/97 12/26/97 03/21/98

Table B1 (continued)...

ADP-5, Julia Tuttle Causeway	25° 48.828' 80° 10.492'	06/28/97	10/22/97
		11/01/97	11/24/97
		12/01/97	03/01/98
		03/25/98	04/21/98
		05/01/98	06/04/98
		07/01/98	07/31/98

C. Weather Data

Convoy Point	25° 27.894' 80° 20.048'	07/17/97	07/08/98
Fowey Rocks C-MAN	25° 35.417' 80° 05.800'	06/05/97	06/29/98



Methodology

a. Weather Data

Weather data from Fowey Rocks and Convoy Point were used to translate wind speed and direction into the magnitude and direction of the corresponding wind stress. The direction of the wind stress force is in the oceanographic convention, rotated 180° from the wind direction, and the magnitude of the wind stress is proportional to the square of the wind speed. We use the algorithm suggested by Wu (1980) for calculating wind stress, τ :

$$\tau = \rho c_d V^2,$$

where ρ is the density of the air, V is the wind speed, in m s^{-1} , measured 10 m above the water surface, and c_d is the drag coefficient, given by:

$$c_d = (0.8 + 0.065 V) \times 10^{-3}.$$

Air density, in turn, is a function of air temperature, surface pressure, and atmospheric moisture (List 1963).

Hourly wind stress vectors can be plotted head-to-tail as progressive vector diagrams (Scientific Programming Enterprises 1985). This approach is well suited for characterizing the general nature of wind stress over the longest time scales covered by the study, but it is inappropriate for identifying wind forcing at a particular time or over the shorter time scales. To emphasize high-frequency variability, wind stress vectors were decomposed into north-south and east-west components and plotted as a function of time.

The similarity of wind stress calculated from the Fowey Rocks and Convoy Point weather records is quantified by calculating the vector correlation coefficient and the mean deflection of the wind stress vector (Kundu 1976). A high degree of similarity would indicate that wind observations from a single location are spatially representative of the entire Biscayne Bay, Card Sound, and Barnes Sound system of coastal lagoons.

Wind stress records are used in spectral analyses (Little and Shure 1988) to examine the wind-forced rise and fall in water level or the wind-forced transport of water past any of the five ADP study sites. At any given location, the response to wind forcing will be a function of the time scale over which the forcing occurs, and it may be highly dependent upon the direction of the wind. Thus, for each study site, we consider several wind directions. Wind vectors are decomposed into components at intervals of 30° , and spectra are computed for each of the six components. Coherences are listed for all periodicities in excess of one day. If the coherence is significant at or above the 95% confidence level, the gain accompanies the coherence in parentheses. The gain, alternately known as the magnitude of the transfer function, is the change in water level that occurs with a unit change in wind stress (in dyne cm^{-2}). If the coherence is significant at or above the 99% confidence level, the coherence and gain values are italicized.

b. Water Level Data

Water level records were analyzed in three ways to (1) obtain an overview of the full time series, (2) characterize the principal tidal constituents, and (3) quantify the response to wind forcing.

To obtain an overview of the full time series, hourly readings have been low-pass filtered to remove the high-frequency variations, including the rise and fall of the tide and the response to the diurnal seabreeze. The numerical filter used for this is the 40-hour low-pass filter described by Bloomfield (1976). With this filter, 63 observations are lost from each end of the record, and the cut-off between what is lost in the filtering process and what is passed occurs at a periodicity

of about 1.5 days. Ten, 50, and 90% of the input variance is passed at periodicities of 30, 37, and 48 hours, respectively.

To identify and characterize the harmonic constants of the principal tidal constituents, the least squares harmonic analysis program developed by the National Ocean Service was used (Schureman 1958). This computer program requires time series at least 180 days in length, and it provides harmonic constants of 37 tidal constituents. In our analyses, we define a tidal constituent to be a “principal” tidal constituent if its amplitude is 1 cm or greater. To provide greater station density, we have incorporated harmonic constants from previous National Ocean Service studies in the same area. When only shorter water level records were available, a 29-day harmonic analysis program was used (Dennis and Long 1971). This same computer program can be used in the model validation exercises. Twenty-nine day model simulations can provide water level records suitable for analysis with the same harmonic analysis programs. Comparison of harmonic constants from model-derived water levels and harmonic constants from observations will indicate how well the model is reproducing amplitudes and phase angles for individual tidal constituents.

To summarize the large collection of harmonic constants for a given tidal constituent, we have constructed co-amplitude and co-phase charts. Co-amplitude charts are constructed by entering the amplitudes for a given tidal constituent on a map of the study area, then contouring. The resulting plot shows regions of high and low amplitudes and thus how the tidal wave is damped as it enters and moves through these coastal lagoons. Co-phase charts are constructed by entering and contouring local phase angles from each of the study sites. Isopleths are at 30° intervals for semidiurnal constituents and at 15° intervals for diurnal constituents. For semidiurnal constituents, a 30° phase lead or lag corresponds very closely to a one-hour time lead or lag. Thus, neighboring isopleths on a co-phase chart can be used to infer the speed and direction of movement of tidal waves through the study area. Similarly, a 15° phase difference for diurnal constituents corresponds very closely to a one-hour time difference, and isopleths can be used to describe the movement of the principal diurnal tidal constituents through the study area.

Harmonic constants are also used to calculate the total amount of water forced into and drawn out of this Bay system with the flood and ebb of the tide. Each study site represents a fraction of the Bay. As the water level in segment i changes, the product of the increase or decrease in height relative to mean sea level, $\Delta\eta_i$, and the surface area it represents, A_i , provides a volume. The hour-by-hour change in volume of the entire Bay system is given by:

$$\Delta V = \sum (\Delta\eta_i A_i).$$

Given the harmonic constants for each segment, hourly water levels can be predicted (Schureman 1958), and a time series of Bay volume relative to mean sea level can be constructed. The result gives the tidal component of the total exchange of water between the bay system and the inner continental shelf. This information is important for estimating flushing rates for the Bay system, and thus it can be an important component of the model validation exercises.

To quantify the response to wind forcing, we employ spectral analysis, using the MatLab software (Little and Shure 1988). Energy density spectra provide information on the magnitude of the rise and fall in water level at a given periodicity. Thus, an increase in the energy density level (similar to the variance) is expected at periodicities corresponding to the diurnal and semidiurnal tides. Also, one can use energy density spectra to determine the relative importance

of, for example, semidiurnal tides, diurnal tides, and low-frequency nontidal variations in water level. Spectral analysis also provides coherence spectra. In this study, spectral analyses of wind stress and water level records will indicate the time scales at which the Bay system responds most clearly to wind forcing. For model validation purposes it is important to know the wind conditions to which the Bay is most responsive because the model Bay should respond in a similar fashion. Finally, as noted above, spectral analysis provides information on the gain. The gain indicates the magnitude of the rise and fall in water level that occurs in response to a given change in wind stress forcing. This can be useful in model testing and validation exercises when wind conditions are specified so the response can be compared to observations in a quantitative way.

c. Acoustic Doppler Profiler Data

The ADP records consist of near-surface to near-bottom profiles of current speed and direction. The ADP profile begins above a “blanking zone” with an observation that is 69 cm above the top of the instrument. Given the height of the ADP above the bottom, it is estimated that the midpoint of the lowest current observation is 84 cm above the bottom. Current speeds and directions are given for layers having a thickness of 29 cm. The number of layers depends on the mean depth at the study site, and on the tidal and nontidal rise and fall of water level. A pressure reading, representing water depth, is included with each current profile. When a partial layer is indicated above the last full layer the current speed and direction from the top full layer is extended into the partial layer. This is important for transport calculations.

ADP records are used to generate two-dimensional transport, which is the vertically summed products of the currents and the layers they represent. The cumulative net transport diagrams are similar to the progressive vector diagrams calculated with wind stress vectors, but transport incorporates the time-varying water depth, and thus it is not just a measure of the current speed at the study site.

ADP data are used in conjunction with wind stress records in spectral analyses to determine the wind conditions most influential in moving water around within these three bays. This is important for model validation, because the model bay should show a similar response to the same wind forcing.

Results

a. Weather Data

A fundamental question at the start of the analysis involves the similarity of the two wind records, and thus the suitability of either wind stress time series to represent conditions at the other location. An 8,333-hour time interval was identified as an overlap period. Data from both locations were available from July 17, 1997, to June 29, 1998, and the two time series were analyzed to determine the similarity of wind conditions. Similarity was quantified by the vector correlation coefficient and by the mean deflection of the wind stress vector at one location relative to that at the other location.

The vector correlation coefficient was +0.868, and the wind stress vector at Convoy Point was 4.3° to the left of the wind stress vector at Fowey Rocks on average. The mean deflection is within the combined accuracies of the wind directions recorded at the two weather stations. The high correlation coefficient and the similar wind stress headings justifies the decision not to

assemble and integrate wind data from several other weather stations in the immediate vicinity of Biscayne Bay, Card Sound, and Barnes Sound.

Scalar average wind speeds were calculated from the hourly wind speeds recorded at each location. Both records were adjusted to a common altitude of 10 m above the surface. The mean wind speed at the Fowey Rocks weather station was 6.8 m s^{-1} , while the mean wind speed at the Convoy Point weather station was 4.7 m s^{-1} . Part of the difference may be a result of the nearshore location of the Convoy Point weather station. When winds were out of the northwest and southwest quadrants, there may have been some “wind shadow” effect produced by nearby vegetation and buildings. To examine the possibility of wind shadow effects, scalar averages were calculated a second time, but using only winds out of the northeasterly and southeasterly quadrants. For this subset of the total, the scalar averages for Fowey Rocks and Convoy Point were 6.9 and 5.2 m s^{-1} , respectively. Thus, for all wind speeds, the Convoy Point average is 68% of the Fowey Rocks average, while for onshore winds the Convoy Point average is 75% of the Fowey Rocks average. This suggests that the wind shadow effect plays a small part in the difference between the two means. An alternate possibility, involving the calibration of either or both of the anemometers, could not be tested.

Figure B2. Progressive vector diagram calculated from hourly Fowey Rocks wind stress vectors, June 5, 1997, to June 29, 1998. Monthly annotations appear on the first day of each month.

During this 389-day time period, the resultant wind stress vector had a magnitude of $0.326 \text{ dynes cm}^{-2}$ and a heading of 287.7° . The June through mid September part of the plot shows relatively steady wind out of the southeast (wind stress toward the northwest). The abrupt counterclockwise deflection that occurs on the first day of October is a common feature of wind stress plots from South Florida and the Keys. Clockwise loops in the plot are formed by winds out of the southerly quadrant, preceding frontal passages, followed by winds out of the westerly and northerly quadrants following the frontal passage. Although wind directions are highly variable over time periods on the order of days, over time scales of months to seasons, wind directions are nearly consistently shoreward.

The scalar average wind speed at this location was 6.8 m s^{-1} . Statistical analyses of Fowey Rocks wind stress and wind stress measured simultaneously at Convoy Point, 15 nautical miles (28 km) southwest of Fowey Rocks, indicate that the correlation coefficient of the wind stress vectors was $+0.868$ and that the average deflection of the Convoy Point wind stress vector was 4° to the left of the Fowey Rocks wind stress vector.

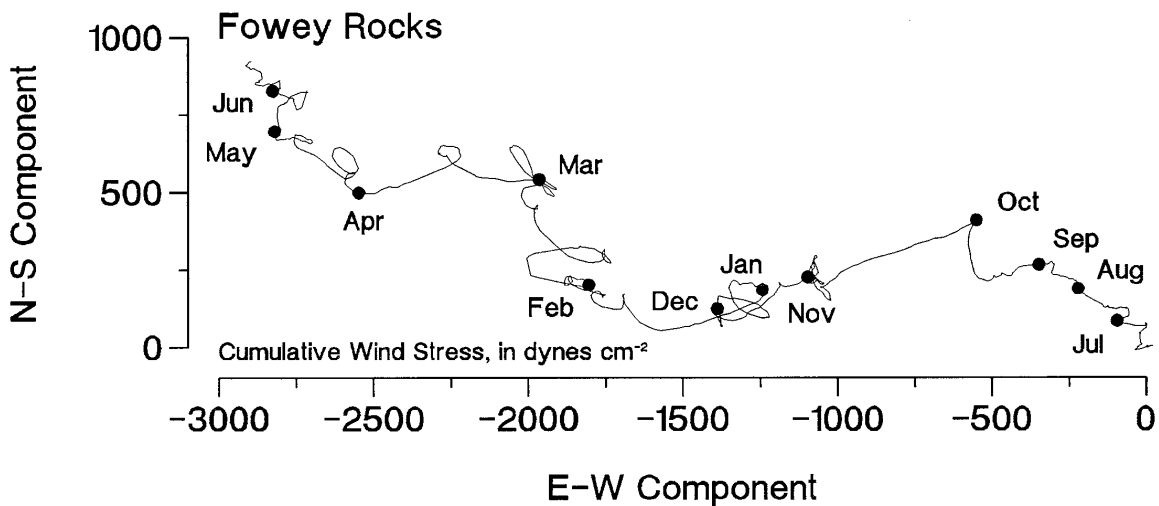


Figure B3. Wind stress data, calculated from weather observations made at Fowey Rocks from June 5, 1997 to June 29, 1998. Shown here are the north-south components (top) and the east-west components (bottom). Data gaps during this time period were short, and with interpolations a continuous record is available for comparison with overlapping segments of water level and ADP data from throughout Biscayne Bay, Card Sound, and Barnes Sound.

Wind events, producing “spikes” in the wind stress record, appear throughout the year in both wind stress components. In general, however, high-frequency fluctuations are greatest during winter months, when cold fronts move through the study area. Wind forcing is noticeably suppressed during summer months.

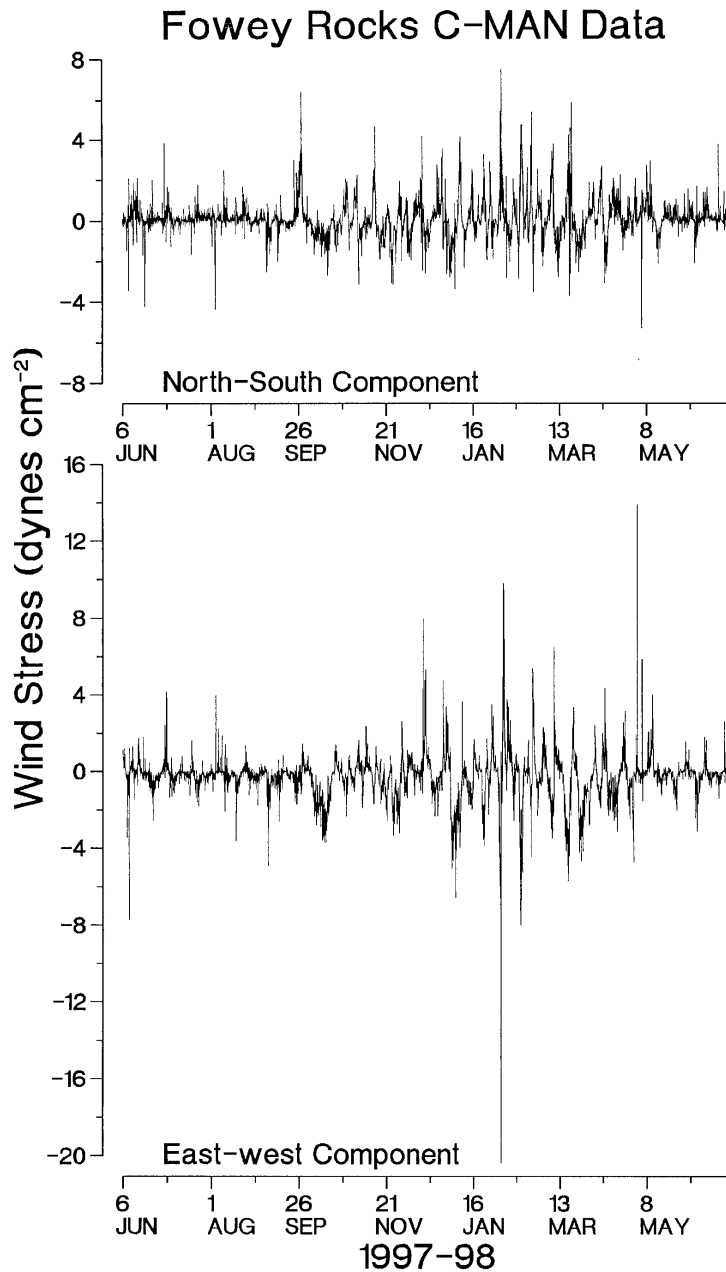


Figure B4. Progressive vector diagram calculated from hourly Convoy Point wind stress vectors, July 17, 1997, to July 8, 1998. Monthly annotations appear on the first day of each month.

During this 356-day time period, the resultant wind stress vector had a magnitude of $0.204 \text{ dynes cm}^{-2}$ and a heading of 283.6° . The scalar average wind speed at this location was 5.1 m s^{-1} . Clockwise loops in the plot are formed by winds out of the southerly quadrant, preceding frontal passages, followed by winds out of the westerly and northerly quadrants following the frontal passage. Many features of the Convoy Point wind stress record are similar to features seen in the Fowey Rocks data.

Statistical analysis of Convoy point wind stress and wind stress measured simultaneously at Fowey Rocks, 15 nautical miles (28 km) northeast of Convoy Point, indicate that the correlation coefficient of the wind stress vectors was $+0.868$, and that the average deflection of the Fowey Rocks wind stress vector was 4° to the right of the Convoy Point wind stress vector.

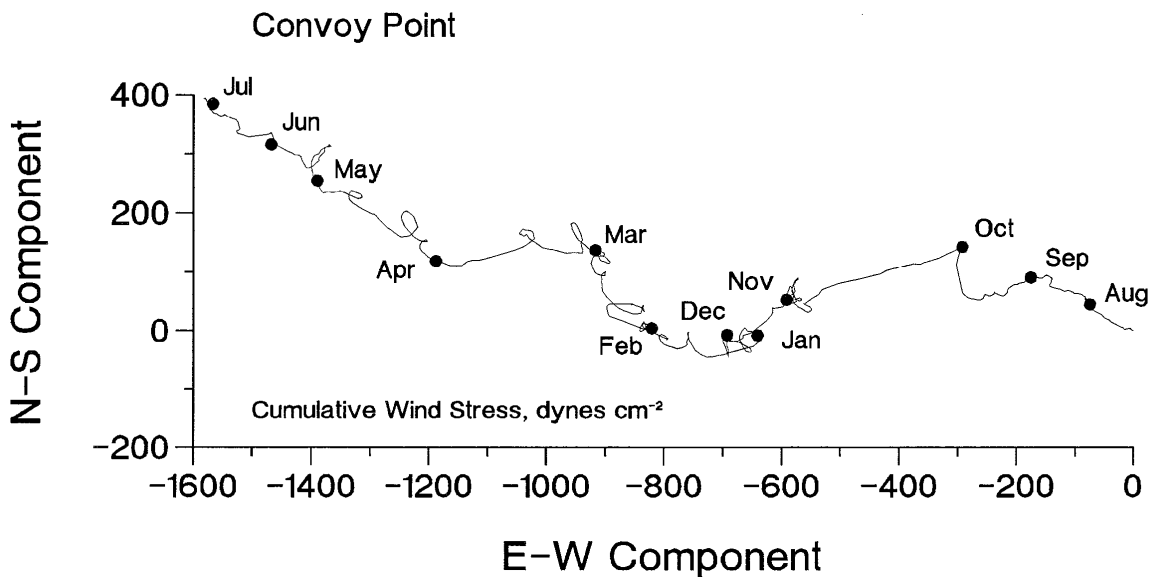
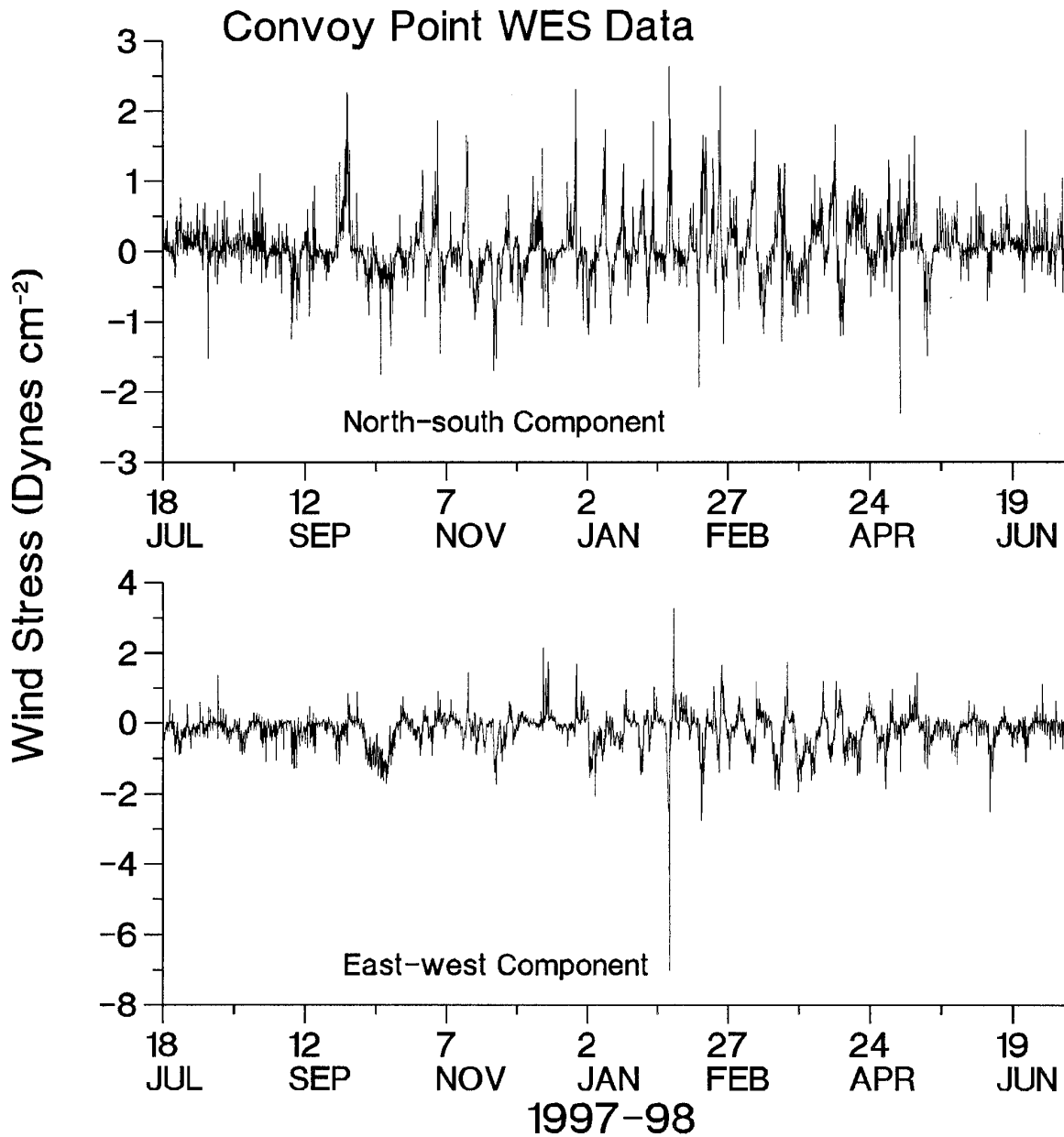


Figure B5. Wind stress data, calculated from weather observations made at Convoy Point from July 17, 1997, to July 8, 1998. Shown here are north-south (top) and east-west (bottom) components. A single continuous record is available for comparison with overlapping segments of ADP data from throughout Card Sound and Biscayne Bay.

Because of the strong westward wind stress in early February, the vertical scales are not the same for the two plots. In general, during summer months both wind stress components show less high-frequency variability. During winter months, variability increases as a result of changes in wind speed and direction associated with frontal passages.



b. Water Level Data

Results of the analysis of the water level data are presented in several ways. First, we provide low-pass filtered plots of the water level records. Each plot is accompanied by a caption that describes the length of the time series, and when and where the data were collected. The analog plots show an increase in the rise and fall in water level during winter months. This is a logical result of cold fronts moving through the study area and producing significant changes in wind speed and direction over time periods on the order of several days. Generally speaking, the plots show that low-frequency fluctuations in water level characteristically occur over time scales on the order of 1-2 weeks.

Second, and accompanying each analog plot, a table summarizes the results of the spectral analysis of the water level record with the Fowey Rocks wind stress data. The table includes the coherence and gain calculated for wind stress components and water level over time scales greater than one day. For example, for the 000-180° (north-south) component, with northward wind stress defined positive, a gain of -0.014 at a periodicity of four days indicates that a wind stress of ± 1 dyne cm^{-2} (produced by a wind speed of approximately 8 m s^{-1}) will produce a 0.014 m (1.4 cm) variation in water level. A negative gain indicates that this will be an inverse relationship. Northward (positive) wind stress will set down water levels. For this same four-day periodicity, a southward wind stress would set up water levels by the same amount. The algebraic sign of the gain is a function of periodicity as much as it is a function of the wind stress component. For example, over relatively short time scales, variations in the north-south wind stress component will set-up and set-down water levels at opposite ends of Biscayne Bay. Over longer time scales, however, the north-south wind stress component will produce an Ekman transport away from or toward the coast, and water level will rise or fall similarly everywhere in the bays.

A third way in which we present results of the analysis of water level data is with co-amplitude and co-phase charts for the five principal tidal constituents: M_2 , S_2 , N_2 , K_1 and O_1 . The semidiurnal (with subscript "2") M_2 constituent occurs as the earth rotates through the high water created by gravitational (near side, directly under the moon) and centrifugal (opposite side) forces that arise as the earth and moon rotate around a common center of mass. The S_2 constituent is created to interact with the M_2 constituent in such a way as to explain the fortnightly fluctuation in tidal range arising from the additive or subtractive effects of the sun's gravitational force—additive at times of new and full moon; subtractive at times of first and third quarter). The N_2 constituent is created to interact with the M_2 constituent in such a way as to explain the monthly fluctuation in tidal range as the moon passes through apogee, then perigee in its elliptical orbit around the earth. The diurnal (with subscript "1") K_1 and O_1 constituents are created to explain the fortnightly increase and decrease in tidal range associated with the moon's declination (the high tides induced by gravitational and centrifugal forces will be in opposite hemispheres).

The fourth way in which we present results of our analysis of the water level database is in the form of histograms of flood and ebb tide volumes. Results should be of use in flushing studies, where flood and ebb intertidal volumes must be compared with the total volumes of the Bay.

Figure B6. Analog plot of low-pass filtered water levels (in meters, relative to NVGD29) from Station TG-1 (**Manatee Bay**), June 6, 1997, to June 30, 1998. Due to breaks in the record, the plot is in three parts: June 6, 1997, to February 14, 1998 (6080 observations), February 17 to March 29, 1998 (960 observations), and April 1 to June 30, 1998 (2172 observations). Quarter-hourly water levels were sub-sampled to obtain a time series of hourly values, and hourly values were low-pass filtered to remove the rise and fall of the tide. As a result of the filtering process 63 hours are lost from both ends of each segment.

Note that the high water level recorded in late January and early February 1998 corresponds to the strong westward wind stress recorded at both weather stations (see Figures B3 and B5).

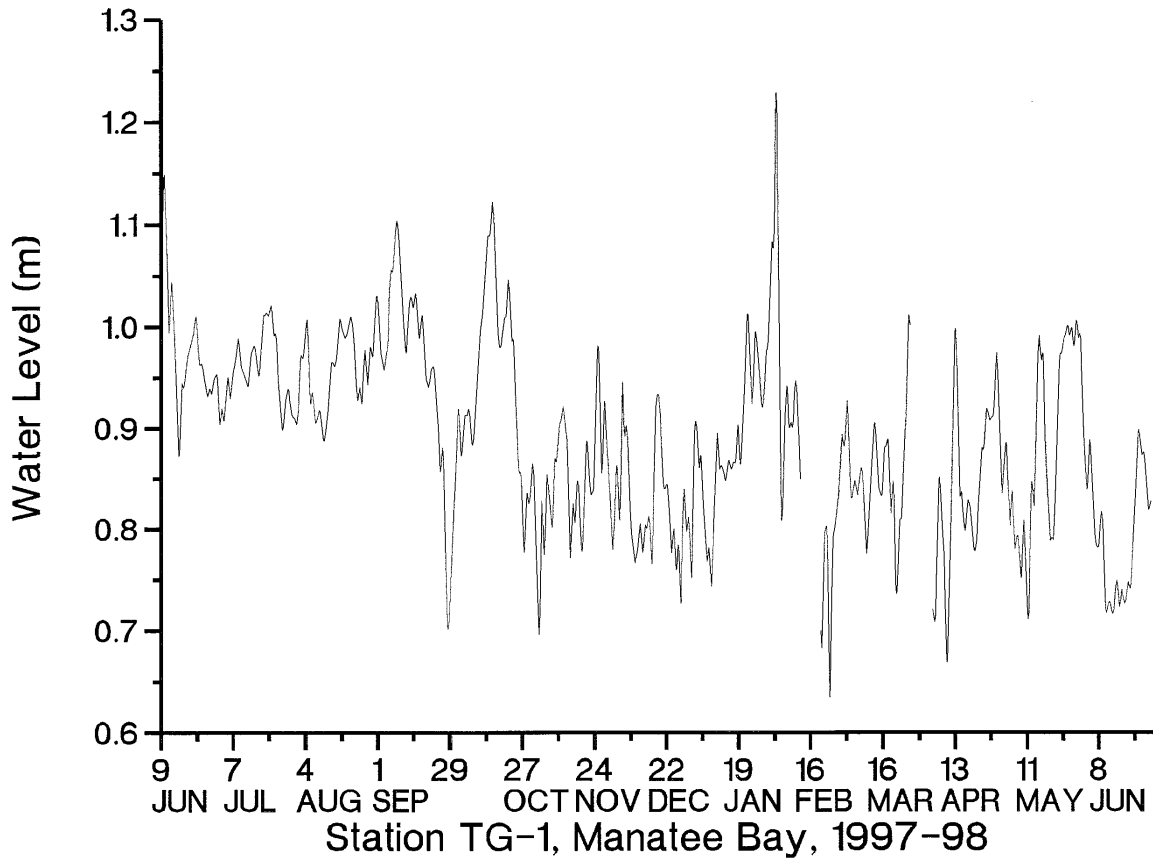


Table B2. Coherence of water levels at Station TG-1 and wind stress, calculated from data recorded June 6, 1997, to February 14, 1998. Bold numbers indicate coherence significant at the 95% confidence limit ($\beta_{05} = 0.307$); bold italicized numbers indicate coherence significant at the 99% limit ($\beta_{01} = 0.376$). The magnitude of the transfer function (“gain”) is shown in parentheses beside coherence values when coherence is statistically significant. Each wind stress column is labeled with two compass headings that are 180° apart. The algebraic sign of the gain corresponds to the first compass heading. For example, a gain of -0.041 indicates that a northward wind stress reaching a magnitude of 1 dyne cm⁻² would produce a set down of water level reaching -0.041 m, or -4.1 cm.

Relatively few coherences are highly significant at this southernmost study site. The mostly negative gains indicate that northward wind stress will set down water levels in Manatee Bay.

Period (d)	<u>000-180°</u>	<u>030-210°</u>	<u>060-240°</u>	<u>090-270°</u>	<u>120-300°</u>	<u>150-330°</u>
16	.273	.291	.198	.154	.159	.199
8	.281	.323(-.041)	.203	.048	.059	.168
5.8	.256	.422(-.037)	.397(-.043)	.135	.054	.119
4	.359(-.014)	.621(-.040)	.668(-.044)	.507(-.034)	.342(-.022)	.261
3.2	.238	.429(-.034)	.458(-.033)	.376(-.028)	.258	.162
2.7	.162	.338(-.024)	.387(-.027)	.391(-.027)	.178	.064
2.3	.264	.470(-.023)	.443(-.025)	.280	.100	.051
2	.354(-.014)	.484(-.022)	.464(-.030)	.233	.047	.172
1.8	.550(-.023)	.622(-.041)	.530(-.048)	.369(-.038)	.322(-.018)	.410(.003)
1.6	.622(-.014)	.642(-.029)	.417(-.035)	.222	.273	.451(.001)
1.5	.408(-.018)	.311(-.021)	.030	.060	.214	.339(.014)
1.3	.621(-.005)	.542(-0.12)	.159	.005	.123	.338(.006)
1.2	.536(-.005)	.475(-.010)	.230	.066	.121	.346(-.001)
1.13	.171	.266	.207	.057	.014	.066
1.08	.033	.075	.071	.020	.002	.008
1.0	.055	.102	.077	.038	.025	.029

Figure B7. Analog plot of low-pass filtered water levels (in meters, relative to NVGD29) from Station TG-2 (**Card Sound Bridge**), June 13, 1997, to June 30, 1998. Due to a break in the record, the plot is in two parts: June 13, 1997, to February 14, 1998 (5913 observations) and February 17 to June 30, 1998 (3203 observations). Quarter-hourly water levels were sub-sampled to obtain a time series of hourly values, and hourly values were low-pass filtered to remove the rise and fall of the tide. As a result of the filtering process 63 hours are lost from both ends of each segment.

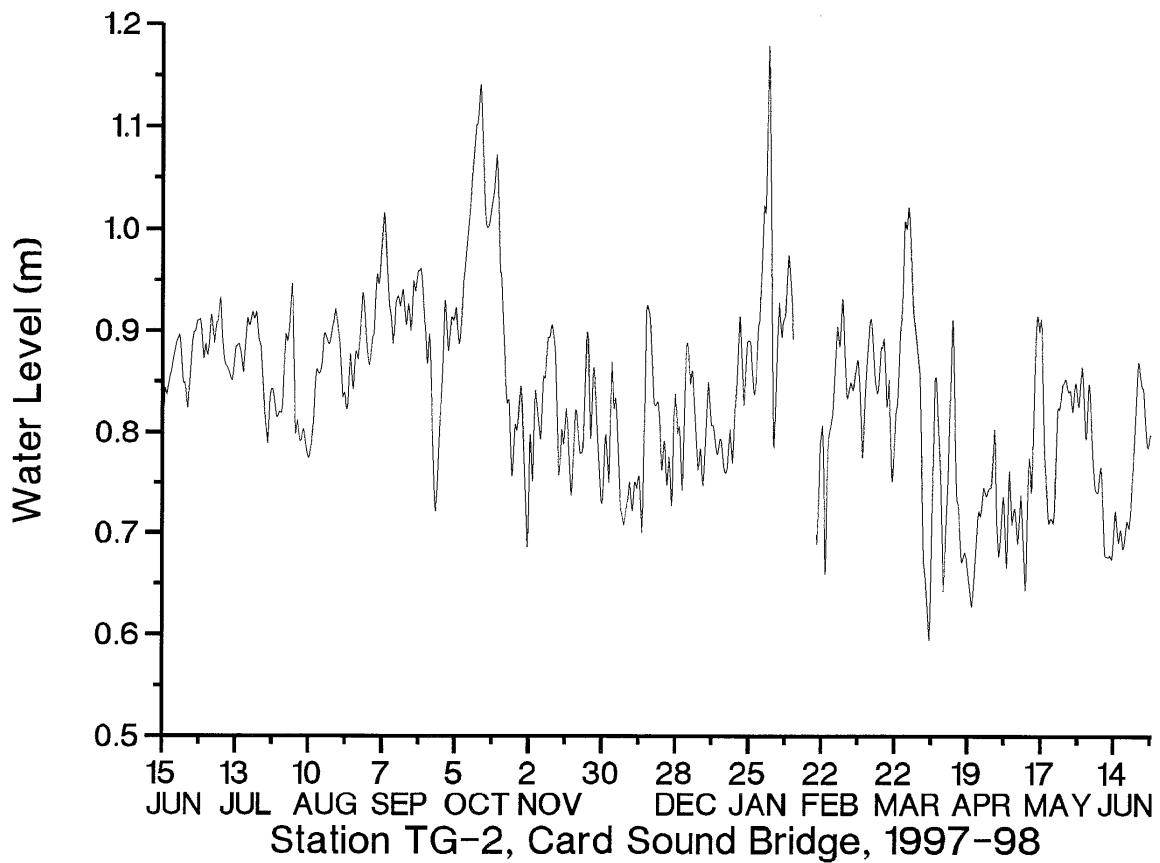


Table B3. Same as Table B1 except for Station TG-2 at Card Sound Bridge, between Little Card Sound and Barnes Sound. The spectral analysis covers the time period from June 13, 1997, to Feb. 14, 1998 ($\beta_{05} = 0.312$, $\beta_{01} = 0.381$).

Highest coherences occur for winds out of the northeasterly quadrant and over time scales on the order 2-8 days. This indicates a response to both a direct downwind transport, and to a shoreward Ekman transport across the shelf forced by southward wind stress.

<u>Period (d)</u>	<u>000-180°</u>	<u>030-210°</u>	<u>060-240°</u>	<u>090-270°</u>	<u>120-300°</u>	<u>150-330°</u>
16	.307	.353(-.044)	.305	.259	.231	.234
8	.527(-.012)	.620(-.044)	.512(-.040)	.420(-.032)	.372(-.026)	.383(-.018)
5.8	.374(.004)	.572(-.028)	.527(-.031)	.426(-.026)	.342(-.024)	.291
4	.407(.002)	.643(-.027)	.601(-.026)	.519(-.024)	.424(-.025)	.316(-.027)
3.2	.194	.556(-.022)	.578(-.022)	.468(-.019)	.348(-.018)	.217
2.7	.097	.446(-.016)	.540(-.017)	.465(-.017)	.317(-.016)	.102
2.3	.397(.004)	.597(-.017)	.605(-.205)	.496(-.026)	.369(-.025)	.292
2	.352(.0004)	.690(-.018)	.532(-.027)	.319(-.023)	.197	.196
1.8	.330(-.004)	.563(-.013)	.456(-.016)	.207	.057	.088
1.6	336(.001)	.452(-.006)	.310	.178	.070	.042
1.5	.339(-.018)	.334(-.014)	.150	.038	.016	.115
1.3	.342(-.010)	.653(-.010)	.575(-.008)	.428(-.007)	.232	.001
1.2	.355(-.022)	.593(-.013)	.521(-.002)	.386(-.003)	.266	.198
1.13	.229	.284	.239	.125	.011	.073
1.08	.084	.078	.045	.017	.007	.038
1.0	.361(.027)	.194	.060	.093	.218	.345(-.033)

Figure B8. Analog plot of low-pass filtered water levels (in meters, relative to NVGD29) from Station TG-3 (**Angelfish Creek**), June 6, 1997, to June 30, 1998. Due to a break in the record, the plot is in two parts: June 6, 1997, to January 24, 1998 (5564 observations) and February 18 to June 30, 1998 (3178 observations). Quarter-hourly water levels were sub-sampled to obtain a time series of hourly values, and hourly values were low-pass filtered to remove the rise and fall of the tide. As a result of the filtering process 63 hours are lost from both ends of each segment.

The seasonal variation in sea level is a more prominent feature of this plot, with high water levels in late fall and low water levels in winter months. The several week period of high water level in March and the several week period of low water level in late April and early May are significant departures from the normal annual cycle in sea level.

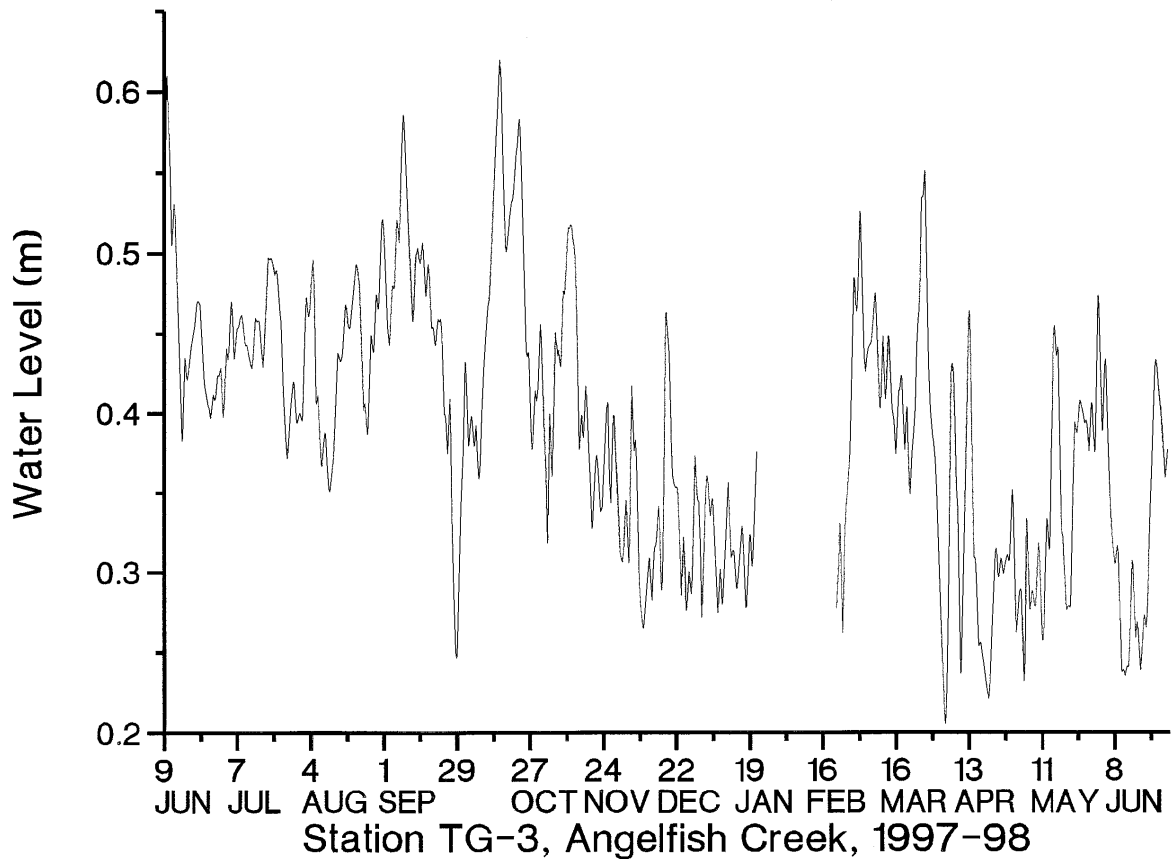


Table B4. Same as Table B1 except for Station TG-3, at the mouth of Angelfish Creek in northern Card Sound. Study period spans June 6, 1997, to Jan. 24, 1998 ($\beta_{05} = 0.321$, $\beta_{01} = 0.393$).

A notable feature of this table is the absence of significant coherence at periodicities in excess of about three days for all wind stress components. This study site is near the western end of Angelfish Creek. Thus, it is likely that water level variations are a response to both local forcing within the Biscayne Bay system and to more regional scale forcing acting on shelf waters and forcing water through Angelfish Creek.

<u>Period (d)</u>	<u>000-180°</u>	<u>030-210°</u>	<u>060-240°</u>	<u>090-270°</u>	<u>120-300°</u>	<u>150-330°</u>
16	.153	.091	.093	.139	.174	.184
8	.158	.127	.053	.022	.088	.144
5.8	.104	.107	.050	.001	.027	.071
4	.107	.247	.276	.164	.055	.027
3.2	.011	.113	.190	.171	.101	.024
2.7	.075	.183	.357(-.016)	.409(-.020)	.323(-.021)	.164
2.3	.129	.371(-.015)	.465(-.019)	.367(-.019)	.166	.022
2	.244	.394(-.025)	.449(-.032)	.281	.027	.073
1.8	.465(-.029)	.486(-.039)	.348(-.038)	.193	.211	.341(.015)
1.6	.443(.014)	.431(-.023)	.253	.114	.183	.331(.005)
1.5	.320	.242	.042	.027	.160	.272
1.3	.613(-.020)	.588(-.018)	.351(-.012)	.062	.090	.405(.019)
1.2	.445(-.006)	.453(-.005)	.304	.074	.029	.263
1.13	.053	.165	.212	.117	.029	.006
1.08	.023	.049	.115	.114	.078	.043
1.0	.109	.139	.052	.002	.011	.049

Figure B9. Analog plot of low-pass filtered water levels (in meters, relative to NVGD29) from Station TG-4 (**Military Canal - East**), June 6, 1997, to June 30, 1998. Due to a break in the record, the plot is in two parts: June 6 to December 8, 1997 (4437 observations) and January 7 to June 30, 1998 (4189 observations). Quarter-hourly water levels were sub-sampled to obtain a time series of hourly values, and hourly values were low-pass filtered to remove the rise and fall of the tide. As a result of the filtering process 63 hours are lost from both ends of each segment.

The seasonal rise and fall in sea level is well defined at this location, with highest water levels in fall months and lowest water levels in late winter and early spring. Highest water level was recorded in early February in response to strong shoreward wind stress (see Figures B3 and B5).

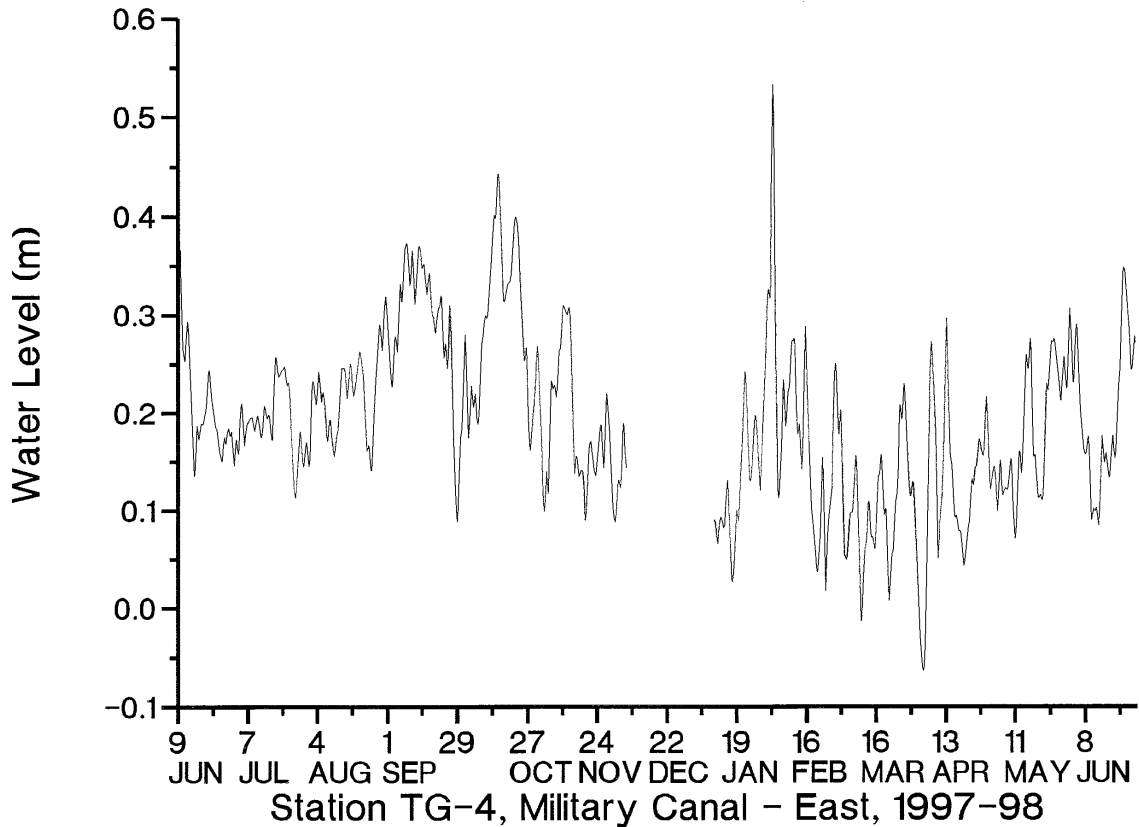


Table B5. Same as Table B1 except for Station TG-4, in south-central Biscayne Bay. This analysis included data from June 6 to Dec. 8, 1997 ($\beta_{05} = 0.360$, $\beta_{01} = 0.438$).

High coherence occurs infrequently and primarily at periodicities on the order of 1-2 days. Water levels seem most responsive to winds out of the northeast and southwest quadrants.

<u>Period (d)</u>	<u>000-180°</u>	<u>030-210°</u>	<u>060-240°</u>	<u>090-270°</u>	<u>120-300°</u>	<u>150-330°</u>
16	.189	.072	.012	.041	.113	.190
8	.198	.147	.077	.019	.034	.156
5.8	.376(.009)	.286	.271	.309	.406(.044)	.486(-.041)
4	.084	.216	.319	.356	.309	.147
3.2	.004	.094	.174	.211	.196	.086
2.7	.163	.228	.321	.433(-.057)	.393(-.066)	.178
2.3	.249	.301	.300	.232	.088	.129
2	.162	.206	.215	.149	.041	.088
1.8	.408(-.035)	.448(-.038)	.396(-.035)	.297	.200	.252
1.6	.477(-.018)	.459(-.035)	.334(-.037)	.247	.256	.359
1.5	.222	.213	.080	.010	.066	.153
1.3	.414(-.029)	.607(-.027)	.655(-.027)	.561(-.029)	.209	.057
1.2	.481(-.012)	.605(-.014)	.649(-.017)	.580(-.025)	.181	.210
1.13	.037	.066	.101	.112	.082	.042
1.08	.081	.059	.089	.139	.154	.126
1.0	.244	.249	.147	.069	.083	.161

Figure B10. Analog plot of low-pass filtered water levels (in meters, relative to NVGD29) from Station TG-5 (**Military Canal - West**), July 10, 1997, to June 30, 1998. Due to a break in the record, the plot is in two parts: July 10, 1997, to March 28, 1998 (6260 observations) and April 1 to June 30, 1998 (2170 observations). Quarter-hourly water levels were sub-sampled to obtain a time series of hourly values, and hourly values were low-pass filtered to remove the rise and fall of the tide. As a result of the filtering process 63 hours are lost from both ends of each segment.

Prominent features in this plot are the seasonal cycle, with autumn high and midwinter low water levels, and the transient high water event in early February, in response to strong shoreward winds.

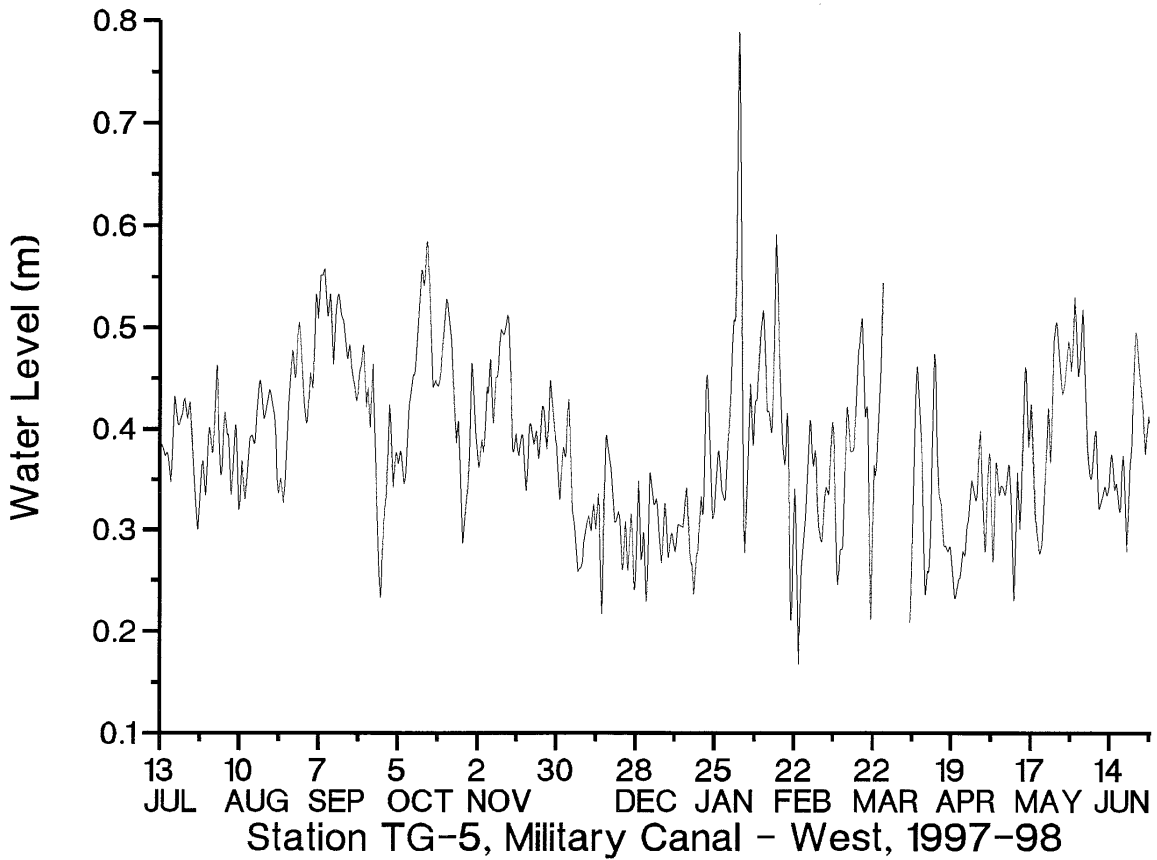


Table B6. Same as Table B1 except for Station TG-5, in west-central Biscayne Bay. Study period spans July 10, 1997, to March 28, 1998 ($\beta_{05} = 0.303$, $\beta_{01} = 0.371$).

Highest coherences are confined largely to periodicities of approximately 2-6 days. The dominance of negative gains for most wind stress components indicates that Bay water levels rise in direct response to westward winds, or southward winds producing a shoreward Ekman transport.

<u>Period (d)</u>	<u>000-180°</u>	<u>030-210°</u>	<u>060-240°</u>	<u>090-270°</u>	<u>120-300°</u>	<u>150-330°</u>
16	.094	.155	.306(-.038)	.312(-.029)	.264	.188
8	.055	.063	.231	.273	.242	.168
5.8	.312(.016)	.321(-.005)	.437(-.027)	.532(-.027)	.491(-.030)	.402(-.025)
4	.346(.007)	.367(-.011)	.396(-.023)	.403(-.018)	.388(-.026)	.361(-.021)
3.2	.245	.342(-.018)	.317(-.021)	.229	.157	.152
2.7	.427(-.001)	.477(-.019)	.516(-.037)	.488(-.040)	.432(-.028)	.409(-.014)
2.3	.574(.013)	.663(-.014)	.684(-.033)	.626(-.037)	.565(-.034)	.537(-.028)
2	.310(-.0003)	.367(-.016)	.435(-.031)	.422(-.033)	.352(-.024)	.305(-.012)
1.8	.113	.219	.407(-.041)	.378(-.033)	.272	.129
1.6	.127	.215	.203	.090	.024	.045
1.5	.023	.164	.293	.197	.099	.035
1.3	.125	.204	.317(-.026)	.307(-.025)	.236	.160
1.2	.070	.223	.382(-.024)	.424(-.029)	.314(-.028)	.119
1.13	.088	.077	.115	.180	.179	.130
1.08	.132	.097	.058	.088	.116	.132
1.0	.097	.135	.055	.012	.007	.031

Figure B11. Analog plot of low-pass filtered water levels (in meters, relative to NVGD29) from Station TG-6 (**Marker 8 - Black Point**) June 6, 1997, to June 30, 1998. There are no breaks in this record, and the 9346 observations are continuous. Quarter-hourly water levels were sub-sampled to obtain a time series of hourly values, and hourly values were low-pass filtered to remove the rise and fall of the tide. As a result of the filtering process 63 hours are lost from both ends of each segment.

The prominent feature in this water level record is the period of sustained high water through most of the month of October. This raises the normal seasonal high water in autumn months by about 0.2 m. The mid-to-late winter low water is shortened by an increase in water level in late January.

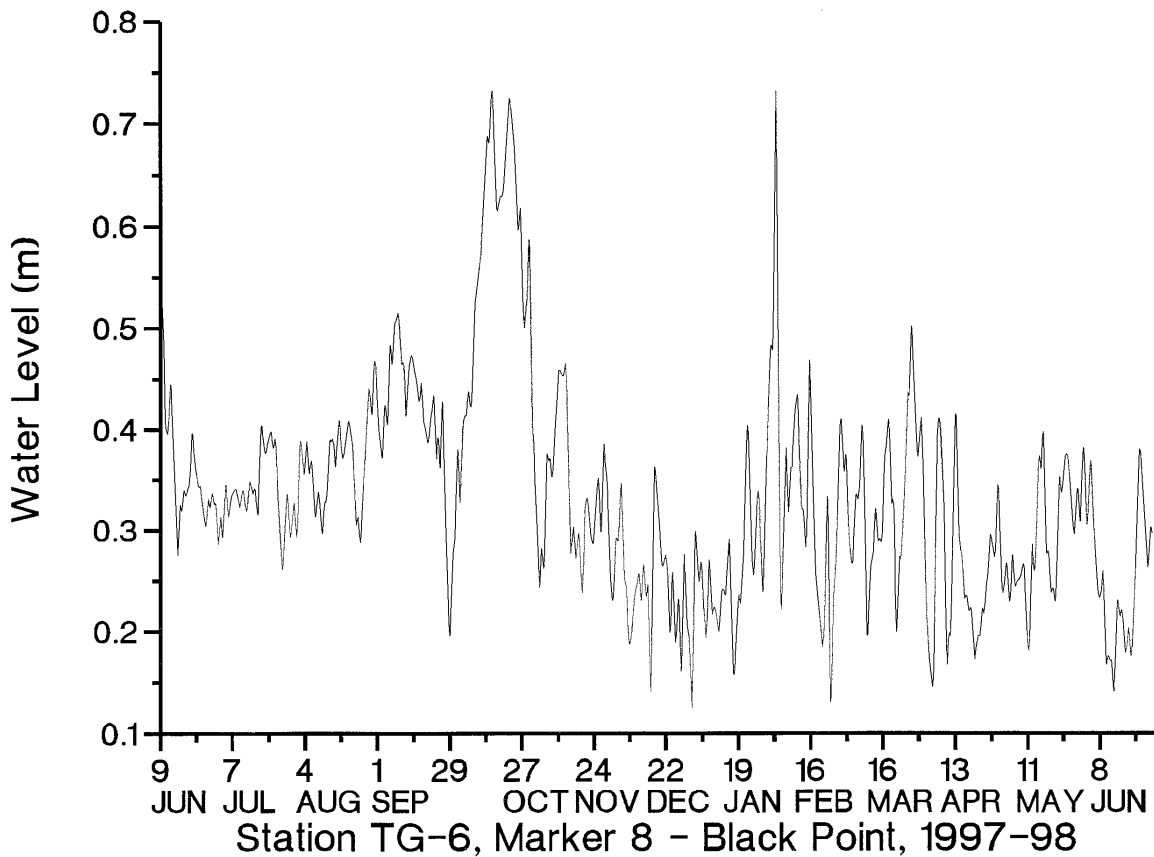


Table B7. Same as Table B1 except for Station TG-6 in west-central Biscayne Bay. The analysis covers the time period from June 6, 1997, to June 29, 1998 ($\beta_{05} = 0.248$, $\beta_{01} = 0.305$).

Highest coherences are broadly distributed, and highly significant relationships occur at nearly all periodicities. The core of highest coherence is found for periodicities on the order of 2-6 days and for winds out of the northeasterly and easterly quadrants. This indicates a response to the direct shoreward transport of water and a shoreward Ekman transport.

<u>Period (d)</u>	<u>000-180°</u>	<u>030-210°</u>	<u>060-240°</u>	<u>090-270°</u>	<u>120-300°</u>	<u>150-330°</u>
16	.193	.257(-.042)	.351(-.049)	.337(-.035)	.293(-.026)	.239
8	.129	.197	.263(-.041)	.224	.163	.127
5.8	.229	.264(-.011)	.431(-.034)	.498(-.039)	.441(-.035)	.329(-.028)
4	.379(.019)	.417(-.016)	.562(-.034)	.627(-.038)	.607(-.039)	.510(-.037)
3.2	.299(.010)	.338(-.014)	.402(-.025)	.418(-.027)	.395(-.026)	.345(-.023)
2.7	.293(.005)	.369(-.019)	.407(-.030)	.388(-.033)	.336(-.032)	.284(-.025)
2.3	.215	.381(-.016)	.466(-.029)	.421(-.031)	.320(-.031)	.214
2	.134	.243	.280(-.021)	.213	.122	.081
1.8	.210	.338(-.028)	.327(-.030)	.212	.114	.104
1.6	.156	.328(-.030)	.407(-.035)	.323(-.030)	.188	.104
1.5	.019	.277(-.033)	.443(-.037)	.358(-.028)	.209	.061
1.3	.259(-.002)	.575(-.021)	.694(-.030)	.523(-.028)	.295(-.022)	.161
1.2	.206	.476(-.019)	.716(-.032)	.659(-.033)	.393(-.027)	.179
1.13	.046	.108	.284(-.036)	.362(-.046)	.269(-.040)	.127
1.08	.049	.039	.160	.213	.183	.121
1.0	.073	.097	.051	.018	.016	.034

Figure B12. Analog plot of low-pass filtered water levels (in meters, relative to NVGD29) from Station TG-7 (**Snapper Creek**), July 10, 1997, to June 30, 1998. Due to breaks in the record, the plot is in three parts: July 10-29, 1997 (456 observations), September 10, 1997, to February 2, 1998 (3487 observations), and February 6 to June 30, 1998 (3469 observations). Quarter-hourly water levels were sub-sampled to obtain a time series of hourly values, and hourly values were low-pass filtered to remove the rise and fall of the tide. As a result of the filtering process 63 hours are lost from both ends of each segment.

The early February 1998 transient peak is missing because of the break in the record. The fall maximum is not much higher than the mid July water levels recorded in the first segment of the data. Midwinter low water levels are broadly distributed between early December and late January.

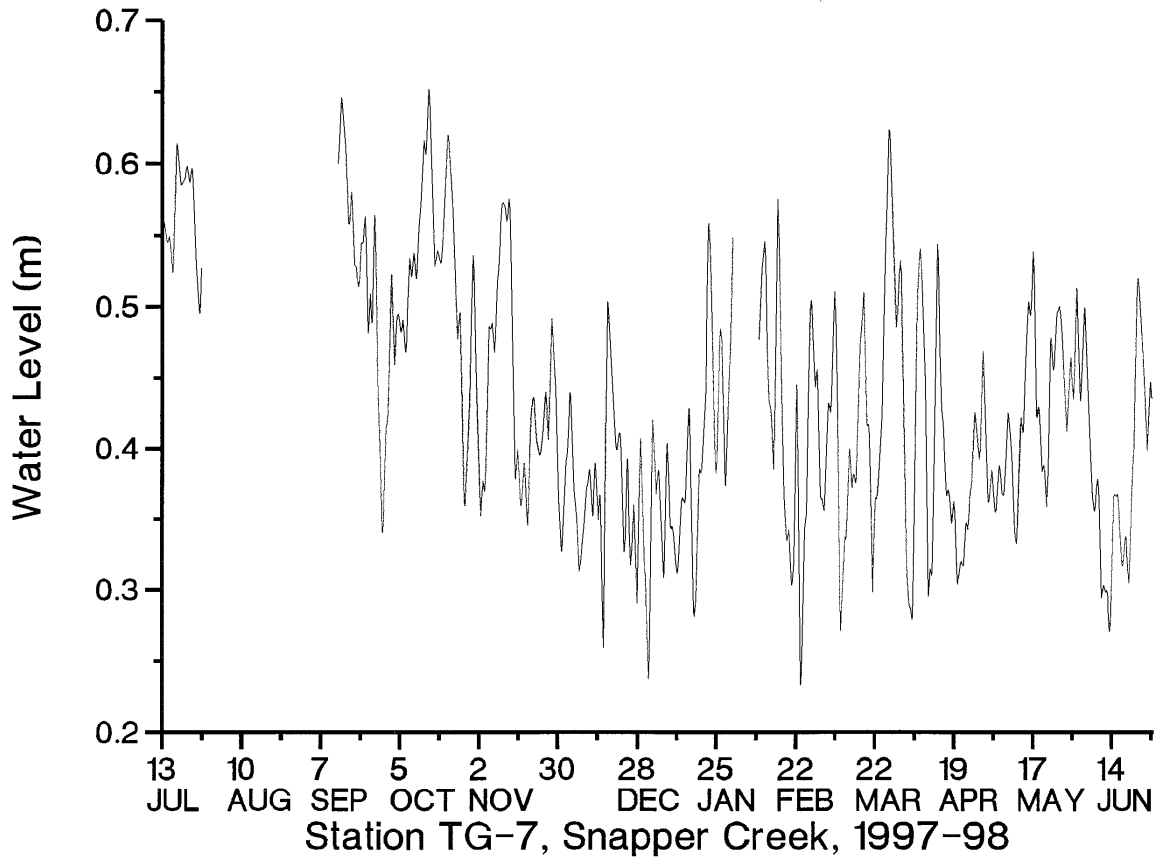


Table B8. Same as Table B1 except for Station TG-7, in west-central Biscayne Bay. The analysis covers the time period from September 1, 1997, to February 2, 1998 ($\beta_{05} = 0.406$, $\beta_{01} = 0.491$).

The table is noteworthy for the relatively small core of high coherences, covering periodicities of 2-6 days and for winds out of the easterly and westerly quadrants. A second region of high coherence is limited to periodicities of just over one day, but it includes some of the highest coherence levels found in data from this study site.

<u>Period (d)</u>	<u>000-180°</u>	<u>030-210°</u>	<u>060-240°</u>	<u>090-270°</u>	<u>120-300°</u>	<u>150-330°</u>
16	.100	.026	.215	.308	.304	.240
8	.083	.020	.017	.111	.156	.136
5.8	.295	.258	.435(-.018)	.589(-.040)	.505(-.034)	.391
4	.341	.377	.631(-.032)	.751(-.038)	.692(-.037)	.523(-.032)
3.2	.184	.263	.483(-.023)	.601(-.028)	.589(-.031)	.418(-.030)
2.7	.234	.171	.331	.504(-.030)	.594(-.036)	.502(-.037)
2.3	.272	.380	.536(-.035)	.585(-.041)	.529(-.043)	.386
2	.074	.134	.210	.247	.123	.049
1.8	.213	.276	.230	.073	.047	.123
1.6	.180	.176	.163	.160	.170	.177
1.5	.079	.011	.070	.161	.154	.125
1.3	.084	.209	.593(-.028)	.623(-.027)	.445(-.021)	.237
1.2	.164	.442(-.020)	.746(-.033)	.774(-.035)	.559(-.031)	.261
1.13	.037	.025	.181	.277	.229	.132
1.08	.230	.201	.105	.141	.187	.215
1.0	.038	.143	.219	.151	.087	.044

Figure B13. Analog plot of low-pass filtered water levels (in meters, relative to NVGD29) from Station TG-8 (**Gables by the Sea**), June 12, 1997, to June 29, 1998. Due to a break in the record, the plot is in two parts: June 12, 1997, to March 18, 1998 (6696 observations) and March 26 to June 29, 1998 (2281 observations). Quarter-hourly water levels were sub-sampled to obtain a time series of hourly values, and hourly values were low-pass filtered to remove the rise and fall of the tide. As a result of the filtering process 63 hours are lost from both ends of each segment.

The fall maximum water level stands out prominently from both midsummer and midwinter levels. The highest water levels, occurring in October, are less clearly defined; they were at Station TG-6 (Figure B11), and the early February spike stands out as the highest point in the series of filtered water levels.

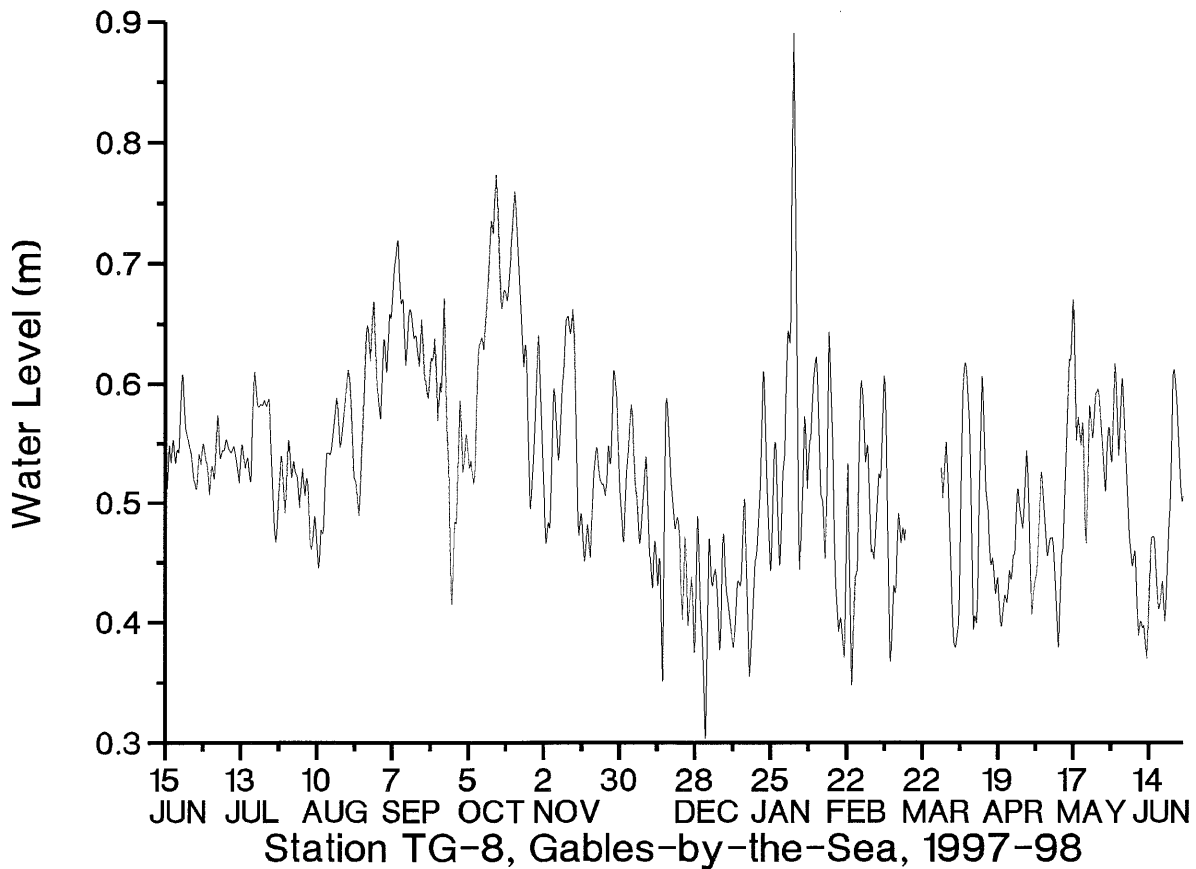


Table B9. Same as Table B1 except for Station TG-8, in north-central Biscayne Bay. The analysis covers the time period from June 12, 1997, to March 18, 1998 ($\beta_{05} = 0.293$, $\beta_{01} = 0.359$).

Highly significant coherences are found for virtually all wind stress components at periodicities of between 2 and 8 days. The negative gains indicate that northward and eastward wind stress will set down water levels along the west side of Biscayne Bay.

Period (d)	000-180°	030-210°	060-240°	090-270°	120-300°	150-330°
16	.365(.011)	.260	.223	.245	.285	.339(-.025)
8	.535(.028)	.518(-.016)	.437(-.034)	.419(-.033)	.432(-.032)	.468(-.034)
5.8	.579(.036)	.548(.003)	.501(-.033)	.510(-.035)	.532(-.034)	.557(-.036)
4	.389(.019)	.427(-.008)	.473(-.024)	.476(-.027)	.543(-.028)	.416(-.028)
3.2	.373(.022)	.413(-.004)	.581(-.026)	.623(-.029)	.577(-.029)	.482(-.028)
2.7	.260	.371(-.009)	.457(-.021)	.428(-.024)	.344(-.023)	.266
2.3	.576(.023)	.587(-.004)	.646(-.027)	.679(-.037)	.667(-.039)	.622(-.036)
2	.488(.027)	.458(-.004)	.623(-.032)	.739(-.042)	.734(-.042)	.635(-.040)
1.8	.240	.137	.338(-.035)	.533(-.044)	.557(-.043)	.444(-.039)
1.6	.279	.197	.283	.369(-.029)	.420(-.033)	.410(-.036)
1.5	.085	.106	.427(-.029)	.500(-.026)	.440(-.024)	.301(-.023)
1.3	.155	.270	.546(-.028)	.657(-.029)	.622(-.032)	.354(-.032)
1.2	.082	.240	58.4(-.030)	.711(-.028)	.638(-.025)	.381(-.019)
1.13	.006	.040	.086	.115	.091	.024
1.08	.009	.023	.044	.054	.049	.027
1.0	.159	.094	.014	.008	.056	.124

Figure B14. Analog plot of low-pass filtered water levels (in meters, relative to NVGD29) from Station TG-9 (**Biscayne Channel - Marker 10**), June 12, 1997, to June 29, 1998. There are no breaks in this record, and the 9167 observations are continuous. Quarter-hourly water levels were sub-sampled to obtain a time series of hourly values, and hourly values were low-pass filtered to remove the rise and fall of the tide. As a result of the filtering process 63 hours are lost from both ends of each segment.

This record from the northern and more isolated part of Biscayne Bay shows the same seasonal cycle in sea level, but the pattern is significantly offset in the direction of higher water levels. The indicated mean water level at Station TG-9 is nearly 1.5 m higher than the means indicated at stations along the west side of Biscayne Bay. This calls into question the leveling and the datum used for the readings, but it does not affect the calculations of tidal amplitudes, nor the spectral analyses with wind data.

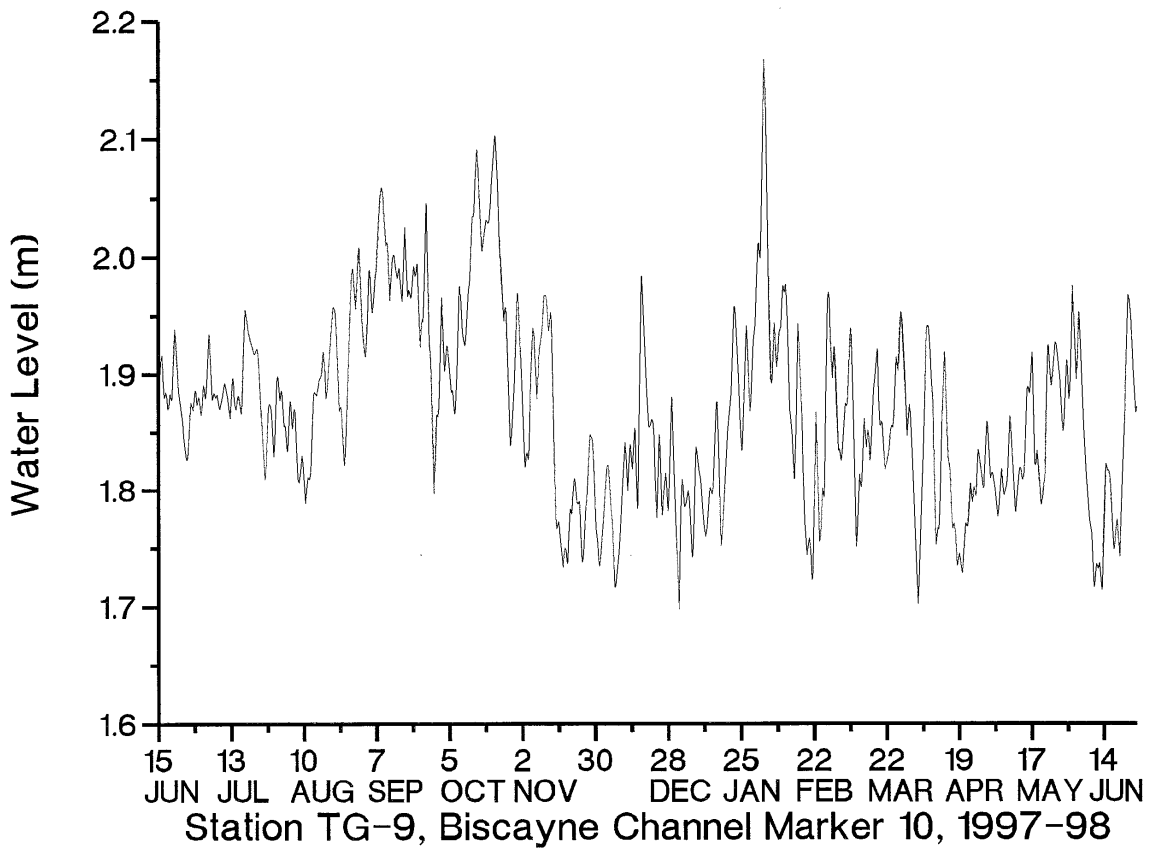


Table B10. Same as Table B1 except for Station TG-9, at the northern end of the Safety Valve and at the entrance to Biscayne Bay. The analysis covers the time period from June 12, 1997, to June 29, 1998 ($\beta_{05} = 0.250$, $\beta_{01} = 0.308$).

Significant coherence levels are relatively infrequent at this location. A band of highly significant coherences occurs at periodicities at and just over two days, and for all wind stress components. Few occurrence of significant coherence are found at the longest periodicities.

<u>Period (d)</u>	<u>000-180°</u>	<u>030-210°</u>	<u>060-240°</u>	<u>090-270°</u>	<u>120-300°</u>	<u>150-330°</u>
16	.121	.061	.056	.078	.103	.126
8	.284(.019)	.228	.161	.159	.178	.219
5.8	.323(.024)	.273(-.001)	.214	.224	.253(-.021)	.288(-.024)
4	.246	.269(.002)	.239	.210	.199	.210
3.2	.202	.165	.185	.217	.233	.231
2.7	.166	.188	.167	.133	.119	.133
2.3	.317(.017)	.342(.003)	.402(-.012)	.420(-.020)	.393(-.022)	.349(-.022)
2	.300(.016)	.294(-.002)	.434(-.021)	.517(-.028)	.489(-.027)	.400(-.024)
1.8	.166	.132	.224	.309(-.026)	.312(-.023)	.254(-.018)
1.6	.190	.140	.126	.151	.184	.206
1.5	.100	.026	.195	.298(-.015)	.311(-.015)	.251(-.016)
1.3	.017	.059	.183	.259(-.010)	.281(-.011)	.202
1.2	.032	.034	.171	.255(-.011)	.251(-.010)	.163
1.13	.067	.059	.054	.059	.070	.074
1.08	.071	.053	.089	.124	.132	.112
1.0	.067	.085	.055	.029	.024	.037

Figure B15. Analog plot of low-pass filtered water levels (in meters, relative to NVGD29) from Station TG-10 (**Miami River**), December 15, 1997, to June 25, 1998. This is an abbreviated record, but there are no breaks and the 4605 observations are continuous. Quarter-hourly water levels were sub-sampled to obtain a time series of hourly values, and hourly values were low-pass filtered to remove the rise and fall of the tide. As a result of the filtering process 63 hours are lost from both ends of each segment.

This approximately six-month time period misses the autumn high water level, but it includes the midwinter low water. The rise in water level starting in mid-April is interrupted in early June, and water levels drop back temporarily to midwinter levels.

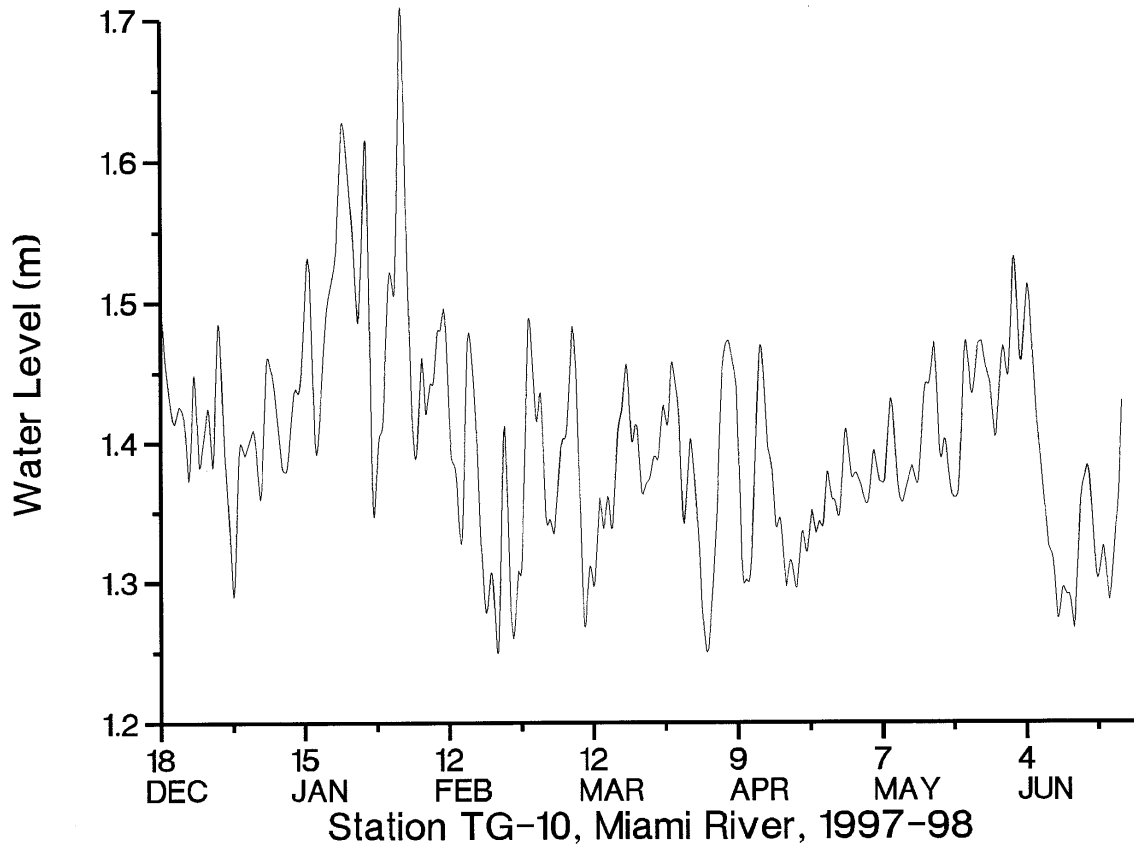


Table B11. Same as Table B1 except for Station TG-10 in northern Biscayne Bay. The analysis covers the time period from December 15, 1997, to June 25, 1998 ($\beta_{05} = 0.353$, $\beta_{01} = 0.430$).

Significant coherences are scattered irregularly through the table, though most occur in the 2-6 day band and for winds out of the easterly quadrant. A second region of high coherence occurs over periodicities on the order of 1-1.5 days, but for the same wind components.

<u>Period (d)</u>	<u>000-180°</u>	<u>030-210°</u>	<u>060-240°</u>	<u>090-270°</u>	<u>120-300°</u>	<u>150-330°</u>
16	.157	.138	.341	.389(-.027)	.360(-.023)	.286
8	.191	.236	.348	.337	.278	.234
5.8	.325	.311	.366(-.015)	.403(-.026)	.396(-.028)	.366(-.028)
4	.550(.040)	.474(.014)	.506(-.012)	.563(-.023)	.602(-.030)	.609(-.038)
3.2	.399(.026)	.436(.018)	.420(.002)	.390(-.007)	.370(-.014)	.369(-.021)
2.7	.283	.246	.152	.117	.138	.205
2.3	.433(.042)	.418(.018)	.374(-.009)	.364(0.019)	.373(-.026)	.398(-.035)
2	.109	.295	.278	.193	.129	.117
1.8	.008	.031	.037	.024	.010	.001
1.6	.136	.086	.018	.009	.043	.099
1.5	.088	.171	.329	.343	.305	.222
1.3	.193	.244	.441(-.014)	.490(-.017)	.435(-.018)	.322
1.2	.368(.017)	.170	.230	.408(-.016)	.510(-.018)	.500(-.019)
1.13	.226	.060	.122	.402(-.062)	.531(-.066)	.430(-.056)
1.08	.183	.031	.152	.316	.357(-.076)	.313
1.0	.093	.137	.094	.050	.036	.048

Figure B16. Analog plot of low-pass filtered water levels (in meters, relative to NVGD29) from Station TG-11 (**Julia Tuttle Causeway - Marker 35**) August 1, 1997, to June 30, 1998. Due to breaks in the record, the plot is in two parts: August 1 to December 3, 1997 (2974 observations) and January 27 to June 30, 1998 (3707 observations). Quarter-hourly water levels were sub-sampled to obtain a time series of hourly values, and hourly values were low-pass filtered to remove the rise and fall of the tide. As a result of the filtering process 63 hours are lost from both ends of each segment.

The midwinter low water levels are missing from this plot, due to the gap during December and January, but an irregular fall maximum is apparent. The record begins again shortly before the transient high water in early February, then water level remains variable but low through the end of the record.

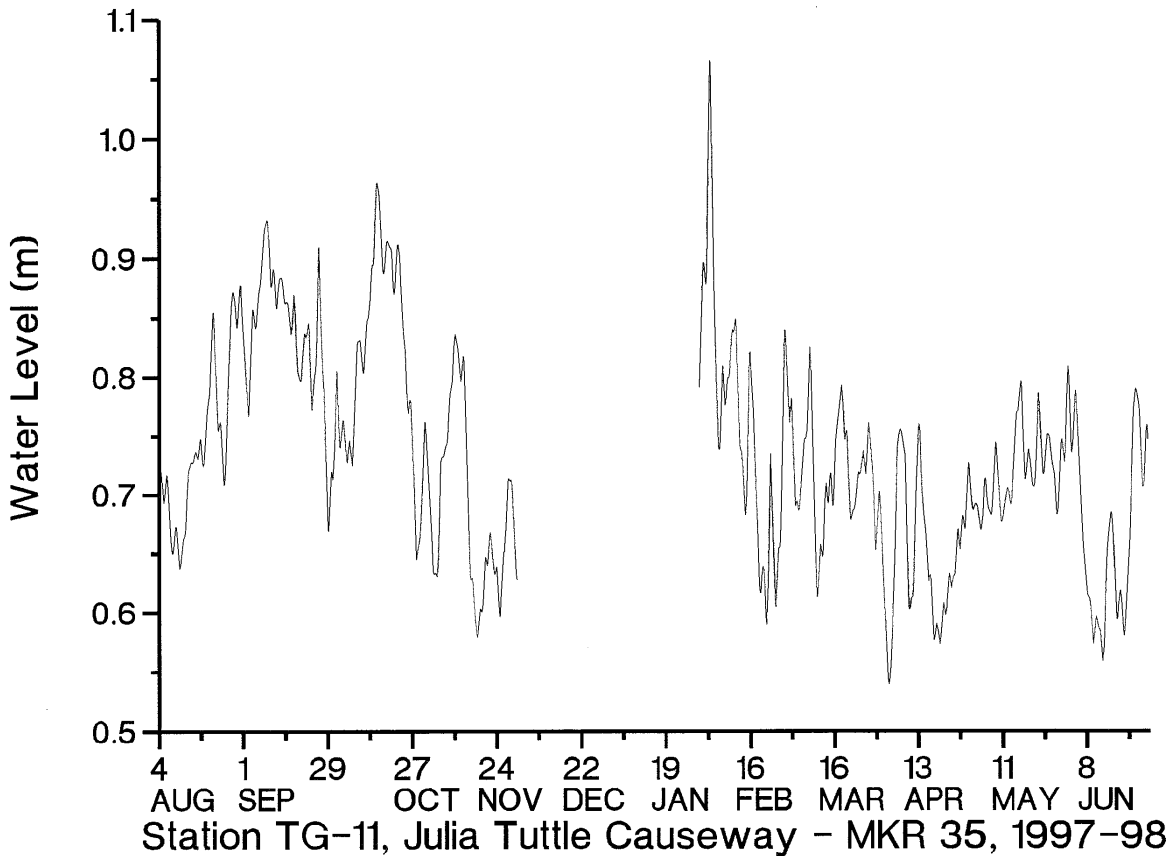


Table B12. Same as Table B1 except for Station TG-11 in northern Biscayne Bay. The spectral analysis covers the abbreviated time period from January 27 to June 29, 1998 ($\beta_{05} = 0.395$, $\beta_{01} = 0.479$).

Statistically significant coherences are clustered relatively tightly at periodicities of just over one day, then again at periodicities greater than about three days. In both cases, however, there is little indication of a preference for a specific range of wind components. In most cases, the gain is negative, indicating that northward and eastward wind stress will set down water levels in the Bay. The positive gains found for the 000-180° components, however, indicate that northward wind stress will have the local effect of forcing water into the northern part of the Bay and raising water levels.

<u>Period (d)</u>	<u>000-180°</u>	<u>030-210°</u>	<u>060-240°</u>	<u>090-270°</u>	<u>120-300°</u>	<u>150-330°</u>
16	.353	.167	.280	.395(-.027)	.459(-.029)	.471(-.033)
8	.689(.039)	.475(-.009)	.533(-.031)	.638(-.033)	.719(-.036)	.767(-.042)
5.8	.589(.030)	.726(-.012)	.742(-.027)	.699(-.027)	.650(-.028)	.599(-.033)
4	.731(.046)	.606(-.003)	.582(-.011)	.589(-.013)	.607(-.017)	.648(-.028)
3.2	.571(.027)	.422(.005)	.491(-.007)	.573(-.011)	.637(-.015)	.673(-.022)
2.7	.371	.135	.220	.344	.439(-.013)	.492(-.017)
2.3	.301	.220	.134	.146	.199	.263
2	.054	.237	.291	.195	.086	.016
1.8	.206	.168	.117	.070	.021	.046
1.6	.062	.012	.058	.120	.185	.205
1.5	.125	.529(-.020)	.618(-.015)	.613(-.014)	.546(-.015)	.306
1.3	.145	.515(-.019)	.635(-.014)	.675(-.013)	.670(-.014)	.510(-.015)
1.2	.011	.354	.564(-.009)	.639(-.010)	.618(-.011)	.374
1.13	.017	.100	.231	.299	.265	.119
1.08	.010	.004	.001	.003	.010	.130
1.0	.121	.045	.015	.080	.130	.146

Figure B17. Analog plot of low-pass filtered water levels (in meters, relative to NVGD29) from Station TG-12 (**Broad Causeway - Marker 13**), June 18, 1997, to June 25, 1998. There were no breaks in the record, and the 8926 observations are continuous. Quarter-hourly water levels were sub-sampled to obtain a time series of hourly values, and hourly values were low-pass filtered to remove the rise and fall of the tide. As a result of the filtering process 63 hours are lost from both ends of each segment.

This northernmost study site produced an annual cycle in sea level that was unlike that found elsewhere during this field study. The fall maximum is subtle, and the winter minimum is short-lived, with late-winter water levels as high as those found in September and October. A very unusual feature of the plot is the sharp rise in water level during the final month of the study, with the highest water levels recorded at the end of the record.

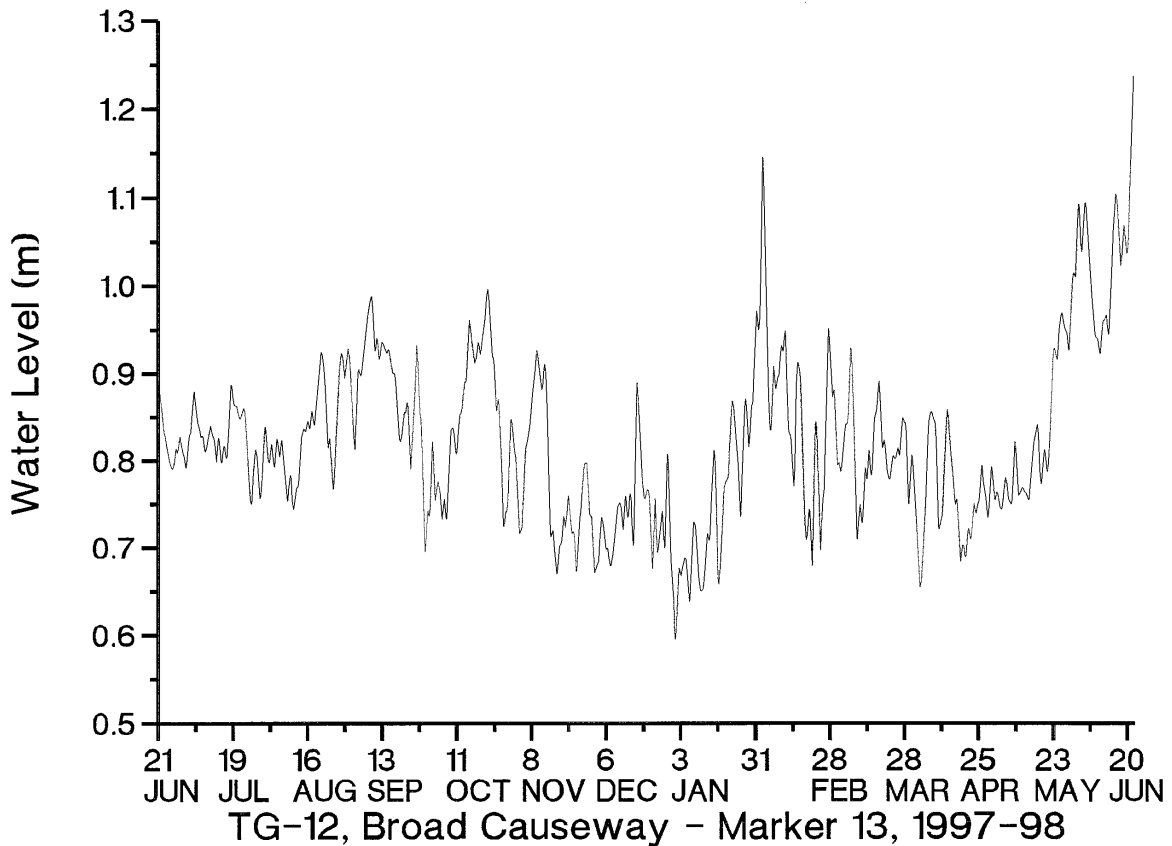


Table B13. Same as Table B1 except for Station TG-12 in northern Biscayne Bay. Study period spans June 18, 1997, to June 25, 1998 ($\beta_{05} = 0.254$, $\beta_{01} = 0.312$).

The pattern of highest coherences is relatively easily summarized, occurring over periodicities of between about 2 and 8 days and for all wind stress components. A second region of high coherence was found for southeasterly winds at periodicities of just over one day.

<u>Period (d)</u>	<u>000-180°</u>	<u>030-210°</u>	<u>060-240°</u>	<u>090-270°</u>	<u>120-300°</u>	<u>150-330°</u>
16	.176	.100	.095	.125	.163	.197
8	.489(.030)	.279(.004)	.223	.310(-.026)	.438(-.032)	.541(-.037)
5.8	.511(.038)	.575(.013)	.502(-.013)	.440(-.021)	.415(-.027)	.429(-.034)
4	.483(.042)	.422(.013)	.382(-.005)	.380(-.010)	.394(-.016)	.428(-.027)
3.2	.497(.035)	.327(.017)	.321(.0001)	.380(-.007)	.450(-.013)	.520(-.024)
2.7	.524(.028)	.301(.014)	.257(-.001)	.322(-.007)	.413(-.012)	.517(-.020)
2.3	.450(.033)	.345(.015)	.251	.257(-.013)	.306(-.019)	.385(-.027)
2	.163	.171	.133	.098	.098	.126
1.8	.044	.024	.019	.026	.046	.062
1.6	.043	.030	.018	.013	.020	.038
1.5	.013	.069	.151	.194	.207	.149
1.3	.033	.177	.320(-.004)	.393(-.006)	.412(-.008)	.291(-.012)
1.2	.161	.119	.172	.224	.269(-.007)	.280(-.013)
1.13	.130	.043	.093	.190	.263(-.029)	.255(-.038)
1.08	.021	.010	.016	.033	.043	.038
1.0	.202	.118	.009	.025	.097	.171

Table B14. Harmonic constants (amplitudes / local phase angles) of the principal tidal constituents at each of the twelve water level stations. Amplitudes are in meters; local phase angles are in degrees.

Station	Tidal Constituent				
	M ₂	S ₂	N ₂	K ₁	O ₁
TG-1	0.061 / 019	0.009 / 029	0.010 / 360	0.011 / 287	0.009 / 315
TG-2	0.083 / 330	0.016 / 353	0.015 / 311	0.013 / 257	0.010 / 276
TG-3	0.101 / 308	0.016 / 342	0.018 / 291	0.016 / 246	0.013 / 260
TG-4	0.217 / 287	0.035 / 335	0.041 / 270	0.028 / 229	0.021 / 239
TG-5	0.193 / 293	0.034 / 324	0.039 / 275	0.021 / 217	0.015 / 234
TG-6	0.220 / 284	0.035 / 321	0.041 / 266	0.024 / 216	0.021 / 233
TG-7	0.260 / 260	0.041 / 295	0.050 / 239	0.029 / 195	0.026 / 218
TG-8	0.274 / 251	0.048 / 283	0.055 / 232	0.029 / 192	0.025 / 210
TG-9	0.297 / 232	0.053 / 260	0.063 / 210	0.032 / 175	0.028 / 195
TG-10	0.311 / 236	0.049 / 264	0.065 / 216	0.034 / 180	0.031 / 198
TG-11	0.308 / 249	0.049 / 283	0.063 / 230	0.035 / 185	0.031 / 208
TG-12	0.296 / 259	0.046 / 297	0.057 / 243	0.032 / 189	0.028 / 210

Figure B18. Map showing the locations of the 38 study sites from which water level records were available to characterize tidal conditions. Water level records that were between one synodic month (29 days) and one year in length were used to calculate amplitudes and local phase angles in degrees. The study sites include 24 NOS sites occupied in the early 1970s, one Harbor Branch site occupied in 1998, one South Florida Water Management District site occupied in 1996, and 12 WES study sites from the 1997-98 field study.

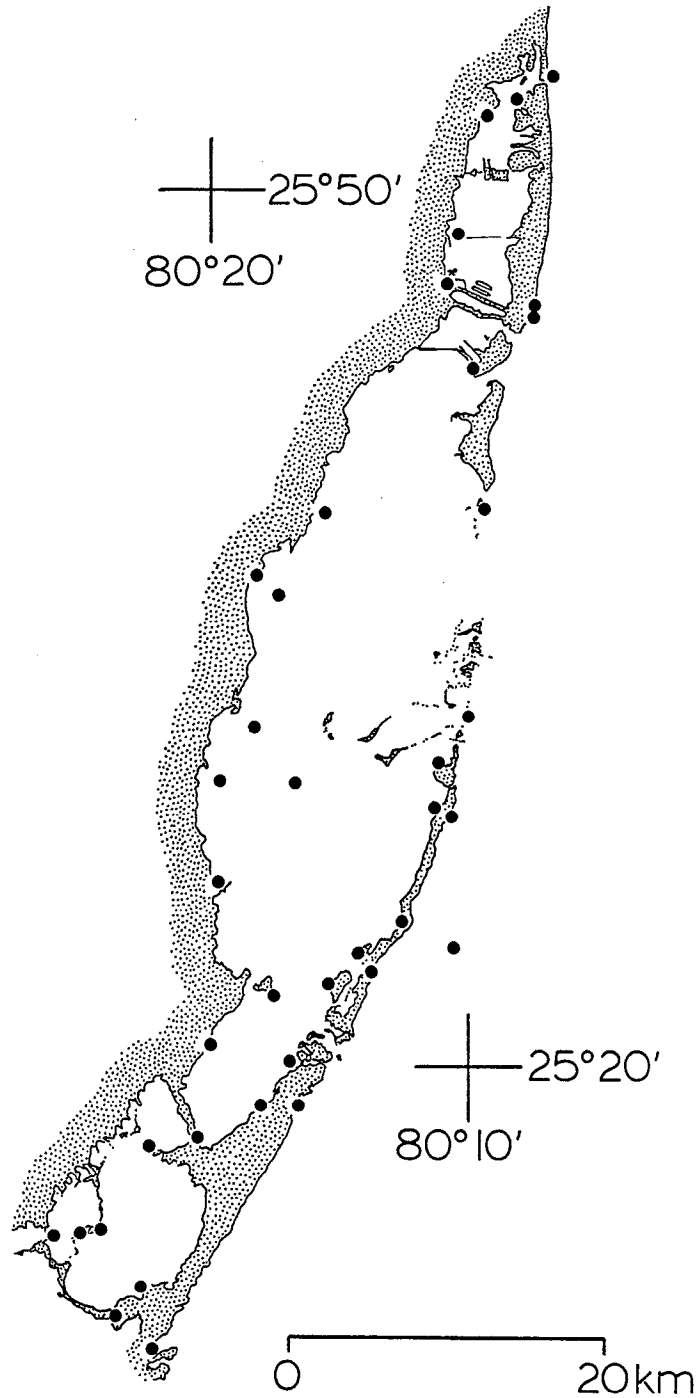


Figure B19. Co-amplitude chart for the M_2 tidal constituent. Amplitudes, in centimeters, are half of the tidal range. M_2 amplitudes are approximately 30 cm in shelf waters and in the northern part of Biscayne Bay. In central Biscayne Bay, amplitudes decrease only slightly, because of the relatively free exchange of water through the Safety Valve. Tidal amplitudes decrease rapidly from north to south in southern Biscayne Bay as tidal waves move over Cutter Bank into Card Sound. Tidal amplitudes in Card Sound and Barnes Sound are approximately 5 cm.

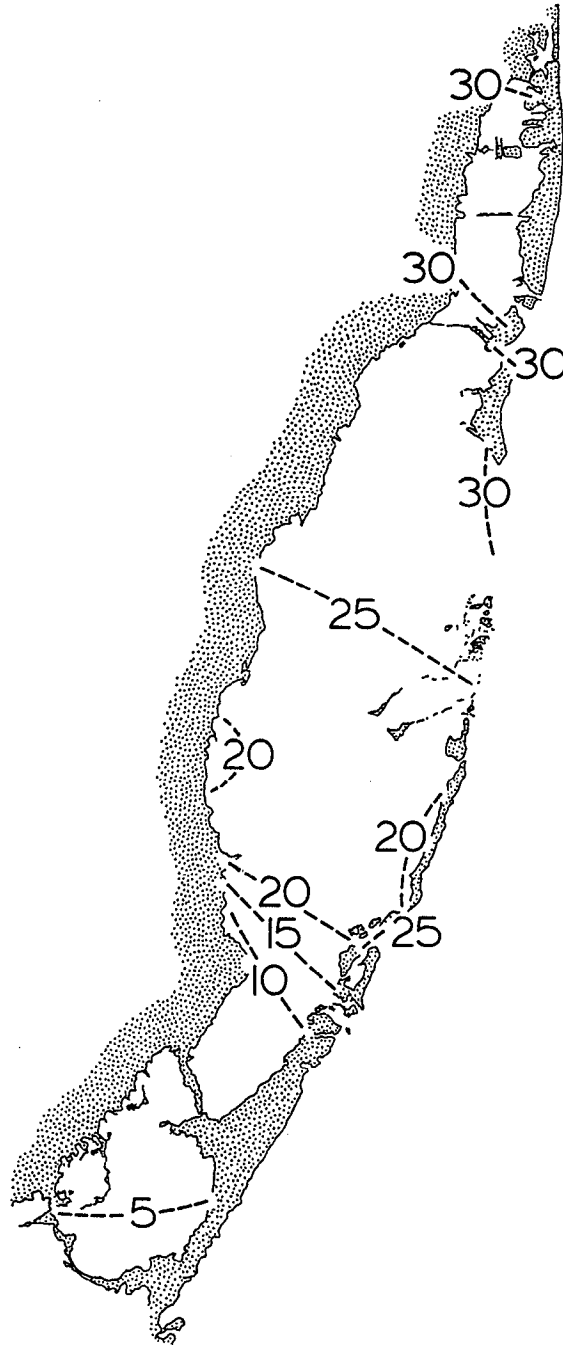


Figure B20. Co-phase chart for the M_2 tidal constituent. Phase angles, in degrees, have been contoured at intervals of 30° because a 30° difference in phase corresponds very closely to a one-hour difference in time. High water along the 260° co-phase line, for example, will have moved to the position of the 290° co-phase line one hour later. Phase differences of less than 30° show that M_2 tidal waves move from the inner shelf into the central and northern part of Biscayne Bay within one hour. The continued movement of the M_2 wave southward through Card Sound and into Barnes Sound is considerably slower as a result of the shallower water. The M_2 wave arrives at the southern end of Barnes Sound and enters Manatee Bay about six hours after entering through the Safety Valve or any of the smaller creeks that connect southern Biscayne Bay or Card Sound with inner shelf waters. The difference in phase angles between shelf waters and southern Barnes Sound is approximately 150° , indicating that high tide in shelf waters occurs within an hour of low tide in southern Barnes Sound, and *vice versa*.

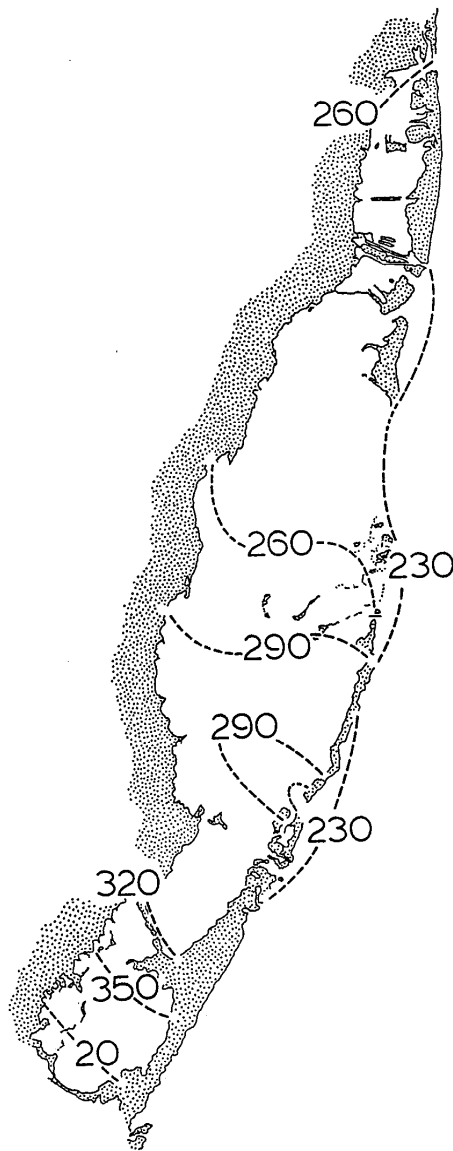


Figure B21. Co-amplitude chart for the S_2 tidal constituent. The interaction of the M_2 and S_2 constituents explains the fortnightly variation in the amplitude of the semidiurnal tide resulting from the relative positions of the sun and moon (i.e., the phase of the moon). Amplitudes of the S_2 constituent are spatially quite uniform at about 5 cm throughout the northern part of Biscayne Bay. Amplitudes decrease from north to south, especially as the tidal waves cross the shallow waters that separate Biscayne Bay and Card Sound. Amplitudes in the southernmost part of the Bay system are on the order of 1 cm.

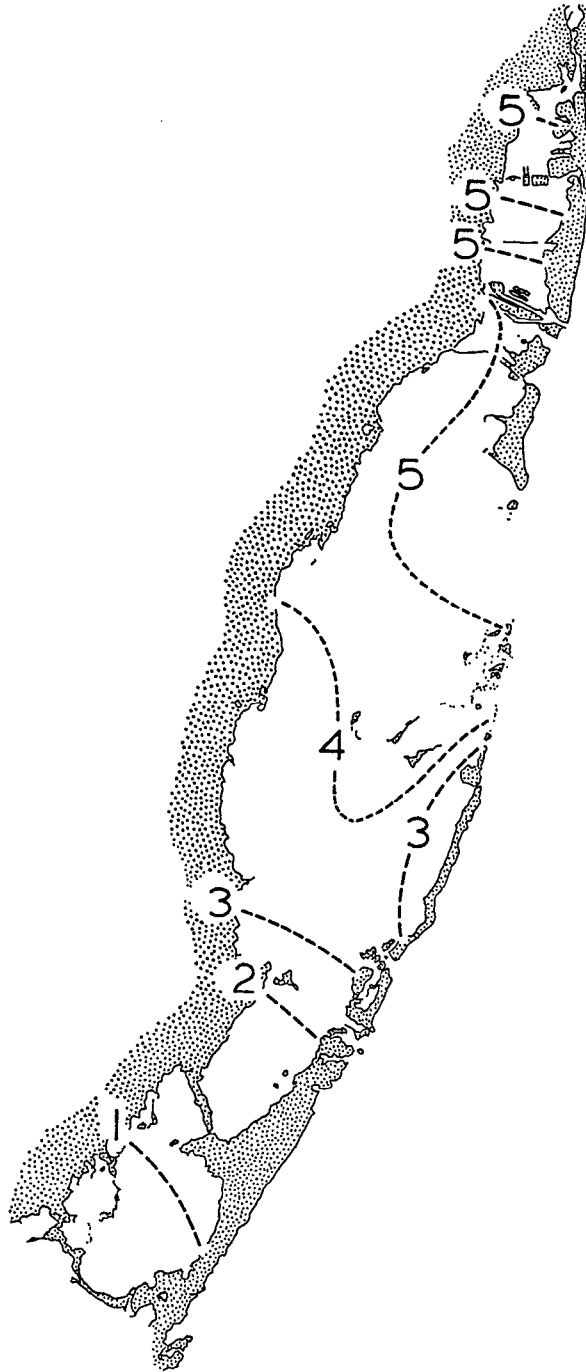


Figure B22. Co-phase chart for the S_2 tidal constituent. Phase differences are relatively small in the northern part of Biscayne Bay, indicating that the S_2 constituent reaches its high tide and low tide levels nearly simultaneously in this area. The 300 and 330° phase angles protruding into Card Sound are the effect of S_2 waves moving in through Angelfish Creek, Broad Creek, and Caesar Creek.

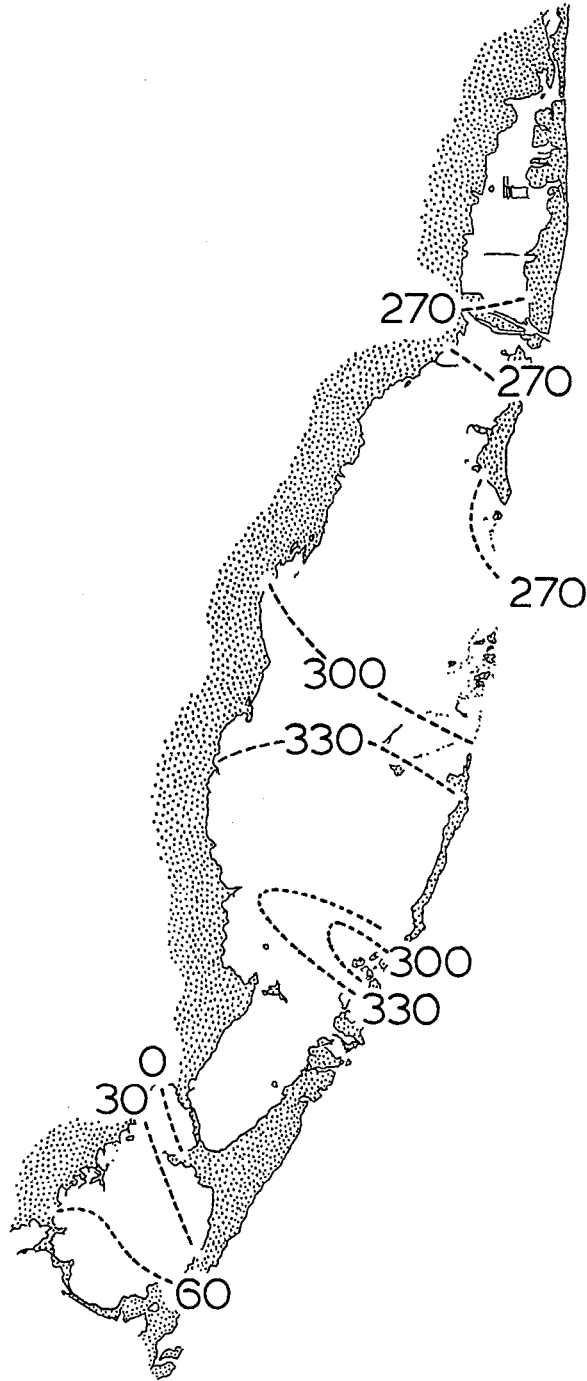


Figure B23. Co-amplitude chart for the N_2 tidal constituent. The combination of the M_2 and the N_2 constituents explains the monthly variation in the amplitude of the semidiurnal tide resulting from changes in the distance from the earth to the moon (apogee and perigee). The N_2 constituent is the second most important in the Biscayne Bay lagoon system. N_2 amplitudes are approximately 8 cm in shelf waters, and amplitudes decrease only slightly to 7 cm in northern Biscayne Bay. Amplitudes are relatively uniform at 5-6 cm in central Biscayne Bay, then decrease quickly as the N_2 waves move southward over Cutter Bank into Card Sound. Amplitudes in Barnes Sound and Manatee Bay are approximately 1 cm.

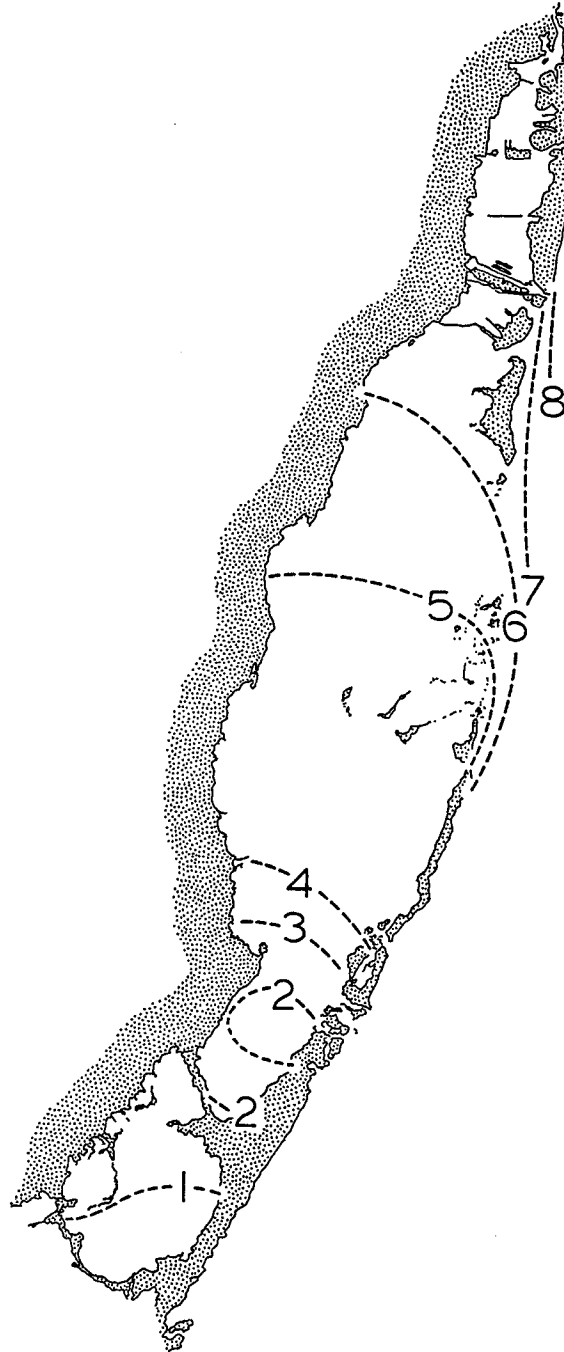


Figure B24. Co-phase chart for the N_2 tidal constituent. Phase angles are delayed by 30° or less throughout much of northern Biscayne Bay, indicating that the N_2 high and low tides occur within approximately one hour of each other throughout this part of the Bay. Tidal waves enter Card Sound and southern Biscayne Bay also through Angelfish Creek, Broad Creek, and Caesar Creek. The approximately 14-nautical-mile separation of the 270° and 300° phase angles in southern Biscayne Bay and southern Card Sound, respectively, suggest that the N_2 wave moves southward at a speed of approximately 26 km h^{-1} (14 knots).

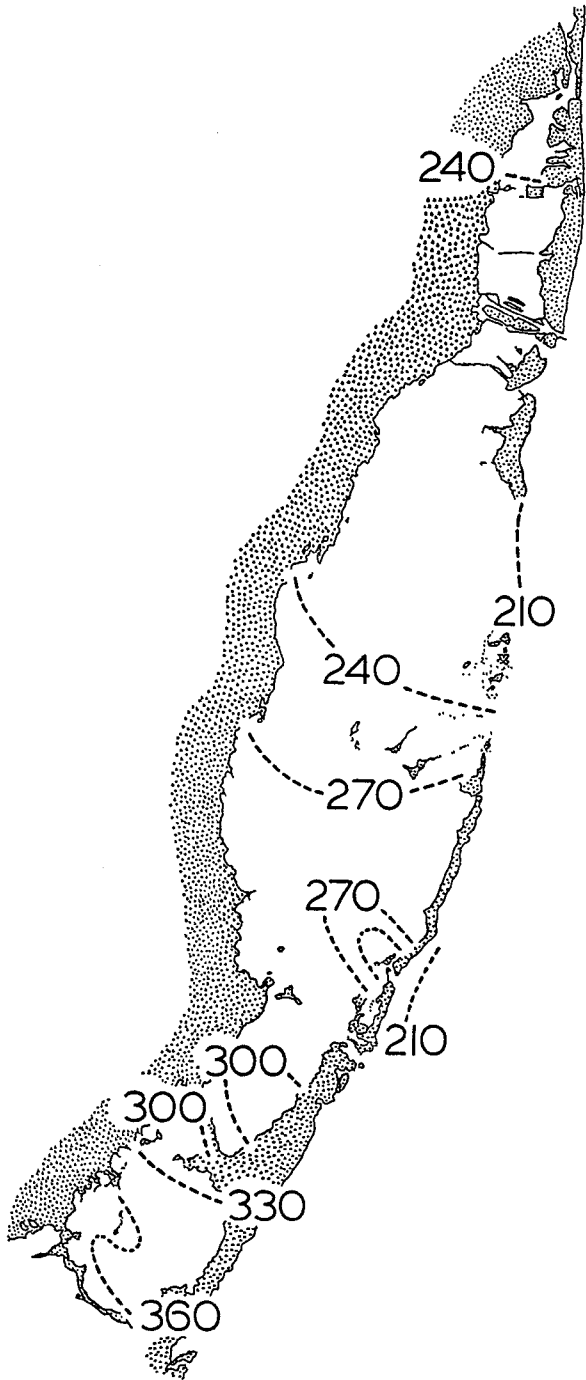


Figure B25. Co-amplitude chart for the K_1 tidal constituent. The pattern is a relatively simple one, because this tidal constituent is quite small everywhere throughout the Biscayne Bay system. K_1 amplitudes are at or just above 3 cm throughout northern Biscayne Bay and at or just below 2 cm throughout central Biscayne Bay, Card Sound, Barnes Sound, and Manatee Bay.

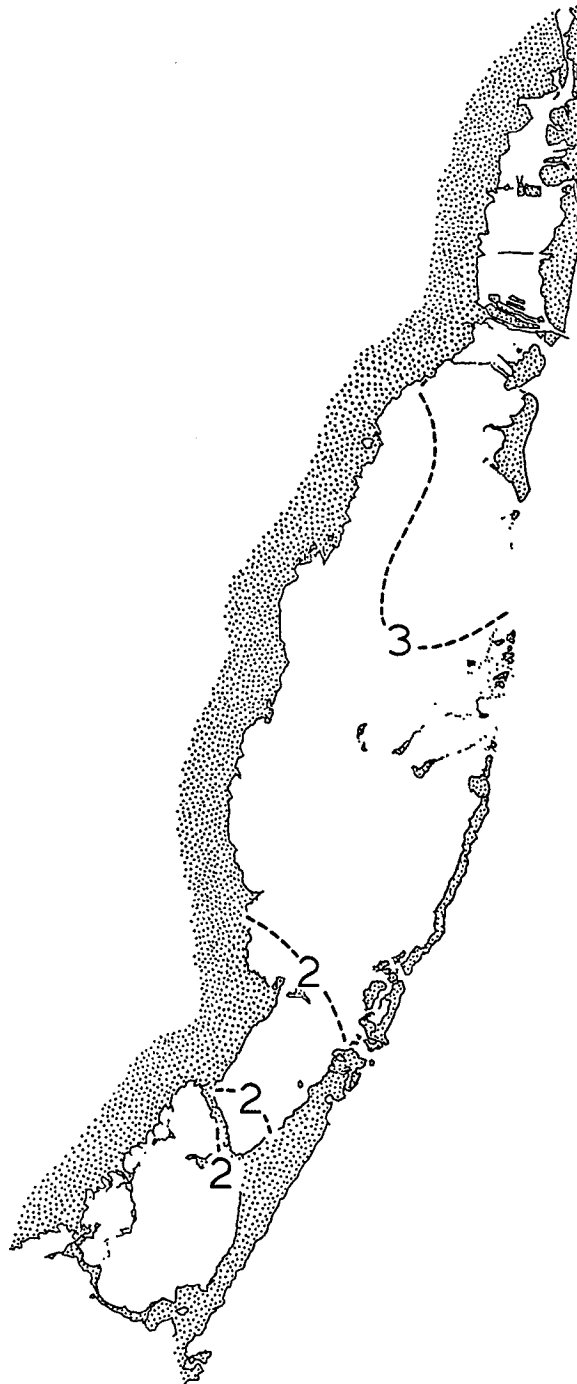


Figure B26. Co-phase chart for the K_1 tidal constituent. In contrast to the K_1 amplitudes, the co-phase chart is relatively complex because the tidal waves move slowly southward from one bay to the next. Phase angles are all in the vicinity of 180° in the northern part of Biscayne Bay, indicating that the N_2 waves reach their high and low tide conditions nearly simultaneously. Because of the slow movement of the tidal waves, especially in Barnes Sound, K_1 waves at the southern end of the bays are very nearly out of phase with those over the inner shelf.

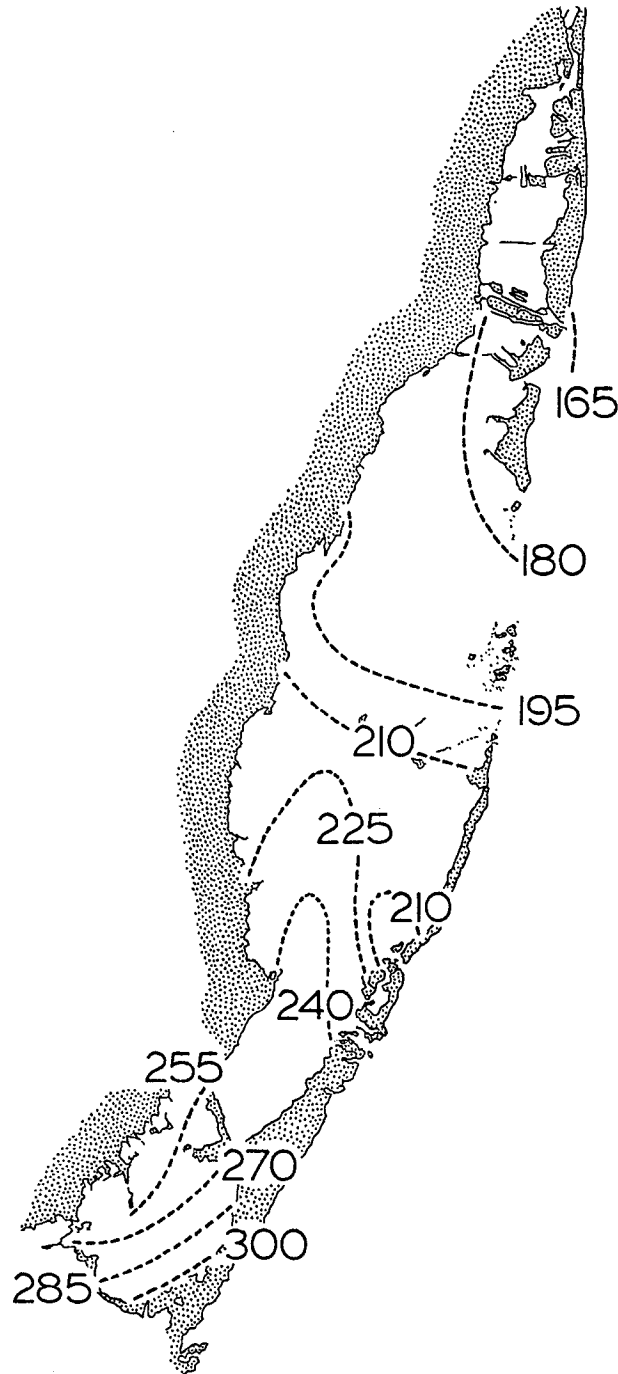


Figure B27. Co-amplitude chart for the O_1 tidal constituent. Amplitudes throughout the central part of Biscayne Bay are all between 2 and 3 cm. Values in the northern part are slightly higher, at or just above 3 cm. Because of the shallow water in Card Sound, Barnes Sound, and Manatee Bay, O_1 waves decrease slightly to amplitudes of about 1 cm.

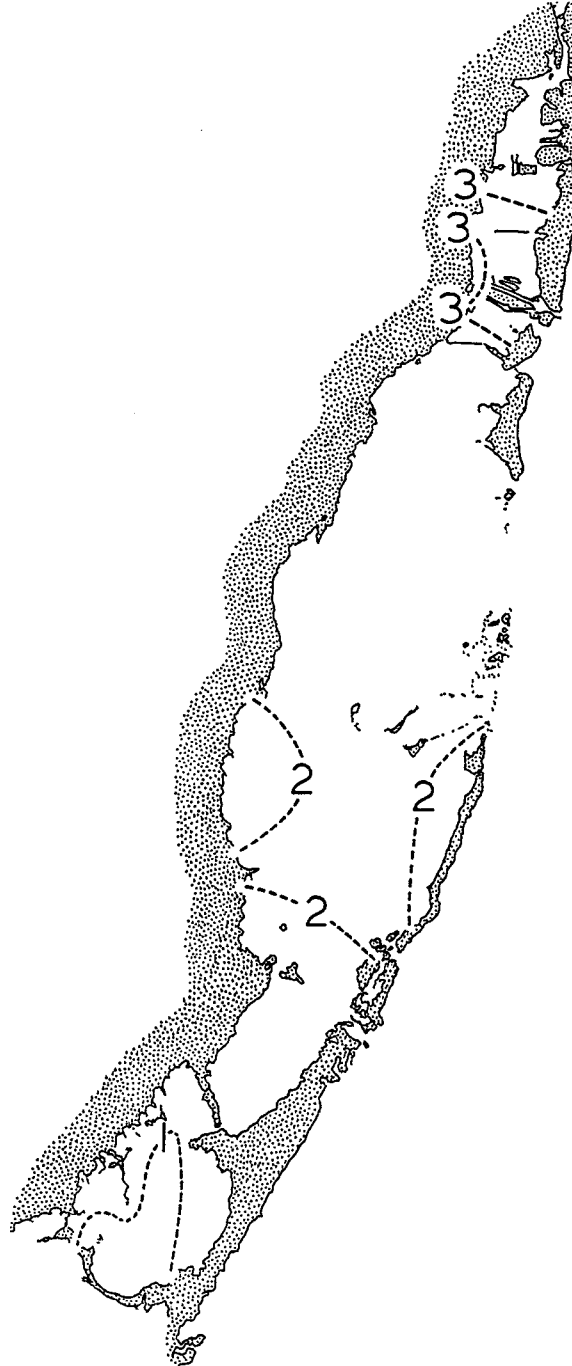


Figure B28. Co-phase chart for the O_1 tidal constituent. This is one of the most complex patterns found for the principal tidal constituents in the Biscayne Bay system. Again, however, phase angles differ only slightly in the northern part of Biscayne Bay, indicating that the O_1 constituent reaches its high and low tide condition nearly simultaneously throughout this area. Isopleths in the southern Biscayne Bay, Card Sound, and, especially, Barnes Sound and Manatee Bay indicate a slowly southward moving O_1 wave that is interacting with the wave moving in through Angelfish Creek, Broad Creek, and Caesar Creek.

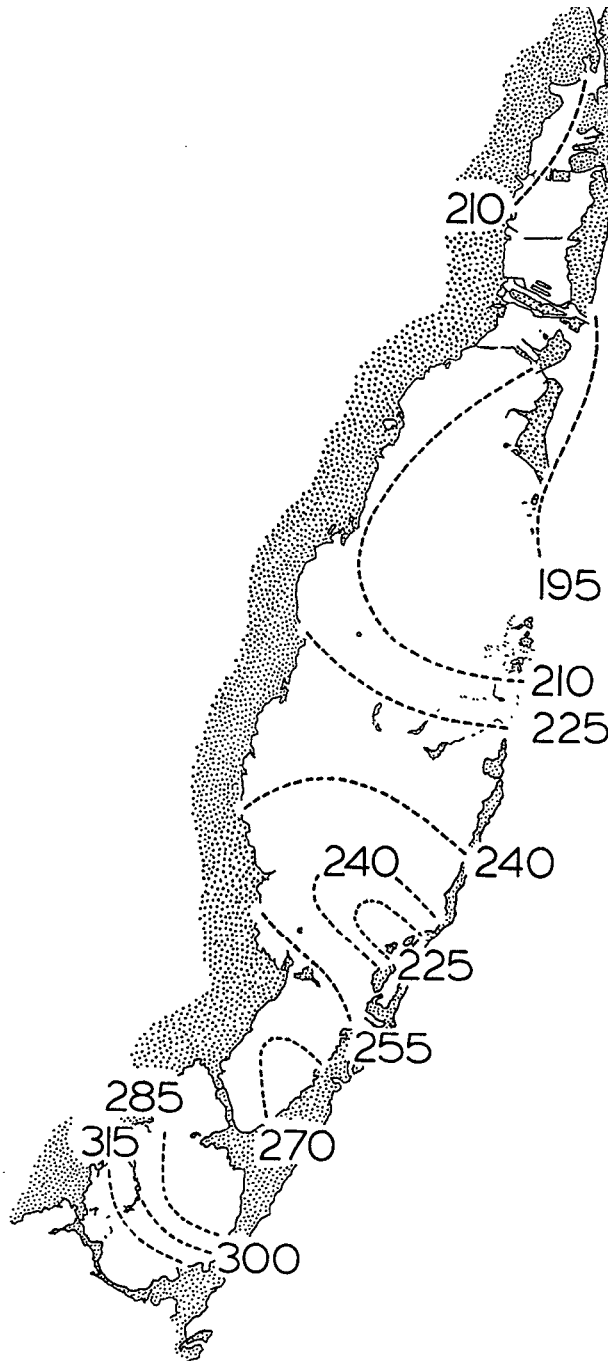
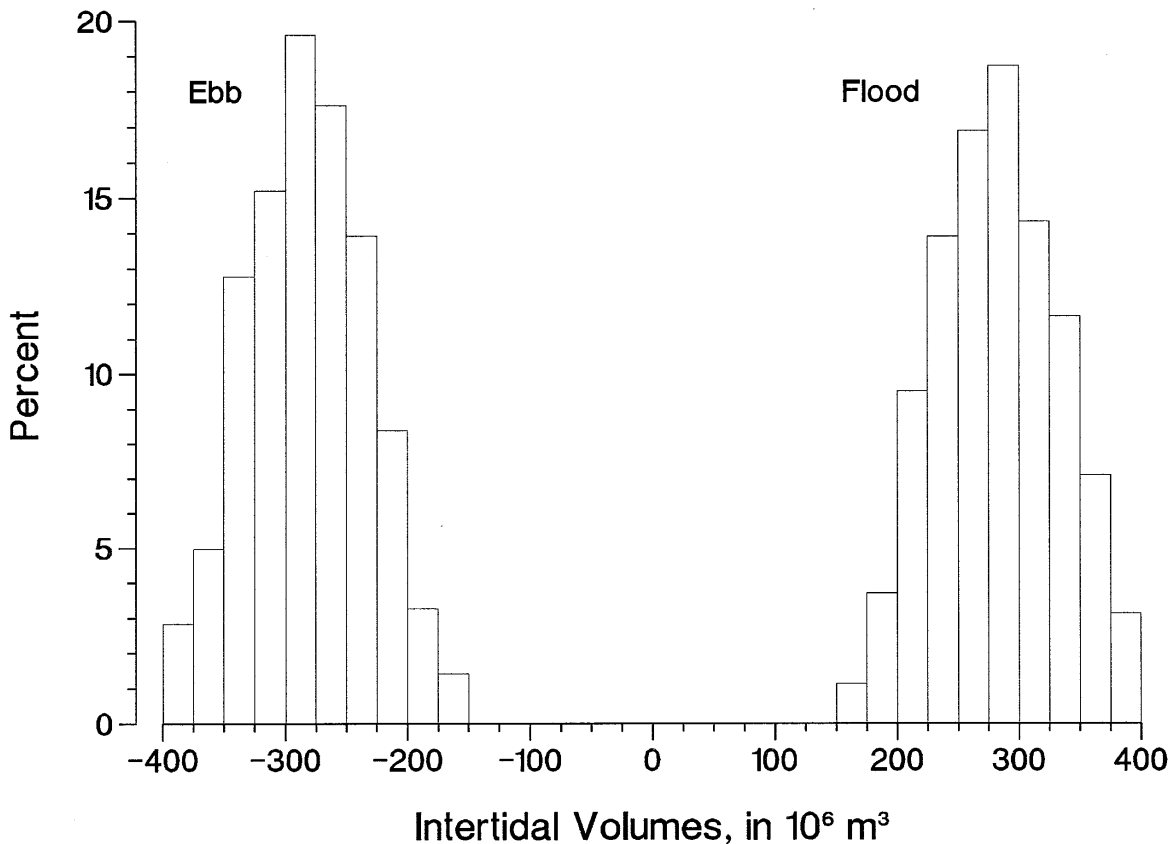


Figure B29. Histograms showing volumes of water, in millions of cubic meters, entering and leaving Biscayne Bay, Card Sound, Little Card Sound, Barnes Sound, and Manatee Bay during the flood and ebb tide cycles. Histograms are based on tidal predictions over a one-year time period. Results are for diurnal and semidiurnal tidal exchanges only. Not included are the long-period tidal constituents, shallow-water (short-period) tidal constituents, and effects of nontidal processes such as winds, rainfall, evaporation, and freshwater runoff. Bin width is $25 \times 10^6 \text{ m}^3$.

Both histograms are characterized by well-defined peaks with frequencies of 18-19% for intertidal volumes between 275 and $300 \times 10^6 \text{ m}^3$. Intertidal volumes of between 200 and $350 \times 10^6 \text{ m}^3$ occur with 85% of the floods and 87% of the ebbs. Extremes, representing neap and spring tide conditions, are in the 150 - 175 and 375 - $400 \times 10^6 \text{ m}^3$ bins, respectively. Harmonic analysis of a one-year simulation of intertidal volumes indicates that the amplitude of the M_2 constituent is $134.2 \times 10^6 \text{ m}^3$. The mean flood and ebb intertidal volumes in the Biscayne Bay System of coastal lagoons are twice the M_2 amplitude, or $268.4 \times 10^6 \text{ m}^3$. The S_2 and N_2 constituents have amplitudes of 24.3 and $26.8 \times 10^6 \text{ m}^3$, and the K_1 and O_1 constituents have amplitudes of 12.8 and $13.8 \times 10^6 \text{ m}^3$, respectively. It is the interaction of these five tidal constituents that produces the neap and spring tide differences and determines the width of the histograms.



c. Acoustic Doppler Profiler Data

It is difficult to form generalizations regarding circulation patterns from the five ADP records. They are all influenced by local topographic features, and thus they are less spatially representative than are the water level records. Also, the ADP time series were the most fragmented. Station ADP-5, for example, was broken into six segments, the longest of which was only 116 days long. Station ADP-4 produced only three short records and the pressure sensor malfunctioned, degrading calculations of both transport and vertically-integrated current speed. Data from Stations ADP-1, 2, and 3 produced long records, but data from every location can be used in some form for model verification purposes, even if they cannot be used in every case to characterize local flow conditions.

Taken together, data suggest a complex net flow pattern for this system of coastal bays. Data from Station ADP-1, though probably influenced significantly by the local effects of exchanges through Angelfish Creek, suggest a south-to-north movement of water along the East Side of Card Sound. Without additional information from elsewhere in Card Sound, however, it cannot be determined whether the observed northward flow represents a movement of water from Card Sound into southern Biscayne Bay or a more localized rotary flow that is contained within Card Sound.

Data from Stations ADP-2 and -3 cover a similar time period, and both study sites are from more open regions of Biscayne Bay. Many features of these two plots, notably the distinct change of direction in early October (see the Fowey Rocks wind stress plot), are very similar in form and timing. Both records indicate relatively little net transport during the few weeks before and after early November. From these two records, the general pattern suggests a transport of water into the northwestern part of Biscayne Bay. It is not clear how water is leaving the landward side of the Bay.

Data from Station ADP-4 included only a small amount of information on water level. The pressure sensor drifted and produced little usable data. Thus, the displacement of water past the study site (i.e., the current speed) must be used to infer transport. Results can be used for model verification, but they are of marginal use for describing the general flow patterns of the Bay.

Data from Station ADP-5 are limited to two segments of 3-4 months in length, but these two records are highly similar in appearance. Flow patterns are clearly constrained by local topographic features (shorelines or channels), but both patterns indicate a relatively steady flow toward the northeast—out of northern Biscayne Bay.

Figure B30. Acoustic Doppler Profiler data from Station ADP-1 in northern Card Sound near the mouth of Angelfish Creek. A single continuous record is available from December 21, 1997, to July 12, 1998. Shown here are vertically averaged north-south (top) and east-west (bottom) current components. Results show maximum speeds for these two components of approximately $\pm 20 \text{ cm s}^{-1}$. Low-frequency fluctuations are more apparent in the north-south component, because tidal fluctuations are smaller. The larger fluctuations in the east-west component of the current are the direct results of exchanges through Angelfish Creek, just east of the study site.

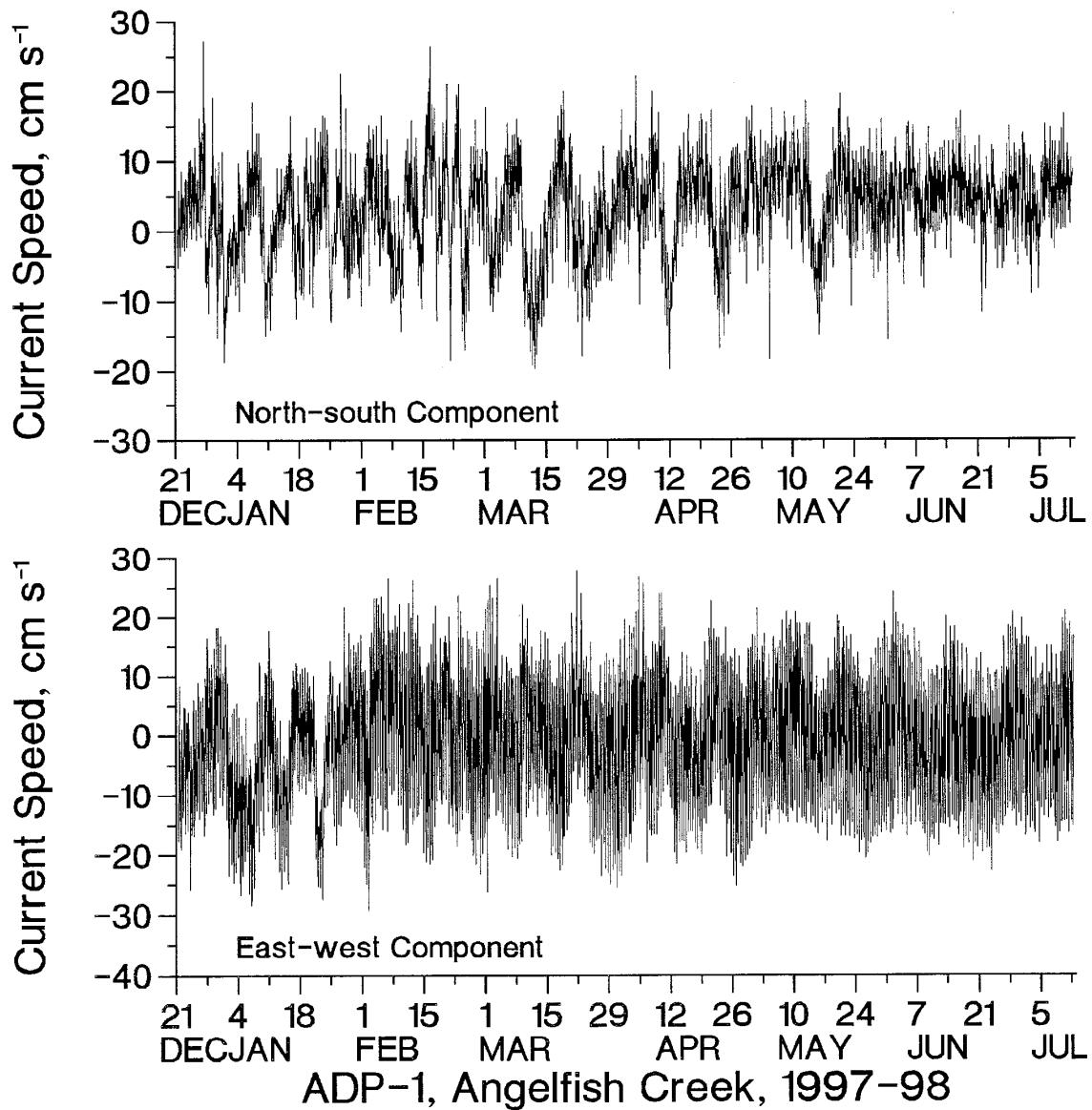


Figure B31. Cumulative net transport diagram constructed from data recorded at Station ADP-1, in northeastern Card Sound near the mouth of Angelfish Creek. Shown here are the data from December 21, 1997, to July 12, 1998. Dots have been entered at the beginning of the first day of each month.

The plot shows a two-part pattern. The first part is an approximately one-month period at the start of the record when the net transport is westward. This suggests a strong inflow through Angelfish Creek. Many tidal cycles are missing a well-defined ebb. The second part, starting in February, consists of a net northward transport that continues through the end of the record. Direct effects of exchanges through Angelfish Creek are apparent only in the form of the east-west flood and ebb of the tide. Wind stress data from Fowey Rocks (Figures B2 and B3) do not indicate a clear seasonal change in wind direction coinciding with the transition from westward to northward transport at Station ADP-1.

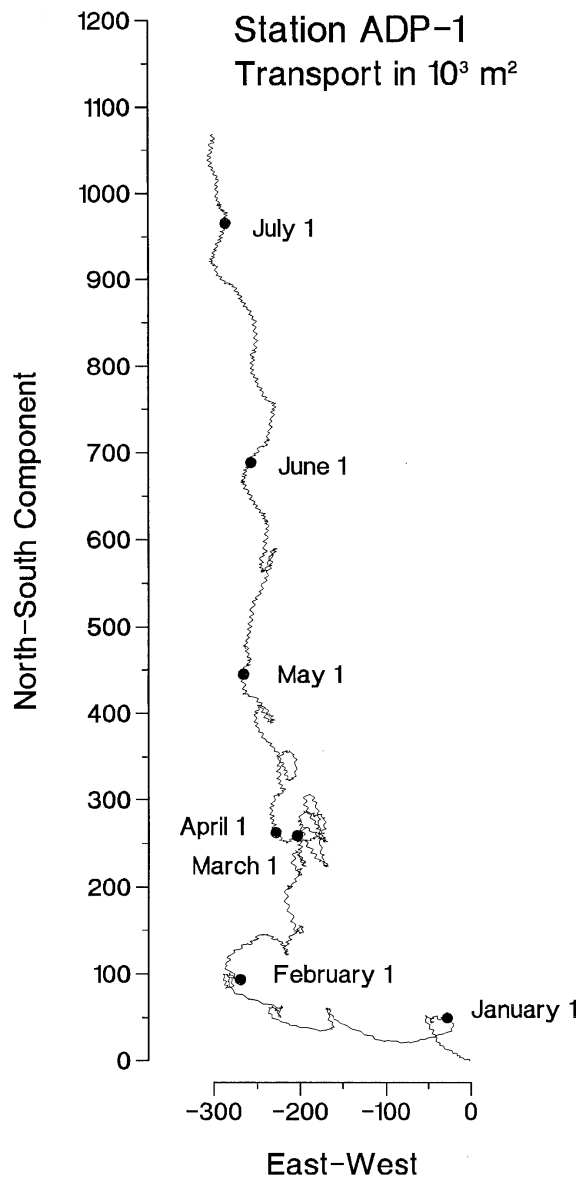


Figure B32. Acoustic Doppler Profiler data from Station ADP-2, in south-central Biscayne Bay. Data are available from three time periods during the June 27, 1997, to June 10, 1998, study. Shown here are vertically averaged north-south (top) and east-west (bottom) current components. The middle and final data segments are too short for a spectral analysis, but the first segment was suitable for analysis of tidal conditions, and for a comparison with Fowey Rocks weather data to quantify the response to wind forcing.

An interesting feature of the north-south component currents is the enhancement of low-frequency variations in the latter part of the record. It is likely that this is because relatively steady shoreward winds during summer months are interrupted by cold-air outbreaks during winter months. The east-west component of the current suggests that low-frequency fluctuations are less seasonal, with variations in shoreward winds occurring throughout the year.

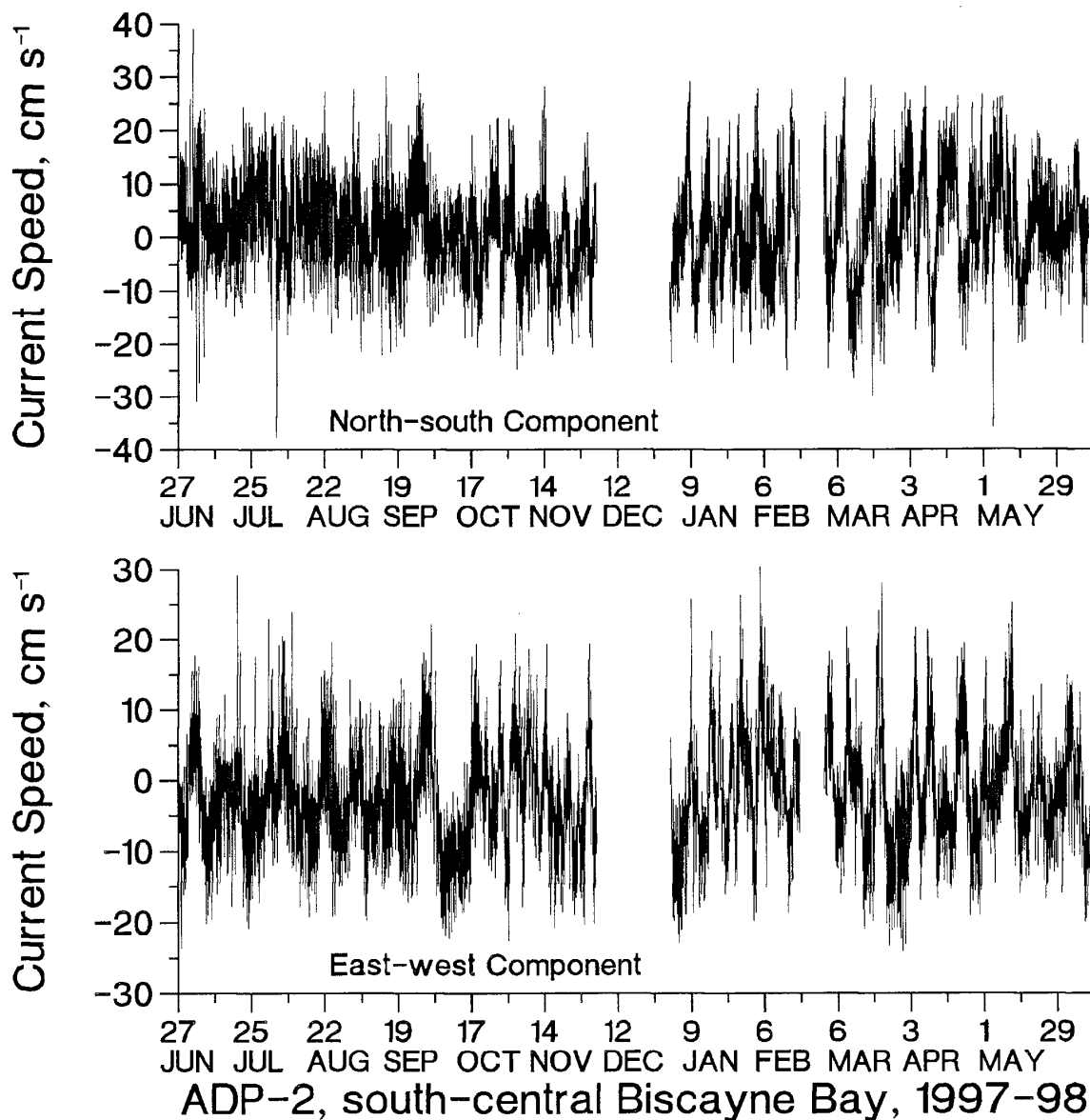


Figure B33. Cumulative net transport diagram constructed from data recorded at Station ADP-2, June 27 to December 3, 1997. Dots have been entered at the beginning of the first day of every month. The plot shows the movement of water past the study site in the south-central part of Biscayne Bay.

The plot begins with a generally northwestward movement of water that continues through early October. Superimposed onto the northwestward flow is a tidal oscillation that reverses the east-west component of the current, but not the north-south component. In early October, and coinciding with a seasonal shift in wind forcing (see Figures B2-B5), transport at the study site becomes westward and relatively steady. This pattern ends in late October and early November, and the net transport is minimal for the next few weeks. Wind forcing is not especially weak during this time (see Figures B3 and B5), but winds are not consistent in direction (see Figures B2 and B4). The net transport is southwestward for the final several weeks covered by this plot.

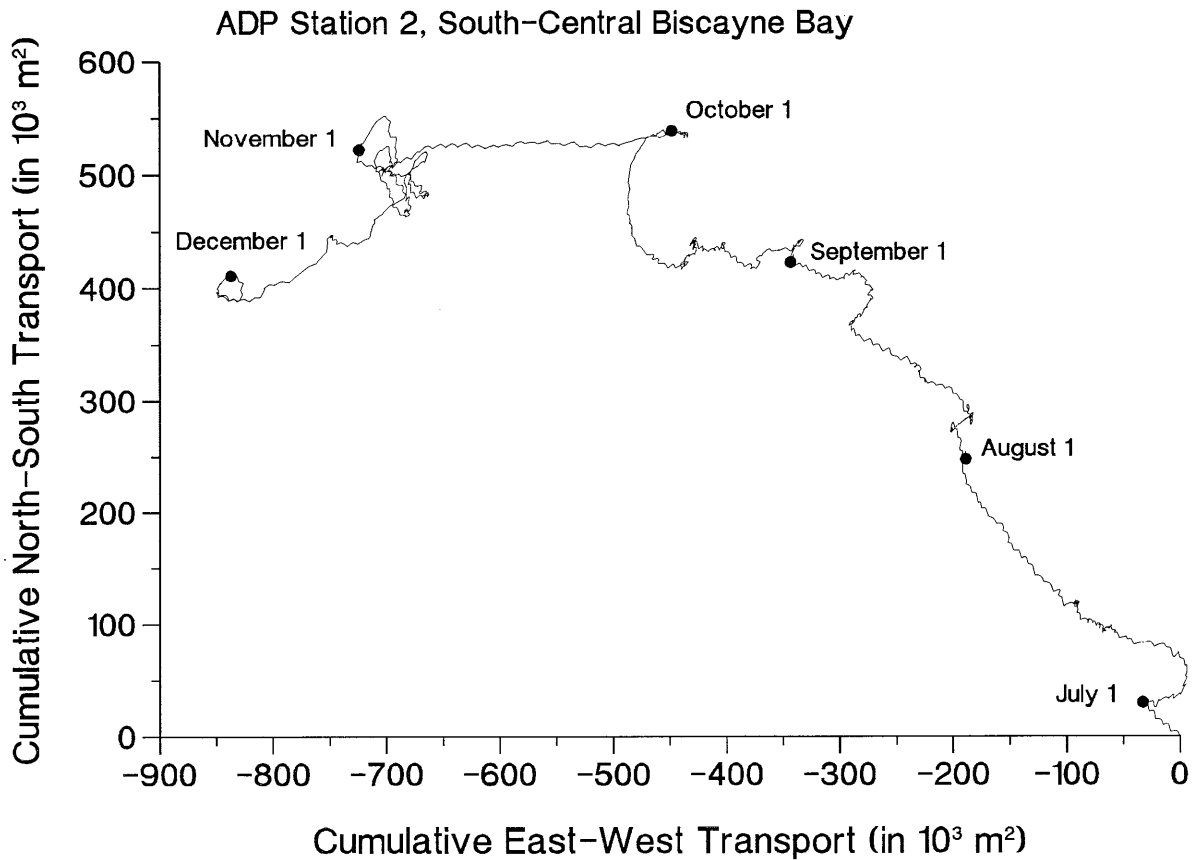


Figure B34. Acoustic Doppler Profiler data from Station ADP-3 in north-central Biscayne Bay, just west of the Safety Valve at Marker 1A. Data are available from three time periods during the June 26, 1997, to July 31, 1998, study. Shown here are the vertically averaged north-south (top) and east-west (bottom) current components. The middle data segment is too short for a spectral analysis, but the first and third segments were suitable for an analysis of tidal conditions, and the first segment is suitable for a comparison with Fowey Rocks weather data to quantify the response to wind forcing.

Data from this location, plotted in this format, show little variation throughout the year. Current speeds are generally between $\pm 10 \text{ cm s}^{-1}$ for the north-south components and $\pm 20 \text{ cm s}^{-1}$ for the east-west components. The slightly more “ragged” appearance of the north-south component currents indicates that nontidal forcing has a greater influence on north-south flow than on east-west flow.

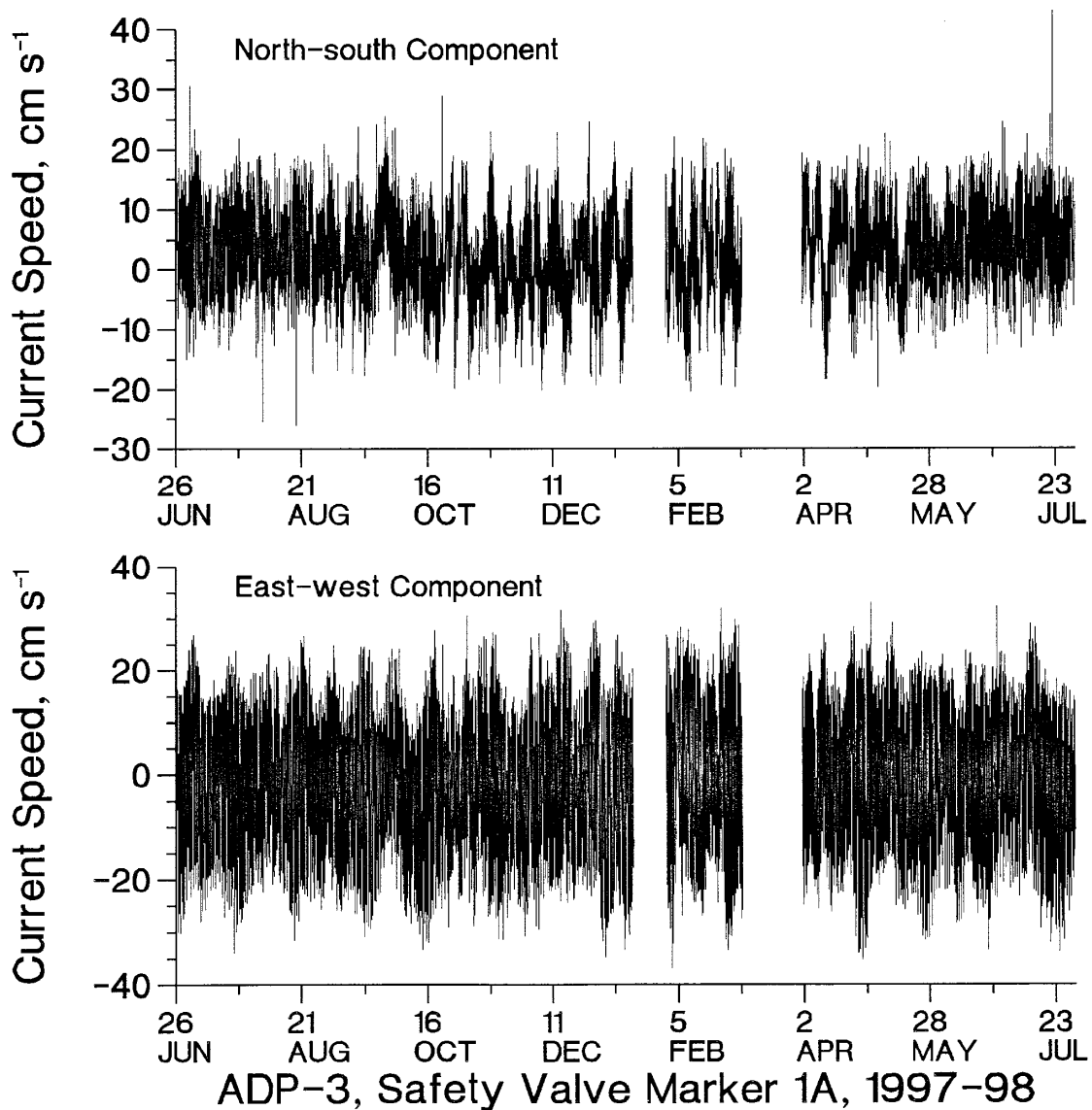


Figure B35. Cumulative net transport diagram constructed from data recorded at ADP Station 3, June 26, 1997, to January 15, 1998. Dots have been entered at the beginning of the first day of every month. The plot shows the movement of water past the study site in Biscayne Bay, directly west of the Safety Valve.

The plot consists of vigorous tidal exchanges superimposed onto a much more gradual inflow--first toward the northwest, then irregularly westward. The transition occurs in early October, shortly after a seasonal change in regional wind stress (see Figures B2-B5). Many features of this plot are similar to those appearing in the cumulative net transport plot constructed using data from Station ADP-2 in south-central Biscayne Bay (see Figure B33).

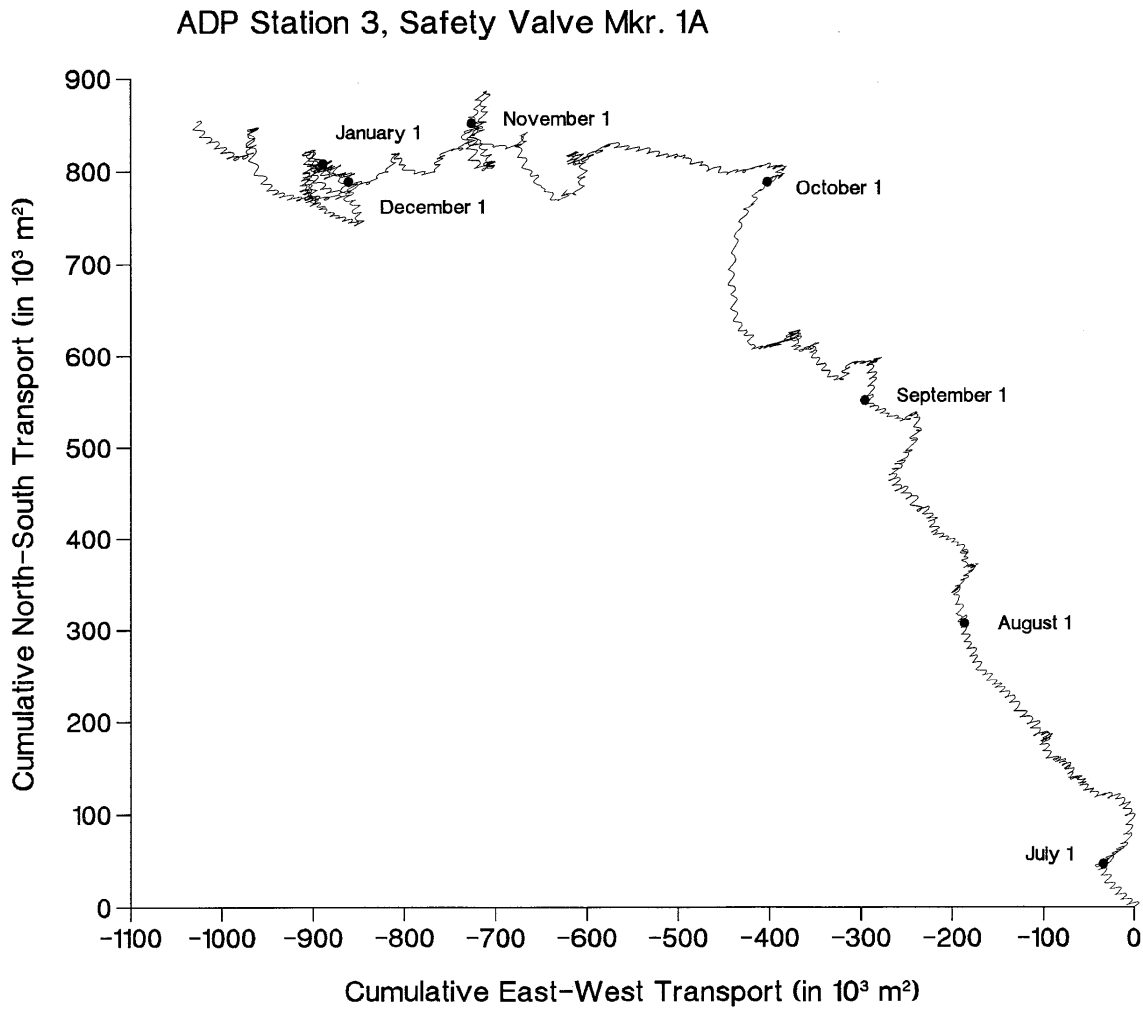


Figure B36. Acoustic Doppler Profiler data from Station ADP-4 in northern Biscayne Bay and just north of West Point at Bear Cut Marker 1. Data are available only from three short time periods during the June 26, 1997, and March 21, 1998, study (a fourth data segment, from May 1-6, was too short to plot). Shown here are the vertically averaged north-south (top) and east-west (bottom) current components. The appearance of the north-south component current speeds changes significantly over the course of the study. Currents in the first segment are generally $\pm 10 \text{ cm s}^{-1}$, while north-south components in the second and third segments commonly reach $\pm 20 \text{ cm s}^{-1}$ as low-frequency fluctuations. Harmonic analyses to isolate tidal currents confirm that the north-south component of the ebb and flood changes unrealistically. It is probable that the second and third segments of north-south flow are contaminated, and they were not used for either harmonic analysis or spectral analysis. Only the first segment of the north-south component flow was used to characterize tides at that location. All three east-west components were used for harmonic analysis, though none was long enough for a meaningful spectral analyses.

Focusing on the first segment of both components, most of the total current is contained in the east-west component, where strongest floods and ebbs commonly reach 20 cm s^{-1} . The transition from neap to spring tide conditions is not well defined, and strongest current speeds rarely exceed 30 cm s^{-1} .

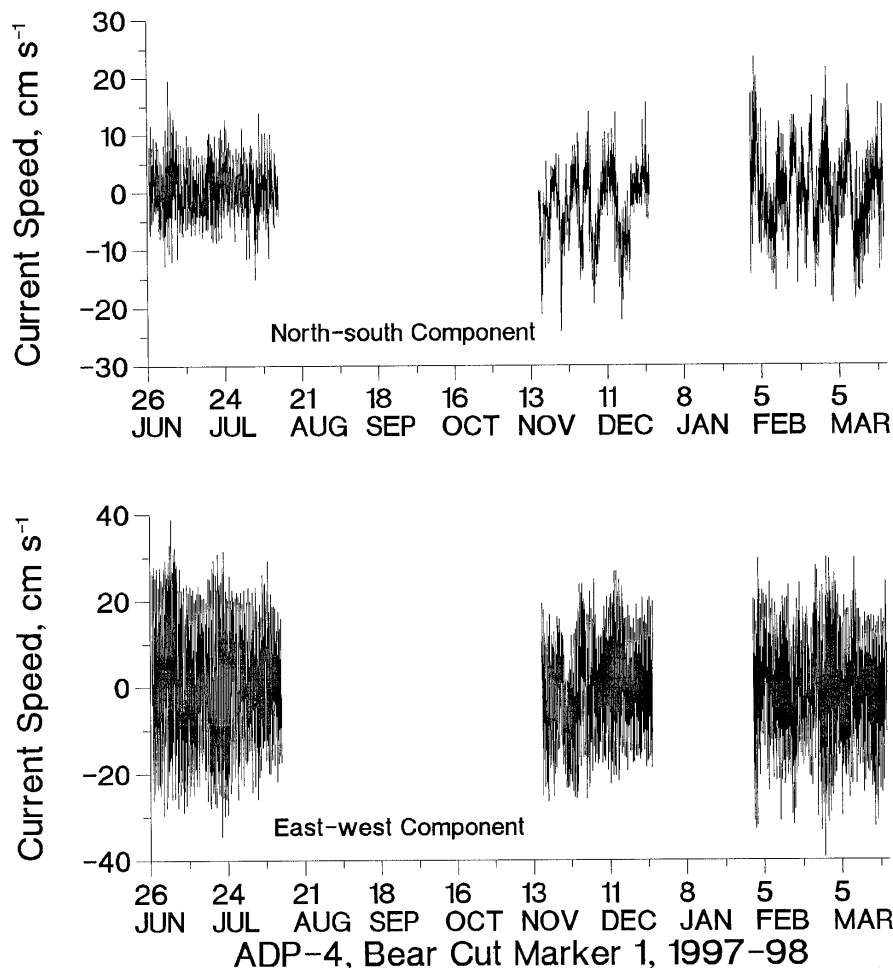


Figure B37. Cumulative net displacement diagrams constructed from data recorded at Station ADP-4, in northern Biscayne Bay, north of West Point on Biscayne Bay. Shown here are data from June 26 to August 12 (left) and from November 15 to December 26 (right), 1997. Dots have not been entered at the beginning of the first day of each month due to the short length of the records.

The two plots are quite different, and the differences should be useful in model verification. The June-August data indicate strong tidal oscillations superimposed onto a relatively weak net displacement toward the north-northeast. The November-December data show poorly defined tidal oscillations superimposed onto a relatively strong net displacement toward the south-southwest. Because of the strong inflow between Virginia Key and Key Biscayne, many tidal cycles have little or no ebb flow. Weather data from Fowey Rocks indicate a weak net northwestward wind stress during the June-August time period and stronger net southwestward wind stress during the November-December time period (see Figure B2).

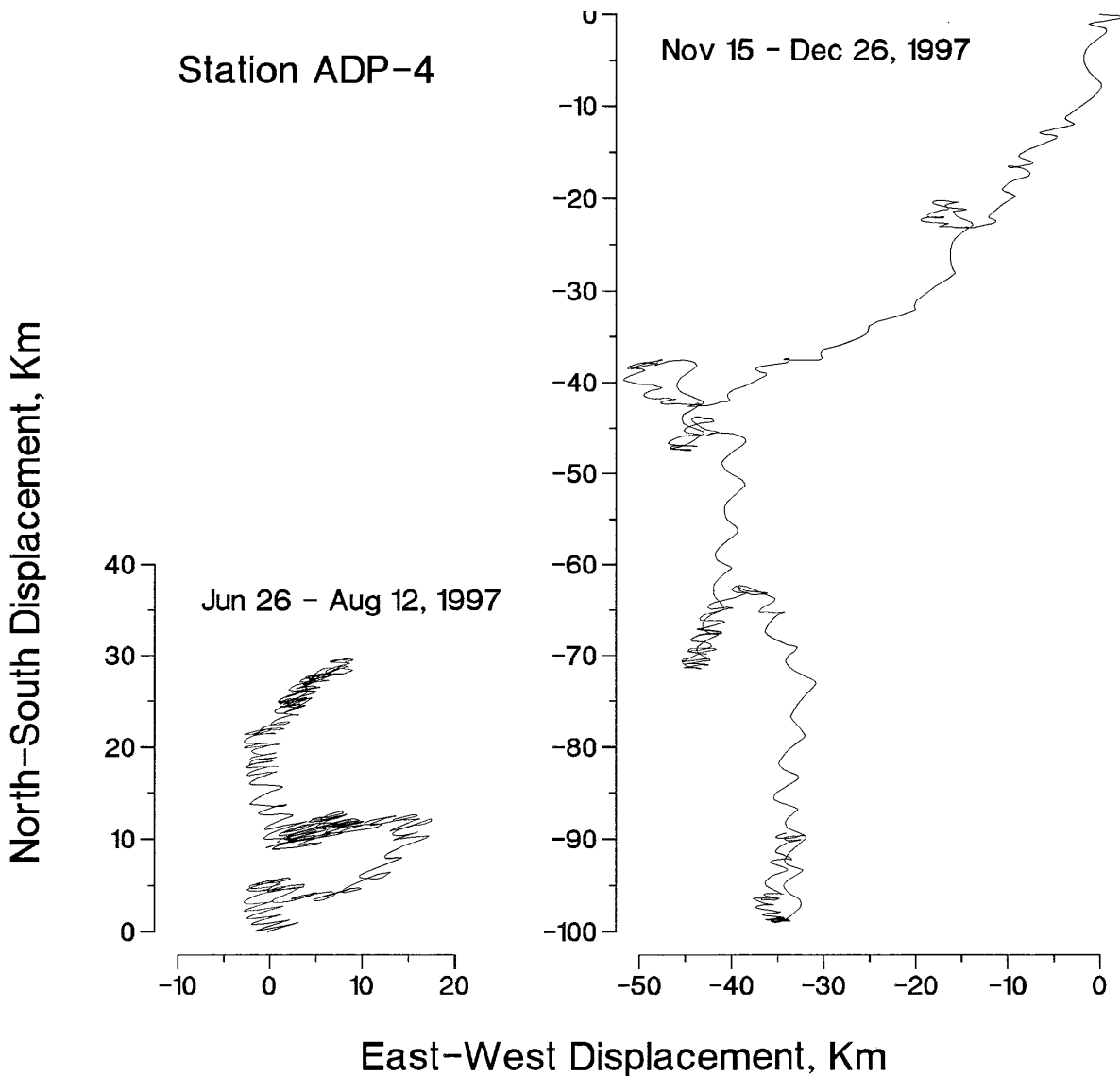


Figure B38. Acoustic Doppler Profiler data from Station ADP-5 in northern Biscayne Bay, at the Julie Tuttle Causeway Marker 35. Data are broken into six time periods during the June 28, 1997, to July 31, 1998, study. Shown here are the vertically averaged north-south (top) and east-west (bottom) current components. None of the segments is suitable for spectral analyses, but only the second segment is too short for a tidal analysis.

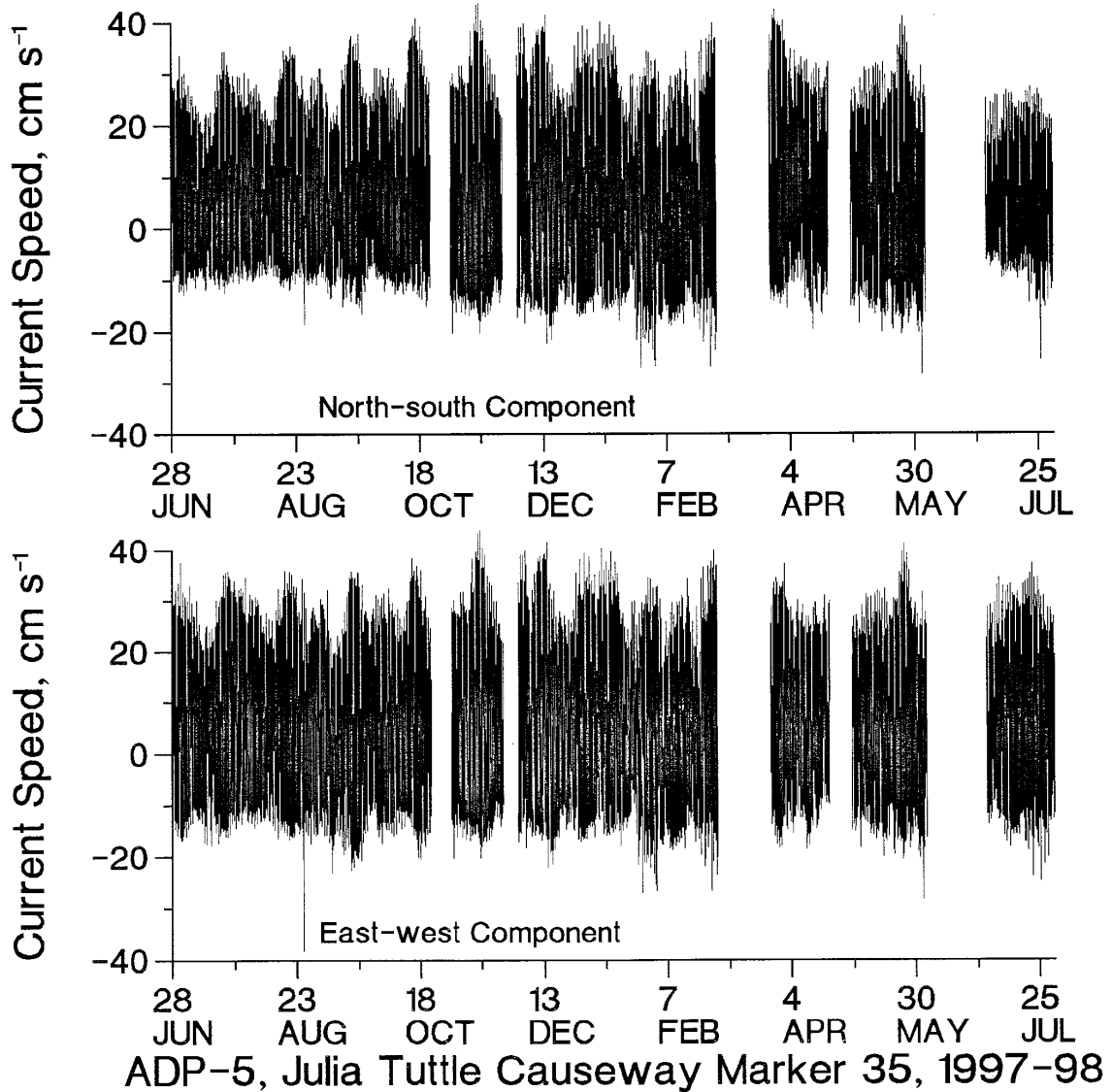


Figure B39. Cumulative net transport diagrams constructed from data recorded at Station ADP-5, in northern Biscayne Bay. Data are available from June 28 to October 22, 1997 (top) and December 1, 1997, to March 1, 1998 (bottom plot). Dots have been entered at the beginning of the first day of each month.

The plots show a remarkably consistent northeastward flow of water past the study site. The nearly constant direction of the flow is a result of the topographic steering produced by channels and nearby shorelines. Superimposed onto the nontidal northeastward flow is the back-and-forth ebb and flood of the tide. Tidal variations are difficult to detect because of the rectilinear nature of both the tidal and the nontidal flow.

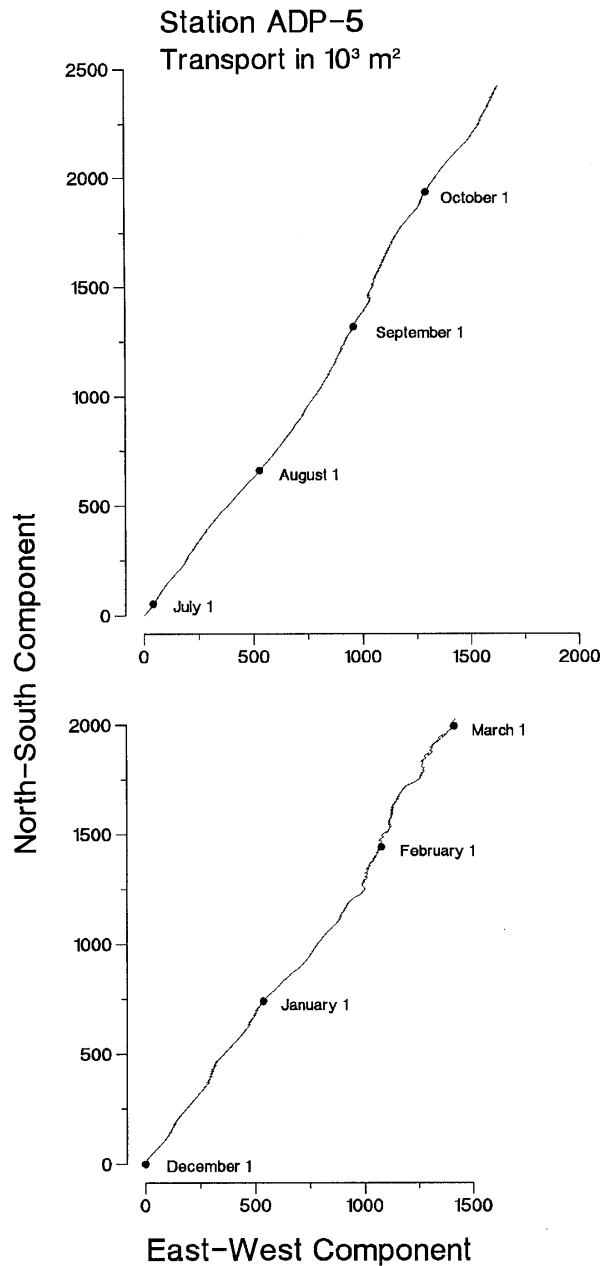


Table B15. Coherence of currents at ADP Station 1 and wind stress at Fowey Rocks, calculated from data recorded December 21, 1997, to July 12, 1998. Bold numbers indicate coherence significant at the 95% confidence level ($\beta_{05} = 0.280$); bold italicized numbers indicate coherence significant at the 99% level ($\beta_{01} = 0.344$). The magnitude of the transfer function (gain) is shown in parentheses beside coherence values when coherence is significant at or above the 95% confidence level. For the north-south components (N-S) northward flow is positive and for east-west components eastward flow is positive. Therefore, northward or eastward winds forcing currents to the north or east result in a positive transfer function. Similarly, southward or westward wind stress forcing currents toward the south or west will produce a positive gain. Alternately, northward or eastward wind stress forcing currents to the south or west result in a negative gain.

The units of gain are cm s^{-1} per dyne cm^{-2} . Thus, in the first example below, a gain of 5.68 indicates that wind stress reaching 1 dyne cm^{-2} with a periodicity of 10.6 days will result in a vertically averaged north-south current speed that reaches 5.68 cm s^{-1} . The positive gain indicates that northward wind stress produces a northward current.

Highest coherences are found for periodicities in excess of about two days. Highest gains occur for downwind flow. For example, north-south currents produced by north-south wind stress.

<u>Period (d)</u>	<u>N-S Winds</u> <u>N-S Currents</u>	<u>E-W Winds</u> <u>N-S Currents</u>	<u>N-S Winds</u> <u>E-W Currents</u>	<u>E-W Winds</u> <u>E-W Currents</u>
10.6	.856 (5.68)	.458 (-2.48)	.431 (-1.84)	.702 (2.88)
5.3	.768 (5.06)	.480 (-2.78)	.440 (-1.58)	.553 (2.78)
3.5	.707 (4.42)	.560 (-1.47)	.317 (-.838)	.374 (1.88)
2.7	.593 (4.15)	.349 (-.473)	.402 (-1.35)	.383 (2.08)
2.1	.482 (4.23)	.355 (-.093)	.305 (-.759)	.450 (2.87)
1.8	.604 (4.89)	.540 (.210)	.252	.465 (3.33)
1.5	.618 (5.32)	.185	.248	.514 (3.17)
1.3	.352 (4.72)	.135	.024	.436 (3.30)
1.2	.661 (5.20)	.299 (-.323)	.009	.312 (3.17)
1.1	.521 (5.89)	.201	.062	.133
1.0	.389 (5.52)	.148	.021	.026

Table B16. Same as Table B15 except for ADP Station 2. The analysis covered the time period from June 27 to December 3, 1998 ($\beta_{05} = 0.317$, $\beta_{01} = 0.387$).

The consistently highest coherences and the highest gains occur for downwind flow. For example, when northward wind stress produces northward currents. Occurrences of wind stress in any direction significantly related to currents 90° to the right or left are much less common, and gains are much less.

<u>Period (d)</u>	N-S Winds <u>N-S Currents</u>	E-W Winds <u>N-S Currents</u>	N-S Winds <u>E-W Currents</u>	E-W Winds <u>E-W Currents</u>
10.6	.810 (6.22)	.116	.249	.711 (7.96)
5.3	.702 (5.73)	.178	.263	.752 (8.13)
3.5	.560 (6.11)	.246	.176	.587 (6.83)
2.7	.352 (4.86)	.120	.488 (-.742)	.636 (5.85)
2.1	.265	.063	.261	.453 (6.01)
1.8	.295	.055	.329 (2.94)	.224
1.5	.372 (4.99)	.012	.219	.349 (4.95)
1.3	.266	.119	.171	.353 (5.34)
1.2	.346 (5.92)	.122	.214	.484 (6.31)
1.1	.402 (7.09)	.079	.081	.076
1.0	.624 (10.7)	.133	.250	.130

Table B17. Same as Table B15 except for ADP Station 3. The analysis covers the time period from June 26, 1997, to January 15, 1998 ($\beta_{05} = 0.280$, $\beta_{01} = 0.344$).

Results are similar to those summarized in Table B16 for Station ADP-2. Highest coherences and highest gains occur for current components parallel to wind stress components. This indicates a direct response to wind forcing in the form of a downwind flow.

<u>Period (d)</u>	<u>N-S Winds</u> <u>N-S Currents</u>	<u>E-W Winds</u> <u>N-S Currents</u>	<u>N-S Winds</u> <u>E-W Currents</u>	<u>E-W Winds</u> <u>E-W Currents</u>
10.6	.842 (5.50)	.222	.247	.759 (3.67)
5.3	.779 (5.72)	.252	.283	.674 (3.78)
3.5	.584 (5.58)	.412 (-.946)	.311 (1.40)	.609 (3.68)
2.7	.541 (5.17)	.259	.406 (1.03)	.570 (3.86)
2.1	.767 (6.25)	.628 (-1.81)	.288 (.313)	.506 (3.02)
1.8	.719 (5.67)	.245	.035	.173
1.5	.597 (5.46)	.155	.000	.306 (2.56)
1.3	.540 (3.73)	.282	.122	.344 (3.42)
1.2	.508 (4.85)	.263	.113	.356 (4.67)
1.1	.351 (6.67)	.171	.105	.039
1.0	.523 (7.95)	.237	.211	.060

Table B18. Harmonic constants (amplitudes / local phase angles) of the principal tidal constituents at each of the five ADP current meter stations. Amplitudes are in cm s^{-1} ; local phase angles are in degrees.

Station	Tidal Constituent				
	M_2	S_2	N_2	K_1	O_1
ADP-1 (N-S)	2.6 / 114	0.6 / 330	0.6 / 131	0.5 / 007	0.5 / 236
ADP-1 (E-W)	12.5 / 044	2.4 / 088	2.2 / 015	0.9 / 366	1.1 / 018
ADP-2 (N-S)	6.8 / 051	2.0 / 062	1.4 / 028	1.2 / 284	0.6 / 313
ADP-2 (E-W)	4.0 / 016	1.1 / 115	1.1 / 001	1.1 / 339	0.1 / 034
ADP-3 (N-S)	7.2 / 046	1.8 / 088	1.3 / 036	1.6 / 279	0.3 / 285
ADP-3 (E-W)	17.5 / 010	2.7 / 040	4.0 / 354	1.7 / 306	0.9 / 306
ADP-4 (N-S)	4.5 / 001	1.2 / 025	0.6 / 001	0.8 / 323	0.6 / 217
ADP-4 (E-W)	20.4 / 017	3.2 / 039	4.2 / 009	2.0 / 296	1.7 / 289
ADP-5 (N-S)	17.7 / 182	2.6 / 219	3.5 / 163	0.9 / 096	1.1 / 117
ADP-5 (E-W)	20.2 / 180	2.7 / 213	3.8 / 161	1.1 / 099	1.0 / 121

Discussion and Summary

The assemblage of weather, water level, and ADP data from the Biscayne Bay series of coastal bays is a database well suited for model verification. Individually, the twelve water level stations and five ADP stations provide data that can be compared with output from the corresponding part of the model domain. Taken together, the water level data, though not the ADP data, characterize tidal conditions throughout the Bay. Wind data are adequate for verifying the model's ability to reproduce the effects of wind stress on water level and circulation. Coherence identifies the broad range of wind directions to which water levels are most responsive, and the transfer function (gain) quantifies the magnitude of the set-up or set-down of water level in response to wind forcing. Comparisons of the five ADP transport records make it clear that five study sites are insufficient for describing bay-wide circulation patterns. However, data from the five locations can be used to verify how well the model is reproducing flow patterns in the corresponding parts of the model domain.

Comparison of the two wind stress records supports the idea that wind data from several locations surrounding the bays were not needed. The high correlation in the long term, and the minimal mean difference in wind direction, suggests that one anemometer with an unobstructed exposure is adequate for recording both landward and seaward directed winds.

Integration of water level data from several sources provides a much better picture of the tidal conditions of the Biscayne Bay system. The co-amplitude and co-phase charts provide a significantly better understanding of tidal conditions than was possible from earlier databases consisting of a smaller number of stations. Although not a part of this study, the WES database makes possible a follow-up investigation of shallow-water and fortnightly tidal constituents.

The progressive vector diagrams of wind stress (Figures B2 and B4) are helpful for understanding the distinct change in transport direction that appears at Stations ADP-2 and -3 in early October. This seasonal change in wind direction has been noted in wind data from several Florida Keys weather stations, and in many cases it has been found to trigger a dramatic change in transport. Similarly, the plots of north-south and east-west wind stress (Figures B3 and B5) are useful for explaining the transient spike in water level in early February.

The analyses of tidal conditions and wind forcing reported here make possible model verification exercises that focus specifically on tides and wind stress. For example, the tables of gain values, presented both with the analyses of water level records and the analyses of ADP records, show a specific response to equally specific wind forcing. If model simulations are forced only by east-west wind stress reaching a magnitude of 1 dyne cm^{-2} , then Tables B2-B13 can be used to test the simulated rise and fall in water level throughout the Bay, and Tables B15-B17 can be used to test the simulated current speeds at three of the ADP study sites. Similarly, if the model is forced by a single tidal constituent in shelf waters, then the five co-amplitude and co-phase charts (Figures B19-B28) can be used to test the simulated rise and fall in water level, or the movement of high or low tide at any point within the Bay specific to that tidal constituent. Forcing the model with observed winds, whether from Fowey Rocks or Convoy Point, introduces a degree of complexity by combining a wide range of periodicities, speeds, and directions. Similarly, a combination of tidal and nontidal water level variations in shelf waters may be a more realistic form of forcing, but it makes an interpretation of the response correspondingly more difficult.

References

- Bloomfield, P. (1976). *Fourier analysis of time series: an introduction*. John Wiley & Sons, New York. 258 pp.
- Dennis, R., and Long, E. (1971). "A user's guide to a computer program for harmonic analysis of data at tidal frequencies," NOAA Tech. Report, U.S. Dept. of Commerce.
- Kundu, P. K. (1976). "Ekman veering observed near ocean bottom," *Journal of Physical Oceanography* 6:238-242.
- List, R. J. (1963). *Smithsonian meteorological tables (6th Edition)*. Smithsonian Institution Publ. No. 4014, Washington, D.C., 527 pp.
- Little, J., and Shure, L. (1988). *Signal processing toolbox, user's guide*. The MathWorks, Inc., Natick, MA, 165 pp.
- Pratt, T. C. (1999). « Biscayne Bay field data report," Waterways Experiment Station. (This reference is superceded by the report to which this Appendix B is attached.)
- Schureman, P. (1958). *Manual of harmonic analysis and prediction of tides*. Spec. Publ. No. 98, U.S. Govt. Printing Office, Washington, D.C., 317 pp.
- Scientific Programming Enterprises. (1985). *PlotIT interactive graphics and statistics reference guide, Version 1.6*. P.O. Box 669, Haslett, Michigan.
- Wu, J. (1980). "Wind-stress coefficients over sea surface near neutral conditions—a revisit," *Journal of Physical Oceanography* 10, 727-40.

Appendix C QA/QC Procedures Used for the Biscayne Bay Feasibility Study

by Richard Curry, Biscayne National Park

Introduction

The National Park Service, Biscayne National Park (BNP) was funded by the U.S. Army Engineer District, Jacksonville (SAJ), to purchase equipment and collect physio-chemical data (temperature, conductivity, and pressure) at various locations in Biscayne Bay. BNP worked in consultation with the U. S. Army Engineer Research and Development Center, Waterways Experiment Station (ERDC-WES), Coastal and Hydraulic Laboratory (CHL) and the Miami-Dade Department of Environmental Resources Management (DERM).

CTD and ADP Deployment

With the assistance of CHL and DERM, twelve conductivity, temperature, and depth (CTD) instrument station locations were selected for these bottom-mounted instruments. CTD station locations ranged from Manatee Bay in the south to near Bakers Haulover Inlet in the north, a distance of approximately 80 km (50 miles). Locations for five bottom-mounted Acoustic Doppler Profiler (ADP) current velocity instruments were also determined. See Table C1 for CTD and ADP coordinates. After the locations were selected BNP installed, or located, mooring pins to which were attached eleven of the twelve multiparameter water quality CTD monitors and the ADP's. CHL personnel used Global Positioning System (GPS) survey equipment and kinematic techniques to establish the horizontal location of the mooring gear to an accuracy of a few centimeters. When necessary for servicing, standard differential GPS equipment was used to relocate the monitoring equipment. Eleven of the twelve CTD deployments were also surveyed to determine the NGVD29 elevation of the instruments' pressure sensors.

Three of the stations had both a multiparameter water quality monitoring CTD unit and an ADP. These three stations were located at Angel Fish Creek (CTD3 and ADP1), Biscayne Bay east of Military Canal (CTD4 and ADP2), and just north of the Broad Causeway Bridge (CTD11 and ADP5). Station CTD10 was located at the mouth of the Miami River on the Atlantic Intracoastal Waterway (AIWW) channel marker "57." It was not mounted on the bottom by divers due to water quality concerns at the site. A stainless steel mounting system was fabricated that could be mounted on the channel marker. After permission was obtained from the U.S. Coast Guard to mount an instrument on the channel marker the mounting system and CTD were placed. The CTD10 location was first occupied on 15 December 1997, about six months after the other CTD stations were first deployed. Because of its unique deployment, the CTD10 location was not surveyed for vertical position. Photographs of the CTD and ADP instruments are located in the main text of this report and in Appendix A.

ADP Discussion

The ADP's are complex monitoring units that are, for the most part, calibrated at the factory. The user is only able to adjust a few parameters such as representative salinity, heading, bin size (see Chapter 3, "ADP Velocity Data" section for a discussion of "bin size"), and sample frequency. The representative salinity is a typical value for salinity of the water at the deployment site and this value, along with the ongoing temperature measurement, is used to calculate the speed of sound in the water. The speed of sound is needed for the velocity measurement. Factory calibration was relied on for depth (pressure), current speed and direction, and temperature since manual calibration was not possible. When the meters were deployed the compass was reset following the simple field procedure recommended by the manufacturer. Some parameters, such as the representative salinity, temperature, pressure, and battery status were checked to verify proper instrument function before leaving the site. If any of these parameters were not within acceptable limits CHL and the manufacturer were consulted, and the meter was returned to the manufacturer if recommended.

Most of the time the ADP's worked reliably, requiring only simple maintenance (wash down and barnacle removal), and down-loading of the data file. The raw data file was sent directly to CHL for assessment and post-processing. Significant amounts of data were lost for three periods of time. These periods were: 11/8 to 12/21/97 at ADP1, 8/12 to 9/11/97 at ADP4, and 11/8 to 11/15/97 at ADP4. Table C2 presents a deployment record for the ADP's.

CTD Discussion

The multiparameter water quality monitors (CTD's) used for this project were the Endeco/YSI Model 6000. These units accurately measure pressure, temperature (thermistor), dissolved oxygen (amperometric), conductivity (salinity by computation), pH, and turbidity. The temperature probe cannot be calibrated and, for the term of this project, neither pH nor turbidity sensors were included. During the calibration phase prior to deployment, the CTD's were put in a crude temperature bath and the temperature was compared to a glass thermometer. If the temperatures differed by more than a degree, the unit was returned to the factory for repair.

CTD conductivity was calibrated using a single point procedure against a secondary seawater standard. The secondary standard was seawater collected from the Gulf Stream from about a meter below the surface. The Gulf Stream water was collected in five-gallon carboys. The conductivity of the water in each carboy was determined against a 0.5 Molar Potassium Chloride (KCl) primary standard using one of the Endeco/YSI CTD units. The process was to calibrate this CTD monitoring unit using the primary standard and then, using this calibrated CTD unit, the specific conductance of the water in the carboy was determined. This water then became the secondary standard used in all subsequent unit calibrations. Periodic recalibration of the secondary standard

water against fresh primary standard showed no measurable drift during the two- to three-month period that the secondary standard water was used. Each new carboy of seawater was always initially calibrated against the primary KCl standard.

Starting, in most cases during July 1997, the pressure transducer/water depth sensor was calibrated by noting the depth indicated while the CTD was “dry in air” and then adjusting the sensor to read 0.0 m when dry in air. A calibration check was then performed by placing the sensor in a 0.5-m bath and noting the depth reading.

Although oxygen was not one of the parameters of interest for this project, it was calibrated anyway. The calibration algorithm is actually internal to the instrument and requires little input from the user. The algorithm is similar to the single point air calibration used for all amperometric meters and requires the user to input the barometric pressure at the time of calibration. No further QA/QC was performed for the dissolved oxygen measurements by BNP.

All CTD’s were allowed to run for a minimum of 12 hours before deployment. This “burn in” period was required to ensure accurate dissolved oxygen data, and to ensure that all parameters were working properly and within expected statistical calibration limits. Deployment information was then stored in memory and the units were taken into the field. An example of the CTD calibration sheet is shown in Figure 4 in Chapter 2. Missing data periods are shown in Table C3 and are discussed further in the main report text.

Instrument Servicing

Once the field study started, monitoring units were almost always on site except when a meter was destroyed or sent to the factory for repairs. In the case of the CTD’s, a newly calibrated meter was taken to a station and deployed along with the existing meter. The two CTD’s were then allowed to collect three or more data values before the old meter was removed and returned to BNP to be cleaned up, have its data downloaded, and be recalibrated for deployment at another site. The purpose of collecting simultaneous data values was to allow for a determination of any drift that might have been due to epiphytic growth on sensor surfaces or other electronic drift. The dissolved oxygen parameter was the most sensitive to distortions by epiphytic growth; temperature and pressure seemed the least sensitive. Epiphytic growth was excessive for all of the northern stations.

Vertical salinity profiles were also obtained during CTD retrieval using a Sea-Bird Electronics CTD unit. If this unit was not available an Endeco/YSI Model 6000 probe was used to determine water column salinity profiles for cross-calibration and post-processing. These profiles provided a third set of values for certain parameters, particularly salinity, being measured by the Endeco/YSI units. Servicing intervals ranged from 10 to 63 days for the CTD’s and from 14 to 103 days for the ADP’s.

BNP was not funded to post-process, or filter, the raw data. Only raw data were sent to CHL for post-processing and use by the modelers. The only review of the data by BNP was to ensure that the instruments were working well when calibrated prior to deployment.

Table C1 Biscayne Bay Feasibility Study CTD and ADP Locations (Pin Locations)					
Station	Type	DGPS-Lat	DGPS-Long	Depth (m)	Description
CTD1	Sonde	25 14.204	080 24.662	1	Manatee Bay
CTD2	Sonde	25 17.310	080 22.113	2	Card Sound Bridge 4 th Dolphin from mn1
CTD3 ADP1	Sonde Current Meter	25 21.167	080 16.816	2	Angel Fish Crk 15 yds NW "14"
CTD4 ADP2	Sonde Current Meter	25 29.683	080 16.702	2.1	Military Canal out
CTD5	Sonde	25 29.780	080 19.528	1	Military Canal close
CTD6	Sonde	25 31.637	080 18.243	1.6	Black Pt. mkr 10oN of "8"
ADP3	Current Meter	25 37.013	080 11.550	3.1	Safety Valve marker 1A
CTD7	Sonde	25 36.245	080 17.354	2	Snapper Crk
CTD8	Sonde	25 39.076	080 15.575	2.4	Gables-by-the-Sea
ADP4	Current Meter	25 42.886	080 10.630	3.2	Bear Cut mkr "1"
CTD9	Sonde	25 39.267	080 09.580	5.2	Biscayne Channel mkr "10"
CTD10	Sonde	25 46.230	080 10.910	3.3	Miami River
CTD11 ADP5	Sonde Current Meter	25 48.828	080 10.492	3.6	Julia Tuttle Cswy Mkr "35"
CTD12	Sonde	25 53.410	080 08.390	2.1	Broad Cswy Mkr "13"

Table C2 ADP Deployment Record for Biscayne Bay Feasibility Study			
Station	Notes	Location Description	Depth (m)
ADP1		Angelfish Creek	2
6/25/97	Deployed.		
8/12/97	Battery too low to collect data so pulled.		
8/14/97	Redeployed with different battery.		
11/8/97	Memory full; brought back to lab because unit acted strange (filled up with headers).		
12/21/97	Redeployed.		
1/29/97	Data download.		
3/18/98	Data download.		
4/23/98	Data download.		
7/23/98	Data download.		
8/24/98	Data download.		
ADP2		Central Biscayne Bay	2
6/25/97	Deployed.		
8/12/97	Data download.		
11/4/97	Data download.		
1/30/98	Data download.		
3/18/98	Data download.		
4/23/98	Data download.		
5/15/98	Changed batteries.		
ADP3		Safety Valve	3.1
6/28/97	Deployed.		
8/12/97	Data download.		
11/4/97	Data download.		
1/30/98	Data download.		
3/18/98	Data download.		
4/23/98	Changed batteries.		
8/4/98	Data download.		
ADP4		Bear Cut	3.2
6/28/97	Deployed.		
8/12/97	Temp & Pres off pulled. Lab: water inside connection. Removed batt & placed in ADCP 1.		
9/11/97	(Redeployed).		
11/4/97	Data download.		
11/8/97	Bad battery connection; pulled for deployment test.		
11/10/97	Lab test.		
11/13/97	Lab test-cable.		
11/15/97	Redeployed.		
1/22/98	Data download.		
3/25/98	Data download.		
5/1/98	Data download.		
5/15/98	Data download.		
8/4/98	Data download.		
ADP5		Julia Tuttle Cswy.	3.6
6/28/97	Deployed.		
8/14/97	Data download.		
11/4/97	Data download.		
1/22/98	Data download.		
3/25/98	Data download.		
5/1/98	(Replaced zinc[sic]).		
8/4/98	Data download.		

Table C3 Missing CTD Data for the Biscayne Bay Feasibility Study		
Dates of Missing Data	Station	Reason
6/5 to 7/10/97	CTD5	Battery compartment flooded
6/6 to 7/10/97	CTD7	Malfunction of unit, cause unknown
6/10 to 7/15/97	CTD11	Malfunction of unit, cause unknown
7/26 to 8/1/97	CTD11	Suspected lightning strike
8/15 to 9/10/97	CTD7	Sonde ripped from pin, unit lost
12/3 to 12/10/97	CTD11	Lock failure, unit lost
12/8 to 1/7/98	CTD4	Malfunction of unit, cause unknown
12/10 to 1/27/98	CTD11	Sonde ripped from pin, unit lost
1/24 to 2/18/98	CTD3	Malfunction of unit, cause unknown
2/2 to 2/16/98	CTD7	Unit programmed improperly
3/28 to 4/1/98	CTD5	Battery power failed
8/15 to 9/2/98	CTD6	Battery power failed
11/6 to //9/98	CTD4	Battery power failed
9/7 to 11/9/98	CTD7	Battery power failed, reverse polarity

Appendix D

Lessons Learned

**by Timothy Fagerburg and Robert McAdory, Coastal and
Hydraulics Laboratory**

Introduction

In the area of field data collection techniques, there can never be too much data collected. The portion of those data intended for use to provide checks and balances on the “main” data quality are especially important. And all of these data are more valuable if adequately documented. The following information provides the data collector with some recommended procedures for calibration, deployment, retrieval, data recording, and quality control checks of data collection instruments.

ADP Current Monitors (with depth sensors)

Logs. All information that may be relevant to aiding in the interpretation and analysis of the instrument long-term data should be collected in a logbook or in log sheets. This information would include pre-deployment check and calibration, deployment, retrieval, post-deployment check and calibration, data downloading, and other information and data as appropriate. It should also include local conditions, especially for the deployed instrument, with photographs (for submerged instruments, especially, if diving is involved). As early as possible, data should be downloaded, processed, and examined by the field personnel for on-the-spot quick quality checks and by end users to determine if the log information and data collected and provided are suitable for their needs. The field and end user personnel should communicate often, in person as often as possible, and with mutual feedback. The best possible formats for organizing the log material should be used. Such formats should be based on previous experience, particularly in the particular system under study, and the formats should be improved while the study is in progress if necessary.

Locations. Locations for each ADP instrument deployment should continue to be identified with the use of Differential Global Positioning Systems (DGPS) as they were in the Biscayne Bay field data collection effort. This enables the redeployment of the instruments at the same or nearly the same location. Any changes in the instrument location should be recorded in the log for each deployment and retrieval interval. If the ADP records depth, the elevation of the ADP instrument should be surveyed in to a datum common to any other deployments in the field exercise. If possible this datum should be one that has known relationships to MLLW and other datums for various locations in the system. This was done for the Biscayne Bay effort CTD instruments, but it was not done for the ADP’s with depth sensors.

Location Description. Physical measurements of the water depths at each sensor location were obtained at the time of the initial deployment of the ADP instruments in Biscayne Bay. The following measurements are recommended for each deployment and retrieval to enhance the record log for data quality control:

Immediately following the initial deployment of each instrument

- record date, time, and DGPS location number
- measure and record depth below water surface to bottom
- measure and record depth below water surface to top of instrument
- measure and record depth below water surface to (vertical) surveyed point
- measure and record wind speed, direction and estimate of wave heights at instrument location; record general weather, water, and other comments as appropriate

Prior to retrieval of each instrument, repeat the above procedure.

In Situ Checks. To enhance the quality of the data, physical measurements of velocity and direction, as well as salinity, at each sensor location should be obtained. This information should be recorded in the field log and provided to the end user. The following procedure is recommended for obtaining the above information:

To obtain an independent check on the velocity and direction data being recorded by the deployed ADP sensor, an alternate velocity recording instrument should be deployed to record the water velocity and direction at a minimum of two depths above the instrument following the deployment of the ADP. These depths should be between the surface and bottom blanking regions, between about 30 cm above the instrument and 30 cm below the surface, depending on local conditions at the time of the check. The instrument used for the check should be documented similarly to the deployed instruments. For the salinity, a probe should measure the salinity profile at the deployment site, since a “typical” salinity must be provided to the ADP for calculation of the speed of sound.

These servicing events should begin with a frequency of one per fortnight. This will allow for on-site and end-user checks before the effort has proceeded very far. As experience and local conditions dictate, the servicing event frequency can be adjusted either up or down, but in no case should the ADP servicing frequency be lower than one per month. “Drift Indices” (see below in Fouling section) and other aids to experience should be used when available to set servicing intervals. Downloaded data should be inspected and transmitted to the end users as soon as possible.

Replacement Instruments. Replacement instruments used as substitutes to enable repair or cleaning of the retrieved sensors should be of the same type with the same settings as are those being removed from service. This effort will ensure consistency in the parameters measured and the format of the recorded data.

Conductivity, Depth, and Temperature (CTD) Sensors

In the Biscayne Bay effort, long-term salinity data were accumulated near the bottom of each CTD site. If possible, near surface data should be recorded as well in future efforts, either at or near the CTD sites.

Logs, Locations, and Location Description. Information for the CTD's should be recorded and logged as described above in the ADP logs section. If the instrument is deployed using a float to maintain its position in the water column, care should be taken that the float line will not become slack during low water. Any slack in the line will allow the instrument to move down in the water column and thus report a larger pressure head (or deeper value of other recorded data) than would otherwise be recorded. If a data location has unavoidably shallow conditions, precautions must be taken to ensure the data can be interpreted properly.

Calibration. The CTD sensors used in the Biscayne Bay field effort (YSI 6000) allow and require much more user calibration than the ADP's used in the Biscayne Bay field effort.

Salinity and Depth. Prior to deployment, each instrument should continue to be calibrated to a known salinity concentration standard and adjustments made to match the calibrated values. Use of a secondary standard in the manner described in Appendix C is fine. However, if salinity, rather than conductivity, continues to be the quantity of interest in CTD measurements, calibration should be with respect to salinity, not conductivity. Depth sensors should continue to be calibrated by the "dry in air" (dia) technique with a 0.5-m bath as a check, as was done in the Biscayne Bay effort. The ambient atmospheric pressure and temperature should also be noted. The dia depth reading of the instrument, along with temperature and pressure should be reported immediately before deployment. In summary:

- conductivity, temperature, salinity, depth, and atmospheric pressure should be reported in the log for calibration. Conductivity, temperature, and salinity should be reported for both the standard and the CTD reading of the standard. The CTD readings before and after any salinity or depth adjustments should be recorded. The dia depth reading and temperature should be recorded right before deployment. If possible, the atmospheric pressure should also be recorded at this time. If the instrument has become hot from lying in the sun in the boat, it should first be cooled in the water before the dia pressure is noted.
- if calibration adjustments cannot be made, or if the instrument reads a temperature more than 1°C different from a standard reading, as was done in the Biscayne Bay effort, the instrument should be replaced.

Immediately after retrieval and removal to the laboratory of each instrument, and prior to downloading or cleaning the instrument:

- immerse the conductivity sensor in a known salinity concentration standard to record the offset caused by any sediment accumulation, biological growth on the sensors, or other cause of instrument drift. Also record the standard salinity, including all the other parameters mentioned above for the pre-deployment calibration, including the dia depth sensor reading.

Extract data from instrument, clean sensors, replenish power source, and re-calibrate prior to redeployment as was done in this study. Downloaded data should be inspected and transmitted to the end users as soon as possible.

In Situ Checks. Physical measurements of conductivity, temperature, and salinity at each sensor location immediately following deployment and prior to retrieval of the instrument were made during the Biscayne Bay Field Data collection effort. This should continue.

- to obtain an independent check on the data being recorded by the deployed sensor, an alternate CTD instrument (i.e. Sea-Bird, YSI 6000, etc.) should continue to be deployed to record the conductivity, temperature, depth, and salinity at the deployment depth of the instrument. If this cannot be done with a recording instrument, an alternate method for the salinity check would be to obtain a sample of water at the depth of the instrument. Laboratory analysis of the water sample would then be performed to obtain the salinity concentrations. Also, as was done in the Biscayne Bay effort, a salinity profile of the site (the “Sea-Bird” data) should be recorded. This profile should include the very near surface portion of the water column. If possible, two like instruments should be deployed simultaneously (the newly deployed instrument and the soon to be retrieved instrument), as was done in the Biscayne Bay effort, to obtain a few overlapping measurements of the CTD output at the site. These checks made at the servicing events for the long-term CTD deployments would be further enhanced if, when possible, the CTD locations are chosen to be the same as the sampling sites of other data collection efforts, such as the Bay Run sites.
- this information should be transferred to the end user at the end of each service interval to aid the data processing and analysis effort.

Fouling. Fouling of the CTD instruments by biological growth is enhanced by seasonal changes in temperature, the salinity concentrations and the depth of water at the deployment site. This fouling introduces errors (drift) in the recorded salinity data due to the alteration of the calibration levels of the sensors. This is usually due to direct growth, (often barnacles) on, around, and in the conductivity sensor. Other sensors are also affected. Time intervals between service intervals of these sensors should be shortened to minimize the fouling errors in the data. There is no exact formula for time periods, but is best determined from local knowledge of the area and observations made at the time the sensor is serviced. The drift indices discussed in Chapter 4 provide some guidance. The recommended time period of 14 days may need to be shortened during long periods of very hot weather and may be lengthened (but never more than 21 days)

during periods of cooler weather. Fouling also can affect the depth measurements, as happened at station CTD1 in Manatee Bay.

Replacement Instruments. Replacement CTD instruments, such as those used as substitutes to enable repair or cleaning of the retrieved sensor should be of the same type as are those being removed from service. This effort will ensure consistency in the parameters measured and the format of the recorded data.

Water-Level Instruments (Tide Gauges)

Tide gauges, *per se*, were not used in the Biscayne Bay effort, though they should be considered in future deployments because of their potential to be paired with surface salinity measurements and the fact that their water level measurements do not require correction for atmospheric pressure.

Logs, Locations and Location Description. Information for the tide gauges should be recorded and logged as described above in the ADP logs section. Additionally, any differences that may be applied to the datum being used as it is affected by the geographical location should be recorded in the log.

Fouling. Fouling of the water level instruments by biological growth may not have as pronounced effect as in the case of the CTD sensors. However, fouling should be a concern as it is enhanced by seasonal changes in temperature, the salinity concentrations, and the depth of water at the deployment site. This fouling, if severe in nature, could ultimately introduce errors (drift) in the recorded data due to the alteration of the calibration levels of the depth sensors. Time intervals between service intervals of these sensors should be shortened to minimize the fouling errors in the data. See the earlier “Fouling” section for deployment length recommendations.

Replacement Instruments. Replacement instruments, those used as substitutes to enable repair or cleaning of the retrieved sensor, should be of the same type as are those being removed from service. This effort will ensure consistency in the parameters measured and the format of the recorded data.

Data Setup

Each instrument should be set up to record the same quantities, with the same units, and in the same format for each deployment. Any necessary changes should be communicated in detail to the end users.

Data Evaluation

After downloading the data from each instrument, it is important that a quick evaluation of the data be performed to determine that the instrument has and will

continue to function properly. The purpose of this evaluation is to provide valuable information to the field crew and the end user on:

- confirmation that the equipment is recording properly
- confirmation that the instrument is within the normal calibration limits

This is in addition to the *in situ* “over the side” information and data recommended earlier. Comparisons should be made of the initial and final values recorded in the data file with any additional “over the side” data obtained at the time of deployment and retrieval.

These comparisons need to be well documented and made available to the final users of the data. A narrative providing insight into and discussion of the recorded material discussed in this appendix is important for use by the data processors, analyst, and end users. This will provide valuable information for determining the quality of the recorded data during the deployment and retrieval intervals.

Data Transfer

After the initial evaluation of the data has been made:

- the data files should be logged, identified, and transferred to the user or users who will perform the data processing and analysis as soon as possible
- all additional information and data which have been obtained, such as during the retrievals, deployments, calibrations and post-deployment checks and information posted on the instrument record logs or in the field notebook should be assembled, copied, and transferred with the data files
- the transfer of this information to the user must be done in a timely manner, not more than 2 weeks following the data retrieval period. This will allow rapid identification of any problems by the data analysts and end users and will expedite resolution of any problems with a minimal loss of data. In addition, this will result in the transmittal of high quality data in manageable quantities for processing in a timely manner by the receiving organization.
- field and processing groups must be in continued and frequent contact concerning the data, its collection and its processing

The level of effort required to obtain, record, and transfer the above recommended information may be high but will ultimately provide the end users of the data with a significantly higher level of confidence when applying the information to achieve the results of the study.

Appendix E

Calculation of Salinity

by Robert McAdory, Coastal and Hydraulics Laboratory

Introduction

This appendix will outline the method used to calculate salinity values to check the calibration of the YSI 6000 CTD's used in the field data collection effort. The salinities calculated were used to determine the post-deployment calibration salinity differences reported as Δ s-type quantities in Tables 69 to 80 of the main text. The raw data were composed of specific conductivity and temperature measurements taken in the laboratory in a bath of Gulf Stream water used as a secondary standard. See Appendix C and the main report text for more discussion of these data. The calculations for salinity made use of the equations used by YSI in the CTD's themselves. Included here will be a discussion of the calibration data collected and the method for calculating the salinity.

Data

During post-deployment checks of the CTD conductivity and temperature measurements, the specific conductivity of a Gulf Stream water sample was measured using the retrieved CTD. The water sample's specific conductivity had been determined previously against a standard 0.5-molar KCl solution for use as a secondary standard. The temperature and specific conductivity were noted for the sample at hand and for the secondary standard batch used. These data were then used to calculate the salinity of the Gulf Stream water as a (secondary) standard and for the secondary standard from parameters measured by the CTD for use in calculating the Δ s quantities.

Method for Calculating

The method of calculating the salinity involved using standard equations as described below. These equations are also those used to calculate salinity by YSI internal to the CTD's. The equations, the approximations used, and a check on the calculations using CTD data are described below.

Equations

Equations used by YSI are those reported by Clesceri, Greenberg, and Trussel (1989), for example, and are the UNESCO methods for the Practical Salinity Scale (UNESCO 1981). See also GOT (2001) or Powell (1986). As provided by YSI (YSI 2001)¹ and supplemented by Clesceri, Greenberg, and Trussel (1989), the salinity as a function of measured electrical conductivity, temperature, pressure, and the standard electrical conductivity of seawater is given by

¹ YSI. (2001). Yellow Springs Instruments, Yellow Springs, OH. Personal Communication.

$$S = a_0 + a_1 R_t^{1/2} + a_2 R_t + a_3 R_t^{3/2} + a_4 R_t^2 + a_5 R_t^{5/2} + \Delta S$$

with

$$R_t = R/(R_p r_t)$$

$$R_p = 1 + P (e_1 + e_2 P + e_3 P^2)/(1 + d_1 T + d_2 T^2 + (d_3 + d_4 T) R)$$

$$r_t = c_0 + c_1 T + c_2 T^2 + c_3 T^3 + c_4 T^4$$

$$R = C(S, T, P)/C(35, 15, 0)$$

$$\Delta S = (b_0 + b_1 R_t^{1/2} + b_2 R_t + b_3 R_t^{3/2} + b_4 R_t^2 + b_5 R_t^{5/2})$$

$$\times (T - 15)/(1 + 0.0162 (T - 15))$$

S is salinity in “practical salinity units,” which are essentially the same as ppt by weight except in very dilute or very saline waters. In these extremes the difference is less than 0.06 units. See NS (2001). The limits of applicability of the above equations are given below. P is the pressure above one standard atmosphere. T is temperature in °C. C(S,T,P) is the electrical conductivity of the sample, depending on salinity (S), temperature (T), and pressure (P), and reported in mS/cm (millisiemens per centimeter). C(35,15,0) is the standard electrical conductivity for seawater, 42.914 mS/cm, as used by YSI. This is the Culkin and Smith (1980) value, and is also used in Sea-Bird instruments (Sea-Bird 2000).

The coefficients in the above equations are as follows:

$$a_0 = +0.008, \quad b_0 = +0.0005, \quad c_0 = +0.6766097, \quad d_1 = +3.426E-02, \quad e_1 = +2.070E-04$$

$$a_1 = -0.1692, \quad b_1 = -0.0056, \quad c_1 = +2.00564E-02, \quad d_2 = +4.464E-04, \quad e_2 = -6.370E-08$$

$$a_2 = +25.3851, \quad b_2 = -0.0066, \quad c_2 = +1.104259E-04, \quad d_3 = +4.215E-01, \quad e_3 = +3.989E-12$$

$$a_3 = +14.0941, \quad b_3 = -0.0375, \quad c_3 = -6.9698E-07, \quad d_4 = -3.107E-03,$$

$$a_4 = -7.0261, \quad b_4 = +0.0636, \quad c_4 = +1.0031E-09,$$

$$a_5 = +2.7081, \quad b_5 = -0.0144$$

If pressure is measured in dbar, as in Sea-Bird (2000) and YSI instruments, the exponents of e_1 , e_2 , and e_3 are, respectively, -5, -10, and -15.

These expressions are intended for use in the temperature and salinity ranges given by

$$-2^\circ\text{C} \leq T \leq 35^\circ\text{C}$$

$$2 \leq S \leq 42$$

Clesceri, Greenberg, and Trussel (1989) discuss extensions to these equations for low salinities that are “valid from 0 to 40 salinity.” At very low “salinities,”

however, the ionic content may not be dominated by NaCl. Other formulae for salinity are examined and compared in Powell (1986).

Conductivity

The standard for seawater given above is the conductivity based on a standard KCl solution at 15°C, rather than the specific conductivity (conductivity corrected to 25°C). The CTD's as used in this field effort reported specific conductivity. The temperature correction between conductivity (C) and specific conductivity (sC) (Clesceri, Greenberg, and Trussel (1989), and the YSI Manual) is given by

$$sC = C / (1 + 0.0191 (T - 25))$$

T is in units of °C. Using this expression, the specific conductivity values reported by the CTD's, particularly those at the post-deployment calibration checks, can be converted to conductivity. These conductivity values can then be used with the recorded temperature values to calculate the salinity readings of the CTD's during the post-deployment calibration checks.

Pressure

The pressure term, R_p , is neglected for the actual calculations. It is uncertain whether YSI uses this term. However, for this term to make a difference of approximately 0.01 in the salinity calculations, the depth of the measurements would need to be 20 m or more. To be precise, for a sample with specific conductivity of 54.37 mS/cm at 19.02°C, 20 m of depth would make a difference of 0.00752 salinity. The depth of the water used in the laboratory was negligible, and the depths of deployment were never greater than about 4 m. Thus, neglecting R_p poses no difficulties for determining the salinity for the post-deployment check and is not an issue for the calculations internal to the CTD's.

Formula Check

Before using the above equations to calculate the salinity for the post-deployment checks, they were used to recalculate salinity values recorded by a CTD *in situ* as a check. These checks showed that the CTD salinities were consistently reproduced to within about 0.00 to 0.02 out of a salinity of about 22. Given that the CTD's report salinity to the 0.01 place, and the exact method (order) and rounding procedure is unknown for the CTD calculations, this degree of reproduction is good. Furthermore, since the goal here is to calculate differences between two similar salinity readings taken at the post-deployment calibration check, these differences in reproduction do not pose a problem.

Conclusions

The standard equations above reproduce the CTD salinities adequately for use in calculating the post-deployment calibration salinities. These salinities can then

be used as a check on the calibration of the retrieved instruments. The resulting differences in salinity, Δs , are given in Tables 69 to 80 of the main text.

References

- Clesceri, L. S., Greenberg, A. E., and Trussel, R. R., eds. (1989). *Standard methods for the examination of water and wastewater, 1989, 17th Edition*, American Public Health Association, 1015 Fifteenth Street NW, Washington, DC 20005.
- Culkin, F, and Smith, N. D. (1980). "Determination of the concentration of potassium chloride solution having the same electrical conductivity, at 15 °C and infinite frequency, as standard seawater of salinity 35.000‰ (chlorinity 19.37394‰)," *IEEE J. Oceanic En.* OE-5:22.
- GOT. (2001). International Cooperative Study of the Gulf of Thailand web site <http://www.start.or.th/got/data/techsupp/pss78.htm>
- NS. (2001). Nova Scotia Museum of Natural History, "Glossary." See salinity entry at <http://museum.gov.ns.ca/mnh/nature/nhns2/glosntoz.htm>
- Powell, G. (1986). "Salinity determination," Interoffice Memorandum, Texas Water Development Board, Austin, TX.
- Sea-Bird. (2000). Application Note No. 14. 1978 Practical Salinity Scale. See entry at http://www.seabird.com/application_notes/AN14.htm
- UNESCO. (1981). "Background papers and supporting data on the Practical Salinity Scale, 1978," UNESCO Technical Papers in Marine Science, No. 37, p. 144.

REPORT DOCUMENTATION PAGE

Form Approved
OMB No. 0704-0188

Public reporting burden for this collection of information is estimated to average 1 hour per response, including the time for reviewing instructions, searching existing data sources, gathering and maintaining the data needed, and completing and reviewing this collection of information. Send comments regarding this burden estimate or any other aspect of this collection of information, including suggestions for reducing this burden to Department of Defense, Washington Headquarters Services, Directorate for Information Operations and Reports (0704-0188), 1215 Jefferson Davis Highway, Suite 1204, Arlington, VA 22202-4302. Respondents should be aware that notwithstanding any other provision of law, no person shall be subject to any penalty for failing to comply with a collection of information if it does not display a currently valid OMB control number. **PLEASE DO NOT RETURN YOUR FORM TO THE ABOVE ADDRESS.**

1. REPORT DATE (DD-MM-YYYY) July 2002		2. REPORT TYPE Final report		3. DATES COVERED (From - To)	
4. TITLE AND SUBTITLE Biscayne Bay Field Data: Volume 1, Main Text; Volume 2, Plates and Appendices				5a. CONTRACT NUMBER	
				5b. GRANT NUMBER	
				5c. PROGRAM ELEMENT NUMBER	
6. AUTHOR(S) Robert McAdory, Thad C. Pratt, Martin T. Hebler, Timothy L. Fagerburg, Richard Curry				5d. PROJECT NUMBER	
				5e. TASK NUMBER	
				5f. WORK UNIT NUMBER	
7. PERFORMING ORGANIZATION NAME(S) AND ADDRESS(ES) U.S. Army Engineer Research and Development Center Coastal and Hydraulics Laboratory 3909 Halls Ferry Road Vicksburg, MS 39180-6199				8. PERFORMING ORGANIZATION REPORT NUMBER ERDC/CHL TR-02-8	
9. SPONSORING / MONITORING AGENCY NAME(S) AND ADDRESS(ES) U.S. Army Engineer District, Jacksonville P.O. Box 4970 Jacksonville, FL 32232-0019				10. SPONSOR/MONITOR'S ACRONYM(S)	
12. DISTRIBUTION / AVAILABILITY STATEMENT Approved for public release; distribution is unlimited.				11. SPONSOR/MONITOR'S REPORT NUMBER(S)	
				13. SUPPLEMENTARY NOTES	
14. ABSTRACT The purpose of this study was to gather field data for Biscayne Bay, Florida, to support the development of a two-dimensional, physical-based numerical model of Biscayne Bay. The data are also appropriate for use in understanding the Biscayne Bay system apart from modeling. The data collection effort was a joint effort by the U.S. Army Engineer Research and Development Center Coastal and Hydraulics Laboratory (CHL) and Biscayne National Park (BNP). Most of the data were collected by BNP, and most of the analysis was done by CHL. The collected data consist of year long sets and Acoustic Doppler Current Profiler intensive inlet transect discharges. Year long data included water surface elevation, temperature, and conductivity values (salinity by calculation) at twelve conductivity, temperature and depth recorders, five additional Acoustic Doppler Profilers to record water surface elevation, temperature, and velocity in 30-cm bins, and one weather station. The intensive transect data included eight to nine approximately hourly transects across 27 inlets and interior channels from which hourly discharge values were calculated. The reliability of the data is considered at length. Additional data necessary for the modeling effort, such as freshwater inflows, were assembled from other sources.					
15. SUBJECT TERMS See reverse.					
16. SECURITY CLASSIFICATION OF:			17. LIMITATION OF ABSTRACT	18. NUMBER OF PAGES	19a. NAME OF RESPONSIBLE PERSON
a. REPORT UNCLASSIFIED	b. ABSTRACT UNCLASSIFIED	c. THIS PAGE UNCLASSIFIED			19b. TELEPHONE NUMBER (include area code)

15. (Concluded).

Biscayne Bay
Current velocity
Discharge data
Drift index
Field data

Freshwater inflow
Instrument calibration
NGVD29 datum
Numerical modeling
Salinity

Salinity calculation
Temperature
Tide
Water surface elevation
Weather data